SYMPOSIUM COMMITTEE

President: Sir Eric K. Rideal, F.R.S.
Chairman: Professor D. H. Everett
Secretary: Dr. R. H. Ottewill

Professor S. Brunauer
Professor J. H. de Boer
Mr. A. S. Joy
Professor J. Th. G. Overbeek
Professor M. Prettre
Mr. M. K. Schwitzer
Dr. H. van Olphen

INTERNATIONAL UNION OF
PURE AND APPLIED CHEMISTRY

in conjunction with

THE SOCIETY OF CHEMICAL INDUSTRY

SURFACE AREA DETERMINATION

Proceedings of the
INTERNATIONAL SYMPOSIUM ON
SURFACE AREA DETERMINATION
held at the
School of Chemistry, University of Bristol, U.K.
16—18 *July*, 1969

Symposium Editors
D. H. EVERETT and R. H. OTTEWILL

LONDON
BUTTERWORTHS

ENGLAND: BUTTERWORTH & CO. (PUBLISHERS) LTD.
LONDON: 88 Kingsway, W.C.2

AUSTRALIA: BUTTERWORTH & CO. (AUSTRALIA) LTD.
SYDNEY: 20 Loftus Street
MELBOURNE: 343 Little Collins Street
BRISBANE: 240 Queen Street

CANADA: BUTTERWORTH & CO. (CANADA) LTD.
TORONTO: 14 Curity Avenue, 374

NEW ZEALAND: BUTTERWORTH & CO. (NEW ZEALAND) LTD.
WELLINGTON: 49/51 Ballance Street
AUCKLAND: 35 High Street

SOUTH AFRICA: BUTTERWORTH & CO. (SOUTH AFRICA) LTD.
DURBAN: 33–35 Beach Grove

Published as a supplement to

Pure and Applied Chemistry

Suggested U.D.C. *number:* 541·18:531·72

Standard Book Number: 0 408 70077 7

Printed in Great Britain by Page Bros. (Norwich) Ltd., Norwich

PREFACE

The proposal to hold the Symposium whose proceedings are reported in this volume was made, on the initiative of Sir Eric Rideal, by the IUPAC Commission on Colloid and Surface Chemistry at its meeting in Prague in August 1967. The objective was to take a first step towards reaching international agreement on methods of determining the surface areas of solids of different kinds, acceptance of which would make feasible the subsequent goal of the establishment of a set of Standards for Surface Area Determination. The project was supported by the Committee of the Colloid and Surface Chemistry Group of the Society of Chemical Industry who collaborated with IUPAC in the organisation of this Symposium.

It would have been over-optimistic to have expected full and complete agreement in such a widely representative Symposium attended by some 289 delegates from 19 different countries. Nevertheless, as these proceedings show, many of the methods proposed in the past for surface area determination are now well established, at least on an empirical basis, and the interrelationships between them are becoming clearer. That the fundamental theoretical basis for these methods is not yet securely established is not very surprising: but there is now a wider appreciation of the nature of the outstanding difficulties facing a more complete general theoretical study.

On the practical side, this Symposium, and the discussions which have arisen from it, have provided a basis for the planning of a project for the establishment of a set of Standards for Surface Area Determination. This is expected to begin as a pilot scheme initiated by the Society of Chemical Industry and then to expand into an international programme under the aegis of IUPAC.

Bristol
March 1970

D. H. EVERETT
R. H. OTTEWILL

OPENING REMARKS

Sir Eric K. Rideal

Physical Chemistry Laboratories, Chemistry Department, Imperial College, London, S.W.7., U.K.

This joint meeting of the Colloid and Surface Chemistry Group of the Society of Chemical Industry and the Commission on Colloid and Surface Chemistry of the International Union of Pure and Applied Chemistry (IUPAC) comes at a very opportune time. The Group has now been in existence for eleven years having previously functioned as a panel for two years, whilst this IUPAC Commission was formed in Montreal in 1961. The same title was chosen for both Group and Commission to reflect the national and international aspects respectively. Whilst the Group has furthered the subject by means of many joint meetings with other groups of the Society and by the holding of symposia on subjects of topical importance, the Commission had definite terms of reference laid down for it by IUPAC at the Montreal meeting.

Since 1961 the Commission has been actively engaged in investigations as to the state of our knowledge, permitting us to make positive recommendations for international usage. Two of the terms of reference were, briefly, (i) Definitions, terminology and symbols; (ii) Conventions in naming colloidal systems.

The fruit of many years of labour requiring the most detailed enquiries and critical examination was presented in the form of a report by the Chairman of our Commission, Professor J. Th. G. Overbeek, to the Council of IUPAC at the meeting at Cortina D'Ampezzo in Italy in July 1969. The Commission in consequence is in a position to commence work on other aspects of the problem laid down in the Montreal terms of reference. Two of these were (i) Definition of pore volumes, bulk density, particle density, types of isotherms, size and sign of phase boundary potential; (ii) Agreement covering the description of finely divided solids and of measuring the adsorption per gramme and per square centimeter of adsorbent.

This Symposium on surface area determination will give the Commission not only a good start but also encouragement to pursue this important phase of its activity.

We are further encouraged by the fact that Professor V. N. Kondratiev, the President of IUPAC, in his Presidential address in 1968 expressed the view that the phenomenon of catalysis was now becoming so important both industrially and from the academic point of view that IUPAC should pay particular attention to this field and in his opinion the Commission on Colloid and Surface Chemistry, possibly with modification, seemed to be the proper vehicle for carrying out this work.

Whilst Professor Kondratiev included both homogeneous and heterogeneous catalysis in his address, the Commission was already aware through the lengthy report of Professor J. Horiuti of the complexities involved in any really adequate treatment of heterogeneous catalysis without completion of the remit in respect to adsorption and surface structure laid down for us at Montreal, and this I regard as an essential priority.

I would like to say a few words about this present meeting. A number of countries in the world have bureaux which are responsible for standards especially those in which commerce is involved. For standards to become international in character we must have a uniform and consistent experimental procedure as well as an agreed method of representing or treating the experimental results. Materials usedfor adsorption are no exception. Perhaps the B.E.T. method of treatment is the nearest approach to this aim. We are honoured in having one of the originators, Dr. S. Brunauer, with us to-day. If we are to adopt this pragmatic approach, we could ask the question, how far should we extend this idea? Should we develop internationally agreed methods for the evaluation of Lewis and Brønsted acidities of alumino-silicates, for the efficiencies of catalysts for various chemical reactions, e.g., SO_3, NH_3, hydrogenation, cyclisation and the like or develop standard methods for the evaluation of supported catalysts? Apart from this utilitarian objective we must attempt to arrive at agreements on concepts regarding surface area since widely different values are obtained when different methods of evaluation are employed. Adsorbents and catalysts are complex systems and in any ultimate analysis of total and available surface we should be able to evaluate the respective contributions of lattice defects, crystal planes and edges as well as Kelvin and sub-Kelvin capillaries and their shapes to the total sorption. We should also seek agreement on the concept of a close-packed monolayer formed on a crystal plane and what P, θ relationship permits us to evaluate it. Whilst it has long been customary to consider that the effective diameter of a Kelvin pore is two molecular thicknesses less than the true diameter, this arbitrary correction must be reconsidered in the light of the possibilities of anomalous values of surface energies and molecular volumes of vapours condensed in what Hardy termed the boundary state. These possible anomalies may likewise affect the validity of computation of the areas determined by methods involving heats of wetting.

Finally, I might mention that within the compass of our task we require to know more about the state of an adsorbed monolayer on a crystal facet. The simplest form, namely, an epitactic configuration, would be revealed by a Langmuir isotherm in which complete atomic coverage could be achieved. In the future the ligand structure and bond strength should be evaluated. In general, lateral interation between the adsorbate molecules causes the growth either of a two phase surface structure, i.e., a patchwise interfacial growth, or repulsive forces may impose regular patterns not coincident with the substrate on the complete monolayer. Dispersion or physisorption is frequently termed van der Waals sorption. We might ask whether critical phenomena, e.g., pressure and temperature, have an objective reality or whether a Boltzmann distribution between bound and free molecules represents the state of affairs more closely, whether the spreading pressure is analogous to osmotic rather than gas pressure and whether two-dimensional diffusion constants could not be evaluated for such systems. If but a few of these observations have any validity it is evident that there is plenty of work ahead of us. The contributions to this meeting show that advance is possible.

INTRODUCTORY LECTURE

J. Th. G. Overbeek

van't Hoff Laboratory, University of Utrecht, Utrecht, The Netherlands

It is my task now to give a brief introduction to this Symposium and perhaps to announce a few subjects that we might want to emphasize in the discussions. The first idea for this Symposium was to obtain a survey of the different methods for surface area determination, to compare their results, and, if possible, to formulate recommendations for methods of measurement or calculation, that could be internationally accepted.

I do not need to stress that area or specific area (= area per unit mass) is an *important* parameter of a finely divided solid (or liquid) phase. But *why* is it *difficult* to measure? The answer is: because it is not well defined. Determining the surface area of a solid is affected with the same difficulties as determining the surface area of *England*, or *Holland* or of the *Italian Dolomites*. On a small scale map the answer is simple, but it is not very accurate and it neglects the structure of the surface completely. So then we have to decide which part of the surface roughness is to be taken into account. Only those features that can be read from the map with elevation contours? Or the actual roughness of the rocks and soil? Or the roughness of the sandgrains and the individual pebbles? There is no unambiguous answer; only an arbitrary choice is possible.

The same is true for the surface area of a finely divided solid. And the choice will depend on the *use we are going to make* of the value of this surface area. Looking at the problem from this point of view, we want to know the complete geography of the surface, accurate to the kind of, and number of, the surface atoms, and including the way in which they are bound to the next lower layer. Such information would be good enough to explain all possible interactions with substances that can be adsorbed, move along the surface, react at the surface, or even move in the gas or liquid phase in the neighbourhood of the surface.

However, this detailed answer is as good as and about as useless as saying that all the properties of a glass of good wine are contained in the Schrödinger equation for its nuclei and electrons.

In the papers for this Symposium, these aspects are mostly not mentioned explicitly, but it will be well to keep them in mind in the discussions. Cases, where indeed this 'molecular' or 'atomic' way to look at the surface becomes preponderant are found when *crystallographic* data are used for surface area determination (assuming that the total surface consists of flat crystallographic surfaces) or also, when instead of asking how many molecules of nitrogen or of another adsorbate are packed on a certain area, one considers how many surface atoms of a given kind of molecule of a certain adsorbate is attached.

But in the main we will discuss surface area in these days from a somewhat simplified point of view, i.e., we form a kind of envelope through the centres of all the surface atoms, and consider the area of this envelope. In a great many cases we are not content to know the area of this envelope, but we want to know also, how it is folded in slits, pores, and other surface irregularities.

In discussing pores, most people will first think of cylindrical pores, but on second thoughts, these are rather improbable. Slits either between two parallel crystal faces, or perhaps wedge shaped slits are already more probable, and in the papers, the old ink-bottle image is used several times to describe a cavity with a narrow entrance. Remarkably enough the image of interstices between a mass of packed and possibly somewhat sintered particles, which might be applicable in several practical cases, is only rarely referred to.

Passing now to the papers presented at this Symposium, we find great emphasis on surface area determination by adsorption methods in different variants.

a_1. The methods used most frequently are based on the determination of the *monolayer capacity* of a given adsorbent by the BET method, by the *t*-method, which is based on it, or by adsorption from solution, using either simple molecules such as benzene or toluene, or large and complicated ones such as dyes. In order to convert the number of molecules in a complete monolayer to a surface area, one needs the area *per adsorbed molecule* and this requires a *calibration* based on the adsorption on a non-porous adsorbent, the surface area of which is known from other data. A very important question is then, whether the surface area per molecule is independent of the chemical nature of the adsorbent.

If the adsorbent is porous, application of the *Kelvin equation* leads in principle to the determination of the volume contained in pores of given sizes and so, with the aid of a pore model, to the distribution of the surface area amongst the pores. However, the method needs several refinements, one of these being the division of pores into *macropores* (too big for capillary condensation), intermediate pores or *mesopores* (typical for capillary condensation) and *micropores* (too small for application of the Kelvin equation).

a_2. Instead of using the adsorption isotherm at about the complete monolayer and higher coverages one may use the *low* (linear) *end of the adsorption isotherm* and when the Henry's law constant for the particular combination of adsorbent and adsorbate is known, derive a surface area from that part of the isotherm. Obviously, surface heterogeneity and the need of calibration with an adsorbent with known area are weak points of this otherwise attractive method.

a_3. For surfaces carrying an electric layer *negative adsorption* of the co-ions can be used to obtain a surface area. This method, which was first proposed by Schofield for clay surfaces, leads to an absolute value of the surface area without the need of a calibration, but it is not applicable to porous solids and in its present form it is not accurate for specific surface areas below a few m^2/g.

b. A completely different approach, leading without calibration to an absolute value for the surface area is based upon the determination of the *heat of immersion*. If the adsorbent is precoated with a sufficiently thick layer of molecules the liquid in which it is to be immersed, immersion results in the destruction of the surface areas containing a surface enthalpy per unit area equal to that of the free liquid and to the liberation of a corresponding amount of heat.

With presently available calorimetric techniques the method requires a non-porous solid with a specific surface area not less than 10 m^2/g.

c. Another method or rather group of methods uses the *flow of a gas or liquid* through a plug or membrane to give information on its surface area. From the steady rate of flow, using the *Kozeny-Carman* method, a relation between porosity and surface area can be obtained. This method, however, does not take the area and porosity connected with blind pores into account. Moreover, a pore model and an estimate of the 'tortuosity' are needed.

Non-steady state methods, in particular the determination of adsorption—and desorption—time lags do give more information and, if judiciously applied, some information on the blind pores. From the adsorption isotherm, the total area can be obtained as in the methods considered under *a*.

d. In the case of expanding clays the surface area can be determined directly from x-*ray crystallographic* data, but this case is a rare exception.

Small angle x-ray scattering, on the other hand, allows the determination of the total surface area in the sample without any separate calibration. Moreover, information can be obtained on pore size or particle size distribution. A remarkable feature of this method is, that it also takes *closed pores* into account, which are inaccessible to all adsorption methods.

e. Finally, mention should be made of the use of the *electron microscope* or of the *ordinary microscope* for determining particle size distributions and surface areas of non-porous particles and of the important case of *carefully drawn glass fibres*, where length, mass, and density are sufficient to allow calculation of the area.

Summarizing, we find that there is quite a variety of methods available and, in favourable cases, more than one method may be applied to the same sample. The methods are of different reliability and of different accuracy; some are absolute, some need a calibration. It is one of the purposes of this Symposium to evaluate these methods critically and perhaps reach a conclusion as to which method or methods and which calibration parameters are to be recommended for particular purposes.

THE BET-METHOD

J. H. DE BOER

Department of Chemistry and Chemical Engineering,
Technological University of Delft, Delft, The Netherlands

1. PHYSICAL AND CHEMICAL ADSORPTION

The equation of Brunauer, Emmett and Teller[1], the BET-equation, is based on van der Waals' attraction forces. These forces may all be considered to be of a physical nature and we may suggest that the conceptions of 'van der Waals' adsorption' and of 'physical adsorption' cover the same phenomena.

Langmuir's original equation[2] may, under certain circumstances, be used to describe certain adsorption phenomena of physical nature, but also those of chemical nature, hence 'chemisorption' fits into this conception.

Both the BET- and the Langmuir-equations can be, and are, used to estimate specific surface areas of adsorbents. In this contribution I shall make use of both conceptions.

2. THE NATURE OF PHYSICAL ADSORPTION

The simplest definition of van der Waals' forces is perhaps the one given by Margenau[3] in 1939, namely that van der Waals' forces are those which give rise to the constant a in van der Waals' equation:

$$\left(p + \frac{a}{v^2}\right)(v - b) = RT \tag{1}$$

This includes: (i) attraction forces caused by the polarization of molecules by static dipole- or quadrupole fields of other molecules, hence Debye's[4] induction effect of 1920; (ii) the forces between molecules possessing dipoles or quadrupoles, hence Keesom's[5] alignment effect of 1921; and (iii) the non-polar van der Waals' forces, also called the dispersion forces since London[6] discovered the close connection between their nature and the cause of optical dispersion.

It is also logical that the forces between a polar surface and dipole molecules and the electrostatic induction of atoms or molecules by polar surfaces are included in the definition of van der Waals' adsorption forces.

Doing this we follow closely Brunauer's[7] concept of physical adsorption. We, therefore, include all cases in which neutral atoms or molecules interact with surfaces *without* sharing of electrons taking place, or *without* exchanging of electrons, thus preserving the individuality of the adsorbed neutral atoms or molecules.

The nature of the thus defined van der Waals' forces does not exclude them from causing intra- or intermolecular bonds in cases which may be considered to belong to the domain of chemistry; I only need to draw the attention to the many co-ordination compounds where H_2O or NH_3 molecules are spacially arranged round central, mostly double-, triple- or higher positively charged ions. This reminder may be sufficient to be somewhat suspicious when it is taken for granted that physical adsorption, contrary to chemisorption, does not alter the surface of an adsorbent seriously. We may be somewhat more confident when the physical adsorption is only caused by the non-polar van der Waals' forces, the third category mentioned above. In the course of this contribution I shall come back to this problem

3. THE BET-EQUATION AND POINT B

I shall not give a derivation of the BET-equation. Derivations can be found in the original literature[1], or in Brunauer's book[7] or if one wants to have a derivation based on the conception of the time of adsorption, I may refer to my own book[8]. In my derivation in that book I follow closely that of the originators of the conception and, of course, in order to come to the practical equation, I have to introduce the same rigid simplifications, which—it must be stated—deviate alarmingly from reality.

The ultimate equation, as given in Brunauer's book[7] is:

$$v = \frac{v_m \, cp}{(p_0 - p)\,\{1 + (c - 1)\, p/p_0\}} \tag{2}$$

which, for practical use is put into the form

$$\frac{p}{v\,(p_0 - p)} = \frac{1}{v_m c} + \frac{c - 1}{v_m c} \cdot \frac{p}{p_0} \tag{3}$$

Apart from the pressure, p, the saturation pressure of the adsorbate, p_0, and the volume of adsorbate, v, adsorbed at the pressure, p, it contains only two constants, v_m, which stands for the volume of adsorbate representing a completely filled monolayer, and, c, given by, approximately,

$$c = e^{(E_1 - E_L)/RT} \tag{4}$$

where E_1 is the average heat of adsorption in the first layer, E_L the heat of liquefaction, and RT has the usual meaning.

The range of relative pressures between which the BET-equation can successfully be used, is from $p/p_0 \sim 0{\cdot}05$ to $p/p_0 \sim 0{\cdot}35$. At higher relative pressures the equation gives figures which are higher than the experimental data; these deviations are increasing at increasing relative pressures. There are other equations known in the literature which describe the experimental data far better than the BET-equation. Contrary to the BET-equation, however, they do not lead to the experimental data of the so-called point B[9] of the isotherm, the point, situated at a relative pressure somewhere between $p/p_0 = 0{\cdot}05$ and $p/p_0 = 0{\cdot}10$, where the first steep part of the isotherm ends and, with a more or less sharp bend, a relatively straight and far less steep part begins.

The aim of the BET-method is to find this point B, either graphically or with the aid of the BET-equation.

4. THE MOLECULAR AREA OF A N_2-MOLECULE

Once point B is found, it is usually taken for granted that the volume (or weight) of the adsorbate, just covering a completely filled unimolecular layer on the surface of a given amount of adsorbent is known. As the aim is to determine the specific surface area of the adsorbent in m^2g^{-1}, a conversion of the volume (or weight) of the adsorbate into a surface area must be found. This means that a specific surface area must be assigned to each molecule of the adsorbate filling the first unimolecular layer. We have arrived, herewith, at the most difficult problem of the practical application of the BET-method.

Considering that it is alleged that the first unimolecular layer is complete at point B (hence before $p/p_0 = 0{\cdot}1$), and that the region of the BET-equation covers the adsorption up to a relative pressure of $p/p_0 = 0{\cdot}35$, where at least a second, but perhaps even higher layers are present, it is logical that the assembly of the adsorbed layers is compared with one of the known condensed states, hence the liquid or the solid state. It is, therefore, also logical to assign the same molecular area to the adsorbed molecules as they have in either the liquid or solid state.

In the practice of BET-determinations nitrogen is mostly taken as the adsorbate and the measurements are done at the temperature of liquid nitrogen, hence at about $-195°C$, and as molecular area of a nitrogen molecule the figures $\sigma_m = 16{\cdot}2$ Å^2 (from liquid nitrogen) or $\sigma_m = 13{\cdot}8$ Å^2 (from solid nitrogen) are used.

Emmett and Brunauer[9] started to use the figure of 16·2 A^2 already with their graphically determined point B. Their most direct evidence that this figure might be the best to use, was that areas computed with this figure were in good agreement with areas derived from the measurements of the mean particle sizes of powders of the adsorbents from electron micrographs.

In a survey article of 1942 Emmett[10] states that 'we have no way of knowing whether the correct value for the area covered by a nitrogen molecule adsorbed on the surface is 16·2 Å^2, as judged from the density of liquid nitrogen, or 13·8 Å^2, as judged from the density of solid nitrogen'. In 1947, however, in an article with Anderson[11] it was stated: 'evidence seems to be accumulating to indicate that the average area occupied by the adsorbed nitrogen molecule is closer to the 16·2 value than to the 13·7 value, but this may well vary somewhat from solid to solid.'

In 1949 Livingston[12] suggested to use the molecular area of 15·4 Å^2, in agreement with the area calculated from the two-dimensional van der Waals' constant. This value, although very nicely situated between the two figures mentioned above, has not been accepted. We will come back on this figure in Section 15.

5. OTHER ADSORBATES

Since the introduction of the BET-method a great many gases other than nitrogen have been used as adsorbates. In a survey-article McClennan and Harnsberger[13] mention recently 107 gases of inorganic and of organic nature, which have been used. They compare the molecular areas of these adsorbates, as calculated or as given by the various authors whose work they cite, with the molecular area of N_2, for which they use $\sigma_m = 16{\cdot}2$ Å^2 at -195°C as the primary standard. From their extensive Table of data, they have chosen 16 substances (benzene, toluene, hexane, butane, ethane, butanol, propanol, ethanol, methanol, ammonia, carbon dioxide, water, oxygen and the noble gases argon, krypton and xenon).

Then the authors select 8 adsorbates for which they give 'recommended molecular areas', and ultimately they narrow their selection down to 5 adsorbates, argon, krypton, water, *n*-butane and benzene.

For comparison, in the present contribution, I shall make use of argon, krypton and water only. According to the study of McClennan and Harnsberger the published molecular areas of *water* vary between 5-6 Å^2 and 23–24 Å^2 with a maximum between 11–12 Å^2 and 14–15 Å^2, whilst those of *argon* vary between 8–9 Å^2 and 16–17 Å^2 with a maximum between 13–14 Å^2 and those of *krypton* vary from 13–14 Å^2 to 25–26 Å^2, with a maximum in the curve between 17–18 Å^2 and 21–22 Å^2.

For argon, krypton and water they give as recommended figures for the molecular area:

Ar at -195°C: 13·8 Å^2

Kr at -195°C: 20·2 Å^2

H_2O at 25°C: 12·5 Å^2

6. A COMPARISON BETWEEN N_2 AND Ar

In an article about uniform graphite surfaces (which we shall discuss in Section 16 of this contribution) Pierce and Ewing[14] describe the work of two Japanese scientists, Kodera and Onishi[15], who measured the surface areas of various carbon blacks, titanium dioxides and silicon dioxides. They compared the surface areas as derived from electron microscopic determinations, with those measured with the use of adsorbed gases. From their comparisons they concluded that the best molecular area of an argon atom at 78°K was $(\sigma_m)_{\mathrm{Ar}} = 13{\cdot}8$ Å^2, a figure which can be computed from the molecular volume of argon at that temperature. Taking this figure as a primary standard, the Japanese scientists conclude that the ratio of the molecular areas of nitrogen and of argon, $[(\sigma_m)_{\mathrm{N_2}}/(\sigma_m)_{\mathrm{Ar}}]$ is $1{\cdot}14 \pm 0{\cdot}03$ on 8 samples of carbon black and $1{\cdot}26 \pm 0{\cdot}02$ on 15 samples of TiO_2 and SiO_2, which would give a molecular area for the nitrogen molecule of 15·7 Å^2 on carbon blacks and of 17·4 Å^2 on TiO_2- and on SiO_2-surfaces.

Corrin[16], comparing the surfaces of 9 varying adsorbents and using both N_2 and Ar as adsorbates at $-195{\cdot}8$ °C gets a better range of linearity for the BET-plot with argon than with nitrogen[17]. He concludes for the molecular surfaces the figures $(\sigma_m)_{\mathrm{N_2}} = 16{\cdot}2$ Å^2 and $(\sigma_m)_{\mathrm{Ar}} = 16{\cdot}6$ Å^2.

As Gregg and Sing[17] conclude in a comparison of the molecular areas of N_2 and of Ar, nitrogen might at some adsorbents be bound by quadrupole forces, in addition to the non-polar van der Waals' forces, whereas argon can only be bound by non-polar forces.

7. ADSORPTION OF N_2 AND OF CO AT TEMPERATURES AROUND 300°K

Menon[18] determined the adsorption of nitrogen on an alumina surface at temperatures around room temperature. At such temperatures one has to apply very high pressures (Menon went to about 3000 atm) to find measurable amounts of adsorbed molecules and one has to correct for the gaseous molecules which would be in the 'adsorption region' because of the high density of the gas. One has, moreover, to define the 'adsorption region'. Because of the relative short range of effective attraction by the surface, this region was defined as the space between the surface of the alumina and a plane, parallel to this surface at a distance of 1·5 diameter of the nitrogen molecule. The gas density in this study was expressed in Amagat Units, an Amagat Unit of density being the density of the gas at 0°C and one international atmosphere pressure. The surface area of the alumina was determined by the normal BET-procedure.

In the region of relatively low pressures, say gas densities up to about 50 Amagat, the amount of adsorbed nitrogen is practically proportional to the pressure. In the region of 150–200 Amagat the 'normal', 'non-adsorbed' gas molecules occupy already so much of the adsorption space, that the curve giving the 'adsorbed amount' rises less strongly, it passes a maximum, but instead of flattening to give a steady amount of 'adsorbed gas', it passes a minimum and rises again.

At zero degree centigrade this *minimum* in the adsorption curve occurs at about 540 Amagat Units corresponding with about 1400 atmospheres. At higher temperatures it occurs with lower pressures, so at 100°C the minimum is found at about 470 Amagat Units.

The only reasonable explanation that we could find for this remarkable phenomenon is that the minimum is caused by an erection of the nitrogen molecules by which they pass from a random position to a position where one of the N-atoms of the N_2-molecule points away from the surface and the other is in close contact with it. Its random rotation is, therefore, stopped. The erection is an endothermic process. This is, however, a net gain of entropy by the erection process.

As the surface area of an erected nitrogen molecule is $12{\cdot}3/15{\cdot}55 =$ about 0·8 of that of a rotating one, there is far more room for adsorption after the erection, which the experiments prove.

It is interesting to note that experiments with carbon monoxide show a similar behaviour as that of nitrogen, *except* for the process of erection. The CO-curves just flatten out at the highest pressures.

8. WATER AS AN ADSORBATE

As I describe[19] in my book *The Dynamical Character of Adsorption*, the saturation pressure p_0 in equations 2 and 3 of the present contribution need not be the normal saturation pressure of the adsorbate. It is especially with water molecules that deviations may occur. If the heat of evaporation of the second and higher layers of the adsorbate is a few per cent higher than the heat of evaporation of the liquid, the adsorption isotherm will not approach asymptotically a vertical at $p/p_0 = 1$, but it will already approach asymptotically a vertical at about $p/p_0 \sim 0{\cdot}9$. On the other hand if the heat of evaporation of the higher layers of the adsorbate is lower than that of the liquid, the asymptote will be found at values of $p/p_0 > 1$.

With water as the adsorbate there are quite a few examples of this behaviour. Water adsorbed on apple pectin[20] approaches a vertical at $p/p_0 < 1$ asymptotically.

The adsorption curve of water on wool gives a sharp intersection with the vertical at $p/p_0 = 1$ and so do also the curves for the adsorption of water on cotton and the adsorption curve of water on maize.

However, also adsorbates other than water may show such behaviour.

9. THE LANGMUIR ISOTHERM

If an adsorbate behaves in such a way that its adsorption isotherm could only approach the vertical at a relative pressure $p/p_0 \gg 1$, we may neglect p with respect to p_0 in equation (3), and obtain[21]

$$v = \frac{v_m\, c p p_0}{p_0\,\{p_0 + cp\}}$$

hence

$$v = \frac{v_m cp}{p_0 + cp} = \frac{v_m\, kp}{1 + kp} \tag{5}$$

where $k = c/p_0$.

Equation (5) is the Langmuir equation.

Admittedly the BET-equation may not be used, generally, outside the relative pressure ranges from 0·05 to 0·35, and the assumptions made in deriving the BET-equation are untenable. It is, nevertheless, interesting to remind ourselves that the Langmuir equation may be considered to be a special case of the BET equation.

10. THE APPLICATION OF THE LANGMUIR EQUATION FOR THE DETERMINATION OF SURFACE AREAS

The Langmuir isotherm equation can, and has in many cases, been used for the determination of surface areas. Unlike the picture underlying the BET-equation, the picture leading to the Langmuir equation may include the phenomenon of chemisorption.

During the years 1927–1939, I used, in the research laboratory of Philips' Eindhoven, the unimolecular chemisorption of some organic substances for the determination of the surface areas of thin alkali- and alkaline earth halide layers, such as used in vacuum incandescent lamps. These salt layers were obtained by evaporation of the corresponding inorganic halides from the tungsten filaments, just before sealing off the lamps from the production machine.

Hydroxy-group containing substances like alizarin were strongly adsorbed on these salt layers, and at a somewhat elevated temperature, they reacted with the outside halide-ions of the salt layer; the resulting hydrogen halide evaporated and the alizarin-ions were chemisorbed on the salt layer. The surplus of physisorbed alizarin could be removed by sublimation followed by rinsing with neutral amyl alcohol and after opening the bulbs the chemisorbed amounts of alizarin could be determined, leading to a very reproducible method for finding the surface area of the salt layers[22].

Also the unimolecular adsorption of hydrogen atoms[23] and the strong adsorption of the first layer of water molecules[24] could be used, and may be considered as applications of the Langmuir isotherm.

All these methods could be and had to be applied on a microscale.

11. COMPARISON OF THE BET AND THE LANGMUIR ISOTHERM ON THE SAME SURFACES

During our work on surface areas and on pore structures, after the 2nd World War, in the chemical laboratory of the Delft University of Technology, we compared the results of the BET-method with those of the Langmuir-adsorption. For the Langmuir-adsorption we used the strongly polar adsorption of lauric acid from a pentane or a hexane solution[25]. As adsorbent, various samples of aluminium hydroxide and of aluminium oxide were used, and somewhat later also dehydrated silicas and rehydrated silicas.

The surface area occupied by fatty acids when spread on water is at least 20·5 Å^2 per molecule. On a dehydrated and then carefully rehydrated silica, however, lauric acid occupied about 66 Å^2 per molecule[26], as derived from the BET-surface area. As the latter was calculated with the N_2-molecular area of 15·4 Å^2, the area per lauric acid molecule is even higher when calculated with the more usual figure of 16·2 Å^2; it then becomes 69·5 Å^2. On a dehydrated silica, however, the lauric acid molecule occupies only 44–46 Å^2 per molecule.

On the surfaces of aluminium hydroxides[25] (11 samples) 0·43 ± 0·01 mmole of lauric acid is adsorbed in a unimolecular layer per 100 m^2 surface area, the latter being estimated by the BET-method and 16·2 Å^2 for the N_2-molecule. In a similar comparison for strongly dehydrated aluminas (dehydrated at temperatures above 800°C) a figure of 0·616 ± 0·016 mmole lauric acid per 100 m^2 was found (9 various samples). The latter figure, assuming the molecular area of N_2 to be 16·2 Å^2, leads to 27 Å^2 per lauric acid molecule.

It may be expected that the lauric acid, because of its strong selective adsorption, will adapt itself to the surface structure of the adsorbent. All aluminas obtained between the decomposition temperatures of the hydroxides and 1000°C have structures based on a nearly closest-packed cubic oxygen lattice, closely related to the spinel-type γ-Al_2O_3. One oxygen atom at the surface may then occupy a surface area of 6·74 Å^2, which leads to the above mentioned molecular surface area of 27 Å^2 for the lauric acid molecule, when one lauric acid molecule is bound to four oxygen atoms of the surface.

In a later study[27] the adsorption of water molecules was studied on strongly dehydrated aluminas. A large amount of water is adsorbed when exposed to a humid atmosphere; most of this water can be expelled by heating at 120°C, but one unimolecular layer of water stays behind. Although this water is very strongly bound, it has not reacted to form hydroxyl groups. When lauric acid is adsorbed on alumina, covered with this strongly bound water layer, nearly the same amount of lauric acid is adsorbed as on the water-free surface (hence far more than on a hydroxide-surface); 0·60 mmole lauric acid is strongly adsorbed, instead of 0·616 on an alumina surface without the strongly bound water layer. Although according to our definition in Section 2 of this paper, the strongly bound water layer is not a chemisorbed one, but a strongly physisorbed layer, we may call it a 'chemisorbed' one, for the same reasons as mentioned in Section 2.

When lauric acid is brought into contact with alumina, covered with a multimolecular water layer, it repels most of the water layers, but it leaves *two* layers on the alumina surface and the lauric acid molecules are adsorbed on top of this bi-molecular layer of water, the first layer of which is the just described 'chemisorbed' layer, whilst the second layer is strongly physisorbed on top of the 'chemisorbed' layer. The number of water molecules in the first 'chemisorbed' layer and in the second strongly physisorbed layer is exactly the same.

12. VISUAL METHODS

The results of many methods of estimating surface areas have been, and are still, controlled by comparing the results with observations made by ultramicroscopic- or electron microscopic methods. The equation(6)

$$\text{area} = \frac{6}{\rho d} \tag{6}$$

is then used to calculate the specific surface area; ρ stands for the density of the substances under investigation and d is an average diameter, calculated from the observation of a great many particles, which are supposed to be of spherical form. This average diameter is calculated[28] by dividing the total sum of the cubes of the measured diameters of the various individual particles by the sum of the squares, hence

$$d = \frac{\Sigma nd^3}{\Sigma nd^2} \tag{7}$$

where n is the number of particles which have been measured; n should be very large.

If all particles were indeed spheres, the calculated area would be correct. A deviation from the spheric form, however, mostly leads to a larger area than indicated by equation 6. This 'visual' method may, therefore, easily lead to too small values of the surface areas.

This is certainly the case when the surface of the particles is not a smooth one, or when narrow capillaries are present. In such a case Abram and Bennett[29], comparing adsorption methods with electron-microscope areas in their investigation of carbon blacks, came to the conclusion that the surface area in 'wide pores' (mostly the room between the individual particles), as determined from the t-plot (see Section 13) gave an excellent agreement with their adsorption experiments.

13. THE t-METHOD

Working with aluminas and aluminium hydroxides, we observed that on such samples where the multimolecular layer of adsorbed nitrogen could be formed freely, the statistical thickness,

$$t = 15{\cdot}47\ V_a/S_{\text{BET}} \tag{8}$$

where V_a is the volume of nitrogen adsorbed in cm^3 STP per gram of adsorbent, is practically independent of the nature of the sample. The thickness t, as a function of the relative pressure, gives one common line for all aluminas.

Experimental values of V_a, measured as a function of the relative pressure, may then be transformed to functions of t. If one then plots V_a for an unknown sample as a function of the experimental t, a straight line is obtained which by extrapolation to $t = 0$ goes through the origin[30, 31]. The slope of this line is a measure of the surface area

$$S_t = 15{\cdot}47\ V_a/t \tag{9}$$

For the construction of the $V_a - t$ plot, the t-values measured by Lippens and given in a table[30, 32] may be used from $p/p_0 = 0{\cdot}08$ with a t-value of 3·51 Å up to a relative pressure of $p/p_0 = 0{\cdot}76$, where the t-value is 9·65 Å.

The t-method is completely based on the BET-conception, but it enables us to obtain more information from the adsorption curves. When the experimental figures of the adsorbed volume of N_2 at liquid nitrogen temperature (-195°C) are plotted as a function of the t-values, given in the table, a straight line may be obtained, the slope of which gives the surface area. If at a certain pressure capillary condensation occurs in pores of certain shapes and dimensions, the adsorption branch lies above the t-curve and, consequently, the V_a–t plot rises above the straight line. When during the adsorption process some pores are filled at a certain relative pressure, the V_a–t plot assumes a less steep slope and again the new slope gives the surface area which is left, that is, the surface area of the wider capillaries or of the outside areas of the granules.

Although the t-method is based on the BET-method, it gives more information. As a matter of fact the experimental V_a–t plot is based on the experimental figures of the adsorbed amounts of nitrogen, as a function of the relative pressure as found on those aluminas or aluminium hydroxides where no capillary condensation, or filling up of narrow pores, takes place. This experimental curve gives then the real data between the relative pressures $p/p_0 = 0{\cdot}08$ and $p/p_0 = 0{\cdot}75$, whereas, as stated in Section 3, the BET-equation covers the experimental curve only between $p/p_0 = 0{\cdot}05$ and $p/p_0 = 0{\cdot}35$.

The dependence of the t-curve on the BET-method demands that at the relative pressure interval between 0·08 and 0·35 both curves coincide. This they indeed do[33].

There are two equations which describe the experimental t-curve relatively well. Anderson's equation[34]

$$v = \frac{v_m\, ckx}{(1 - kx)\ \{1 + (c - 1)\ kx\}} \tag{10}$$

where $x = p/p_0$ and with $c = 53$ and $k = 76$ gives a good fit[34] and so does the equation of Harkins and Jura[35], which may be written as:

$$\log p/p_0 = 0{\cdot}034 - \frac{13{\cdot}99}{t^2} \tag{11}$$

Later we found[36] that the common *t*-curve which we found for aluminas, can also be used with MgO, SiO_2, TiO_2, ZrO_2, $BaSO_4$, Nickel-antigorite and with three graphitized carbon blacks.

Recently Broekhoff[37] found, by careful measurements, that the *t*-method could be extended to higher relative pressures than 0·75. His values go up to a relative pressure of 0·92.

The common *t*-curve for the oxides and some other oxidic substances, mentioned above, and for the carbons, cannot be used for *all* substances. When one plots *t*-values, as calculated by equation (8), as a function of the relative pressure p/p_0 for a great variety of non-porous substances, and one tries to draw one average curve through the various points, this average curve may easily show deviations of 10 per cent or more from the experimental values. When the *t*-value is only used for pore analysis, as e.g. described by Barrer, Joyner and Halenda[38], the *t*-correction in such an analysis is usually small enough and an average *t*-curve drawn through the measuring points of widely varying substances may be used. Such curves have been given by Shull[39], by Cranston and Inkley[40] and recently by Pierce[41]. For our purpose, in the case of the *t*-method, however, we need a common *t*-curve with smaller deviations[42], say not more than about 3–4 per cent. Such a common *t*-curve exists, as we saw, for the oxidic substances and the graphites, and we may expect that such a common curve—a slightly different one—will also exist for halides, and perhaps also for a group of metals. Further experimental research has to be done in this direction. In some of our publications about the *t*-method our curve for the oxidic substances and the carbons was indicated as the 'universal' *t*-curve; we should not have used that word!

14. HOMOGENEOUS SURFACES

Graphitized carbon blacks, prepared by heating to temperatures round about 3000°C, show chiefly basal graphite planes. It was already noted by Joyner and Emmett[43] that the nitrogen adsorption isotherms at liquid nitrogen temperature showed an unusual step-like rise between the relative pressures 0·2 and 0·4. Some years ago Conway Pierce and Bland Ewing[44] measured carefully the adsorption isotherms of N_2, CO and various organic molecules, such as ethyl chloride, *n*-hexane, benzene, etc., on such carbon surfaces. They concluded that at point B of those isotherms the nitrogen molecules were not packed with their usual molecular area of 16·2 Å^2, but that their area is larger in this case, and that the extra rise in the adsorption isotherm—the Joyner-Emmett step as they call it—is due to additional adsorption in the first layer, along with the start of the second layer adsorption.

They also note that BET-plots cannot be used with such homogeneous graphite surfaces, because such plots are only linear over such a short range that they are not reliable for the estimation of V_m; hence, according to these authors, the point-B-method has to be used. In view also of the work of Kodera and Onishi[15], Pierce and Ewing do not feel it 'as yet possible to assign an absolute value to any cross-sectional area'. Their estimate is that, at the point B of the isotherms of N_2 on graphitized carbons the molecular area of the nitrogen molecule is about 20 Å^2, and they conclude that the surface area of these carbons is, therefore, about 1·2 to 1·25 times as large as according to the 'conventional estimation'.

The last two sentences of the valuable article of Pierce and Ewing may be cited: 'But as noted by Brunauer' (our citation 7) 'nitrogen adsorption can give the absolute surface area within 20 per cent. They conclude then by writing: 'It is perhaps unrealistic to expect better absolute values.'

15. THE TWO-DIMENSIONAL VAN DER WAALS' EQUATION

The two-dimensional analogue[45] of the van der Waals' equation (see Section 2) is:

$$\left(F + \frac{a_2}{A^2}\right)(A - b_2) = RT \tag{12}$$

where F is the two-dimensional pressure, e.g. in dynes/cm, A is the surface area occupied e.g. by one molecule and a_2 and b_2 are the two-dimensional analogues of the van der Waals' a and b respectively, whilst RT has the usual meaning. a_2 and b_2 are related with the three-dimensional constants:

$$a_2 = \frac{3\,a}{8\,d} \tag{13a}$$

$$b_2 = \frac{3\,b}{4\,d} \tag{13b}$$

where d is the diameter of the molecules.

These equations show that the influence of a_2 in a two-dimensional gas is relatively less than that of a in a three-dimensional gas. This causes the two-dimensional critical temperature ${}_2T_c$ to be only half the three-dimensional critical temperature T_c:

$$\left.\begin{aligned} {}_2T_c &= \frac{8\,a_2}{27\,R\,b_2} \\ \text{and} \qquad T_c &= \frac{8\,a}{27\,R\,b} \end{aligned}\right\} \tag{14}$$

whence

$${}_2T_c = \tfrac{1}{2}\,T_c \tag{15}$$

This concept is, of course, only approximate but more refined formulations of the equations of state of the three-dimensional and the two-dimensional gases, also lead to the result that the two-dimensional critical temperature of a two-dimensional gas is approximately half that of the three-dimensional gas. Lennard Jones and Devonshire[46] e.g. give the relation ${}_2T_c = 0{\cdot}53\ T_c$.

These relatively simple equations may be used only if the molecules in the adsorbed (two-dimensional) state have lost only one degree of translation by the act of adsorption; they should have two degrees of translation left across the surface and moreover they should retain their rotations.

If the adsorbed N_2-molecules do not retain their complete freedom of rotation at -195°C when they are adsorbed, we must, probably, expect that a_2 and b_2 twice have different values. For a completely flat, or a completely vertically oriented position on the surface, we may then expect the following values for a_2 and b_2, as compared with the average ones:

Flat position: $a_2 = 4500 \times 10^{-32}$ erg cm^2
$b_2 = 17{\cdot}1 \times 10^{-16}$ cm^2
${}_2T_c = 56{\cdot}8$°K
Vertical position: $a_2 = 5250 \times 10^{-32}$ erg cm^2
$b_2 = 12{\cdot}3 \times 10^{-16}$ cm^2
${}_2T_c = 92$°K
Average (rotating): $a_2 = 4570 \times 10^{-32}$ erg cm^2
$b_2 = 15{\cdot}55 \times 10^{-16}$ cm^2
${}_2T_c = 63$°K

For krypton, where no special orientation can be expected, the two-dimensional critical temperature, calculated as half the three-dimensional temperature, may be expected to be 105°K, the a_2 and b_2 being

$$a_2 = 7600 \times 10^{-32} \text{ erg cm}^2$$
$$b_2 = 15{\cdot}7 \times 10^{-16} \text{ cm}^2$$

16. THE ADSORPTION OF KRYPTON AND OF NITROGEN ON HOMOGENEOUS CARBON SURFACES

The adsorption of krypton on a homogeneous carbon surface was measured by Singleton and Halsey[47], our own measurements on the same homogeneous carbon led to identical results[48]. Two-dimensional condensation was clearly observed, the temperature of the experiment (77·5°K) being distinctly lower than the two-dimensional critical temperature. There was also two-dimensional condensation clearly observable in the second adsorbed layer, on top of the first one. The higher layers did not show the phenomenon clearly; there seemed to be some intermixing of the layers already.

Duval and Thomy[49], possessing a still more homogeneous graphite, obtained by what they call exfoliation, observed two-dimensional condensation in 5 successive layers.

The adsorption of nitrogen on one of the homogeneous carbons (Sterling F.T.) showed no sharp condensation phenomena, but there was a 'dip' in the curve for the first and for the second adsorbed layer, as can be expected for a two-dimensional gas, not far above its two-dimensional critical temperature[36, 48, 50]. The same curve was found by Kiselev, whose measurements were made on the same carbon[51]. With reference to the data in Section 15, we may conclude that the nitrogen moledules are *not* oriented in a vertical position, but probably in average positions. The adsorbed nitrogen molecules may be considered as rather mobile molecules which by rotating behave as if they were of spherical shape.

The description of the successive multimolecular layers (at least two) of nitrogen (super-critical) and of krypton (sub-critical) by the two-dimensional van der Waals' equation, leads to the possibility of calculating the monolayer volume of these gases, and together with their b_2-values (which should then be used for the molecular surface area) also the surface area. Doing this with krypton we obtained[52] 13·6 m^{2}g^{-1} for Sterling F.T. carbon and with nitrogen 13·5 m^2g^{-1}. Recently the curves have been measured again by Broekhoff[53] in order to obtain a higher precision and the results are that krypton gives a surface area of 13·9 m^2g^{-1} and nitrogen 13·2 m^2g^{-1}. For the same homogeneous carbon the *t*-plot—based on the BET-equation—gives 13·3 m^2g^{-1}.

These latter two values, obtained with nitrogen as an adsorbent, but with two completely independent methods and with two different values for the molecular area, viz. 15·55 Å^2 for the van der Waals' method, and 16·25 Å^2 for the *t*-method, give practically the same figure of the surface area of the homogenous carbon, which is a striking result.

A direct application of the BET-equation gives a lower value, viz. 12·2 m^2g^{-1}, because of the low scope of the isotherm in the 'dip' between the relative pressures of 0·05 and 0·30; the *t*-method, based on the BET-method, can use the upper parts of the isotherm.

17. THE RESULTS OBTAINED WITH HOMOGENEOUS SURFACES APPLIED TO THE PROBLEM OF HETEROGENEOUS SURFACES

A careful study of the gradual building-up of the adsorbed layers on homogeneous carbon surfaces shows that, at 77·5°K, nitrogen behaves as a super-critical two-dimensional fluid. The first adsorbed layer of nitrogen is, at a relative pressure of 0·08, two-dimensionally compressed to such a high degree of coverage of about 0·85, that nitrogen behaves as a condensed phase. The degree of coverage in this first layer increases at higher relative pressures and it is about 0·90 at a relative pressure of 0·60 and it becomes more compressed at higher relative pressures, while at the same time the second and higher layers are formed.

This behaviour depends strongly on the heat of adsorption and there are certainly less strong adsorbing surfaces, such as e.g. polythene, which show such behaviour, only at far higher relative pressures.

The BET-equation, in its application, locates the B-point mostly at about $p/p_0 \sim 0{\cdot}1$; the monolayer is certainly not complete at that point, but together with the molecules adsorbed already in the second layer, etc., the amount of N_2 may approximately be equal to that of a well compressed monolayer.

Following an example given by Ross and Olivier[54], we tried to compute the isotherms which would result if heterogeneous surfaces were made up from a great number of small homogeneous patches, distributed along gaussian distribution curves, with a mean adsorption energy, E_{ads} and various standard deviations. These 'synthetic' isotherms were then analysed by means of the BET-equation. Although the procedure which we followed may only be considered as an idealized way of arriving at a heterogeneous surface, the results are interesting enough to be studied. We shall give the range of *c*-values (*c* being the constant of the BET-equation, see e.g. 2 and 3) and the range of molecular areas of the nitrogen molecules, caused by the standard deviations of distribution which we gave. The complete table has already been published[52], *Table 1* shows the main results.

These figures may warn us that the results of a BET-determination of a surface area may be seriously influenced by the mean heat of adsorption and by the form and the width of the adsorption energy distribution curve.

The B-point does *not* give the monolayer capacity of a 'statistical monolayer'. The degrees of coverage at the B-points as found with our 'synthetical' heterogeneous surfaces can be calculated by dividing the two-dimensional van der Waals' constant $b_2 = 15{\cdot}55$ Å^2 by the apparent molecular area of N_2, as given in the last column of the table. For $E = 1800$ cal mole^{-1} and a standard deviation of 100, therefore, this degree of coverage would be $\sim 0{\cdot}81$ and for $E = 2600$ cal mole^{-1} and a standard deviation of 600, it would be $\sim 1{\cdot}2$.

Table 1.

E_{ads}	*Standard Deviation*	*c*	N_2 *molecular area*
1800 cal mole^{-1}	100–600	515–72	19·2–19·8 A^2
2000 cal mole^{-1}	100–600	358–72	18·0–17·4 A^2
2200 cal mole^{-1}	100–600	175–66	16·6–15·6 A^2
2400 cal mole^{-1}	100–600	83–59	14·9–14·1 A^2
2600 cal mole^{-1}	100–600	42–53	12·6–13·0 A^2

18. CONCLUSIONS

The differential heat of adsorption of the first molecules of nitrogen on a homogeneous carbon surface was found to be 2·22 kcal mole^{-1} (ref. 55). Comparing this with the table in Section 17 we come to the conclusion that the molecular area of nitrogen should be between 16·4 and 15·5 Å^2, depending on the deviation of the adsorption energies along the various parts of the adsorbent. A standard deviation of 200 would give 16·2 Å^2 for the surface area of the nitrogen molecule, whilst the *c*-value of the BET-equation would be about 140; quite reasonable figures.

The results of Section 7 may assure us that, at − 195°C, the adsorbed nitrogen molecules will be still rotating, and will certainly not erect themselves. Even if perhaps rotation has stopped altogether, they will be adsorbed in averaged positions; their b_2-value and the corresponding (larger) apparent molecular area will be the average one ($b_2 = 15{\cdot}55$ Å^2).

In Section 11 we learned that a comparison of the adsorption of lauric acid and of water on various aluminas, with the adsorption of nitrogen on the same adsorbents leads to the result that in this case 16·2 Å^2 should be taken for the molecular area of nitrogen, when using the BET-equation.

In Section 13 we learned that the *t*-curves, which as we saw are based on the BET-equation, are the same for several other oxidic substances and for graphitized carbons. We are inclined to conclude from this fact that the molecular area of nitrogen will be the same in all these cases.

Although the data in the table[30, 32] used for the *t*-method on these substances is based on a molecular area of nitrogen of 16·27 Å^2, the molecular area may vary from adsorbent to adsorbent and be $n \times 16{\cdot}27$ Å^2, where n does not differ too seriously from unity. The original 16·27 Å^2 was calculated from the density of liquid nitrogen at $-195°C$, assuming that the dimensions of the nitrogen molecule when adsorbed on the oxidic adsorbents, would not deviate too seriously from this figure. We know, however, that the adsorbed nitrogen in the first adsorbed layer is, two-dimensionally, in a super-critical state and that we, therefore, may not expect the molecular surface area to be exactly 16·27 Å^2, as in the three-dimensional liquid state at that temperature.

The common t-curve, however, means that the table for the t-values, as published[30, 32] may be used, provided one is aware of the fact that all figures have to be multiplied with a factor n which does probably not deviate from unity seriously.

If our conclusion, mentioned in Section 11, that the comparison of the adsorption of lauric acid and of water with that of nitrogen on strongly dehydrated alumina leads to exactly the same surface area if the molecular area of nitrogen is 16·2 Å^2 is a right one, then the factor n is 0·995 in this case, and probably also for all substances for which *this* common t-curve holds.

As stated in Section 13, other groups of adsorbents may be expected to show deviating t-values as a function of relative pressure. For these adsorbents we must, provisionally, accept an uncertainty of, say, 20 per cent on both sides of the surface area as expressed in m^2/g, unless a comparison with a Langmuir isotherm such as that of the adsorption of lauric acid, described in Section 11, narrows the uncertainty down to far smaller percentages.

Other methods, such as e.g. an estimation of the surface area from the adsorption of gases at high temperatures as described by Barker and Everett[56], include also an uncertainty of about 20 per cent on both sides.

I may express the hope that future work will lead to the finding of other t-tables for the adsorption of nitrogen on other groups of substances, such as halides, metals, organic materials, etc., and that such tables can be used for the analysis of the adsorption curves on substances belonging to such a group, in the same way as it has successfully been done in recent times by various investigators working with adsorbents belonging to the group for which our present t-table of the mentioned oxides and hydroxides and the carbons holds. In such a way far more use can be made from the BET-method, on which the t-method is based, then measuring total surface areas only.

References

[1] S. Brunauer, P. H. Emmett and E. Teller. *J. Am. Chem. Soc.* **60**, 309 (1938).

[2] I. Langmuir. *Phys. Rev.* **8**, 149 (1916); *J. Am. Chem. Soc.* **40**, 1361 (1918).

[3] H. Margenau. *Rev. Modern Physics* **11**, 1 (1939).

[4] P. Debye. *Physikal. Z.* **21**, 178 (1920).

[5] W. H. Keesom. *Physikal. Z.* **22**, 129 (1921).

[6] F. London. *Z. Physik.* **63**, 245 (1930).

[7] S. Brunauer. *The Adsorption of Gases and Vapours*, Chapter VI, Oxford University Press, London, 1943.

[8] J. H. de Boer. *The Dynamical Character of Adsorption*, Clarendon Press, Oxford, 1953, sec. ed. 1968, Chapter V.

[9] S. Brunauer and P. H. Emmett. *J. Am. Chem. Soc.* **59**, 1553 (1937).

[10] P. H. Emmett. In *Advances in Colloid Science, Vol. I*, p. 24. Interscience Publ. Inc., New York, 1942.

[11] R. B. Anderson and P. H. Emmett. *J. Applied Physics* **19**, 367, 370 (1948).

[12] H. K. Livingston. *J. Colloid Sci.* **4**, 447 (1949).

[13] A. L. McClennan and H. F. Harnsberger. *J. Colloid and Interface Sci.* **23**, 577 (1967).

[14] C. Pierce and B. Ewing. *J. Phys. Chem.* **68**, 2562 (1964), see esp. p. 2568.

[15] K. Kodera and Y. Onishi. *Bull. Chem. Soc. Japan* **32**, 356 (1959); **33**, 338 (1960).

[16] M. L. Corrin. *J. Am. Chem. Soc.* **73**, 4061 (1951).

[17] See S. J. Gregg and K. S. W. Sing, *Adsorption, Surface Area and Porosity*, pages 91 and 98, Academic Press, London and New York, 1967.

[18] P. G. Menon, Thesis at Delft University of Technology, 1961;
A. Michels, P. G. Menon and C. A. ten Seldam, *Rec. Trav. Chim. Pays Bas* **80**, 483 (1961).
J. H. de Boer and P. G. Menon. *Proc. Kon. Ak. Wet., Amsterdam* **65**, 17 (1962).
P. G. Menon. *J. Am. Chem. Soc.* **87**, 3057 (1965); *Chem. Rev.* **68**, 277 (1968).

[19] J. H. de Boer, Ref. 8, Chapter V, Sections 48 ff., especially 55.

[20] These figures are taken from a Progress Report of the Department of Scientific and Industrial Research (1943), by R. Gave.

[21] J. H. de Boer, Ref. 8, Chapter V, Section 56.

[22] J. H. de Boer. *Z. physikal. Chem.* **B 15**, 281, 300 (1932).
J. H. de Boer and L. A. H. Wolters. *Z. physikal. Chem.* **B 17**, 161 (1932).

[23] J. H. de Boer and J. J. Lehr. *Z. physikal. Chem.* **B 24**, 98 (1934).

[24] J. H. de Boer and C. J. Dippel. *Z. physikal. Chem.* **B 25**, 237 (1934).

[25] J. H. de Boer, G. M. M. Houben, B. C. Lippens, W. H. Meys and W. K. A. Walrave. *J. Catalysis* **1**, 1 (1962).

[26] J. H. de Boer, M. E. A. Hermans and J. M. Vleeskens. *Kon. Ned. Ak. v. Wet., Proceedings* **B 60**, 54 (1957).

[27] J. H. de Boer, J. M. H. Fortuin, B. C. Lippens and W. H. Meys. *J. Catalysis* **2**, 1 (1963).

[28] see e.g. R. B. Anderson and P. H. Emmett. *J. Applied Physics* **19**, 367 (1948).

[29] J. C. Abram and M. C. Bennett. *J. Colloid and Interface Sci.* **27**, 1 (1967).

[30] B. C. Lippens, Thesis at Delft University of Technology, 1961.

[31] B. C. Lippens and J. H. de Boer. *J. Catalysis* **4**, 319 (1965).

[32] B. C. Lippens, B. G. Linsen and J. H. de Boer. *J. Catalysis* **3**, 32 (1964).

[33] J. H. de Boer, B. C. Lippens, B. G. Linsen, J. C. P. Broekhoff, A. van den Heuvel and Th. J. Osinga. *J. Colloid and Interface Sci.* **21**, 405 (1966).

[34] R. B. Anderson. *J. Am. Chem. Soc.* **68**, 686 (1946).

[35] W. D. Harkins and G. Jura. *J. Am. Chem. Soc.* **66**, 1366 (1944).

[36] J. H. de Boer, B. G. Linsen and Th. J. Osinga. *J. Catalysis* **4**, 643 (1965).

[37] J. C. P. Broekhoff, Thesis at Delft University of Technology, 1969.

[38] E. P. Barrett, L. G. Joyner and P. P. Halenda. *J. Am. Chem. Soc.* **73**, 373 (1951).

[39] C. G. Schull. *J. Am. Chem. Soc.* **70**, 1405 (1948).

[40] R. W. Cranston and F. A. Inkley. *Adv. Catalysis* **9**, 143 (1957).

[41] Conway Pierce. *J. Phys. Chem.* **72**, 3673 (1968).

[42] J. H. de Boer. *J. Phys. Chem.*, to be published.

[43] L. G. Joyner and P. H. Emmett. *J. Am. Chem. Soc.* **70**, 2353 (1948).

[44] C. Pierce and B. Ewing. *J. Am. Chem. Soc.* **84**, 4070 (1962); *J. Phys. Chem.* **68**, 2562 (1964).

[45] J. H. de Boer, Ref. 8, Chapter VII.

[46] J. E. Lennard-Jones and A. F. Devonshire. *Proc. Roy. Soc.* **A 163**, 53, 132 (1937).

[47] J. H. Singleton and G. D. Halsey. *J. Phys. Chem.* **58**, 1101 (1954).

[48] J. H. de Boer, J. C. P. Broekhoff, B. G. Linsen and A. L. Meyer. *J. Catalysis* **7**, 135 (1967).

[49] X. Duval and A. Thomy. *C.R. Acad. Sci. Paris* **259**, 4007 (1964).

[50] J. H. de Boer and J. C. P. Broekhoff. *Proc. Kon. Ned. Ak. Wet.* **B 70**, 317 (1967).

[51] A. A. Isirikyan and A. V. Kiselev. *J. Phys. Chem.* **65**, 601 (1965).

[52] J. H. de Boer and J. C. P. Broekhoff. *Proc. Kon. Ned. Ak. Wet* **B 70**, 342 (1967).

[53] J. C. P. Broekhoff, Thesis, Delft Technological University, 1969.

[54] S. Ross and J. P. Olivier. *On Physical Adsorption*, Interscience, New York 1964, Chapter IV.

[55] J. H. de Boer and J. C. P. Broekhoff. *Proc. Kon. Ned. Ak. Wet.* **B 70**, 354 (1967).

[56] J. A. Barker and D. H. Everett. *Trans. Faraday Soc.* **58**, 1608 (1962).

DISCUSSION

Dr. A. Lecloux (*Solvay et Cie, Belgium*) said: At the end of his lecture, Prof. de Boer said that some experimental work had to be carried out to determine *t*-curves which can be used for the analysis of the nitrogen adsorption isotherms when the adsorbents are neither oxides nor hydroxides. In our laboratory, we have obtained some interesting results in this field and I would like to make some comments about them. We determined, with a classical volumetric apparatus, the nitrogen adsorption isotherms on a great number of solids, belonging to three chemical groups: oxides, chlorides and organometallic materials. The analysis of the adsorption curves was usually done by the t-method, but, for all substances belonging to the last two groups and also for some oxide samples, we obtained anomalous t-plots when the t-curve proposed by de Boer was used. In fact, in the region of low relative pressure, the experimental points lie on a straight line, but this straight line does not pass through the origin; it cuts the v-axis for a negative value of the adsorbed volume. On the other hand, we calculated for all these samples, the BET specific surface area and the value of the c-BET constant and we came to the conclusion that the t-curve proposed by de Boer may not be used if the value of the c-BET constant was lower than 100. We separated our samples, which were characterized by a c-BET constant lower than 100, in two main groups; the first one included the samples with a c-value between 50 and 70 and the second one, the samples with a c-value between 20 and 30. Using the relation of de Boer, $t = 15{\cdot}47\ v/S_{\mathrm{BET}}$, we determined the common t-curve for each group of samples. In the first case, from 22 isotherms and, in the second case, from 8 isotherms, we obtain t-curves which show deviation from the experimental values which are never greater than 5 per cent. In the *Figure A* the t-curve of de Boer is compared to the new t-curves we have obtained. Their range of validity is limited by c values. These ranges have been experimentally determined, by using these three curves for the construction of t-plots from

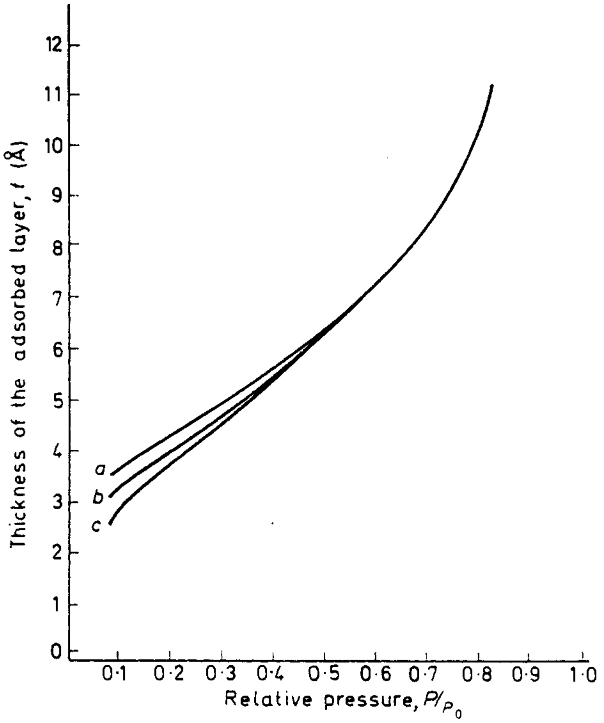

Figure A. Variation of the thickness of the adsorbed layer of nitrogen with the relative pressure. These t-curves have to be used when: $a = 300 > c_{\mathrm{BET}} \geqslant 100$ (from de Boer;) $b = 100 \geqslant c_{\mathrm{BET}} \geqslant 40$; and $c = 40 \geqslant c_{\mathrm{BET}} \geqslant 20$.

adsorption curves with different *c*-BET values. For high pressure ($p/p_0 > 0{\cdot}6$) the new *t*-curves follow the curve proposed by de Boer. The differences between the three curves increase with decreasing pressure.

I think it is more correct to group the solids on the basis of the *c*-BET constant values than on the basis of their chemical nature, because there are some oxidic samples, the *c*-constant of which is lower than 100, and also some chloride compounds which have a *c*-value higher than 100. For these particular samples, the *t*-plots are normal only if the *t*-curve is selected on the basis of the *c*-BET value.

Professor J. H. de Boer replied: The remark of Monsieur A. Lecloux is a very interesting one and I shall certainly give it serious attention. The *t*-method, using the *t*-curve which holds for those oxides and hydroxides which we have specifically mentioned in various publications, although originally based on the BET method of estimating surface areas, is practically independent of the BET method, since we estimated the surface area of the adsorbed nitrogen molecule with the lauric acid method, using, therefore, the Langmuir conception rather than the BET equation.

We know that for metals a slightly different *t*-curve has to be used, whilst also alkali and earth alkali halides show a slightly different *t*-curve; organic materials, such as plastics show even larger deviations.

The BET equation covers only a small part of the *t*-curves, the part between relative pressures of $\sim 0{\cdot}08$ to $\sim 0{\cdot}25$ to 0·30, which part contains, however, the B-point.

Our attempts have been directed on making the *t*-method independent from the BET equation. The approach now given by Monsieur Lecloux falls back on the BET equation again, and it gives a special significance to the constant *c*. It is, certainly, an interesting approach.

UTILISATION OF ADSORPTION DATA IN THE BET REGION

K. S. W. Sing

Department of Chemistry, Brunel University, Acton, London, W.3, U.K.

Adsorption isotherms of nitrogen, carbon tetrachloride and neopentane vapours are analysed by means of a graphical procedure similar to the *t*-method of Lippens and de Boer[5]. The amount adsorbed is plotted against α_s (instead of t) for a non-porous reference solid, where α_s is the ratio of the amount adsorbed (at the given p/p_0) to the amount adsorbed at $p/p_0 = 0{\cdot}4$. Deviations of α_s-plots from linearity are explained in terms of capillary condensation, which may accompany multilayer formation (at $p/p_0 > 0{\cdot}4$), and micropore filling, which only occurs at low p/p_0. If micropore filling is absent, the surface area is readily calculated from the slope of the α_s-plot by using a normalising factor, obtained from the standard isotherm on the non-porous reference material of known surface area.

In general, surface areas calculated from the nitrogen α_s-plots on a wide variety of non-microporous samples of alumina, silica and chromia are shown to agree well with the corresponding BET areas. The carbon tetrachloride and neopentane, α_s-plots on non-microporous silicas are also found to give surface areas in good agreement with the BET-*nitrogen* areas.

The α_s-plot provides a means of separating a complex experimental isotherm into its component parts. With a microporous solid, the slope of the α_s-plot in the *multilayer* region is directly proportional to the area of the *external* surface. The usefulness of this approach is illustrated by reference to nitrogen and carbon tetrachloride isotherms on microporous chromium oxide gels.

INTRODUCTION

Routine adsorption measurements for the determination of surface area by the BET method[1] are generally made within the range of relative pressures, $p/p_0 \sim 0{\cdot}05$–$0{\cdot}5$. The adsorption in this region of the isotherm may depend on three different mechanisms: (a) monolayer-multilayer coverage, (b) micropore filling, and (c) capillary condensation. We may regard (a) and (b) as the primary stages of adsorption and (c) as a secondary process, which involves the formation of a liquid-like meniscus. If the complete close-packed monolayer is well-defined and micropore filling is absent, the monolayer capacity may be identified with the uptake at point B on an isotherm of Type II or IV in the BDDT classification[2] (see *Figure 1*). The appearance of the isotherm may be somewhat misleading, however, if monolayer adsorption and micropore filling occur side by side at $p/p_0 < 0{\cdot}1$. Then, neither the uptake at point B nor the BET monolayer capacity is strictly valid. In our view this situation, where the processes (a), (b) and (c) all contribute

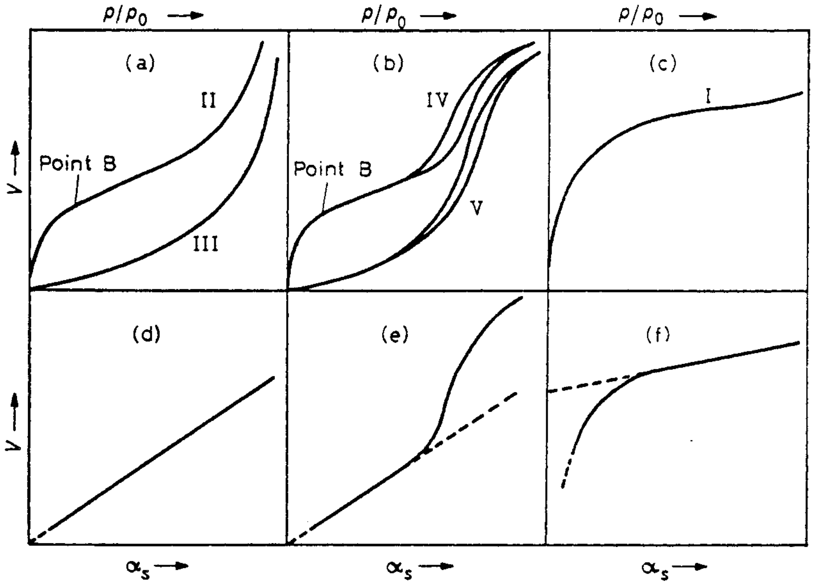

Figure 1. Types of adsorption isotherms and α_s plots

to the measured adsorption, is not uncommon, but in fact it is one which has received little attention. The present paper sets out to examine how we may identify and separate these processes and to consider how far they impose limitations on the use of the adsorption method for the determination of surface area.

A procedure for detecting the effect of micropore filling in the simplest case of the Type II isotherm was used by Harris and Sing[3]. First it was established[4] that nitrogen isotherms obtained at −196°C on a wide range of non-porous (or macroporous) silicas and aluminas could be reduced to a common curve when plotted in the form V/V_m against p/p_0, where V is the amount adsorbed at the relative pressure, p/p_0, and V_m the BET monolayer capacity; then the reduced isotherms on porous gels were compared with the standard curve. It was argued that since the process of micropore filling must be complete at some point on the isotherm (probably at $p/p_0 = 0{\cdot}1$–$0{\cdot}2$) the multilayer formation on the remaining part of the surface will result in a *lower* overall uptake of nitrogen than is given by a non-porous solid of the same BET area. Deviation of the reduced isotherm below the standard was found with a number of alumina precipitates and exposure to water vapour caused the reduced isotherm to move closer to the standard curve—indicating the closure of micropores. 'Activation', by heat treatment, on the other hand, caused the reduced isotherm to rise above the standard curve; this indicated pore widening, i.e. the conversion of micropores to transitional pores with consequent capillary condensation of the nitrogen vapour.

In recent years, the *t*-method of Lippens and de Boer[5] has attracted a good deal of attention as a simple and direct means of interpreting nitrogen isotherms. In this method, the amount of nitrogen adsorbed by the test sample is plotted against t, the statistical multilayer thickness for the adsorption of nitrogen on a non-porous solid. The t-plot has the advantage over the older method in that departure from a linear relation is more easily detected and quantitatively assessed than is the deviation from a complex curve.

de Boer and his coworkers[6] have adopted as their standard a multilayer thickness curve, which they call 'the universal t-curve'. It appears that this was based on their original isotherm for nitrogen on non-porous alumina, with slight correction at $p/p_0 > 0{\cdot}75$. In fact, the exact form and location of a physical adsorption isotherm depends to some extent on the chemistry of the solid surface as well as on its area and porosity; for example, dehydroxylation of a silica surface causes point B of the nitrogen isotherm to become less distinct[7], whereas graphitization of carbon results in a tendency for the isotherm of nitrogen (and especially that of krypton and argon) to become stepwise[8,9].

Other limitations of the t-plot are: (1) that it is not strictly independent of the BET method, since t is itself calculated from V/V_m and (2) that it cannot be readily applied to a Type III isotherm, or a Type II isotherm with a very small knee at low pressure. To avoid these difficulties, the method of Lippens and de Boer was modified[10] and t replaced by $(V/V_X)_S$, which we shall now call α_s (in place of V_S, the symbol previously used[10,11]), where V_X is the amount adsorbed at a selected relative pressure, $(p/p_0)_X$. The reduced standard isotherm for the non-porous reference solid is, therefore, arrived at empirically and not via V_m.

The location of $(p/p_0)_X$ is not entirely arbitrary; with a number of vapours (including nitrogen at $-196°$), it seems reasonable to place $\alpha_s = 1$ at $p/p_0 = 0{\cdot}4$. Both monolayer coverage and micropore filling usually occur at $p/p_0 < 0{\cdot}4$, whereas capillary condensation (at least in association with hysteresis) takes place at $p/p_0 > 0{\cdot}4$. Furthermore, greater precision is achieved by locating $\alpha_s = 1$ in the middle range of the isotherm rather than at, say, $p/p_0 = 0{\cdot}1$ (especially so if the BET parameter c is low, i.e. $c < 10$).

Three hypothetical α_s-plots are shown in (d), (e) and (f) of *Figure 1*, with the corresponding isotherms in (a), (b) and (c). The linear plot in (d) is the result of unrestricted monolayer-multilayer adsorption on a non-porous or macroporous solid (pore width, $d > 200$ Å); in this case the isotherm may be of Type II or Type III (or stepwise) and is, of course, identical in shape to the standard. The α_s curve in (e), providing clear evidence of capillary condensation taking place in transitional pores ($d = 20$–200 Å), is derived from isotherms IV or V in (b). In the case of (f), the α_s-plot is obtained from a Langmuir type of isotherm [I in (c)] and now pronounced micropore filling is followed by multilayer adsorption (the linear branch) on a small external surface.

Values of surface area, A_s, are readily calculated from the slopes of the linear regions of the α_s-plots in (d), (e) and (f) by using a proportionality (or normalising) factor, which is obtained from the standard isotherm on the non-porous reference material of known BET surface area. We shall see later that under certain conditions A_S agrees closely with A_{BET}, but there are circumstances where A_S provides a more reliable estimate of the surface area than A_{BET}. The micropore volume can be obtained by the backward extrapolation[10,12] of the linear branch of the α_s-plot in (f) to $\alpha_s = 0$; the intercept on the V-axis gives the effective origin for the monolayer–multilayer adsorption on the external surface.

In this paper, the α_s method is used to analyse isotherms of nitrogen, carbon tetrachloride and neopentane on various porous and non-porous solids. The adsorption isotherms will be presented and discussed in detail elsewhere; here we are only concerned with the application of the new method for the determination of surface area.

SELECTION OF NON-POROUS REFERENCE MATERIALS

Clearly, the successful exploitation of the new method must depend on careful selection of non-porous reference solids. The uptake of vapour by non-porous crystalline materials is usually small and difficult to measure with high accuracy. The search has, therefore, continued for suitable relatively high area solids with low porosity and uniform surfaces.

Other workers[6,7] have used the Aerosil grades of silica, assuming them to be non-porous; detailed investigation[13], however, has shown that samples of Degussa Aerosil are often porous, the exact pore dimensions depending on the conditions of pre-treatment and storage, e.g. compaction or exposure to water vapour. Two Degussa products, TK 70 and TK 800 ($A_{\mathrm{BET}} = 36$ and $154\ \mathrm{m^2g^{-1}}$, respectively) are currently under investigation in these and other laboratories and they have been found to consist of discrete spherical particles, the degree of aggregation being lower than in the commercial grades of Aerosil. Another satisfactory grade of non-porous hydroxylated silica was found to be Fransil EL. Values of the surface area of this material as determined by nitrogen adsorption and electron microscopy[13] were $A_{\mathrm{BET}} = 38{\cdot}7\ \mathrm{m^2g^{-1}}$, $A_{\mathrm{EM}} = 35\text{–}36\ \mathrm{m^2g^{-1}}$. The reduced α_s isotherms of nitrogen[13] on samples TK 70, TK 800 and Fransil are in excellent agreement over a wide range of p/p_0, as are those of carbon tetrachloride[14]. In addition, the α_s data for nitrogen agreed well with those obtained on crystalline quartz and other low area silicas[4] ($A_{\mathrm{BET}} = 1\text{–}10\ \mathrm{m^2g^{-1}}$).

de Boer, Linsen and Osinga[6] report that their t-curve for nitrogen on Degussa alumina (flame hydrolysis product) is in reasonable agreement (at $p/p_0 < 0{\cdot}75$) with the original t-curve obtained on calcined alumina. In our view, the original data of Lippens, Linsen and de Boer[15] do not provide a satisfactory standard for alumina and it would appear that their sample contained transitional pores. We prefer to adopt Degussa Aluminiumoxid C as standard ($A_{\mathrm{BET}} = 111\ \mathrm{m^2g^{-1}}$), which gives a reduced nitrogen isotherm in excellent agreement with that on other samples of non-porous amorphous alumina and aluminium hydroxide (*Table 1*). It will be seen later that the situation is more complicated with high-temperature α-alumina.

ADSORPTION OF NITROGEN ON ALUMINA

Nitrogen isotherms have been determined[11,16,17] at −196°C on a wide variety of calcined and uncalcined aluminium hydroxide gels; a representative selection of the results is included in *Table 1*. The BET surface areas, A_{BET}, were calculated in the usual way, assuming the nitrogen molecule in the close-packed monolayer to occupy an average area, ω_{N}, of $16{\cdot}2\ \text{Å}^2$.

Table 1. Surface areas of aluminas calculated by the BET and α_s methods from nitrogen adsorption isotherms

*Sample**	*Surface area* (m^2g^{-1})		*Linearity of α_s-plot, range of p/p_0*	*Reference*
	A_{BET}	A_S		
B(Pc)1	9·9	10·0	0·04–0·9	16
B(Pc)2	8·2	8·5	0·005–0·9	16
G1	541	537	0·10–0·85	16
Pc	389	390	0·03–0·40	16
Pc(500)5	277	272	0·03–0·14	11
Pm(1000)5	132	133	0·10–0·40	11
C(1200)6	74·8	74·8	0·005–0·75	17
C(1200)114	5·9	5·9	0·26–0·48	17
C(1300)6	4·5	4·0	0·40–0·75	17
C(1400)6	2·5	2·2	(0·4–0·8)	17
Gb	38	39	0·01–0·36	17
Gb(300)6	361	307	0·005–0·03	17
Gb(1200)6	5·0	4·7	0·32–0·65	17
Gb(1400)6	2·0	2·0	0·22–0·40	17
IG3(1200)6	5·1	4·8	0·36–0·50	17
I(1200)6	4·3	4·4	0·14–0·77	17
CGb(1200)6a	6·6	6·2	0·28–0·65	17
CGb(1200)6b	5·4	5·6	0·14–0·77	17

†Figure in brackets represents temperature of calcination. Time of calcination is indicated by figure after bracket. Thus, Sample Gb (1400)6 is gibbsite, heated at 1400°C for 6 hours.

The α_s-plots were constructed by taking Degussa Aluminiumoxid C as the reference solid. The range of linearity of each α_s-plot is shown in the fourth column. The value of A_s has been calculated from the slope of the linear part of the α_s-plot (taking a line through the origin), using the relation

$$A_S = 2{\cdot}87\ V/\alpha_s \tag{1}$$

where V is the volume of nitrogen adsorbed, expressed in cm^3 (s.t.p.), and the factor 2·87 has been obtained by calibration against the BET area of Degussa Aluminiumoxid C.

The first two samples, B(Pc)1 and B(Pc)2, in *Table 1* are of well-defined bayerite, prepared by ageing pseudoboehmite under controlled conditions. Electron microscopy has shown these to contain small regular particles of bayerite. Sample G1 was an amorphous alumina prepared in the presence of glycerol; it is particularly striking that this high area material is essentially non-porous and it appears that the glycerol molecules are held at the surface to provide an effective barrier and prevent the cementation of neighbouring particles[16].

The values of A_{BET} and A_S in *Table 1* are generally in good agreement, although in some cases the range of linearity of the α_s-plot is very restricted. The results on sample Gb(300)6 are noteworthy; this sample, prepared by heating gibbsite to 300°C, was microporous since the α_s-plot was somewhat similar to that in *Figure 1*(f) and the *initial* linear branch very short. It is not surprising, therefore, that the values of A_{BET} and A_S are found to be in poor agreement with this material.

With some of the high temperature samples of α-Al_2O_3, e.g. C(1300)6, C(1400)6, Gb(1200)6, the agreement between the two sets of values is also unsatisfactory. Clearly, in these cases the shape of the nitrogen isotherm has changed from that on the reference material and strictly a different standard α_s curve should have been employed. Until an appropriate standard has been found, we cannot use the nitrogen α_s plots on these materials to characterise porosity.

ADSORPTION OF NITROGEN, CARBON TETRACHLORIDE AND NEOPENTANE ON SILICA

Adsorption isotherms of nitrogen[19,20] were measured at -196°C and those of carbon tetrachloride[14,19] at 20° and neopentane[19] at 0°C on a range of porous and non-porous hydroxylated silicas. The values of surface area, calculated from these isotherms by the BET and α_s methods, are given in *Table 2*. The BET areas, A^{N}_{BET} and A^{C}_{BET}, were obtained from the nitrogen and carbon tetrachloride isotherms, assuming $\omega_N = 16{\cdot}2$ Å^2 and $\omega_C = 37$ Å^2, respectively. The α_s-plots were based on the standard adsorption data for the three vapours on Fransil (assuming this to be truly non-porous and to have a representative surface). The values of the areas A^{N}_{S}, A^{C}_{S} and A^{P}_{S} (from nitrogen, carbon tetrachloride and neopentane respectively) in *Table 2* were calculated from the slopes of the α_s-plots, taking the line through the origin and using the simple equations

Table 2. Surface areas of silicas calculated by the BET and α_s methods from isotherms of nitrogen, carbon tetrachloride and neopentane

Sample	*Porosity*	*Surface area* (m^{2}g^{-1})				
		BET–nitrogen A^{N}_{BET}	α_s-nitrogen A^{N}_{S}	BET–carbon tetrachloride A^{C}_{BET}	α_s-carbon tetrachloride A^{C}_{S}	α_s-neopentane A^{P}_{S}
Fransil	N	38·7	—	18	—	—
TK 70	N	36·3	35·6	27	35·8	—
TK 800	N	154	153	69	153	154
Aerosil 200	N	194	193	116	190	187
Gel A	T	300	299	150	280	—
Gel B	M + T	(500)	(500)	(640)	(1000)	(860)
Gel C	M + T	(576)	(552)	—	(590)	—
Gel D	M	(767)	(809)	(680)	(2800)	(2200)

N, non-porous; T, transitional porous; M, microporous; M + T, micro- and transitional porous.

$$A^{N}_{S} = 2{\cdot}89\ V_N/\alpha^{N}_{S} \tag{2}$$

$$A^{C}_{S} = 1{\cdot}92 \times 10^3\ X_C/\alpha^{C}_{S} \tag{3}$$

$$A^{P}_{S} = 3{\cdot}24 \times 10^3\ X_P/\alpha^{P}_{S} \tag{4}$$

where V_N is the volume of nitrogen adsorbed [in cm^3 (s.t.p.)], and X_C and X_P are the amounts of carbon tetrachloride and neopentane adsorbed (both in g). The BET–nitrogen area of Fransil was used to obtain the various factors in Equations (2), (3) and (4). As might be expected[4], because of the similarity in the surfaces of alumina and silica, the values of the normalising factors (2·87 and 2·89) in Equations (1) and (2) are nearly equal.

The Degussa sample TK 800 gave linear α_s-plots over the following ranges of p/p_0:0·001–0·9 for nitrogen, 0·001–0·75 for carbon tetrachloride and 0·001–0·5 for neopentane. It is believed that the upward departure from linearity shown by carbon tetrachloride at $p/p_0 = 0{\cdot}75$ and by neopentane at $p/p_0 = 0{\cdot}5$ is the result of interparticle capillary condensation. The linearity of the α_s-plots at lower p/p_0 confirms that both TK 70 and TK 800 are non-microporous and similar in character to Fransil.

The values of $A^{\mathrm{N}}_{\mathrm{BET}}$ are likely to be reliable (within, say, ± 5 per cent of true areas), apart from those in brackets which refer to microporous samples. The poor agreement between $A^{\mathrm{N}}_{\mathrm{BET}}$ and $A^{\mathrm{C}}_{\mathrm{BET}}$ is not unexpected and is related to the Type III character of the carbon tetrachloride isotherms (The BET parameter c is c. 3 for both carbon tetrachloride and neopentane). More interesting is the good agreement shown between $A^{\mathrm{N}}_{\mathrm{BET}}$, $A^{\mathrm{N}}_{\mathrm{S}}$, $A^{\mathrm{C}}_{\mathrm{S}}$ and $A^{\mathrm{P}}_{\mathrm{S}}$; this demonstrates that the α_s method can be used with systems having weak adsorbate–adsorbent interactions. Indeed, there appears to be some advantage in employing carbon tetrachloride or neopentane over nitrogen because the near-Type III isotherms of these comparatively bulky and highly polarisable molecules are more sensitive to pore narrowing than are the Type II isotherms of nitrogen. The figures in brackets are not real values of surface area, but they do serve to illustrate the marked effect of pore narrowing on the slope of the initial part of the α_s-plot. It is clear that the *apparent* surface areas of the microporous solids calculated from the carbon tetrachloride and neopentane α_s-plots are considerably greater than the corresponding values from the nitrogen α_s-plots. Thus, the adsorption of carbon tetrachloride or neopentane provides a sensitive probe for the detection of microporosity. The effect helps to explain the variation in apparent area per carbon tetrachloride molecule (cf. nitrogen), found on, a series of calcined aluminas[21].

ADSORPTION OF NITROGEN AND CARBON TETRACHLORIDE ON CHROMIUM OXIDE

Chromium oxide provides an example of a complex gel system in which changes occur on calcination in both the degree of surface oxidation[22] and the pore structure[23]. This leads to a difficulty in selecting the most suitable non-porous reference solids for the analysis of the adsorption data. Ideally, a different standard isotherm would be used for each well-characterized oxidation state (e.g. Cr^{3+} or Cr^{6+}). As in the case of high-temperature alumina, this problem has not yet been solved; fortunately, however, the evidence obtained so far suggests that the standard data for silica may be used, at least for the determination of surface area of chromium oxides by the α_s method. Thus, the α_s-plot of nitrogen on high temperature α-$\mathrm{Cr_2O_3}$ (sample (a) in *Table 3*), taking Fransil as the standard, was linear over the p/p_0 range 0·02–0·85. Values of the surface areas, $A^{\mathrm{N}}_{\mathrm{S}}$ and $A^{\mathrm{C}}_{\mathrm{S}}$, of samples (a) and (b) were calculated from the slopes of the α_s-plots with the aid of Equations (2) and (3). The agreement shown in *Table 3* between $A^{\mathrm{N}}_{\mathrm{BET}}$, and $A^{\mathrm{N}}_{\mathrm{S}}$ for sample (a), and between $A^{\mathrm{N}}_{\mathrm{BET}}$, $A^{\mathrm{N}}_{\mathrm{S}}$ and $A^{\mathrm{C}}_{\mathrm{S}}$ for sample (b) appears

Table 3. Surface areas of chromium oxide gels calculated by the BET and α_s methods from isotherms of nitrogen and carbon tetrachloride

Gel	*Porosity*	*Surface area* (m^2g^{-1})				
		BET–nitrogen	α_s-nitrogen		α_S-carbon tetrachloride	
		A^N_{BET}	A^N_S	A^N_S (ext)	A^C_S	A^C_S (ext)
(a) α-Cr_2O_3 (880)	N	10·9	10·7	10·7	—	—
(b) I(180)	N	40·3	41·1	41	44·5	45
(c) I(180)-soaked	M	143	—	43	—	54
(d) V	M	224	—	5·2	—	5·0

N, non-porous; M, microporous

to justify this approach. Samples (c) and (d) are microporous gels and now the procedure must be modified.

External surface areas, A^N_S(ext) and A^C_S(ext), were calculated from the slopes of the upper linear parts of the nitrogen and carbon tetrachloride α_s-plots, respectively, using the equations

$$A^N_S(\text{ext}) = 2{\cdot}89\ \Delta V_N / \Delta \alpha^N_s \tag{5}$$

and

$$A^C_S(\text{ext}) = 1{\cdot}92 \times 10^3\ \Delta X_c / \Delta \alpha^C_s \tag{6}$$

In employing Equations (5) and (6) to calculate the external areas from the slopes, $\Delta V_N / \Delta \alpha^N_S$ and $\Delta x_c / \Delta \alpha^C_s$, we are, of course, assuming that the multilayer adsorption process is proceeding as on an open surface. The linearity of the α_s-plots over the range $p/p_0 = 0{\cdot}40$–$0{\cdot}85$, confirms that capillary condensation is not contributing to the measured adsorption.

Sample (c) was prepared from (b) by soaking it in water to remove the CrO_3, which had been deposited in the micropores[23]. The estimated values of external area in *Table 3* are hardly changed—in marked contrast to the BET area. Sample (d) clearly has a small external area and the agreement between A^N_S(ext) and A^C_S(ext) may be considered rather striking.

ISOSTERIC HEAT OF ADSORPTION OF CARBON TETRACHLORIDE

Related to the influence of pore narrowing on the shape of the isotherm is its effect on the heat of adsorption[24]. Thus, the process of micropore filling is often (perhaps always) accompanied by an enhanced differential heat over that given by coverage (under the same conditions of p and T) of the open surface. Preliminary results are shown in *Table 4* for isosteric heats of adsorption of carbon tetrachloride on selected silicas. The heats were calculated from isotherms measured gravimetrically[18, 19] over the temperature range 5–25°C and for the present purpose of comparison they are expressed as a function of p/p_0 (rather than surface coverage). It is noteworthy that whereas the carbon tetrachloride isosteric heats remain reasonably constant on both TK 800 and the wide-pore silica gel (Gel A), they show a significant variation on the two microporous solids (Gels B & D). In the latter two cases, micro-

Table 4. Isosteric heat of adsorption of carbon tetrachloride on silicas

	Isosteric heat (kcal mole^{-1})			
p/p_0	TK 800	Gel A	Gel B	Gel D
0·02	—	—	11·5	12·4
0·05	9·0	9·2	10·8	10·4
0·10	9·0	9·2	10·0	10·0
0·20	9·0	9·2	9·6	9·2
0·40	8·9	9·4	9·7	9·1

pore filling enhances the isosteric heat over the low pressure end of the isotherm, i.e. to at least $p/p_0 = 0{\cdot}1$. Although further work is clearly required before any firm conclusions can be drawn, the results in *Table 4* do appear to confirm the importance of micropore filling prior to, and within, the BET range of the isotherm.

GENERAL CONCLUSIONS

The BET method has proved remarkably successful but it is not infallible[25]. Many attempts have been made to adjust the areas assigned to adsorbed molecules to bring BET surface areas into better agreement. This arbitrary manipulation is somewhat unsatisfactory as it assumes the validity of the BET monolayer capacity. For example, it is very doubtful whether the BET procedure serves any useful purpose when applied to a Type III isotherm. One important case where it seems justified, however, is for the adsorption of nitrogen on non-porous hydroxylated silica and alumina; on these solids, nitrogen forms a well-defined close packed monolayer in which each molecule appears to occupy an average area of about 16 Å^2. All the values of A_s, calculated from the α_s-plots, are based on the BET-nitrogen areas of the two non-porous reference solids (Fransil and Aluminium-oxide C) and it has been established that this procedure is at least self-consistent.

Once the standard isotherm has been obtained for a particular adsorbate-adsorbent system, the α_s method may be employed for routine determinations and indeed has certain advantages over the BET method. The linearity of the α_s-plot depends directly on the degree of conformity of the isotherm with the standard and, therefore, provides a simple diagnostic test for micropore filling or capillary condensation.

An advantage of the α_s method is that it can be used with Type III isotherms, or Type II isotherms having a small or indistinct knee ($c \longrightarrow 2$). The present work demonstrates that such isotherms can be employed on an empirical basis to provide surface areas in excellent agreement with BET-nitrogen areas. Moreover, these isotherms can be applied as a sensitive test for microporosity[27], which may not always be easy to recognise from the nitrogen isotherms (e.g. if compensation occurs between micropore filling and reversible capillary condensation[26]).

Care is, of course, required to ensure that the α_s-plots are restricted to that part of the isotherm covered by *reliable* standard data for the particular adsorbate–adsorbent system. At very low pressures, the effect of the surface chemistry becomes important (e.g. the presence of surface impurities or active centres); at high pressures ($p/p_0 > 0{\cdot}9$ for nitrogen), interparticle condensation and surface curvature introduce complications.

ACKNOWLEDGEMENTS

The author wishes to thank the following for help and encouragement in the preparation of this paper: Dr. S. J. Gregg, Dr. R. E. Day, Mr. P. A. Cutting and Mr. D. A. Payne. Thanks are also due to Degussa Forschung Chemie F.C.Ph., Laporte Industries Limited and the Unilever Chemical Development Centre for supplying materials and information.

References

[1] S. Brunauer, P. H. Emmett and E. Teller. *J. Am. chem. Soc.* **60**, 309 (1938).
[2] S. Brunauer, L. S. Deming, W. S. Deming and E. Teller. *J. Am. chem. Soc.* **62**, 1723 (1940).
[3] M. R. Harris and K. S. W. Sing. In *Third International Congress of Surface Activity* (Cologne) 1960, II, p. 42.
[4] M. R. Harris and K. S. W. Sing. *Chem. & Ind.* 487 (1959).
[5] B. C. Lippens and J. H. de Boer. *J. Catalysis.* **4**, 319 (1965).
[6] J. H. de Boer, B. G. Linsen and Th. J. Osinga. *J. Catalysis* **4**, 643 (1965).
[7] B. G. Aristov and A. V. Kiselev. *Koll. Zhur.* **27**, 299 (1965).
[8] M. H. Polley, W. D. Schaeffer and W. R. Smith. *J. phys. Chem.* **57**, 469 (1953).
[9] C. Pierce and B. Ewing. *J. phys. Chem.* **68**, 2562 (1964).
[10] K. S. W. Sing. *Chem. & Ind.* 1520 (1968).
[11] D. Aldcroft, G. C. Bye, J. G. Robinson and K. S. W. Sing. *J. appl. Chem.* **18**, 301 (1968).
[12] K. S. W. Sing. *Chem. & Ind.* 829 (1967).
[13] J. D. Carruthers, P. A. Cutting, R. E. Day, M. R. Harris, S. A. Mitchell and K. S. W. Sing. *Chem. & Ind.* 1772 (1968).
[14] P. A. Cutting and K. S. W. Sing. *Chem. & Ind.* 268 (1969).
[15] B. C. Lippens, B. G. Linsen and J. H. de Boer. *J. Catalysis* **3**, 32 (1964).
[16] G. C. Bye, J. G. Robinson and K. S. W. Sing. *J. appl. Chem.* **17**, 138 (1967).
[17] D. A. Payne and K. S. W. Sing. *Chem. & Ind.* 918 (1969).
[18] P. A. Cutting. *Seventh Vacuum Microbalance Techniques Conference*, 1968 to be published.
[19] P. A. Cutting and K. S. W. Sing. unpublished work.
[20] J. D. Carruthers, R. E. Day and K. S. W. Sing. unpublished work.
[21] S. J. Gregg and K. S. W. Sing. *J. Phys. Chem.* **55**, 597 (1951).
[22] J. D. Carruthers, J. Fenerty and K. S. W. Sing. *Sixth International Symposium for the Reactivity of Solids*, 1968, 127.
[23] J. D. Carruthers and K. S. W. Sing. *Chem. & Ind.* 1919 (1967).
[24] A. V. Kiselev. In *Second International Congress of Surface Activity* (London) 1957, II, p. 179.
[25] S. J. Gregg and K. S. W. Sing. *Adsorption, Surface Area & Porosity*, p. 35, Academic Press, London, 1967.
[26] G. C. Bye and K. S. W. Sing. *Chem. & Ind.* 1139 (1967).
[27] C. Pierce and R. N. Smith. *J. Phys. Chem.* **54**, 784 (1950).

DISCUSSION

Dr Th. J. Osinga (*Unilever Research Laboratorium, Vlaardingen, Netherlands*) said: Professor Sing started his paper, by explaining that his graphical procedure was an improvement over the *t*-method of Lippens and de Boer. He also stated that the *t*-method being based on the BET method was on a questionable basis. Therefore Prof. Sing introduces a reference curve without any particular basis. I feel however, that an analysis should be made of the differences between the two methods and I would like to contribute by giving my view on the matter and I look forward to have Prof. Sing's reactions.

First I would like to give the essential feature of the *t*-method of Lippens and de Boer. It was noted by several investigators, besides Lippens and de Boer, *e.g.*, Schüll, Cranston and Inkley and others, that on many nonporous substances a similar N_2 sorption isotherm was found, which turned out to be more or less the same, when related to the same surface area. This means, that the thickness of the adsorbed layers is a unique function of the relative pressure for many adsorbents which, as we have learned here, are characterised by a c value (from the BET equation) higher than 100.

Lippens and de Boer have suggested that all isotherms, measured on similar adsorbents, but now possibly containing pores, should be referred to the statistical thickness of the adsorbed layer, that would have been found at the same relative pressure in the absence of pores

$$\left(t = \frac{V_a}{V_m} t_1\right)$$

This procedure has shown to give valuable information on the presence of micropores. So far the method of Lippens and de Boer is in principle independent of the BET method. However they have chosen the BET method for the calculation of the thickness of the adsorbed layer (via V_m). As at present it is believed that the BET equation gives good surface areas, a fact also nicely demonstrated here by Dr Deitz, and as I understand is also adopted by Prof. Sing, this choice still seems acceptable. If in the future better methods, generally accepted, are available to characterise the surface area (or V_m) the t-curve of Lippens and de Boer might be revised easily by multiplication of the whole curve with a constant factor $V_m\mathrm{BET}/V_m\mathrm{NEW}$ and I feel that Dr Lippens and Prof. de Boer will agree that this should be done then.

When we now analyse the proposition of Prof. Sing to relate the sorption isotherms to an adsorbed value at a relative pressure of 0·4 we see, that his standard curve is essentially the same, but only differs by a constant factor $V_m/t_1 V_{0\cdot4}$. It is my opinion, that all analysis of isotherms, carried out using the curve of Prof. Sing on adsorbent-adsorbate systems with $c \sim 100$ can also be carried out with the t-method.

However the method of Prof. Sing is more restricted as only indications can be obtained of the presence of micropores or pores causing condensation effects. To relate the slopes of the curves with surface areas, also in the approach of Prof. Sing an equation like the BET equation must be adopted.

An advantage of the Lippens–de Boer method is, according to my opinion, that as they plot V_a vs. the thickness t, it is directly clear, that the slope of the curve gives that surface area, still taking part in the adsorption process which makes it easier to visualise the meaning of the curves.

The point made by Prof. Sing, that the t-curve proposed by Lippens and de Boer cannot be applied to type III isotherms is right, while the c values of these adsorbents are appreciably lower than 100 ($c < 1$). This means that a separate t-curve must be measured for such adsorbent-adsorbate systems, possibly based on another method to determine V_m instead of the BET method. However in my opinion the same applies to the standard curve of Prof. Sing. He also will have to measure a separate new standard curve on a non-porous sample for such an adsorbent-adsorbate system. Furthermore it should still be assessed that for these c values standard curves do exist.

It is my feeling, that a very valuable remark was made during this symposium by Dr Lecloux viz. that the t-curve of Lippens and de Boer can only be applied to samples with a c value of approx. 100, as the t-curve is a function of c. It might be possible to decide directly which t-curve must be used when the c value of the adsorbent-adsorbate system is known from a BET plot determined on a non-porous sample.

Professor K. S. W. Sing replied: I agree with Dr Osinga that the t-method has provided a useful means of analysing nitrogen isotherms on some oxides and other solids. As already stated by Prof. de Boer, it is based on the BET method since V_m must be located before t can be obtained; further application of the t-method is restricted therefore to those adsorption systems where the monolayer capacity is well defined. On the other hand, the standard α_s isotherm is not directly related to V_m and can be established even when V_m is unknown. The application of the new method is illustrated in the paper by the analysis of the near—Type III isotherms of carbon tetrachloride and neopentane. These molecules were chosen because their bulky size and high polarisability make the dispersion interactions especially sensitive to pore narrowing. Indeed, the α_s-plots reveal that the carbon tetrachloride and neopentane isotherms are considerably influenced by micropore filling and it seems reasonable to conclude that the resulting increase in the value of c cannot be taken as evidence in favour of the validity of V_m or t.

Dr Osinga suggests that the standard α_s curve is essentially the same as the standard t curve and that the values of α_s can be converted to those of t by the use of a constant factor. It follows from the above reasoning that this is only true for Type II isotherms, and only then if the shape of the isotherm (*e.g.* as indicated by the magnitude of c) remains reasonably constant from one *non-porous* solid to another. It so happens that the standard α_s curves for nitrogen on a number of hydroxides and hydrous oxides are in close agreement and, as already mentioned, in these cases the BET method appears to provide a reliable estimate of V_m (when $c \sim 100$). Since the validity of the BET monolayer capacity is questionable for many (perhaps most) other adsorption systems it seems prudent at the present time to adopt the α_s-plot rather than the t-plot as an empirical method of isotherm analysis.

Dr R. S. Mikhail (*Ain Shams University, U.A.R.*) said: The paper presented by Professor Sing is of particular interest, and carries certain advantages over the simpler V_l–t plot of Lippens and de Boer. However, I am worried about a few points, which I hope Professor Sing will clarify for me.

1. The values of A_{BET} and A_S in *Table 1* show disagreement in certain cases. I wish that the BET c constants had been included in the table. Brunauer and myself have shown, in 1968, that in order to get an agreement between A_{BET} and A_t obtained for the usual Lippens–de Boer plot, the c value approximately should be the same for adsorption on the non-porous reference material as that for the material to be analysed. It seemed to me that this also should be necessarily the case to obtain agreement between A_{BET} and A_S. If the C values are not nearly identical in the cases which showed a disagreement, then this might be the cause. This seems to be a necessary condition in both the A_S method or the A_t method.

2. Regarding type III isotherms, these are sometimes obtained for water vapour adsorption as well as for other vapours on solid surfaces. For water vapour this usually occurs when the surface is hydrophobic, or, in certain cases, when the surface shows a composite character, *i.e.* being partly hydrophobic and partly hydrophilic. If through physical or chemical treatment you are able to change the hydrophilic/hydrophobic character of the surface without altering the surface area of the solid, then an increase of this ratio will lead to a series of isotherms with steeper early regions. Consequently, one would expect to get steeper V_s plots. I believe that in such particular cases one is measuring the area of the hydrophilic fraction of the surface and not the total surface area of the solid. It seems to me that the development presented by Professor Sing is still unable to solve this particular problem, and to measure the total surface area of a composite surface showing a type III isotherm; neither can it be applied for analysis of the hydrophilic function of the surface.

Professor K. S. W. Sing replied: In my paper I have given the range of linearity of the α_s-plots rather than the values of c. I agree with Dr Mikhail that in attempting to assess the validity of BET areas it is useful to consider the corresponding values of c. In a contribution to this discussion, Payne and I give the values of c for nitrogen and argon adsorption isotherms on certain non-porous aluminas and silicas. Reference to *Table 1* of my paper will indicate that in general a high value of c is associated with rather poor agreement between A_{BET} and A_{S}. If the α_s-plot is linear in the *multilayer* range (and extrapolates back to the origin) we may take this as a good indication of the validity of A_{S} rather than A_{BET}. In my view, the α_s method has a clear advantage over the t-method in this respect since in principle it can be made independent of the BET method.

I accept the reservation expressed by Dr Mikhail that a Type III water isotherm may result through the fractional coverage of a composite surface and in that case cannot be employed to give a measure of the *total* surface area. The adsorption of water vapour is a complex process, but it is possible that by the correct choice of standards the α_s method could be applied to water (and other adsorbates undergoing *specific* adsorption) to estimate the area of the hydrophilic fraction of the surface.

Professor M. M. Dubinin (*Academy of Sciences, Moscow*) said: Professor Sing's paper described a modification of de Boer's method in which the mean statistical thickness of the adsorption layer t was replaced by α_s:

$$\alpha_s = V/V_{\mathrm{X}} \qquad (1)$$

where V_{X} is the adsorption value at a selected equilibrium relative pressure x. For a number of vapours, including nitrogen at a temperature of −196°C, the value of x was set at 0·4, assuming that at this relative pressure the filling of micropores terminates, but capillary condensation does not begin yet.

In the introduction to my paper, which I will present at the next session, I will try to substantiate the fact that the lower boundary of capillary condensation in transitional pores is matched by meniscus curvature radii of about 15–16 Å. Proceeding from this it is easy to calculate by the Kelvin equation the characteristic relative pressures for various vapours corresponding to 15–16 Å:

$$x = \exp\left[-\frac{2\sigma v}{RTz}\right] \tag{2}$$

According to Eq. (2) the values of x depend on the surface tension σ and the molar volume of the adsorptive V.
Table A lists the calculated values of x.

Table A. $z = 15$ Å

Vapour	t (°C)	$\sigma \frac{\text{erg}}{\text{cm}^2}$	$v \frac{\text{cm}^3}{\text{mol}}$	$x = p/p_s$
N_2	−196	8·85	34·65	0·53
H_2O	20	72·75	18·05	0·49
C_6H_6	20	28·88	88·79	0·25
CCl_4	20	26·8	96·45	0·24

For nitrogen at −196°C and for water at 20°C the values of x do not differ essentially from 0·4. For benzene and carbon tetrachloride at 20°C, however, the value of x is almost half that value. In the light of the foregoing, in Sing's empirical a_S-method it is expedient to adopt for various vapours relative pressures x close to the tabulated characteristic equilibrium relative pressures for the beginning of capillary condensation. Then the values for various vapours will have the nature of the corresponding values.

Professor K. S. W. Sing replied: There are two comments I wish to make concerning Academician Dubinin's observation that the lower limit for the capillary condensation of a particular vapour should be taken into account when deciding the α_s scale. Firstly, the selection of the point on the *standard* isotherm corresponding to $\alpha_s = 1$ is not strictly governed by any consideration of capillary condensation because only monolayer-multilayer adsorption should be taking place on the non-porous reference solid. It is therefore a matter of convenience as to where $(p/p_0)_x$ is located. However, it should be remembered that when c is low the accuracy of the adsorption data in the low p/p_0 range is likely to be limited; again, at high p/p_0 there is the possibility of interparticle capillary condensation—especially with high area non-porous solids. For these reasons the choice of $(p/p_0)_x$ in the middle range of the isotherm may be desirable.

Secondly, it is perhaps worth noting that an upward deviation of the nitrogen α_s-plot from linearity at $\alpha_s < 1$ (*i.e.* $p/p_0 < 0{\cdot}4$) has been found with certain calcined aluminas [D. Aldcroft, G. C. Bye, J. G. Robinson and K. S. W. Sing. *J. appl. Chem.* **18**, 301 (1968)]. At present, it is not clear whether this is due to a form of reversible capillary condensation (perhaps in wedge-shaped pores), a second stage of micropore filling or a third, intermediate process which has not yet been properly characterised.

Dr B. C. Lippens (*Texaco Belgium N.V., Ghent*) said: Concerning the question of sorption in the microporous materials I would like to draw the attention to the behaviour of some gelatinous aluminium hydroxide preparations described in my thesis [Delft (1961, p. 29)]. The samples were prepared by reacting ammonium alum with a concentrated solution of ammonium sulphate in aqueous ammonia during different reaction times. After filtration, washing and drying at 120°C samples were obtained of which the BET surface area and the specific volumes in water, carbon tetrachloride and mercury were measured.

A remarkable difference was found between the specific volumes measured in water (V_W) and those measured in carbon tetrachloride (V_C). Therefore we also measured the pore volume V_{pN} using nitrogen at 78°K and a relative pressure of 0·98 and the sorption capacity for water V_{pW} at room temperature and a relative water vapour pressure of 0·98. The results are shown in *Table B*.

Table B

Sample No.	W	SO_3	S_{BET}	V_w	V_c	V_{Hg}	V_{pw}	V_{pN}	V_p	$V_c + V_{pN}$
1	27·6	10·9	2	0·486	0·757	0·771	0·420	0·004	0·285	0·761
2	26·8	9·6	49	0·478	0·692	0·759	0·424	0·053	0·281	0·745
3	26·2	7·6	183	0·461	0·535	0·737	0·427	0·198	0·276	0·733
4	25·8	5·2	244	0·449	0·482	0·742	0·446	0·257	0·293	0·739
5	26·0	3·6	289	0·442	0·439	0·735	0·448	0·301	0·293	0·740

W : water content in g/100g Al_2O_3
SO_3 : SO_3 content in g/100g Al_2O_3
S_{BET} : in m^2/g Al_2O_3
Other quantities in ml/g Al_2O_3.

The sum of the specific volume in carbon tetrachloride V_c and the nitrogen pore volume V_{pN} is approximately equal to the specific volume in mercury V_{Hg} (which may be put equal to the granular volume of the material [W. H. Meijs, thesis Delft (1961), p. 36]. V_c will be equal to the sum of the real specific volume of the material and the volume of those pores in which carbon tetrachloride cannot penetrate. From the fact that $V_c + V_{pN}$ is equal to the volume of the granules it follows that there are no pores into which nitrogen can penetrate and carbon tetrachloride cannot. This was to be expected as the mean size of the pores accessible to nitrogen is about 21 Å (radius), which is large compared with the size of carbon tetrachloride molecule.

Assuming that V_w will not differ much from the real specific volume [J. J. Steggerda, thesis, Delft (1955), p. 60] the total pore volume V_p can be calculated taking the difference between V_{Hg} and V_w.

All five preparations possess a pore volume of 0·28 to 0·29 ml/g Al_2O_3, fully accessible for water but only partly for nitrogen or carbon tetrachloride. Whether the pore volume inaccessible for nitrogen corresponds to very narrow pores or to wider ones with very narrow or blocked openings, it will be clear tha phenomena like this complicate the application of the *t*-method to various adsorbates.

Another point should be stressed, namely the difference between pore volumes V_p and the sorption capacity for water V_{pw}, which is about $1\frac{1}{2}$ times as large as V_p. It is very unlikely that the sorbed water in the pores would have a density of about 1·5 and it must therefore be assumed that part of the sorbed water is taken up in the solid itself with simultaneous swelling.

Both phenomena, swelling and a pore volume accessible to certain adsorbates and not accessible to others, are certainly not limited to the case described here. It shows that one must be careful by assuming the presence of a micropore volume in the case that the adsorbate is not completely "indifferent" to the adsorbent.

Mr D. A. Payne and **Professor K. S. W. Sing** said: Argon adsorption is less well established than nitrogen for the determination of specific surface area. The results expressed in *Table C* serve to illustrate the difficulty encountered in attempting to bring BET nitrogen and argon areas into agreement. The values of A^{Ar}_{BET} were calculated by assuming the area per molecule of argon, Ω_{Ar}, to be 16·5 Å^2; (values of 16·0, 16·5 and 16·6 Å^2 have been obtained by Harkins [*The Physical Chemistry of Surface Films*, Reinhold (1952), p. 227], Harris and Sing [*Chem. & Ind.* 757 (1967)] and Corrin [*J. Am. Chem. Soc.* **73**, 4061 (1951)] respectively. The lack of good agreement between A^{N}_{BET} and A^{Ar}_{BET} appears to be related to the low C values for argon. It is noteworthy, therefore, that excellent agreement is obtained between A^{N}_{BET}, A^{N}_{S} and A^{Ar}_{S} when the α_s-plots for nitrogen and argon are calibrated with Fransil.

Table C. Surface areas of silicas

Sample	Nitrogen–BET ($\Omega_N = 16{\cdot}2$ Å^2)		Nitrogen–α_s	Argon–BET ($\Omega_{Ar} = 16{\cdot}5$ Å^2)		Argon–α_s
	A^{N}_{BET}/m^{2}g^{-1}	c	A^{N}_{S}/m^{2}g^{-1}*	A^{Ar}_{BET}/m^{2}g^{-1}†	c	A^{Ar}_{S}/m^{2}g^{-1}*
Fransil	38·7	102	—	35·6	32	—
TK 70	36·3	82	35·7	32·4	34	35·4
Silica Gel	216	75	217	194	47	218

* Based on A^{N}_{BET} of Fransil.
† P_0 of solid argon used in BET equation.

The results obtained on certain samples of high temperature alumina are given in *Table D*. The c values for both nitrogen and argon are considerably higher than those in *Table C*, and it is somewhat surprising that the agreement between A^{N}_{BET} and A^{Ar}_{BET} is improved. This agreement might be taken as a strong indication of the reliability of the BET areas but for the fact that the values of A^{Ar}_{S} are consistently higher than those of A^{N}_{BET} or A^{Ar}_{BET}. Reliance is placed on the values of A^{Ar}_{S} since the argon α_s-plots are of good linearity in the *multilayer* region (unlike those of nitrogen) and show a deviation only at low relative pressure. We, therefore, favour the

Table D. Surface areas of high temperature aluminas

	Nitrogen–BET ($\Omega_{\mathrm{N}} = 16{\cdot}2$ Å^2)		Argon–BET ($\Omega_{\mathrm{Ar}} = 16{\cdot}5$ Å^2)		Argon–α_s
Sample	$A_{\mathrm{BET}}/\mathrm{m^2g^{-1}}$	c	$A_{\mathrm{BET}}^{\mathrm{Ar}}/\mathrm{m^2g^{-1}}$†	c	$A_{\mathrm{S}}^{\mathrm{Ar}}/\mathrm{m^2g^{-1}}$*
C(1200)114	5·9	283	6·1	78	6·6
C(1300)6	4·5	388	4·4	81	4·9
C(1400)6	2·5	342	2·5	75	2·7
Gb(1200)6	5·0	600	5·1	101	5·5
Gb(1400)6	2·0	742	2·1	82	2·2
CGb(1200)6	6·6	332	6·8	88	7·3

* Based on $A^{\mathrm{N}}_{\mathrm{BET}}$ of alumina standard.
† P_0 of solid argon used in BET–equation.

explanation that both nitrogen and argon exhibit localised adsorption on high temperature alumina, but that argon behaves normally in the multilayer region.

Dr S. J. Gregg (*Brunel University*) said: It will bear emphasis that the a_s method represents a very neat means of comparing an experimental isotherm with the standard isotherm, with the minimum number of assumptions. If the experimental isotherm has exactly the same shape as the standard then the two isotherms can be brought into coincidence by scaling the experimental one up or down by using a normalising factor, f, say. If one then makes the single assumption (which is basic to the very concept of adsorption) that the uptake at a given pressure is proportional to the surface area of the adsorbent, then the surface area of the experimental solid is merely equal to $f x A_{\mathrm{standard}}$, where A_{standard} is the area of the standard specimen. If the value of A_{standard} is known (*e.g.* from nitrogen adsorption), then the value of A for the experimental solid can be at once calculated.

Various workers have in essence adopted this device down the years. The well-known *t*-method of de Boer and Lippens provides an elegant means of carrying out the comparison of isotherms with the standard, but it is still tied to the BET method (through the use of monolayer capacity) and it also involves an assumption as to the thickness of the adsorbed layer. The a_s-method is free of these limitations; it can therefore be applied immediately to adsorbates other than nitrogen—even if the isotherm should be of Type III—and it does not necessitate any assumption as to the value of cross-sectional area ω_m.

Dr R. B. Gammage (*Oak Ridge National Laboratory*) said: There appears to be a common *t*-curve describing the adsorption of nitrogen on heterogeneous, metallic oxide powders. We find, however, that for the special case of a non-porous thorium oxide [E. L. Fuller, Jr., H. F. Holmes, and C. H. Secoy. *J. Phys. Chem.* **70**, 1633 (1966)] with a homogeneous surface [H. F. Holmes, E. L. Fuller, Jr., and C. H. Secoy. *J. Phys. Chem.* **72**, 2095 (1968)] the common aspect is no longer true for surface outgassed at 25°. In *Figure A* are shown the adsorption isotherms of nitrogen for the same surface outgassed at 25° and 1000°. The surface retains the gravimetric equivalent of three layers of water after the 25° outgassing whereas it is completely stripped of water at 1000°. As can be seen, the effect of surface water is to reduce the adsorptive capacity by 20–25 per cent in the multi-layer region. On this oxide a well ordered water structure is formed[2] and on the surface so presented the energy of interaction of nitrogen is low ($c \sim 30$). The uptake of nitrogen is also unusually low. The ordered water structure is rapidly broken up by outgassing at temperatures higher than 25° with an increase in the uptake and energy of interaction of nitrogen. After outgassing at 100°, the isotherm of nitrogen approximates to the upper one shown in *Figure A*. Essential to the reasoning is the knowledge that the oxide is truly non-porous. Three more important pieces of evidence can be recited to support a non-porous character; no slow kinetics, no adsorption hysteresis and agreement between the nitrogen BET specific surface after 500° outgassing and the Harkins Jura absolute specific surface determined by the heat of immersion in water.

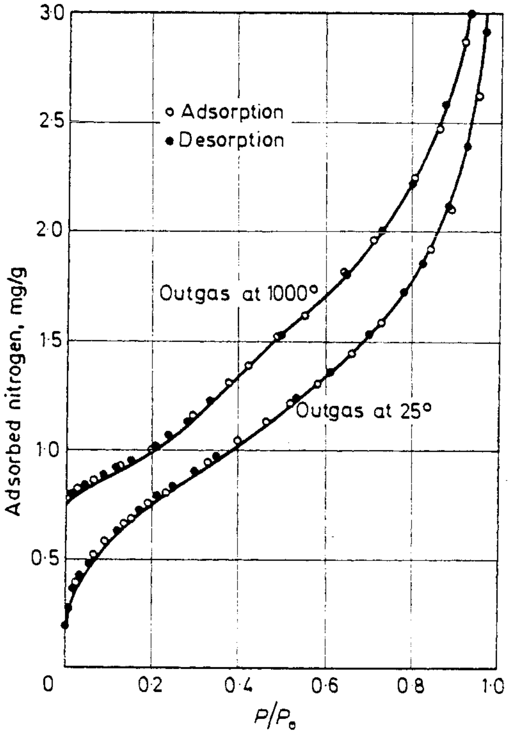

Figure A. Adsorption of nitrogen at 77°K on non-porous thorium oxide I.

CROSS-SECTIONAL AREA OF ADSORBED GASES ON PRISTINE E-GLASS FIBRE OF KNOWN AREA

VICTOR R. DEITZ and NOEL H. TURNER

U.S. Naval Research Laboratory, Washington, D.C. 20390, U.S.A.

A pristine E-glass fibre (a silica alumina borate glass) was drawn directly from the melt under highly controlled conditions. This sample offered an unmodified glass fibre surface of known diameter and length for adsorption studies. Adsorption isotherms were determined for krypton, nitrogen, and argon at 77·4°K and 90°K and the cross-sectional areas of the adsorbed molecules were calculated for the monolayer coverage determined from the BET plots. These values are compared with various values reported in the literature. Subsequent contact of the E-glass sample with liquid water for only one hour modified significantly the adsorption properties of the glass fibre. The great importance of the pretreatment (i.e., 'cleaning') on the surface properties of glass is emphasized.

INTRODUCTION

It has long been considered desirable to compare a known geometric area of a solid with the BET surface area derived from the BET monolayer coverage and an assumed cross-sectional area of the adsorbed molecule[1,2]. One experimental difficulty is the selection of a material that has a boundary with a surface roughness less than the diameter of the adsorbate molecule. Not only is such a material difficult to prepare, but it is also difficult to maintain. A pristine E-glass fibre of known length and constant diameter should be a good approximation to this ideal behaviour. As the molten glass leaves the opening in the platinum crucible during the fibre-drawing process, surface tension draws the melt into a cylindrical shape before the mass has solidified. At the drawing speeds employed in this investigation it is estimated that the fibre travelled 3 mm in 100 μsec and solidification most probably took place after this period[3,4]. This is ample time for the molecular groups in the glass surface to be pulled by surface tension into a position of minimum free energy. A smooth surface is indicated by electron microscopy but the residual roughness of present concern must be of an atomic magnitude.

Some adsorption measurements are reported using krypton, nitrogen and argon with samples of E-glass fibre drawn directly from the melt under closely controlled conditions. The monolayer coverage is then calculated from the BET plots and combined with the known area of the E-glass fibre to obtain the cross section of the adsorbed molecule.

EXPERIMENTAL

Formation of E-glass fibre

The facility for drawing a single glass fibre located at the U.S. Naval

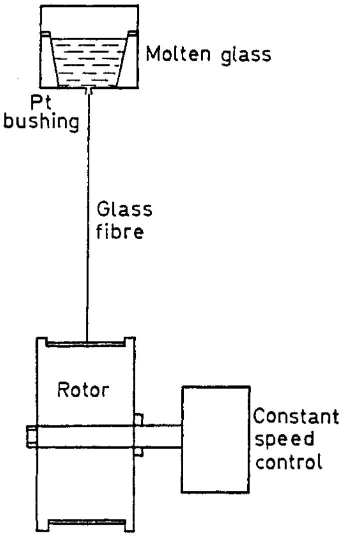

Figure 1. Schematic drawing of the equipment for Fibre-pulling

Ordnance Laboratory was kindly made available for this work. A schematic drawing of the apparatus is shown in *Figure 1.* The E-glass in the form of marbles was introduced into the platinum crucible which served as the resistance element of a high amperage furnace. When the covered crucible was heated to the drawing temperature, the glass flowed through an orifice in the bottom of the crucible and was then attenuated into a fibre by winding on a stainless steel wheel driven by a constant speed motor. The fining temperature of the E-glass was about 1400°C and the drawing temperature was controlled at 1260° ± 3°C.

In order to realize a fibre of known area (A), the following must be known: the speed of the rotor (ω), the drawing time (t), the diameter (D) of the rotor, the average depth (d) of the glass fibre collected on the rotor, the fibre weight (W), and the density (ρ) of the glass fibre. The area is then given by

$$A = 2\pi \left(\frac{W\,(D + d)\;\omega t}{\rho}\right)^{\frac{1}{2}} \tag{1}$$

Alternatively, if the average diameter of the fibre (Δ) were known, then

$$A = \pi^2\,(D + d)\,\Delta\,\omega t$$

One of the basic assumptions of equation (1) is the formation of a fibre of constant diameter. Thomas[5] has shown that in general six variables must be controlled in order to realize constant diameter. Of these, the temperature of the glass melt, the drawing speed, and the depth of glass in the crucible are important to the present work. The remaining variables are fixed for a given operation, namely, the design of the crucible, the diameter (1·8 mm) of the opening in the crucible, and the composition of the glass. The results of Thomas for a type E-glass fibre at a drawing speed of 4000 ft/min and a temperature of 1260°C showed that the fibre diameter varied 0·03 μ for a change of 1°C. At the same temperature and a drawing speed of 4000 ft/min the fibre diameter varied with drawing speed in an amount 0·001 μ per linear ft per min.

The linear speed of the fibre preparation used in the present measurements was greater than that mentioned above, approximately 6600 ft/min. The speed of the rotor was controlled with a precision of 10 parts per 5000 as determined by frequent measurements with a stroboscope (Type 1531-A Strobatac, General Radio Company, Concord, Mass.). This corresponds to an uncertainty of the 13 parts in 6600. Therefore, the change in fibre diameter due to this parameter is too small to be significant.

Similarly, the amount of glass contained in each sample of fibre (15 to 20g) was not sufficient to change the depth of the glass melt (approximately 50 mm) in the crucible to an appreciable extent during the sample collection.

From equation (1) the fractional variation in the area is given by

$$\frac{\delta A}{A} = \frac{1}{2}\left[\frac{\delta W}{W} + \frac{\delta(D + d)}{D + d} + \frac{\delta W}{\omega} + \frac{\delta t}{t} + \frac{\delta \rho}{\rho}\right]$$

The weight of the fibre was known to 0·001 g in 15 g total. The uncertainty in $D + d$ is in the depth of the packing of glass fibre accumulated on the rotor; this is estimated to be 0·05 cm in a total of 18·45 cm. The running speed could be rapidly reached and the time of fibre collection may have been uncertain to about 0·5 min in 100 min. The density of the fibre was determined by pyconometer measurements to be 2·568 ± 0·001 g/cm³.† Using these values for the uncertainties of δW, $\delta(D + d)$, $\delta\omega$, δt, and $\delta\rho$, the value of $\delta A/A$ is 0·005.

The details of a typical preparation of E-glass fibre are given in *Table 1.* Since the rotor speed was measured at various time intervals, the summation

Table 1. Collection of E-glass fibre (Series 1)

Time	*Crucible* temp. (°C)	*Rotor speed* (rpm)	*Time interval* (min)
11:55	Start		0
12:05	1260	3540	10
12:13	1260	3542	8
12:20	1260	3542	7
12:25	1260	3542	5
12:30	1260	3540	5
12:35	1262	3542	5
12:44	1262	3542	9
12:53	1262	3538	9
13:00	1263	3535	7
13:06	1262	3538	6
13:14	1262	3540	8
13:21	1262	3540	7
13:27	1262	3540	6
13:31	Stop	3540	4

$\Sigma\omega t = 339\,840.$

---

†The authors wish to acknowledge the measurements of J. L. Bitner for the density of the E-glass fibre samples used in the present work.

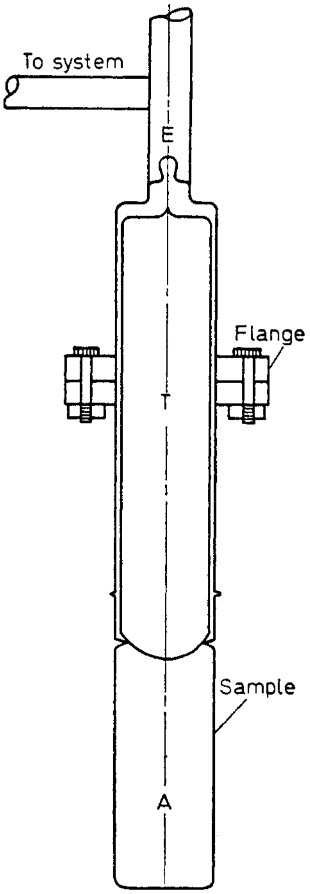

Figure 2. Adsorption container for a large sample of E-glass fibre

of the product ωt was determined instead of averaging. The weight of the fibre was 22·055 g, $D + d$ was 18·5 cm, and A, calculated from equation (1) was 4·61 ± 0·02 m^2.

Immediately after the rotor was stopped, the accumulated fibre was removed and transferred to the container shown in *Figure 2*. 'Clean-room' procedures were used in these operations. The evacuated tube 'T' was inserted to diminish the dead space and the closure was quickly made using a copper gasket between the two stainless steel flanges. About 30 sec were required for these manipulations. The container was furnished with a seal-off bubble 'E' which was broken with a glass hammer after sealing to the vacuum apparatus.

Adsorption measurements

The adsorption of nitrogen, argon, and krypton were determined volumetrically. The essential parts of the apparatus were enclosed and maintained at 26·8 ± 0·05°C; the region in the vicinity of the liquid nitrogen or liquid oxygen was vented directly to the room. A Wallace–Tiernan gauge (Model FA 145), calibrated against a mercury manometer, was used for pressures greater than 5 torr. A capacitance manometer (Granville-Philips Co.), calibrated with a McLeod gauge, was used for the lower pressures.

The apparatus was greaseless and free of mercury. At the high pressures Dahl metal valves were employed in which the valve body and the thin metal diaphragm were made of stainless steel; the gasket was of Teflon. For the krypton measurements, Granville-Phillips C valves were used having seats of stainless steel to silver and welded diaphragms. The inlet and outlet connections of stainless steel were welded and joined by Kovar seals to Pyrex tubulation. A diagramatic sketch is shown in *Figure 3*.

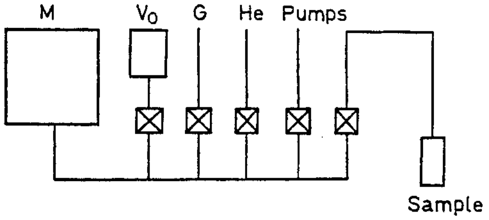

Figure 3. Schematic drawing of the gas adsorption apparatus: Manometer M, known volume V_0, Gas inlet G, Helium inlet He, Metal valves X

The liquid nitrogen or oxygen was maintained at constant level by an automatic levelling device. An oxygen manometer served as the standard for the determination of the temperature of liquid nitrogen. Purified tank nitrogen or argon was used and the krypton (mass spectrometric grade) was expanded directly from a litre flask.

The areas concerned are between 4 and 6 m^2 per sample and it is necessary to strive for high precision in the pressure measurements. In order to minimize the accumulation of error in the determination of the amounts adsorbed, only 1 to 3 adsorption points were determined for a given experiment. The dead space was calculated from the known volume of the empty container minus the volume of the fibre (W/ρ). The sample was outgassed at 300°C before each series of measurements. The outgassing was continued until the pressure increase (with the sample at 300°C and isolated from the pumps) due to the evolved gases amounted to no more than 5 nmole h^{-1}m^{-2}.

RESULTS

The results are presented in the form of BET plots,

$$\frac{p/p_0}{N_a\,(1 - p/p_0)} \text{ versus } p/p_0$$

where p/p_0 is the relative pressure and N_a is the amount adsorbed at 77·4°K, *Figure 4* for krypton, *Figure 5* for nitrogen, and *Figure 6* for argon. *Table 2* is a summary of the calculated adsorbed cross sectional areas using the known E-glass surface of 4·61 m^2. Values have also been obtained using liquid oxygen and the available results for 90·2°K are also given in *Table 2*. *Table 3* summarizes the krypton measurements with four different samples of E-glass fibre. The average cross-sectional area of krypton from these measurements is 20·6Å^2.

Table 2. Adsorbate areas using a known area of E-glass fibre

		(Å²)	*Literature values*[7] (Å²)
Nitrogen	N_2 77·4	16·4	16·2
	90·2	16·6	
Argon	Ar 77·4	13·4	13·8
	90·2	13·9	
Krypton	Kr 77·4	20·4	20·2
	90·2	20·4	

Table 3. Krypton adsorption on E-glass fibre

Series	A (m²)	n_m (μ moles)	Kr 77·4°K (Å²)
I	3·96	33·1	19·9
II	6·30	49·2	21·2
III	4·50	35·7	20·9
IV	4·61	37·5	20·4

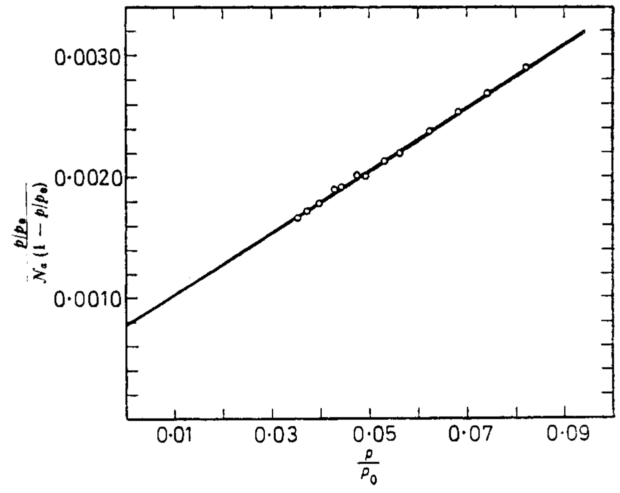

Figure 4. BET plot for krypton at 77·4°K on E-glass fibre

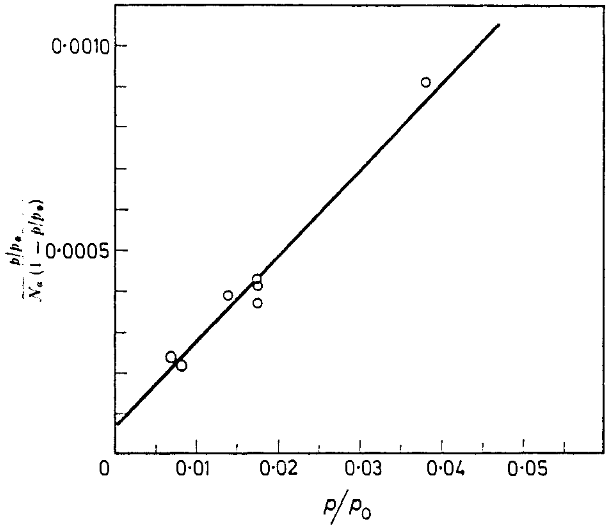

Figure 5. BET plot for nitrogen adsorbed at 77·4°K

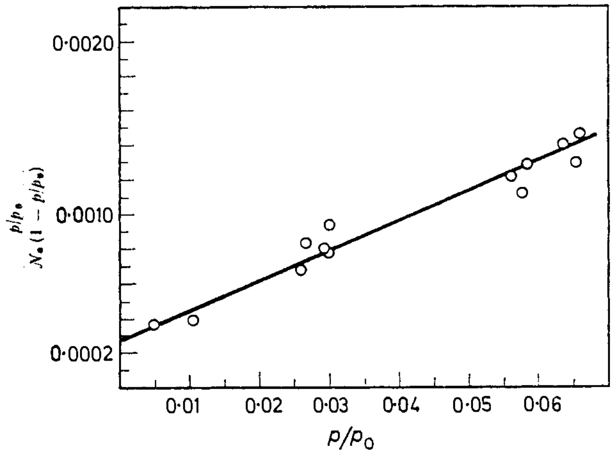

Figure 6. BET plot for argon adsorbed at 77·4°K

CONCLUDING REMARKS

Although the uncertainties that must be ascribed to the cross-sectional areas of adsorbed N_2, Ar, and Kr are not small, definite conclusions can be reached concerning the surface of pristine E-glass fibre. First the surface is not appreciably rough. A value for σN_2 less than 16·2Å^2 places the burden of proof on the investigator to demonstrate that the surface is not rough. A value greater than 16·2Å^2 could raise questions regarding the packing of nitrogen in the monolayer. In the present measurements, a linear BET plot for the pristine fibre is realized for values of p/p_0 less than 0·08. This is similar to the behaviour reported by MacIver and Emmett[6] for the adsorption of nitrogen on NaCl; the straight line drawn in the 0·01–0·07 region avoids the embarrassment of a negative intercept that would otherwise be obtained.

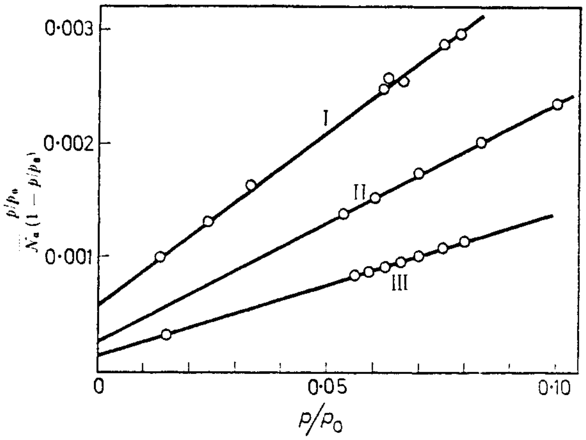

Figure 7. Influence of the roughness of E-glass fibre shown by change in the BET plots for krypton at 77·4°K

Second, the unique behaviour of pristine fibre is readily appreciated from the BET plots of *Figure 7.* These are based on the adsorption of krypton at 77·4°K and are concerned with three sequence operations on another sample (Series I) of E-glass fibre (15·88 g). I designates the plot for the pristine E-glass fibre. Subsequently, the container was removed and the sample contacted with distilled water. After 1 hour the water was withdrawn, and the container after drying in an air oven at 105°C was attached to the adsorption apparatus; II is the resultant plot for this water-treated sample. The container was again removed and the sample treated with hydrochloric acid (3 N) at 0°C for 1 h. After cold water washing to neutral pH, the container was dried and returned for another series of krypton adsorption measurements; III is the resulting BET plot. The corresponding values for the krypton monolayer coverage are 33, 46, 84 μmoles, respectively. Obviously, the surface of the pristine E-glass can be readily roughened by the relatively mild chemical treatment associated with the contact of distilled water. This was not found to take place with limited exposure to water vapour. In view of the short exposure of the pristine E-glass to water vapour in the environment during fibre drawing, it is probable that the pristine glass fibre is reasonably free of roughness due to this source.

On the basis of the deviation of the observed points from the least-square line in the BET plots, the uncertainty in the slope is least for krypton. A statistical analysis of all the results must await the completion of extended measurements with independent samples of E-glass fibre that are now in progress. The overall reproducibility of the krypton cross section is shown in *Table 3* for four different E-glass fibre samples.

It is gratifying that the results agree with accumulated experience for a variety of materials as recently summarized by McClellan and Harnsberger[7].

References

[1] R. B. Anderson and P. H. Emmett. *J. Applied Phys.* **19**, 367 (1948).
[2] S. J. Gregg and K. S. W. Sing. *Adsorption, Surface Area and Porosity,* Academic Press, London (1967), 371 pp.
[3] O. L. Anderson. *J. Applied Phys.* **29**, 9–12 (1958).
[4] S. Bateson. *J. Applied Phys.* **29**, 13–21 (1958).
[5] W. F. Thomas. *Phys. & Chem. Glasses* **1**, 4–18 (1960).
[6] D. S. MacIver and P. H. Emmett. *J. Phys. Chem.* **60**, 824 (1956).
[7] A. L. McClellan and H. F. Harnsberger. *J. Colloid & Interface Sci.* **23**, 577–99 (1967).

DISCUSSION

Dr. P. Bussière (*Institut de Recherches sur la Catalyse du C.N.R.S., Villeurbanne, France*) said: (i) Within what precision can you assume a perfect smoothness of the surface of your glass fibres? (ii) What saturation pressure do you take for krypton when given its cross sectional area?

Dr. V. R. Dietz replied: Electron microscope observations of the replica surface of pristine glass fibres, limited to an overall precision of 25 Å, showed no surface structure and we are, therefore, concerned with dimensions on an atomic scale.

At this level we do not consider pristine glass to be very rough for the following reasons: (i) It was prepared directly from the melt and the large surface tension at the instant of fibre formation most likely draws the molten glass into a cylindrical shape, (ii) there is an immediate response to chemical roughening of pristine glass by liquid water and dilute cold hydrochloric acid as shown by krypton adsorption, (iii) the adsorption of water vapour at 25°C and desorption with slow heating to 300°C does not change the krypton adsorption, (iv) quite reasonable values were obtained for the cross sectional areas of adsorbed Kr, N_2, and Ar.

While we believe that the geometrical surface of the pristine E glass is not very rough, the *composition* of the surface is rather indefinite. It is our belief that both geometrical and chemical descriptions of the surface are important. Current work indicates that both factors can be varied over wide ranges in the pretreatment of the glass fibre.

We use the equilibrium vapour pressure of solid Kr for reasons expressed in our reply to Dr J. M. Haynes.

E. Robens (*Battelle-Institut e.V., Frankfurt/Main, W. Germany*) said: I would like to report briefly on measurements of the molecular areas of some adsorbed gases [E. Robens, G. Sandstede, G. Walter. In *Vacuum Microbalance Techniques*, Vol. 8, A. W. Czanderna (ed.): New York: Plenum Press (1970)]. The sorption measurements were made using electromagnetic microbalances, following Gast. The quantity of monolayer sorbate was determined by the BET method. The area required by the molecules (σ) was determined by measuring isotherms both with the gas under investigation and with nitrogen at 77°K, assuming 16·2 Å^2 as the molecular area of nitrogen, or krypton at 90°K assuming 26·0 Å^2 as the molecular area of krypton.

For propane on PTFE at 0°C we obtained 34 Å^2, for neopentane on gold at 0°C 36 Å^2, for acetic acid on aluminium at 20°C a mean value of 23 Å^2, for oxygen on gold 11 Å^2 (oxidation), for acetic acid on oxidised gold 9 Å^2, for krypton on glass and aluminium at 77°K we found a mean value of 26 Å^2 (using the saturation pressure of the solid condensate).

We also compared the surface areas obtained by nitrogen adsorption (S_{BET}) of several samples with those determined geometrically (S_g). In the case of gold foils the BET surface was 13 per cent, in the case of aluminium foils 27 per cent larger than S_g. In the case of glass spheres, the BET value was only 5 per cent higher than the value obtained by microscopic grain size analysis. The results are summarized in *Table A*.

Table A. Results of surface area determination

Sorbent	*Dimensions*	S_g (m^2)	*Weight* (g)	*Sorbate*	*Temperature* (°K)	S_{BET} (m^2)	Å^2
Al foil	0·0100 m^2 × 20 μm	0·200	0·488	N_2 Kr	77·5 77·5	0·0226	28
Al foil	0·8170 m^2 × 1 μm	1·6340	1·981	N_2 CH_3COOH	77·5 292·2	2·07	23
Al powder			0·198	N_2 Kr	77·5 77·5	0·853	25·2
Au foil	0·1800 m^2 × 0·5 μm	0·3600	1·993	N_2 O_2 CH_3COOH	77·5	0·332*	11 9
Au powder (99·999 %)	80 % 0·05– 5 μm 20 % 6–10 μm		1·000	Kr 2,2-Dimethyl-propane	90·3 273	0·144	35·6
PTFE (Hostaflon TF 14)				N_2 Propane 2,2-Dimethyl-propane	77·5 273 273	2·03†	34·0
Glass spheres	20–60 μm	0·1105	1·826	N_2 Kr	77·5 77·5	0·1165	26·7

* Probably sintered during bake-out oxidation on the oxidized foil.
† Absorption.

Dr V. R. Dietz replied: The values reported by E. Robens demonstrate the importance of a full knowledge of sample preparation and sample origin. Aluminium foil or powder is oxide-covered to varying degrees and the large surface area of this type of alumina would greatly influence the measurements with foil and powder.

Gold foil and gold powder may or may not be free of base-metal oxides, but the possibility of introducing surface roughness in their preparation require additional information as to the source and experimental procedure.

Dr V. R. Dietz (*U.S. Naval Research Laboratory, Washington*) said: Haynes has pointed out [*J. Phys. Chem.* **66**, 182 (1962)] the influence of uncertainties in p_0 (the saturation vapour pressure of Kr) on the monolayer coverage calculated from the BET plot. The dependence on p_0 is obvious since the required slope $(c - 1)/v_m c$ and intercept $(1/v_m c)$ depend on $x = p/p_0$ in the BET equation $x/v(1 - x) = Ax + B$. Haynes assumes that there is a change in x given by $x' = \phi x$, where ϕ is a parameter and accordingly $\phi = p_0/p_0'$. We wish to comment on the physical reality of this postulate and to reject its use.

A physical adsorption process may be specified by the transition from one of the three states of Kr (1. gas, 2. liquid, 3. crystal) to the adsorbed state as indicated in *Figure A*. At 90·1°K or 77·4°K, both below the normal melting point of Kr 115·6°K, Haynes would use a greater p_0 than the equilibrium value. The original suggestion of P. H. Emmett [*J. Am. Chem. Soc.* **67**, 1555 (1945), footnote 11] was to use a value of p_0 given by extrapolating the liquid state to the lower temperature. This is equivalent to using the supercooled liquid as the reference level for the transition to the adsorbed state.

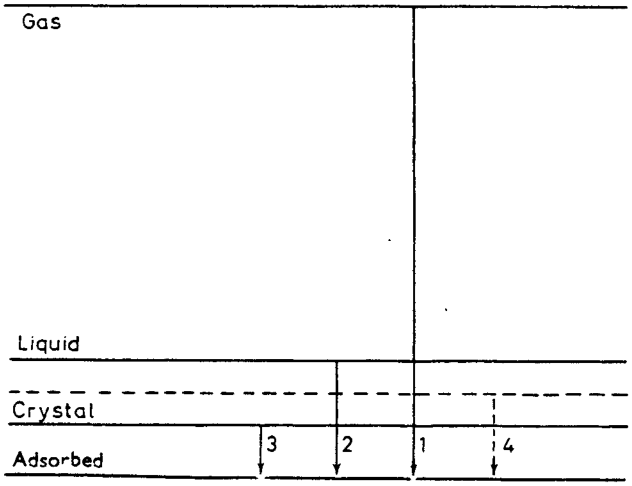

Figure A.

The assumption of Haynes in his definition of ϕ is equivalent to postulating superheated and supercooled levels (evaluated relative to the equilibrium vapour pressure) corresponding to the values of ϕ. This procedure is a bit arbitrary. It is more fundamental to consider that all of the change brought about by adsorption resides in the interaction of Kr with the surface. This is equivalent to the use of transitions 1, 2, or 3, these reference states being related among each other by the known heats of vaporization and fusion of Kr.

The cross-sectional area of adsorbed Kr is 20·2 Å^2 for a large number of surfaces, and this value is significantly different from that calculated from the density of the liquid or the solid. It appears to the writer to be more helpful to seek interpretations in terms of the strong polarizability of Kr and the surface atoms of the solid than it is to modify the reference level of non-adsorbed Kr by arbitrary changes in p_0.

Dr J. M. Haynes (*University of Bristol*) replied: It is important to recognize that *any* choice of the parameter ϕ (including the value unity) is arbitrary, because of the non-thermodynamic character of the Langmuir/BET approach. The suggestion that ϕ might be chosen not equal to unity was made for the utilitarian purpose of obtaining straight BET plots, in order to facilitate intercomparisons of the *empirical* BET parameter v_m. The idea that ϕ might have relevance to any real physical property of the adsorbate was explicitly excluded [*J. Phys. Chem.* **66**, 182 (1962)]; nevertheless, Guggenheim [*Applications of Statistical Mechanics*, Oxford University Press (1966), Chap. XI] has since given an interpretation which involves the spacing of adsorption sites in relation to interatomic spacings in the bulk liquid adsorbate.

COMPARISON OF DKR AND BET MONOLAYER VALUES

D. F. KLEMPERER

University of Bristol, Bristol, U.K.

Mr. J. C. Snaith and I have studied the adsorption of xenon over a wide range of relative pressures on various metal films prepared under ultra-high vacuum conditions. The low pressure data were analysed using the Dubinin–Kaganer–Radushkevich (DKR) method and data in the region of relative pressure equal to 0·01 to 0·35 were analysed by the BET method.

Table 1. Ratio of V_{m} values for adsorption of xenon at −196° Con evaporated metal films

	$\dfrac{V_{\mathrm{m}}\ \text{(DKR)}}{V_{\mathrm{m}}\ \text{(BET)}}$	BET *c* factor
Run 20 Cu/Na	0·87	53
	1·04	70
	0·74	15
Run 21 Na	1·11	105
	0·93	77
	0·70	30
Run 23 Fe/Na	1·13	3348
	1·16	493
	1·11	730
	0·99	141
	0·98	33
Run 24 Fe/Na	0·64	44
	0·73	30

	$\dfrac{V_{\mathrm{m}}\ \text{(DKR)}}{V_{\mathrm{m}}\ \text{(BET)}}$	BET *c* factor
Run 29 Fe/Na	1·30	−135
	1·10	582
	1·16	−192
	1·22	−187
	1·21	14 600
Run 37 Fe/Na	1·16	−369
	1·08	−740
	1·10	947
	1·10	532
	1·09	363
	1·00	176
	0·97	122

The ratios of V_{m} values extracted by these two methods are shown in *Table 1*, together with the corresponding BET *c* values. The average of the 25 ratios shown is 1·025 and, as has been remarked by other authors[1], it is certainly remarkable that such similar v_{m} values should come out of the two completely different models.

There is, however, a tendency for the ratio of v_{m} values to decrease with falling *c* value and this may reflect the influence of the *c* value on the relative pressure at which the monolayer is filled: we recall that the mathematical nature of the BET equation is such that as *c* falls, so higher relative pressures are needed to fill the monolayer and the equation must be applied in the vicinity of the point B if a monolayer value is to be extracted. It is, in fact well known that BET v_{m} values are sensitive to the range of relative pressure which is adopted. Ricca and Bellardo[2], for instance, found that the difference in v_m arising from two contiguous pressure ranges could amount to as much as 35 per cent.

In each of the runs tabulated, except Run 21, an increasing amount of sodium was presorbed. Pure sodium films were used in Run 21. Bearing in mind that the BET c value is also a rough guide to the value of E_1, the heat of adsorption in the first layer, it is interesting to notice that c shows a tendency to fall as the coverage of presorbed sodium rises. Runs 20 and 23 show this effect clearly. No experimental values of the isosteric or the calorimetric heat of adsorption on sodium are available, but it is possible to estimate the isosteric heat from the slope of the DKR plot. As sodium is presorbed in increasing amounts, so the slope does, in fact rise, corresponding to a falling heat. We evaluate a heat of adsorption on pure sodium which is about 1 kcal mol^{-1} less than the value obtained on iron.

On the other hand, the effect may be connected with the progressive and large fall in apparent area which we have observed as sodium is presorbed. The main effect of sodium could therefore be to smooth over the most active high-heat sites. The v_m ratio is anyway known to fall as iron films are sintered[3].

In a broader context, it would be nice to be able to deduce v_m values from isotherms without recourse to any mathematical analysis, and without looking for a point B or a kink in surface potential plots[4]. With this goal in mind, Mr. P. A. Williams and I have made some preliminary experiments using a xenon titration method, which is due to Singleton and Halsey[5].

Following this method, xenon was presorbed on an evaporated iron film in steadily increasing amounts. After each addition, a krypton isotherm was

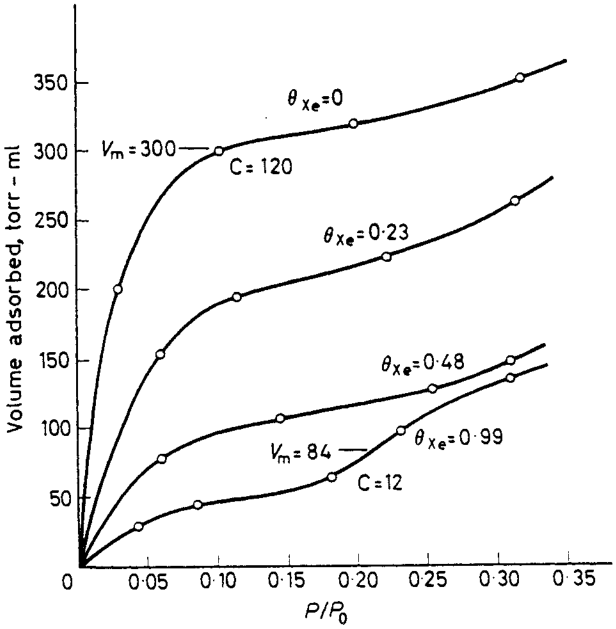

Figure 1. Krypton isotherms on evaporated iron film at −196°C.

recorded. When the amount of presorbed xenon is just equal to the monolayer volume, then the initial knee in the krypton isotherm should finally disappear.

Figure 1 shows what happens. The initial knee does, in fact, fall away as xenon is presorbed and the BET c value falls steadily, demonstrating the tendency for a classical type III isotherm, without a knee, to be approached. In these runs, the BET v_m value for krypton is also falling. Presumably this is the result of presorbed xenon filling up some of the internal film structure—these films had a roughness factor of about 50. The isotherms bring to mind those shown by Professor Gregg in an earlier contribution to this discussion. This effect should not, however, influence the viability of the titration method which is based on xenon molecules forming the first adsorbed layer.

References

[1] Y. Delaunois, A. Frennet and G. Lienard. *Disc. Far. Soc.* **41,** 114 (1966); *J. Chim. Phys.* **63,** 906 (1966).
[2] F. Ricca and A. Bellardo. *Z. phys. Chem. N.F.* **52,** 318 (1967).
[3] A. Granville and P. G. Hall. *J. Chem. Soc. A*, 64 (1968).
[4] J. Pritchard. *Nature* **194,** 38 (1962).
[5] J. H. Singleton and G. D. Halsey. *J. Phys. Chem.* **58,** 330 (1954).

COMPARISON OF MONOLAYER CAPACITIES FROM BET AND DUBININ–KAGANER–RADUSHKEVICH (DKR) ISOTHERMS

B. A. Gottwald

Technische Universität, Hannover, Germany

A fundamental problem in surface area determination from adsorption data is the determination of monolayer capacities in terms of different adsorption models and their comparison. Such a comparison can be carried out conveniently by considering the slope α of double-logarithmic plots of the adsorption isotherms (v or θ vs. p or p/p_S) and its dependence on surface coverage[1].

For the DKR-isotherm

$$\log \theta_{\mathrm{DKR}} = -D.\,[\log (p/p_S)]^2 \qquad (1)$$

a plot of $\alpha/\sqrt{D}$ vs. degree of coverage θ_{DKR}, both in logarithmic scale, is shown in *Figure 1*. Moreover *Figure 1* shows a plot of α vs. amount adsorbed

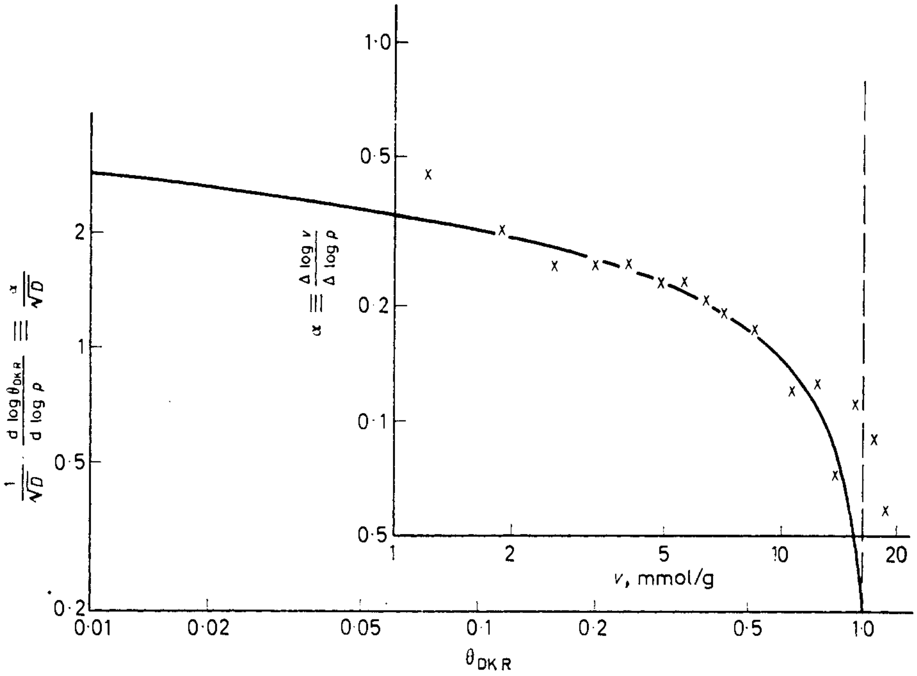

Figure 1. Comparison of DKR-model [(solid line) ($\alpha/\sqrt{D}$ vs. θ_{DKR})] with experimental data [(X) (α vs. v)]

v, calculated from the data of Kaganer[2] for the adsorption of nitrogen on coconut charcoal at 77·6°K; this is a typical experimental result. On comparing the experimentally observed data with the DKR-model, v is related to θ_{DKR} through the monolayer capacity v_{mDKR}, which appears graphically as a scale factor for the abscissa axis. Similarly $\sqrt{D}$ is a scale factor for the ordinate axis. Both scale factors can be determined when the double-logarithmic plots of the experimental data and the DKR-model are brought into coincidence, as shown in *Figure 1*. This comparison gives a value of about 16 mmol/g for the DKR monolayer capacity.

Figure 2 shows a plot of α vs. degree of coverage θ_{BET} for the BET-isotherm

$$\theta_{\mathrm{BET}} = \frac{C \, . \, p/p_{\mathrm{s}}}{(1 - p/p_{\mathrm{s}}) \, . \, [1 + (C - 1) \, . \, p/p_{\mathrm{s}}]} \tag{2}$$

for several values of the constant C. This family of curves is brought into coincidence with the experimental data which gives a value of about 16 mmol/g for the BET monolayer capacity, a value in agreement with the DKR monolayer capacity.

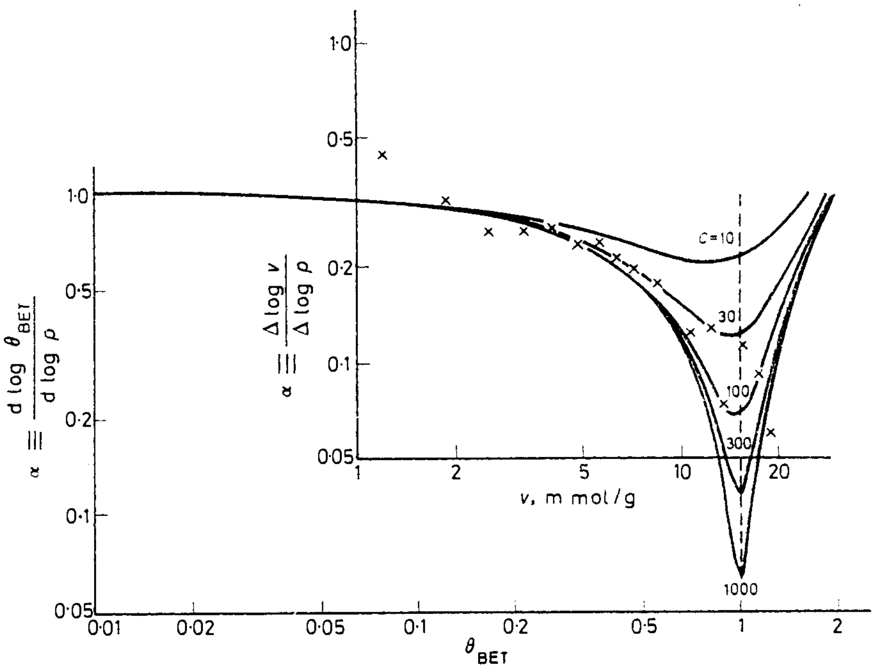

Figure 2. Comparison of BET-model [(solid line) (α vs. θ_{BET})] with experimental data [(X) (α vs. v)]

This close correspondence of the monolayer capacities was first reported by Kaganer and has since been frequently described in the literature. A comparison of the models shows that when the DKR-curve and the family of BET-curves are brought into coincidence, the scale factor for the abscissa is almost equal to unity for C-values between approximately 30 and 300 and coverages between 0·1 and 0·6. Thus the superposition of experimental data with double-logarithmic plots of a vs. degree of coverage in terms of either model, must necessarily, give almost identical monolayer capacities.

It is the purpose of this brief contribution to show that the close correspondence between the BET and DKR monolayer capacities is caused merely by the mathematical form of equations (1) and (2) and its underlying models and has otherwise no further significance.

References

[1] B. A. Gottwald and R. Haul. *Proc. 4th Int. Vacuum Congr.*, Manchester (1968) 96–100.
[2] M. G. Kaganer. *Zhur. Fiz. Khim.* **33**, 2202–2210 (1959).

SURFACE AREAS OF POROUS SOLIDS

STEPHEN BRUNAUER

Institute of Colloid and Surface Science and Department of Chemistry, Clarkson College of Technology, Potsdam, New York, U.S.A.

Examples are cited to show that the BET method, with nitrogen or other adsorbates, can give reliable surface area values for porous solids which contain no micropores (pores less than 16–20 Å in width). On this point there is general agreement among surface chemists working in the field. Examples are also cited to show that the BET method, with nitrogen, water vapour, or other adsorbates, can give reliable surface area values for porous solids which contain micropores. This conclusion is in opposition to the present concensus of opinion.

INTRODUCTION

This paper is not intended to be a review of the subject. A detailed and very good review is found in a recent book of Gregg and Sing[1]. My manifold activities have prevented me even from reviewing the complete literature of the less than two years that have elapsed since the appearance of the book; consequently, my discussion is partly concerned with the contributions which, together with my coworkers and students, I have made to the field in the last two years, and partly with other work, old and new, that I consider pertinent to the subject.

SOLIDS WITHOUT MICROPORES

1. In the BET paper[2], two equations were proposed by the authors: a two-parameter equation for adsorption on a free surface, and a three-parameter equation for adsorption in a parallel-plate pore. The former equation has become known as *the* BET equation, and I will follow the customary usage. However, the three-parameter equation will also play a role in this paper.

Dubinin classified the pores into three groups: micropores, having widths or radii less than 15–20 Å; macropores, having widths or radii greater than 200–1000 Å; and transition pores, in the intermediate size range. On the basis of the broad experience he has gathered in four decades of research on adsorption, he has come to the conclusion that the BET equation gives the correct surface area, with nitrogen as the adsorbate, for porous solids which contain no micropores. A similar conclusion was reached by Gregg and Sing[1] and on the basis of my own experience, I also concur in this conclusion. The differences in view will come in the discussion of solids which contain micropores.

The surface areas obtained from v_m values of nitrogen adsorption isotherms, using 16·2 Å^2 for the area occupied by a nitrogen molecule, have received numerous confirmations for nonporous solids, among which perhaps the agreements with electron microscopic results are the most striking. It is obvious from the form of the BET equation, that a linear plot can only be obtained if c is constant in the so-called BET region; i.e., between $\theta = 0{\cdot}5$ and $1{\cdot}5$; and tens of thousands of linear BET plots give some indication that c is actually constant. This, in turn, means that the free energy of adsorption is constant. As the statistical number of adsorbed layers increases from 0·5 to 1·5, the heat of adsorption decreases, but the entropy increase just balances this effect. Because of the highly nonspecific nature of nitrogen adsorption, this happens to be true for practically all adsorbents.

2. The correctness of the BET surface for porous adsorbents has no such obvious confirmation as that for non-porous adsorbents. In our early research, the confirmation we could offer was the agreement between surface area values obtained by using different adsorbates for the same adsorbent. Good agreements were obtained when the molecules did not differ greatly in size (e.g., N_2, O_2, Ar, CO and CO_2), but butane gave smaller areas than the others. This could easily be explained by the assumption that the area covered by a butane molecule was larger than what we had calculated from the liquid density assuming spherical molecules, or by assuming that butane could not penetrate into the smallest pores, or by both of these effects. Even so, the agreement between surface area values obtained with different adsorbates can be considered only a necessary but not a sufficient proof of the correctness of the BET surface.

A theoretical contribution to the subject came from the three-parameter BET equation. This equation contains a third parameter, n, which is the maximum number of layers that can be adsorbed on one wall of a parallel-plate pore. The three-parameter equation, for $n > 3$, gives results indistinguishable from the two-parameter equation in the BET region of the isotherm, i.e., for p/p_0 values between 0·05 and 0·35. Pickett[3] derived a simpler equation for adsorption in a parallel-plate pore; this equation also reduces to the BET equation in the BET region. The result is reasonable; if the pores are sufficiently wide, the adsorption is similar to adsorption on a free surface. The dividing line is approximately $n = 3$; which is a 21 Å wide pore for nitrogen. (If adsorbed nitrogen is assumed to be a film of hexagonally close packed spheres, the thickness of one layer is 3·5 Å.) Actually, for $n = 3$, the BET equation gives approximately 3 per cent smaller surface than the three-parameter equation, as was shown by Joyner, Weinberger, and Montgomery[4].

3. Further important contributions to the problem came from pore structure analysis. Wheeler[5] introduced the method of analysis based on nitrogen isotherms in 1945, and numerous modifications of the method have been advanced in the subsequent years. The analysis is performed on the desorption or the adsorption branch of the hysteresis loop, which is the region in which multilayer adsorption is augmented by capillary condensation. It is assumed that all pores in the adsorbent are either cylindrical or that all pores are parallel plates, and the Kelvin equation is used to calculate a radius or a width at each relative pressure. The Kelvin equation is

$$RT \ln \frac{p}{p_0} = -\frac{2\gamma V}{r_k} \qquad (1)$$

where γ and V are the surface tension and molar volume of the adsorbate, assumed to be the same as those of the liquid, and r_k is either the radius of the cylinder or the distance between the parallel plates corresponding to the relative pressure p/p_0.

Because the adsorbent has a multilayer of adsorbed film on its pore walls, the r_k value in Eq. (1) does not represent the radius of the pore, but the radius of that part of the pore in which capillary condensation or evaporation takes place. I have called this the *core* of the pore. In order to obtain the radius of the pore, the thickness of the adsorbed film, t, must be added to the pore radius. (If the parallel-plate idealization is used, the pore width is $r_k + 2t$.) The values of t are obtained from a so-called t-curve, which is a plot of the statistical thickness of the adsorbed film vs. p/p_0 for non-porous adsorbents. A variety of such t-curves for nitrogen are available in the literature. Shull[6] was the first to determine a t-curve; he used a number of non-porous adsorbents and plotted an average curve for almost the entire relative pressure range. The t-curves of different investigators differ from each other, depending on the group of adsorbents used for their determinations; if one group of adsorbents has higher heats of adsorption than another, the t-curve will indicate a thicker film at the same relative pressure. In the analysis one should use that t-curve which corresponds to the heat of adsorption of the adsorbent to be analyzed. Nevertheless, the choice of the correct t-curve is not critical, partly because the t-curves do not differ from each other greatly, and partly because the t-values constitute only a part of the pore radius. The situation is quite different in micropore analysis, as will be seen later.

The analysis consists in determining the pore volumes and pore surfaces of groups of pores that have radii between $r + \Delta r$. Volume and surface values are then summed up, and the cumulative pore volume and cumulative pore surface can be compared with the 'total' pore volume (obtained from the adsorption at a pressure close to p_0) and with the BET surface. I put the word 'total' in quotes, because the Kelvin radius at p_0 is infinite; consequently, the analysis starts or ends at a relative pressure less than p_0. Thus, the largest pores are left out of consideration, which fact introduces probably a negligible error into the cumulative pore surface, but may introduce a sizeable error into the cumulative pore volume. The analyses based on the adsorption and on the desorption branches of the nitrogen isotherms, of course, give different results. Because the desorption values are higher than the adsorption values (except at the two ends of the hysteresis loop), the cumulative volume and surface are also higher.

Cranston and Inkley[7], using the cylindrical idealization and their own t-curve, analyzed 14 porous adsorbents both on the basis of the adsorption and desorption branches of nitrogen isotherms. The highest point of the isotherms used in the analysis was at $p/p_0 = 0{\cdot}931$. For the adsorption branch the cumulative pore volume values ranged from 89 to 106 per cent of the 'total' pore volume; for the desorption branch from 89 to 113 per cent. For the adsorption branch, the cumulative pore surface values ranged from 86 to 126 per cent of the BET surface; for the desorption branch from 86 to 157 per cent.

Practically all investigators have used the agreement between the cumulative pore surface and the BET surface as the criterion of the correctness of their pore structure analysis. A criterion was badly needed, because in many instances true capillary condensation equilibrium is not reached either on the adsorption side or on the desorption side or on both sides[8]. In addition, (a) the idealizations are bound to give erroneous values for the pore surfaces, and (b) the micropores and the largest pores are left out of consideration. Under such circumstances, the type of agreement cited above may be considered a semi-quantitative mutual confirmation of the correctness of the pore structure analysis and of the BET surface for porous solids.

4. Important further advances have been made in the last few years. In the first place, Lippens and de Boer[9] developed a method for separating micropores from wider pores; thus, we can now test whether an adsorbent contains micropores. There is no capillary condensation in micropores; so the capillary condensation method can perform a complete analysis only for adsorbents which contain no micropores. In the second place, the present writer and his coworkers have developed a more rational approach to pore structure analysis in the capillary condensation region[10].

The precursor of our method of pore structure analysis was a method that Kiselev[11] developed for the determination of the surface areas of porous solids. By thermodynamic reasoning he derived a general equation for capillary condensation, which is valid for pores of any shape. The equation, when solved for the surface area within the pores, is

$$s = \frac{1}{\gamma} \int_{a_{\mathrm{H}}}^{a_{\mathrm{s}}} - RT \ln \frac{p}{p_0} \, da \tag{2}$$

where γ is the surface tension of the adsorbate, considered as liquid, a_{H} is the number of moles adsorbed at the beginning of the hysteresis loop, and a_{s} is the number of moles adsorbed at p_0. Graphical integration of Eq. (2) gives the surface. However, s gives the surface area of the *cores* of the pores, and not of the pores, and so the method is applicable only if the pores are so wide that the thickness of the adsorbed film on the walls can be neglected. The external surface is also neglected, but this seldom introduces an appreciable error for porous solids.

Kiselev employed his method successfully for the determination of the surface areas of a number of adsorbents possessing wide pores. For example, for a silica gel seven adsorbates gave a mean surface area of 298 m^2/g, and the largest deviation from the mean was 10 per cent. The nitrogen BET area for this silica gel was 315 m^2/g. The Kiselev area is smaller than the BET area, as it should be, because the core areas are smaller than the pore areas, except for parallel-plate pores. For a group of six adsorbents he obtained areas that were 1 to 18 per cent lower than the BET areas. However, for two very narrow pore adsorbents he obtained areas with three different adsorbates that ranged from 7 to 57 per cent of the BET areas.

5. Whereas Kiselev's method has limited applicability for the determination of total surface areas, Eq. (2) has no such limitation for determining the core surface area of a group of pores. For example, if we perform a pore structure analysis using a nitrogen desorption isotherm, we can determine the area of the cores of the largest pore group by integrating Eq. (2) from

a_s to $a_{0 \cdot 95}$, where the latter quantity is the number of moles adsorbed at $p/p_0 = 0{\cdot}95$. There is no need here to go into all the details of our method of pore structure analysis. Suffice it to say, that we can obtain the surface areas of all the groups of cores by this method. The volumes of the core groups are obtained from the isotherm, just as in the older methods. The volume divided by the surface gives the hydraulic radius of the core group. In our method, the distribution of the surfaces and volumes of the cores (and of the pores) is made in terms of hydraulic radii and not Kelvin radii.

I called this method 'modelless', by which I meant that no idealized pore shape was assumed when the analysis was made in terms of the cores. The method in this modelless form may be well suited for many practical uses; it is especially suitable for comparing similar adsorbents and catalysts in industrial operations. However, if we want to convert the core parameters into pore parameters, by using an appropriate t-curve for the thickness of the multilayer film, a model must be assumed. A cylindrical model will give a different structure curve from a parallel-plate model[10] or from a spherical pore model.

If the 'modelless' method winds up with cylindrical or parallel-plate pores, why should we not use these idealizations right from the start, as in the older methods? There is a simple answer to this. The older idealizations used only *one* experimental value obtained from the isotherm, the volume of the core group (the volume adsorbed or desorbed between two relative pressures), but the hydraulic radius and the surface of the core group were hypothetical; whereas the new method is based on *two* values obtained from the isotherm, the volume and the surface of the core group, which automatically gives the third core parameter, the hydraulic radius.

If one has only one experimental core parameter, one can go very far wrong in calculating the two others. For example, if a pore has a narrow entrance and a wide body, the Kelvin radius will be that of the entrance and the calculated pore surface will be much larger than the actual surface if the desorption branch of the isotherm is used. (Almost all investigators use the desorption branch.) On the other hand, when one has the values for *all three* core parameters, one cannot go too far wrong in calculating the pore parameters, regardless whether parallel-plate, cylindrical or spherical pore shape is assumed[8].

In a paper published in 1968[12], we discussed among other things the analyses of two silica gels, which contain no micropores. The test for micropores was made by the Lippens-de Boer method[9]. The cumulative pore surface and pore volume, obtained by our new method, were in excellent agreement with the BET surface and the total pore volume. This time the word *total* is not in quotes, because if the analysis is made in terms of hydraulic radii, one can go up to p_0[10]. We have made many analyses since which are not published as yet, and the results are very satisfactory.

One other interesting and as yet unpublished result may be mentioned here. We analyzed the pore structures of the same two silica gels also by water vapour adsorption. The BET surface areas obtained by water vapour were roughly one half as large as those obtained by nitrogen. The reason for this is, in our interpretation, that about half of the silica surface is hydrophobic, and the adsorption of water vapour on this part of the surface in the BET region of the isotherm is small, possibly negligible. However, the pore structure analysis by water vapour in the capillary condensation region gave a cumulative surface in excellent agreement with the *nitrogen* BET surface.

The results obtained from pore structure analysis present a strong mutual confirmation of both the BET nitrogen surface and the method of analysis. The parts of the isotherm used in the two methods are different, and the principles on which the determinations are based are also entirely different. Thus, I come back to the conclusion with which I started—the BET method, with nitrogen as the adsorbate, *usually* gives reliable surface area values for porous adsorbents which contain no micropores.

SOLIDS WITH MICROPORES

1. Naturally, if a molecule cannot penetrate into a pore, we cannot measure the surface area of the pore with it. I used the word 'usually' in the previous paragraph, because I know of one case, where nitrogen was unable to penetrate even into pores that were considerably larger than micropores. The total porosity of hardened portland cement paste, the product of the chemical reaction between portland cement and water, increases when the weight of water mixed with unit weight of cement increases. We hydrated a cement paste, with a water–cement ratio of 0·7, and after complete hydration we measured the total pore volume and the BET surface both by water vapour adsorption and nitrogen adsorption. The water surface was 200 m^2/g, the nitrogen surface was 136 m^2/g, the water porosity was 0·401 ml./g, the nitrogen porosity was 0·276 ml./g. From these data, I calculated that the hydraulic radius of the pore system accessible to water (which is the total pore system, as we shall see) was 20·1 Å, that of the pore system accessible to nitrogen was 19·8 Å, and that of the pore system inaccessible to nitrogen was 20·8 Å[13].

It is interesting to note that the hydraulic radius of the pore system inaccessible to nitrogen was greater than that of the pore system accessible to nitrogen. A hydraulic radius of 20·8 Å means that the average width of the pores inaccessible to nitrogen was 41·6 Å if we visualize the pores as parallel plates, or the average radius was 41·6 Å if we assume cylindrical pores. The explanation of the above results is that many of the larger pores have narrow entrances; the entrances are either too small to admit nitrogen molecules, or nitrogen molecules are so strongly adsorbed in the constrictions that they prevent other nitrogen molecules from entering. I discount the 'activated entry' explanation[1], because no increase in adsorption could be noticed between 15 min and 15 h or longer times.

Hopefully, such examples are rare, and nitrogen can enter the total pore systems of most adsorbents that contain no micropores. I will cite examples later which show that nitrogen can correctly measure the surfaces of some adsorbents which contain only micropores or both micropores and wider pores. But let us stay now with hydrated portland cement. The BET surface area obtained by water vapour was confirmed by small angle x-ray scattering, and by calculation of the surface from x-ray diffraction data. (These two methods are completely independent.) Thus, the water vapour BET surface measures the total surface area; consequently, the uptake at p_0 measures the total porosity. The important additional information is that the cement pastes have a large number of micropores, and in fact, if the porosity is low, by far the greatest part of the surface is in micropores. Another hardened cement paste, which was made from the same cement as the paste I discussed above, but with the much lower water–cement ratio of 0·35, had a surface area of 208 m^2/g as measured by water vapour adsorption, but only 57 m^2/g by nitrogen adsorption. The total porosity by water was 0·126 ml/g, by nitrogen it was 0·075 ml/g. The hydraulic radius of the total pore system, measured by water vapour, was 6·1 Å; that of the pore system accessible to nitrogen was 13·2 Å, and that of the pore system inaccessible to nitrogen was 3·4 Å. Here we are very much in the micropore region, yet the water surface area was very nearly the same as that of the paste containing much larger pores. Thus, for these hydrophilic surfaces, and probably other, possibly all hydrophilic surfaces, correct surface areas can be obtained by the BET method using water vapour as the adsorbate even if the pore system contains predominantly or solely micropores.

2. The isotherms of solids which contain *only* micropores usually look like Type I or Langmuir type isotherms. It has been frequently pointed out that these isotherms are not really Langmuir type isotherms, and they do not represent monolayer adsorption. For example, occasionally the plateau of the isotherm leads to an absurdly high surface area value[1]. It is seldom, if ever, pointed out that what looks like a Langmuir isotherm may actually be a Langmuir isotherm. An example of this is a charcoal, for which we obtained perfect straight line plots, using the Langmuir equation, for six gases: N_2, Ar, O_2, CO, CO_2 and C_4H_{10} (n-butane)[14]. The average surface area obtained on the basis of the first five gases was 840 m^2/g, and the maximum deviation from the average was 6·4 per cent. I did not bother with calculating the Gurwitsch volumes from the plateaus of the isotherms in the subsequent 32 years, but I did it for this paper. If we assume that the plateaus represent not monolayers but filling of the pores with liquids, the average for the five gases is 0·273 ml/g and the maximum deviation from the average is 14·3 per cent. This, in itself, means something, but the most interesting item was the butane result. Calculated as surface, the butane value was 25 per cent lower than the average of the five other gases, which is not unreasonable, as I discussed earlier in this paper. However, calculated as pore volume, the butane result was 16·5 per cent *higher* than the average, and 6·4 per cent higher than the next highest value, that obtained for oxygen. There was no evidence of the 'activated entry' effect in this work. The *smallest* pore volume was obtained for carbon dioxide, the largest for butane, and the four others were between them. Nitrogen at $-195{\cdot}8°C$ and at $-183°C$ gave identical surface area values (not identical v_m values).

On the basis of the above examples we can conclude that it is possible to obtain reliable surface area values for solids containing micropores. Further evidence will be cited from two other lines of approach, entirely different from the previous ones and from each other.

3. Recently, together with my coworkers, I have developed a method for determining the pore volume and pore surface distributions of micropores[15]. I have called this the micropore analysis method or 'MP-method'; it is based on ideas developed by de Boer and his coworkers[9].

As I stated earlier, a *t*-curve is a plot of the statistical thickness of the adsorbed film vs. p/p_0, obtained for non-porous adsorbents. The statistical thickness is defined as

$$t = 10^4 v_l / S_{\mathrm{BET}} \qquad (3)$$

where v_l is the volume adsorbed *as liquid* in ml/g, and S_{BET} is the BET surface area of the adsorbent in m^2/g. With these units, t is obtained in Angstroms. In all pore structure analyses it is assumed that the thickness of the adsorbed film at any relative pressure is the same in the pores as on non-porous adsorbents.

Any isotherm for a non-porous solid can be converted into a straight line plot according to Eq. (3). For a given point on the isotherm, the volume or weight adsorbed is converted into v_l by assuming that the density of the adsorbate is the same as the density of the liquid. The t-value for the corresponding p/p_0 is read from the t-curve, and v_l is plotted against t. Furthermore, even in pores the amounts adsorbed at low pressures should be in agreement with the amounts adsorbed on a free surface, except when the width of the pore approaches the diameter of a molecule (3·5 Å for nitrogen). The v_l–t plot should, therefore, be a straight line even for most porous solids in the low pressure region. The slope of the line gives the surface area of the adsorbent, and it is designated S_t.

When some of the narrow pores are filled up by multilayer adsorption, further adsorption does not occur on the entire surface because a part of the surface has become unavailable. The points of the v_l–t plot then begin to deviate downward from the straight line. This fact was used by de Boer and his coworkers to separate the pore system into narrow and wide pores, and it enabled them to calculate the surface areas and volumes of the totality of narrow pores and the totality of wide pores. They called their method t-method, and the MP-method is an extension of the t-method. In the MP-method, the downward deviations from the v_l–t plot are used to evaluate the pore volume and pore surface distributions of micropores.

I will not go into the details of the method; those interested can read the original paper[15]. Some points, however, need mentioning here. (1) In the analysis the lower part of the isotherm is used, from about $p/p_0 = 0{\cdot}1$ to 0·5. (2) The pores are idealized as parallel plates; however, it is shown in the paper that the cylindrical idealization would give the same results for the surface, volume and hydraulic radius of each pore group. (3) Whereas in the capillary condensation methods of analysis the t-values appear as correction terms only, in the MP-method the t-values determine the entire volume of a pore group. (4) It is, therefore, vitally important that the correct t-curve be used for the analysis.

The correct t-curve is not a t-curve determined for adsorbents which are chemically similar to the adsorbent to be analyzed, but a t-curve which is based on adsorbents that have approximately the same heats of adsorption as the adsorbent to be analyzed. The BET c constant is frequently adequate for testing the appropriateness of the t-curve. The c constant of a silica gel may be the same as that of a certain carbon black, whereas one carbon black may have an order of magnitude greater c constant than another. Because it is difficult to determine large c constants accurately, a more reliable test is the agreement between S_{BET} and S_t. If the wrong t-curve is used, S_t may be larger or smaller than S_{BET}[15].

4. By the MP-method we have analyzed a silica gel, Davidson 03, which contains only micropores. The nitrogen isotherm looks like a Langmuir isotherm, but it is a pseudo-Langmuir isotherm. The BET plot gave a surface area of 793 m^2/g and S_t was 792 m^2/g, showing that the correct *t*-curve was used. (Such close agreement is naturally very rare.)

When an adsorbent contains only micropores, the nature of the method of analysis is such that the cumulative pore surface is bound to agree with S_t within experimental error. Because S_{BET} is equal to S_t, the agreement between cumulative pore surface and BET surface cannot be considered a mutual confirmation. However, the agreement between cumulative pore volume and total pore volume can be used as a criterion of the correctness of the pore structure analysis. The cumulative pore volume was 0·409 ml./g, and the total pore volume was 0·403 ml./g. In the analysis, the volume of each pore group is calculated from the surface and the hydraulic radius of the same pore group; consequently, correct volumes can be obtained only if the surfaces are correct. Thus, the correctness of the cumulative pore volume indicates that the BET surface area was correct for this adsorbent. The pores of greatest frequency had a width of 9·2 Å, and the largest pores had a width of 16 Å.

The same silica gel was analyzed also by water vapour adsorption, but the results are unpublished as yet. Water vapour, like nitrogen, gave a pseudo-Langmuir isotherm. The cumulative pore surface was 794 m^2/g, the cumulative pore volume was 0·410 ml./g, and the pores of greatest frequency were at 8·4 Å. (There is obviously no 'activated entry' here.)

5. We next analyzed by nitrogen isotherms the pore structures of two silica gels which contained both micropores and larger pores. The MP-method was used for the micropore analysis, and the 'modelless' method for the wider pores. The isotherm of Mallinckrodt's Special Bulky silicic acid was Type II. This gel had almost 90 per cent of its total surface but only 19 per cent of its total pore volume in micropores. The cumulative pore volume and the cumulative pore surface (including micropores and wider pores) differed from the total pore volume and the BET surface by less than 1 per cent. The other silica gel, Mallinckrodt's Standard Luminescent grade silicic acid, had a Type IV nitrogen isotherm; in this gel 75 per cent of the total surface and 31 per cent of the total pore volume was in micropores. The results of the analysis were almost as good as for the other gel. The results obtained with water vapour were in agreement with the nitrogen results.

On the basis of the analyses of the three silica gels which contain micropores, we can conclude that the results confirm both the BET surface area values and the methods of pore structure analysis.

6. Kaganer[16] has developed a theoretical approach, very different from the BET method, for the determination of specific surface areas of adsorbents. Furthermore, the method is applicable at very low relative pressures, orders of magnitude below the BET region. The surface area values obtained by him for silica gels, charcoals and aluminas by nitrogen, argon and krypton adsorption were within 3 per cent of the values obtained by the BET method. Armstrong and Hobson[17] tested the Kaganer method using pyrex glass specimens of known surface areas, with nitrogen at −195°C as the adsorbate.

The results they considered their best ones confirmed the Kaganer surface areas.

The question here is not whether the Kaganer theory or the BET theory is right. As far as I can see, the two theories are not mutually exclusive; both are approximations, and both may be right as far as they go. The important fact is that two very different methods lead to the same surface area values for adsorbents which contain micropores. I consider this a strong mutual confirmation of the reliability of the surface area values obtained for micropores.

7. Gregg and Sing[1] point out the well-known fact that the heats of adsorption in very narrow pores are higher than on a free surface, because the adsorbate is attracted to more than one surface. They argue that the increased adsorption should give too high v_m values, and they conclude that the BET equation is of doubtful validity for microporous adsorbents. I also shared this view until I found out that the BET method was valid for microporous adsorbents. After I found this out, it was not difficult to find the reason for the validity of the method.

There is an effect which works in the opposite direction from the one brought up by Gregg and Sing. Joyner, Weinberger and Montgomery[4] compared the v_m values obtained by the customary two-parameter BET equation and the three-parameter BET equation for values of n less than 4·5, using a c constant of 100. The c constant for nitrogen at $-195{\cdot}8^\circ$C is close to 100 for many adsorbents. I mentioned already that for $n = 3$ the BET equation gives a v_m value which is 3 per cent smaller than the three-parameter v_m value. For $n = 1{\cdot}4$, the BET v_m is 20 per cent smaller than the three-parameter value. Thus, as we go to narrower and narrower pores, the BET equation gives lower and lower v_m values, *provided* that the heat of adsorption remains the same as on a free surface. This is implied in assuming the same c constant for all of the calculations. However, the heat of adsorption does not remain the same; it increases as we go to narrower pores. The two effects may partly or wholly compensate for each other.

In the examples I have brought up in this paper to support the validity of the BET surface areas for adsorbents which contain micropores, the compensation appears nearly perfect. I do not claim that in every single case such a perfect compensation will occur, but I hope and expect that we will find similar situations in many instances, especially when nitrogen is used as the adsorbate. At the beginning of this paper I pointed out the remarkably accurate compensation of enthalpy by entropy as evidenced by the constancy of c in the BET region. This seems to happen for practically all adsorbents when nitrogen is used as the adsorbate. I have attributed this to the highly non-specific nature of nitrogen adsorption. This highly non-specific adsorption may manifest itself also in frequent occurrence of the compensation discussed in the previous paragraph.

Naturally, if nitrogen cannot penetrate into a pore, it cannot measure the surface of the pore. The smaller water molecules may be able to penetrate into the pores in this case, and if the surface is hydrophilic, reliable surface values can be obtained for micropores. If the pores are so small that even water molecules cannot penetrate into them, for most practical purposes they do not exist.

ACKNOWLEDGEMENTS

The author gratefully acknowledges his indebtedness to the National Science Foundation for Grant GP–7746, which is supporting the work on which this paper is based.

References

[1] S. J. Gregg and K. S. W. Sing. *Adsorption, Surface Area and Porosity*. Academic Press, London and New York (1967).
[2] S. Brunauer, P. H. Emmett and E. Teller. *J. Am. Chem. Soc.* **60**, 309 (1968).
[3] G. Pickett. *J. Am. Chem. Soc.* **67**, 1958 (1945).
[4] L. G. Joyner, E. B. Weinberger and C. W. Montgomery. *J. Am. Chem. Soc.* **67**, 2182 (1945).
[5] A. Wheeler. *Advan. Catalysis* **3**, 250 (1951).
[6] C. G. Shull. *J. Am. Chem. Soc.* **70**, 1405 (1948).
[7] R. W. Cranston and F. A. Inkley. *Advan. Catalysis* **9**, 143 (1957).
[8] S. Brunauer, R. Sh. Mikhail and E. E. Bodor. *J. Colloid and Interface Sci.* **25**, 353 (1967).
[9] B. C. Lippens and J. H. de Boer. *J. Catalysis* **4**, 319 (1965).
[10] S. Brunauer, R. Sh. Mikhail and E. E. Bodor. *J. Colloid and Interface Sci.* **24**, 451 (1967).
[11] A. V. Kiselev. *Usp. Khim.* (in Russian), **14**, 367 (1945).
[12] R. Sh. Mikhail, S. Brunauer and E. E. Bodor. *J. Colloid and Interface Sci.* **26**, 54 (1968).
[13] R. Sh. Mikhail, L. E. Copeland and S. Brunauer. *Can. J. Chem.*, **42**, 424 (1964).
[14] S. Brunauer and P. H. Emmett. *J. Am. Chem. Soc.* **59**, 2682 (1937).
[15] R. Sh. Mikhail, S. Brunauer and E. E. Bodor. *J. Colloid and Interface Sci.* **26**, 45 (1968).
[16] M. G. Kaganer. *Zh. fiz. Khim.* (in Russian), **33**, 2202 (1959).
[17] R. A. Armstrong and J. P. Hobson. *J. Phys. Chem.* **67**, 2000 (1963).

DISCUSSION

Professor R. A. W. Haul (*Technical University, Hannover, Germany*) said: In recent years a number of studies have been reported in the literature on low pressure and low temperature physisorption, particularly on pyrex glass surfaces and evaporated metal films. It has been frequently found that the adsorption data can be well represented by a Dubinin–Kaganer–Radushkevich (DKR) plot. We have studied [R. Haul and B. A. Gottwald. *Surface Sci.* **4**, 321, 334 (1966). B. A. Gottwald and R. Haul. *Surface Sci.* **10**, 76 (1968); also *Proc. Fourth Intern. Vacuum Congress* (1968)] transient molecular flow of rare gases through a single pyrex glass capillary at low pressures under u.h.v. (ultra high vacuum) conditions over a wide temperature range. Although the main objective was a study of residence times of adsorbed molecules, the results have some bearing on the problem of monolayer capacities. For example argon adsorption at temperatures ranging from 83 to 100°K results in a cross section area obtained from the DKR monolayer capacity which is in agreement with the value adopted in the BET procedure. In a number of cases, however, drastic differences may occur. Some typical examples for pyrex glass surfaces (assumed roughness factor 1) are listed in *Table A*.

Inspection of the data reveals that in the case of abnormally high apparent cross section area the experimental temperatures were below approximately one half of the corresponding critical temperature. As is known two-dimensional condensation phenomena may occur under such conditions which can lead to the formation of clusters on parts of the surface.

Table A. Apparent cross sectional area from DKR plots for molecules adsorbed on pyrex glass surfaces at temperatures above and below one half of the critical temperature of the adsorbate

Adsorbate	$\frac{T_{\mathrm{crit}}}{2}$ [°K]	*Exp. temp. range* [°K]	*Cross sectional area* [Å²/*molecule*] *from DKR plot*	*Cross sectional area* [Å²/*molecule*] *adopted BET value*	*Reference*
Ar	75	83–100	15	~15	*a, b*
		63–77	143		*c*
		77	103		*f**
Kr	105	98–130	14	~21	*a*
		77–90	108		*d*†
		77, 90	145		*f*†
Xe	145	130–158	52	~25	*a*
		77–90	162		*d*
		77, 90	360		*f*†
N_2		63–90	16	~16	*c*
CO	67	77, 90	16	~16	*g*
CH_4	95	77–90	69	~16	*e*

* Calculated with vapour pressure of solid adsorptive; for supersaturated liquid the values are somewhat smaller.

† Experimental data evaluated by DKR plot.

[a] R. Haul and B. A. Gottwald. *Surface Sci.* **4**, 334 (1966).

[b] B. A. Gottwald and R. Haul. *Proceedings of the Fourth International Vacuum Congress* (1968).

[c] J. P. Hobson and R. A. Armstrong. *J. Phys. Chem.* **67**, 2000 (1963).

[d] B. G. Baker and P. G. Fox. *Trans. Faraday Soc.* **61**, 2001 (1964).

[e] F. Ricca and R. Medana. *Ric. Sci.* **34**, 617 (1964).

[f] F. Ricca, R. Medana and A. Bellardo. *Z. Phys. Chem. N.F.* **52**, 276 (1967).

[g] F. Ricca, R. Bellardo and R. Medana. *Ric. Sci.* **36**, 460 (1966).

On the other hand for u.h.v. evaporated metal films, e.g. with Xe even at 77°K agreement is found between BET and DKR monolayer capacities [Y. Delamois, A. Frennet and G. Lienard. *Disc. Faraday Soc.* **41**, 114 (1966); *J. Chim. Phys.* **63**, 906 (1966). D. F. Klemperer, this volume, page 55]. This may suggest that the above mentioned phenomena are absent because either of large surface heterogeneity of the metal films and/or relatively strong adsorbate/adsorbent interaction. At pyrex glass surfaces, on the other hand, lateral interaction between adsorbed molecules may lead to condensation effects if the temperatures are sufficiently low.

Professor Brunauer has stressed in his paper the agreement between BET and DKR monolayer capacities. In his contribution Dr Gottwald discussed the significance of this correspondence.

Professor S. Brunauer replied: I am not sure that I understand Dr Gottwald's comments fully, but if I do, I disagree with him.

If the BET equation is 'desensitized' in the manner shown in his *Figure 4* or *Figure 5* (*loc. cit.*) it seems that one can obtain the same value for v_m whether $c = 30$ or 1000. By desensitizing I mean the following. If the true value of an adsorption point is 1000, and one obtains a value of 900, then the error is 10 per cent. However, log log 1000 = 0·477, and log log 900 = 0·470, so the error in such desensitized plot is less than 1·5 per cent.

According to the BET equation, $v = v_m$ at about $p/p_s = 0{\cdot}03$ when $c = 1000$, and at about $p/p_s = 0{\cdot}16$ when $c = 30$. The adsorptions at $p/p_s = 0{\cdot}03$ and $0{\cdot}16$ may differ by a factor of 2 or more or less. No one plots the BET equation in Dr Gottwald's desensitized version; consequently, the BET values of Kaganer can be in error by a few per cent only.

As I look at Kaganer's plot for nitrogen on coconut charcoal at 77·3°K, I cannot see how his intercept can be in error by more than a few per cent. His v_m may possibly be 15 or 17 mmol/g instead of 16. Thus, the two methods give remarkably close agreement.

The BET model and the Kaganer model are quite different, and the adsorption data from which v_m is evaluated are also quite different. I repeat, therefore, my conviction that the results constitute a mutual confirmation of the correctness of the v_m values. I may also add that by converting any number of equations into sufficiently desensitized forms, one can wash out all the experimental differences.

Professor M. M. Dubinin (*Academy of Sciences, Moscow*) said: The most debatable part of Professor S. Brunauer's interesting paper is the method for determining the distribution of the micropore volume and surface area, or the MP-method. This method is described in detail in his published work [R. Sh. Mikhail, S. Brunauer and E. E. Bodor. *J. Colloid Interface Sci.* **26**, 45 (1968)] and applied to a specimen of silica gel Davidson O3 possessing only micropores.

The fact that this silica gel is a microporous adsorbent does not cause any doubt. A similar silica gel specimen designated as No. 8 and having a somewhat smaller limiting volume of the adsorption space has been studied by A. V. Kiselev and E. V. Khrapova [*Kolloidnyi Zhurnal* **19**, 572 (1957)]. *Figure A* depicts isotherms of low-temperature adsorption of nitrogen for various ranges of equilibrium relative pressures; the isotherms are reduced to a unit surface. If the experimental points for non-porous quartz and silica gels of the transitional-pore type fit one and the same reduced curve, the reduced isotherm for silica gel 8 represents a more convex curve testifying to a considerable departure from affinity of the isotherms under review in the range of small equilibrium relative pressures. It would be noted that for silica gel 8 the adsorption and desorption branches of the nitrogen isotherm coincide, as well as for silica gel Davidson O3. For silica gel 8 a sharp difference in specific surface areas for nitrogen (510 m^2/g) and water (800 m^2/g) determined by the BET-method is observed, which is typical for microporous adsorbents.

Brunauer sees the principal confirmation of the MP-method in the remarkable coincidence of the specific surface areas of silica gel Davidson O3 determined by the BET-method and the MP-method based on the use of de Boer's t-method, and also in the coincidence of the sum of the volumes for the group of pores with an experimental limiting adsorption volume. Determination of the specific surface area of this silica gel by the BET method has been carried out by the four first points of the adsorption isotherm of nitrogen, i.e. for a very narrow range of equilibrium relative pressures from 0·05 to 0·2. The basic condition for the application of the MP-method adopted by the authors was the equality of the constant c of the

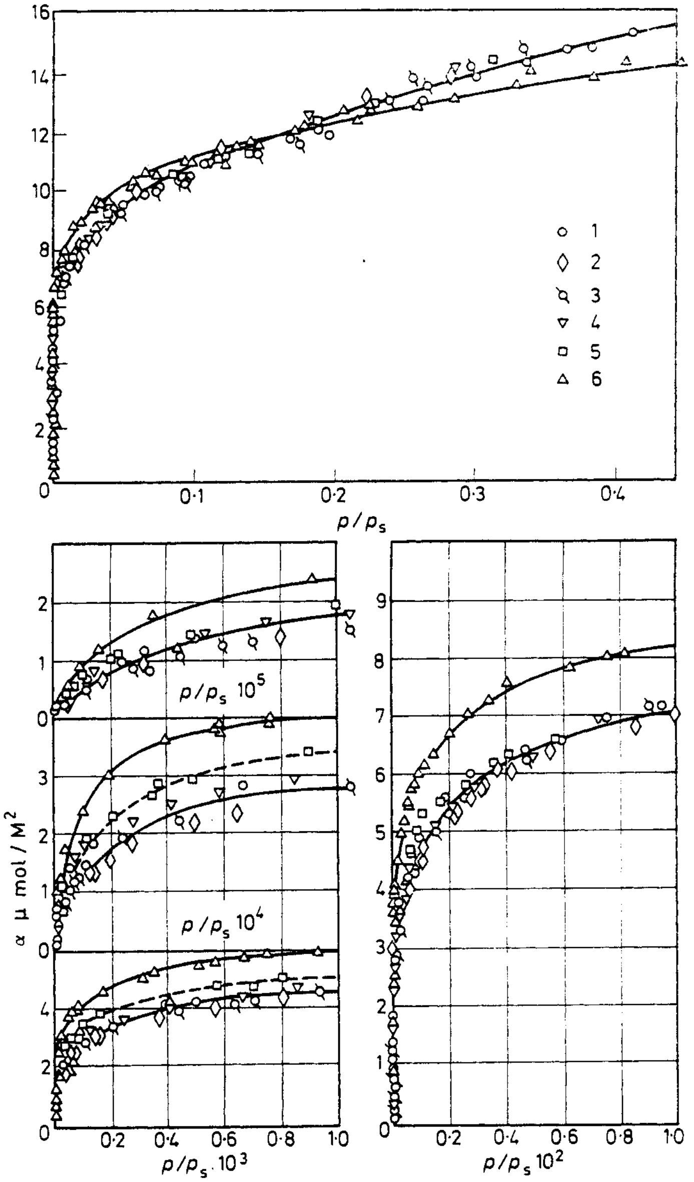

Figure A. Isotherms of low-temperature adsorption of nitrogen for various ranges of equilibrium relative pressures

BET-equation for the adsorption isotherm of nitrogen on silica gel and the constant *c* corresponding to de Boer's *t*-curve. Therefore in the indicated narrow range of equilibrium relative pressure the adsorption isotherm of nitrogen for silica gel and the nitrogen isotherm reduced to a unit surface and corresponding to de Boer's *t*-curve were similar. The affinity factor was automatically equal to the specific surface area of silica gel determined by the BET-equation. Therefore the coincidence of the specific surface area of silica gel Davidson O3 determined by the BET method (793 m^2/g) and that obtained by the *t*-method (792 m^2/g) is a direct consequence of the initial propositions and points exclusively to the fact that the applied graphical methods for calculating these values have been carried out with maximum accuracy.

In the case of the MP-method the tangents to the curve expressing the dependence of the filled micropore volume in cm^3 of the bulk liquid on the mean statistical thickness of the adsorption layer (de Boer's V–t plot in *Figure B*) are limited by the straight line 1 passing through the origin of the straight line with an angular coefficient of 792 m^2/g and by the straight line 9 with an angular coefficient practically equal to zero. Any method of drawing tangents between the lines 1 and 9 will yield differences of the specific surface areas for groups of pores whose sum must absolutely coincide with 792 m^2/g.

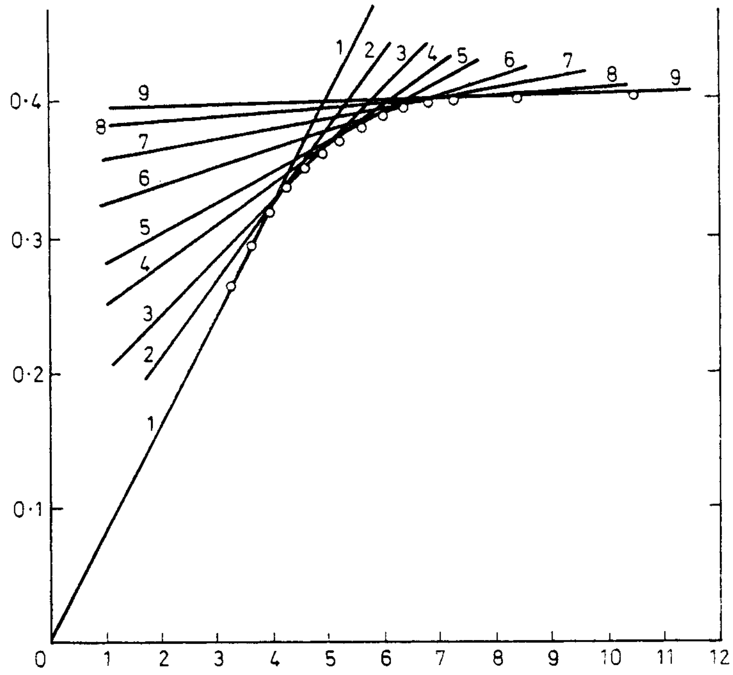

Figure B. de Boer's V–t plots

According to the scheme for calculating the total pore volume adopted in the MP-method

$$V = \sum_{i=1}^{n} V_i = \sum_{i=1}^{n} (S_i - S_{i+1}) \left(\frac{t_i + t_{i+1}}{2}\right) \qquad (1)$$

where n is the number of pore groups and the expression under the summation sign represents the volume of the ith pore group.

If r is sufficiently large, i.e. if each group of pores corresponds to a very small range of their sizes which tends to zero in the limit, then summation (Eq. 1) may be replaced by integration, and in this case a tangent at any point of the curve $V = f(t)$ expresses the specific surface area of the pores remaining unfilled:

$$S = \frac{\mathrm{d}V}{\mathrm{d}t} \tag{2}$$

On the basis of the solution of the integral and expression (1) we obtain:

$$V = -\int_{S_1}^{S_2} t\,\mathrm{d}S \tag{3}$$

and, using partial integration, we get:

$$V = -S_n t_n + S_1 t_1 + \int_{t_1}^{t_n} S\,\mathrm{d}t \tag{4}$$

According to Eqs. (4) and (3)

$$V = -S_n t_n + S_1 t_1 + V_{mi} - V_1 \tag{5}$$

where V_{mi} is the total micropore volume. Since the real curve is characterized by a linear initial section and a limiting value $V = V_{mi}$ = constant, then

$$S_n = 0 \qquad \text{and} \qquad S_1 = \frac{\mathrm{d}V}{\mathrm{d}r} = \frac{V_1}{t_1} \tag{6}$$

according to Eqs. (5) and (6)

$$V = V_{mi} \tag{7}$$

with any shape of the curve $V = f(t)$ characterized by the above-mentioned features.

On the whole the coincidence of the sum of the volumes of pore groups with the volume of the micropores of silica gel is a geometrical sequence of the adopted scheme for calculating the total volume of a pore group by the MP-method.

The application of de Boer's t-method automatically implies the assumption that for the adsorbent under study nitrogen molecules in a continuous monolayer have a molecular area identical with that adopted in calculating the t-curve. For microporous adsorbents whose pore sizes are commensurate with those of nitrogen molecules this assumption cannot be true. The diagram presented in *Figure C* is a qualitative illustration of this conclusion. Therefore the application of the t-method for determining the specific surface area of a microporous adsorbent or a group of its pores is not physically justified.

In conclusion I would like to point out that each method has limits of applicability. For decades we have been witnessing the triumph of Brunauer's method for determining specific surface areas. The new versions, which have been developed in de Boer's and later in Sing's works are based on the use of the BET-method. The application of the BET-method can be considered justified for many cases of non-porous and porous bodies, i.e. for non-porous, macroporous and transitional-pore adsorbents. The microporous

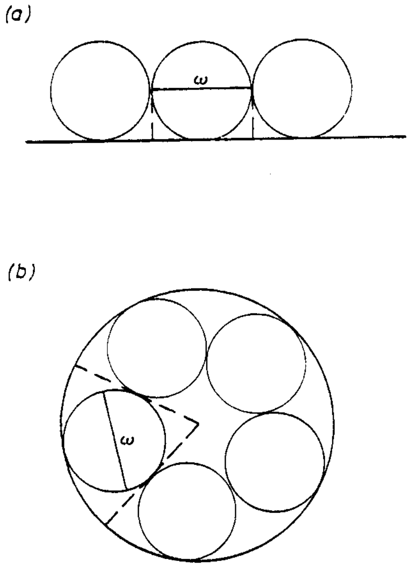

Figure C. Nitrogen area in (*a*) ultra-micropore, (*b*) micropore

adsorbents, or adsorbents containing micropores lie beyond the boundaries of applicability of the BET-method or of the versions of the methods proposed by de Boer and Sing, which are also based on the BET-method.

Professor S. Brunauer replied: Academician Dubinin first compares our Davidson O3 with Kiselev's silica gel 8, and agrees that both are microporous adsorbents. The main difference between the two silica gels is that Kiselev found a great discrepancy between the BET areas obtained with nitrogen and water, whereas our silica gel had the same surface area as measured by nitrogen and water. However, this point has little, if any, bearing on the subject.

According to Academician Dubinin 'Brunauer sees the principal confirmation of the MP-method in the remarkable coincidence of the specific surface areas of silica gel Davidson O3 determined by the BET-method and the MP-method based on the use of de Boer's *t*-method, and also in the coincidence of the sum of the volumes for the group of pores with an experimental limiting adsorption volume'. The first part of this sentence is incorrect, and is based on incomplete reading of the paper. It is stated in our paper that 'The fact that S_t agreed with S_{BET} was bound to lead to agreement between the cumulative pore surface and the BET surface in this particular analysis, because all pores were micropores, and the slopes of the straight lines in *Figure 2* decreased step by step from the slope giving S_t to almost zero.' [R. Sh. Mikhail, S. Brunauer and E. E. Boder. *J. Colloid Interface Sci.* **26**, 45 (1968)] Thus, Dubinin's discussion of this point was unnecessary. However, he is right in saying that we considered the agreement between the cumulative pore volume and total pore volume as ev idence of the correctness of the MP-method and the BET surface.

STEPHEN BRUNAUER

Some time ago Professor Lee Brown of the University of Colorado submitted to me a derivation, not identical with but similar to that of Dubinin, leading to the same conclusion; namely, that the cumulative pore volume must be equal to the total pore volume. Although I have a slight misgiving about one point in both derivations, I will not go into that but, for the sake of argument, I accept the criticism as valid. However, this is not the end of the story.

The paper just discussed (*loc. cit.*) is immediately followed by another paper, which was left out of consideration by Academician Dubinin [R. Sh. Mikhail, S. Brunauer and F. E. Bodor. *J. Colloid Interface Sci.* **26**, 54 (1968)]. That paper contains the pore structure analysis of two silica gels, which contain both micropores and larger pores. Contrasting the analyses with the first paper in which we deal with a silica gel that contains only micropores, we have stated, 'The situation is different here. When an adsorbent contains both micropores and larger pores, the cumulative surface in the narrow pores cannot be equal to S_t or S_{BET}'. Thus the objections raised by ourselves against the cumulative pore surface argument and by Professors Brown and Dubinin against the cumulative pore volume argument lose their validity when only a part of the pore system is in micropores. The fact that the cumulative pore surface for the *entire* pore system agreed with the BET surface, and the cumulative pore volume for the *entire* pore system agreed with the total pore volume can be considered as evidence of the correctness of the MP-method and of the BET surface. Since the publication of the two papers, many additional pore structure analyses were performed by us for a variety of adsorbents, using both nitrogen and water vapour as adsorbates, and these have confirmed our conclusions. If the MP-method gives good results for adsorbents which contain both micropores and wider pores, I believe that it is safe to conclude that the method gives good results also when the adsorbent contains only micropores.

In addition to the above, I should like to point to my discussion of the problem in the second half of my present symposium paper. As I discussed earlier, Dr Gottwald's objection to my citing the agreement between the BET and Kaganer surface areas, in my opinion, is not valid. I should like to repeat also the agreement found between BET areas obtained for hardened portland cement pastes and calcium silicate pastes by water vapour adsorption, by small angle x-ray scattering, and by x-ray diffraction data. These adsorbents have most of their surface areas in micropores.

Academician Dubinin points out in his *Figure C* that the usual nitrogen area is inapplicable in micropores. In our first paper (*loc. cit.*), we distinguished between ultra-micropores and micropores, and pointed out that difficulties may be introduced if the adsorbent contains ultra-micropores. Dubinin's *Figure C(a)* is an ultra-micropore. The MP-analysis starts with pores that have radii equal to twice the diameter of the adsorbate molecule. Even in this case the area will be somewhat larger than 16·2 Å^2 for nitrogen and *for a cylindrical pore*, but the discrepancy will be much smaller than that shown by Dubinin. For parallel-plate pores, there will be no discrepancy.

For ultra-micropores, such as we find in molecular sieves, the geometrical surface of the pore walls has little significance for a chemist. The important thing is how many adsorbate molecules can we get into the pores, if any.

Dr B. C. Lippens (*Texaco Belgium N.V.*) said: With respect to the filling of a micropore system with an adsorbate I would like to mention some results we obtained about ten years ago when we studied the adsorption of lauric acid on aluminas. Some of the results have been published [J. H. de Boer, G. M. M. Houben, B. C. Lippens, W. H. Meijs, and W. K. A. Walraeve. *J. Catalysis* **1**, 1 (1962)] but most of them can be found in my thesis [Delft (1961), p. 152].

Lauric acid will be adsorbed on an alumina surface from a pentane solution with the carboxyl group bound to the surface and the long hydrocarbon chain in upright position; this of course provided the sizes of the pores do not form a restriction. Each lauric acid molecule occupies a surface of 27 Å^2, or 0·617 mmol lauric acid is adsorbed per 100 m^2 of BET-surface area. If the pores are narrow the quantity of lauric acid adsorbed per 100 m^2 of surface area is lower. This property we used to obtain somewhat more information on the micropore system of some aluminas.

With the t-method we found the surface area in the wide pores (S_w) from the slope of the V_a–t plot in the intermediate relative pressure region and the total surface area S_t from the initial slope. The difference $S_t - S_w = S_n$ represents the surface in the micropore system. The volume of the narrow pores were calculated with a method similar to the MP-method as described by Brunauer and his coworkers from the slope of the tangents of the V_a–t plot (ref. 2 page 152). We divided the V_a–t curve into a number of steps each corresponding to an increase of 0·2 Å in the thickness of the adsorbed layer. At the beginning and at the end of such a step we drew the tangent to the curve, determined its slope and calculated the corresponding surface area with

$$S = 15{\cdot}47 \times \frac{dV_a}{dt}$$

The difference between the surface area at the beginning and at the end of the ith step, ΔS_i, represents the surface area of the group of pores having a width between $2(t_i - 0{\cdot}1)$ and $2(t_i + 0{\cdot}1)$. Assuming that the mean width of the pores of this group is equal to $2t_i$ the volume of these pores is given by

$$V_i = t_i \times \Delta S_i$$

The total volume V_n of the narrow pores then is:

$$V_n = \Sigma\, \Delta V_i = \Sigma\, (t_i \times S_i)$$

Now we assumed that the pores corresponding to S_w are wide enough that lauric acid is freely adsorbed in them and will occupy 27 Å^2 of surface area per molecule. We calculated the amount adsorbed on this part of the surface (LA_w).

The difference with the total measured amount of lauric acid adsorbed on the sample (LA_{tot}) is the amount of lauric acid adsorbed in the micropores (LA_n).

The results for various samples are shown in *Table B*:

Table B

Sample	S_t	S_w	S_n	V_n	LA_{tot}	LA_w	LA_n
BY 200	26·6	8·7	17·9	0·0075	0·082	0·054	0·028
BY 250	483	20·1	463	0·1965	0·998	0·124	0·874
BY 270	440	20·6	419	0·1972	0·994	0·127	0·867
BY 450	386	21·5	364	0·1982	1·003	0·132	0·871
BOG 450	17·2	5·1	12·1	0·0051	0·055	0·032	0·023
BOG 580	65·0	17·2	47·8	0·0260	0·219	0·106	0·113
		m^2/gAl_2O_3		ml/gAl_2O_3		$mmol/gAl_2O_3$	

By comparing the values of V_n with those of LA_n we found that 1 mmol of lauric acid occupies a volume of 0·226 ml in the micropore system, which corresponds with a density of 0·88. Comparing this with the literature data (solid 0·883, liquid 0·868) we may conclude that the micropore volume can equally be filled with either nitrogen or lauric acid. Where here apparently a volume filling occurs, it follows that of course a value for the surface of micropores can be calculated, but that for all practical purposes only the micropore volume has any significant meaning.

Professor S. Brunauer replied: My only remark on Dr Lippen's comments is concerned with his last sentence, 'Where here apparently a volume filling occurs, it follows that of course a value for the surface of micropores can be calculated, but that for all practical purposes only the micropore volume has any significant meaning.'

At the Parma Research Laboratory of Union Carbide very great interest was expressed in the MP-method for determining the surface distribution in the micropores *for practical purposes*. Similar interest was manifested in other industrial laboratories, likewise for practical purposes. But the most important thing is this: one cannot compare the cumulative surface of the pores of solids which contain micropores with the BET surface or any other surface unless one determines the surface in the micropores.

Dr W. de Vleesschauwer (*Texaco Belgium N.V.*) said: This comment deals with pore structure analysis without adopting a pore shape model, called briefly the modelless method. Professor Brunauer stated in his presentation that this method is based on Kiselev's equation and does not depend on the Kelvin equation. Kiselev's equation is given by

$$S_c = -\frac{1}{\gamma}\int_{a_H}^{a_s} RT \ln p/p_0 \, da \tag{1}$$

where S_c is the surface area of the adsorbed film at the beginning of the hysteresis loop. a_H and a_s are respectively the number of moles of nitrogen adsorbed at that point and at saturation pressure. It is obvious that the surface area thus calculated is not based on any adopted pore model.

In the pore structure analysis proposed by Brunauer, the above equation is not used in the integral form but rather in a differential form, since one is interested in the core surface area of a group of pores which lose their capillary condensate when the relative pressure is decreased by a small amount.

In that case Eq. (1) reduces to:

$$\Delta S_c = -\frac{RT}{\gamma} \ln p/p_0 \, \Delta a \tag{2}$$

in which equation Δa can be represented by

$$\frac{\Delta V_c}{V_{\text{spec}}}$$

Equation (2) can be rearranged to:

$$\frac{2\Delta V_c}{\Delta S_c} = -\frac{2\gamma V_{\text{spec}}}{RT \ln p/p_0} \tag{3}$$

The right-hand term is well known from the Kelvin equation:

$$r_k = -\frac{2\gamma V_{\text{spec}}}{RT \ln p/p_0} \tag{4}$$

Consequently, the core surface area of a group of pores which lose their capillary condensate is actually calculated in the modelless method from the simple equation

$$\Delta S_c = \frac{2\Delta V_c}{r_k} \tag{5}$$

Hence use is made of the Kelvin equation for the calculation of ΔS_c. Since ΔV_c is not the volume actually desorbed, but the volume corrected for multilayer evaporation in previously emptied pores, a pore volume must be adopted to allow for this correction. It is clear, especially in the case of pores of the ink-bottle type, that Eq. (5) will give rise to serious errors, for the simple reason that the Kelvin radius where emptying occurs corresponds with that of the narrow neck. Therefore, we are of the opinion that the 'modelless method' is not to be preferred to the 'older idealisations' as they are called in Brunauer's paper.

Yet we must be grateful to Professor Brunauer for reintroducing Kiselev's equations. This equation offers indeed a modelless method for calculating the surface area of the adsorbed film at the beginning of the hysteresis loop.

Another method which allows that is the *t*-method. Therefore I would suggest a comparison of the value of S_t at the lower end of the hysteresis loop where the area is given by the slope of the V_a–t plot at that particular pressure, with the core surface area calculated from the higher part of the hysteresis loop by Kiselev's equation. Both methods are independent and do not rely on any pore model. As far as we know such a comparison has never been made.

Professor S. Brunauer replied: In answer to Dr de Vleesschauwer's comments, I should like to make the following remark:

(a) We did not use his equation (2), but the integrated form

$$S_c = -\frac{RT}{\gamma}\int_{a_1}^{a_2} \ln\frac{p}{p_0}\,da$$

(b) Because Kiselev's equation is valid for pores of any shape it must be valid also for cylindrical pores. Kiselev himself showed that his equation reduces to the Kelvin equation for cylindrical pores.

(c) The core surface area is not calculated from his equation (5). It is actually equal to

$$S_c = \frac{\Delta V_c}{r_h}$$

where r_h is the hydraulic radius. If the pore is *really* cylindrical, this equation reduces to Dr de Vleesschauwer's equation (5). However, our equation is valid for cores of any shape.

(d) I do not understand the statement that 'This equation offers indeed a modelless method for calculating the surface area of the adsorbed film at the beginning of the hysteresis loop.' It seems to me that the method is modelless, as far as the cores are concerned for the entire hysteresis loop [S. Brunauer, R. Sh. Mikhail and E. E. Bodor. *J. Colloid Interface Sci.* **24**, 451 (1967)].

Professor K. S. W. Sing in conjunction with **Dr R. E. Day** and **Dr L. J. Stryker** (*Brunel University*) said: Recently Carruthers and Sing have compared water vapour isotherms for samples of silicas, alumina and chromia and observed a comparatively large uptake on chromium oxide [J. D. Carruthers and K. S. W. Sing. *Discussions of the Wetting Symposium*, S.C.I. Monograph No. 25, p. 412 (1967)]. These results indicated a highly specific interaction between the solid and the adsorbate water molecules and an explanation was proposed in terms of a rehydration within the surface layers with probable rearrangement of the coordination state of the surface chromium ion complexes.

In our latest studies on chromium oxide we have found much larger differences in the uptake of water vapour relative to nitrogen than those found for the portland cement paste examples cited by Professor Brunauer. A comparison of two water isotherms determined at 20°C and a nitrogen isotherm measured at -196°C on a chromium oxide sample (Gel V) is given in *Figure D*. The water vapour isotherms (I and II) are Type I (BDDT classification) characteristic of a microporous adsorbent. A pronounced hysteresis is observed on desorption (darkened symbols) over the entire pressure range. There is also a considerable quantity of water retained by the gel (indicated in *Figure D* by the respective arrows) which could not be removed by outgassing at room temperature for a period of several days. In contrast the nitrogen uptake (isotherm III) was barely detectable on the same chromium oxide sample. The comparative BET areas and the micropore volumes obtained from α_s plots for water vapour and nitrogen on gel V

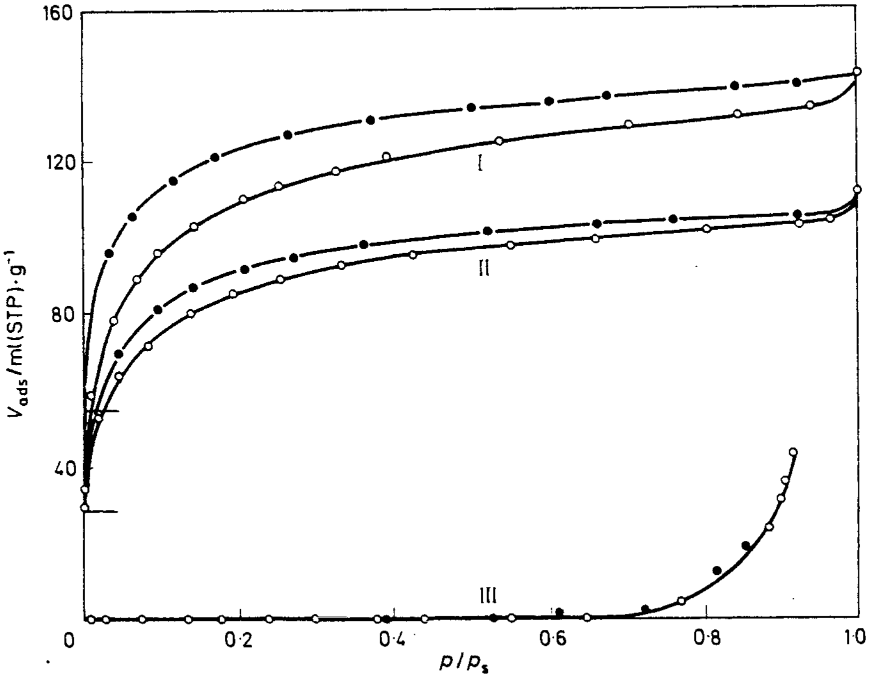

Figure D. Sorption isotherms for water vapour at 20°C and nitrogen at −196°C. I Water sorption on gel V heated at 115°C for 2 hours in vacuum. II Water sorption on gel V heated at 115°C for 2 hours in water vapour. III Nitrogen sorption on gel V outgassed at 20°C for 40 hours

are shown in *Table C* demonstrating the large differences in the adsorptive capacities of the two molecules. Also tabulated are some unpublished results of J. D. Carruthers and K. S. W. Sing on other chromium oxide gels showing less striking examples in the comparative uptake for the two adsorbates. However, in every case the adsorption of water vapour exceeds that of nitrogen. The results on gel V were obtained on the same sample, the successive treatments being performed without removing the sample from the silica spring apparatus. The temperature of calcination is given by the figure immediately following the particular sample and the time of calcination in the indicated environment is shown in brackets. The reduction in the

Table C

Chromia Sample	S_{BET} (m^2 . g^{-1})		*Micropore volume* (ml . g^{-1})	
	H_2O	N_2	H_2O	N_2
Gel V, 20(70) vacuum	294	<1	0·108	undetectable
Gel V, 115(2) vacuum	267	<1	0·097	undetectable
Gel V, 115(2) water vapour	210	—	0·073	undetectable
Gel V, 115(2·5) vacuum	246	<1	0·086	undetectable
Gel A, 180(2) air[2]	197	84	0·086	0·049
Gel A, 345(0) air[2]	118	45	0·042	0·012
Gel C, 240(0) air[2]	250	230	0·120	0·112

water BET values and micropore volumes for gel V with successive heat treatment at 115°C indicates that considerable ageing takes place at this temperature. Also the isotherm obtained after heating in a water vapour atmosphere (corresponding to approximately 1·75 cm Hg at 20°C) exhibited considerably less hysteresis and the sample retained a smaller proportion of water after the final room temperature outgassing.

It is clear that the sorption of water vapour on these chromium oxide gels is highly specific and involves special considerations when applying the conventional methods of analysis. In the case of gel V the difference between the water vapour and nitrogen uptakes is rather large to be explained wholly in terms of micropores which are accessible only to water molecules. The large quantities of water retained which can not be removed by room temperature outgassing for prolonged periods, support the conclusions of Carruthers and Sing (*loc. cit.*) that rehydration of the chromium complexes takes place. These workers suggested that this rehydration involves penetration of water molecules into the solid, a process which may account in part for the large differences between the water vapour and nitrogen adsorption levels. Consequently, in such complex systems it is doubtful whether the BET area represents a reasonable estimate of the available surface area.

Professor S. Brunauer replied: My only remark about the interesting contribution of Stryker, Day and Sing is that I agree completely with the authors. In their system, and doubtless in others of similar nature, the apparent BET surface obtained by water vapour adsorption may be completely wrong because of reaction of water with the surface or even the body of the adsorbate.

Dr J. M. Haynes (*University of Bristol*) said: The applicability of Eq. (2) of Brunauer:

$$S = \int_{a_{\mathrm{H}}}^{a_{\mathrm{S}}} \frac{RT}{\gamma} \ln \frac{p_0}{p} \, \mathrm{d}a$$

appears to be limited to certain classes of pore structure, since it involves the integration of a differential equation

$$\gamma \, \mathrm{d}s = \Delta\mu \, \mathrm{d}a$$

which is valid only for reversible processes. Whilst pores of some shapes, such as wedges, may fill and empty reversibly, others, such as open-ended cylindrical pores, and the pore space between packed spheres, involve spontaneous processes both in filling and in emptying. It is therefore worth enquiring into the seriousness of this limitation. Theoretical estimates of the excess energy dissipation attributable to irreversible condensation or evaporation processes are feasible only for pores of simple geometry; here, we have instead chosen to use the experimental data of C. B. Ferguson and W. H. Wade [*J. Colloid Interface Sci.* **24**, 366 (1967)], who measured BET areas of pre-adsorbed water films in porous Vycor. Water was adsorbed in their sample at 25°C, and carefully cooled to −196°C before measuring nitrogen adsorption on the system (substrate + pre-adsorbed water). Their data thus give core areas as a function of degree of pore filling.

Ferguson and Wade also published a complete water isotherm for the same sample, which we have analysed first according to the Kelvin equation, from which a cumulative core area distribution may be obtained, assuming cylindrical pore geometry. This can then be 'corrected', using the *t*-curves of J. Hagymassy, S. Brunauer and K. Sh. Mikhail [*J. Colloid Interface Sci.* **29**, 485 (1969)], to give pore areas. Corresponding results have also been obtained using the interpreted Kiselev equation, assuming a constant (bulk) value for γ. Combination with the Kelvin data permits calculation of hydraulic radii, to which Brunauer's 'modelless' method may be applied. Finally, we have also used the related equation of I. Bakardjiew [*Z. phys. Chem.* **225**, 273 (1964)]:

$$S = -RT\int_{a_\mathrm{H}}^{a_s} \ln\frac{p}{p_0}\left[\frac{\partial a}{\partial \ln \frac{p}{p_0}}\right]_\mathrm{T} \mathrm{d}\ln\frac{p}{p_0}$$

The results, shown in *Figures E*, *F*, *G*, lead to the following conclusions:

(i) The integrated Kiselev equation provides good agreement with measured core areas along the adsorption branch, suggesting that no large energy dissipation due to spontaneous pore filling occurs in this particular pore geometry.

(ii) Results obtained by the Kiselev equation are almost indistinguishable from those given by the Bakardjiew method for the adsorption branch (*Figure E*).

(iii) Application of the Kiselev equation to the desorption branch (*Figure F*) seriously overestimates the core area at almost all degrees of pore filling. We believe that this is due in part to irreversibility in the desorption process, although it is possible that Ferguson and Wade's results are too low in certain ranges because of a 'pore-blocking' effect.

(iv) Data calculated with the Kelvin equation show that it underestimates the surface area in the adsorption branch, but overestimates it in the desorption branch. This suggests that cylindrical pore shapes + simple Kelvin equilibria do not represent the system accurately.

(v) In *Figure G*, the pore area calculated by Brunauer's 'corrected modelless method' [S. Brunauer, R. Sh. Mikhail and E. E. Boder. *J. Colloid Interface Sci.* **24**, 451 (1967)] is compared with that obtained by correcting the Kiselev areas for the thickness of the multilayer film, using the cylindrical pore model. It should be noted that the cumulative area ought not to exceed the specific surface of the material (126 $\mathrm{m^2\,g^{-1}}$ by nitrogen BET).

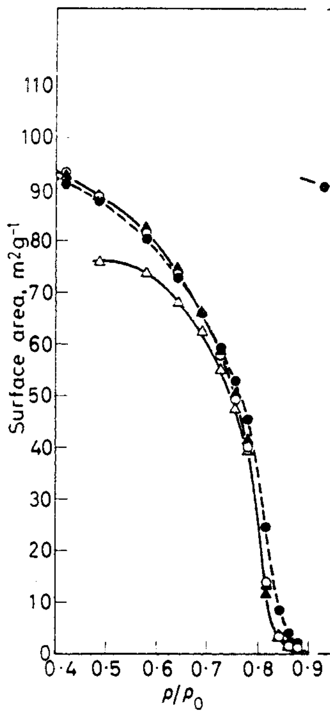

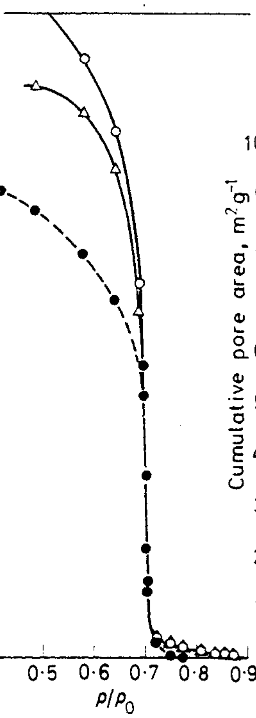

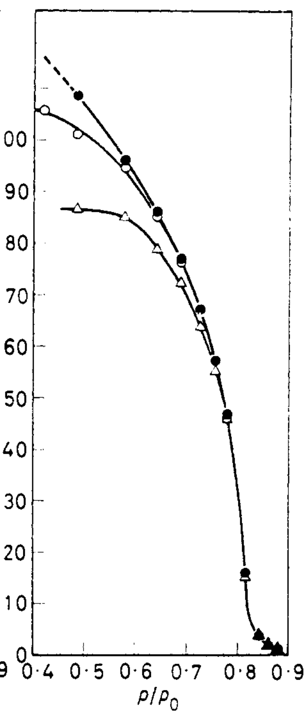

Figure E. Adsorption data of water/vycor at 25° [●, N_2 BET; ○, Kiselev equation; ▲, Bakardjiew equation; △, Kelvin equation (Robert's method) + cylindrical pore model]

Figure F. Desorption data of water/vycor at 25° [●, N_2 BET; ○, Kiselev equation; △, Kelvin equation + cylindrical pore model]

Figure G. Cumulative pore area distributions using cylindrical pore model (Absorption data of water/vycor at 25°) [●, Brunauer *et al.* 'corrected modelless method'; ○, Kiselev equation; △, Kelvin equation (Robert's method)]

Professor S. Brunauer replied: I should like to add to the interesting and valuable conclusions of Dr Haynes the following: (a) It is very clear that the Kelvin equation and the 'corrected modelless' method do not give the same results. Note especially *Figure G.* I am making this statement as an additional response to Dr de Vleesschauwer's comments. (b) In conclusion (v) of Dr Haynes, he states that 'the cumulative area ought not to exceed the specific surface of the material (126 m^2 g^{-1}) by nitrogen BET'. He does not state, however, what is very important, that the cumulative area obtained by the corrected modelless method with water vapour adsorption is almost exactly equal to the nitrogen BET area in *Figure G.* (c) I agree with Dr Haynes that for the adsorbent–adsorbate system he is considering the adsorption branch represents true capillary condensation equilibrium (or close to it).

Dr S. J. Gregg (*Brunel University*) said: A decision between the rival views that the plateau corresponds to capillary filling or to monolayer coverage respectively is difficult to make by testing the constancy of the Gurvitsch volume or of the specific surface.

$$v_{\mathrm{s}} = \frac{a_{\mathrm{s}}}{\rho_{\mathrm{T}}} \tag{1}$$

$$A = \frac{a_{\mathrm{s}}}{M} . N . \omega_{\mathrm{m}} = \frac{a_{\mathrm{s}}}{M} . N \left(\frac{M}{\rho_{\mathrm{T}} N}\right)^{\frac{2}{3}} f \tag{2}$$

Here ω_{m}, the area of the adsorbate molecule, is calculated from the liquid density without adjustment (A = specific surface; M = molecular weight; N = Avogadro's constant; f = packing factor).

From Equations (1) and (2) by inserting the values $N = 6{\cdot}0 \times 10^{23}$ and $f = 1{\cdot}09$ one obtains

$$A = 8{\cdot}4 \times 10^7 . \frac{v_{\mathrm{s}}}{V^{\frac{1}{3}}}$$

where V = molar volume.

Thus if v_{s} is constant for a number of adsorbates on a given solid, A will also appear constant to within the limits of variation of $V^{1/3}$; and conversely if A is constant with the different adsorbates, v_{s} will also appear constant to within the limits of variation of $V^{1/3}$. Actually for the adsorbates referred to above, except butane, $V^{1/3}$ varies only from 3·03 to 3·30 cm mol$^{-1/3}$ except for butane ($V = 4{\cdot}55$). It is interesting therefore that (according to my calculation) the Gurvitsch volume for butane does not fall out of line, whereas the specific surface must do so unless the ω_{m} value is arbitrarily adjusted.

One should not of course expect absolute constancy of the Gurvitsch volume for microporous solids, since packing effects are bound to obtrude.

Professor S. Brunauer replied: Dr Gregg is right; I made a numerical mistake in calculating the Gurvitsch volume of butane. He is also right in stating that it is difficult to make a decision between volume filling and monolayer capacity on the basis of the plateau of the isotherm. His proof appeared already in the excellent book of S. J. Gregg and K. S. W. Sing [*Adsorption, Surface Area and Porosity*, Academic Press, London and New York, p. 210 (1967)], and I read it, but I forgot it. I apologize.

Professor R. M. Barrer (*Imperial College*) said: In Dr Brunauer's paper and in other papers in this meeting there has been considerable reference to micropores and to the meaning of micropore areas. Sorbents such as the molecular sieves consist almost wholly of micropores, the external surface having about 1 per cent of the sorption capacity of the internal pores. This is clearly the limiting case of micro-porosity, and the associated pore sorption capacity can be expressed either as a volume or as a monolayer equivalent area, a term which I introduced some years ago. If all the sorbate filling the micropores are removed and spread as a close packed monolayer on a molecularly smooth surface the area covered is the monolayer area equivalent to the micropore capacity. I suggest that no other meaning is possible for micropore area, and that it would be helpful and avoid confusion if the term were employed widely where micropores are involved.

At the other limit, where there are no micropores, but only non-porous particles, the monolayer equivalent area obviously becomes the true area.

In Dr Brunauer's paper there is reference to the high 'surface' area of cements measured using water and to the much lower area sometimes obtained using nitrogen. Because of its dipole moment there is a large field-dipole energy component in the binding energy of water to ionic and polar substrates. Water is therefore very energetically bound in such a polar material as cement, and one is not surprised that at or near room temperatures it will penetrate into the cement to parts of the medium which are quite inaccessible to N_2 at $-196°C$. This situation is often found in the less open of the molecular sieve zeolites.

Earlier in this meeting Dr Gregg referred to the device of blocking micropores in carbon by sorbing hydrocarbons and then determining the remaining area by the BET method. It is therefore worth noting that a similar procedure has been employed for some time for molecular sieve crystals. Here the micropores are filled with water and the Kr or N_2 area is then determined. This area is the small external area of the crystals, and may be required *inter alia* for the interpretation of intracrystalline diffusion kinetics.

Dr Gammage (elsewhere in this publication) has reported a slow process for Ar uptake in a thoria containing some micropores, in which however N_2 was taken up considerably more rapidly. If the tempo of this slow process is governed by molecule-sized entrances into micropores then the difference between N_2 and Ar is just as expected, and as found for various molecular sieves (Caand Ba-mordenites, levynite, Na-chabazite, Na–A etc.). The van der Waals dimensions for N_2 are 3·0 Å normal to its long axis and 4·1 Å along this axis, while Ar is a sphere of diameter $3{\cdot}8_3$ Å. Clearly in an end-on orientation N_2 will penetrate much more rapidly through suitably small apertures than will Ar, just as observed in the molecular sieves. If this explanation of Dr Gammage's experiment is correct then it would not be true to say that N_2 should always be preferred to Ar in monolayer equivalent area determinations. Many micropore systems would have openings large enough to admit either gas freely.

Professor S. Brunauer replied: Perhaps the difference between Professor Barrer's view and my own lies in the definition of micropores. As I stated in our paper on micropore analysis [R. Sh. Mikhail, S. Brunauer and E. E. Bodor. *J. Colloid Interface Sci.* **26**, 45 (1968)], and in my answer to Academician Dubinin's comments, the MP-method breaks down for ultra-micropores. I am completely willing to accept Professor Barrer's concept of monolayer equivalent area for ultra-micropores. The MP-method starts with analysing the surface and volume distributions of micropores which have radii equal to twice the diameter of the adsorbate molecule if the pores are cylindrical, or have widths equal to twice the diameter of the adsorbate molecule if the pores are parallel plates. At this lower limit of micropores, about 7 Å for nitrogen adsorption, which is also the upper limit of ultra-micropores, there is no difference between Professor Barrer's view and mine. However, the micropores range to an upper limit of five or six molecular layers in a parallel plate pore, and if we use the monolayer equivalent area, we may make the serious mistake of overestimating the surface.

What Professor Barrer says about nitrogen vs. water area of cement pastes, we have known and accepted for two decades. The fact that water can penetrate into pores inaccessible to nitrogen was always attributed by us not only to the difference between the sizes of the molecules, but also to the strong attraction between an ionic surface and the large dipole of water.

I should like to make a few remarks in connection with Professor Barrer's comment on the experiments of Dr Gamage. The explanation of Professor Barrer is very reasonable, but not his conclusion. It is true that many micropore systems have openings large enough to admit both nitrogen and argon, but since ordinarily we do not know *a priori* the sizes of the openings, it seems to me safer to use nitrogen.

There are two other items that bother me about argon adsorption. Since the bulk phase at 77·3°K is the solid and not the liquid, the question is whether one should use the vapour pressure of the solid or that of the extrapolated liquid? I, and most others, have used the extrapolated liquid vapour pressure, but this could not be used in pore structure analysis, where we have to go up to p_0. The second point is even more bothersome. A value of 16·6 Å^2 is frequently used for the area covered by an argon atom. Why is argon in a complete monolayer so much more loosely packed than in the liquid state? I personally belong to the 'nitrogen-party'.

Dr B. Rand (*University of Birmingham*) said: Professor Dubinin has already criticized Brunauer's micropore (MP) method of analysis. I would like to make some additional comments. *Figure H* shows the essentials of the method, which is described in detail in the original paper.

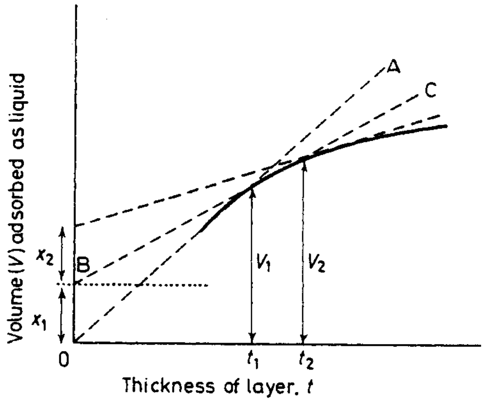

Figure H. Volume adsorbed as liquid against thickness of layer

After V_2 cm^3 of adsorbate have been adsorbed a certain volume of the micropore structure is filled with adsorbate. According to Brunauer this volume is given by the expression,

$$\text{Pore volume filled} = 10^4(S_1 - S_2)\,\frac{(t_2 - t_1)}{2} \qquad (1)$$

(S_1 and S_2, the slopes of lines OA and BC, are respectively the total surface area of the micro-pores and of those micropores not yet filled with adsorbate at V_2 cm^3 adsorbed).

It can easily be shown that

$$10^4(S_1 - S_2) = \frac{x_1}{t_1} \tag{2}$$

and, therefore, since $t_2 - t_1$ will in practice be a small interval, the pore volume filled in this interval is approximately equal to x_1, the intercept of the extrapolated section of the t plot (BC). Since the cumulative pore volume, according to Brunauer, is determined by summing the intercepts of successive extrapolations ($x_1 + x_2 + \ldots$ etc.) it is not surprising to find that good agreement is obtained with the Gurvitsch pore volume. Such agreement is therefore no criterion that the initial slope of the t plot (S_1) is a true measure of the surface area of the adsorbent when it contains micropores.

Furthermore, since $t_2 > t_1$ the pore volume calculated by equation (1) will always be greater than x_1 and hence the cumulative pore volume will be greater than the Gurvitsch pore volume. It is significant that, for the analysis of a silica gel, Brunauer quotes the figures: Cumulative pore volume = 0·409 cm^3 g^{-1}, Gurvitsch pore volume = 0·403 cm^3 g^{-1}.

Professor Haul has shown that the mathematical nature of the BET and Dubinin–Kaganer–Radushkevich (DKR) equations is such that they will yield similar values for the monolayer capacity. I would like to add a word of caution about the application of the DKR method to the determination of the monolayer capacity of non-porous solids.

The DKR equation,

$$t = \frac{V}{V_0} = \exp\left(\frac{-k\,\Delta G^2}{\beta^2}\right) \tag{3}$$

assumes that the distribution of differential adsorption free energy (ΔG) is of the form,

$$f(\Delta G) = -\frac{2k\,\Delta G}{\beta}\exp\left(\frac{-k\,\Delta G^2}{\beta^2}\right) \tag{4}$$

Thus, a linear plot of

$$\log V = \log V_0 - k\,\Delta G^2 \tag{5}$$

will be obtained only when the distribution of differential adsorption free energy is of this form. *Figures I* and *J* show the type of Dubinin–Radushkevich plot which is obtained when the distribution of adsorption free energy is of the normal and log-normal forms. It can be seen that, if the distribution of adsorption free energy approximates to either of these distributions, extrapolation of data determined only at low relative pressures (high ΔG) can result in erroneous value of V_0.

In *Figure K* the D–R plot of CO_2 adsorbed at 195°K on microporous polymer carbons is shown. The plot shows two linear regions. Extrapolation of the high ΔG^2 data would result in a limiting adsorption value in excess of that measured experimentally. In this case the intercept on the log V axis is not a measure of the monolayer capacity but of the micropore volume.

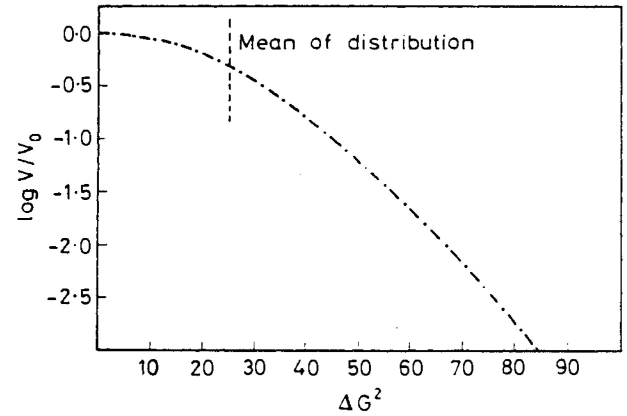

Figure I. A Dubinin plot synthesized from a log-normal distribution of V (volume adsorbed) with ΔG.

$$f(\Delta G) = \frac{1}{\log \sigma \sqrt{2\pi}} \exp\left[-\frac{(\log \Delta G - \log x)^2}{2 \log^2 \sigma}\right]$$

where $x = 1{\cdot}35$ kcal mol^{-1} and $\sigma = 5{\cdot}0$ kcal mol^{-1}

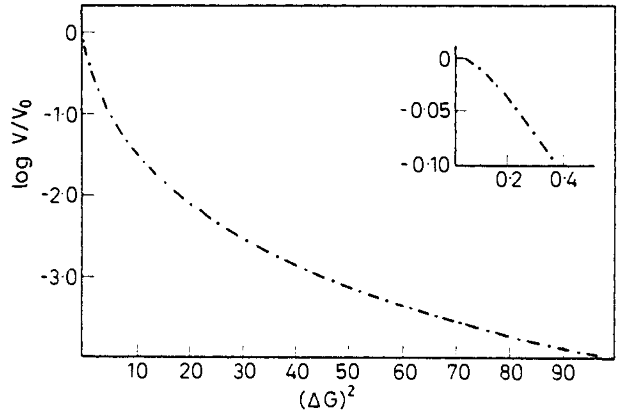

Figure J. A Dubinin plot synthesized from a log-normal distribution of V (volume adsorbed) with ΔG.

$$f(\Delta G) = \frac{1}{\log \sigma \sqrt{2\pi}} \exp\left[-\frac{(\log \Delta G - \log x)^2}{2 \log^2 \sigma}\right]$$

where $x = 1{\cdot}0$ kcal mol^{-1} and $\sigma = 1{\cdot}86$ kcal mol^{-1}

However, data of the type shown in *Figure L* has been observed for adsorption of N_2 at 78°K on non-porous TiO_2 (B. Rand, unpublished results).

The section ABC describes the build up of the monolayer whilst CD is due to multilayer formation. It can be seen that extrapolation of AB will result in a V_0 value which is too high, the correct extrapolation being BCE. The point B corresponds approximately to the mode of the distribution of AT with V, which resembles a normal distribution rather than that predicted by the DKR equation. It is therefore important that in using this method to

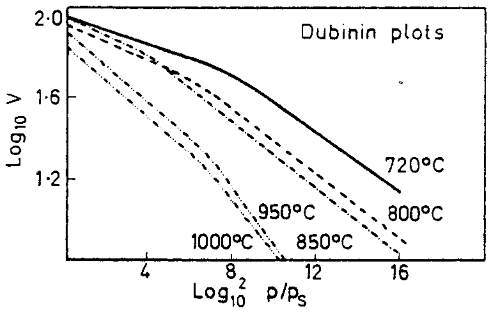

Figure K. Adsorption of carbon dioxide, at 195°K, on polyfurfuryl alcohol carbons. A heat treated series

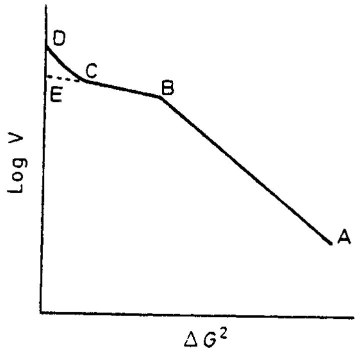

Figure L. Type of curve obtained for the adsorption of nitrogen on non-porous TiO_2 at 78°K

estimate the monolayer capacity of a non-microporous adsorbent the data be extended into the multilayer region so that any deviations from linearity in the DKR plot are observed.

Professor S. Brunauer replied: I note that according to Dr Rand we should obtain for adsorbents which contain only micropores a somewhat greater cumulative pore volume than the Gurvitsch volume, whereas according to Academician Dubinin we should obtain the Gurvitsch volume. For the rest, I refer to my answer to Academician Dubinin's comments.

Dr Rand's warning about determining the monolayer capacity by the DKR method is doubtless well taken, but it does not seem to apply to the isotherm discussed by Dr Gottwald, nor to many other isotherms of Kaganer.

Professor J. M. Holmes (*Carlton University, Ottawa*) said: In the preprints of your paper no reference is made to the recent work of C. Pierce [*J. Phys. Chem.* **72**, 3673 (1968)] in which he raises questions as to the actual *t*-values used in the work of Lippens and de Boer. I presume most of your work on this was done before Pierce's work was published and I am wondering if applying his *n* values to your data would make any difference in the interpretation of your result?

Also throughout your paper and in many others at the symposium numerous references were made to the use of the BET *c* value as an adequate test of the appropriateness of the *t*-curve or of the energetics of the surface under investigation. The *c* value is a measure of the energy of adsorption and I believe it is agreed it gives order of magnitude values only because of the fact that it is calculated from isotherm data and is extracted from an exponential expression in the BET equation. It would appear to me that a direct measurement of heats of adsorption by calorimetry would give a much better characterization of the surface under consideration than many of the *c* values reported. Why has comparatively little work been done on direct measurement of heats of adsorption? Is it because of the difficult and time consuming experimental techniques or is it because of interpretation of the results obtained from such measurements? I realize that much work has been done on heats of wetting and immersion of solids with adsorbed gases but very few direct measurements of heats of adsorption of nitrogen on the various solids reported by you and others have been carried out. In addition I would expect that more modern methods of measuring low pressures should yield meaningful isosteric heats of adsorption at coverages below the statistical monolayer and should give heats of adsorption which would characterize surfaces more exactly than *c* values. It is surprising that more of this type of research has not been reported.

Professor S. Brunauer replied: In response to Professor Holmes, I wish to say that I was fully aware of Professor Pierce's criticism of the *t*-curve of Lippens and de Boer. Professor Pierce is under the misapprehension that there is only one correct and universal *t*-curve, which applies to all adsorbents. Actually, I know of at least five *t*-curves (Shull, Pierce, Harris and Sing, Cranston and Inkley, Lippens and de Boer), and all of them are correct. In several friendly exchanges of letters, I tried to convince Professor Pierce, but I had no success. He also tried to convince me, likewise without success.

The *c* constant of the BET equation is frequently adequate for the testing of the appropriateness of the *t*-curve, but not always. Often it is difficult to obtain a good *c* constant because of the uncertainty in the intercept of the BET plot. A much more reliable test is the agreement between S_{BET} and S_{t}.

There is no question about the fact that calorimetric measurements give a very better characterization of the surface than the *c* constant. However, the question presently discussed is the selection of the appropriate *t*-curve for the pore structure analysis of a given adsorbent. For this purpose, calorimetric data for the adsorbent are not needed.

THE SURFACE AREA IN INTERMEDIATE PORES

J. C. P. BROEKHOFF and J. H. DE BOER

Laboratory of Chemical Technology, Delft University of Technology, Delft, The Netherlands

In many adsorbents, micropores as well as intermediate pores are found. The BET method leads to an overall estimation of the surface area. It is often necessary to determine the intermediate pore surface area separately. Two methods of estimation are discussed, both based on the common *t*-curve of multimolecular adsorption. The simple *t*-method is especially suited for the estimation of external surface area and surface area in intermediate slit-shaped pores. The validity of the *t*-method for intermediate tubular and spheroidal pores is discussed. The estimation of cumulative surface areas from the adsorption- and the desorption-branch of the hysteresis-loop also leads to acceptable intermediate pore surface area values, if the influence of the free energy of adsorption on the capillary condensation and evaporation of nitrogen is taken into account. Methods of calculation are discussed in some detail.

1. INTRODUCTION

Several classifications of pores according to their shapes and sizes have been proposed. According to Dubinin[1], we may distinguish between macropores (> 2000 Å), intermediate pores (from 20 Å up to 2000 Å), and micropores ($<$ 15 to 20 Å). In recent times, it has become clear that there are important differences in behaviour between macropores, intermediate pores and micropores. For example, hysteresis-phenomena in physical adsorption occur neither in macro- nor in micro-pores, but nearly exclusively in intermediate pores. In heterogeneous catalysis, intermediate pores and micropores may behave completely different. For example, it was found by Linsen[2] that hydrogenation of fatty oils with the aid of nickel–silica catalysts, takes place at the surface of intermediate pores (wider than 20 Å) whereas micropores are completely inactive. Catalysts used in his study had surface areas of about 300 m^2/g, but less than 10 per cent of the surface was found actually to participate in the reaction.

In many cases it is therefore not sufficient to determine the total surface area of an adsorbent. It is often required to make separate estimations of the surface area present in micropores and in intermediate pores respectively. One step further is the estimation of a complete pore surface area distribution function. For non-porous adsorbents, the BET-method, which will be discussed by de Boer in detail, is a convenient and probably reasonably accurate means of surface area estimation. From the recent review of Gregg and Sing[3] it appears that, if nitrogen is used as the adsorbate, the BET-method gives estimates which agree within 20 per cent with estimates based on such methods as electron-microscopy.

On the other hand, in the BET-theory the adsorbent surface is supposed to be non-curved. Although this does not necessarily invalidate the use of the BET-method for porous adsorbents, it is no longer possible to obtain independent evidence on the reliability of the BET-method from methods such as electron microscopy. Moreover, the BET-method cannot be used to yield separate estimates of the surface area present in micropores and in intermediate pores respectively. In many a case, both types of pores occur together in the same adsorbent.

The *t*-method of de Boer and Lippens[4, 5], which is ultimately based on the BET surface area as a primary standard, can give valuable information concerning the presence of micropores. Moreover, the *t*-method can be used to estimate the surface area not present in micropores in cases where different types of pores occur simultaneously. On the other hand, the *t*-method is based on the assumption, that the thickness of an adsorbed layer is solely a function of the relative pressure and not influenced by the curvature of the pore walls. This assumption clearly is at variance with the observed occurrence of capillary condensation phenomena in the intermediate and high relative pressure range if intermediate pores are present. Therefore, our first problem is: What is the influence of capillary effects on the applicability of the *t*-method to adsorption in intermediate pores? This question is closely connected with the second one: Is it possible to estimate the surface area in intermediate pores from the observed capillary condensation and evaporation phenomena?

The principle of the calculation of cumulative surface areas from the pore size distribution, obtained on the basis of the Kelvin-equation, is well-known[6, 7]. In general, a certain fixed pore model is used in the calculation. Cumulative surface areas have been obtained either from the adsorption- or from the desorption branch of the isotherm. Many authors have used equality of BET surface areas and cumulative surface areas as a criterion for the validity of the calculated distribution. It is clear, that there is no sense in comparing BET surface areas and cumulative surface areas unless the absence of micropores has been demonstrated. The calculation of cumulative surface areas as an independent way of estimating intermediate pore surface areas was introduced by Kiselev[8]. This author used a generalised form of Kelvin's equation for reversible condensation and evaporation processes. In this way, a surface area may be calculated without actually assuming a pore model. As Brunauer *et al.*[9] have pointed out, the area obtained is not the true pore wall surface area but rather the area of the interface between the adsorbed layers at the walls of the pores and the vapour phase, the so-called 'core surface area'. In not very wide pores with curved walls, the difference in magnitude between core surface area and pore surface area may be appreciable. Conversion of core surface areas into pore surface areas necessitates the asumption of a discrete pore model. Moreover, both Kiselev and Brunauer had to assume that the capillary condensate has essentially bulk liquid properties. Yet it is clear that the fact, that multi-layer adsorption takes place at non-curved adsorbent surfaces below saturation, indicates that at least the *chemical potential* of a liquid layer in contact with a solid adsorbent surface cannot be equal to that of the bulk liquid. It is therefore clear that in calculations of pore surface areas from either the adsorption- or the desorption-branch of the hysteresis-loop we have to account for the influence of pore geometry as well as for the influence of adsorption on the state of the capillary condensed liquid. This is only feasible, if simplified pore models are adopted.

2. COMMON t-CURVE AND ITS APPLICATIONS

It was found by de Boer *et al.*[10] that the amount of nitrogen adsorbed per unit of surface area of non-porous adsorbents, is a unique function of the relative pressure $x = p/p_0$, for a large number of inorganic oxides and hydroxides as well as for graphitised carbon blacks. If it is assumed that the adsorbed nitrogen multi-layer has the same molar volume as the bulk liquid at the same temperature, then the common isotherm may be represented in the form of a t-curve, representing the thickness of the adsorbed layer (in Å) as a function of x. The t-curve for nitrogen at these oxides and hydroxides, is represented in *Figure 1.* Other groups of materials may obey different t-curves. It is clear that nitrogen adsorption isotherms at porous adsorbents belonging chemically to the class of adsorbents constituting the common t-curve, may be plotted against the thickness of the adsorbed layer t, as derived from the common t-curve, instead of p/p_0. Three characteristic types of behaviour are found[11] (see also *Figure 2a, b* and *c*).

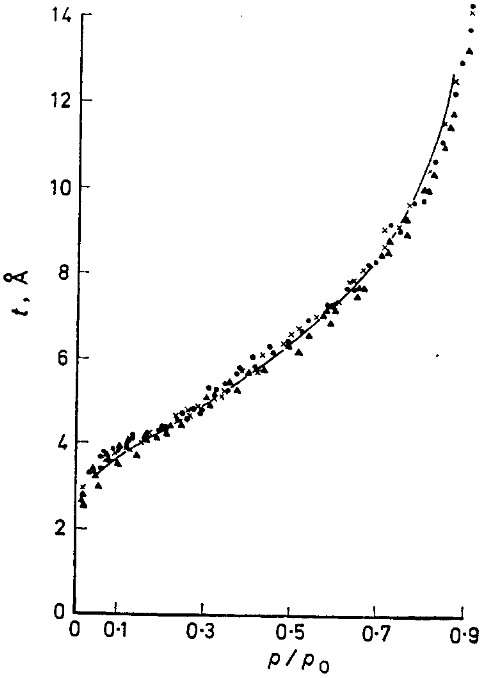

Figure 1. The common t-curve of multi-molecular nitrogen adsorption on oxidic and hydroxidic adsorbents[10].

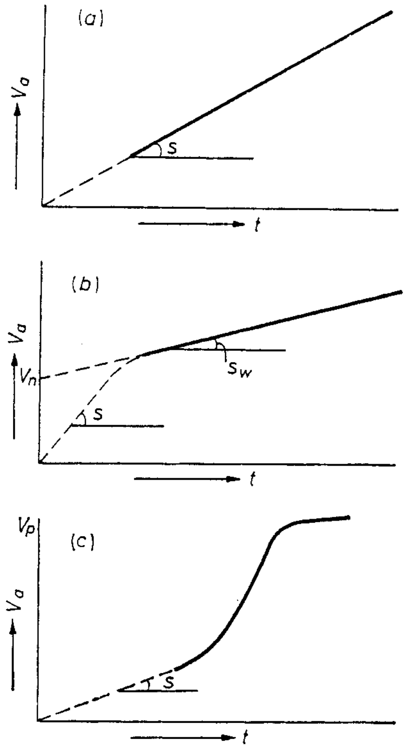

Figure 2. Three characteristic types of *t*-plots. (*a*) external surface area or intermediate slit-shaped pores; (*b*) micropores and external surface area; (*c*) intermediate pores with curved walls.

(*a*) A straight line extrapolating through the origin indicates the absence of micropores, as well as the absence of capillary condensation phenomena at the adsorption branch of the isotherm. The latter may be due to either the absence of intermediate pores with radii small enough to invoke capillary condensation or to the occurrence of slit-shaped pores.

(*b*) Downward deviations at comparatively low relative pressures are commonly taken as an indication of decrease of the accessible surface area through blocking of micropores by the adsorbed layer. Commonly, a second straight part in the *t*-plot is found at intermediate relative pressures, corresponding with the unhindered growth of the adsorbed layer either in intermediate pores or at the external surface area of the adsorbent.

(*c*) Upward deviations are taken as an indication of the onset of capillary condensation in intermediate pores. After complete blocking of the pores with capillary condensate, a second straight part is found in the *t*-plot, corresponding to unhindered growth of the adsorbed layer at the external surface area of the adsorbent.

In case (*a*) the total surface area of the adsorbent is simply found from the slope of the *t*-plot, through the relation

$$S_t = 15{\cdot}47 \, \mathrm{d}V_a/\mathrm{d}t \qquad (1)$$

where V_a is the amount of nitrogen adsorbed, expressed in ml at s.t.p., t is expressed in Å and S in m^2. In case (*b*), the second slope of the t-plot corresponds with S_w, the surface area present either in intermediate pores or as external surface area. On the other hand, it is highly questionable whether the initial slope of the t-plot at low relative pressures corresponds with the total surface area of the adsorbent, including the micropore surface area. It is highly improbable that in micropores the thickness of the adsorbed layer is still the same as on non-porous adsorbent surfaces. Therefore, the micropore surface area cannot be estimated from the t-plot. The initial slope probably leads to a *minimum* estimate of the micropore surface area. In case (*c*) the surface area of the intermediate pores may be estimated from the initial slope only. If no capillary condensation effects intervened, then we should have expected downward deviations in the t-plot with increasing layer thickness. This may be easily demonstrated by assuming either tubular or spheroidal pores of radius r. If we assume the actual thickness t to be independent of the pore geometry, then from simple geometric considerations we find the following relations between S_t, as derived from the slope of the t-plot through Eq. (1), and S, the true surface area of the pore walls:

$$S_t = S\,(1 - t/r) \quad \text{(tubular pores)}$$

$$S_t = S\,(1 - t/r)^2 \quad \text{(spheroidal pores).}$$

Actually, capillary condensation effects an upward deviation of the t-plot, indicating that in pores where capillary condensation takes place, the thickness of the adsorbed layer is increased, ultimately leading to complete pore filling. Application of the t-method to adsorption in this type of pore necessitates estimation of the influence of pore geometry on the increase in layer thickness in pores. Such estimates may be obtained from the thermodynamic theory of capillarity, after making some simplifying assumptions. In the first place we will adhere to the assumption of bulk liquid density for the adsorbed layer. In the second place, we will assume the existence of a surface tension γ at the adsorbate-vapour interface. The magnitude of γ will be taken equal to that of the bulk liquid. It is however impossible to assume that the chemical potential of the adsorbed layer μ_a is equal to that of the bulk liquid, μ_L, as this would lead to the consequence that no adsorbed layer may ever be stable[12]! Clearly, μ_a will depend on the distance to the pore wall, viz. on the thickness of the adsorbed layer t. Formally, we may write

$$\mu_a = \mu_L - F(t) \tag{2}$$

For non-curved surfaces, $F(t)$ may be derived from the t-curve as for every point on the t-curve, $\mu_a = \mu_g$. This leads to the relation

$$-RT\ln(x) = F(t) \tag{3}$$

(where x is the relative pressure p/p_0).

It may be shown, that the common t-curve of multi-molecular nitrogen adsorption of *Figure 1* is adequately described by the empirical relation

$$F(t)/(2{\cdot}303RT) = 16{\cdot}11/t^2 - 0{\cdot}1682\exp(-0{\cdot}1137\,t) \tag{4}$$

if t is larger than 5 Å. Combination of Eqs. (2) and (4) results in a useful, although strictly empirical, relation between chemical potential and layer thickness. In intermediate pores with curved walls, Eq. (3) is no longer valid, but we may assume that Eqs. (2) and (4) remain valid, apart from the additional contribution of the curvature of the adsorbate-vapour interface to the chemical potential of the adsorbed liquid. As we will show, a quantitative treatment of capillary condensation and evaporation of nitrogen from intermediate pores, may be based on the empirical relation (4), enabling surface area estimations from the adsorption-and the desorption-branch of the hysteresis-loop. It is however inevitable to assume a certain fixed pore model for the calculations.

3. CHOICE OF A PORE MODEL

In practice pore shapes may be quite complicated. Qualitative descriptions of pore shapes and of adsorption in pores in actual porous systems have been proposed by Everett[13]. For a more quantitative description, one has to revert to more simple pore models in order to keep the mathematics of the analysis tractable. On the other hand, the choice of a simplified pore model for the description of adsorption in intermediate pores is neither unimportant nor completely arbitrary. The shape of the hysteresis-loop may provide us with useful information concerning the appropriate choice of a pore model. According to de Boer[14], five fundamentally different types of hysteresis-loops may be observed. Three of them, the types A, B and E, indeed are frequently encountered in practice. Combinations of these types do occur, but only occasionally. In *Figure 3*, these three types are sketched. According to de Boer, the A-type hysteresis-loop, is connected with a variety of pore shapes which may be conveniently approximated by the model of tubular pores. Hysteresis may either be due to the occurrence of tubular pores which are open at both ends, or to 'bottle-neck' effects during evaporation. If these bottle-neck effects are more pronounced, then an E-type hysteresis-loop is found. In this case one may envisage the pores to consist of wide cavities with varying radii, connected to the vapour phase through narrow 'necks'. This, of course, is a simplification. E-type hysteresis-loops may be caused by the interconnection of pores of different radii giving rise to 'cooperative effects' during capillary evaporation (see the discussion by Everett[15] on hysteresis). Probably, in A-type hysteresis-loops, cooperative effects are relatively unimportant, due to the uniformity in pore radius found in these cases. Both A- and E-type hysteresis-loops have in common, that upward deviations in the t-plot of the adsorption branch are found (*Figure 2b*). These deviations often start at relative pressures below that of the closing

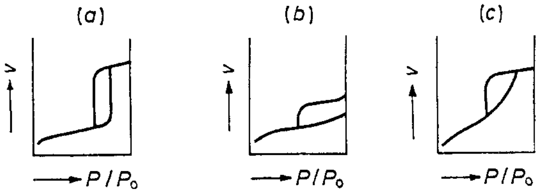

Figure 3. Classification of hysteresis-loops. (*a*) A-type; (*b*) B-type; (*c*) E-type.

point of the hysteresis-loop, indicating either the onset of reversible capillary condensation or the increase in layer thickness of the adsorbed layer due to curvature of the pore walls. On the contrary, these upward deviations in the t-plot are not found in B-type hysteresis-loops. This would point to the absence of pore wall curvature, viz. slit-shaped or wedge-shaped pores. The same behaviour may be found in 'ink-bottle' pore structures with extremely wide bodies and short necks. This sort of behaviour is easily detected by comparing the mean pore radius as computed from $(2\ V_p/S)$, with the pore radius as deduced from the steepest part of the desorption branch of the hysteresis-loop with the aid of relations of the Kelvin-type.

For A- and E-type hysteresis-loops, we will assume the pores to be tubular in shape, although spheroidal pores may be an adequate model for describing E-type hysteresis-loops. Unless stated otherwise, B-type hysteresis-loops will be associated with the existence of slit-shaped intermediate pores.

4. SURFACE AREA IN INTERMEDIATE SLIT-SHAPED PORES

In intermediate slit-shaped pores, the thickness of the adsorbed layer during adsorption is not influenced by capillary condensation effects. Thus, the intermedate pore surface area may be obtained from the slope of the t-plot at intermediate and high relative pressures, even in the presence of micropores. In this section, we will compare this surface area with the surface area obtained from the desorption branch of the hysteresis-loop with the aid of a refinement of Kiselev's method[8].

Kiselev started from the consideration that along an equilibrium branch of an isotherm the free energy gained in evaporating dN moles of capillary condensed or adsorbed liquid is compensated by the free energy needed in creating an adsorbed layer-vapour interface of magnitude dA

$$(\mu_a - \mu_g)\, dN = \gamma dA \tag{5}$$

Eq. (5) in fact is a generalised form of Kelvin's equation. This may be seen by considering the reversible evaporation of dN moles of capillary condensate from a slit-shape pore of diameter d. For such an evaporation dA/dN is equal to $2v_m/(d - 2t)$, where v_m is the molar volume of the adsorbate, and t the thickness of the adsorbed layer remaining at the pore walls. If it is assumed that μ_a, the chemical potential of the capillary condensed liquid, is equal to μ_L, then Eq. (5) reduces to the well-known equation

$$- RT \ln(x) = 2\gamma v_m/(d - 2t) \tag{6}$$

For slit-shaped pores, dA, the created core surface area, is equal to dS, the corresponding pore surface area. Thus, Eq. (5) might in principle be directly used to evaluate pore surface areas from the desorption branch of the isotherm if it could be assumed that μ_a is equal to μ_L. Eq. (5) has been used for this purpose by Brunauer *et al.*[9] in the form

$$A \text{ (or } S) = \int_{N_{x=1}}^{N_{x_c}} - (RT/\gamma) \ln(x)\, dN \tag{7}$$

where x_c is the lower relative pressure closing point of the hysteresis-loop.

As was pointed out by Brunauer, Eq. (7) is of restricted accuracy as the number of moles dN evaporated over the relative pressure interval dx has to be corrected for the change in thickness $\mathrm{d}t$ of the adsorbed layer for all pores already emptied:

$$dN = dN_a - S_c \mathrm{d}t/v_m \tag{8}$$

where S_c is the cumulative surface area in all pores emptied at the relative pressure x, and dN_a is the change in total number of moles adsorbed over the relative pressure interval dx. In Eq. (8), explicit use has been made of the slit-shaped pore model.

More accurate results may be obtained by introducing Eq. (2) into Eq. (5). Consider the reversible evaporation of ΔN moles of capillary condensate from a slit-shaped pore of diameter d, resulting in the creation of a core surface area of magnitude ΔA. It may be shown[17] that this process is equivalent to a decrease in thickness of the adsorbed layer from $d/2$ to t_e at the surface area ΔS, accompanied with the creation of a core surface area ΔA. The free energy balance [Eq. (5)] then may be written as:

$$\gamma \Delta A = \int_{N_i}^{N_f} [\mu_L - \mu_g - F(t)] dN \tag{9}$$

where N_f and N_t are the number of moles adsorbed at the pores surface area ΔS, before and after the reversible evaporation process respectively. Eq. (9) is of quite general validity (compare a similar derivation by Deryagin[16]), independent of the actual pore shape, provided evaporation is a truly reversible process. For slit-shape pores, Eq. (9) may be integrated by change of variable from N to t. In this type of pores the relation

$$N = \Delta S\, t/v_m$$

holds. Consequently, Eq. (9) may be written as

$$\gamma \Delta S = -RT \ln(x) \Delta N - \Delta S/v_m \int_{t_e}^{d/2} F(t)\, dt,$$

which may be rearranged to

$$\Delta S\left[\gamma + 1/v_m \int_{t_e}^{d/2} F(t)\, dt\right] = -RT \ln(x)\, \Delta N \tag{10}$$

For sufficiently large values of d, Eq. (10) may be approximated by

$$\Delta S\left[\gamma + 1/v_m \int_{t_e}^{\infty} F(t)\, dt\right] = -RT \ln(x)\, \Delta N \tag{11}$$

For nitrogen at about 77·6°K, Eq. (4) may be used to give a numerical solution of Eq. (11) in the form

$$\Delta S = 15{\cdot}47\, \Delta V \times \frac{-\log(x)}{[2{\cdot}051 + 16{\cdot}11/t_e - 1{\cdot}483 \exp(-0{\cdot}1137\, t_e)]} \tag{12}$$

where ΔV is the volume desorbed from the pores emptying at the relative pressure x, expressed in ml s.t.p. In practical application of Eq. (12), the desorption branch of the hysteresis-loop is divided into a suitable number of intervals. At each interval, the volume desorbed ΔV_a is transformed to ΔV by means of Eq. (8), making use of the surface area obtained in the previous steps of the calculation. The surface area present in the pores emptying over the interval with mean relative pressure x, is subsequently computed from Eq. (12), where t_e can be taken directly from the common t-curve of multimolecular adsorption (*Figure 1*). Of course, Eq. (12) is only valid for the adsorbents of the group which obeys the common t-curve. Although Eq. (12) does not refer explicitly to the pore diameter d, in fact it is only a rearrangement of the corrected Kelvin-equation[17]

$$d = 2t_e + \frac{4{\cdot}102 + 32{\cdot}22/t_e - 2{\cdot}966 \exp\left(-\,0{\cdot}1137\, t_e\right)}{-\log(x)} \tag{13}$$

Therefore, application of Eq. (12) is equivalent to calculation of pore surface areas with the aid of the Steggerda-Innes[18] equation

$$\Delta S = 2/(d - 2t_e) \times (15{\cdot}47\,\Delta V_a - S_c \Delta\, t_e) \tag{14}$$

where d, the mean pore diameter of pores emptying at the mean relative pressure x of the interval ΔV_a, is determined separately from Eq. (13). In the common procedure of estimating pore size distributions and cumulative pore surface areas for slit-shaped pores, the role of the free energy of adsorption in the capillary evaporation process is neglected, which simply means that Eq. (14) is applied to the desorption branch of the isotherm in combination with Eq. (6) instead of Eq. (13).

We will now consider the application of both procedures (with and without the inclusion of the free energy of adsorption terms) to the evaluation of intermediate pore surface areas in some practical cases. Van Doorn[19] determined nitrogen adsorption isotherms on graphitic oxide samples. It is known e.g. from electron-microscopy, that graphitic oxide consists of laminar sheets, indicating the appropriateness of the slit-shaped pore model. A t-plot analysis[17] showed however that a considerable part of the total surface area was present in micropores. Surface areas of intermediate pores were determined from the slope of the t-plots after complete filling of the micropores (S_w), as well as from the desorption branches of the isotherms. All isotherms showed perfect B-type behaviour in the hysteresis-region. The cumulative surface areas as determined from Eq. (12) (denoted by S_c) and from the combination of Eqs. (6) and (14) respectively (denoted by S_c) are compared with S_w and S_{BET} in *Table 1*. The cumulative calculations

Table 1. Examples of the analysis of isotherms with B-type hysteresis-loops on basis of the model of slit-shaped pores

Sample	*Code*	*ref.*	S_{BET}	S_w	S_c	S_c class.
			m²/g			
Graphitic oxide	4H	(19)	81·8	22·2	21·3	31·9
Graphitic oxide	5R I	(19)	81·8	19·5	20·4	29·1
Graphitic oxide	5R II	(19)	96·2	23·5	19·5	27·0
Dehydrated boehmite	BoG 580	(20)	65·7	19·1	20·7	29·1
Dehydrated boehmite	BoG 750	(20)	19·1	19·1	15·9	21·1
Nickel silicate	Pr 21	(21)	212	207	213	288

have been performed from saturation downwards until the lower relative pressure closing point of the hysteresis-loop has been reached. (Further extension downwards leads to inclusion of micropores, for which all the concepts of capillarity lose their meaning, and so to results which have no physical significance). The same procedure has been followed for two samples of dehydrated boehmite, the isotherms of which have been published by Lippens[20], and for an isotherm on a nickel-silicate catalyst as published by Linsen[21]. In all these cases, the slit-shaped pore model was a reasonable one on crystallographic grounds. With reference to *Table 1*, we may conclude that estimation of S_w from the t-method leads to results which are in good agreement with the S_c-values found along the desorption branch of the isotherms, if the influence of the free energy of adsorption on the capillary evaporation process is accounted for in the proposed manner. Neglect of the free energy terms, leading to the estimates S_c column of *Table 1*, results in surface area values which are by far too high. On the other hand, it is clear that the cumulative surface area method leads to estimates of the surface area of intermediate pores, and therefore is particularly suited for an analysis of the contribution of intermediate pore surface area to the porosity of an adsorbent. The cumulative surface area method directly leads to an estimate of the distribution of available surface area of pore width as well as to an estimate of the overall intermediate pore surface area. The t-method, which in the case of slit-shaped pores can be applied unambiguously, only leads to an estimate of the latter quantity. Both methods, on the other hand, are not strictly independent. Both utilise, if in a completely different manner, the common t-curve of multi-molecular nitrogen adsorption. Therefore, calculation of S_c with the aid of Eq. (12) may be viewed as an extension of the t-method in order to account for capillary phenomena.

5. THICKNESS OF ADSORBED LAYER IN PORES WITH CURVED WALLS

As we have seen, upward deviations in the t-plot of the adsorption branches of A- and E-type isotherms, are always found. This indicates that in e.g. tubular pores there is an extra increase in thickness of the adsorbed layer with increasing relative pressure, ultimately leading to spontaneous pore filling by capillary condensation. This is easily explained by assuming the existence of an adsorbate–vapour interfacial tension of magnitude γ, even for an adsorbed layer of only a few molecular diameters, [in fact the same assumption has been made in deriving Eqs. (10)–(13)]. Eq. (5) then states that for an adsorbed layer in a tubular pore, which is in equilibrium with its vapour phase, a virtual evaporation of dN moles from the adsorbed layer results in a decrease in free energy, which is exactly compensated by the increase in free energy due to the increase in core surface area of the adsorbed layer. The equilibrium thickness in a pore with curved walls may then be found by substituting Eq. (2) into Eq. (5), resulting in

$$\gamma\, v_m\, dA/dV = -RT\ln(x) - F(t_e) \tag{15}$$

Only for very simple and regular pore models, there can be assigned a simple meaning to t_e. In slit-shaped, cylindrical and spheroidal pores with smooth walls, t_e is the thickness of the adsorbed layer, viz. the distance of the adsorbate–vapour interface from the pore wall. For tubular pores, dA/dV is equal to $1/(r - t_e)$, and the equilibrium thickness t_e becomes a solution of the equation

$$- RT \ln(x) = F(t_e) + \gamma\, v_m/(r - t_e) \tag{16}$$

As $F(t_e)$ of necessity is a positive, continuously decreasing, function of t_e, it is clear that for finite values of r, t_e is always larger than the corresponding value of t on a non-porous adsorbent at the same relative pressure. For spheroidal pores, this line of reasoning leads to the equation

$$- RT \ln(x) = F(t_e) + 2\gamma\, v_m/(r - t_e) \tag{17}$$

In the derivation of Eq. (16) we have assumed that $F(t)$ itself is independent of r, the pore geometry. Equations similar in form as Eq. (16) and (17) may be derived from the line of reasoning forwarded some seventeen years ago by Foster[22]. In a more qualitative fashion Everett has discussed the formation of adsorbed layers in more irregular pore shapes[13]. Both authors came to the conclusion that the adsorbed layer in pores with curved walls is only stable over a restricted range of relative pressures. The general condition of stability for an adsorbed layer may be written as

$$\mathrm{d}x/\mathrm{d}t \geqslant 0 \quad \text{for } t = t_e \tag{18}$$

Application of this condition to Eq. (16) leads to the stability conditions for adsorption in tubular pores

$$- dF(t)/dt\ _{t=t_e} - \gamma v_m/(r - t)^2 \geqslant 0 \tag{19}$$

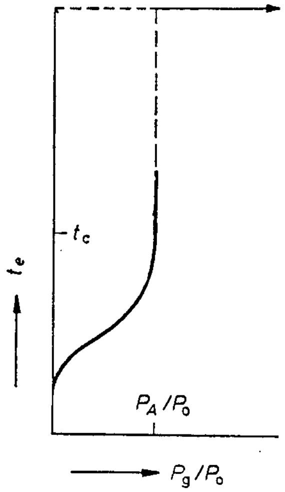

Figure 4. Variation of thickness of the adsorbed layer with relative pressure in a tubular pore.

The general behaviour of the thickness of an adsorbed layer in a tubular pore of radius r, is represented in *Figure 4*. Once the critical thickness t_c is surpassed, spontaneous and irreversible pore filling takes place. The irreversible character of the process causes the adsorption branch of the hysteresis-loop to be a non-equilibrium branch, so Eq. (5) cannot be applied to pore filling along the adsorption branch of the isotherm in the case of tubular pores. For nitrogen at 77·6°K, the equilibrium thickness t_e is found by combining Eqs. (17) and (4) to yield

$$-\log(x) = 16{\cdot}11/t_e^2 - 0{\cdot}1682 \exp(-0{\cdot}1137\, t_e) + 2{\cdot}051/(r - t_e) \qquad (20)$$

subject to the condition:

$$32{\cdot}22/t_e^3 - 0{\cdot}01912 \exp(-0{\cdot}1137\, t_e) \geqslant 2{\cdot}051/(r - t_e)^2 \qquad (21)$$

In connection with the construction of t-plots, we are however not so much interested in the value of t_e, but rather in the value of t_f, where t_f is defined as: $t_f = V_s/S$, where V_s is the volume of the adsorbed layer at the surface area S. For simple pore models, t_f and t_e are related to each other by

$$t_f = t_e \qquad \text{(slit-shaped pores)}$$

$$t_f = t_e\,(1 - t_e/2R) \qquad \text{(tubular pores)}$$

$$t_f = t_e\,(1 - t_e/R + t_e/3R^2) \qquad \text{(spheroidal pores).}$$

In constructing t-plots of the adsorption branch in tubular pores, a straight line relation between V_a and t_f rather than t_e is obtained. As appears from *Table 2*, estimates of t_e in tubular pores do seriously deviate from the t-values of the common curve of *Figure 1*. On the other hand, t_f-values are found to be of the same order of magnitude as the common t-values, as long as t_e is distinctly smaller than t_c, the critical value of t at the onset of irreversible pore filling.

As we do not know, in advance, the pore size distribution of a porous sample containing tubular pores only, it is impossible to construct t-plots using calculated t_f-values. Therefore it is extremely fortunate that at low relative pressures t_f from *Table 2* is found to be of the same order of magnitude as the common t-values. This means that we can go on using simple t-plots in estimating the intermediate pore surface area even for tubular pores. Approximately the same conclusion results from an analysis of the spheroidal pore model[23]. On the other hand, the noted compensational effect of geometrical and thermodynamical influences on the thickness of the adsorbed layer, is rather accidental. For more complicated pore shapes, the agreement between t_f and t_e is less satisfactory. For example, de Boer *et al.*[24] studied the formal thickness of the nitrogen adsorbed layer in packings of non-porous silica particles with different radii. It was found in this case, that t_f was substantially less than the t-values of the common curve. This deviation could be explained by the combined effect of curvature of the particles and the geometry of the region of contact between adjacent particles. (For spherical particles, Eq. (15) predicts a decrease in thickness of the adsorbed layer, instead of the increase found for tubular and spheroidal geometries).

It may thus be concluded, that in pores with curved walls, the increase in thickness due to capillary effects is roughly compensated by the decrease in available space for the adsorbed layer with increasing layer thickness. As

Table 2. Calculated equilibrium thickness t_e and formal thickness t_f (Å), as a function of r (Å) and p/p_0
(Formal thicknesses t_f have been indicated in italic)

p/p_0	*t-common curve*	*Radius of tubular pore*											
		128·1		96·5		63·8		46·7		34·8		23·2	
0·9	*14·3*	18·6	*17·3*	25·3	*22·0*								
0·8	*10·4*	11·4	*10·9*	11·9	*11·1*	13·3	*11·9*						
0·7	*8·6*	9·1	*8·7*	9·2	*8·8*	9·7	*9·0*	10·5	*9·3*	13·0	*10·5*		
0·6	*7·4*	7·7	*7·4*	7·8	*7·5*	8·0	*7·5*	8·4	*7·6*	8·6	*7·8*		
0·5	*6·5*	6·7	*6·5*	6·7	*6·5*	6·9	*6·5*	7·1	*6·5*	7·4	*6·6*	8·6	*7·0*
0·4	*5·7*	5·8	*5·7*	5·9	*5·7*	6·0	*5·7*	6·1	*5·7*	6·3	*5·7*	6·8	*5·8*
0·3	*5·0*	5·1	*5·0*	5·1	*5·0*	5·2	*5·0*	5·3	*5·0*	5·4	*5·0*	5·7	*5·0*
0·2	*4·4*	4·4	*4·3*	4·4	*4·3*	4·5	*4·3*	4·5	*4·3*	4·6	*4·3*	4·8	*4·3*
0·1	*3·7*	3·7	*3·7*	3·7	*3·6*	3·7	*3·6*	3·8	*3·6*	3·8	*3·6*	3·9	*3·6*

a consequence, the *t*-method may be used with the common *t*-values, as an approximate method of surface area estimation in intermediate pores.

6. CUMULATIVE SURFACE AREA ESTIMATIONS FROM A-TYPE HYSTERESIS-LOOPS

As we have seen, in pores with curved walls the core surface area A is no longer equal to the pore surface area S. Both quantities are related to each other through the pore radius and the thickness of the adsorbed layer. For tubular pores we have

$$S = r/(r - t_e)A$$

and for spheroidal pores

$$S = r^2/(r - t_e)^2\mathrm{A}$$

Thus, for not very wide pores, the difference between S and A is far from negligible.

Reversible evaporation from tubular pores takes place along the desorption branch of the isotherm, and intermediate pore surface areas may be found from this branch with the aid of Eq. (9). This equation may be integrated in terms of t, as for tubular pores the number of moles $\mathcal{N}$ adsorbed at part of the pore wall with surface area ΔS, is given by

$$\mathcal{N} = \Delta S(t - t^2/2r)/v_m.$$

Consequently, Eq. (9) may be written as

$$\gamma\Delta A = \gamma\Delta S(r - t_e)/r = - RT\ln(x)\Delta\mathcal{N} - \frac{\Delta S}{v_m r}\int_{t_e}^{r} F(t)\ (r - t)dt \qquad (22)$$

where $\Delta\mathcal{N}$ is the number of moles evaporated during the formation of the core surface area ΔA, in a pore of radius r.

It will be clear that Eq. (22) cannot be applied to the calculation of ΔS from the desorption branch of the isotherm, unless r is evaluated explicitly. This may be done by using the geometrical relation $\Delta\mathcal{N}/\Delta S = (r - t_e)^2/(2v_m r)$ (tubular pores). It is then found that Eq. (22) is equivalent to the corrected Kelvin-equation[25,26]:

$$r = t_e + \frac{2\gamma v_m\ r—t_e + \int_{t_e}^{r} 2F(t)\ (r - t)dt}{- RT\ln(x)\ (r - t_e)} \qquad (23)$$

where t_e is given by Eq. (16). At each relative pressure x, the Eqs. (16) and (23) may be solved simultaneously by using the numerical relation (4) for $F(t)$. Again, it is then assumed that $F(t)$ is independent of the pore radius r. In tubular pores this cannot be strictly true, but deviations are probably small, at least for not very narrow pores. The numerical expression of Eq. (23) for nitrogen at 77·6°K and the substances of the common *t*-curve, is somewhat complicated[27]

$$r = t_e + \frac{4{\cdot}102r - t_e + 32{\cdot}22\ [r/t_e - 1 - \ln(r/t_e)]}{- (r - t_e)\ \log(x)}$$

$$- \frac{2{\cdot}964\exp(- 0{\cdot}1137\ t_e)\ (r - t_e - 8{\cdot}795) + 26{\cdot}06\exp(- 0{\cdot}1137\ r)}{- (r - t_e)\log(x)} \qquad (24)$$

Simultaneous solution of Eqs. (20) and (24) proceeds e.g. with the aid of a two-dimensional Newton-Raphson iteration method. Calculation of cumulative surface areas then is straightforward, although lengthy. The desorption branch of the isotherm is again divided into a suitable number of intervals, and for each interval, r_k, the mean radius of pores emptying, is determined from Eqs. (24) and (20). The surface area of the pores emptying over the k-th interval, ΔS_k, is then determined from the relation

$$\Delta S_k = \frac{2\,r_k}{(r_k - t_{r_k,x_k})^2}\left\{ 15{\cdot}47\,\Delta V_a - \sum_{i=1}^{k-1} \frac{\Delta S_i}{2r_i}\left[(r_i - t_{r_i,x_k})^2 - (r_i - t_{ri,xk_{-1}})^2\right]\right\} \tag{25}$$

where t_{r_i,x_k} and $t_{r_i,x_{k-1}}$ is the thickness of the adsorbed layer at the walls of a tubular pore with radius r_i at the lowest relative pressure of the kth and the $(k - 1)$th interval respectively, to be estimated from Eq. (20). Application of Eq. (25) has to be effected with the aid of an electronic computer, as it is too tedious for hand computing.

Before illustrating this procedure with practical examples, we must pay some attention to the adsorption branch of the isotherm. As we have explained in the preceding section, the adsorption-branch of the hysteresis-loop for tubular pores is essentially metastable with respect to the desorption branch, and pore filling is an irreversible process, for which Eq. (9) is not valid. The relative pressure of pore filling for a certain pore radius r, can however be computed from Eqs. (20) and (21). First, the critical thickness of the adsorbed layer, t_c, is determined from Eq. (21) for a given pore radius, and then the corresponding relative pressure of adsorption may be determined from Eq. (20). At an arbitrary relative pressure x, the pore radius r of pores spontaneously filling, can be determined by interpolation. These radii r, may be used in Eq. (25) to calculate cumulative surface areas from the *adsorption* branch of the hysteresis-loop, as Eq. (20) for the thickness of the adsorbed layer in pores not yet filled with capillary condensate, remains valid, despite the metastable character of the adsorption branch. In actual porous systems, pores will not be exactly tubular in shape, but we get an impression on the adequacy of the tubular pore model. A requirement of consistency is, that both the adsorption- and the desorption-branch of the hysteresis-loop should lead to the same values for the surface area in intermediate pores, S_c, if each calculation is made with the appropriate pore radius. Of course, cumulative surface areas in intermediate pores may also be calculated from pore size distributions based on the application of the classical Kelvin equation for evaporation from cylindrical pores:

$$r = t - 2\gamma v_m/RT\ln(x) \tag{26}$$

where t now is the t-value derived from the common t-curve. The adsorption branch of the isotherm must then be analysed with the aid of Cohan's equation[28]

$$r = t - \gamma v_m/RT\ln(x) \tag{27}$$

while the calculational procedure may then be based on the method of Barrett, Joyner and Halenda[6] for the calculation of pore size distributions. Such a procedure is equivalent to neglecting all contributions of the free energy of adsorption in the capillary evaporation process. Differences in outcome between both procedures may serve as an indication of the importance of accounting for free energies of adsorption in estimating pore surface areas from the adsorption- and desorption branches of the hysteresis-loops.

We will now discuss some practical examples. Lippens[29] studied the dehydration of micro-crystalline boehmite. The starting material had a surface area of 68 m²/g; the adsorption isotherm showed an A-type hysteresis-loop. After heating at 450°C, the surface area was found to increase from 68 to 93·5 m²/g. The *t*-plot analysis, however, showed that the intermediate pore surface area had remained at 68 m²/g, the excess surface area of 25·5 m²/g being present in micropores (of course the significance of this last number is questionable). An analysis of the hysteresis-loop of the isotherm by means of the tubular pore model leads to values for S_{cum}, which are in excellent agreement with the S_w-value as derived from the *t*-plot, see *Table 3*. Moreover, both the adsorption- and the desorption branch of the isotherm lead to the same value of S_c, where in the case of the desorption-branch Eq. (23) was used, and for the adsorption branch Eq. (21) for the emptying, respectively filling, of pores. In this case, analysis of the hysteresis-loop leads to a consistent interpretation. In *Figure 5*, the cumulative surface area distribution

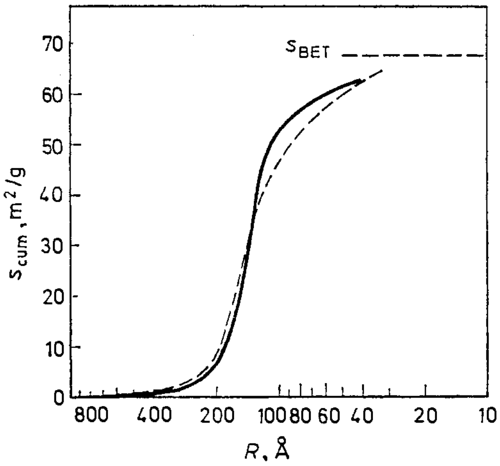

Figure 5. Surface area distribution curve for dehydrated micro-crystalline boehmite BoW 450 (solid line: desorption, broken line adsorption).

curve is shown, as derived from the desorption-branch (solid line) and the adsorption-branch (broken line) respectively. The consistency between both branches is quite satisfactory. It is to be noted, however, that consistency between both branches is only obtained *if* all equations of capillarity are properly corrected for the influence of the free energy of adsorption on the capillary condensation and evaporation processes. In order to do this, we had to sacrifice the simplicity of the starting equation (5) and to make the

Table 3. Examples of the analysis of isotherms with A-type hysteresis-loops on basis of the model of tubular pores and of spheroidal pores

Sample	*Code*	*ref.*			*Tubular pores*		*Spheroidal pores*		*Tubular pores class*	
			S_{BET}	S_w	S_c† ads	S_c† des	S_c† ads	S_c† des	S_c† ads	S_c† des
			(m²/g)							
Dehydrated microcrystalline boehmite	BoW 450	(29)	93·5	68·0	65·5	63·4	68·1	67·7	107	79·6
Porous zirconia	ZrO_2 390	(30)	100	100	106	97·6	104	111	202	132
Porous zirconia	ZrO_2 450	(30)	64·0	64·0	67·2	62·0	61·6	66·1	119	83·2
Magnesia from magnesite	M 800	(31)	33·6	33·7	35·5	32·8	31·6	34·9	61·1	41·8
Magnesia from nesquehonite	N 800	(31)	22·8	22·4	21·0	22·0	21·6	23·3	34·2	27·1
Magnesia from nesquehonite	N 700	(31)	44·5	44·0	49·5	50·1	48·4	52·1	78·0	62·2

† $S_{c\,\mathrm{ads}}$ and $S_{c\,\mathrm{des}}$ denote cumulative surface areas from the adsorption- and from the desorption branch of the hysteresis-loop respectively.

approximation of the introduction of a simplified pore model. The failure of the equations (26) and (27), where the free energy of adsorption contribution is neglected, seems to be a justification of the adopted procedure. On the other hand, the particular assumption made for the pore model, seems to be not a very critical one. For example, we may consider capillary condensation in and evaporation from a spheroidal pore. The growth of the adsorbed layer in such a pore qualitatively follows the trend as sketched in *Figure 4*. The thickness of the adsorbed layer is determined by Eq. (17), whereas spontaneous capillary condensation does not take place until a critical thickness t_c has been reached, determined by the relation

$$- dF(t)/dt_{\,t=t_c} = 2\gamma v_m/(r - t_c)^2 \qquad (28)$$

It may be shown that integration of Eq. (9) for this pore model leads to the corrected Kelvin equation

$$r = t_e + \frac{3\gamma v_m r - t_e^2 + \int_{t_e}^{r} 3(r-t)^2 F(t)\, dt}{- RT \ln(x)(r - t_e)^2} \qquad (29)$$

This is a relation between the radius of the cavity and the relative pressure below which the capillary condensed liquid thermodynamically becomes unstable towards evaporation. It may be solved for r at a given relative pressure in combination with Eq. (17). [There is a distinct difficulty here: Eq. (29) only applies to a hypothetical reversible process of pore emptying. Such a process is difficult to envisage for spheroidal pores, where 'bottle-neck' effects seem to be inherent to the model. For the present we will neglect this difficulty and assume evaporation to be controlled by thermodynamic rather than mechanistic factors].

Cumulative surface areas for the model of tubular pores may now be calculated in a manner exactly analogous to that just discussed for cylinders, with the aid of the equation

$$S_k = \frac{3\, r_k^2}{(r_k - t_{r_k,x_k})^3} \left\{ 15{\cdot}47 \Delta V_a - \sum_{i=1}^{k-1} \frac{S_i}{3 r_i^2} \left[(r_i - t_{r_i,x_k})^3 - (r_i - t_{r_i,x_{k-1}})^3 \right] \right\} \qquad (30)$$

Eq. (30) may be applied to the adsorption branch in combination with pore radii r_k found from combination of the Eqs. (28) and (17). The physical significance of applying Eq. (30) to the desorption branch of the isotherm, where r_k is calculated from Eqs. (29) and (17), is, that we suppose 'bottle-neck' effects to be absent during desorption. In applying the spheroidal pore model to the adsorption- and desorption-branch of the isotherm, it is found that the resulting cumulative surface areas are of the same order of magnitude as the ones found before for the model of tubular pores (see *Table 3*).

The procedures just discussed have been applied to a large number of isotherms with approximately A-type hysteresis-loops[27]. In general, it is found that cumulative surface areas from the adsorption-branch as well as from the desorption-branch, each with its proper choice of pore radii, are well in agreement with each other and with BET surface areas if *no* micropores are present and with S_w-values as derived from the *t*-plot if micropores are also present. On the other hand, neglect of the free energy of adsorption contributions, leads to cumulative pore surface areas which not only are mutually inconsistent, but also higher (often far higher) than the values found from the *t*-plot. As we have discussed in Section 5 it may be expected that the *t*-plot analysis remains approximately valid in intermediate pores, so any serious discrepancy between S_w and the cumulative surface areas points to fallacious cumulative results. In *Table 3* this is illustrated with some more examples of cumulative calculations performed on isotherms published elsewhere. Rijnten[30] prepared a number of porous zirconias by dehydration of hydrous zirconia prepared by precipitation. For preparations formed at temperatures of 390°C and 450°C the nitrogen isotherms show A-type hysteresis-loops. A *t*-plot analysis indicated the absence of micropores. Also in these cases, satisfactory agreement is found between S_{BET}, S_w and the cumulative surface areas obtained from both branches of the hysteresis-loop. Moreover the cumulative surface area distribution functions are mutually consistent, as is shown in *Figure 6* and *Figure 7*.

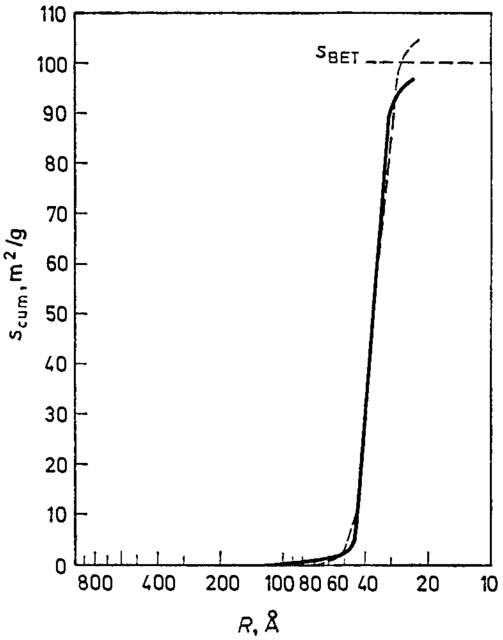

Figure 6. Same as *Figure 5* but for dehydrated zirconia after heat treatment at 390°C.

De Vleesschauwer[31] studied the formation of porous magnesias from magnesite and nesquehonite. At the highest temperatures of decomposition, A-type hysteresis-loops develop. Again, cumulative surface areas are then in reasonable agreement with S_{BET} (and thus with S_w as no micropores are present), as illustrated for one of these samples in *Figure 8*.

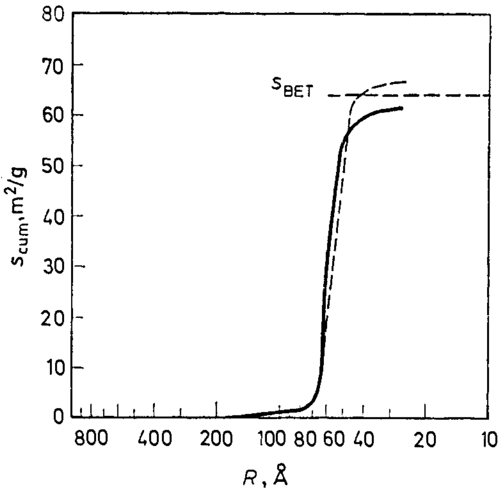

Figure 7. Same as *Figure 6,* but after heat treatment at 450°C.

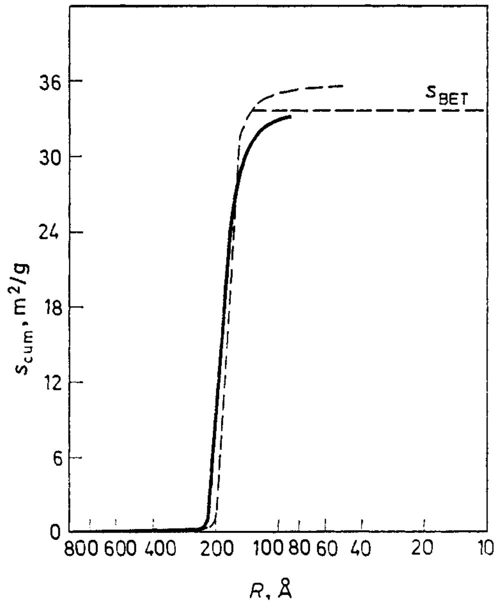

Figure 8. Same as *Figure 5* but for porous magnesia, after sintering at 800°C.

7. INTERPRETATION OF E-TYPE HYSTERESIS-LOOPS

Although A-type hysteresis-loops readily lend themselves to quantitative analysis in terms of simple pore models, the situation is less simple for E-type hysteresis-loops. As we have discussed in Section 3, the E-type hysteresis-loop may be connected with the simple 'ink-bottle' pore model or alternatively, and more generally, with mutual dependence of pores in capillary evaporation and condensation processes[15]. Upward deviations in the t-plot of the adsorption branch, commonly found in E-type hysteresis-loops, indicate that in this case also, the intermediate pores must be described in terms of tubular or spheroidal pores. It is however no longer possible to obtain a consistent interpretation of both the adsorption- and the desorption branch of the isotherm. In the classical 'bottle-neck' theory of hysteresis, the desorption branch may certainly not be used for the calculation of intermediate pore surface areas. In general, it is found that the desorption branch leads to cumulative surface areas which are by far too high, if we suppose the S_t-estimates from the adsorption-branch to be reasonable ones. In many cases, it is found that the adsorption-branch may be used for the estimation of intermediate pore cumulative surface areas, if it is assumed that adsorption here is a *reversible* process, which may be described with Eq. (5). Cumulative surface areas and surface areas from the t-plot then become reasonably consistent. This is in accordance with the work of Kington and Smith[32] who found that for a certain porous glass sample the adsorption-branch is the thermodynamic equilibrium one. In general we should expect along the adsorption branch also, combinations of reversible and irreversible pore filling. In that case neither the adsorption- nor the desorption-branch corresponds to true thermodynamic equilibrium and we should expect cumulative pore surface area distribution curves to be severely distorted. It might be supposed, that the t-plot analysis remains valid for such irregular pore systems, but the cumulative surface areas can no longer be used as an independent check on the S_t-values. Recent scanning studies on A-, E-, and B-type hysteresis-loops, made in this laboratory[33], indicate that A- and B-type hysteresis-loops may be fairly well described in terms of simple models, but that the interpretation of E-type hysteresis-loops is not straightforward.

8. CONCLUDING REMARKS

The t-method of surface area determination was originally intended for the surface area estimation of non-curved adsorbent surfaces only, viz. for the estimation of the total surface area of non-porous solids or the 'external' surface area of micropores solids. The application to systems with slit-shaped pores presents no difficulty, even in the presence of micropores. An alternative method of surface area estimation of intermediate pore surface areas, even in the presence of micropores, is the calculation of 'core' surface areas from the desorption branch of the hysteresis-loop. For slit-shaped pores, 'core' surface areas are directly comparable to pore surface areas. Agreement between S_c (from the desorption branch) and S_w (from the t-plot of the adsorption branch) was found to be satisfactory for a number of typical B-type isotherms. If we had applied the tubular pore model to the desorption branch of *these* isotherms, we would have found considerably higher cumulative surface areas. The conversion of core surface areas to pore surface areas, inherent to the model of tubular pores, leads to an overestimate which must be fallacious for B-type isotherms, where the straight t-plot indicates the absence of any appreciable pore surface curvature. This point is illustrated for the previously discussed examples, in *Table 4*. Indeed, cumulative pore surface areas for B-type isotherms estimated with tubular pore models, are not in agreement with S_w-values.

For A-type isotherms, on the other hand, the upward deviations in the t-plot indicate the occurrence of capillary condensation phenomena, which are probably associated with the existence of curved pore walls. The 'core' surface area is then bound to be lower than the pore surface area. The assumption of tubular (or spheroidal) pores then leads to S_c-values, which are in reasonable agreement with the S_w-values from the t-plot. In this case, both the adsorption- and the desorption-branch may be used. In the absence of any capillary effects, we would expect the S_w-values for pores with curved surfaces to be too low, due to the decrease in adsorption space with increasing layer thickness. As we have shown, capillary effects result in an increase in thickness of the adsorbed layer, which probably roughly compensates the geometrical effect just mentioned, at least for simple pore models. Therefore, it is probable that for tubular (and spheroidal) intermediate pores, the values of S_w as derived from the t-plot in the region before spontaneous pore filling starts, remain valid estimates of the intermediate pore surface areas. Thus a consistent interpretation of A-type isotherms may be based on the simple model of tubular pores. If, on the other hand, we had analysed the desorption branch of the isotherm with the aid of the slit-shaped pore model, then for the reasons just discussed we would have obtained S_c-estimates which were distinctly too low. That this is indeed the case, is illustrated by the examples of *Table 4*.

Table 4. Comparison between cumulative surface areas as calculated along the desorption branch of the isotherm, for the tubular pore model and for the slit-shaped pore model respectively

Sample Code (see tables 1 and 3)	*Shape of hysteresis-loop*	S_w	S_c slit-shaped pores	S_c tubular pores
			(m^2/g)	
graphitic oxide 4H	B	*22·2*	*21·3*	31·9
BoG 580	B	*19·1*	*20·7*	30·6
Pr 21	B	*207*	*213*	294
BoW 450	A	*68·0*	54·3	*65·5*
ZrO_2 390	A	*100*	73·7	*97·6*
ZrO_2 450	A	*64·0*	44·2	*62·0*

A drawback of the present approach is the necessity to assume a discrete pore model. As is illustrated by the given examples, it is indispensable to account for the free energy of adsorption contribution to the condensation- and evaporation-process in calculating cumulative surface areas. This cannot be properly done without assuming a simple pore model. While this procedure is not very satisfactory for E-type isotherms, the analysis of A- and B-type isotherms in terms of simple pore models leads to satisfactory results, enabling the estimation of the total intermediate pore surface area as well as the detailed intermediate pore surface area distribution curve.

References

[1] M. M. Dubinin. *Pure Appl. Chem.* **10**, 309 (1965).
[2] B. G. Linsen. Thesis, Delft, 1964, p. 88.
[3] S. J. Gregg and K. S. W. Sing. *Adsorption, Surface Area and Porosity*, chapter II, Academic Press, London 1967.
[4] B. C. Lippens and J. H. de Boer. *J. Catalysis*, **4**, 319 (1965).

[5] J. H. de Boer, B. G. Linsen, Th. van der Plas and G. J. Zondervan. *J. Catalysis* **4**, 649 (1965).
[6] E. P. Barrett, L. P. Joyner and P. P. Halenda. *J. Am. Chem. Soc.* **73**, 373 (1951).
[7] R. W. Cranston and F. A. Inkley. *Adv. Catalysis* **9**, 143 (1957).
[8] A. V. Kiselev. In *The Structure and Properties of Porous Materials*, p. 130 (D. H. Everett and F. S. Stone, Eds), Butterworths, London 1958.
[9] S. Brunauer, R. S. Mikhail and E. E. Bodor. *J. Colloid Interface Sci.* **24**, 451 (1967).
[10] J. H. de Boer, B. G. Linsen and Th. J. Osinga. *J. Catalysis* **4**, 643 (1965).
[11] J. H. de Boer, B. C. Lippens, B. G. Linsen, J. C. P. Broekhoff, A. v.d. Heuvel and Th.J. Osinga. *J. Colloid Interface Sci.* **21**, 405 (1966).
[12] J. C. P. Broekhoff and J. H. de Boer. *J. Catalysis* **9**, 15 (1967).
[13] D. H. Everett. In *The Structure and Properties of Porous Materials*, p. 95 (D. H. Everett and F. S. Stone, Eds), Butterworths, London 1958.
[14] J. H. de Boer. In *The Structure and Properties of Porous Materials*, p. 68 (D. H. Everett and F. S. Stone, Eds), Butterworths, London 1958.
[15] D. H. Everett. In *The Solid-Gas Interface* p. 1055 Vol. II, New York 1967.
[16] B. V. Deryagin. *Proc. 2nd. Intern. Congr. Surface Activity*, Vol. II, p. 112, Butterworths, London 1957.
[17] J. C. P. Broekhoff and J. H. de Boer. *J. Catalysis* **10**, 391 (1968).
[18] J. J. Steggerda. Thesis, Delft 1955, p. 92.
W. B. Innes. *Analyt. Chem.* **29**, 1069 (1957).
[19] A. B. C. Van Doorn. Thesis, Delft 1957, pp. 63 and 65.
[20] B. C. Lippens. Thesis, Delft 1961, p. 129.
[21] B. G. Linsen. Thesis, Delft 1964, p. 51.
[22] A. G. Foster. *J. Chem. Soc.* 1806 (1952).
[23] J. C. P. Broekhoff and J. H. de Boer. *J. Catalysis* **10**, 153 (1968).
[24] J. H. de Boer, B. G. Linsen, J. C. P. Broekhoff and Th. J. Osinga. *J. Catalysis* **11**, 46 (1968).
[25] J. C. P. Broekhoff and J. H. de Boer. *J. Catalysis* **10**, 378 (1968).
[26] B. V. Deryagin. *Acta Physicochim. U.R.S.S.* **12**, 139 (1940).
[27] J. C. P. Broekhoff and J. H. de Boer. *J. Catalysis* **10**, 377 (1968).
[28] L. H. Cohan. *J. Am. Chem. Soc.* **60**, 433 (1938).
[29] B. C. Lippens. Thesis, Delft 1961, p. 130.
[30] J. H. de Boer. *Proc. British Ceramic Society*, **5**, 5 (1965). H. Th. Rijnten. Thesis, Delft 1969.
[31] W. F. M. N. de Vleesschauwer. Thesis , Delft 1967.
[32] G. L. Kington and F. S. Smith. *Trans. Faraday Soc.* **60**, 705 (1964).
[33] J. H. de Boer, L. F. Brown and J. C. P. Broekhoff, to be published.

DISCUSSION

Professor M. M. Dubinin (*Academy of Sciences of U.S.S.R., Moscow*) said: The paper of Broekhoff and de Boer is of great fundamental importance. It represents a rational synthesis of our conceptions of the distinguishing features of adsorption in micropores and of de Boer's original ideas about polymolecular adsorption in transitional pores with due allowance for the shape of transitional pores. The paper formulates more rigorous methods for determining the specific surface area of transitional pores, presents a further development of the *t*-method and demonstrates its potentialities, for instance in the presence of micropores, i.e. for adsorbents of the micro-transitional-pore type. I agree with the basic propositions of the paper and wish the authors further successes in the development of this fruitful and important line of research.

Professor J. Lyklema (*Agricultural University, Wageningen, The Netherlands*) said: In your derivations you had to assume that—although the chemical potential of the adsorbed material is different from its bulk value—still the bulk value for the surface tension could be used. Would you please comment on these points, especially on the question whether or not you consider them mutually consistent?

Dr J. C. P. Broekhoff replied: The general differential equation for a meniscus at the adsorbed phase- gas interface may be written as:

$$1/R_1 + 1/R_2 = (\mu_a - \mu_g)/(\gamma v_a) \qquad (1)$$

where μ_a and v_a are the chemical potential and the local molar volume of the adsorbed phase, and R_1 and R_2 are the radii of curvature [J. C. P. Broekhoff, Thesis, Delft (1969)]. In general, μ_a and v_a, as well as γ, may be dependent on the distance to the pore surface as well as to some extent at least, on the pore geometry. So, R_1 and R_2 are not constant but dependent on the distance to the pore surface. Eq. (1) may be integrated to yield the shape of the meniscus only if μ_a, v_a and γ are known functions of the distance to the pore surface. Now only μ_a may be experimentally determined as a function of the distance to the pore wall (strictly spoken for infinite wide pores only) from the *t*-curve of multi-molecular adsorption. Nothing is known experimentally about v_a and γ. It has become general practice to assume that v_a is constant and equal to its bulk value at measuring conditions. Both the BET-method of surface area determination and the *t*-plot analysis are based on this assumption. At low layer thicknesses, this assumption probably breaks down. As we have shown elsewhere [J. H. de Boer and J. C. P. Broekhoff. *Proc. Kon. Ned. Akad. Wetenschap.* **B70**, 342 (1967)], the state of the, e.g. the second layer at relative pressures below 0·3 is that of a supercritical 2-D gas. At higher layer thicknesses, the assumption of liquid density may be a reasonable approximation.

The assumption of bulk liquid density is commonly coupled with the assumption of liquid structure for the adsorbed layer. The differences between μ_a and the bulk value of μ for the liquid may then be viewed to result from the potential field emanating from the surface. The assumption of a liquid structure, without any change in density or molecular orientation in the liquid film suggests the assumption of a constant value of γ. Note that this value of γ is distinctly different from the overall value of γ_{sg}, the interfacial tension at the solid–vapour interface. This last value is directly connected with μ_a, and so a function of the thickness of the adsorbed layer. Eq. (10) of our paper may also be derived on basis of γ_{sg}, if it is assumed that merging of the adsorbed layer from opposite walls results in a decrease in free energy, equal to γ times the core surface area.

The actual value of γ, apart from the structure of the adsorbed layer, will also depend on the layer thickness and the curvature of the adsorbed layer. A molecule in the surface of an adsorbed layer has a smaller number of non-nearest neighbours than a molecule in the surface layer of a bulk liquid. T. L. Hill [*J. Am. Chem. Soc.* **72**, 3923 (1950)] estimated this effect to be very small, at least in the case of small drops of liquid, where there is an additional effect of the curvature of the surface. On purely thermodynamic grounds, the influence of curvature on surface tension has been estimated by a number of workers [F. P. Buff. *J. Chem. Phys.* **23**, 419 (1955). F. O. Koenig. *J. Chem. Phys.* **18**, 449 (1950). R. Defay, I. Prigogine and A. Bellemans. *Surface Tension and Adsorption*, p. 258, Longmans, London (1966)]. According to Defay *et al.*, the influence of curvature on surface tension is small for curvatures larger than 100 Å, but becomes appreciable for curvatures of the order of magnitude of 10 Å. According to these authors, the surface tension of water at this curvature has increased by 45 per cent. Now during evaporation from a pore, the curvature of the meniscus has been shown by me (*loc. cit.*) to be maximal in the centre of the pore, and to decrease towards the walls of the pore. Thus, it is possible that the surface tension at the centre of the pore is substantially larger than that in the neighbourhood of the pore walls. This would severely affect the integration of Eq. (1). It is to be noted, that stable capillary condensed liquids during evaporation at relative pressures below 0·4, are never observed in pores smaller than 30 Å. This may be connected with the existence of large negative pressures occurring in such small pores at the centre of the pores. Quantitatively, for pores wider than 30 Å, this increase in surface tension does affect the prediction of pore widths (Eq. 13 of our paper), only to some extent. At a relative pressure 0·5, Eq. (13) predicts a pore width of 34 Å. A rough estimation indicates that an overall increase in γ of 30 per cent leads to an estimation pore width of about 38 per cent, so an increase of only about 12 per cent.

In our opinion, the assumption of liquid density for the adsorbed phase is an even more vital one that the assumption of a constant surface tension. As I have shown before (*loc. cit.*), for a pore system with pores of a radius of 80 Å, the assumption of liquid density for the capillary condensed phase leads to an estimate for the pore volume which exactly equals the pore volume determined from the solid density in combination with imbibition in mercury. At small layer thicknesses, deviations may however become appreciable. The assumption of constant layer density is so vital to the interpretation of adsorption data that it deserves more attention.

ON THE SURFACE OF NON-POROUS AND POROUS ADSORBENTS

M. M. Dubinin

Institute of Physical Chemistry, Academy of Sciences of the U.S.S.R., Moscow

The surface and porosity of adsorbents are not abstract notions. They are expressed in certain values or in the corresponding distribution functions, which, as a rule, cannot be measured directly, but can be calculated by applying theoretical or semiempirical equations to experimental data, usually on adsorption, capillary condensation or mercury penetration. Therefore the physical reality of the calculated parameters of the surface, or porosity, of adsorbents depends primarily on whether the initial premises of the theoretical description of the observed phenomena are true to life. This is determined not only by the degree of approximation of the theoretically adopted model of the phenomenon, but also by the range of applicability of the relevant process mechanism.

VARIETIES OF ADSORBENTS AND SOME OF THEIR PROPERTIES

Irrespective of their chemical nature adsorbents are usually classified as non-porous or porous. The non-porous adsorbents include adsorbents the radii of curvature of whose surfaces are very large and basically tend to infinity. In actual fact, however, in most cases study is made of non-porous adsorbents with a specific surface area of the order of tens m^2/g, which are already highly dispersed solids. Such adsorbents are also regarded as non-porous. A typical example is graphitized carbon black with spherical particles having radii of about 150 Å and a specific surface close to 100 m^2/g.

Adsorbent pores are voids or cavities in solids which usually communicate with each other. Their shapes and sizes differ widely and depend on the nature of the adsorbent and the method by which it is obtained. The linear sizes of pores of any cross-sectional shape are characterized by the ratio of the area of the normal cross section of the pore to its perimeter. This ratio has the dimension of length and is termed the hydraulic radius. Use is usually made of the so-called effective, or equivalent pore radius, r, equal to twice the hydraulic radius.

From the point of view of pore sizes, which essentially determine the mechanism of adsorption and capillary phenomena occurring in them, it is expedient to divide the adsorbent pores into three basic varieties, which are most clearly defined in porous carbonaceous adsorbents with a polymode pore volume distribution according to the effective radii: macropores ($r \gtrsim$ 1000–2000 Å), transitional, or intermediate pores, and micropores ($r <$ 15–16 Å). Classifying the adsorbents proper by the same token, we will have the following structural types of porous adsorbents limiting in the sense of individuality: macroporous, transitional-porous, and microporous. Adsorbents of mixed structural types may contain two or all the three pore varieties, i.e. they may be micro-transitional-porous, macro-transitional-porous, etc. The substantiation of the above classification of pores and porous adsorbents, and numerous examples and methods for determining the parameters of the porous structures of adsorbents are given in the literature[1].

In connection with the use of highly dispersed solids in investigations as non-porous adsorbents the division of the adsorbents into non-porous and porous becomes conventional. Thus, graphitized carbon black with a specific surface area of the order of tens of m^2/g loosely poured into an ampoule of an adsorption unit, or pellets pressed from it, acquire the so-called secondary porous structure formed by the spaces between the contacting particles. Depending on the size of the carbon black particles and the degree of its compaction the effective radii of the secondary pores are of the order of hundreds or even tens of Å near the contacts between particles. As a result the primary phenomenon of vapour adsorption on the surface of the carbon black particles in the region of sufficiently high relative pressures will be complicated by capillary vapour condensation in the secondary porous structure. Therefore the non-porous adsorbents under consideration will not differ in their properties from the adsorbents of the transitional-pore type.

For physical adsorption, two characteristic schemes of the filling of the adsorption field should be considered. The first scheme involves successive formation of adsorption layers, i.e. layer-by-layer coverage of the surface by the molecules adsorbed (monomolecular and polymolecular adsorption). This scheme is valid for adsorbents the radii of curvature of whose surfaces are relatively large compared with the sizes of the molecules adsorbed, i.e. for non-porous, macroporous, transitional-pore and macro-transitional-pore adsorbents. The second scheme involves adsorption in micropores whose linear sizes are commensurable with those of the molecules adsorbed. The whole volume of the micropores is a space in which an adsorption field exists. When dispersion forces predominate the adsorption energy and adsorption potentials in the micropores are substantially higher than for adsorption in large pore varieties. Since there is an adsorption field in the entire micropore volume, the concept of layer-by-layer surface coverage loses its physical meaning. Adsorption in micropores is characterized by the volume filling of their adsorption space (volume filling of micropores). The micropore parameters for carbonaceous adsorbents have been studied[2,3] and the specific features of adsorption in micropores have also been considered in detail[4,5].

SPECIFIC SURFACE AREA OF ADSORBENTS

By definition the specific surface area of an adsorbent is the surface of unit mass. It is usually expressed in m^2/g. At present it is possible to state with full confidence that the concept of specific surface area has a physical meaning only for adsorbents having no micropores, i.e. for non-porous, macroporous, transitional-porous, and macro-transitional-porous adsorbents.

The methods of theoretical analysis of experimental data on adsorption and capillary† phenomena are divided into two groups. The first group includes those which make it possible to determine the amount of substance adsorbed per unit mass of adsorbent necessary for the formation of a continuous monomolecular layer, or the so-called monolayer capacity. The calculation of the specific surface area requires an assumption concerning the area occupied by a molecule in a continuous monomolecular layer, i.e. the magnitude of the 'molecular area'. The methods of the second group lead directly to the determination of the specific surface area of adsorbents.

Let us first consider the principal methods of the first group. If a_m is the capacity of a monolayer in mmol/g, and ω a molecular area in Å^2, the specific surface area of the adsorbent, s, in m^2/g is expressed as

$$s = 6{\cdot}02\ a_m\omega \tag{1}$$

The first approach of Emmett and Brunauer[6] to the evaluation of a_m was based only on general considerations about polymolecular physical adsorption. The characteristic point, B, of the transition of the steep initial section of the isotherm curve for low-temperature adsorption of nitrogen to a flatter, almost rectilinear section, was interpreted as indicative of the formation of a continuous monomolecular layer. This was based on the assumption that the adsorption energy for the first monomolecular layer substantially exceeds the adsorption energy for the subsequent adsorption layers. This semi-empirical approach represented the principal solution. All subsequent development of the method amounted essentially to a more accurate determination of the position of point B.

An important stage in the development of the method for determining a_m was the elaboration by Brunauer, Emmett, and Teller (BET) of the foundations of the theory of polymolecular physical adsorption on homogeneous surfaces[7]. The BET isotherm equation for adsorption in an adsorption space not restricted by walls has two constants, a_m and c. The latter is associated with 'pure' heat of adsorption for the first adsorption layer and the experimental temperature. Later this equation was extended to the case of porous adsorbents (BDDT equation) when adsorption is limited by the formation of n adsorption layers[8]. The BET equation will lead to reliable values of a_m only at the large values of c which are typical of low-temperature adsorption. Due to the greatly simplified adsorption model, thermodynamic functions (heats and entropies of adsorption) calculated on the basis of the BET equation are in semiquantitative agreement with those determined from experimental data. In the general case the BET equation does not yield a quantitative picture of the temperature dependence of adsorption. As a result it rather expresses the analytical method for determining the position of point B[9], i.e. a_m. In this case considerably fewer experimental points of the isotherm are required than for the graphical method of locating point B.

According to the deduction scheme the BDDT equation corresponds to porous adsorbents. In practice, however, its application to low-temperature adsorption of nitrogen on non-porous adsorbents produces values of n from

† Capillary vapour condensation, mercury penetration.

3 to 5, and the range of applicability is considerably broader than with the BET equation[9]. As a result the reliability of determination of a_m is increased, since at $n > 3$ the BET and BDDT equations lead to practically coincident values of a_m. Thus the BDDT equation complements the BET equation in the sense of the analytical method for determining the position of point B[9].

To calculate s by Eq. (1) it is necessary to know the molecular areas, ω, of the substances adsorbed. For molecules of simple substances whose shape is not essentially non-spherical it is usually assumed that the adsorbed molecules have compact hexagonal packing as in bulk solid or liquid phases. The molecular area ω can then be calculated from the density of the bulk phase[10]. For nitrogen at $-196°C$, $\omega_0 = 16{\cdot}2$ Å^2. This value is in good agreement with the data of the independent absolute method of Harkins and Jura[11] and is usually adopted as standard for nitrogen.

Many authors give 'corrected' values of molecular areas, ω, obtained under the assumption that the BET method for low-temperature adsorption of nitrogen at $\omega = 16{\cdot}2$ Å^2 yields correct values of specific surface areas. Then

$$\omega = 16{\cdot}2\,\frac{a_m^0}{a_m} \tag{2}$$

where a_m is the capacity of the monolayer for the adsorbate in hand and a_m^0 for nitrogen. The corrected values so obtained for ω not only differ substantially (up to 45 per cent) from the values of ω even for the simplest substances (Ar, Kr) but also depend on the nature of this adsorbent. Thus, the specific surface areas for 11 samples of various adsorbents determined from adsorption isotherms of n-butane at 0°C with the use of the BET equation and Eq. (1) with $\omega = 32{\cdot}1$ Å^2 are from 0·56 to 1·32 of the values of the specific surface areas of the same adsorbents obtained from low-temperature adsorption of nitrogen[9] at $\omega_0 = 16{\cdot}2$ Å^2.

These deviations may be caused by the chemical or geometrical non-homogenity of the adsorbent surface and by the different orientation of polyatomic molecules, if their shape is essentially non-spherical. In a particular case, a change in the chemical nature of the surface of silica adsorbents can be achieved by partial replacement of hydroxyl groups by other radicals, for instance fluorine atoms. *Table 1* lists the results of our joint experiments with Neimark for an initial uniformly wide-pore silica gel CK, an adsorbent of the transitional-pore type, and for specimens of CK-1 and CK-2 obtained from CK by increasing the degree of chemical modification of the surface by fluorine atoms. The specific surface areas, s, were determined from low-temperature adsorption of nitrogen. For all the substances studied the BET equation was in good agreement with the experimental

Table 1

Adsorbent	S (m^2/g)	S' (m^2/g)	ω, Å^2		
			Ar, $-196°C$	C_6H_6, 20°C	H_2O, 20°C
CK	326	338	17·6	52·7	31
CK-1	276	283	18·4	136	72
CK-2	236	293	18·8	292	93

adsorption isotherms in the usual range of equilibrium relative pressures. In passing from CK to CK-2, the constants c remained practically unchanged for argon and benzene, but increase for water. The molecular areas, ω, were calculated by Eq. (2); s' denotes the specific surface areas of adsorption films calculated by Eq. (5) from the desorption branches of capillary condensation of cyclohexane at 20°C.

According to *Table 1*, ω is practically constant for non-specific adsorption of Ar. For specific adsorption of benzene and water the molecular areas increase abruptly with progressing chemical modification of the silica gel surface. These experiments are of basic importance. They indicate that the concept of the molecular area has two different limiting meanings. In the case of relatively weak localization on the surfaces of adsorbed molecules, such as nitrogen and argon the calculated values of a_m correspond to continuous monomolecular layers. In this case the molecular areas are determined by the sizes of the molecules adsorbed. In specific adsorption, for instance, of benzene or water, the more widely spaced active centres of the surface, i.e. hydroxyl groups remaining unsubstituted by fluorine atoms, exhibit a stronger effect of molecule localization. In this case molecular areas calculated from the experimental values of a_m essentially express the average surface of the absorbent per adsorption centre. This explains the considerable increase of the molecular areas of benzene and water calculated from Eq. (2) in passing from CK to CK-2.

Of more approximate nature are the relative methods for determining the specific surface area. These are based on the assumption of the chemical and geometrical identity of the surface of the different adsorbent specimens being studied. This assumption is equivalent to the constancy of c in the BET equation or to the use of its average value. In any version of the relative method use is made of a calibration curve which is constructed from experimental adsorption isotherms of vapour on adsorbent specimens with a known specific surface area, usually determined by the BET method. Kiselev[12] used as a calibration curve the adsorption isotherm $\alpha = f(p/p_s)$ referred to a unit surface area of the adsorbent which he called the absolute curve.

Then for an adsorbent specimen with a specific surface area s the adsorption isotherm will be given by

$$a = sf(p/p_s) \tag{3}$$

de Boer[13], assuming that the molecules in a polymolecular adsorption layer are packed with the same density as in a bulk liquid phase, adopted a calibration curve in the form of the dependence of the average statistical thickness of the adsorption layer, t, on p/p_s. If v is the volume of one millimole of the adsorbate in the bulk liquid phase, then Eq. (3) is reduced to

$$t = \frac{av}{s} = vf(p/p_s) \tag{4}$$

Since according to Eq. (4) the adsorption values, a, for any adsorbent of the type under study with an unknown specific surface area are directly proportional to t, a graph for the dependence of a on t (to each point of the graph there correspond different values of p/p_s) plotted on the basis of the experimental adsorption isotherm. The calibration curve will take the shape of a straight line passing through the origin. The value of s is determined from the angular coefficient of the straight line which is equal to s/v. The t-method was further developed by Sing.[21]

Microporous adsorbents sometimes exhibit formal agreement of experimental adsorption isotherms with the BET or BDDT equation for a relatively small range of p/p_s usually in the region of lower pressures. Since the volume filling of micropores practically occurs at small p/p_s, the calculated values of a_m are close to the limiting adsorption values corresponding to volume filling of micropores[4]. On the other hand, formal geometrical calculation of the values of ω for molecules filling the micropores leads to values which not only differ considerably from ω_0 but also depend on the size of both the molecules and the micropores themselves. The 'specific surface areas' of microporous adsorbents (which often range from 1000 to 2000 m^2/g) estimated with the use of molecular areas ω_0 have no physical meaning, nor has Eq. (1) which served for their estimation.

Real non-porous, even crystalline adsorbents have surface defects which often reach molecular dimensions. Such geometrical surface inhomogeneities can be regarded as relatively shallow 'surface' micropores. In analysing adsorption isotherms of nitrogen at $-196°C$ and those of water at 25°C on crystalline powder of pure rutile by the use of the t-method it was shown[14] that the straight lines $a = \varphi(t)$ cut short intercepts on the y-axis which correspond to a surface micropore volume of about 0·004 cm^3/g filled in the region of considerably smaller p/p_s. In spite of the smallness of this volume of micropores, their presence resulted in a 22 per cent increase in the specific surface area being determined and impaired the accuracy of the linear form of the BET equation. The filling of surface micropores by preadsorbed water led to a clearly defined picture of polymolecular adsorption of nitrogen on a geometrically uniform surface. On the whole methods of this group are characterized by conventional results. More reliable and coinciding data (provided micropores are practically absent in the adsorbent) can be obtained from isotherms of non-specific adsorption of nitrogen, argon or krypton vapours due to dispersion interaction. The experimental conditions should ensure considerable values of the constant c (relatively low temperatures, and substantial differences in the energies of adsorbate–adsorbent and adsorbate–adsorbate interaction).

The methods of the second group make it possible to determine, not the specific surface area of the adsorbent proper, but the specific surface area of the adsorption film. For non-porous and relatively large-pore adsorbents (macro and transitional-pore adsorbents with effective pore radii of at least 30–40 Å) these specific surface areas practically coincide. The basic idea of these methods consists in direct determination or calculation from experimental isotherms or vapour capillary condensation of changes in enthalpy or free energy as a result of the disappearance of the adsorption film surface on application of a liquid or on volume filling of the pores by the capillary condensation mechanism. In principle, these methods are applicable to non-porous, macroporous and transitional-pore adsorbents for which the adsorption layer concept has a physical meaning.

The absolute method of Harkins and Jura[11] is based on the previous formation on the surface of non-porous dispersed bodies of thick adsorption layers as a result of vapour adsorption at high relative pressures and on the subsequent calorimetric determination of the heat of wetting. The quotient of the heat of wetting by the total surface energy of the liquid expresses the specific surface area of the adsorption film, s'. This method should be used with care for highly dispersed non-porous bodies because of the possible capillary condensation in the secondary porous structure of the powder during the formation of thick adsorption layers on its surface. If this is controlled then the absolute method leads to specific surface areas, s', in good agreement with s determined by the BET method from low-temperature adsorption of nitrogen. In principle, the absolute method makes it possible to determine the specific surface area of transitional pores and macropores in adsorbents containing any volume of micropores which are filled completely during the formation of adsorption layers in transitional pores and macropores.

The thermodynamic principles of calculating s' from the isotherm of capillary vapour condensation date back to Hückel[15]. The method was formulated[16,17] and refined by Kiselev[18]. The differential molar work of adsorption, A, of the vapour of a substance whose initial state corresponds to saturated vapour at a temperature T is expressed by $A = RT\ln p_s/p$. The quotient of the integral work of vapour adsorption in the adsorption value range from the beginning of capillary condensation, a°, up to its completion, a_s, at $p/p_s = 1$ divided by the free surface energy of the adsorption film, σ, expresses the specific surface area of the adsorption film in transitional pores which disappears as a result of the filling of the total pore volume:

$$s' = \frac{1}{\sigma}\int_{a^\circ}^{a_s} A\,\mathrm{d}a \tag{5}$$

According to Bering *et al.*[19] the beginning of capillary condensation corresponds to the filling of pores with effective radii of 15–16 Å, i.e. at the lower limit of applicability of the Kelvin equation. The assumption adopted in deducing Eq. (5) to the effect that σ coincides with the corresponding value for a bulk liquid phase to a satisfactory approximation is valid only when the number of adsorption layers, n, is equal to or more than 3. At $n = 2$, σ is about 30 per cent higher for a film than for a liquid. Recently Rusanov[20], using a more rigorous thermodynamic analysis, confirmed the indicated evaluation of deviations of σ for thin adsorption films. He also showed that the concept of the practical constancy of the surface tension for concave liquid menisci, as contrasted to convex ones, can be extended to the region of considerably smaller curvature radii; this favours the applicability of the Kelvin equation for description of capillary vapour condensation in transitional pores with small effective radii[20].

Despite the rather crude assumption, s' calculated by Eq. (5) for the example of a uniformly wide-pore silica gel from capillary condensation isotherms of various vapours are in satisfactory agreement with the specific surface area of the adsorbent determined from low-temperature adsorption of nitrogen by the BET method[18]. There is less agreement for fine-pore silica gels containing substantial micropore volumes[1].

The specific surface area of macropores and of part of the transitional pores being filled can be evaluated from experiments on mercury penetration. It is easy to show that

$$s = \frac{1}{\sigma \cos\theta} \int_0^V P \mathrm{d}V \tag{6}$$

where V is the mercury-filled pore volume at a hydrostatic pressure P, σ the surface tension of mercury, and θ the contact angle. This method is particularly convenient in investigating macroporous adsorbents and catalysts with a specific surface area of several m^2/g. On the other hand, if the macropores have narrower entrances as compared with the voids, i.e. if they are bottle-shaped, the values assessed from Eq. (6) may be considerably overstated[1].

In this paper we have described and discussed the most widespread methods for determining or estimating specific surface areas of adsorbents. In view of the lack of space we could not even mention more specific methods or less substantiated modifications of the basic methods. In spite of a certain conventionality, each of the basic methods, with a rational choice of objects and conditions of investigation, leads to sufficiently satisfactory and reproducible results. Particular attention in our discussion was given to reasonable limits of applicability of each method when the results obtained have a physical meaning. In the author's opinion the main trouble is the loose extension of the methods to adsorbents of incompatible structural types or to the region of experimental parameters where the starting premises of theoretical models underlying the methods clearly cease to apply.

References

[1] M. M. Dubinin. *Adv. Colloid and Interface Sci.* **2**, 217 (1968).

[2] M. M. Dubinin, G. M. Plavnik and E. D. Zaverina. *Carbon* **2**, 261 (1964).

[3] M. M. Dubinin and G. M. Plavnik. *Carbon* **6**, 183 (1968).

[4] M. M. Dubinin. *J. Coll. and Interface Sci.* **23**, 487 (1967).

[5] M. M. Dubinin. *Chemistry and Physics of Carbon*, Vol. 2, p. 51, Marcel Dekker, New York (1966).

[6] P. H. Emmett and S. Brunauer. *J. Amer. Chem. Soc.* **59**, 1553 (1937).

[7] S. Brunauer, P. H. Emmett and E. Teller. *J. Amer. Chem. Soc.* **60**, 309 (1938).

[8] S. Brunauer, L. S. Deming, W. E. Deming and E. Teller. *J. Amer. Chem. Soc.* **62**, 1723 (1940).

[9] D. M. Young and A. D. Crowell. *Physical Adsorption of Gases*, Butterworths, London, 1962.

[10] S. Brunauer. *The Adsorption of Gases and Vapors*, Princeton University Press, Princeton, 1945.

[11] W. D. Harkins and G. Jura. *J. Chem. Phys.* **11**, 430 (1943); *J. Amer. Chem. Soc.* **66**, 919, 1362 (1964).

[12] A. V. Kiselev, *The Structure and Properties of Porous Materials*, p. 195, Butterworths, London (1958).

[13] B. C. Lippens and J. H. de Boer. *J. Catalysis* **4**, 319 (1965).

[14] R. E. Day and G. D. Parfitt. *Trans. Faraday Soc.* **63**, 708 (1967).

[15] E. Hückel. *Adsorption und Kapillarkondensation*, A. V., Leipzig, 1928.

[16] S. S. Kistler, E. A. Fischer and I. B. Freeman. *J. Amer. Chem. Soc.* **65**, 1909 (1943).

[17] E. N. Harvey. *J. Amer. Chem. Soc.* **65**, 2343 (1943).

[18] A. V. Kiselev. *Proc. of the Second International Congress of Surface Activity*, Vol. 2, p. 189, Butterworths, London (1957).

[19] B. P. Bering, M. M. Dubinin and V. V. Serpinsky. *J. Coll. and Interface Sci.* **21**, 378 (1966).

[20] F. M. Kuni and A. I. Rusanov. *Phys. Letters* **25A**, 577 (1967); **26A**, 577 (1968).

[21] S. J. Gregg and K. S. W. Sing, *Adsorption, Surface Area and Porosity*, Academic Press, London, New York, 1967.

DISCUSSION

Professor M. M. Dubinin (*Academy of Sciences, Moscow*) said: Since the complete text of my paper is in the possession of the members of the Symposium I will avail myself of the time accorded to me to make an addition of radical importance for the conception of adsorption in micropores.

In the general case real porous adsorbents may contain three varieties of pores: micropores, transitional or intermediate pores and macropores. The concept of transitional pores is associated with the occurrence on their surface of mono- and polymolecular adsorption and their subsequent volume filling in the region of higher relative pressures according to the capillary condensation mechanism. A question of principle arises as to the lower limit for the linear dimensions of transitional pores, i.e. their effective radii, which are equal to the doubled hydraulic radii of the pores. This problem has been considered in a work performed by B. P. Bering, M. M. Dubinin and V. V. Serpinsky [*J. Coll. Interface Sci.* **21**, 378 (1966)].

Under conditions of complete wetting, the following expression may be written in accordance with the Kelvin equation for a spherical meniscus of radius r:

$$A = RT \ln p_s/p = 2\sigma v/p \tag{A}$$

where A is the differential molar work of adsorption ($A = -\Delta G$; G is Gibbs free energy), σ is the surface tension and v is the molar volume of the adsorbate. At a constant degree of filling of the sorption space, i.e., at av = constant, the radius of curvature of the meniscus is also constant, i.e., r = constant, and therefore

$$\left(\frac{\partial A}{\partial T}\right)_{av} = \frac{2}{p}\left(\frac{\partial \sigma v}{\partial T}\right)_{av} = A\left(\frac{\partial \ln \sigma v}{\partial T}\right)_{av} = A\frac{\mathrm{d}\ln \sigma v}{\mathrm{d}T} \tag{B}$$

We also assume that in the region where the Kelvin equation (A) is valid, the temperature coefficient of the product σv for liquid in capillaries is equal to the corresponding coefficient for bulk liquid.

As is well known, the product σv for liquids is a decreasing function of temperature, i.e.

$$\frac{\mathrm{d}\ln \sigma v}{\mathrm{d}T} = K(T) = \frac{\mathrm{d}\ln \sigma}{\mathrm{d}T} + \frac{\mathrm{d}\ln v}{\mathrm{d}T} < 0 \tag{C}$$

and therefore

$$\left(\frac{\partial A}{\partial T}\right)_{\mathrm{av}} = A\frac{\mathrm{d}\ln \sigma v}{\mathrm{d}T} = AK < 0 \tag{D}$$

From Eq. (D) it follows that the derivative $\mathscr{P} = (\partial A/\partial T)_{av}$, in a region where the Kelvin equation is valid for capillary condensation, should be proportional to A. *Figure A* exhibits the dependence of $\mathscr{P}$ on A plotted from the desorption branch of the isotherm for the case of adsorption of benzene on silica gel [S. Z. Muminov, B. P. Bering and V. V. Serpinsky. *Izv. Akad. Nauk. SSSR, Ser. Khim.* No. 1, 43 (1966)]. In the temperature interval studied the value of σv for benzene decreases linearly with T and K being equal to $-$ 0·0041 deg^{-1}. The straight line OK in *Figure A* is drawn at a theoretical slope equal to K. It is evident from the figure that as A grows, the experimental values of the derivative $\mathscr{P}$ first fall on the line OK, and then, in the vicinity of point K sharply deviate from this line upwards and pass into the region of positive values. In the same figure values of r, calculated from Eq. (A), are also plotted along the axis A. The point K lies approximately at 15–16 Å, and defines the lower limit of the values of r below which the

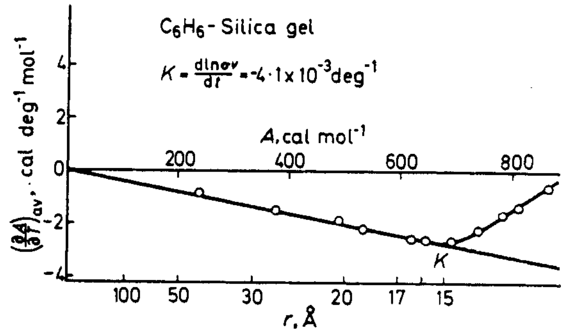

Figure A. Dependence of P on A in the case of adsorption isotherm of benzene on silica gel

Kelvin equation is evidently invalid. Similar results have been obtained from Lambert and Clark's experiments [B. Lambert and A. M. Clarke. *Proc. Roy. Soc.* **A122**, 497 (1929)] for capillary condensation of benzene on ferric oxide-gel (*Figure B*). Thus, the curves of *Figures A and B* are especially remarkable in that they make possible purely thermodynamical determination of the lower limit radius r of the applicability of the Kelvin equation.

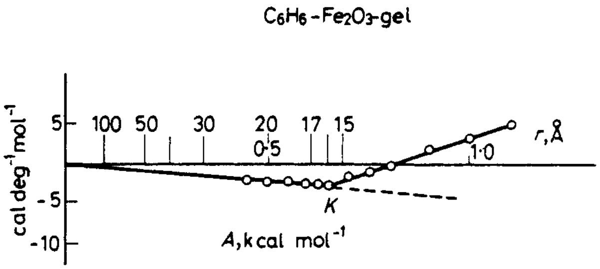

Figure B. Lambert and Clark's experiments for capillary condensation of benzene on ferric-oxide gel

Proceeding from the foregoing considerations the lower boundary of the effective radii of transitional pores has been set at about 18–19 Å. It corresponds to effective meniscus curvature radii of about 15–16Å or to a characteristic equilibrium relative pressure of 0·24 for the standard vapour–

benzene. The respective characteristic relative pressures for nitrogen and water are 0·53 at − 196°C and 0·49 at 20°C.

In joint investigations with G. M. Plavnik with the use of an independent method of small-angle scattering we have determined the effective radii or radii of inertia of the micropores of carbonaceous adsorbents [M. M. Dubinin and G. M. Plavnik. *Carbon* **2**, 261 (1964); **6**, 183 (1968)]. For the majority of active carbons characterized by a narrow distribution of micropores they were within the range from 5 to 7 Å. At high degrees of activation, however, active carbons exhibited a wider distribution of micropores in the range of effective radii between 5 and 14 Å. In contrast to the transitional pores, adsorption in micropores is characterized, not by the successive formation of adsorption layers, but by their volume filling.

Thus, the distinction between the micropores and transitional pores is drawn on the basis of the different mechanisms of the sorption processes occurring in them.

Professor R. Sh. Mikhail (*Ain Shams University, Cairo*) said: The contradictory statements made by Professor Dubinin and Professor Brunauer regarding the mechanism by which micropore filling takes place is of special interest to most of us, and I am going to report to this symposium some of the results we obtained recently in our laboratories. These will show that both the volume filling mechanism of Dubinin and the surface coverage mechanism of Brunauer are not quite satisfactory when being dealt with separately, and micropore filling takes place through both volume filling as well as surface coverage. As a matter of fact it is very hard to imagine volume filling taking place without surface coverage. However, applying the BET equation to the adsorption in narrow pores, as well as on plane surfaces needs a knowledge of the area occupied by a single molecule on the surface. This in itself is a major problem because this means that the BET method uses only one parameter of the molecule which is the area in contact with the surface. For adsorption on plane surfaces, or for the adsorption of nearly spherical molecules in different pores this does not seem to be a serious problem. But for non-spherical molecules, this area depends on the actual orientation on the surface, and in narrow pores, where the opposite wall field effect is stronger than on plane surfaces, this orientation is more likely to occur. Apparently, therefore, the use of a wrong molecular area due to this effect, will vitiate the computation of the surface area in narrow pores.

On the other hand, the second parameter of the molecule, namely its thickness on the surface, finds its means of evaluation through the use of the V_{1-t} plot of de Boer *et al.* The surface area obtained from the BET (S_{BET}) equation will coincide with the surface area obtained from the V_{1-t} plot (S_t) only if the orientation of non-spherical molecules is properly deduced.

Even for spherical or nearly spherical molecules, then packing might change more in narrow pores than on a plane surface, and S_{BET} will agree with S_t when the correct packing is assumed.

It is evident therefore that a combination of both the BET method, which deals with one parameter of the molecule, and the V_{1-t} plot, which deals with its other parameter of the molecule, might lead to a better understanding of the mechanism of adsorption particularly in narrow pores.

We measured the adsorption of two non-spherical molecules, namely benzene and cyclohexane, and two nearly spherical molecules, namely carbon tetrachloride and isopropanol on the narrow pore silica gel Davidson O3.

Table A. BET *c* constants and V_m values calculated for the adsorption of benzene, cyclohexane, isopropanol and carbon tetrachloride

Adsorbate	BET *c constants*	V_m *value* (g/g)
Benzene	21	0·2274
Cyclohexane	17	0·1988
Isopropanol	29	0·1667
Carbon tetrachloride	89	0·4444

In *Table A* we summarized the V_m BET values obtained by the use of the four vapours, as well as their BET '*c*' constant. For the two non-spherical molecules, benzene and cyclohexane, *Table B* shows that S_{BET} agrees with S_t fairly well only when the molecular areas as well as their thicknesses are calculated on the basis of a vertical orientation on the walls of the pores. In the same table, the surface areas were also evaluated by a completely independent method which is Kaganar's method, shown as S_K, which also shows excellent agreement with S_t and S_{BET}. It is worth mentioning that the agreement between S_t and S_{BET} is not only valid internally for one and the same adsorbate, but between both adsorbates as well.

Table B. Surface area of silica gel Davidson 03 from benzene and cyclohexane adsorption

Adsorbate	*Orientation*	a(Å^2)	S_{BET}(m^2/g)	σ(Å)	S_t(m^2/g)	S_k(m^2/g)	*c* (non-porous)
Benzene	vertical	25	438·0	5·9	460·0	451·6	4–58
	flat	42	721·0	3·6	1140·0		
Cyclo-hexane	vertical	30	429·0	6·0	420·0	418·7	3–18
	flat	39	524·8	4·6	780·0		

For the other two nearly spherical molecules namely carbon tetrachloride and isopropanol, *Table C* shows that both vapours can give the same surface areas obtained from cyclohexane and benzene when the right packing factors are chosen for them. It is worth mentioning that a low packing factor (for carbon tetrachloride) assumes a denser mode two dimensionally than three dimensionally, as should be expected to be the case for the adsorption in narrow pores due to the opposite wall effect.

Table C. Surface area of silica gel Davidson 03 from isopropanol and carbon tetrachloride adsorption

Adsorbate	*Packing factor*	a(Å^2)	S_{BET}(m^2/g)	σ(Å)	S_t(m^2/g)	S_k(m^2/g)	*c* (non-porous)
Isopropanol	1·091	27·7	444·2	4·6	400·0	466·1	2–145
Carbon tetra-chloride	1·091	30·0	524·0	5·2	508·0	515·2	4–32
	0·866	25·0	438·5	6·3	436·0		

In *Figure C*, benzene is taken as an example to show the steric effects which might lead in very narrow pores to its orientation with its larger axis being parallel to the surface, and as soon as the pore becomes wide enough to accommodate the molecule perpendicular on the surface it will acquire that position. However, in pores with radii wider than 2–3 layers on the surface it is most likely that the molecule will lie flat again on the surface. The figure is drawn to scale, and in our opinion the definition of the term 'narrow' and 'wide' is definitely connected to the size of the adsorbate molecule. A pore which is considered as 'narrow' to cyclohexane or benzene might behave as wide to nitrogen or water. However, if this representation shown in *Figure C* is near to what actually happens in a range of narrow pores, then it would mean that the area occupied by a single molecule on its surface is variable in a wide range, and would actually show a minimum as represented in *Figure D*. The same effect was noticed by Kiselev, and was shown in the 1958 Symposium in Bristol.

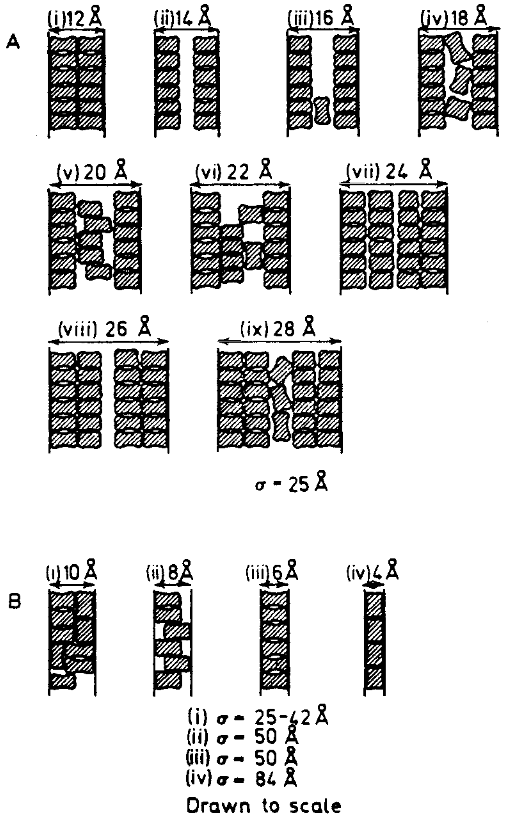

Figure C. Orientation of benzene molecules in micropores

It is mentioned here that the opposite wall effect which would lead to the orientation of the benzene molecule vertically on the surface might extend to 2–3 layers on the surface. The evidence for this was obtained by studying the adsorption of benzene on two other silica gels, silica gel Davidson 81, and silica gel Davidson 59. Their pore volume distribution analysis curves are shown in *Figure E*. For Davidson 81, the most frequent size of pores lies at a value of 18–19 Å, and for this silica gel the evidence was collected to the effect that the benzene molecule still occupies a vertical orientation on the surface. For the other silica gel which contains much wider pores, the evidence is in favour of the benzene molecule lying flat on the surface. These results will shortly be published in more detail in the *Journal of Colloid and Interface Science*.

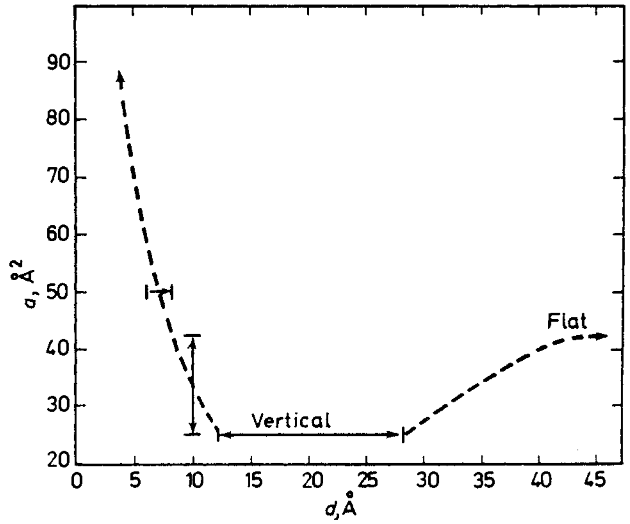

Figure D. Apparent area per benzene molecule as a function of the pore-width

Finally, I would like to comment on Professor Dubinin's criticism on the MP-method for micropore analysis. Apparently his criticism is valid, and it is true that whatever the slope of the straight line of the V_{l-t} plot is, one should expect S_{cum} to agree with S_t. However, two other points strongly support the validity of the MP method for use in narrow pore analysis: (a) that in the MP method, the surfaces are merely used to calculate the volumes of the specific groups of pores of known width. This would lead to the direct conclusion that the criterion of the argument between V_{cum} and V_p is still valid as shown before in the original paper, and as is shown here in *Table D*. (b) I wish also to point to the fact that if one uses different adsorbates of different sizes, shapes and characteristics, and still get the same surface volume and pore sizes (cf. *Table D*), then this by itself stands in favour of the MP method.

I do agree with Professor Dubinin that the agreement between S_{cum} and

S_t should not be taken as a criteria for the correctness of the analyses, but this in itself does not disprove the validity of the MP method for micropore analysis.

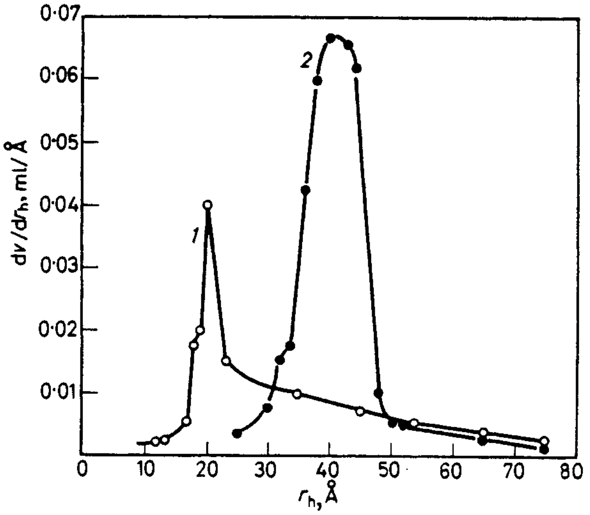

Figure E. Pore volume distribution curves of the two wide-pore silica gels [*1*, Silica gel Davidson 81 based on parallel plate model; *2*, silica gel Davidson 59 based on parallel plate model].

Table D. The cumulative surface and cumulative volume of silica gel Davidson 03

Adsorbate	S_t(m^2/g)	S_{cum}(m^2/g)	Vp(ml/g)	V_{cum}(ml/g)
Benzene	460	457	0·3336	0·3382
Cyclohexane	420	415	0·3306	0·3262
Isopropanol	400	390	0·3355	0·2997
Carbon tetrachloride	436	432	0·3193	0·3365

Dr S. J. Gregg (*Brunel University, London*) said: I have some confirmatory evidence as to the effect of the presence of micropores on the adsorption isotherm.

If a solid possesses both micropores and an appreciable external surface, the experimental isotherm will represent the sum of two individual isotherms, a Type I corresponding to the micropores and a Type II corresponding to the external surface; it will therefore also be a Type II isotherm but with a steep initial portion. To test this view Dr Langford working in my laboratory took a carbon black with an external area known from electron microscopy and produced micropores in it by high temperature oxidation [S. J. Gregg and J. F. Langford. *Trans Faraday Soc.* **65**, 1394 (1969)]. He then determined the isotherms of nitrogen at — 195° (a) after outgassing at 1000° (Curve E†); (b) after outgassing, exposing to nonane vapour at

---

†For Curves A—E see *Figure 2* in *Trans. Faraday Soc.* **65**, 1394 (1969)

− 195° to fill up the micropores and pumping off the excess (Curve A); (c) after progressively emptying the pores of nonane by pumping at elevated temperature (Curves D, C and B). In the region to the right of point B the graphs are all parallel and the isotherm E corresponding to filled micropores gives a BET area in agreement with the geometrical area. It seems clear therefore that this part of all the isotherms corresponds to multilayer formation and the vertical separation of Curves A and E to the micropore contribution.

The heat of adsorption should be noticeably higher in the micropore than on the open surface. Mr Diano, working with me, has demonstrated that this is so for hexane by calculating the heat of adsorption from measurements of the heat of immersion in hexane of samples of the black charged with different amounts of hexane (as in the paper by Goodman and collaborators See p. 299). The adsorption isotherm of hexane, measured in a separate experiment, was of Type II with a steep initial rise. The differential heat of adsorption was much higher in this region.

Professor D. H. Everett (*University of Bristol*) said: In Professor Dubinin's paper micropores are defined as those whose radii are less than 15–16 Å. This is the same as the lower limit set for the onset of capillary condensation and for the applicability of the Kelvin equation; and it is also the point from which the integration of equation (5) begins. Attempts have been made to understand the factors which determine this limit. Dubinin and Kadlec in a paper which, I understand, is in the process of publication†, discuss the possibility that one reason, or perhaps *the* reason why the Kelvin equation breaks down is that in pores of a certain critical size the negative pressure or tension within the liquid exceeds the tensile strength of the liquid. Capillary condensation and the associated hysteresis effects cannot then occur in pores smaller than this size. It is argued, on the basis of a rather crude theory of intermolecular forces in liquids, that this radius should be approximately independent of adsorbate and independent of temperature. Mr Burgess at Bristol has adopted a somewhat different approach, namely that of calculating the critical tension in the liquid directly from the closure point of the hysteresis loop. The Kelvin equation is not used as such: the lowering of hydrostatic pressure in the liquid is estimated from the observed decrease in its vapour pressure. We were particularly interested to see how this limiting tensile strength depended upon temperature and upon the substance concerned. To make a comparison between various substances, it is convenient to plot the critical tension (or the tensile strength) divided by the critical pressure of the material concerned as a function of the reduced temperature. The figure shows the available data calculated from published isotherms where closure points have been determined with adequate precision. Unfortunately only a small range of T/T_c is covered because most work has been done between the melting point and the boiling point of the adsorptive, but the somewhat scattered points indicate that there is a relationship between these quantities. One possible interpretation of the critical tensile strength is to identify it with the depth of the minimum of an equation of the van der Waals type for

---

† now published: O. Kadlec and M. M. Dubinin, *J. Colloid Interface Sci.*, **31**, 479 (1969).

the substance concerned. From a known or assumed equation of state, such as the van der Waals equation, one can calculate the dependence of τ/p_c on T/T_c. The curves corresponding to the van der Waals equation, the Berthelot equation, and a modified van der Waals equation which, according to E. A. Guggenheim (*Thermodynamics*, 5th Edn., p. 142, North Holland Pub. Co., Amsterdam, 1967), fit real liquids rather well, are shown in *Figure F*.

The data are not very extensive. They are derived from experiments which were not primarily designed to locate the closure point of the hysteresis loop, but they cover a wide range of substances from argon to pentane, hexane, benzene and so on. They all fall quite close to the line corresponding to the modified van der Waals equation and it seems that this interpretation of the lower limit of capillary condensation at least makes sense. What we now need of course are data at higher temperatures. Such measurements are being made in various laboratories and it will be interesting to attempt to interpret them in this way. It so happens of course that in the lower range of temperatures the radii corresponding to the critical tensions are in the range 12 to 15 Å and in effect this represents the empirical division between micro- and meso-pores; but at higher temperatures the critical radii will be much higher.

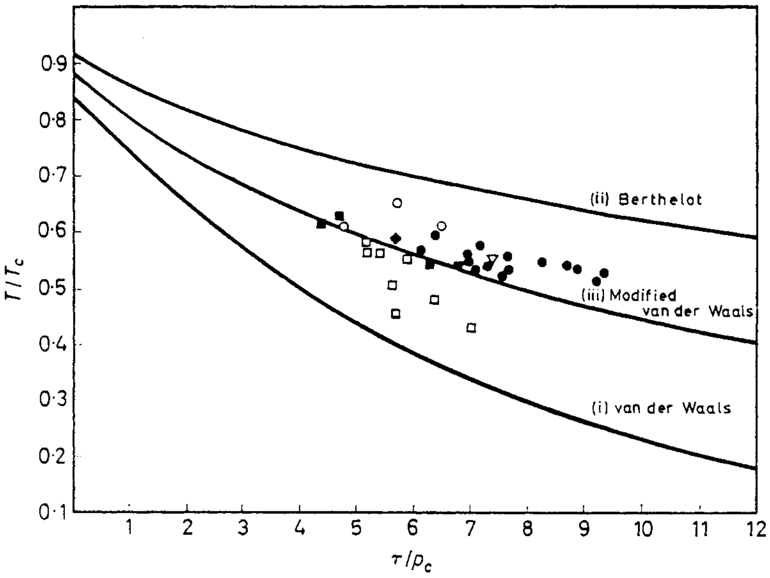

Figure F. Limiting tensile strength divided by critical pressure as a function of reduced temperature for various substances. Curve (i) according to the van der Waals equation; (ii) according to the Berthelot equation; (iii) according to Guggenheim's modification of the van der Waals equation [● benzene; ○ 2,2-dimethylbutane; ■ nitrogen; □ xenon; ▲ cyclohexane; △ 2,2,4-trimethylpentane; ♦ n-hexane]

ON THE APPLICATION OF THE t–PLOT METHOD TO REAL MICROPOROUS SYSTEMS

A. P. Karnaukhov

Institute of Catalysis, Novosibirsk, U.S.S.R.

As I see it, the *t*-plot method is based on an ideal model of adsorption on the surface, which either does not restrict the amount adsorbed or restricts it step by step. I think that this condition is mainly satisfied in macro- and transitional-porous systems or in the case of solids with slit-like pores of one or several sizes. There are many real microporous systems for which this assumption does not apply. If the slit-like pores have numerous different sizes then the *t*-curves, as shown in *Figure 1*, have no linear section. With Professor Kiselev[1] we studied globular systems with very small particles and high packing density, e.g. microporous silica gel, in which the exposed surface was reduced during adsorption. The sorption isotherm of the type shown in *Figure 2* would have a corresponding *t*-curve of the shape shown in *Figure 1*.

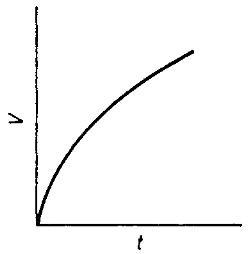

Figure 1

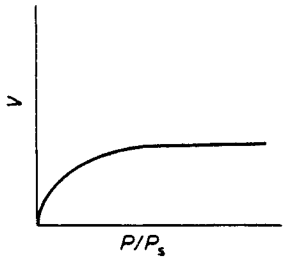

Figure 2

In our laboratory we have also studied the adsorption of benzene on alumina samples and applied the *t*-method to these data[2]. The *t*-curves were again non-linear as shown in *Figure 1*. We explained this by the presence of slit-like pores of different sizes.

Probably, for very many microporous systems the *t*-plot method cannot be applied because of the effect of restriction of the exposed surface area as the adsorption process proceeds. Possibly an exception exists with solids containing narrow cylindrical pores, for which a restriction of the surface area of the adsorbed film is more or less compensated by the greater thickness of the film in the pore as compared with the film thickness on a non-porous adsorbent at the same *p*/*ps* values (*Figure 3*). For such systems the *t*-curves are very likely close to a straight line.

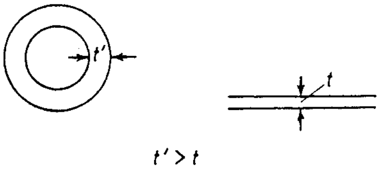

Figure 3

References

[1] A. P. Karnaukhov and A. V. Kiselev. *Zh. fiz. chimii.* **34**, 2176 (1960); **43** (1969), to be published.

[2] K. G. Ione and A. P. Karnaukhov. *Kinetike i kataliz*, to be published.

THE EFFECT OF SUBSTRATE HETEROGENEITY ON THE DETERMINATION OF SURFACE AREA BY GAS ADSORPTION

SYDNEY ROSS

Rensselaer Polytechnic Institute, Troy, New York, U.S.A.

The theory on which the BET determination of surface area is based does not take into account any heterogeneity of the substrate. In fact, as with the theory of the Langmuir equation, which is its source and origin, the substrate is supposed to be energetically uniform. We know, of course, that when one tries to meet the condition of an energetically-uniform solid substrate in actual practice, an S-shaped adsorption isotherm is obtained[1], which cannot be described by the Langmuir equation. On the other hand, when one turns to measurements of the surface tension of solutions, which provide substrates that are undeniably homogeneous, the use of the Langmuir equation to describe the adsorption of the solute is widely accepted, and has recently received the accolade of recognition from the thermodynamic treatment of van den Tempel and his associates[2]. Since this situation is really anomalous it demands discussion and further investigation.

The way in which the Langmuir equation for the adsorption isotherm enters into the description of the surface tension isotherm arose historically with the discovery by von Szyszkowski of the following empirical equation for the surface tension isotherm:

$$\pi = \sigma_0 - \sigma = a \ln (1 + bc) \tag{1}$$

where the lowering of the surface tension of a solution of concentration c is given by $(\sigma_0 - \sigma)$. It was thereafter soon revealed that by introducing Gibbs adsorption theorem in its qualified form, viz.,

$$\Gamma = \frac{1}{RT} \frac{\mathrm{d}\pi}{\mathrm{d} \ln c} \tag{2}$$

where Γ is the Gibbs excess concentration at the surface in moles cm^{-2}, the Szyszkowski equation would yield the Langmuir equation for adsorption:

$$\theta = \frac{\Gamma}{\Gamma_m} = \frac{bc}{1 + bc} \tag{3}$$

The connexion between the empirical von Szyszkowski equation for the surface-tension isotherm and the Langmuir equation for the adsorption isotherm was persuasively presented by Freundlich in his celebrated book *Colloid and Capillary Chemistry*, and was no doubt interpreted by many readers and students to mean that Langmuir's theoretical model of the adsorption equilibrium was applicable to adsorption at a liquid surface. Nevertheless, in a third cognate field of experimental investigation, namely, the measurement of the force–area relations of insoluble monolayers on aqueous substrates, the equations of state that are employed to describe the observed data rarely include the one corresponding to the Langmuir equation, which would be:

$$\pi = \left[\frac{kT}{A_0}\right] \log \frac{A}{A - A_0} \tag{4}$$

Instead of that we have the Volmer equation:

$$\pi(A - A_0) = kT; \tag{5}$$

the van der Waals equation:

$$\left(\pi + \frac{\alpha}{A^2}\right)(A - A_0) = kT; \tag{6}$$

and the Schofield–Rideal equation:

$$\pi(A - A_0) = ikT \tag{7}$$

Equations (5), (6) and (7) all bear obvious analogies to equations of state of non-ideal gases. Equation (5), it is true, when brought into its equivalent form for adsorption expressed as a relation between Γ and c, does resemble the Langmuir equation, but de Boer[3] has demonstrated that one of the constants in the final result does not have the same meaning as it has in the Langmuir equation, so the resemblance is merely accidental. Jura and Harkins[4] have suggested a further number of different equations of state relating π, A, and T for insoluble monolayers, to be applied to the different states of aggregation that they distinguished on the evidence of painstaking measurements of force–area diagrams, but again none of them corresponds to the Langmuir equation. So here is another anomaly that deserves more discussion and investigation.

Part of the mystery is dissipated if we recall another of de Boer's demonstrations, to the effect that *under certain conditions* the two-dimensional van der Waals equation [equation (6)] can be made to coincide with the Langmuir equation. The coincidence pertains to the higher range of monolayer coverage, to values of θ greater than one-sixth to one-third. Here again one of the two constants, namely, the constant that describes the initial slope of the isotherm, which can be directly measured only at very low values of θ, is not the same for the two equations. But if the observed data do not extend to the range of low coverage they could be quite adequately described by the Langmuir equation without any conflict, contradiction, or anomaly being revealed. Now this is precisely the situation with the reported surface tension data for solutions of soaps, detergents, wetting agents and other surface active solutes[5]. The standard free energy change on adsorption out of solution is about 0·7 kcal per carbon atom[6], which gives a total value for a typical solute of about six times that for the adsorption of a gas of low molecular weight on a solid substrate. Only recently have measurements of the surface tension of solutions of surface active solutes been made at concentrations sufficiently dilute to reach the initial linear part of the isotherm, which has received the name of the Henry's law region. Insoluble monolayers of long-chain aliphatic derivatives of 16 to 36 carbon atoms have likewise only rarely been measured in the Henry's law region, where they would be described by the two-dimensional ideal-gas law

$$\pi A = kT \tag{8}$$

When this formidable task was successfully accomplished by Guastalla[7] he received the plaudits of the scientific community. With insoluble monolayers of rigid polycyclic molecules that lie flat on the surface because of two hydrophilic groups located at opposite ends of the molecule, the experimental difficulties are not as great, and Cadenhead and Phillips[8] were able to observe the Henry's-law behaviour of a surface film of estradiol diacetate with relative ease. With adsorption of gases on solids, the attainability of the Henry's law region depends on the degree of substrate heterogeneity: nearly-uniform substrates such as those of graphitized carbon black, boron nitride, alkali-metal halides, and polyurethane foam display Henry's law behaviour at pressures well within the reach of normal high-vacuum apparatus, but a substrate with a wide distribution of adsorptive energies, such as has glass as an adsorbent, may remain outside the best of modern ultra-high vacuum techniques[9]. Thus the three different experimental techniques, though related by a common theory, have not always yielded results that agree, because of the wide variation in the molecular weight of adsorbate best suited for a given approach.

A recent publication of Hauxwell and Ottewill[10] reports the measurement of the surface-tension isotherm of water as a function of the pressure of a gaseous adsorbate of low molecular weight. Similar measurements are also in progress in my laboratory. Gases that are not particularly surface active, such as nitrogen and carbon dioxide, show Henry's law behaviour on adsorption at pressures lower than one atmosphere. But toluene vapour, a much more surface active adsorbate, already shows deviation from Henry's law at a pressure of 2 mm; and the deviation is in a direction that can be ascribed to intermolecular attraction (*Figure 1*). In other words, the adsorption isotherm of the monolayer is S-shaped, just as it is for the adsorption of a low-molecular weight adsorbate such as ethane on graphitized carbon black. This result indicates that to the many known similarities of behaviour of two-dimensional and three-dimensional matter, similarities such as ideal-gas behaviour at low pressures, non-ideal gas behaviour at higher pressures, condensation to a liquid phase, and a critical temperature above which such condensation cannot occur; to all these similarities should be added the phenomenon of the two-dimensional Boyle temperature. Heretofore the negative deviation from ideality of the product πA to values lower than kT has been observed only with gases adsorbed on homotattic solids and with some insoluble monolayers, but not with surface active solutes as measured by the surface tension isotherm. These latter have shown only a positive deviation, and until the occurrence of a negative deviation was observed, either by reducing the temperature or by using an adsorbate of much lower adsorptive potential, the existence of a two-dimensional Boyle temperature for adsorbed solutes had not been demonstrated. But for my present purpose, the point requiring emphasis is that adsorption isotherms that can be characterized as being below the two-dimensional Boyle temperature, i.e. showing a negative deviation from ideality, as demonstrated by their initial convexity to the concentration (or pressure) axis, cannot be described by means of the Langmuir equation, at least at low concentrations. And where the Langmuir equation is employed as a description at higher concentrations it is to be regarded merely as a useful empirical approximation, without any theoretical implications. Logically, the same warning holds when the Langmuir equation is applied to adsorption isotherms above their two-dimensional Boyle temperature, although here the empirical character of the Langmuir description is not as evident.

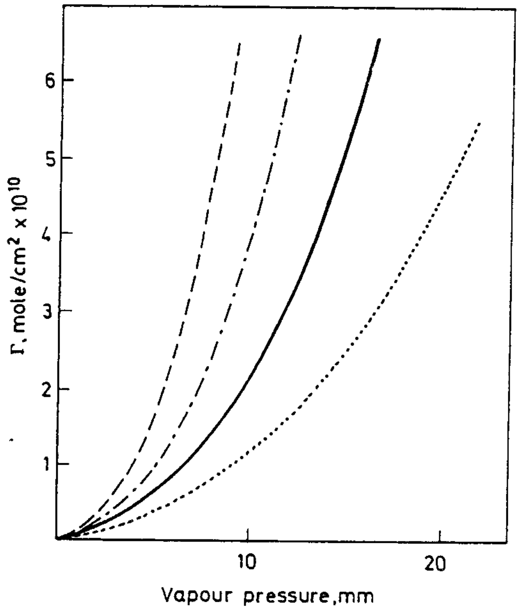

Figure 1. Adsorption isotherms |Γ *vs* p| at temperatures of 5·0, 10·0, 15·0 and 20·0°C for toluene on a water substrate, derived by an application of the Gibbs adsorption theorem to the surface tension isotherm. Data and calculations by Hauxwell and Ottewill[10]

The foregoing considerations are relevant to the question of how we are to construct a theoretical model of physical adsorption that will take into account the heterogeneity of a solid substrate. As a model for the heterogeneity we can suppose the substrate to consist of a continuous distribution of energies, approximated for the purpose of calculation as a large number of discrete patches, each one of which has a uniform adsorptive potential designated U_1, U_2, U_3, etc., and each of them contributing to a different extent to comprise the whole substrate. It is important to emphasize, because of a common misunderstanding, that the model is not that of a patchwork of substrates but of a continuous distribution of energies; that is, a gently rising slope rather than a series of terraces. The patches are introduced as an approximation for ease of calculation, and should not be literally interpreted. It is, nevertheless, convenient to continue to talk of uniform patches, although they are only approximately uniform. When each patch is in equilibrium with an adsorbate at a given pressure and temperature, the concentration of adsorbed monolayer on that patch would be related to the values of U_1, U_2, U_3, etc. No mental difficulties should arise from surface concentrations of adsorbate existing, as it were, side by side on the substrate, as a familiar analogous situation is the unequal distribution of a common solute between adjacent but immiscible solvents; or borrowing a graphic image from Professor Aston, co-existing puddles and patches of different degrees of wetness on the uneven surface of a tennis court after a shower. Supposing then that we treat the heterogeneity in this way, a more controversial question concerns the selection of the isotherm equation to relate the surface concentration of adsorbate on each uniform patch to its adsorptive potential. One could follow Brunauer, Emmett and Teller in selecting the Langmuir equation, and this course of action has indeed been adopted by some[11]. It has the advantage of providing a simple mathematical expression for θ as a function of p, whereas almost any other choice (with the trivial exception of equation (8)) leads to an infinite series for the explicit expression for θ. An expression for θ as a function of p is a necessary step in the mathematical development of the model, and there is, therefore, a strong inclination in favour of an equation that leads to a tractable solution. I trust I shall not be considered as lacking in respect towards the authors of the BET theory, or of failing to recognize the historical importance of their contribution, if I nevertheless suggest that their selection of the Langmuir adsorption equation was, perhaps unconsciously, determined by this psychological factor. In 1938, when electronic computers were still over the horizon, it may indeed have been Hobson's choice, as no other adsorption equation could have led so readily to a solution of the multilayer model. Thirty years later, not only has the computer released us from an aversion to intractable integrals but, as I have shown above, we are more aware of the unsuitability of the Langmuir model of physical adsorption and of the limitations of the Langmuir equation as a description of the adsorption isotherm for a uniform substrate. Instead of trying to extend the BET theory to include heterogeneity of the substrate, a different approach seemed to be demanded.

The general form for an adsorption isotherm for a heterogeneous substrate is

$$\mathrm{d}\theta = \phi(U)\,\psi(p, U)\,\mathrm{d}U \tag{9}$$

where $\phi(U)$ is a continuous function describing the distribution of adsorptive potential energies of a heterogeneous substrate, and $\psi(p, U)$ is an isotherm equation describing the coverage of the substrate patch of adsorptive potential U, as a function of p. Ross and Olivier[12] selected a Gaussian distribution of adsorptive potentials for the first function $\phi(U)$, and the Hill–de Boer adsorption equation, which is based on a two-dimensional van der Waals equation [equation (6)], for the second function $\psi(p, U)$. The reasons for making these particular selections have already been stated elsewhere[13] and need not be repeated here. The description of the adsorption on a heterogeneous substrate that is provided by these selections is both reasonable and simple in concept. It has four temperature-independent molecular parameters having clear physical significance. The function $\phi(U)$ includes the mean potential energy of adsorption and the Gaussian variance of adsorptive potentials of the substrate; the function $\psi(p, U)$ includes the two van der Waals constants α and A_0, which are two-dimensional analogues of the familiar a and b of the van der Waals equation for non-ideal gases. A number of computed model isotherms are tabulated in the book by Ross and Olivier[12]. The experimentally determined isotherm is fitted to its closest match among the calculated model isotherms; the matched isotherm then yields values of the four molecular parameters. This mode of data reduction enables interpretation of the adsorption isotherm to be made along rational molecular lines.

A determination of the monolayer capacity, the well known V_m of the BET symbolology, can also be obtained from the matched isotherm, thus providing an alternative to the BET method of measuring the specific surface of a finely divided solid from its adsorption isotherm. The portion of the isotherm that is matched is restricted to the first layer of adsorbate, or the monolayer region, which usually is found at relative pressure less than one-tenth; this is to be compared with the BET theory of multilayer adsorption, which uses the isotherm up to relative pressures of three-tenths. Another point of comparison worth noting lies in the calculation of the specific surface of the adsorbate from the derived monolayer capacity, V_m, according to the following equation:

$$\Sigma = V_m N_0 A_0 / 22\,400 \times 10^{20} \tag{10}$$

where Σ is the specific area in m^2/g, V_m is the monolayer capacity of the substrate in cm^3 (S.T.P.)/g, N_0 is Avogadro's number, and A_0 is the limiting area per molecule of adsorbate in Å^2/molecule. By the method of Ross and Olivier, V_m is determined from the matching isotherm and A_0 is defined as the two-dimensional analogue of the b-constant in the van der Waals equation. The definition in question follows from the definition of θ as A_0/A. With the BET method, equation (10) is still used, but there is room for some manipulation of the value of A_0 to adjust the result in accordance with extraneous knowledge that may influence the judgment of the investigator. Nigrogen is most frequently used as the adsorbate in applications of the BET method, and comparisons of specific surface areas thus determined with determinations by other methods yield values of A_0 for nitrogen ranging from 15·2 to 16·4 Å^2 per molecule. Harkins and Jura[14] have put forth that an even wider variation is possible, from 13 to 17 Å^2 per molecule, as c in the BET equation varies from 25 to 250. I shall advert later to the possible significance of these variations.

An interesting feature of the computed isotherms is the influence of substrate heterogeneity on their shape, as illustrated in *Figure 2*, taken from reference 12. The top curve $\gamma = \infty$ represents the isotherm for a completely uniform substrate; as more and more heterogeneity is introduced into the model, everything else being kept constant, the isotherms become less sigmoidal, and soon assume the more familiar shape of common observation, which is concave throughout its course to the pressure axis. These isotherms resemble descriptions by the Langmuir equation, and in fact such a description has

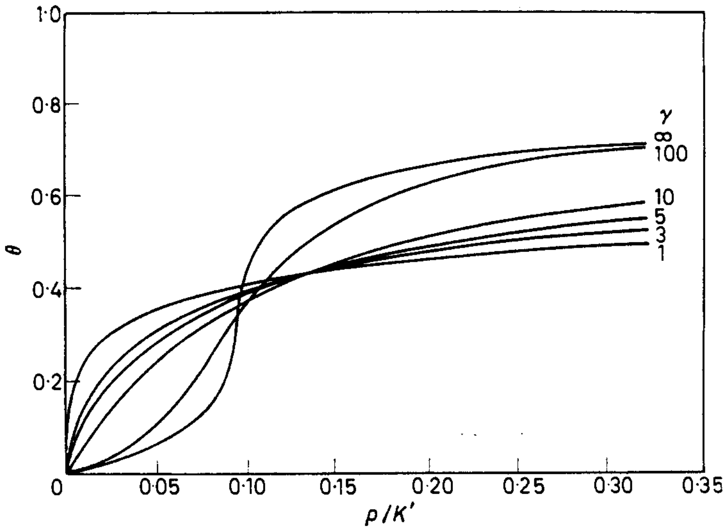

Figure 2. Computed model isotherms for heterogeneous substrates of different degrees of deviation from the mean, corresponding to the distribution curves shown in *Figure 4*. (From Ross and Olivier[12])

been shown to be possible. *Figure 3* shows the customary p/V *vs* p plot that tests the fit of the Langmuir equation to experimental data. In this case the data are not experimental, but computed from the model of a two-dimensional non-ideal gas distributed in patches of different concentration on a heterogeneous substrate. If we treat them as if they were experimental data, however, we can derive values of V_m, the monolayer capacity, from the constants of the straight lines of *Figure 3*. On doing so, we find that the values obtained are lower than that of the model, ranging from about 88 per cent for the less heterogeneous substrates down to 75 per cent for the most heterogeneous substrate.

The story that is told by applying the Langmuir equation to the monolayer range of the adsorption isotherm should be the same as that told by applying the BET equation to the multilayer range. In practice, where enough low-pressure data are available, I have always found the two accounts to agree in the determination of V_m. The Langmuir plots of *Figure 3* are therefore duplicates of what would be revealed by BET plots of the same model if the computations had been continued into the multilayer region. Hence, we should expect that when V_m is determined from an experimentally-observed isotherm by both methods, that of Ross and Olivier and of BET, that the BET determination will have a value of only about 75 to 90 per cent of the Ross–Olivier determination. The few direct comparisons that are on record[12] bear out this expectation. For diamond and rutile, two extremely heterogeneous substrates, the observed disparity is even greater than the percentages quoted above, which are based on models.

The reason for the disparity may perhaps be seen by examining *Figure 2*, where the shape of the isotherms accurately reflects the shape of the distribution curve of the adsorptive potentials (*Figure 4*). As the distribution is

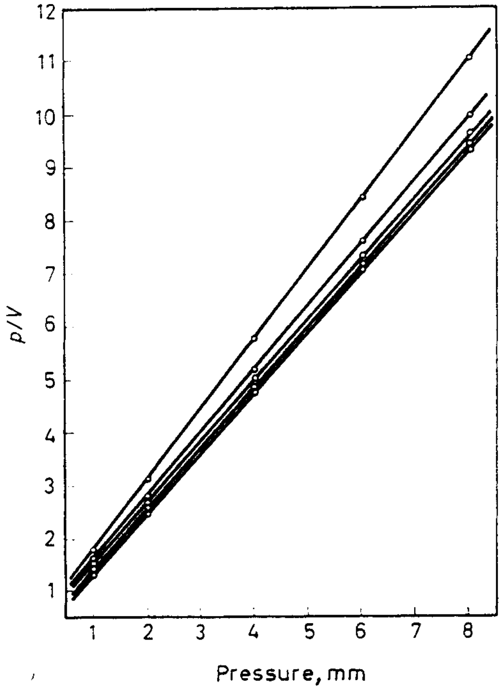

Figure 3. Plots made in accordance with the Langmuir equation of the computed isotherms shown in *Figure 2*

made wider, it includes more of the higher potentials and also more of the lower potentials; the inclusion of more of the higher potentials increases the calculated amount of adsorption at low pressures, and the inclusion of more of the lower potentials decreases the calculated amount of adsorption at higher pressures. The presence of a significant fraction of substrate of low adsorptive potential in a real adsorbent would require the attainment of high pressures to cause adsorption to occur on the low energy sites or patches. A Type III adsorption isotherm would result, unless co-existing high-energy patches were also present. When it comes to matching actual isotherms against models computed on the supposition of Gaussian distributions, if the presence of high-energy patches is confirmed by good matching at low coverage, there will always be included, by virtue of the Gaussian symmetry, an equivalent range of low-energy sites, the actual evidence for which cannot be observed, since the formation of multilayers at higher pressures obscures the monolayer contribution that is still taking place on low-energy patches. If there were in actuality no such low-energy patches at all, the Ross–Olivier method would count them in anyway. On the other hand, if there are such low-energy patches, the Langmuir equation and the BET equation would fail to detect them. Here, then, we have the reason, in the symmetry of the Gaussian distribution that was assumed to describe the heterogeneity of adsorptive energies of the substrate, why the method of Ross and Olivier gives higher results for V_m than does the Langmuir or the

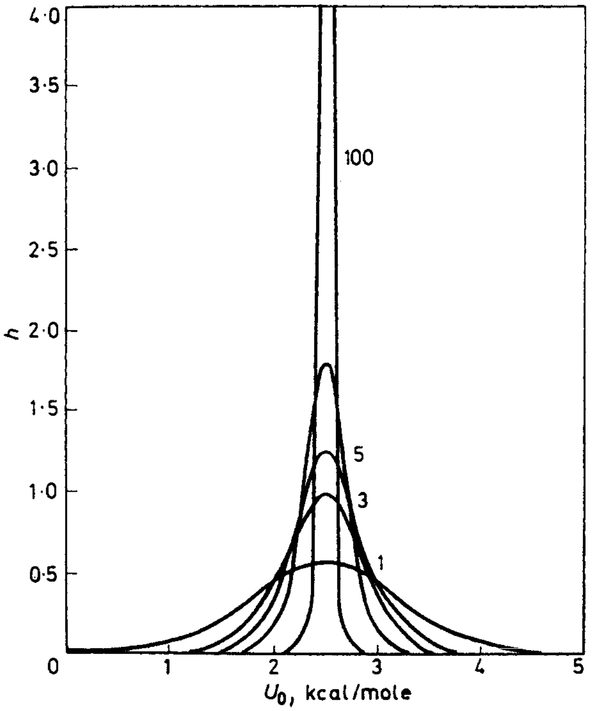

Figure 4. Gaussian adsorptive-energy distribution curves for several degrees of deviation from the mean

BET equations, and why the difference between the results of the two methods increases with the standard deviation from the mean energy. *Figures 2*, *3* and *4* do not tell the whole story because they are postulated on a fixed value for the mean adsorptive potential of 2·5 kcal/mol. When the experimentally-determined isotherm is matched with its closest model isotherm, the correct value for the mean adsorptive potential is determined, and it is clear that if it should be less than 2·5 kcal/mol the difference between the results of the Ross–Olivier and the BET methods would be even greater.

Now it might be said by an advocate of the BET method that for a very heterogeneous substrate, particularly one having a low value for the mean potential, the method of Ross and Olivier gratuitously adds to the specific surface area a certain percentage for which the adsorption isotherm (because of multi-layer formation) provides no evidence. And indeed, as de Boer and Broekhoff[15] have also shown, if the BET method is then constrained to give the same value of Σ by means of equation (10), its low value of V_m must be compensated by an inflated value of A_0. But the evidence, accumulated over the years of ever-growing employment of the BET method, is that an inflated value of A_0 is the general rule. The method of Ross and Olivier is held by an intrinsic definition of its theory to a single value of A_0, based on the van der Waals constant b of the adsorbate in the form of a gas. For nitrogen this value is $A_0 = 15{\cdot}5$ Å^2 per molecule. At one time, Livingston[16] suggested that for the BET method the best value of A_0 for nitrogen is 15·4 Å^2 per molecule, but this was not widely accepted. Currently, the standard accepted value for nitrogen is 16·2 Å^2 per molecule at -195°C. The calculations of Harkins and Jura[14], already referred to, were to the effect that A_0 for nitrogen should vary from 13 to 17 Å^2 per molecule, as c in the BET equation varies from 25 to 250. This result is in perfect accord with the comparison we have just drawn between the Ross–Olivier and the BET methods, because a high value of c in the BET equation corresponds to a low value of the mean adsorptive potential, which as we have seen requires A_{0x} to be inflated for use with the BET derived value of V_m. The calculations of Harkins and Jura, it should be noted, were not based on models of heterogeneous substrates but on actual comparisons of the results of the BET method with that of their own completely independent method of determining specific surface area. The accepted $A_0 = 16{\cdot}2$ Å^2 per molecule of the BET method is already 5 per cent greater than the Ross–Olivier value, which almost concedes that practice has demonstrated that at least 5 per cent of the gratuitous boost in V_m conferred by the Gaussian distribution is based on reality. And suggestions to use even higher values of A_0 for nitrogen in BET applications for special classes of adsorbents are sometimes reported. Such cases, if substantiated by independent measurements of the surface area, and if correlated with high values of c in the BET equation, would demonstrate that a fraction of the substrate might really consist of surface of such low energy that its contribution to the adsorption is not evident in the isotherm in the range below 35 per cent relative pressure.

References

[1] S. Ross and W. Winkler. *J. Colloid Sci.* **10**, 330 (1955).

[2] E. H. Lucassen-Reynders and M. van den Tempel. *Fourth Int. Congress of Surface Activity*, Brussels, 1964; M. van den Tempel, J. Lucassen and E. H. Lucassen-Reynders, *J. Phys. Chem.* **69**, 1798 (1965).

[3] J. H. de Boer. *The Dynamical Character of Adsorption*, Clarendon Press, Oxford, 1963, sec. ed. 1968.

[4] G. Jura and W. D. Harkins. *J. Amer. Chem. Soc.* **68**, 1941 (1946).

[5] S. Ross and E. C. Chen. *Ind. Eng. Chem.* **57**, No. 7, 40 (1965).

[6] H. Freundlich. *Colloid and Capillary Chemistry*, H. S. Hatfield, transl., Methuen and Co. Ltd., London, 1926, p. 68.

[7] J. Guastalla. *C.R. Acad. Sci. Paris* **206**, 993 (1938).

[8] A. Cadenhead and M. C. Phillips. *J. Colloid and Interface Sci.* **24**, 491 (1967).

[9] J. P. Hobson. *J. Chem. Phys.* **34**, 1850 (1961).

[10] F. Hauxwell and R. H. Ottewill. *J. Colloid and Interface Sci.* **28**, 514 (1968).

[11] A. W. Adamson and Irene Ling. *Advances in Chemistry Series* **33**, 51 (1961).

[12] S. Ross and J. P. Olivier. *On Physical Adsorption*, Wiley-Interscience, New York, 1964.

[13] S. Ross, 'The Homotattic Surface' In *The Solid-Gas Interface*, E. A. Flood ed., vol. 1, p. 491, Marcel Dekker, Inc., New York, 1967.

[14] W. D. Harkins and G. Jura. *J. Amer. Chem. Soc.* **66**, 1366 (1944).

[15] J. H. de Boer and J. C. P. Broekhoff. *Proc. Kon. Ned. Ak. Wet* **B70**, 342 (1967).

[16] H. K. Livingston. *J. Colloid Sci.* **4**, 447 (1949).

DISCUSSION

Dr V. R. Deitz (*Naval Research Laboratory, Washington, D.C.*) said: Is it not desirable in theoretical treatments to take into account three factors in consideration of surface heterogeneity, namely, geometrical, chemical composition and energetics? There are wide ranges for each category as listed below:

	Limit 1	*Limit 2*
geometrical	atomically smooth	atomically rough
chemical	constant composition	indefinite composition
energetic	homotattic	broad composition

An example is the basal plane of graphite which is smooth, of fixed composition and of constant energy. Another is the pristine glass fibre that has a smooth surface but has an indefinite surface composition. The three factors are not independent of each other, but they do serve to organize a considerable number of observations.

Professor S. Ross replied: I welcome the distinctions introduced by Dr V. R. Deitz as they indicate that the progress of our science demands more exact definitions of the terms in use. Instead of *chemical* in his listing, I should like to substitute *crystallographic*, as the same material may nevertheless present different crystal faces. Sodium chloride normally shows 100-faces with the net composition of the substrate being $Na^+ Cl^-$, but it can also be obtained with 111-faces, which are either all Na^+ or all Cl^-. An element, on the other hand, will have the same composition of substrate (all carbon atoms, for example) on every crystal face, but in a different arrangement on different crystal faces. Crystalline homogeneity was what the late Col Chris Sanford and I had in mind when we coined the word *homotattic* [C. Sanford and S. Ross. *J. Phys. Chem.* **58**, 288 (1954)], as indeed the etymology of the word would imply. We did not intend it to mean *iso-energetic*, in the sense of equal adsorptive energies throughout, but it has subsequently fallen into this use, as the place given to it by Dr Deitz in his Table testifies. This is not the first time in the history of science that a technical term has drifted into a meaning other than its original definition, as I found out myself when I had occasion to look into the origin of Faraday's terms *anode* and *cathode* [S. Ross. *Notes and Records of the Royal Society* **16**, 187 (1961)]. But let us try to preserve the distinction between *homotattic* and *iso-energetic* because even although they may often turn out to be equivalent in practice, they represent two distinct mental concepts. For example, a celebrated diagram of J. Lennard-Jones [*Trans. Faraday Soc.* **28**, 333 (1932)] could be precisely defined as: 'Iso-energetic contour lines on a homotattic substrate.' The lines may be real enough, even though the differences in adsorptive energy between them are not to be detected by too large an adsorbed molecule. The differences can be detected, however, by an adsorbed molecule sufficiently small, though this operation is not always practicable.

Finally, a note about the spelling of *homotattic*. The Oxford English Dictionary contains the noun *homotaxis* and its corresponding adjective *homotaxic*, which are technical terms coined by Huxley for use in the science of geology. Our word *homotattic*, derived from the same Greek sources for another purpose, was spelled so in order to avoid confusion with *homotaxic*, both spellings being equally correct formations from the Greek. The spelling *homotatic* is not a correct transliteration, although it does appear in Webster's all-permissive Dictionary as a variant of *homotaxic*. Let us not, on our part, encourage another Anglo-American diversity in spelling.

SURFACE CONCENTRATION OF HYDROXYL GROUPS ON AMORPHOUS SILICAS HAVING DIFFERENT SPECIFIC SURFACE AREAS

L. T. Zhuravlev and A. V. Kiselev

Institute of Physical Chemistry, Academy of Sciences, Moscow, U.S.S.R.

The adsorption[1] and other surface properties of various silicas are known to depend, especially in the cases of molecules capable of specific interactions, on the presence of silanol hydroxyl groups on the surface. The concentration of hydroxyl groups in silica a_{OH}/s, where a_{OH} and s are, respectively, the analysed hydroxyl group content per gram of solid and the specific surface area, has been determined by various methods[2–22]. Hydroxyl groups are shown[7, 16–18, 21, 23–25] to be present both on the surface ($a^{(v)}_{OH}$) and in the bulk of the silica network ($a^{(s)}_{OH}$).

We have measured the a^{s}_{OH} values for more than 40 different samples of amorphous silicas (silica gels, aerosils, aerosilogels) by the method of isotope exchange[21] between D_2O and the surface OH groups. At room temperature, only the surface hydroxy groups enter the deuterium exchange reaction whereas the internal hydroxyls are practically unaffected. The exchange method has shown that the $\alpha^{0}_{OH} = a^{0*}_{OH}/s$ values for amorphous samples of silicas having fully hydroxylated surfaces lie in the rather narrow range from 7 to 9·5 μmole OH/m² (from 4·2 to 5·7 OH groups/100 Å²) independently of the specific surface area value s and other structural characteristics. The fully hydroxylated state of the surface was retained after prolonged treatment *in vacuo* at ~200°C of samples given a preliminary surface hydration. In this case practically all the adsorbed water is removed from the surface while hydroxyl groups bonded to the silica atoms remain unaffected.

In *Figure 1* the values are given of the concentration of surface hydroxyls group on silica, determined by ourselves and by A. Agzamkhodzhaev. These values, $a^{(s)}_{OH}$ (mmole OH/g), are referred to unit weight of the samples having different s values. The experimental values of $a^{(s)}_{OH}$ are bounded by two slightly diverging straight lines passing through the origin of coordinates. This shows that the quantity of hydroxyl groups $a^{(s)}_{OH}$ on the surfaces of all these samples, as determined by the method of isotope exchange (unaffecting the hydroxyl groups within the silica particles), is proportional to the specific surface area of the amorphous silica investigated.

The $a^{(s)}_{OH}$ value is only a part of the total content of hydroxyl groups a_{OH} in silica; the other part, $a^{(v)}_{OH} = a_{OH} - a^{(s)}_{OH}$ is contained within the bulk. From this point of view it is of interest to examine the a_{OH}/s (μmole/m²) values for fully hydroxylated silicas having different specific surface areas (treated at 120–200°C). These values, shown in *Figure 2*, have been collected from data of various authors[3–22] and were obtained by different

---

*The superscript refers to a fully hydroxylated surface

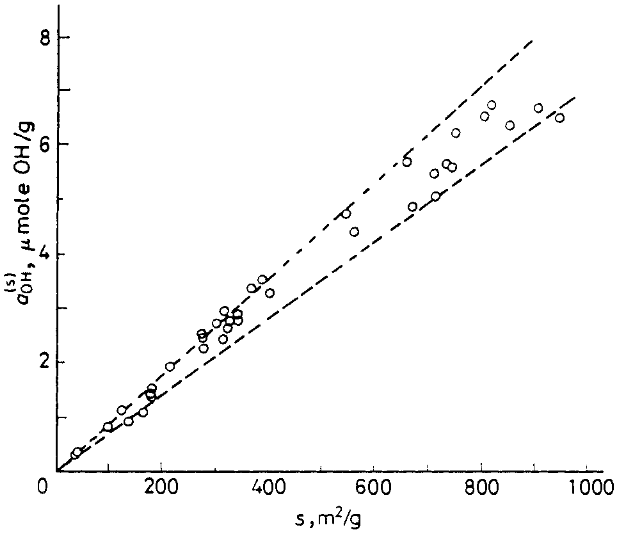

Figure 1. Dependence of concentration of surface hydroxyl groups determined by deutero exchange on the surface area of silica

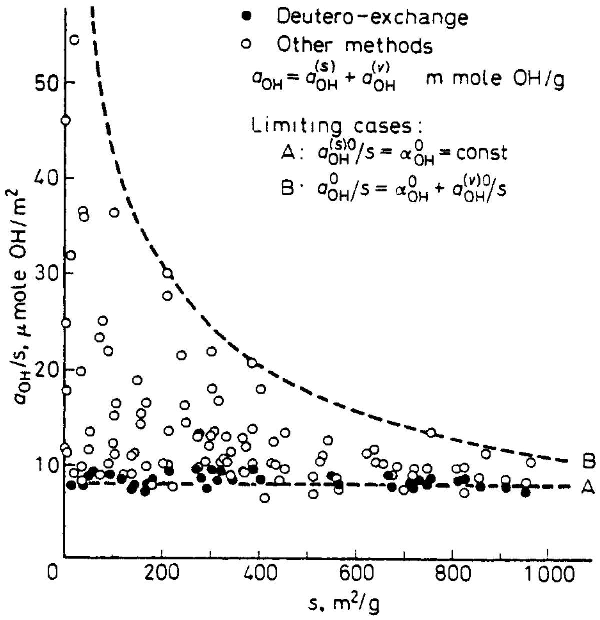

Figure 2. Concentration of surface and bulk hydroxyl groups for silicas of different surface areas

methods (thermogravimetrical, chemical, n.m.r., deuterium-exchange) for both amorphous and crystalline samples of silicas. From *Figure 2* one can see that the a_{OH}/s values obtained by the deuterium exchange method (for various silica samples in our investigations[21] and for the aerosil samples in the work of Boehm[22]), black points, lie near the straight line A, parallel to abscissa and are independent of the s value. From above, this region is bounded by the curve B, which, as the s value increases, gradually approaches the straight line A. The straight line A represents the constant mean concentration of hydroxyl groups on the silica surface $a^{(s)0}_{OH}/s = \alpha^0_{OH}$. The region of experimental points, confined between the curves A and B (*Figure 2*), shows the content of internal hydroxyl groups and, hence, the ordinate of any point in the region between the straight line A and curve B represent the total quantity of hydroxyl groups (on the surface and in the bulk) referred to unit surface of the sample. On the other hand, the ordinate of the straight line A, which is independent of the s value, is the value of the surface concentration of silanol groups for the fully hydroxylated state of the silica surface. These minimum experimental values $a^0_{OH}/s = \alpha^0_{OH}$, are in good agreement with the minimum values of α_{OH} estimated on the basis of crystallographic data[9, 11, 15, 26] assuming that every Si atom coming to the surface binds one OH group (the minimum values for various crystalline and amorphous silicas are 7·6–9·9 μmole OH/m^2). According to the experimental data of de Boer *et al.*[15] approximately the same constant value, $a^0_{OH}/s = 7{\cdot}7$–$8{\cdot}0$ μmole OH/m^2, is obtained on prolonged heating of the initial silica samples to rather high temperatures, followed by rehydroxylation of the surface with liquid water and final treatment at 100–200°C.

It should be emphasized that the experimental points in the region between the straight line A and the curve B are obtained by various authors, mainly, by the thermogravimetric method which gives the total content of the 'structural water' liberated both from the surface and out of the bulk of the silica network on heating the sample to high temperature (1000–1200°C). The chemical methods give experimental values of the quantity a_{OH}/s, in general, close to the lower boundary straight line A, but they sometimes considerably deviate from this, since some of these chemical reactions are influenced by steric factors.

The constancy of the $a^{(s)0}_{OH}/s = \alpha^0_{OH}$ values obtained by the deuteroexchange method (black points in *Figure 2*) shows that the fully hydroxylated state of the silica surface is practically independent of the specific surface area of the sample within the limits studied by us. One should certainly bear in mind that in the case of microporous silicas the estimation of the α^0_{OH} value cannot be made with the same accuracy since the determination of the magnitude of the specific surface area of the network of such samples is difficult.

The nature of the curves A and B corresponds to the simplest model of amorphous silica as an ensemble of globules having a fully hydroxylated surface and internally saturated by hydroxyl groups[21, 26–29]. The total content of hydroxyl groups g_{OH}, in one globule of radius R may be represented, in the framework of this model, as a sum[21]

$$g_{OH} = K^0_{OH}V + \alpha^0_{OH}S \approx \tfrac{4}{3}\pi R^3 K^0_{OH} + 4\pi R^2 \alpha^0_{OH} \tag{1}$$

where V and S are the volume and the surface area of one globule while K^0_{OH} is the concentration of the OH groups in the bulk of the globule. If the K^0_{OH} and α^0_{OH} concentrations for fully hydroxylated silica are constant and independent of R, i.e. of s, specific surface area, the following equations for the corresponding boundary curves are obtained

$$a^{(s)0}_{OH}/s = \alpha^0_{OH} = \text{constant} \qquad (2)$$

and

$$a^0_{OH}/s = K^0_{OH}/s\delta + \alpha^0_{OH} = a^{(v)0}_{OH}/s + \alpha^0_{OH} \qquad (3)$$

where δ is the density of the silica network and $a^{(v)0}_{OH}$ = bulk content of hydroxyl groups per gram of silica. In this model the straight line of equation (2) corresponds to the straight line A in *Figure 2*, and the hyperbola (3) to curve B.

Figure 2 shows that the surface concentration of OH groups on fully hydroxylated amorphous silicas $\alpha^0_{OH} \approx$ 7–9·5 μmole OH/m^2 (4·2–5·7 groups OH/100 Å^2) may be regarded as a reproducible constant.

It is of interest to further consider the dependence of the surface concentration of hydroxyl groups α_{OH}, on the temperature of the vacuum treatment of silicas, initially fully hydroxylated. As an example, such a dependence is shown in *Figure 3* for the seven samples of aerosils investigated by us by means of the deuterium exchange method at various temperatures

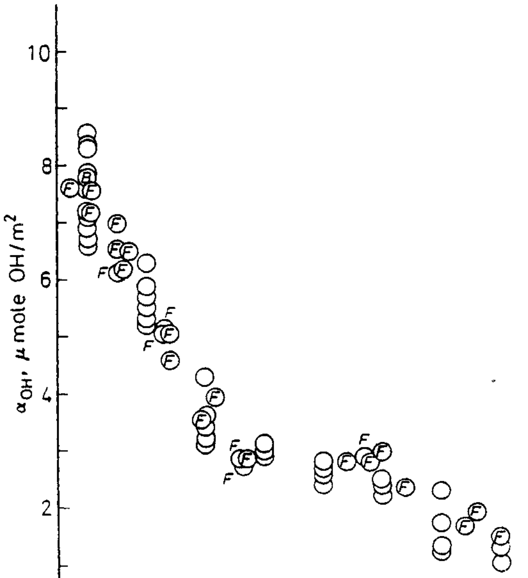

Figure 3. Dependence of surface concentration of hydroxyl groups of aerosils on temperature of heat treatment [*F*. Fripiat *et al.*; *B*. Boehm and Wisstober]

from 200°C (the fully hydroxylated state of the surface) to 900°C (the highly dehydroxylated state). In *Figure 3* are also given the α_{OH} values determined according to the reaction with $LiCH_3$ and $MgCH_3I$ for the Degussa aerosil sample, $s = 178$ m^2/g, by Fripiat *et al.*[17] and values determined by deuterium exchange for an aerosil with a specific area $s = 145$ m^2/g by Boehm and Wisstober[22]. Despite the difference in the specific surface areas of the aerosil samples, the α_{OH} values at the given temperature of the vacuum treatment are close to each other and the decrease in α_{OH} under similar conditions of heating of the various aerosils, occurs to approximately the same degree: α_{OH} decreases rapidly over the range of 200–400°C, and then continues to decrease at slower rate. Spectroscopic investigations show[30, 31] that a curve of this form may be accounted for by the ease of removal of the surface hydroxyls, bounded by mutual hydrogen bonds, on heating from 200 to 400°C, after which the dehydroxylation process becomes slower, mainly because of the increase in the mean distance between the neighbouring free (non-interacting) hydroxyl groups on the surface of the non-sintering aerosil samples.

Thus, the values of the surface concentration of hydroxyl groups in amorphous silicas in the fully hydroxylated surface state α^0_{OH}, and in practically dehydroxylated states (derived from the fully hydroxylated state) are reproducible constants. In this case the α^0_{OH} value corresponds to the number of surface silicon atoms and may be determined from the structural data independently of adsorption measurements of the surface area. This fact permits the $a^{(s)}_{OH}$ determination by the deuterium exchange method to be considered as an independent means of estimating silica specific surface area (in the absence of microporosity) according to formula

$$s = a^{(s)}_{OH}/\alpha^0_{OH} \tag{4}$$

In this case the $a^{(s)}_{OH}$ values are determined by the deuterium exchange method for the fully hydroxylated state of the silica surface when $\alpha^0_{OH} \approx 8{\cdot}0$ μmole OH/m^2 (5·0 groups OH/100 Å^2).

SUMMARY

Using the deuterium exchange method the quantities of surface hydroxyl groups, $a^{(s)}_{OH}$, have been estimated on the fully hydroxylated surfaces of more than 40 samples of amorphous silica (aerosils, aerosilogels, silica gels). The surface concentration of hydroxyls, $\alpha^0_{OH} = a^{(s)0}_{OH}/s$, is about 8·0 μmole OH/m^2 (5·0 OH groups/100 Å^2) independent of the specific surface area, s, of these samples. An examination of literature data has shown that referring the values of ignition loss to unit surface area often gives higher values of $a^{(s)}_{OH}/s$. This is accounted for by the fact that, on annealing, hydroxyl groups attached to the surface and also those contained in the bulk of the silica network are lost. All the results obtained previously lie between a constant value corresponding to α^0_{OH} and a value which decreases as the sizes of the particles composing the silica diminishes (i.e. when s increases); this corresponds to the hydroxylation both of the surface and the bulk of the silica.

Knowing $\alpha^{0}_{OH} \approx 8{\cdot}0$ μmole/m^2 from independent crystallographic data and measuring the surface hydroxyl group content $a^{(s)0}_{OH}$ by deutero-exchange of the fully hydroxylated surface of the silica sample with D_2O, it is possible to determine the specific surface area of the sample, $s = a^{(s)}_{OH}{}^{0}/\alpha^{0}_{OH}$, without any adsorption measurements.

References

[1] R. K. W. Sing, This Symposium.
[2] A. V. Kiselev. *Kolloid. Zhur.* **2**, 17 (1936).
[3] S. Brunauer, D. L. Kantro and C. H. Weiss. *Can. J. Chem.* **34**, 1483 (1956).
[4] V. A. Dzisko, A. A. Vishnevskaya and V. S. Chesalova. *Zhur. Fiz. Khim.* **24**, 1416 (1950).
[5] J. Bastick. *Bull. Soc. chim. France* 437 (1953); *Chemie et Industry* **78**, 9 (1957).
[6] D. Papee. *Bull. Soc. chim. France* 14 (1955).
[7] J. Shapiro and H. G. Weiss. *J. Phys. Chem.* **57**, 219 (1953);
H. G. Weiss, J. A. Knight and J. Shapiro. *J. Am. Chem. Soc.* **81**, 1823 (1959).
[8] H. W. Kohlschutter and J. Kampf. *Z. anorg. allg. Chem.* **292**, 289 (1957).
[9] W. Stober. *Kolloid. Z.* **145**, 17 (1956).
[10] L. D. Belyakova, O. M. Dzhigit and A. V. Kiselev. *Zhur. Fiz. Chim.* **31**, 1577 (1957).
[11] S. P. Zhdanov and A. V. Kiselev. *Zhur. Fiz. Khim.* **31**, 2213 (1959).
[12] M. M. Egorov, K. G. Krasilnikov and V. F. Kiselev. *Zhur. Fiz. Khim.* **32**, 2448 (1958).
[13] V. I. Kvlividze, N. M. Ievskaya, T. S. Egorova, V. F. Kiselev and N. D. Sokolov. *Kinetika i kataliz* **3**, 31 (1962).
[14] S. A. Greenberg. *J. Phys. Chem.* **60**, 325 (1956).
[15] J. H. de Boer and J. M. Vleeskens. *Proc. Kon. Ned. Ak. Van Wetensch* **B60**, 234 (1957);
J. H. de Boer, M. E. Hermans, J. M. Vleeskens. **B60**, 45, 54 (1957).
[16] C. Naccache, J. Francois-Rossetti and B. Imelik. *Bull. Soc. chim. France* 404 (1959);
C. Nassache and B. Imelik. *Bull. Soc. chim. France* 553 (1961).
[17] J. Fripiat and J. Uytterhoeven. *J. Phys. Chem.* **66**, 800 (1962);
J. Uytterhoeven, M. Sleex and J. J. Fripiat. *Bull. Soc. chim. France* 1800 (1965);
M. V. Tongelen, J. B. Uyterrhoeven and J. J. Fripiat. *Bull. Soc. chim. France* 2318 (1965).
[18] V. M. Chertov, D. V. Dzhambaeva, A. S. Plachinda and I. E. Neimark. *Dokl. Akad. nauk SSSR* **161**, 1149 (1965).
[19] V. U. Chertov, D. V. Dzhambaeva, A. S. Plachinda and I. E. Neimark. *Zhur. Fiz. Khim.* **40**, 520 (1966).
[20] N. V. Akshinskaya, V. Ya. Davydov, A. V. Kiselev and Yu. S. Nikitin. *Kolloid. Zhur.* **28**, 3 (1966).
[21] L. T. Zhuravlev and A. V. Kiselev. *Kolloid. Zhur.* **24**, 23 (1962);
V. Ya. Davydov, A. V. Kiselev and L. T. Zhuravlev. *Trans. Faraday Soc.* **60**, 2254 (1964);
L. T. Zhuravlev and A. V. Kiselev. *Zhur. Fiz. Khim.* **39**, 453 (1965);
A. A. Agzamhadzhayev, L. T. Zhuravlev and A. V. Kiselev. *Izv. Akad. nauk SSSR, ser. Khim.* 1186 (1968);
A. A. Agzamhadzhayev, L. T. Zhuravlev, A. V. Kiselev and K. Ya. Shengelya. *Izv. Akad. nauk SSSR, ser. Khim.* (1969).
[22] H. P. Boehm. *Advances in catalysis and related subjects*, vol. 16, Academic Press, New York and London (1966).
[23] M. R. Basila. *J. Chem. Phys.* **35**, 1151 (1961); *J. Phys. Chem.* **66**, 2223 (1963).
[24] J. Young. *J. Colloid Sci.* **13**, 67 (1958).
[25] V. Ya. Davydov and A. V. Kiselev. *Zhur. Fiz. Khim.* **37**, 2593 (1969).
[26] R. K. Iler. *The colloid chemistry of silica and silicates.* New York (1955).
[27] A. V. Kiselev, V. M. Lukyanovitch and E. A. Porai-Koshic. *Methods of studying the structure of highly dispensed and porous bodies* Adademy of Sciences USSR, p. 161 (in Russian) (1958).
[28] C. R. Adama and H. H. Vuge. *J. Phys. Chem.* **61**, 722 (1957).
W. G. Schlaffer, C. R. Adams and J. N. Wilson. *J. Phys. Chem.* **69**, 1530 (1965).
[29] A. V. Kiselev, Ya. S. Nikitin and E. B. Oganesyan. *Kolloid. Zhur.* **28**, 667 (1966).
[30] A. V. Kiselev and V. I. Lygin. *Uspekhi Khimii* **31**, 361 (1962).
[31] R. M. Donald. *J. Phys. Chem.* **62**, 1168 (1958).

ON THE ADSORPTION OF NITROGEN AND ARGON BY THORIUM OXIDE

R. B. Gammage, E. L. Fuller, Jr. and H. F. Holmes

Oak Ridge National Laboratory, Oak Ridge, Tennessee, U.S.A.

In a succinct manner, Harris and Sing[1] have summarized the difficulties associated with the use of argon adsorption for surface area determinations of oxides. Our work with thorium oxide finds us in general agreement with their findings. We are able to pinpoint, however, a further complicating factor in argon, and also nitrogen adsorption, which hitherto has received little attention, namely surface hydration[2–7]. It will be shown that surface water can affect the apparent specific area of the open surface and in addition can block or hinder the access of nitrogen and argon molecules to a system of fine pores. In the latter case nitrogen proves itself better able than argon, at 77°K, to penetrate the pore system.

To assess the uptake of nitrogen and argon by a porous thorium oxide (sample B[6]), comparative adsorptions have also been made on a non-porous thorium oxide (sample I[7]). At each one in a series of selected outgassing temperatures, repetitive sorption cycles in water vapour were carried out to produce a surface in the equilibrium state of hydration prior to adsorbing nitrogen or argon. The extent of surface hydration, for various temperatures of outgassing, has been dealt with previously[7]. All adsorption measurements have been made with the Cahn microbalance[8].

Table 1. Specific surface area of non-porous thorium oxide I measured by the adsorption of nitrogen and argon at 77°K

Outgassing temperature (°C)	*Surface area* (m^2/g)		BET "*c*"	
	S_{N_2} (16·2 Å^2/N_2)	S_{Ar} (16·6 Å^2/Ar)	c_{N_2}	c_{Ar}
25	2·38	2·38	32·6	21·8
500	2·69	2·69	520	385
1000	2·82	2·70	3150	2220

The heat of immersion in water at 25°C (Harkins Jura absolute method) was 120 ± 3 ergs/cm$_2$ using the area measured after outgassing at 500°C. The surface enthalpy of liquid water at 25°C is 118·5 ergs/cm^2.

In *Table 1* the results are given for nitrogen and argon adsorptions on sample I (non-porous). Adopting the procedure of taking the value of P_0 as that of super-cooled liquid and $A_m{}^{Ar} = 16{\cdot}6$Å^2, [9] an excellent match is obtained between S_{N_2} and S_{Ar} except for surface outgassed at 1000°C. The very high value of C_{N_2} could reflect a state of localized adsorption. Heat of immersion measurements with sample I[3] have already indicated that nitrogen adsorption on the surface outgassed at 500°C gives the most acceptable value of the specific surface area (see footnote to *Table 1*). Having shown previously that sample I is composed of open surface[3], the 12 per cent reduction in both S_{N_2} and S_{Ar}, when adsorptions are conducted on the water saturated surface (25°C outgassing), suggests that each adsorbate adopts a more open structure than is the case for adsorption on the well outgassed surface (500°C outgassing). For a rutile surface, Isirikyan and Kazmenko[10] have reported the same characteristic of increased adsorptive capacity for nitrogen and argon as the extent of surface hydration is reduced. At the same time they observed that S_{N_2}/S_{Ar} remained constant over a large range of outgassing temperature as is the case for thorium oxide surface.

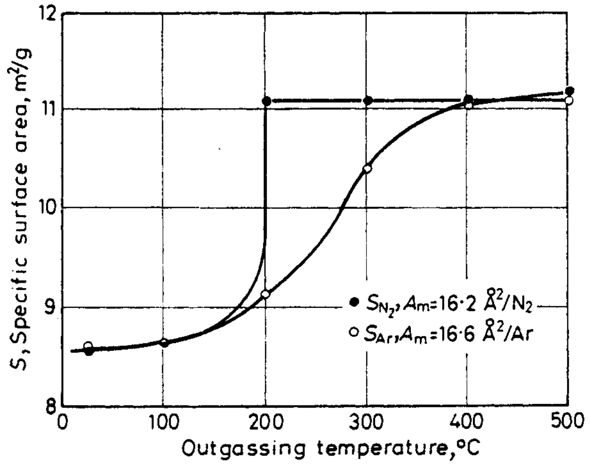

Figure 1. Specific surface area of porous thorium oxide B determined by the adsorptions of nitrogen and argon at 77°K

The variations in the specific surface area of sample B (porous), as a function of outgassing temperature, are shown in *Figure 1.* As observed for the non-porous oxide, S_{N_2} and S_{Ar} match for outgassing temperatures of 25°C and 500°C. It is also evident at intermediate temperatures of outgassing (200°C and 300°C) that $S_{N_2} > S_{Ar}$. Apparently the nitrogen molecules are better able than argon atoms to penetrate the partially hydrated pore structure despite their similarity in size. With the surface in the 400°C or 500°C outgassed condition (partially hydroxylated[7]), both nitrogen and argon experienced little difficulty in penetrating the pore structure; there were no unduly drawn-out kinetic effects. A blocking problem caused by adsorbed water can be evidenced first after the 300°C outgassing. Lowering the outgassing temperature from 400°C to 300°C also marks the onset of much slower kinetics of adsorption with each adsorbate. It should be mentioned that at this and lower temperatures of outgassing, equilibration at a given relative pressure is more rapid with nitrogen than argon. The differential kinetic effect can be presented in a striking fashion for a surface outgassed at 100°C, as shown in *Figure 2.* Nitrogen reached all of the hydrated pore structure available to it in the first day of the adsorption experiment. To achieve the same degree of penetration with argon, continuous adsorption was required over a period of one week after which time

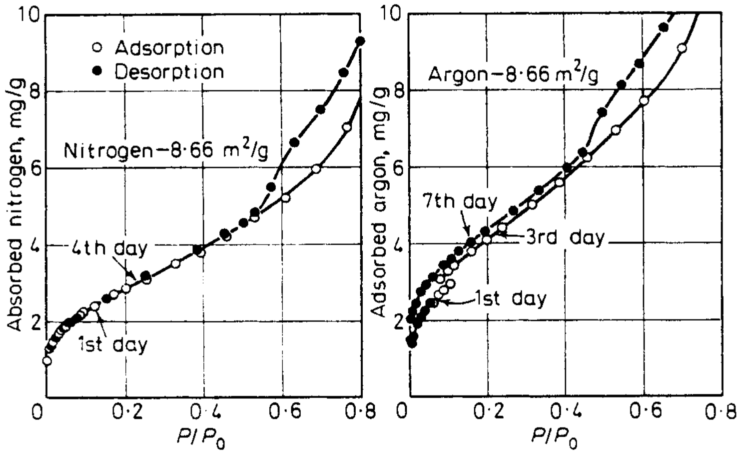

Figure 2. Adsorption of nitrogen and argon at 77°K on porous thorium oxide B outgassed at 100°C

S_{Ar} became equal to S_{N2} at 8·66 m^2/g. The inferior penetrating power of argon can be linked plausibly to the fact that the stable phase of argon at 77°K is solid while that of nitrogen is liquid.

t-plots have also been constructed from the adsorption of nitrogen on porous and non-porous thorium oxide. The information they gave helped to explain quantitatively the change which occurs in the specific surface area of sample B between the outgassing temperatures of 500°C and 25°C. For 500°C outgassing, the *t*-plot could be extrapolated to give a positive intercept whose equivalent apparent micropore area was 1·36 m^2/g. For the 25°C outgassed condition, an extrapolation of the *t*-plot passed through the origin showing that the micropore volume has remained full of water. The BET area of sample B was 11·24 m^2/g following outgassing at 500°C. Subtracting the apparent micropore area of 1·36 m^2/g leaves an area of 9·88 m^2/g. Our experience with the non-porous oxide indicates that a further reduction of 12 per cent in the remaining area is to be expected on lowering the outgassing temperature from 500°C to 25°C—this leaves 8·74 m^2/g. The area of sample B, in the 25° outgassed condition, measured directly from the adsorption isotherm of nitrogen was 8·56 m^2/g. Thus we have been able to account satisfactorily for the magnitude of the surface area change shown in *Figure 1*. At the same time it has been shown that it is essentially the pores of microsize which are filled with water at low outgassing temperature and whose volume is denied to nitrogen molecules. This still holds true for outgassing at 100°C when S_{N_2} is 8·66 m^2/g.

Our experience with thorium oxide has shown that the method of nitrogen adsorption has definite advantages over that of argon adsorption as a probe of surface area and pore structure. Whether the surface is open or contained within fine pores, the results also show clearly the importance of taking into account the state of hydration of the oxide surface.

---

† Research sponsored by the U.S. Atomic Energy Commission under contract with the Union Carbide Corporation.

References

[1] M. R. Harris and K. S. W. Sing. *Chem. and Ind.* 757 (1967).
[2] E. L. Fuller, Jr., H. F. Holmes, and C. H. Secoy. *J. Phys. Chem.* **70**, 1633 (1966).
[3] H. F. Homes, E. L. Fuller, Jr., and C. H. Secoy. *J. Phys. Chem.* **72**, 2095 (1968).
[4] H. F. Holmes, E. L. Fuller, Jr. and C. H. Secoy. *J. Phys. Chem.* **72**, 2293 (1968).
[5] H. F. Holmes, E. L. Fuller, Jr., R. B. Gammage and C. H. Secoy. *J. Coll. Interface Sci.* **28**, 421 (1968).
[6] H. F. Holmes, E. L. Fuller, Jr. and C. H. Secoy. *J. Coll. Interface Sci.* **70**, 436 (1966).
[7] E. L. Fuller, Jr., H. F. Holmes, C. H. Secoy and J. E. Stuckey. *J. Coll. Interface Sci.* **72**, 573 (1968).
[8] E. L. Fuller, Jr., H. F. Holmes and C. H. Secoy. *Vacuum Microbalance Tech.* **4**, 109 (1965).
[9] M. L. Corrin. *J. Am. Chem. Soc.* **73**, 4061 (1951).
[10] A. A. Isirikyan and I. A. Kazmenko. *Kolloidn. Zh.* **30**, 220 (1968).

HIGH PRODUCTIVE CHROMATOGRAPHIC METHODS FOR DETERMINATION OF THE TOTAL AND ACTIVE SURFACE AREA OF CATALYSTS

A. P. KARNAUKHOV and N. E. BUYANOVA

Institute of Catalysis, Academy of Sciences, Novosibirsk, U.S.S.R.

As long as the activity of catalysts depends directly on the value of their surface area, determination of this characteristic is very important in the study of the processes of heterogeneous catalysis and its commercial application. If a catalyst is an individual substance, it is necessary to determine its total surface area S_t; if it consists of several components, it is necessary to know the surface area of its active part S_a.

DETERMINATION OF THE TOTAL SURFACE AREA OF CATALYSTS

The existing vacuum adsorption methods for the determination of S_t no longer correspond to the present-day scope of catalytic investigations. Highly increased needs for investigation of properties of various catalysts cannot be secured with complicated glass vacuum apparatus which have very low productivity and insufficient sensitivity for coarsely dispersed solids. Practically, these apparatuses are not at all suitable for the commercial determination of S_t of manufactured catalysts or for the control of its change in the course of a technological process.

At the Institute of Catalysis (Novosibirsk), where the need for S_t determination is about 3500 measurements a year, the authors have developed a gas chromatographic apparatus[1] based on Nelsen–Eggertsen's method of thermal desorption[2]. Argon is used as adsorbate in place of nitrogen. Of all the gases usually used for S_t determination (N_2, Ar, Kr, Xe), argon has the smallest spherical molecule, and its adsorption has a low sensitivity to the chemical nature of the surface. The use of argon makes it possible to increase the accuracy of chromatographic measurements since, in order to obtain the same relative pressures (0·05–0·25), one may use smaller concentrations of adsorbate in the carrier gas (1·5–8% for argon instead of 5–25% for nitrogen). This decreases errors due to deviation from linear dependence between the signal of the katharometer and the concentration of adsorbate and makes the base line more stable during cooling or warming of the adsorber with the catalyst.

High productivity is provided by: (i) parallel performing of training and adsorption processes on all catalyst samples loaded in the apparatus, and (ii) reduction of measurements to a minimum during desorption.

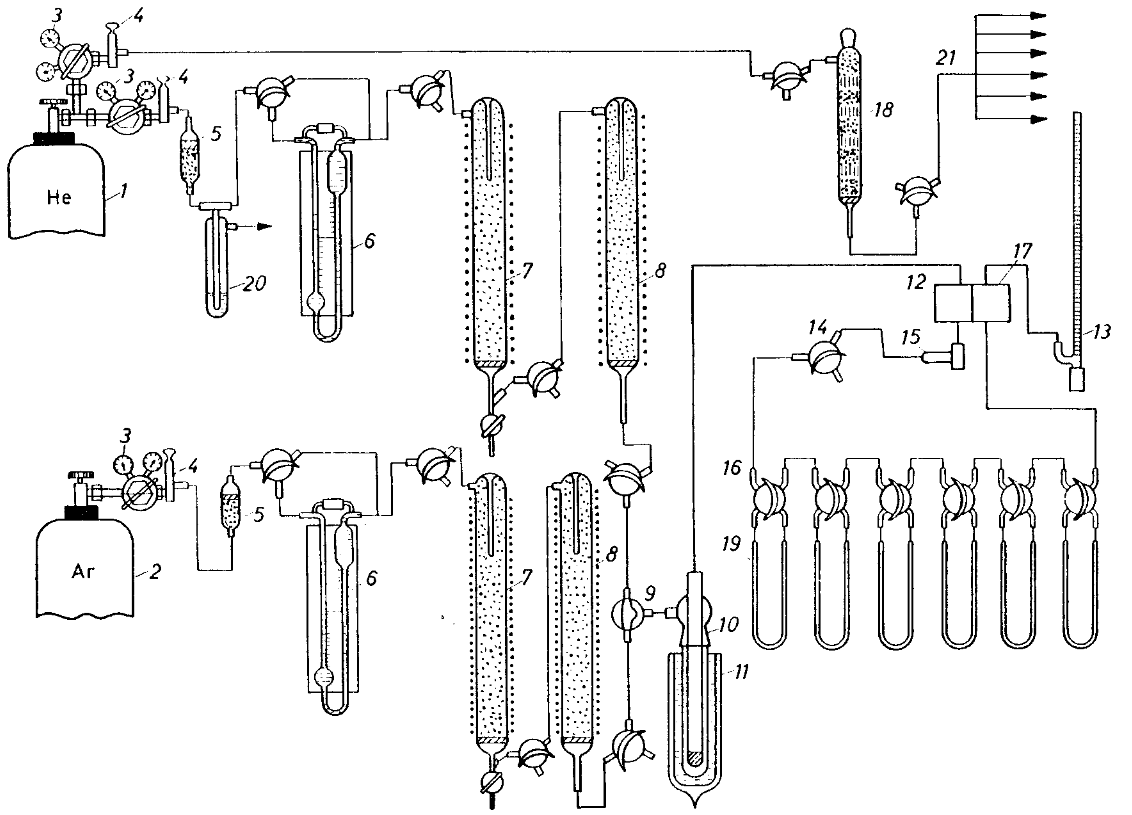

Figure 1. Schematic diagram for determination of total catalyst surface area. *6,* flowmeters; *7,8,18,* columns for drying and purification of gases; *10,* trap for water freezing; *12, 17.* katharometer; *16,* four-way stop-cocks; *19,* adsorbers; *13,* film flowmeter; *21,* comb for joining adsorbers during training.

Six samples (*Figure 1*) loaded in adsorbers (U-shaped tubes) and pretrained separately in the flow of helium through the comb *21*, upon heating are joined to the four-way stopcocks *15* without breaking the gas flow. Argon–helium mixture of invariable composition purified in the columns *7,8* is run simultaneously through all the six adsorbers cooled by liquid nitrogen until adsorption equilibrium is reached. This corresponds to the deviation of the recorder's pen connected with the katharometer *12,17* on the base line. Then by turning the four-way stopcocks, five adsorbers are switched off and the Dewar's vessel is taken away from under the sixth. The amount of argon desorbed from the sample is determined from the area of the recorded peak (*Figure 2*). A similar procedure is carried out with the other five samples. The surface area is calculated from the amount of desorption by means of Temkin's 'one-point' method[3] in which the constant *c* of the BET equation for the given adsorbate is assumed to be independent of the adsorbents' nature. For argon this constant, determined by us as the mean quantity from many experiments, is taken to be equal to 60.

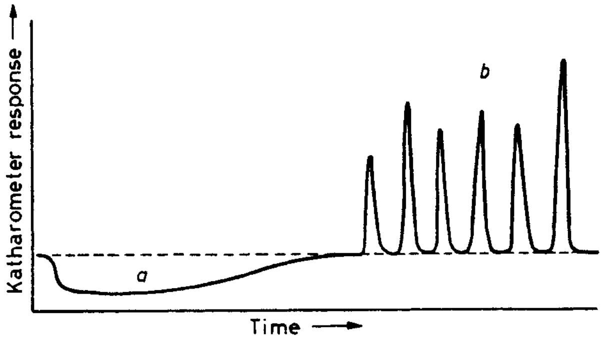

Figure 2. Chromatogram of argon adsorption and desorption peaks.

The output of the apparatus is 12 samples per six hours. It is convenient for numerous measurements of S_t due to its universality for various adsorbents and catalysts having different chemical nature, dispersity and porous structure. The apparatus permits one to measure S_t having values from 0·01 to 1000 m^2/g; the porous structure has practically no effect on the accuracy of the S_t determination because adsorption and desorption equilibrium is checked for any catalyst by appearance of the recorder's pen on the base line. The average discrepancy between the measured quantities of S_t and those obtained by static method equals 3·5 per cent. The apparatus described is being successfully used in many research and industrial laboratories in the Soviet Union.

DETERMINATION OF THE ACTIVE SURFACE AREA OF CATALYSTS

Since the first works by Emmett and Brunauer[4], Burstein[5], Boreskov and Karnaukhov[6], the methods of separate determination of the component surface area S_a of complex catalysts by chemisorption of carbon oxide and hydrogen have been often in use. These methods require more complicated static apparatus than are needed for S_t measurements. For simplification and acceleration of S_a determinations for Ni, or Fe, or Pt on SiO_2 and Al_2O_3 the authors have used chromatographic measurements of oxygen chemisorption[7,8,9] by the impulse method at room temperature. First the catalyst is reduced in hydrogen and trained in the inert gas flow. Then small portions of oxygen are successively introduced into the carrier gas passing through the sample. As chemisorption of oxygen is irreversible, the katharometer does not detect its appearance in the outflow from the adsorber until adsorption saturation on the catalyst surface is reached. The amount of oxygen chemisorbed is determined by summing up all portions of oxygen until the first peaks start to appear (*Figure 3a*). Since in blank experiments it has been found that carriers in fact did not adsorb oxygen at room temperature (*Figure 3b*), it could be suggested that all oxygen adsorbed by catalysts was chemisorbed by the metal. S_a of the supported metal in the case of iron and nickel catalysts was estimated from comparison of the oxygen chemisorption value on supported metals and on pure Ni and Fe with the known surface area (measured by the BET method) under the same conditions: $S_a = A/\alpha$ where A is adsorption per 1 g of supported metal and α that per 1 m^2 of pure metal. Assumed identity of chemisorption properties of pure and supported metals was justified by the facts that these metals were on the surface

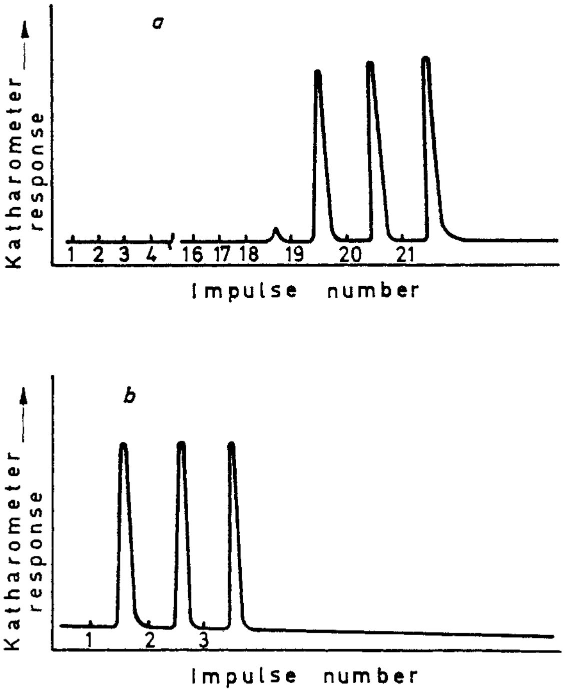

Figure 3. Chromatograms of oxygen adsorption: (*a*) on catalyst Ni–Al_2O_3; (*b*) on the carrier Al_2O_3.

of the carriers in the form of comparatively coarse crystals; this was tested by the X-ray method. For a platinum catalyst, containing a small amount of platinum, in which the metal is highly dispersed, determination of S_a would be formal. Therefore it is better to determine its dispersity by the ratio of the number of atoms available for adsorption to the total number of atoms of the metal Pt*: Pt; one atom of oxygen is assumed to be chemisorbed on two atoms of platinum[8,10]. Only a small number of the results that have been obtained are listed in *Table 1*†. Here one can see that: (i) the chromatographic method gives the results close to those obtained by the static method; (ii) in the case of large concentrations of Ni and Fe on the support they form crystals of 50 to 100 Å size; (iii) in the case of small concentrations of Pt on the support every (or almost every) atom of the metal is available for chemisorption of oxygen. This corresponds to either very fine crystals or two-dimensional platinum.

Table 1. Surface area and dispersity of Ni, Fe and Pt catalysts

No.	*System*	*Metal content* (%)	*Reduction temperature* (°C)	S_t (m^2/g)	S_a (m^2/g of metal)		O*:M	M*:M	*Size of the crystal from* S_a (Å)
					Static method	*Chromatographic method*			
1	Ni–SiO_2	20	300	260	59·5	60	0·15	0·08	95
2	Ni–Al_2O_3	15	300	170		105	0·26	0·14	55
3	Fe–Al_2O_3	5·5	400	200	107	115	0·42	0·12	72
4	Fe–Al_2O_3	8·35	400	200	98	110	0·40	0·11	79
5	Pt–Al_2O_3	2·04	700	170	170	199	0·36	0·72	12
6	Pt–Al_2O_3	1·27	500	200	243	254	0·46	0·92	9
7	Pt–Al_2O_3	0·69	500	205	(276)	(276)	0·59	1·0	
8	Pt–Al_2O_3	0·16	500	180	(276)	(276)	1·03	1·0	

The apparatus for S_a determination is simpler than that for S_t determination. It is used for characterization of the dispersity of nickel catalysts not only at the Institute but also at some chemical plants.

References

[1] N. E. Buyanova, G. B. Gudkova and A. P. Karnaukhov. *Kinetika i kataliz* **6**, 1085 (1965).

[2] F. M. Nelsen and F. T. Eggertsen. *Analyt. Chem.* **30**, 1387 (1958).

[3] M. I. Temkin. *Zh. fiz. chimii* **29**, 1610 (1955).

[4] P. H. Emmett and S. Brunauer. *J. Am. Chem. Soc.* **59**, 310, 1553 (1937).

[5] R. H. Burstein, P. I. Levin and S. M. Petrov. *Zh. fiz. chimii* **5**, 209 (1934).

[6] G. K. Boreskov, and A. P. Karnaukhov. *Zh. fiz. chimii* **26**, 1814 (1952).

[7] N. E. Buyanova, A. P. Karnaukhov, L. M. Kefili, I. D. Ratner and O. N. Cherniavskaya. *Kinetika i kataliz* **8**, 868 (1967).

[8] N. E. Buyanova, N. B. Ibragimova and A. P. Karnaukhov. *Kinetika i kataliz*. **10**, 397 (1969).

[9] N. E. Buyanova, A. P. Karnaukhov and O. N. Cherniavskaya. *Kinetika i kataliz* (to be published).

[10] A. V. Khasin and G. K. Boreskov. *Dokl. A.N. SSSR* **152**, 1387 (1963).

---

† For certain samples with particularly highly dispersed Pt chemisorption occurs to a greater extent (see the table). It is natural to expect a change of chemical properties of Pt if its particles consist of a small number of atoms.

DETERMINATION OF SMALL SURFACE AREAS BY NITROGEN ADSORPTION

G. H. B. Lovell

Atomic Energy Board, Pretoria, South Africa

Measurements of surface areas less than 500 cm^2 g^{-1} using a Nelsen and Eggertsen type apparatus[1] were rendered inaccurate by small inverse peaks appearing before the desorption peaks, *Figure 1(a)*. These inverse peaks varied in size inversely with the surface area of the sample, becoming equal to the desorption peak when no sample was present, *Figure 1(b)*. Methods of eliminating the effects of these peaks were deemed necessary before accurate measurements could be made.

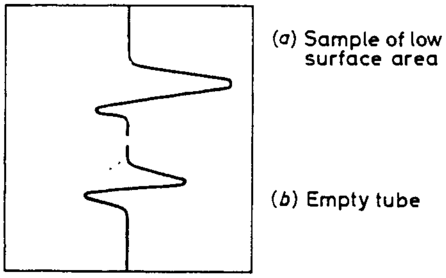

Figure 1. Desorption curves (not to scale)

TRANSVERSE THERMAL DIFFUSION

When a sample holder is removed from liquid nitrogen, pre-cooling of the gas stream in the thin inlet leg soon ceases, and the gas enters the still cold sample container sensibly at room temperature. Partial separation of the gases takes place by transverse thermal diffusion, nitrogen moving to the walls of the container and helium to the centre. Here the gas flow is more rapid and sweeps away the helium enriched gas to the katharometer, the trace recording an inverse peak. As the container approaches room temperature conditions for thermal diffusion cease, and the separated nitrogen diffuses into the gas stream producing a normal peak immediately following the inverse peak, and necessarily of the same area.

A further difficulty is the disturbance of the recorder base line caused by the rush of gas through the katharometer that accompanies the warming up of the sample holder. To overcome these difficulties the desorption apparatus (*Figure 2*) was designed.

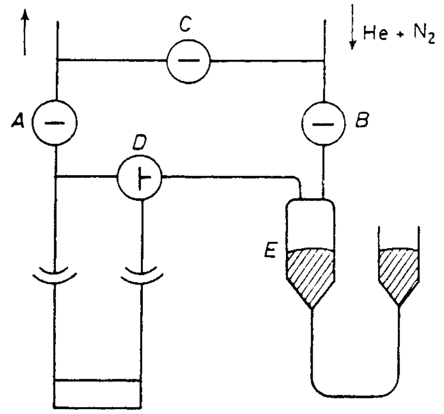

Figure 2. Adsorption apparatus after desorption

USE OF DESORPTION APPARATUS

During adsorption, stopcocks *A* and *B* are open, *C* closed and *D* in the position to direct the gas stream over the sample. Desorption is carried out with stopcocks *A* and *B* closed and *C* open, the expanding gas being accommodated in the vessel *E*. The pressure in the system is finally brought to atmospheric by adjustment of the mercury level in *E*. By opening stopcocks *A* and *B* and closing *C* the gas in the system can be passed to the katharometer with virtually no disturbance of the recorder base line. To reduce thermal diffusion effects the sample holder should be rapidly warmed up by immersion in room temperature water.

If the inverse peak is small it is permissible to subtract its area from that of the normal peak, but if it is of a size comparable to that of the normal peak it is advisable to remix the gases before passing to the katharometer. This can be accomplished by raising and lowering the mercury level in *E* whilst turning stopcock *D* so that gas is alternately drawn from the sample container up one leg and returned down the other.

LONGITUDINAL THERMAL DIFFUSION

Thermal diffusion can take place along the legs of a sample holder cooled in liquid nitrogen, helium diffusing towards the stopcocks *A* and *D* (*Figure 2*) and nitrogen to the cold sample container. Up the inlet leg, helium diffusion is against the gas stream of about 37 cm^3/min and can be minimized by reducing the leg diameter to 2 mm with a consequent increase in gas velocity.

The gas velocity in the 3 mm diameter outlet leg is probably sufficient to prevent the slower nitrogen diffusion, but the complete elimination of thermal diffusion effects is difficult and they are probably the major factor in determining the practical lower limit of measurement.

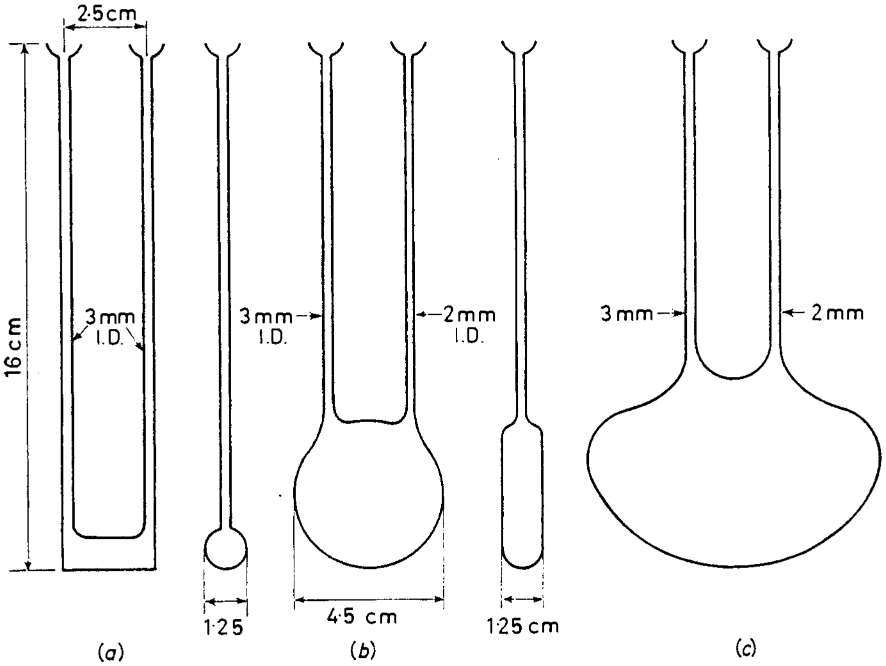

Figure 3. Sample holders (*a*) Nelson and Eggertsen; (*b* and *c*) Larger holders

SAMPLE HOLDERS

Large sample holders that contain the sample as a thin vertical bed to ensure uniform cooling and rapid warming are compared with the 'standard' holder in *Figure 3.* The largest holder, *c*, is designed to limit the maximum distance desorbed gas has to diffuse to enter the gas stream.

SIZE OF TRANSVERSE THERMAL DIFFUSION PEAKS

The area of the transverse thermal diffusion peak varies with the area of the cold sample container surface freely exposed to the gas stream. Holders should contain the maximum amount of sample without the gas flow being impeded sufficiently to cause a pressure increase in the katharometer reference cell and accompanying base line drift.

Sample holders completely filled with granules approximately 0·5 mm to 1·5 mm in diameter give minimal thermal diffusion peaks. Coarser particles often provide easy passage of gas between the grains and in consequence the thermal diffusion peaks can be large.

SPIRAL TUBE DESORPTION APPARATUS

With the desorption apparatus described (*Figure 2*) mixing between the desorbed gas and the instrument gas stream takes place in chamber *E* resulting in rather flat peaks. To improve the peak shape the vessel *E* was replaced by a vertical glass spiral (*Figure 4*) to which are attached a number of stopcocks connected to the instrument gas stream via a manifold *M* and three-way cock *B*.

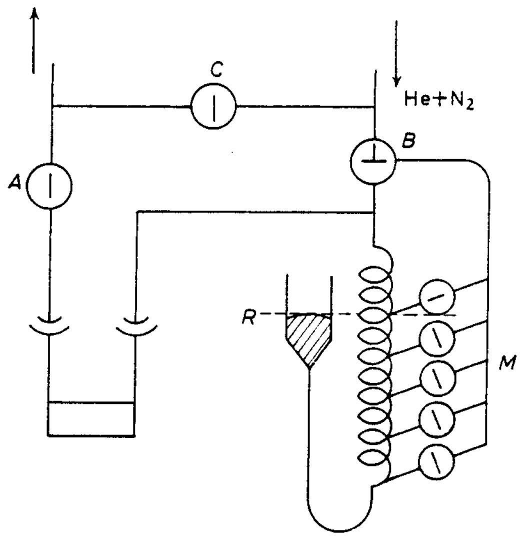

Figure 4. Spiral desorption apparatus showing desorbed gas passing to katharometer

Adsorption is carried out as before, and desorption with *C* open, *A* closed and *B* turned so that only the manifold is connected to the gas stream. After desorption is complete the pressure in the system is adjusted to atmospheric, and then the level of mercury in *R* moved so that when stopcock *A* is opened the mercury level in the spiral will move to just below one of the stopcocks attached to it.

On opening cock *A* followed by the selected spiral stopcock and closing *C*, the contained gas is passed to the katharometer.

Very sharp peaks are obtained and it can be inferred that the initial rush of gas observed on warming the sample holder is due to the expansion of the interstitial gas and it is only later that the adsorbed gas is released.

The apparatus cannot be used for re-mixing and hence is only of use when the inverse peak is small. In view of these limitations it is doubtful if the added complexity is justified.

Suitably small injection valves were made from 4-way glass stopcocks with single bore keys, the bore measuring the volume of nitrogen (*Figure 5*). For accurate measurement the nitrogen supply should be turned off before injecting.

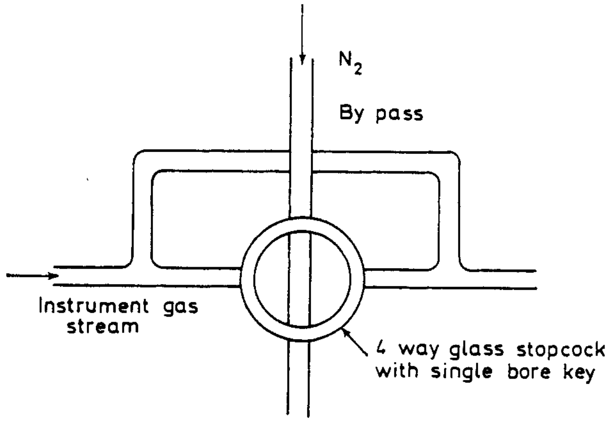

Figure 5. Injection valve capacity (approx. 0·01 ml)

RESULTS

The results of determinations on silica rock, crushed and wet-graded $-10 + 28$ mesh (1·68 to 0·6 mm dia.) using the spiral desorption apparatus, and on 2 mm diameter glass spheres using the mixing techniques are given in *Table 1.*

Table 1

	Silica rock ($-10 + 28$ mesh)	*Glass spheres* (2 mm dia.)
Surface area ($cm^2\ g^{-1}$)	227	81
	207	106
	222	78
	212	89
	207	126
	187	91
Mean	210·4	95·2
Standard deviation	14·0	18·0
Coefficient of variation	6·7	18·9

Reference

[1] F. M. Nelson and F. T. Eggertsen. *Anal. Chem.* **30**, 1387–1390 (1958).

ESR METHODS FOR THE ACTIVE SURFACE AREA DETERMINATION OF CATALYSTS

J. L. GARNETT and A. T. T. OEI

University of New South Wales, Kensington, Australia

A fundamental problem in current catalytic research is to determine the number of active sites on a catalytic surface and to relate these sites to the actual chemical reaction occurring on the surface. Conventional methods of surface area determination such as the BET method, need to be interpreted with caution since these procedures normally give surface areas based on the physical adsorption characteristics of nitrogen, or a rare gas, rather than their chemisorption properties.

It is thus important to be able to measure surface areas by other independent methods and to compare the results with conventional procedures. On sensitivity considerations, electron spin resonance (ESR) spectroscopy is a potentially powerful tool for the determination of unpaired spins in a catalytic surface. For most catalysts, it is useful to distinguish between bulk and surface paramagnetic properties. Thus current ESR methods can be used (i) directly to estimate the *total* unpaired spins in a system, or (ii) indirectly to measure the free radical species *at the surface* only. This communication summarises preliminary work using three different types of ESR procedure which appear to be attactive for the estimation of the active surface areas of various catalysts.

ESR METHODS

(i) Hydrogenation and exchange catalysts—Pre-reduced systems

A valuable class of catalysts are the pre-reduced Group VIII transition metals which are used for hydrogenation and isotopic hydrogen exchange reactions. For the deuteration of aromatic compounds with heavy water, platinum is the most active general catalyst[1]. These exchange reactions occur readily at room temperature. However, if the pre-reduced catalyst is exposed to oxygen, prior to exchange, the deuteration reaction is poisoned at room temperature, i.e. all active sites are combined with oxygen. If this oxygen is scavenged by hydrogen prior to exchange (a special example of 'self-activation'[2]) the deuteration reaction is not poisoned. If the scavenger is diphenyl picrylhydrazine ($DPPH_2$), the oxygen is readily removed quantitatively from the surface to give the radical DPPH which can be rapidly analysed by ESR.

In preliminary published work[3], the reaction of $DPPH_2$ with an oxygen-poisoned pre-reduced platinum catalyst was described and from the DPPH generated an active catalyst surface area of $0{\cdot}17$ m^2g^{-1} was calculated using a value of 8 $Å^2$ for the oxygen atom. In recent, more refined kinetic experiments, on a different batch[4] of $Pt + O_2$ where the catalyst was reduced slowly to minimize sintering, active surface areas of 1·1 m^2g^{-1} were obtained. This value is lower than the order of magnitude obtained for the surface area measurement of these catalysts by the carbon monoxide method[5]. These preliminary experiments show that the oxygen on the surface poisons the catalyst sites for isotopic exchange at room temperature. The present ESR technique of quantitatively scavenging this oxygen thus gives a direct measure of the number of sites which are catalytically active. Further, under the conditions of measurement, the correction for radical DPPH adsorption is relatively insignificant.

(ii) Oxidation catalysts—O_2 scavenging by $DPPH_2$

A modification of the above procedure (i) involves the estimation of active oxygen surface areas of inorganic oxides such as MnO_2, PbO_2 and $Pt + O_2$ etc. which are used for oxidation reactions. In this method[6], $DPPH_2$ in benzene is converted to DPPH by reaction with the oxygen on the inorganic oxide. The stationary state yield of DPPH can be related to the active oxygen scavenged on the oxide surface and thus to the number of active sites in these catalysts available for oxidation reactions. Using a sample of MnO_2, a surface area of 41·5 m^2g^{-1} was obtained by this ESR technique[6]. This compares with a value of 44 m^2g^{-1} by the BET method using nitrogen[6]. The limiting factor, again, in the procedure is the correction for residual DPPH adsorption on the surface, however this effect is only significant for concentrations of DPPH $> 6 \times 10^{-4}$ moles l^{-1} and experiments can be designed to work below this critical concentration.

(iii) DPPH adsorption from solution

A third modification of the above procedures is to measure directly the adsorption of DPPH from solution onto the surface of a catalyst. The same batch of MnO_2 as for procedure (ii) has been used[6] and the surface area determined from the DPPH adsorption isotherm. The value of 46 m^2g^{-1} obtained by this method is in good agreement with data from procedure (ii) and the BET method. For this calculation hexagonal close packing of spheres on the surface is assumed and thus the effective surface area of a DPPH molecule can be calculated to be 160 Å^2.

Misra[7] has already used an analogous technique for determining the surface areas of carbon blacks, his ESR value of 198·5 m^2g^{-1} being in good agreement with the electron micrographic area of 200 m^2g^{-1}. For carbon blacks it may even be possible to separate bulk and surface paramagnetism by the ESR method and experiments of this type are at present in progress[8]. This is important in gas phase pyrolysis studies of organic compounds where carbon films may be deposited and it is essential to establish possible *heterogeneous* contributions from the active sites in the surface of the carbon to the pyrolysis. Such studies are at present being finalised[8].

CONCLUSION

Three representative type systems have been summarised for the active surface area determination of catalysts by ESR methods. Where possible the results have been compared with surface area determinations by other methods including the BET method. The predominant advantages of the ESR method are high sensitivity and specificity.

ACKNOWLEDGEMENT

The authors thank the Australian Research Grants Committee and the Australian Institute of Nuclear Science and Engineering (Mr E. A. Palmer) for continued support.

References

[1] J. L. Garnett and W. A. Sollich-Baumgartner. *Adv. Catalysis* **16**, 95 (1966).
[2] J. L. Garnett and W. A. Sollich-Baumgartner. *J. Phys. Chem.* **68**, 436 (1964).
[3] J. L. Garnett, A. T. T. Oei and W. A. Sollich-Baumgartner. *J. Catalysis* **7**, 305 (1967).
[4] A. T. T. Oei and J. L. Garnett. *J. Catalysis*, in the press.
[5] J. W. Hightower and P. H. Emmett. *J. Colloid Sci.*, in the press.
[6] A. T. T. Oei and J. L. Garnett, submitted for publication.
[7] D. M. Misra, *J. Phys. Chem.* **71**, 1552 (1966).
[8] J. L. Garnett, D. Johnson, A. T. T. Oei and J. Sherwood, unpublished work.

THE APPLICATION OF HIGH TEMPERATURE/ LOW COVERAGE GAS ADSORPTION MEASUREMENTS TO THE DETERMINATION OF THE SURFACE AREAS OF SOLIDS

D. H. Everett

Department of Physical Chemistry, School of Chemistry, University of Bristol, Bristol, U.K.

This paper reviews critically the applicability to the determination of surface areas, of adsorption studies at temperatures above the bulk-phase critical temperature of the adsorptive, and at low surface coverages. Particular attention is paid to the limiting (Henry's law) behaviour, and to investigations of the deviations of the adsorbed phase from ideal two-dimensional gas behaviour.

1. INTRODUCTION

The use of gas adsorption methods for the determination of the surface areas of solids inevitably involves a series of compromises. In the absence of a universal theory of adsorption applicable over wide ranges of temperature and pressure, we are forced to employ one or more partial theories, each within the limited range of conditions to which it is appropriate. A step towards a more complete theory will have been taken when the parameters of one partial theory which satisfy the experimental data within one range of conditions also account for the behaviour of the system in other circumstances when used in conjunction with another partial theory. A key parameter which should remain invariant if various partial theories are valid is the area of the surface of the solid.

Each partial theory faces difficulties which limit the degree to which it can be regarded as a faithful representation of the physical situation. For example, theories which are concerned with relatively high adsorptions, at pressures up to about one atmosphere, and at temperatures below the boiling point of the adsorptive, have to deal with a fluid-like condensed phase in a steep potential gradient[1,2]. A detailed absolute theory relating to these conditions is likely to be at least as complex as that of a liquid in the absence of an external field. This difficulty is in part circumvented in the BET theory[3] by taking the liquid as a reference state whose properties such as its chemical potential and molar volume are known experimentally. By relating the properties of the adsorbate to those of the liquid, and assuming that a complete monolayer corresponds to close packing of molecules on the surface, it is possible to identify the degree of adsorption corresponding to monolayer coverage and so relate the surface area of the solid with some confidence to the size of the molecules of the adsorptive. It is, however, well known that the theory underlying the BET equation deals inadequately with the lateral interactions between adsorbed molecules[4], and has other shortcomings. From a practical standpoint, however, the experimental methods employed for the determination of surface area by the BET technique are well established and not unduly sophisticated.

On the other hand, at temperatures above the critical temperature of the adsorptive, and at adsorptions corresponding to less than one per cent of the monolayer capacity, it is possible[5–8] to derive a theory which is, in the limit, dependent only on adsorption forces and is independent of the interactions between adsorbed molecules and of their size. This theory, which applies to the 'Henry's law region' of the isotherm, is, however, markedly sensitive to energetic heterogeneity of the surface and requires for its quantitative application a detailed understanding of the nature of adsorption forces. This method has nevertheless the important practical advantage that Henry's law constants can be measured rapidly using gas chromatographic techniques.

A third approach[9,10] considers the region, again at high temperatures, but at pressures just above the Henry's law region in which deviations from Henry's law arise from interactions between pairs of adsorbed molecules. In this case what is needed (and can in large part be derived from the data themselves) is a knowledge of the laws governing the forces between adsorbed molecules. The theory is very largely independent of any detailed theory of adsorbent/adsorbate interactions, and, if the energetic heterogeneity of the surface is randomly distributed, or is periodic with a wavelength comparable with the molecular size of the adsorbate, it should be relatively insensitive to heterogeneity. If the surface consists of a number of uniform patches, however, then significant effects may be expected. This third approach to the problem has a number of apparent advantages, but these have not yet been fully explored experimentally, and they are in any case offset to some extent by the more sophisticated experimental techniques required to obtain reliable data.

The present review is concerned with a critical appraisal of the two high temperature methods mentioned above.

2. ADSORPTION IN THE HENRY'S LAW REGION (2ND ORDER INTERACTIONS)

We consider first the interaction of a dilute gas with a solid surface at temperatures where the adsorption is small enough for the potential energy of the system to arise solely from contributions from adsorbent/adsorbate interactions. Under these circumstances the problem may be discussed in terms of Boltzmann's distribution law[9]. In the simplest case of the adsorption of a monatomic gas by a plane surface the surface excess, n^{σ}, defined as the excess of the number of moles of gas actually present in the system over the number of moles which would be present if the bulk gas concentration, c^0, were uniform up to a chosen surface separating the solid and gas phases, is given by

$$n^{\sigma} = \underset{\substack{\text{all}\\\text{surface}}}{\int\int} \int_{z_0}^{\infty} (c - c^0)\, \mathrm{d}z\mathrm{d}x\mathrm{d}y + \underset{\substack{\text{all}\\\text{surface}}}{\int\int} \int_{0}^{z_0} c\,\mathrm{d}z\mathrm{d}x\mathrm{d}y, \qquad (1)$$

where c is the concentration of gas molecules in the element of volume $\mathrm{d}x\mathrm{d}y\mathrm{d}z$, and the adsorbing surface (defined, for example, by the plane of the nuclei of the surface atoms of the solid) is the xy-plane. z is then the perpendicular distance of the element $\mathrm{d}x\mathrm{d}y\mathrm{d}z$ from the adsorbing surface. The Gibbs dividing surface with respect to which the surface excess is defined is parallel to the xy-plane and cuts the z-axis at z_0. It is convenient to choose z_0 as the collision diameter between the gas atom and the surface i.e. the distance at which the adsorption potential energy, ϵ, is zero (*Figure 1*).

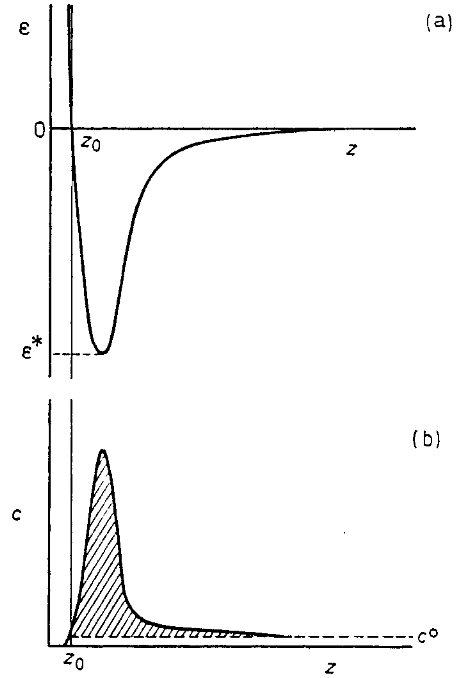

Figure 1. (a) Potential energy of interaction (ϵ) of gas atom with surface as function of perpendicular distance (z) from the surface. z_0 is the collision diameter of the atom with the surface; ϵ^* the depth of the potential energy minimum.
(b) concentration (c) of gas atoms as function of z. c^0 is the gas concentration far from the surface where ϵ is zero. Shaded area gives adsorption per unit area relative to a Gibbs dividing surface at z_0.

According to Boltzmann's distribution law

$$c = c^0 \mathrm{e}^{-\epsilon(x,y,z)/kT}, \qquad (2)$$

where ϵ, the mutual potential energy of the solid and a single gas atom at (x,y,z) is, in general, a function of all three variables.

It follows that, neglecting the small second term in Eq. (1),

$$n^{\sigma} = c^0 \underset{\substack{\text{all}\\\text{surface}}}{\int\int} \int_{z_0}^{\infty} [\mathrm{e}^{-\epsilon(x,y,z,)/kT} - 1]\, \mathrm{d}z\mathrm{d}x\mathrm{d}y\,. \qquad (3)$$

In the particular case in which the surface is energetically uniform i.e. ϵ is independent of x and y, the integration over these variables can be carried out immediately to give $\int \int \mathrm{d}x\mathrm{d}y = A$, the surface area. Furthermore, if the gas phase behaves as an ideal gas, $c^0 = p/\boldsymbol{R}T$, where p is the gas pressure, so that

$$n^\sigma = \frac{Ap}{\boldsymbol{R}T} \int_{z_0}^{\infty} [\mathrm{e}^{-\epsilon(z)/kT} - 1]\,\mathrm{d}z\,. \tag{4}$$

If the adsorption potential energy can be written in the reduced (or conformal) form

$$\frac{\epsilon}{\epsilon^*} = f\left(\frac{z}{z_0}\right), \tag{5}$$

where ϵ^* is the depth of the minimum in the curve of ϵ against z, then it follows that the integral in equation (4) can be written

$$z_0 \int_1^{\infty} [\mathrm{e}^{-\epsilon(z/z_0)kT} - 1]\,\mathrm{d}\,(z/z_0) = z_0\,F\left(\frac{\epsilon^*}{\boldsymbol{k}T}\right), \tag{6}$$

where the form of F is immediately deducable from that of f.

Equation (4) predicts that the isotherm of n^σ against p is linear. The slope is the so-called Henry's law constant, k_{H}, which is thus given by

$$k_{\mathrm{H}} = \frac{Az_0}{\boldsymbol{R}T} F\left(\frac{\epsilon^*}{\boldsymbol{k}T}\right) \tag{7}$$

A quantitative theory of adsorption forces can, in principle, yield values of z_0 and ϵ^* and the form of F so that from a measured value of k_{H} the surface area A can be calculated. In the present state of knowledge, while reasonably based theories exist to evaluate the contribution to ϵ from attractive dispersion forces, there is no adequate theory of repulsive forces. Consequently it is necessary either to combine experimental data with theoretical equations to obtain z_0, or to estimate z_0 from other considerations (e.g. collision or crystal radii).

First, an appropriate algebraic form for the adsorption potential has to be selected. For example, most attention has so far been paid to potentials of the following form:

$$\frac{\epsilon}{\epsilon^*} = \frac{n}{m-n}\left(\frac{m}{n}\right)^{-\frac{m}{m-n}} \left[\left(\frac{z_0}{z}\right)^m - \left(\frac{z_0}{z}\right)^n\right] \tag{8}$$

where $m > n$. If interactions between the atom of adsorbate and a single atom of the solid is characterised by $n = 6$, $m = 12$, (the 6:12 potential) then integration throughout a continuous semi-infinite solid with a planar surface leads to $n = 3$, $m = 9$ for the adsorption potential energy. If the solid has a layer structure (e.g. graphite) so that most of the interaction energy comes from the first layer of atoms, then $n = 4$, $m = 10$.

Values of $F(\epsilon^*/\boldsymbol{k}T)$ have been tabulated for a variety of values of $(n{:}m)$ including $(3{:}\infty)^{7}$; $(3{:}12)^{11,14}$; $(3{:}9)^{11,12,13,15}$; $(4{:}10)^{11}$.

For a given chosen form of F it is now possible by various fitting techniques to find the values of Az_0 and ϵ^* which best represent the experimentally observed variation of k_H with T. It is important to stress that this analysis gives only the product Az_0 and that some means must be found of estimating z_0 before the surface area can be calculated.

From a theoretical standpoint, if it is possible to evaluate the attractive contribution to the adsorption potential:

$$\epsilon^{att} = -C/z^3 \tag{9}$$

by calculating C absolutely, then from a knowledge of the experimental value of ϵ^*, z_0 can be found from the relationship

$$z_0 = \sqrt[3]{\frac{g(m)C}{\epsilon^*}}, \tag{10}$$

where $g(m)$ is a numerical constant equal to $(3/[m-3])\ (m/3)^{m/(m-3)}$. In effect we employ the experimental value of ϵ^* together with the theoretical equation (9) to evaluate the repulsive part of the potential.

Sams, Constabaris and Halsey[17], as well as others, have examined the applicability of a number of alternative theoretical equations for determining the constant C. The results of calculations of A based on experimental data on the adsorption of noble gases by graphitised carbon are summarised in *Table 1*. The variation in the calculated values of A for P33 (2700) graphitised carbon shown in the table emphasises the unsatisfactory state of the theory of adsorption forces. It is well known that the theory of dispersion forces between like atoms in the gas phase is far from complete[18]. When applied to the interaction between unlike atoms an added problem arises, namely that of the appropriate 'combining rule' to be applied. Sams[19] has shown that a further selection of discrepant results are obtained if different combining rules are selected. It is thus claimed that the rather satisfactory agreement found by Crowell and Steele[20] for ϵ^* calculated using the geometric mean combining rule for the attractive constants was somewhat fortuitous. Attention is also drawn to the work of Poshkus and Kiselev[21] whose calculations of the energy of interaction between graphite and noble gas atoms yield values of ϵ^* in excellent agreement with experiment. These authors employ rather more sophisticated equations which include terms for dipole-quadrupole interactions and evaluate z_0 (and its variation from point to point over the surface) from consideration of the van der Waals radii of the adsorbed atom and of a carbon atom in graphite.

An alternative method[17] of factorising Az_0 which has the advantage of not calling upon a theory of adsorption forces, but depends on the additivity of collision radii, is to plot Az_0 for a series of noble gas atoms against the collision radius $(r_0/2)$ of the noble gases derived from gas phase measurements. Since as an approximation

$$z_0 = \frac{(r_0)_C}{2} + \frac{r_0}{2} \tag{11}$$

Table 1. Analysis of high temperature gas adsorption data

Henry's law analysis

(a) P33(2700) (BET area 12·5 m^2g^{-1})

EXPERIMENTAL DATA OF SAMS, CONSTABARIS AND HALSEY[17]

	Model†	ϵ^*/k K	$Az_0 \times 10^3$ cm^3g^{-1}	A/m^2g^{-1}‡				
				KM	SK	L	B	MP
Ne	3: 9	382	2·199	8·00 (7·94)§	12·09	14·87(14·34)	12·65	11·77
	3:12	383	2·541	8·64 (8·52)	13·11	16·10(15·31)	13·68	12·72
	4:10	367	3·117	8·45 (8·37)	10·91	13·45(13·23)	—	—
Ar	3: 9	1107	2·393	8·64	12·80	14·96	12·80	11·81
	3:12	1110	2·762	9·33	13·81	16·15	13·81	12·73
	4:10	1071	3·278	8·86	11·38	13·38	—	—
Kr	3: 9	1460	2·406	8·44	12·73	14·76	12·66	11·68
	3:12	1463	2·797	9·17	13·81	15·98	13·78	12·71
	4:10	1403	3·399	8·97	11·76	13·65	—	—
Xe	3: 9	1919	2·625	8·75	13·53	15·44	13·26	12·38
	3:12	1923	3·042	9·48	14·63	16·71	14·42	13·40
	4:10	1860	3·549	9·05	12·11	13·81	—	—
H_2	3: 9	574(614)	—	12·88¶(11·26)	—	17·45	—	—
	3:12	576(617)	—	13·87 (12·01)	—	18·86	—	—
	4:10	552(587)	—	12·65 (11·05)	—	15·93	—	—
D_2	3: 9	579(601)	—	12·72 (11·82)	—	17·12	—	—
	3:12	580(606)	—	13·79 (12·62)	—	18·54	—	—
	4:10	556(574)	—	12·54 (11·70)	—	15·53	—	—
CH_4	3: 9	1483(1486)	—	6·74 (6·71)	—	12·96	—	—
	3:12	1487(1490)	—	7·28 (7·25)	—	13·99	—	—
	4:10	1432(1435)	—	7·20 (7·16)	—	11·74	—	—
CD_4	3: 9	1450(1452)	—	7·37 (7·36)	—	14·13	—	—
	3:12	1454(1456)	—	7·96 (7·94)	—	15·20	—	—
	4:10	1399(1402)	—	7·90 (7·85)	—	12·87	—	—

† Analysis was also made in terms of (3:∞) potential[17]; the areas calculated on this basis are widely different from those tabulated and have been omitted from this summary.

‡ Abbreviations refer to equation used for calculating adsorption energy: KM, Kirkwood-Müller; SK, Slater-Kirkwood; L, London; B, Bardeen; MP, Margenau-Pollard.

§ Figures in brackets include corrections for quantum effects[11, 16].

¶ The figures given here are taken from ref. 11 and differ substantially from those given in ref. 17b: the reason for this difference is said[11] to arise from the use of different values for the susceptibility of P33 in the two sets of calculations: however, the value for this susceptibility quoted in ref. 11 is the same as that used in earlier papers by Halsey and his co-workers.

Table 1 continued on p. 187

Table 1 continued from page 186

(b) P33(2700) EXPERIMENTAL DATA OF EDMONDS[52]

	Model	ϵ^*/k K	$Az_0 \times 10^3$ cm^{3}g^{-1}	A/m^{2}g^{-1} KM	 Coll. diam.†
Kr	3:9	1450	2·54 ± 0·03	8·89	7·24
Xe	3:9	1905	2·637 ± 0·001	8·78	7·02

†z_0 taken as ½ layer spacing in P33 (1·71 Å) + ½ r_0, where r_0 is the gas collision diameter

(c) P33(2700) EXPERIMENTAL DATA OF THOMAS[53]

	Model	ϵ^*/k K	$Az_0 \times 10^3$ cm^{3}g^{-1}	A/m^{2}g^{-1} KM	 Coll. diam.
Ar	3:9	1150 ± 20	2·08 ± 0·03	7·60	6·10
N_2	3:9	1185 ± 5	2·094 ± 0·003	—	5·90

(d) BLACK PEARLS No. 71 (BET AREA 337 m^{2}g^{-1})
EXPERIMENTAL DATA OF STEELE AND HALSEY[7] AND OF FREEMAN AND HALSEY[35]

		ϵ^*/k K	$Az_0 \times 10^3$ cm^{3}g^{-1}	z_0 Å	A_{KM} m^{2}g^{-1}	Ref. No.
He	3:∞	302	114	2·47	462	7
	3:9	231·67	80·1	1·96	409	13
	(3:9)QM	243·86	76·6	1·93	397	13
	(3:9)	270	51·3	2·18	235	12
Ne	3:∞	685	99·3	2·70	367	7
	3:9	646·83	40·4	2·00	202	13
Ar	3:∞	2185	71·9	2·75	262	7
	3:9	2049·14	23·45	2·04	115	13
	3:9	1921	39·64	2·45	162	12

(e) *Sterling MT*(*2800*) (BET area 7·5 m^{2}g^{-1}) EXPERIMENTAL DATA OF THOMAS[53]

	Model	ϵ^*/k K	$Az_0 \times 10^3$ cm^{3}g^{-1}	z_0(KM) Å	A_{KM} m^{2}g^{-1}	z_0(coll. diam.) Å	$A_{coll.}$ m^{2}g^{-1}
Kr	3:9	1430 ± 30	1·06 ± 0·09	2·81	3·8	3·51	3·0
Xe	3:9	1928 ± 10	1·01 ± 0·04	2·94	3·4	3·76	2·7

where $\frac{(r_0)_C}{2}$ is the collision radius of the carbon surface, this graph should be a straight line of slope A (*Figure 2*)†. If the collision radii are those corresponding to a (6:12) potential in the gas phase, then $A = 7{\cdot}41$ m^{2}g^{-1}, while the use of crystal radii gives $A = 8{\cdot}38$ m^{2}g^{-1} for P33(2700) graphitised carbon.

It is clear that even when applied to the determination of the surface areas of homogeneous surfaces the use of the Henry's law constant is subject, at the present time, to many uncertainties. Even greater uncertainties arise when the adsorptive is non-spherical and the surface is either heterogeneous or non-planar. It is not necessary to give the detailed theory since the general problems can be indicated qualitatively.

---

†It is interesting to note that essentially this method was advocated by Williams[22] fifty years ago, using values of r_0 calculated from van der Waals constants.

First, if the molecule is non-spherical the potential energy of interaction with the surface will depend not only on the location of its centre of mass, but also on its orientation[8]. If α, β and γ are appropriate angular co-ordinates defining the orientation of the molecule then $\epsilon(x,y,z,\alpha,\beta,\gamma)$ instead of $\epsilon(x,y,z)$ and equation (3) now has to be integrated over all six variables.

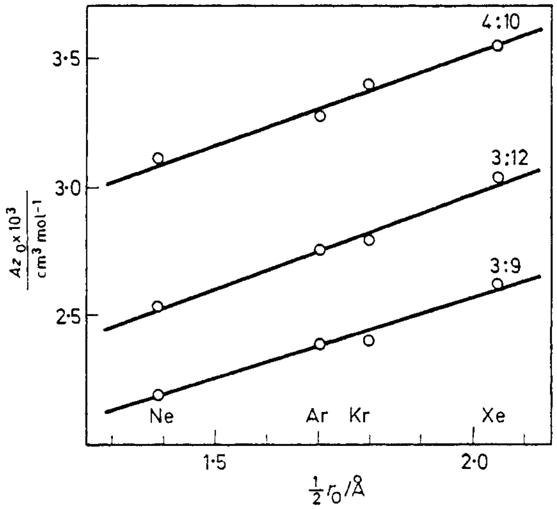

Figure 2. Az_0 for adsorption by P33(2700) graphitised carbon black as a function of the collision radius of rare gas atoms ($r_0/2$). Az_0 calculated for (3:9), (3:12) and (4:10) forms of adsorption potential energy; r_0 is the collision diameter calculated from the second virial coefficient of the bulk gas. Areas derived from the slopes of these lines are given in *table* (*3b*) (ii).

Secondly, if the surface is planar but energetically heterogeneous then the integration over (x,y) in equation (3) leads not to the area but an 'apparent area' which is a weighted average area[23].

Thirdly, if the solid is porous, then again the interaction energy $\epsilon(x,y,z)$ depends on all three variables together, and the integration has to be carried out throughout the pore volume of the system.

The result of a more complete analysis of the problem can now be written in general terms in the form

$$k_{\mathrm{H}} = \frac{Az_0}{kT} F_0 \left(\frac{\epsilon_0^*}{kT}\right) \phi_{\mathrm{rot}}\ \phi_{\mathrm{het}}\ \phi_{\mathrm{cap}} \tag{12}$$

where F_0 is a reference function applicable to a plane surface and ϵ_0^* is a reference energy of interaction. ϕ_{rot} is a factor which depends on the orientation dependence of the interaction energy; ϕ_{het} is a factor depending on the heterogeneity of the surface and includes a term dependent on the difference between ϵ_0^* and the mean interaction energy; ϕ_{cap} takes account of the modification to F_0 by the geometry of the system. If both heterogeneity and porous structure are simultaneously present then the two effects cannot easily be disentangled.

The effect of these factors have been examined in a preliminary way by several authors. Thus ϕ_{cap} has been calculated by Steele and Halsey[24] for parallel-planar walls and cylindrical capillaries (*Figure 3*).

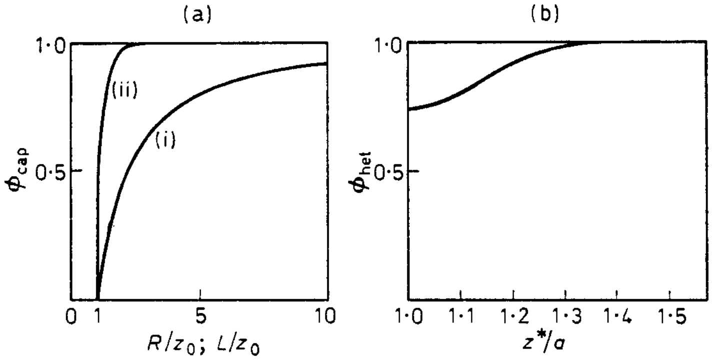

Figure 3. (a) ϕ_{cap} as a function of size of capillaries: (i) for cylindrical capillaries of radius R: (ii) for parallel slot capillaries of width L.
(b) ϕ_{het} for heterogeneity caused by periodic fluctuations across the 100 face of a simple cubic lattice of identical atoms, as a function of z^*/a. z^* is the value of z at the minimum of the adsorption energy curve, and a is the lattice parameter. $z^*/a \rightarrow \infty$ corresponds to a structureless solid.

Heterogeneity may manifest itself either through a periodic variation of ϵ^* over distances comparable with the lattice spacing of the solid; a random distribution of adsorption sites of differing adsorption energies; or in terms of a patchwise distribution of areas of solid (e.g. crystal faces) to which correspond different energies. As far as the Henry's law constant is concerned the spacial distribution of adsorption energies is irrelevant. One particular case which has been computed[24] is that in which ϵ^* depends on the location of the adsorbate atom over an array of atoms of a simple crystal lattice. The results for the (100) plane is shown in *Figure 3* (*b*) in which ϕ_{het} is plotted as a function of z^*/a where a is the lattice parameter.

Finally, we consider ϕ_{rot}. It has been recognised experimentally[25-27] that when Henry's law constants for a series of molecules of increasing complexity are considered, then the values of A calculated for a given surface fall off as the molecule increases in size. Thus in the extreme case of the adsorption of benzene on graphitised carbon[28,29] the experimental data suggest that $\phi_{rot} \approx 1/100$. When the orientation dependent ϵ calculated by Kiselev and Poshkus[30] is employed in equation (3), however, the calculated value of k_H is consistent with the accepted value of the surface area of P33(2700)[29]. Similarly, Freeman and Kolb[25] found that the surface areas calculated from k_H determined gas-chromatographically for several alkanes, decreased as the size of the molecule increased and hence, presumably, ϕ_{rot} decreased. Similar results were reported by Hansen, Murphy and McGee[26]. It may be commented in passing that Freeman and Kolb in fact attempted to interpret their data by assuming that the surfaces of the charcoals they studied were heterogeneous and possessed two types of surface A_1 and A_2 for which the adsorption energies were ϵ^* and $2\epsilon^*$ respectively. They thus threw the blame for the variation of the apparent surface area with molecular size on ϕ_{het}, whereas it is probable that ϕ_{rot} is the main factor, and ϕ_{cap} may also have played some part.

We conclude that, from the point of view of surface area determination, the use of Henry's law constant measurements is of value only if the measurements are made with monatomic gases; and that more careful study of the influence of heterogeneity is needed before this method can be considered to have any absolute status. On the other hand, studies of adsorption of a variety of gases on a surface of well defined area are of value in elucidating the nature of the adsorption phenomenon for different molecules.

It remains only to comment on the special case of adsorption in the Henry's law region of gases by microporous solids. Here we may regard the problem as one of micro-pore filling, assuming that within each pore the adsorption potential energy is essentially constant. Equation (3) then leads to the simple relationship

$$k_{\mathrm{H}} = \frac{V^p}{RT}\,[\mathrm{e}^{-\epsilon/kT} - 1] \tag{13}$$

where $V^p = \int \mathrm{d}x\mathrm{d}y\mathrm{d}z$ = pore volume of the solid accessible to the centres of mass of the adsorbed molecules. In this case, of course, adsorption measurements in this region can tell us relatively little about the surface area of the solid, although it may be possible to gain some information by studying the change of V^p with the diameter of the adsorbate: in the absence of a molecular sieve effect, the variation of V^p with molecular size may give some information about the size of the capillaries.

3. ADSORPTION IN THE SLIGHTLY IMPERFECT TWO-DIMENSIONAL GAS REGION (3RD ORDER INTERACTIONS)

In the previous section we have examined the problems which arise when an attempt is made to calculate the surface area of a solid from the Henry's law constant characterising its interaction with a dilute gas. We now consider adsorption equilibrium at somewhat higher pressures where deviations from Henry's law become important. Provided that the temperature is high enough, relative to the potential barriers hindering free translation over the surface, but not too high relative to the adsorption energy, then the adsorbed molecules will form an approximately two-dimensional mobile phase which may be treated as a slightly non-ideal two-dimensional gas. It was shown by Barker and Everett[9] and by Constabaris, Halsey and Sams[10] that by considering deviations from Henry's law it is possible to develop a new method of deriving surface areas which does not require a prior knowledge of the potential energy of interaction of adsorbed molecules with the surface, but relies on knowledge gained from the adsorption data themselves about the interactions between adsorbed molecules.

Ignoring for the moment the effects of non-ideality of the bulk gas, and of deviations of the adsorbed phase from exact planarity, it can be shown that†

$$\ln \frac{n^\sigma}{p} = \ln k_{\mathrm{H}} - \frac{2n^\sigma B^*}{A}, \tag{14}$$

where B^* is the two-dimensional virial coefficient which describes the deviation of the spreading pressure π of the adsorbed gas from the ideal equation:

$$\pi A = n^\sigma RT\left[1 + \frac{n^\sigma B^*}{A} + \frac{(n^\sigma)^2 C^*}{A^2} + \ldots\right]. \tag{15}$$

According to equation (14) a graph of $\ln(n^\sigma/p)$ against n^σ should be linear with a slope of $-2B^*/A$. An alternative method of analysis is to plot n^σ/p against p: if this is linear so that

$$\frac{n^\sigma}{p} = k_1 + k_2 p, \tag{16}$$

(k_1 is, of course, equal to k_{H}), then it follows that

$$\frac{2B^*}{A} = -\left(\frac{k_2}{k_1^2}\right). \tag{17}$$

Thus if B^* can be evaluated independently, the surface area A can be found.

The two-dimensional second virial coefficient is related to the energy of interaction $u^*(r)$ between two adsorbate molecules a distance r apart on the surface by the following equation‡, analogous to that for the bulk second virial coefficient:

$$B^* = -\frac{N_{\mathrm{A}}}{2}\int_0^\infty 2\pi r\,[\mathrm{e}^{-u^*/kT} - 1]\,\mathrm{d}r. \tag{18}$$

As a first approximation we might assume that $u^*(r)$ is the same as $u(r)$ in the bulk gas phase§. If, for example, the Lennard-Jones (6:12) potential appropriate to gaseous Ar is inserted in Eq. (18), then the relation between B^* and T shown in *Figure 4*, curve (i) is obtained. However, taking the experimental data[10] for adsorption of Ar by P33(2700), assuming provisionally an area of about 10 $\mathrm{m^2 g^{-1}}$, and calculating B^*, we obtain the experimental points shown in the figure. The main discrepancy between the theoretical and experimental values of B^* lies in the wide difference between the temperatures at which B^* passes through zero (two-dimensional Boyle temperature, T_B^*). No adjustment of the surface area can rectify this discrepancy, so that we are led immediately to the conclusion that the interaction energy u^* is different from that, u, between molecules in the gas. It is well known that the dispersion energy between a pair of gas atoms is

---

† The earliest derivation of this equation seems to have been by Williams[22], although on rather different grounds. Virial equations of this type were, however, derived also by Bradley[31], and by Wilkins[33].

‡ First derived by Mitchell[34] although clearly hinted at by Bradley[31].

§ Wilkins[33] adopted this view but used a very crude non-attracting hard sphere model for both gas and adsorbed phases. Freeman and Halsey[35] in their preliminary work also used the same model and obtained 'surprisingly close agreement' between theory and experiment.

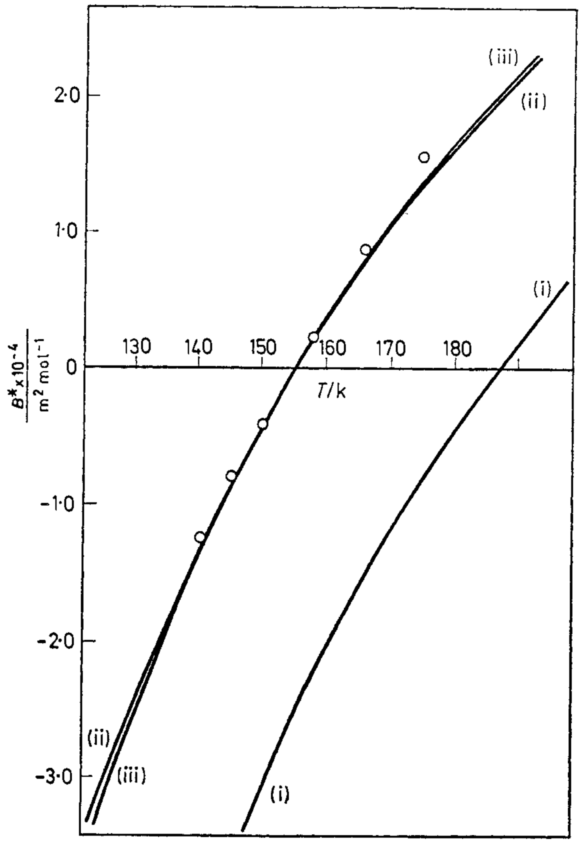

Figure 4. Two-dimensional second virial coefficient B^* as a function of T. Points: experimental points for Ar adsorbed on P33(2700) taking $A = 10{\cdot}2\ m^2g^{-1}$. Curve (i): calculated from (6:12) interaction potential between adsorbed atoms, using bulk gas phase parameters. Curve (ii): (6:12) potential with perturbed attraction term. Curve (iii): (6:12:3) potential with bulk gas phase parameters for terms in r^{-6}, r^{-12} and coefficient of r^{-3} repulsion fitted to experimental data.

perturbed by the presence of a third atom (three-body effect), and it can be shown[36–38] that in the same way the energy of interaction between a pair of adsorbed molecules will be perturbed by the presence of a surface with which the adsorbed molecules are interacting simultaneously.

There are several ways in which this effect can be incorporated into the present theory, of which four are discussed below[39].

(i) We may follow Sams, Constabaris and Halsey[10] in assuming, empirically, that perturbation by the surface changes the depth of the minimum (u^*_{min}) of the interaction potential between adsorbed molecules but does not change the collision diameter, r^*_0.

(ii) The alternative empirical approach of Everett and Barker[9] is to assume that the presence of the surface influences the attractive part of the potential function, reducing it by a factor ξ, while leaving the short range repulsive contribution unaffected.

(iii) The theoretical conclusions of Pitzer and Sinanoglu[36] may be accepted, and the perturbation may be expressed in terms of a long-range repulsion proportional to $1/r^3$ which is added to the bulk gas (6:12) potential.

(iv) The more complex theoretical equation of McLachlan[37] may be employed which predicts a perturbation which at short distances is proportional to $1/r^3$, but which changes steadily to a $1/r^6$ term at larger separations.

Values of B^* corresponding to all these cases have been computed and tabulated [9,10,14,40–43]. As might have been expected from experience in the fitting of bulk gas virial coefficients to different forms of interaction potential, when the parameters of the various equations are chosen to give the same Boyle temperature, the calculated values of B^* as a function of temperature do not differ significantly from one another, as shown by curves (ii) and (iii) in *Figure 4*. This figure shows also that, when an appropriate value is chosen for the surface area, any one of these potentials gives an adequate representation of the experimental data. Furthermore, it has also been shown[44,45] that the inclusion of quantum effects does not lead, for Ar and heavier noble gases, to any significant contribution to B^*.

Thus, although adsorption measurements of this kind demonstrate clearly that the forces between adsorbed molecules are very substantially modified by the presence of a solid surface, it is not possible to distinguish between alternative forms of equation to represent the perturbed potential. If it were possible to derive theoretically the absolute values of the parameters of the theoretical equations, then the validity of the alternative theories could be assessed: the preliminary conclusions are that neither theoretical treatment is adequate to provide a quantitative explanation of the observed results[46,41,47,42].

However, from the point of view of surface area determination, this lack of sensitivity to the exact form of the perturbed potential is a major advantage since it is unlikely that the correct form of this potential will lead to values of B^* substantially different from those corresponding to the equations discussed above.

In the practical application of the method outlined above, it is necessary to eliminate the approximations implied in the above discussion, since they can introduce errors of more than 10 per cent. There are three main correction terms to be included. These take account of the non-ideality of the bulk gas phase, of interactions between 'adsorbed molecules' and adjacent gas phase molecules, and the fact that the adsorbed molecules are not confined exactly to a plane but have a component of motion normal to the surface. A simple correction for gas phase imperfection[9] gives the equation

$$\frac{2B^*}{A} = -\frac{(k_2 - Bk_1/RT)}{k_1^2}, \tag{19}$$

where B is the bulk second virial coefficient, while the more complete theory, taking account of the first and third of the above effects[9] gives

$$\frac{2(B^* - \alpha)}{A} = -\frac{(k_2 + 3Bk_1/RT)}{k_1^2}\,, \tag{20}$$

where α is a term which corrects for the deviation of the adsorbed phase from exact planarity†. The value of α depends on the adsorption energy ϵ^* (which as seen in Section 2 can be evaluated from an analysis of k_1 as a function of T), T, z_0, $u^*_{\min}$ and on r^*_0, the collision diameter of the adsorbed molecules. Computed values of α are given by Barker and Everett[9] together with an interpolation formula which Wolfe and Sams[14] have used to prepare a more complete table.

There are still too few experimental data available to enable a critical test to be made of this method of determining surface areas. The work of Sams, Constabaris and Halsey[10,47,49–51] has been analysed and reanalysed many times. Different authors have included the various correction terms in various combinations, and have used several forms for the perturbed potential $u^*(r)$ between adsorbed molecules. The published results of these analyses are summarised in *Table 2*. In addition, similar, though less extensive, measurements have been made by Edmonds[52] and Thomas[53]: an analysis of their work is included in the table.

Table 2. Analysis of high temperature gas adsorption data: imperfect two-dimensional gas method

	Eqn. for $u^*(r)$	Eqn. for B^*/A (*see footnote*)	$u_{\min}/k$ K	r_0 Å	$u^*_{\min}/k$ K	r^*_0 Å	A m^{2}g^{-1}	Ref. No.
	P33(2700) EXPERIMENTAL DATA OF REF. 10 AND REF. 52 FOR Xe							
	Square well	(b)	69·4	3·16	53·7	3·16	9·3 ± 0·4	39
Ar	6:∞	(a)	—	—	222		9·3	48
	6:12	(a)	124	3·40	96	3·40	8·96 ± 0·5	10
		(b)	119·8	3·41	99·4	3·41	9·8 ± 0·3	39
		(b)	119·8	3·41	99·4	3·46	10·2 ± 0·3	39,40
		(c)	119·8	3·41	98·1	3·47	8·95 ± 0·5	46
		(b)	119·8	3·41	99·4	3·46	10·08	42,48
	6:12:3	(b)	119·3	3·45	—	—	10·59	42
		(b)	119·8	3·41	110·0	3·43	10·4 ± 0·3	39
		(b)	119·8	3·41	109·9	3·43	10·36	42,48
		(b)	119·8	3·41	110·0	3·43	10·7 ± 0·3	40,41
		(b)	122·0	3·40			10·36	42
	McLachlan	(b)	119·8	3·41			10·5 ± 0·3	41
	6:12	(d)	119·8	3·41	95	3·47	8·54	14
		(e)	119·8	3·41	94·6	3·48	8·32 ± 0·5	46
	6:12		166·7	3·68	142·8	3·73	9·73	

Table 2 continued on page 195

---

†k_1 and k_2 are here the intercept and slope of a graph of n^σ/p against p; if the data are expressed in terms of V_{ex}[7], and k_1' and k_2' refer to a graph of V_{ex}/p against p, then Eq. (20) becomes[46]

$$\frac{2(B^* - \alpha)}{A} = -\frac{(k_2' + 2Bk_1'/RT)}{(k_1')^2}\,.\,RT\,. \tag{20'}$$

It is not always clear whether authors have analysed data through n^σ or V_{ex}, nor whether, when V_{ex} has been converted to n^σ, a bulk gas imperfection correction has been included.

Table 2 continued from page 194

	6:12:3	(b)	158·7	3·60	151·2	3·61	9·30	42
		(b)	165·2	3·66	154·6	3·68	9·69	42
		(b)	166·7	3·68	155·4	3·70	9·81	42
		(b)	172·7	3·59	158·5	3·61	9·44	42
	6:12	(d)					8·2	14
Xe	6:12	(b)	225·3	4·07	194·0	4·12	10·86	42
		(e)	221·0	4·10	207	4·12	10·6 ± 1·0	46†
	6:12:3	(b)	224·5	4·06			11·02	42
			225·3	4·07			11·11	42
			229·8	3·97			10·65	42
			230·2	3·97			10·63	42
	6:12	(d)			184	4·14	8·68	14
		(e)	221·0	4·10	195·6	4·14	9·8 ± 1·0	46†
CH_4	6:12	(b)	148·2	3·82	129·2	3·86	11·3	42
	6:12:3	(b)	148·2	3·82	139·2	3·84	11·48	42
	6:12	(d)					8·8	14
		(e)	148·2	3·82	135 ± 7	3·85	8·5 ± 1·0	46
CD_4	6:12	(b)	146·9	3·82	129·3	3·86	9·4	42
	6:12:3	(b)	146·9	3·82	138·6	3·84	9·43	42
	6:12	(d)					7·3	14
BLACK PEARLS 71 (BET AREA = 337 m^2g^{-1}; E.M. area = 130 m^2g^{-1}) EXPERIMENTAL DATA OF FREEMAN[12]								
	6:∞	(a)	119·8	3·41	222	—	98	48
	6:12	(b)	120	3·41	80	3·52	123	9
	6:12	(a)	119·8	3·41	97	3·47	111	48
	6:12:3	(a)	119·8	3·41	109		111	48
GRAPHON (BET AREA = 85 m^2g^{-1}) EXPERIMENTAL DATA OF EDMONDS[52]								
Kr	6:12	(c)	171·0	3·60	102·5	3·76	43·3 ± 5	
Xe	6:12	(c)	221·0	4·10	131	4·28	39·9 ± 5	
STERLING MT(2800) (BET AREA = 7·5 m^2g^{-1}) EXPERIMENTAL DATA OF THOMAS[53]								
Kr	6:12	(c)	221	4·10	206·5	4·12	6·5 ± 2·5	
	6:12	(e)	221	4·10	202·5	4·13	5·5 ± 2	

(a) $2B^*/A = -k_2/k_1^2$ (see eqn. 17)
(b) $2B^*/A = -(k_2 - Bk_1/RT)/k_1^2$ (see eqn. 20)
(c) $2B^*/A = RT(k_2' + 2Bk_1'/RT)/k_1^2$ (see eqn. 20′)
(d) $2(B^* - \alpha)/A = -k_2/k_1^2$
(e) $2(B^* - \alpha)/A = -(k_2 + 2Bk_1/RT)/k_1^2$ (see eqn. 20)

† Experimental data of Edmonds[52]

This table demonstrates that the final calculated value of the surface area is insensitive to the values chosen for the bulk gas parameters, and to the exact form of $u^*(r)$. Thus for Ar adsorption by P33(2700) the 6:12, 6:12:3 and McLachlan potentials, used with a range of bulk gas parameters, lead (with the same form of bulk gas imperfection correction) to calculated surface areas of 10·3 ± 0·5 m^2g^{-1}. Even the unrealistic square well and 6:∞ potentials give an area of 9·3 m^2g^{-1}.

The bulk gas imperfection correction has a significant effect: the use of Eq. (20) (neglecting α) in place of Eq. (19) decreases the calculated area by about 12 per cent to 8·95 m^2g^{-1}, while the inclusion of the α-correction reduces the value by a further 6 per cent to about 8·4 m^2g^{-1}.

Surface areas determined with various gases also agree quite well (*Table 3c*). Thus the overall average for Ar, Kr, Xe and CH_4 adsorption is 10·6 ± 1·0 m^2g^{-1} if α is neglected, or 8·8 ± 1·0 m^2g^{-1} including the correction for non-planarity (data for gases other than Ar are less extensive so that the areas calculated from them are less reliable).

Table 3. Summary of surface area estimates for P33(2700)

(a) BET METHOD

Gas	*Molecular area* (a/Å^2)	A/m^2g^{-1}	*Remarks*
N_2	16·2	12·5	
Ar	13·8	11·4	ref. (50)
	13·1	10·9	$a = 2^{1/3}(\sqrt{3}/2)(r_0^*)^2$
Xe	20·2	14·8	ref. (50)
	18·7	13·7	$a = 2^{1/3}(\sqrt{3}/2)(r_0^*)^2$

(b) HENRY'S LAW METHOD (mean of results foi Ne, Ar, Kr, Xe)

(i) z_0 from KM

Model	A/m^2g^{-1}
3:9	8·46
3:12	9·40
4:10	8·83

(ii) from slope of Az_0 against $r_0/2$ (*Figure 3*)

Model	A/m^2g^{-1}	
	r_0 *from gas 2nd virial coefficient*	r_0 *from crystal radii*
3:9	6·26	
3:12	7·38	8·38
4:10	7·04	

(iii) from $Az_0/(1{\cdot}70 + r_0/2)$

Model	A/m^2g^{-1}
3:9	7·0
3:12	8·0
4:10	9·6

(c) TWO-DIMENSIONAL IMPERFECT GAS METHOD

Gas	*Eqn. for* u^*	*Mean* A/m^2g^{-1}		
		uncorr. for α		corr. for α
		(eqn. 19)	(eqn. 20, with $\alpha = 0$)	(eqn. 20)
Ar	6:12	10·3	8·95	8·43 ± 0·5
	6:12:3			
	McLachlan			
Kr	6:12	9·6	—	8·2 ± 1·0
	6:12:3			
Xe	6:12	10·86	—	9·8 ± 1·0
	6:12:3	10·6	—	8·7 ± 1·0
	6:12†			
CH_4	6:12	11·4	—	8·6 ± 1·0
	6:12:3			
Overall mean		10·6 ± 1·0		8·8 ± 1·0

† Experimental data of Edmonds[52]

The surface area of P33(2700) determined using the BET equation applied to N_2, Ar and Xe adsorption[50] is generally accepted as 12·5 ± 2 m^2g^{-1} (*Table 3a*). The discrepancy between this area and that derived from high temperature adsorption is probably only just outside the errors of the two methods.

For other carbons, especially the less homogeneous Black Pearls 71 and Graphon, the discrepancy between the BET and high temperature adsorption values is, however, much greater. One cannot yet be certain of the origin of this difference: the fact that the area derived from high temperature adsorption on BP 71 (mean ~120 m^2g^{-1}) agrees with the electron microscope value (130 m^2g^{-1}) but is widely different from the BET value (337 m^2g^{-1}) may suggest that in some instances the high temperature method leads to more significant values†. But there is undoubtedly need for an independent study of several more graphitised carbons to establish whether or not this difference is general; and if so to seek an explanation of the discrepancy.

In this connection it is important to consider the effect, on the present method, of heterogeneity and of hindered rotation of non-spherical molecules.

First, unlike its effect on k_1, the influence of heterogeneity on the third order interaction depends on the spacial distribution of adsorption energies. Because the theory applies only to adsorption at relatively high temperatures one may expect periodic fluctuations of ϵ^* of short wavelength compared with the size of the adsorbate to have a small effect[39] and to be exerted mainly through a perturbation of the correction term α.

On the other hand, in the case of a patchwise distribution (homotattic surface) each area will be associated with a different value of n^σ and the deviations from ideality of the two-dimensional gas will vary from patch to patch. It is readily shown that, ***provided all patches are in the region where equation (16) applies to each patch,***

$$\frac{k_2}{k_1^2} = -\frac{2B^*}{A_{\mathrm{app}}}\,, \tag{21}$$

where A_{app}, the apparent surface area, is related to the real surface area by

$$A_{\mathrm{app}} = \frac{\langle k_1^0 \rangle^2}{\langle (k_1^0)^2 \rangle} \cdot A\,. \tag{22}$$

Here

$$\left.\begin{aligned} \langle k_1^0 \rangle &= \frac{\sum_i k_{1,i}^0 A_i}{\sum_i A_i}\,, \\ \langle (k_1^0)^2 \rangle &= \frac{\sum_i (k_{1,i}^0)^2 A_i}{\sum_i A_i}\,; \end{aligned}\right\} \tag{23}$$

$k_{1,i}^0$ is the Henry's law constant per unit area for the patch of type i, having an area of A_i:

$$k_{1}^0i, = k_{1,i}/A_i\,.$$

---

†It may be noted also that application of the Henry's law analysis to the adsorption of Ar by BP 71 using a 3:9 expression for ϵ^* gives areas of 115 and 162 m^2g^{-1} (*Table I*).

$\langle k_1^0 \rangle$ and $\langle (k_1^0)^2 \rangle$ are thus the mean values of $k_{1,i}^0$ and $(k_{1,i}^0)^2$ weighted according to the areas with which they are associated. Since in general the square of a mean quantity is less than the mean square value, the presence of patchwise heterogeneity will be expected to lead to apparent surface areas which are less than the true surface area. This effect could contribute to the much larger discrepancies between the BET area and the high temperature area, found for the somewhat heterogeneous carbons, Black Pearls and Graphon, when compared with the nearly homogeneous P33 (2700): but this must be a tentative conclusion until more data are available.

A different problem arises if the heterogeneity is present in the form of a small area of very highly active surface ('hot spots'). Here it may not be possible to make accurate experiments at pressures low enough for the adsorption on these areas to approach the Henry's law region, so that the experimental isotherm fails to show limiting Henry's law behaviour. This phenomenon is of course now well recognised in the low adsorption region at low temperatures[54,55], but one might hope that it would be less serious in high temperature work. Indeed the isotherms obtained by Sams, Constabaris and Halsey for the adsorption of Ar on P33(2700) (their data for Kr, Xe, CH_4, CD_4 are hardly extensive enough to draw any conclusions from) seem, when due allowance is made for the rapidly decreasing accuracy of low pressure adsorption points, to tend to Henry's law (i.e., graphs of equations (14) and (16) are linear and can be extrapolated reliably to give k_1). On the other hand, the recent careful measurements of Thomas[53] on the adsorption of Ar by P33(2700) using a differential technique which is believed to be rather more precise than that of Constabaris, Singleton and Halsey[49], failed at lower temperatures ($\sim$175 K) to approach Henry's law in the limit of low pressures: similar discrepancies were found at 0°C by Edmonds[52] using Xe + Graphon and, for Xe + MT 3100 and Graphon, by Friedman[56]. Thomas's data can, however, be accounted for quantitatively if one assumes that the sample of P33(2700) which he used contained 0·05 per cent of its area in the form of hot spots which were saturated at the lowest pressures he employed ($\sim$4 cm Hg). It is interesting that Graham[56] estimated that his sample of P33(2700) contained 0·1 per cent of high activity heterogeneity; while Casanova, De Paz, Dondi, Klein and Scoles[57], whose experiments on Ar isotope separation were made on a portion of our sample of P33(2700), were unable to obtain agreement with their theoretical predictions and suggested that this might arise from heterogeneity of the carbon surface. These results indicate that different samples of P33(2700) may have slightly different properties, or may be in different degrees contaminated with very small amounts of highly active (e.g., porous or very finely divided) material. For example, the presence of 10 ppm of highly active material of surface area 600 m^2g^{-1} in our sample would be sufficient to cause the effect observed by Thomas. Provided that hot spots present in the sample remain saturated at the lowest pressures studied, their presence can be detected and their influence eliminated by suitable analysis of the data; but if this condition is not fulfilled, one faces difficulties in attempting to make an unambiguous analysis.

We may also expect to meet problems when this method is applied to the analysis of the adsorption of non-spherical molecules. The two-dimensional second virial coefficient will differ from that calculated from the interaction potential corresponding to the bulk gas not only because of the presence of three-body effects, but also because hindered rotation on the surface may modify the form of $u^*(r)$. Thus Pierotti and Smallwood[28] found that B^* for benzene adsorbed on P33(2700) is positive and decreases with increasing temperature: this is impossible for spherical molecules in this temperature range and probably indicates, as suggested by Kiselev[59], that the attractive potential between benzene molecules adsorbed 'flat' on the surface is small so that the main contribution to B^* comes from repulsive forces. Measurements of this kind on the adsorption of non-spherical molecules are likely to be of more interest in connection with studies of the interactions between adsorbed molecules than in relation to surface area determination.

Finally, we consider the case of adsorption in micropores. In the limiting case in which the micropores provide an essentially constant adsorption field, it is readily shown that

$$\ln \frac{n^\sigma}{p} - \frac{B^p}{RT} = \ln k_\mathrm{h} V^p - \frac{2n^\sigma B^p}{V^p}, \tag{24}$$

where B^p is the second virial coefficient of the material within the pore. This may be expected to differ from the bulk virial coefficient not only because of perturbation of the intermolecular interactions by the solid but also because the integration in Eq. (18) is limited to the region within a pore and cannot be taken to infinity. It remains to be seen whether any useful information about pore structures and the interactions between molecules adsorbed in pores can be derived from the application of Eq. (24), or more sophisticated forms of it, to adsorption data for noble gases at high temperatures in micro-porous media.

4. CONCLUSIONS

The main conclusions to be drawn from the present review are the following:

(i) Measurements of Henry's law constants for the adsorption of spherical molecules on homogeneous surfaces can in principle lead to reliable estimates of surface area. But before this can be achieved in practice further progress needs to be made in the calculation of the absolute magnitudes of adsorption energies.

(ii) The interpretation of measurements of the deviations from Henry's law, expressed in terms of B^*, are less dependent upon absolute theoretical calculations and provided that measurements can be made at temperatures approaching the Boyle temperature of the two-dimensional gas, reliable estimates of surface area can be made for homogeneous surfaces.

Indeed it is a remarkable feature of this method that the only information about the system needed in advance is of the approximate values of the parameters which, in conjunction with a Lennard-Jones (6:12) potential, account for the properties of the bulk gas.

(iii) Surface heterogeneity probably has a much greater influence on Henry's law constants than on the apparent areas derived from measurements of B^*. Further work is needed to elucidate the reasons for the discrepancies between BET surface areas and those calculated from high temperature adsorption.

(iv) Experiments using gases other than the noble gases have their main value in the investigation of topics such as hindered rotation, and the forces between molecules oriented at surfaces. They are of limited value for the determination of surface areas.

(v) Further work is needed to establish the applicability of high temperature adsorption studies to the investigation of porous materials.

References

[1] T. L. Hill and S. Greenschlag. *J. Chem. Phys.* **34**, 1538 (1961).
[2] W. A. Steele and M. Ross. *J. Chem. Phys.* **35**, 850 (1961).
[3] see, e.g., S. Brunauer, *Physical Adsorption of Gases* chap. 3, Oxford University Press, 1943.
[4] e.g., T. L. Hill. *J. Chem. Phys.* **14**, 263 (1946); **15**, 767 (1947).
[5] S. Ono. *J. Chem. Phys.* **18**, 397 (1950); S. Ono and S. Kondo. In *Handbook of Physics*, Vol. 10, p. 231. ed. S. Flügge, (Berlin, Göttingen, Heidelberg), 1960.
[6] T. L. Hill. *Statistical Mechanics* (New York) 1956, Appendix 10.
[7] W. A. Steele and G. D. Halsey. *J. Chem. Phys.* **22**, 979 (1954).
[8] W. A. Steele. *Adv. Coll. Interface Sci.* **1**, 3 (1967).
[9] D. H. Everett. *Soc. Chem. Ind. Monographs*, No. 14 (*Powders in Industry*), 98 (1960);
J. A. Barker and D. H. Everett. *Trans. Faraday Soc.* **58**, 1608 (1962).
[10] J.R. Sams, G. Constabaris and G. D. Halsey. *J. Chem. Phys.* **36**, 1334 (1962).
[11] R. Yaris and J. R. Sams. *J. Chem. Phys.* **37**, 571 (1962).
[12] M. P. Freeman. *J. Phys. Chem.* **62**, 723, 729 (1958).
[13] W. C. de Marcus, E. Hopper and A. M. Allen, *U. S. Atomic Energy Comm., Report K-1222* (Oak Ridge, Tenn.), 1955.
[14] R. Wolfe and J. R. Sams. *J. Phys. Chem.* **69**, 1129 (1965).
[15] W. R. Hansen. *J. Phys. Chem.* **63**, 743 (1959).
[16] J. R. Sams and R. Yaris. *J. Phys. Chem.* **67**, 1931 (1963).
[17] (a) J. R. Sams, G. Constabaris and G. D. Halsey. *J. Phys. Chem.* **64**, 1689 (1960);
(b) G. Constabaris, J. R. Sams and G. D. Halsey. *J. Phys. Chem.* **65**, 367 (1961).
[18] K. S. Pitzer. *Adv. Chem. Phys.* **2**, 59 (1959).
[19] J. R. Sams. *Trans. Faraday Soc.* **60**, 149 (1964).
[20] A. D. Crowell and R. B. Steele. *J. Chem. Phys.* **34**, 1347 (1961).
[21] A. V. Kiselev and D. P. Poshkus. *Trans. Faraday Soc.* **59**, 176 (1963).
[22] A. M. Williams. *Proc. Roy. Soc. A*, **96**, 287 (1919).
[23] D. H. Everett. *Gas Chromatography* 1964 (ed. A. Goldup) (London 1965), 219.
[24] W. A. Steele and G. D. Halsey. *J. Phys. Chem.* **59**, 57 (1955).
[25] M. P. Freeman and K. Kolb. *J. Phys. Chem.* **67**, 217 (1963).
[26] R. S. Hansen, J. A. Murphy and T. C. McGee. *Trans. Faraday Soc.* **60**, 597 (1964).
[27] A. L. Myers and J. M. Prausnitz. *Trans. Faraday Soc.* **61**, 755 (1965).
[28] R. A. Pierotti and R. E. Smallwood. *J. Coll. Interface. Sci.* **22**, 469 (1966).
[29] R. A. Pierotti. *Chem. Phys. Lett.* **2**, 420 (1968).
[30] A. V. Kiselev and D. P. Poshkus. *Trans. Faraday Soc.* **59**, 428 (1963); D. P. Poshkus, *Disc. Faraday Soc.* **40**, 195 (1965).
[31] R. S. Bradley. *Phil. Mag.*, Ser. 7, **11**, 690 (1931).
[31] D. C. Henry. *Phil. Mag.*, Ser. 6, **44**, 689 (1922).
[33] F. J. Wilkins. *Proc. Roy. Soc. A*, **164**, 496 (1938).
[34] J. S. Mitchell. *Trans. Faraday Soc.* **31**, 980 (1935).
[35] M. P. Freeman and G. D. Halsey. *J. Phys. Chem.* **59**, 181 (1955).
[36] K. S. Pitzer and O. Sinanoglu. *J. Chem. Phys.* **32**, 1279 (1960).
[37] A. D. McLachlan. *Mol. Phys.* **7**, 381 (1964).
[38] R. Yaris, *Thesis*, University of Washington (1962).
[39] D. H. Everett, J. D. Johnson and M. L. Klein. *Colloqu. Phys. Chem. of Processes at Solid Surfaces* (Madrid 1964) (C.S.I.C. Madrid 1965), p. 73.
[40] J. D. Johnson and M. L. Klein. *Trans. Faraday Soc.* **60**, 1964 (1964).
[41] J. D. Johnson and M. L. Klein. *Trans. Faraday Soc.* **63**, 1269 (1967).
[42] R. Wolfe and J. R. Sams. *J. Chem. Phys.* **44**, 2181 (1966).
[43] J. E. Krizan and A. D. Crowell. *J. Chem. Phys.* **41**, 1322 (1964).
[44] J. R. Sams. *Mol. Phys.* **9**, 195 (1965).
[45] T. B. MacRury. *J. Chem. Phys.* **49**, 1543 (1968).
[46] D. H. Everett. *Disc. Faraday Soc.* **40**, 177 (1965).
[47] J. D Johnson. *J. Phys. Chem.* **72**, 3697 (1968).
[48] R. Wolfe and J. R. Sams. *Canad. J. Chem.* **46**, 1781 (1968).
[49] G. Constabaris, J. H. Singleton and G. D. Halsey. *J. Phys. Chem.* **63**, 1350 (1959).

[50] J. R. Sams, G. Constabaris and G. D. Halsey. *J. Phys. Chem.* **66**, 2154 (1962).
[51] J. R. Sams. *J. Chem. Phys.* **37**, 1883 (1962).
[52] T. Edmonds, Ph.D. Thesis, University of Bristol, 1964.
[53] H. E. Thomas, Ph.D. Thesis, University of Bristol, 1969.
[54] J. P. Hobson and R. A. Armstrong. *J. Phys. Chem.* **67**, 2000 (1963).
[55] B. A. Gottwald and R. Haul. *Surface Sci.* **10**, 76 (1968).
[56] H. C. Freidman, *M.S. Thesis*, Penn. State 1965; cf. H. Cochrane, P. L. Walker, W. S. Diethorn and H. C. Freidman. *J. Coll. Int. Sci.* **24**, 405 (1967).
[57] D. Graham. *J. Phys. Chem.* **62**, 1210 (1958).
[58] G. Casanova, M. De Paz, M. G. Dondi, M. L. Klein and G. Scoles. *Disc. Faraday Soc.* **40**, 188 (1965);
G. Casanova, M. G. Dondi, G. Scoles and M. L. Klein. In *Fundamentals of Gas-Surface Interactions*, p. 258. ed. H. Saltsburg, J. N. Smith and M. Rogers, (New York, London.) 1967.
[59] A. A. Isirikyan and A. V. Kiselev. *J. Phys. Chem.* **65**, 6016 (1961); *Russ. J. Phys. Chem.* **38**, 821 (1964); cf. C. Pierce and B. Ewing. *J. Phys. Chem.* **71**, 3408 (1967).

DISCUSSION

Professor M. M. Dubinin (*Academy of Sciences, U.S.S.R.*) said: Professor Everett has devoted his paper to the exposition of two methods for determining specific surface area, which are based on very general physical concepts and are not connected with the very imperfect adsorption theories. This, of course, is an extremely attractive feature of the concepts described.

The practical potentialities of the first method are regarded very pessimistically by Everett himself. He considers that the existing theory of intermolecular interactions which, in principle, yields a solution to the problem still needs many improvements and adjustments. I believe that at present there is no quantitative theory of intermolecular interactions for intermolecular distances of the order encountered in physical adsorption. The semi-empirical approaches to the calculation of adsorption energy described in the paper lead to estimates of specific surface area which differ by almost a factor of three (see *Table 1* of the paper). I think that until a basically new step is made (not in adsorption theory, but in theoretical physics) in the theory of intermolecular interactions, which is equal in scope, for instance, to London's works of 1930, we cannot count on anything more than an estimate of the order of magnitude of adsorption energy.

The second method, in which an adsorbate is regarded as a slightly imperfect two-dimensional gas, is free from the need to evaluate adsorption energy. Therefore, it makes sense even now to discuss the practical potentialities of this method, and this is corroborated convincingly enough by the satisfactory agreement of the specific surface areas calculated and determined by the BET-method for adsorbents with energetically uniform surfaces (see *Table 2* of the paper). Two problems associated with this method, however, require discussion.

1. According to Everett, the criterion of applicability of the second method is the correspondence of the experimental data to the equation

$$\frac{n^\sigma}{p} = k_1 + k_2 p \qquad \text{(A)}$$

The question arises, however, whether this criterion is sufficient. Let us consider the case of adsorption according to the classical Langmuir mechanism in the absence of interaction of adsorbate molecules.

$$\frac{n^\sigma}{p} = \frac{n^\sigma_m b}{1 + bp} = n^\sigma_m b - n^\sigma_m b^2 p + n^\sigma_m b^3 p^2 \tag{B}$$

or, approximately, for small pressures:

$$\frac{n^\sigma}{p} \approx n^\sigma_m b - n^\sigma_m b^2 p = k_1 + k_2 p \tag{C}$$

Eq. (C) shows that Everett's criterion is satisfied for non-interacting molecules. Of course, purely formally one may consider that the Langmuir mechanism is equivalent to interaction according to the law:

$$\begin{aligned} u^*(z) &= 0 \quad \text{at } z \geqslant z_0 \\ u^*(z) &= \infty \text{ at } z < z_0 \end{aligned} \tag{D}$$

In this case, however, the value of z_0 is entirely unrelated to the size of the adsorbing molecules and is equal to the distance between the discreet adsorption centres on the adsorbent surface. It is evident that in this case it is impossible to approximate, even to the roughest extent, the interaction energy between two adsorbate molecules by the energy $u^*(z)$ for the bulk gas phase.

2. Even ideal crystals, for instance those of rutile, according to R. E. Day and G. D. Parfitt [*Trans. Faraday Soc.* **63**, 708 (1968)], possess surface defects which have a substantially higher adsorption energy. These defects may be regarded as 'shallow micropores' and they can play an essential role precisely for high-temperature adsorption. Real adsorbents generally possess a clearly defined energetically non-uniform surface. The possibility of application of the second method requires not only discussion, but also experimental evaluation for real non-porous and wide-porous adsorbents whose specific surface area is previously determined by the BET-method.

Professor D. H. Everett replied: It is, of course, well known that adsorption isotherms can be expressed as power series in the pressure, and that in general we may expect to be able to represent any experimental isotherm in a short interval of pressure sufficiently near the origin by $n^\sigma/p = k_1 + k_2 p$. This, in itself, is not therefore a sufficient criterion for the applicability of the method of analysis outlined in my paper. It can be applied only when there are adequate reasons for believing that the adsorbed molecules are fully mobile: that is at sufficiently high temperatures. One may make reasonable guesses as to the temperature range implied by this condition for a given system: whether or not we are justified in analysing a given set of data in this way will be determined, ultimately, by whether the parameters derived from the analysis are self-consistent and make sense physically.

Dr J. G. T. Aken (*National Defense Research Organisation, T.N.O., Netherlands*) said: With the aid of equation (13):

$$k_{\mathrm{H}} = \frac{V^p}{RT}\left(\exp\left(-\epsilon/kT\right) - 1\right)$$

I tried to predict the temperature dependence of helium adsorption on activated carbons. This phenomenon is important in the case of density determinations by means of helium dead space measurements; the temperature at which the helium adsorption may be neglected has to be known.

The data of F. A. P. Maags, P. H. Schwabe and J. H. Williams [*Nature, Lond.* **186**, 956 (1960)] and K. A. Kini and W. O. Stacy [*Carbon* **1**, 17 (1963)] were used for this purpose. It appeared that with $V^p = 0{\cdot}3$–$0{\cdot}5$ ml/g, which is the order of the micropore volume of the activated carbons, and $-\epsilon = 200$–300 cal/mol, the experimental data at low temperatures correspond with the theoretical ones, but at high temperatures they are considerably lower.

The rather strong decrease of the experimentally determined helium adsorption at high temperatures should mean—in terms of equation (13)—a decrease of V^p or of $-\epsilon$. I do not know any reasons for this but I hope you can offer an indication for the solution of this problem.

Professor D. H. Everett replied: The problem of helium adsorption by porous carbons is interesting because of its importance in establishing the dead-space correction in adsorption systems and in the determination of the density of porous solids. It is usually assumed that the adsorption of helium tends to zero symptatically as the temperature increases. However, at high temperatures gas molecules are able to penetrate further into the repulsive force field of the solid so that, as R. A. Pierotti [*Vacuum Microbalance Technique* **6**, 1 (1967)] has pointed out, when the total adsorption is small it is no longer possible in applying the Gibbs definition to ignore the last term on the right hand side of Eq. (1) of my paper. Eq. (13) is then no longer adequate to describe helium adsorption quantitatively. With regard to the data of Kini and Stacey, the rapid variation of the apparent isosteric heat of adsorption of helium with temperature is difficult to understand and warrants, I believe, further careful investigation.

Professor J. Th. G. Overbeek (*van't Hoff Laboratory, Utrecht, Netherlands*) said: Since the method proposed both in its Henry's law form and in the two-dimensional virial approach, is quite sensitive to heterogeneity of the surface, could this aspect not be used for obtaining quantitative information on the heterogeneity, especially in the case of surfaces containing a small fraction of highly active adsorption sites or adsorption regions?

Professor D. H. Everett replied: I agree that the sensitivity to surface heterogeneity of the methods I have discussed, which limits their value for the determination of surface areas, may be turned to advantage, and that careful measurements of this kind may prove useful in studying the heterogeneity itself.

Dr F. A. P. Maggs (*C. D. E., Salisbury*) said: Interest in the interpretation of gas adsorption isotherms at temperatures well above the critical has led me to consider an approach resembling that given in Professor Everett's paper, but of a less comprehensive nature.

The Gibbs equation, in gas/solid interface terms may be written as $d\Delta G = d\pi = RT/MS\, v\, d\ln p$; ($\pi$ = two-dimensional surface pressure, p = equilibrium gas phase pressure; S = specific surface, v = volume gas adsorbed). D. H. Bangham [*J. Chem. Soc.* 1324 (1931)] has shown that this may be combined with the Rideal–Schofield two-dimensional equation of state, namely, $\pi(A - B) = RT$ to give:

$$\ln p = \ln \frac{v}{v_m - v} + \frac{v}{v_m - v} + I$$

where $A =$ area occupied by an adsorbed molecule, $B =$ area occupied by the adsorbed molecule under high surface compression, $I =$ integration constant.

Two-dimensional properties are thus ascribed to the adsorbed film following this isotherm equation. The equation is, however, only soluble with tedium (e.g. successive approximations), and has not been used.

If, however, we expand the equation and neglect powers of v/v_{m} (assuming low coverage) the following tractable equation is obtained:

$$\ln p/v = 2v/v_m - \ln v_m + I$$

A plot of $\ln p/v$ against v will therefore have a gradient of $2/v_{\mathrm{m}}$; $v_{\mathrm{m}} = 0{\cdot}869 \times$ gradient, if $\log_{10} v/v_m$ is used.

Adsorption isotherms of argon and nitrogen adsorbed on carbon black, and charcoals at 273 K do in fact yield linear plots of this equation. Values of v_m are lower than those derived from a BET using nitrogen at 77 K, and for the carbon black are in agreement with areas calculated from electron micrographs. Areas given by this equation are proportional to the heats of wetting and these are proportional to electron micrograph areas for both high and low area carbon blacks.

Professor D. H. Everett replied: The equations used by Maggs are, of course, closely related to those in my paper. His B is in effect a temperature-independent second virial coefficient related to the area excluded by a molecule: for a filled monolayer $V_m = A/B$ moles. In general B^* is a function of T and A/B^* cannot be identified with the monolayer capacity. In the case of porous adsorbents, where the concept of monolayer adsorption may lose its validity, we prefer to use Eq. (24) of my paper. It turns out [Dr A. R. Paniego and Dr F. Rodriguez-Reinoso (University of Bristol), unpublished results] that for the adsorption of Ar, Kr, Xe by microporous carbons B^p is positive and almost independent of temperature so that one is tempted to identify it with a molecular co-volume: however, attempts to correlate B^p with molecular size are not entirely convincing and a more sophisticated analysis will probably be needed.

Sir Eric K. Rideal (*Imperial College, London*) said: (1) Is there any real experimental proof that there are cases of a two-dimensional gaseous state on solid surfaces? Surface diffusion is, of course, well known. (2) Is the transition from a fixed to a mobile two-dimensional state a critical process, *i.e.* with critical T and π values, or is there a Boltzmann transition from fixed to mobile molecules?

Professor D. H. Everett replied: (1). Sir Eric, in his usual perceptive manner, asks a simple question to which there is, I think, no simple satisfactory answer. Indeed we must first answer the question: how can we recognise a two-dimensional gaseous state experimentally? Let me only, therefore, indicate how one can justify a two-dimensional model on theoretical grounds. The concentration profile of molecules near an adsorbing surface is sharply peaked, and below a certain temperature (T_1), characteristic of each system, its extent normal to the surface does not exceed the diameter of an adsorbate molecule. The motion of a molecule parallel to the surface is hindered by energy barriers characteristic of the underlying solid structure, and becomes effectively a free translation above a second characteristic temperature (T_2). For most crystallographically smooth surfaces $T_2 < T_1$ and there is a range of temperatures between T_2 and T_1 in which it is reasonable to treat the adsorbed molecules as though they are free to move over the surface in the (x, y) plane but are effectively restricted to a monolayer in the z-direction. The upper limit T_1 can, however, be relaxed somewhat since Barker and Everett have evaluated a correction term to take account of deviations from a strictly two-dimensional gas.

(2). There is good reason to expect, and some experimental evidence to support the view that a smooth transition can occur from mobile to localised adsorption as either the temperature or the surface concentration is changed. But in many cases it is difficult to distinguish between a mobile → localised transition and a two-dimensional condensation which, as is well-known, is sharp only on a very homogeneous surface.

Dr V. R. Dietz (*U.S. Naval Research Laboratory, Washington*) said: As this instructive paper points out, the problems of surface heterogeneity are very complex. In the case of ideal single crystals there is a built-in heterogeneity that depends on structure. A measure of this atomic roughness may be had from the number of terms required to sum a 6–12 potential between a gas molecule and all atoms in the surface. An example is graphite. Summing over 25 000 atoms and relative to a position over a carbon atom in the basal plane, 95 per cent of the total interaction energy is contributed by summing only the carbon atoms in the first layer, *i.e.* the basal plane. However, over a carbon atom in an edge plane of the *abab* hexagonal lattice, only 66 per cent of the interaction is contributed by all of the boundary atoms even though they do not lie in a true geometrical plane. Accordingly, the edge plane of the graphite lattice may be viewed as one having a greater atomic roughness than the basal plane.

Professor D. H. Everett replied: I agree that the very small residual heterogeneity which we have detected in our samples of P33 (2700) may be an intrinsic property of graphitised carbon particles and attributable to edge planes of the graphite lattice.

Professor S. Ross (*Rensselaer Polytechnic Institute, U.S.A.*) communicated: While the present Symposium was taking place at the University of Bristol, a famous London company performed the operettas of Gilbert and Sullivan at the Bristol Hippodrome. At the performance of *Ruddigore* I heard a direct and melodious invocation to introduce the subject of my own work at the Symposium:

> "You must stir it and stump it
> And blow your own trumpet;
> Or, trust me, you haven't a chance."

I notice, somewhat to my chagrin, that while Professor Everett lists three approaches, or partial theories as he calls them, for the analysis of gas-adsorption isotherms, he ignores a fourth approach, that of S. Ross and J. P. Olivier (*On Physical Adsorption*, Wiley-Interscience, New York, 1964), which is as fully worked out as any of the others and even has its own independent estimate of the surface area of P33 (2700) for comparison in his *Table 3*. I wish to repair this omission, not for the reason given by Gilbert, but because the results of the Ross–Olivier treatment offer an explanation of the discrepancy between the evaluations of the specific surface of P33(2700) by the BET method and by the other two methods.

The Ross–Olivier treatment analyses the portion of the isotherm from just above the Henry's-law region to the onset of multilayers. This range of first-layer adsorption exists for argon at 77·5 K at pressures between 0·1 and 10 mm, so that the data can be conveniently measured without unduly sophisticated experimental techniques and without requiring any correction for the non-ideality of the bulk gas. A body of data pertaining to argon and nitrogen at temperatures of 77·5 and 90·1 K adsorbed by carbons of varying degrees of graphitization has been collected by Ross and co-workers at the Rensselaer laboratory, and these data were used by Ross and Olivier in their book. In this book the estimations of surface areas are not reported in the usual form of m^2/g but only as monolayer capacities, designated V_β but corresponding in meaning to the BET parameter V_m: the numbers for V_β are converted into specific surface area (A) by the formula:

$$A = V_\beta \,.\, N_0 \,.\, \beta^{1d} \,.\, 10^{-20}/22\,400$$

where N_0 is Avogadro's number and β^{1d} is the cross-sectional area of the adsorbate molecule calculated from the b-constant of the van der Waals equation for the gas concerned. The results presented in *Table A* for argon, nitrogen, and krypton adsorbed by P33(2700) are taken from Table VII-2, and the values of β^{1d} from Table VI-I of Ross and Olivier's book.

Table A. Ross–Olivier estimates of the surface area of P33(2700)

Gas	*Temp.*/(K)	$\beta^{1d}/(A^2)$	V_β	A/(m^2/g)	γ
Ar	77·5	13·6	3·68	13·4	170
Ar	90·1	13·6	3·68	13·4	170
N_2	77·5	15·5	3·15	13·1	120
N_2	90·1	15·5	3·15	13·1	120
Kr	90·1	15·7	3·41	14·7	330

These results are uncorrected, in the sense that they are based on two-dimensional van der Waals constants calculated directly from the gas constants, *i.e.*, assuming that the interaction energy (U^*) of the adsorbate is not different from that, U, between molecules in the gas. We shall suppose that we do not know the observed values for the two-dimensional critical temperature (${}_aT_c$) or the two-dimensional Boyle temperature (${}_aT_B$), so we can still blissfully expect that each of them will be exactly one-half their respective bulk-gas values. This then is our first approximation, from which, by matching observed *versus* computed isotherms, are estimated certain key parameters, namely, the average interaction energy (U_0'), the degree of heterogeneity of the substrate (γ), and the monolayer capacity (V_β). The heterogeneity is expressed as a symmetrical distribution of adsorptive energies (U_0) around an average U_0', and the parameter γ controls the width of the distribution: *i.e.*,

$$\Phi\,(U_0) = \frac{1}{n} \exp\,[-\,\gamma\,(U_0 - U_0')^2]$$

Iso-energetic substrates would have γ equal to infinity; the smaller the value of γ the more heterogeneous is the distribution of adsorptive energies. The adsorptive heterogeneity of a substrate is not an absolute quantity but depends on the adsorbate. Most investigators agree in ascribing a high degree of crystallographic uniformity, or homotaxy, to the surface of the graphitized carbon black designated P33(2700). But a homotattic substrate is not necessarily iso-energetic, as I have had occasion to mention elsewhere in this book. The larger the adsorbed molecule, the less sensitive it is to the differences between the iso-energetic contour lines on a homotattic substrate. The data in *Table A* show, quite reasonably, that the graphite substrate is progressively more energetically uniform as we go from nitrogen to argon to krypton. For an adsorbate such as chloroform or carbon tetrachloride, this substrate is effectively iso-energetic, as is made evident by the vertical discontinuity marking the two-dimensional condensation of these high-molecular-weight adsorbates on P33(2700). This feature of the adsorption isotherm responds sensitively to energetic heterogeneity of the substrate, by departing from verticality immediately the substrate departs from being iso-energetic. With easily-condensed vapours the adsorption can be measured readily at temperatures around 300 K and the high temperature also contributes to make the substrate less heterogeneous. Thus, while this substrate is not iso-energetic towards adsorbed argon at 77·5 K, it behaves as an iso-energetic substrate towards adsorbed carbon tetrachloride at 300 K.

The investigator can exploit the iso-energetic character of P33(2700) towards carbon tetrachloride by treating these adsorption data by means of the well-developed body of theory that has been based on the postulate of an iso-energetic substrate. Ross and Olivier did just this, to evaluate the perturbation introduced by the graphite to the attractive forces between the adsorbed molecules of carbon tetrachloride. The perturbation was described by them as the effect of a substrate field that reduced the molecular attraction of adsorbed molecules by inducing parallel induced dipoles upon them. But the mechanism of the perturbation does not need to be described so explicitly: the same purpose is served by a pragmatic approach similar to that of Everett and Barker, in which the proportional reducing factor that affects the attractive part of the adsorbate–adsorbate potential is merely obtained empirically from the carbon tetrachloride adsorption. The perturbation, no matter how described, can be observed without ambiguity only where no obscuring effects are introduced by heterogeneities of the adsorptive energies. Adsorbed argon on P33(2700) is not free from this obscuring influence.

The perturbation observed and evaluated from the adsorption isotherms of large adsorbates at high temperatures was then applied to the low-temperature isotherms for adsorbed argon and nitrogen on P33(2700). It resulted, of course, in a reduced value of α, the two-dimensional van der Waals constant; and so required a new search among a different series of computed isotherms to discover the best match, and thence to evaluate the corrected parameters. The corrected values for γ, V_β, and A are given in *Table B* for the argon and nitrogen isotherms, taken from Tables VII-9 and VII-10 of Ross and Olivier.

The magnitude of the perturbation correction can be reported most usefully and appropriately in this place in terms of its reduction of the two-dimensional Boyle temperature: Professor Everett's *Figure 4* shows 195 K as the Boyle temperature of argon as a two-dimensional gas; the Ross–Olivier correction for the perturbation of the Ar-Ar attraction would reduce the Boyle temperature to 178 K. This is much less of a correction than Professor Everett's calculations for the same effect, for which he finds three different methods of estimation to agree. "Never saw such unanimity on a point of law in all my life!" to quote Gilbert again. Still, its impressiveness is a little spoiled since he was aware of the answer he needed, namely, 155 K.

Comparison of the results reported in *Tables A* and *B* shows that after correcting for perturbation we get slightly higher values for the surface area, and rather higher values for γ. The average value obtained for the surface area agrees best with the BET equation applied to the N_2, Ar, and Xe adsorption data in the multilayer range of the isotherm, and is substantially larger than that derived from high-temperature adsorption. But another discrepancy awaits explanation: the experimental observations appear to locate the two-dimensional Boyle temperature of argon adsorbed on P33(2700) at 155 K (Everett, *Figure 4*) and not at 178 K as predicted by the Ross–Olivier correction for perturbation. The energetic heterogeneity of the Ar-P33(2700) system provides the explanation. Small as the distribution is, it has a profound effect on the locating of the two-dimensional critical temperature and of the two-dimensional Boyle temperature. Chapter V of Ross and Olivier's book is entitled 'Implications of the concept of surface heterogeneity;' it explores the characteristic features of the computed isotherms to find out the effects of heterogeneity on the results obtained by the unwary theorist who would treat nearly-iso-energetic substrates as

Table B. Corrected Ross–Olivier estimates of the surface area of P33(2700)

Gas	*Temp.*/(K)	$\beta^{\mathrm{1d}}/(\mathrm{A}^2)$	V_β (corr.)	A/(corr.) $\mathrm{m^2g^{-1}}$	γ (corr.)
Ar	77·5	13·6	3·83	14·0	400
Ar	90·1	13·6	3·75	13·7	400
N_2	77·5	15·5	3·30	13·8	300
N_2	90·1	15·5	3·28	13·8	300

wholly iso-energetic. By doing so, he has then to ascribe to perturbation what is actually due to heterogeneity. If now the two-dimensional van der Waals equation should be used to describe the isotherm, it appears to have undergone a great diminution of the a-term, which in extreme cases changes sign, thus leading some authors to deduce repulsive interactions between the adsorbed molecules; or if the two-dimensional virial equation should be used, the values of B^* all become larger, with a consequent apparent reduction in the two-dimensional Boyle temperature. The model isotherms give us a quantitative relation between the degree of heterogeneity and the magnitude of the mis-ascription:

$$_{a}T_{\mathrm{B}}^{*} = {}_{a}T_{\mathrm{B}}\left(1 - \frac{2{\cdot}43}{\sqrt{\gamma}}\right)$$

where $_{a}T_{\mathrm{B}}^{*}$ is the apparent Boyle temperature and $_{a}T_{\mathrm{B}}$ is the actual Boyle temperature of the adsorbed non-ideal gas. This equation is equation V-2 of Ross and Olivier, cleared of an obvious mistake in arithmetic and made to relate to $_{a}T_{\mathrm{B}}$ instead of $_{a}T_{c}$. If we apply this equation to the parameters reported in *Table A* ($_{a}T_{\mathrm{B}} = 195$ K; $\gamma = 170$) or to the corrected ones reported in *Table B* ($_{a}T_{\mathrm{B}} = 178$ K; $\gamma = 400$) we find the apparent Boyle temperature coming out quite near to 155 K, in agreement with the value shown in *Figure 4*. (*Table A* gives 158·7 K, *Table B* gives 156·4 K).

The foregoing analysis of the adsorption of argon by graphitized carbon black seems to dispose of the discrepancy in the estimates of surface area (ah! but wait); and, what is more important, it shows that adsorption measurements at 77·5 K, made with no more elaborate apparatus than is common in physical chemistry laboratories, can be extrapolated to yield the same value for the *apparent* two-dimensional Boyle temperature that is to be measured by interpolation only by the utmost in precision techniques. Presumably, after a time, the mythical Chinese learnt that you *could* roast a pig without burning down your house.

And now for the surprise *dénouement*, at the end of the third act as it were.

The treatment outlined by Professor Everett for the analysis of high-temperature adsorption isotherms is to obtain from the data the second virial coefficient of the adsorbate, which is considered as a non-ideal gas with mobility in two dimensions on the substrate. This treatment is essentially the same as that suggested by de Boer in his book on adsorption (1953), using as an equation of state the less-refined description of a non-ideal gas provided by the two-dimensional van der Waals equation. Neither de Boer nor Everett included the heterogeneity of the substrate as a factor in their analyses, which omission severely restricts their applicability. But if we do consider for the nonce the substrate as iso-energetic, both treatments should show general agreement in the results obtained, even if we do not accept these results as correct. In order to investigate this point, the adsorption isotherm for argon at 77·5 K on P33(2700) was matched against the Hill–de Boer equation

$$p = K\frac{\theta}{1-\theta}\exp\left(\frac{\theta}{1-\theta} - \frac{2a\theta}{kT\beta}\right)$$

at increasingly lower values of a/β. Not unexpectedly, quite a good match could be made; it came out at $2a/RT\beta = 5{\cdot}4$, which is considerably less than the unperturbed-adsorbate parameters at $2\alpha^{id}/RT\beta^{id} = 6{\cdot}50$. The reduction in α given by this match corresponds to a two-dimensional Boyle temperature of 159°K, which is probably a satisfactory agreement between the two methods. Surprisingly, however, the estimated surface areas are not in agreement: the Hill–de Boer equation giving $V_\beta = 3{\cdot}90$ ml at s.t.p./g adsorbent, or $A = 14{\cdot}3$ m^2/g. This result follows the general trend we have observed before (cf. *Tables A* and *B*) that when matches of the data to computed isotherms are made at increasingly lower values of α/β, the necessary compensation of the other constants is to make both γ and V_β increase. The original discrepancy in the estimation of A therefore persists even when the Ross–Olivier treatment is adjusted to conform with the Everett perturbation and the supposition of an iso-energetic substrate. This unexpected result suggests to me that samples of P33(2700) can perhaps be found with different specific surface areas, ranging from 8 to 14 m^2/g, but not differing in the characteristics of their surfaces, which by virtue of the same thermal conditioning are practically entirely comprised of homotattic basal planes of graphite. The sample that I have at Rensselaer, with which all the data discussed here were obtained, seems to be the same as the one used for the BET determination, but the sample used by Halsey and co-workers in Seattle may really have less specific surface. If this is so, all the discrepancies in the estimation of surface areas have a trivial cause, but the differences I have pointed out between the theories of de Boer, Everett and Barker, Halsey and co-workers, and others, on the one hand, and Ross–Olivier on the other hand, are fundamental.

Professor D. H. Everett replied: Professor Ross will I think agree that the approach used by Ross and Olivier is appropriate only to the analysis of adsorption data at temperatures well below the critical temperature of the adsorptive: this is why my paper, which considered adsorption at temperatures well above the critical, did not discuss their work. Nevertheless he is right to draw attention to the possibility of estimating the two-dimensional Boyle temperature from low temperature adsorption data. However, his application of Ross and Olivier's equation V-2 to T_B seems to be unjustified for reasons which will be published separately.

I wish only to make one other comment on his remarks, because he has apparently misunderstood part of my paper. My estimate of the Boyle temperature of Ar + P33 (2700) is derived directly from experimental data, and, apart from minor variations depending on how, for example, the correction for bulk gas imperfection is applied, the figure of 155 K is not open to adjustment and I was certainly not 'aware of the answer needed'! This figure is then employed to calculate the parameters of various equations used to represent the perturbed inter-molecular potential. No attempt is made to calculate the values of these parameters from quantum mechanical theory: indeed, as stressed by Dubinin, further progress in the theory of intermolecular forces is needed before this becomes worthwhile. There is, I think, little reason to expect, as Ross and Olivier assume, that the reducing factor to be applied to the attractive potential will be the same for all molecules, nor does it now seem likely that it can be interpreted in terms of an electrostatic field over a graphite surface.

HELIUM ADSORPTION AT ROOM TEMPERATURE AND ADSORPTION ISOTHERMS

JEAN-BAPTISTE DONNET

Ecole Supèrieure de Chimie, Mulhousè, France

and

BERNARD LESPINASSE

Institut National des Sciences Appliquè, Villeurbanne, France

Volumetric or gravimetric determinations of adsorption isotherms are only possible when the quantities of adsorbed gas are measurable. To overcome this limitation, we propose a new method on the indirect estimation of the adsorption isotherm. The experimental results were performed by Couderc and Papirer in the laboratories of Professor Donnet[1, 2]. Lespinasse[3–5] proposed a satisfactory theoretical explanation of the results.

The experimental procedure is outlined in *Figure 1*. Let V be the volume of the enclosure (A) and V_0 the particular value of V when piston is at its initial position. It follows that V and V_0 are related by the expression (1).

$$V = V_0 - Sx \tag{1}$$

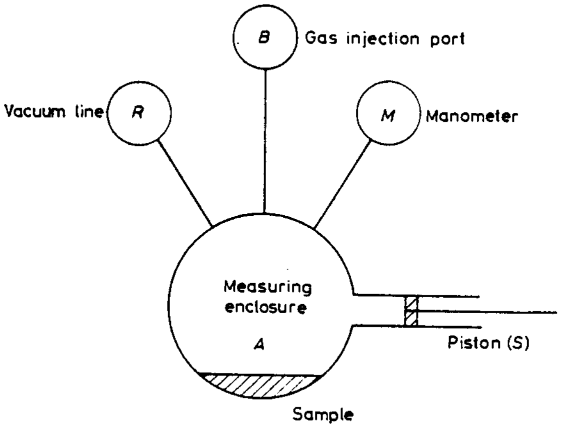

Figure 1. Helium adsorption apparatus: (A) measuring enclosure; (R) vacuum line; (B) injection port for the introduction into (A) of a known number n_t moles of gas; (M) manometer giving the pressure p of the gas. The small piston with a cross-sectional area S is connected with (A). The position of the piston can be varied by $\pm x$ around an arbitrarily selected initial position

Let us distinguish the two cases in which the enclosure (A) is either empty or contains an adsorbing sample.

For the empty enclosure into which we introduce a number n_t of moles of gas, supposed to be ideal, equations (2) holds. By using an orthogonal

$$pV = n_tRT \quad \text{or} \quad \frac{n_tRT}{p} = V = V_0 - Sx \tag{2}$$

system of axes (n_tRT/p versus V) the compressibility isotherm is represented by a straight line having a slope equal to unity.

Consider now the case when the enclosure contains an adsorbing sample of volume V_E. The sample will adsorb gas following a law, say:

$$n_a = G(p) \tag{3}$$

If n_t is the total number of moles of gas introduced into A, x the position of the piston and p the equilibrium pressure, it follows that:

$$n_t = n_a + n_g = n_a + \frac{p}{RT}(V - V_E) \tag{4}$$

where n_g is the number of gas moles in the volume ($V - V_E$). If we compress the gas by a slight variation of the position of the piston, we determine the tangent to the compressibility isotherm. Lespinasse[4–7] related the slope $K_v(p)$ of the tangent to the number n_a of adsorbed gas moles by the equation (5), where B is a constant equal to $RT/(V_0 - V_E)$

$$K_v(p) = \frac{1 + B\,(n_a/p)}{1 + B\,(\mathrm{d}n_a/\mathrm{d}p)} \tag{5}$$

Experimentally, we measure p and x and replace the axes system

$$\left(\frac{n_tRT}{p} \text{ versus } V\right) \quad \text{by} \quad \left(\frac{n_tRT}{p} \text{ versus } x\right)$$

The slope of the line in the new axes is now:

$$K_x(p) = S\,\frac{1 + B\,(n_a/p)}{1 + B\,(\mathrm{d}n_a/\mathrm{d}p)} = f(x, p) \tag{6}$$

$K_x(p)$ is equal to S in 3 cases: (i) for $n_a = 0$, in other words if the enclosure is empty or if the sample does not adsorb gas; (ii) for $n_a/p = \mathrm{d}n_a/\mathrm{d}p$, that is every time the tangent to the adsorption isotherm goes through the origin, or if a segment of the isotherm itself can be represented by a straight line through the origin; (iii) for $p = 0$ since $n_a/p \rightarrow \mathrm{d}n_a/\mathrm{d}p$.

Some possible theoretical forms of the curves $K_x(p)$ and the corresponding adsorption isotherms are shown in *Figure 2.* Stepped isotherms appear when $\mathrm{d}n_a/\mathrm{d}p = \infty$ for a given pressure $p = p_s$. At this pressure the tangent to the curve $K_x(p)$ is vertical.

As an example of the application of this method to experimental data, *Figure 3* shows the behaviour of a non-porous solid like Graphon (graphitized carbon black)[5, 7].

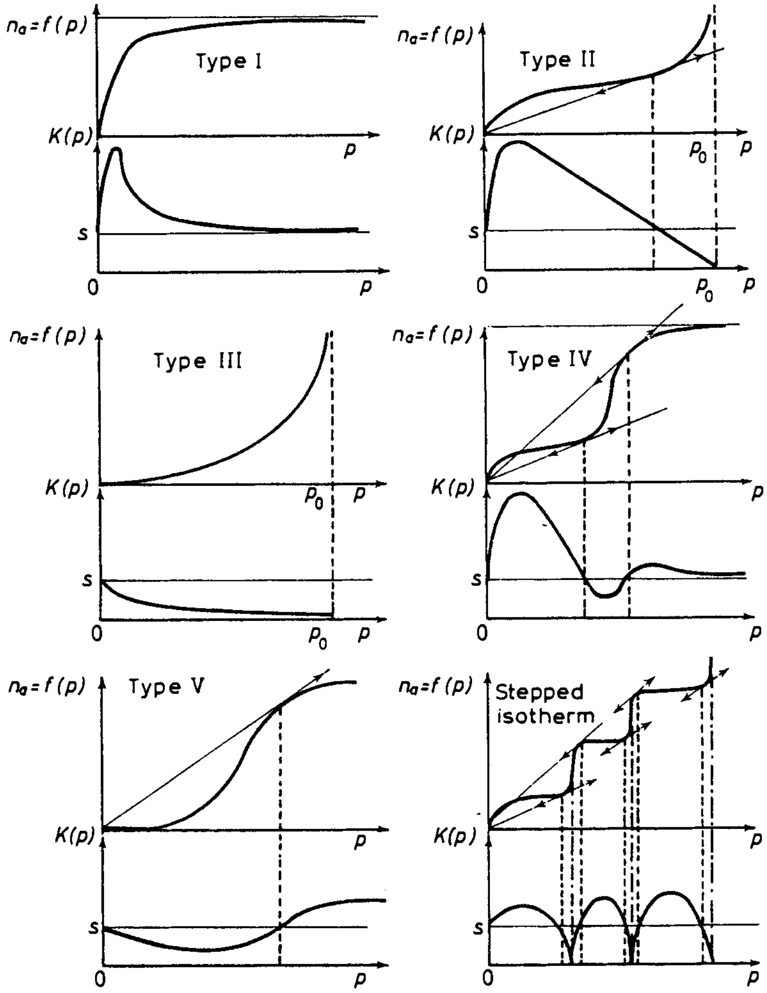

Figure 2. Relationship between isotherm type and $K_x(p)$: in each diagram the upper curve shows the isotherm and the lower the corresponding form of $K_x(p)$

The curve $K_x(p)$ obtained on Graphon is a hyperbola and this is supported by the transform $K_x(p) = f(1/p)$, which is a straight line. It follows that:

$$K_x(p) = S\frac{1 + B\,(n_a/p)}{1 + B\,(\mathrm{d}n_a/\mathrm{d}p)} = A + \frac{C}{p}, \tag{6}$$

where A and C are positive constants.

Noting that A is practically equal to S, we obtain on integration the linear law: $n_a = A'P + C'$, where A' and C' are positive constants. The constant C' arises probably from the Graphon surface irregularities (which are actually detected by nitrogen adsorption at low temperature) and which adsorb gas immediately at the beginning of the experiment. As a first approximation, it appears that helium adsorption on Graphon is a

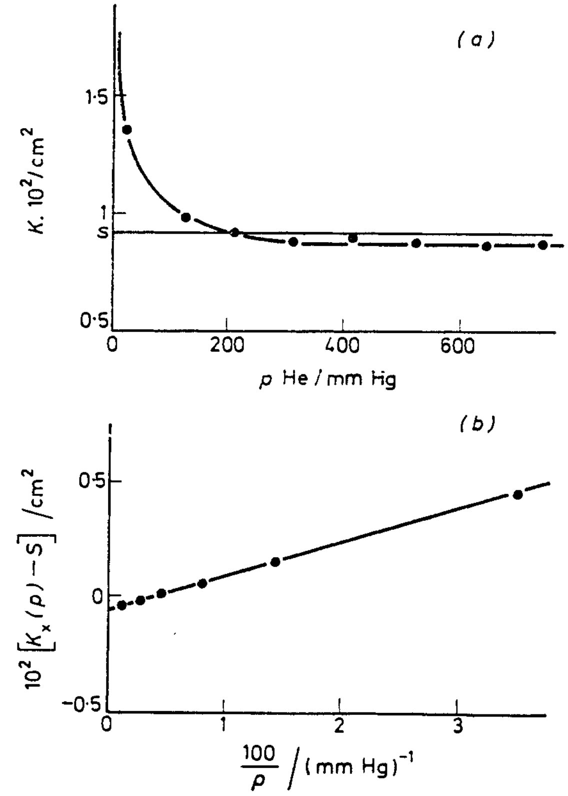

Figure 3. Adsorption of helium by Graphon. (*a*) $K_x(p)$ as function of p; (*b*) $[K_x(p) - S]$ as a function of $1/p$

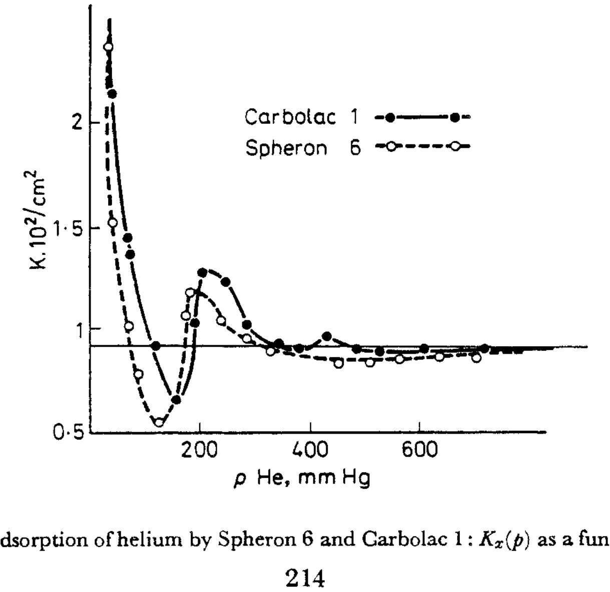

Figure 4. Adsorption of helium by Spheron 6 and Carbolac 1 : $K_x(p)$ as a function of p

linear function of the pressure. Different results are obtained on porous substances like carbon blacks or activated coals.

Figure 4 shows results for Spheron 6 which contains pores of about 7 Å diameter and Carbolac 1 which has a distribution of pore sizes between 7 and 20 Å. The curves $K_x(p)$ of these samples are no longer hyperbolas. The curve for Spheron 6 has a minimum around 140 mm of Hg and for Carbolac 1 a minimum situated near 170 mm of Hg. According to the above theory these minima correspond to non-vertical stepped isotherms and the experimental results indicate that the steps are shifted towards higher pressures when the pore diameter increases.

Our investigations were repeated with samples of a mineral coal progressively activated with steam at 900°C. Our results confirmed that activation increases the pore sizes since the minima in the $K_x = f(p)$ curves are shifted toward higher pressures with increasing activation. We have

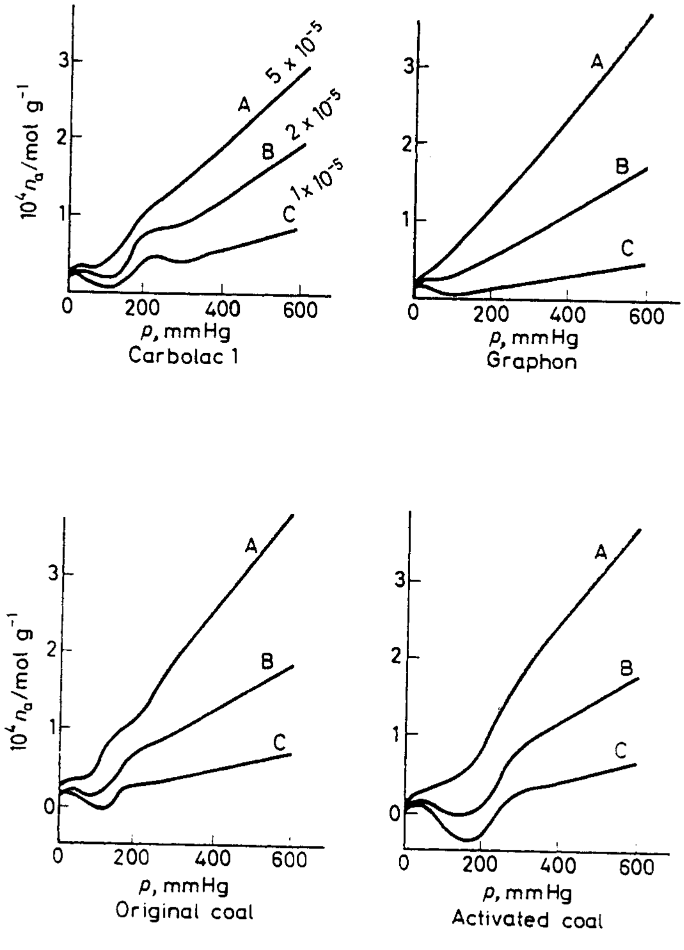

Figure 5. Isotherms calculated by integration of $K_x(p)$ assuming that the absolute adsorption at 600 mm Hg have chosen arbitrary values, e.g. for Carbolac 1 : 1, 2, 5 × 10^{-5} mol g^{-1}

extended this kind of experiment to numerous samples of very low specific surface area, including silica, alumina, glass fibres and so on.

To calculate the isotherms by integration of the function $K_x(p)$, it is necessary to know a particular value of the function $n_a = G(p)$. However, at this time, it is not possible to measure accurately, with our apparatus, the small amounts of adsorbed helium. Therefore, in order to try a calculation, for the carbon samples studied, we choose arbitrary quantities, say 1, 2 and 5×10^{-5} mol g^{-1}, at a pressure of about 600 mm Hg, values that are advanced in current literature for carbonaceous materials.

The integrations performed with an IBM computer give the curves shown in *Figure 5*. These are not the true adsorption isotherms but they show the general appearance of the isotherms. The curves (A) look like the classical isotherms while the curves (B) and (C) obtained when the smaller amounts of adsorbed helium are assumed, are obviously not adsorption isotherms since their slopes and even the adsorbed quantities are sometimes negative.

At higher pressures, the adsorbed quantities are proportional to the pressure, a result already mentioned in the literature.

In conclusion, it appears that our method can be of great interest where the classical method fails.

References

[1] J. B. Donnet, P. Couderc and E. Papirer. Eighth Biennial Conference on Carbon. Buffalo 19–23 June, 1967.

[2] J. B. Donnet, P. Couderc and E. Papirer. *J. Chim. Phys.* **64**, 1656 (1967).

[3] B. Lespinasse. *C. R. Acad. Sci.* **267**, *Serie C*, 359 (1968).

[4] B. Lespinasse. *J. Chim. Phys.* **65**, 1772 (1968).

[5] B. Lespinasse. *C. R. Acad. Sci.* **267**, *Serie C*, 1268 (1968).

[6] B. Lespinasse, M. Otterbein, E. Brousse, J. B. Donnet, P. Couderc and E. Papirer. *C. R. Acad. Sci.* **267**, *Serie C*, 1441 (1968).

[7] B. Lespinasse, M. Otterbein, E. Brouse, J. B. Donnet, P. Couderc, E. Papirer. *J. Chim. Phys.* in press (1969).

LOW SURFACE AREA DETERMINATION

G. Beurton and P. Bussière

Institut de Recherches sur la Catalyse du C.N.R.S., Villeurbanne, France

1. INTRODUCTION

What is a low surface area? As usual in metrology, this concept must be connected to some method of determination. Since the extensive development of the remarkable BET method[1], it seems convenient to say that a surface area is low if it cannot be measured with reasonable accuracy by means of the physical adsorption of nitrogen. For powdered solids, we therefore put the region of 1 m^2/g as the upper limit. With massive solids and films, the determination of the roughness factors involves samples with a surface area which is lower than some hundreds of square centimeters and cannot be measured by the BET method with nitrogen.

The measurement of such low surface areas is interesting, both for fundamental research and for industrial reactions and products, because it can be applied to problems of adsorption, catalysis, physics of solids, chemical reactions in the solid state, sintering, electrochemistry, heat exchange, friction, etc. For this reason each method of surface area determination needs to improve its sensitivity, and we shall attempt to review a number of methods. Fortunately some methods have been discussed at this Symposium by eminent reviewers, and we shall mention these very briefly. We have an interest mainly in the use of radioactive tracers, which is a general source of micromethods, in particular the physical adsorption of krypton 85.

2. DESCRIPTION OF METHODS[2-5]

2.1. Direct examination of surface

Since the linear dimensions of the particles of a solid with a specific surface area of 1 m^2/g and unit density are of the order of microns, one can expect *optical* and *electron microscopy* to be suitable methods for the determination of low surface areas and indeed this is so[6, 7].

The first is at its worst when the solid is polydispersed, somewhat transparent, and with one dimension lower than the other, as it is for instance in the case of needles of metaldehyde[8], with a measured specific surface of 3·7 m^2/g. As a rule this method provides interesting results in the upper region of our range, but it has some limitation in estimating eventual roughness factors.

Electron microscopy enables one to see many more details of the solid. Difficulties arise from the absorption of electrons by matter, but they can, in some cases, be overcome by an examination of thin sections. The usual practical field seems to be the same as that for optical microscopy.

Profilography. It is possible to obtain values of the roughness factors from profiles of the surfaces, which are described by the movement of a microbead on them, using for instance Erbacher's approximtaion of roughnesses to tetrahedrons[9]. Roughness factors as low as 1·006 can be obtained[10]. Here is at least the limitation of the diameter of the bead (usually about 1 micron).

2.2. Methods involving porosity

Permeametry[11] is well known as a suitable method for the study of coarse particles. In the absence of narrow pores it is possible to measure down to hundreds of cm^2/g by the steady state procedure or to thousands by the transient state procedure; the experiments are quick. It must be noted that absolute values of the areas are dependent on the choice of the shape factor.

Mercury porosimetry[12] was recently used down to 0·1 m^2/g.

Low angle x-ray diffraction[13] is said to have the lower limit of 1 m^2/g, and it was able to determine the specific surface area of 0·34 m^2/g for a silicon carbide. It is very useful to measure surface areas due to very narrow and even closed pores.

2.3. Heterogeneous isotopic exchange

Isotopic exchange reactions between fluid phases and solids can be studied by means of tracers. The easiest procedure can be used when it is possible to determine the steady state conditions, since, if the isotopic effects are negligible, the isotopic composition x of the fluid phase is equal to that, y, of the solid surface, i.e.:

$$\frac{n_f'}{n_f} = \frac{n_s'}{n_s}$$

n_f': number of atoms of the tagged species in the fluid phase,
n_f: total number of exchangeable atoms in the fluid phase,
n_s': number of atoms of the tagged species on the solid surface,
n_s: total number of exchangeable atoms on the solid surface.

Suitable equilibration times and concentrations can be obtained from a plot of log $(1 - F)$, where F is the degree of evolution of the exchange, against time. The equation above enables one to calculate n_s from the measurements of the isotopic concentration in the fluid phase only. When it is possible to establish a value of σ for the solid area corresponding to one exchangeable atom of the surface, the total area S can easily be deduced from the relation:

$$S = n_s \,.\, \sigma$$

Using the simple procedure requires that there is neither change of the surface during an experiment, nor rate controlling diffusion in the fluid phase, nor quick process of exchangeable atom transfer from the surface to the inner layers of the solid. If any troublesome processes occur, an alternative is to develop equations, which can be solved for S, as for instance the one recently published[14, 15]. Another problem of course is the knowledge of the elementary area σ.

The first studies were performed about fifty years ago[16], by *solid/solution* exchange, and a few years later success was achieved in measuring surface areas as low as some tens of cm^2/g[17]. A number of inorganic compounds were assayed in this way prior to 1951[18]. Further studies are few; uranium dioxide (0·13 m^2/g) by uranium exchange[19], lead sulphate (0·80 m^2/g) by sulphur exchange[20], calcium carbonate (some m^2/g) by calcium exchange[21], strontium sulphate (about 2 m^2/g) by strontium or sulphur exchange[15], chromium oxide gels (some m^2/g or less) by chromium exchange[22], silver oxide (about 1 m^2/g) by silver exchange[23]. The reproducibility of an experimental procedure can be good, within a few per cent, but the actual accuracy depends strongly on the processes mentioned above, and we often miss comparison with other methods.

The rate of *solid/gas* exchange becomes appreciable at relatively high temperatures, where disturbances from the above mentioned effects often are severe. This procedure therefore was not extensively used, although the exchange between oxygen and solid inorganic oxides provided some measurements of specific surface areas of a few m^2/g[24].

2.4. Adsorption from solutions

Adsorption from solution provides some very attractive methods, as far as it studies solids in liquid media, and supplies reproducible results from easy and quick procedures. It succeeds in determining surface areas as low as some cm^2.

Dye adsorption[25] was used some thirty years ago to measure areas of 0·1 m^2/g. Some correlations have been possible between the area per molecule found and that expected theoretically.

Adsorption of long chain compounds[26], providing monomolecular compact adsorbed films, has been used from solutions in different solvents. The use of ^{14}C-labelled molecules is the easiest procedure and gives measurements of surface areas as low as 0·5 m^2/g for numerous solids by counting the solution[27], or to 2·45 cm^2 by counting the sample[28–30]. It is necessary to ensure a high purity for the solvent and the surface, in particular with respect to water and compounds similar to the adsorbate. The solvent must be chosen so that its affinity for the solid does not compete with that of the adsorbate.

These conditions and the necessity of knowing exactly the interactions involved are imperative in *ion adsorption*, and this must be the reason why research workers were not very eager to utilise it for measuring surface areas. After the use of natural radioelements, with the help of which metallic reas of some cm^2 were obtained[31], about thirty years were needed before any further work was reported. These data provided interesting values for metal plates or coarse powders by using anion adsorption[32–35].

In addition to sensitivity, radioactivity gives the possibility of studying the distribution of adsorbed species on surfaces by means of autoradiography. In some systems preferential adsorption occurs at microcracks[28] or joins[33].

2.5. Physical adsorption of gases

It has been known for a long time that solids would trap gases at low temperature[36], but only in the twentieth century has the nature of the interactions involved and the laws of the phenomenon become somewhat clearer. Electrostatic forces are responsible for the so-called physical adsorption, which is most efficient near the liquefaction temperature of the gas, and requires energies of the same order as the heats of liquefaction. Adsorbed amounts are functions of the relative gas pressure and of the solid surface area[37–41]. The latter can be derived with the help of experimental data from a suitable law for the isotherm, such as the BET[42], HJ[43] or DKR[44] expressions; these provide the amount adsorbed as a monomolecular layer. Hence knowing the elementary area σ[45] occupied by one molecule of the adsorbate on the solid surface the surface area can be calculated. This method is attractive, because it can be used either as a relative method with a good accuracy or as an absolute method within the precision of σ. It was therefore adapted to low surface area determination.

2.5.1. *Experimental techniques and results*

Improvements in sensitivity were obtained by using suitable techniques for the measurements of low pressures and/or adsorbate amounts.

In the conventional *volumetric procedure* a limitation in sensitivity arises from the 'dead' volume, which it is necessary to reduce as much as possible[46]. For this purpose adsorbates, the saturation pressure of which is low at liquid nitrogen temperature, have been used instead of nitrogen: argon[47], krypton[48], xenon[49], or hydrocarbons[50–56]. Another improvement is to use dilution of nitrogen by helium[57, 58]. It is also interesting to determine the amount of an adsorbate by means of a thermodesorption procedure[59, 60]. As to *low pressure determinations*, these have been achieved with the help of precise instruments involving low volume probes: ionization gauges[61], thermocouple gauges[62], thermistor gauges[63, 64], membrane micromanometers[65], and radioactivity detectors connected with the use of a gas tracer such as ^{85}Kr [66, 67] or ^{133}Xe [68]. A special feature of the latter technique was to provide a means of measuring partial pressures of the adsorbate in a mixture with helium, which can be convenient not only for volumetric requirements but also to ensure correct temperature of the samples. With these procedures low specific surface areas can be determined in the range from some m^2/g down to 0·01 m^2/g, and the smallest sample areas can be some tens of cm^2 with krypton or some cm^2 with xenon.

Gravimetric measurements of the adsorbed amounts are possible even with nitrogen by using very sensitive balances[69] and this method could give areas of some tens of cm^2; the only limitation is the weight of the samples.

Vapour phase chromatography introduces several possibilities. Each point of an isotherm can be obtained by determination of the areas of a desorption peak[70], and the whole isotherm provided either by frontal analysis[71] or by peak analysis[72]. Wit hthe first technique specific surface areas as low as 49 cm^2/g and areas down to some tens of cm^2 have been measured[73]. The second method was applied to samples of 130 cm^2 [74].

Using *radioactive tracers* enables one to obtain directly the amount of an adsorbate with the help of the emitted radiation. Krypton 85 is the most convenient radioelement because of its long half-life, 10·6 years, and its interesting decay scheme, giving one β particle with a maximum energy 0·67 MeV per decay and one γ photon of 0·52 MeV per 250 decays. The photons can be detected even through a Dewar flask, providing a quick and easy procedure[75–77], with the only disadvantage of involving rather high activities. Specific surface areas were obtained down to 0·04 m^2/g. We also constructed a cell for the use of the β-rays[67], where only low activities were needed, and could measure specific surface areas in the range 6–0·08 m^2/g on samples smaller than 0·5 g.

2.5.2. Discussion

In the low pressure devices *the temperature of the sample* is somewhat different from that of the cryogenic bath[78]: it may continuously decrease when the pressure increases during an adsorption experiment. However, this deviation can be reduced by supplying a suitable amount of helium[79] and we constructed a cell which avoids this defect[80]. Uncertainty can exist about the *temperature of some parts of the gas volume*. Eventual deviations of the true low pressure above the sample from the farther measured value, due to *thermomolecular flow*, can generally be corrected for.

The most severe experimental limitation in determining the lowest areas is the *adsorption on the walls of the cell*.

Theoretical limitations are not typical of low surface area determination, and we will only mention them briefly. The largest error can arise from a poor knowledge of the cross-sectional area σ of an adsorbed molecule, due either to a misleading assumption on the physical state of the adsorbate or to a dependence of σ on the chemical nature of the surface. Krypton gives a typical instance of the first case, since it can be thought to adsorb in the state of a supercooled liquid[48] or in the solid state[81]. Fortunately the resulting data for the areas are not very different when an adequate value of σ is associated with the saturation vapour pressure for each state[82, 83]: 19·5 Å^2 for the supercooled liquid with $p_s = 2{\cdot}72$ torr, and 21·5 Å^2 for the solid with $p_s = 1{\cdot}88$ torr. However, larger values of p_s have been proposed[84] and seem to give a correction for the erroneous curvatures of linear BET plots[85]. The influence of the chemical nature of the surface[45, 86] and the influence of some previous chemisorption[87–89] are more serious and cannot be easily corrected for. At least some chemisorption can compete with physisorption when using hydrocarbons as adsorbates[90].

For low surface area determination, *texture* does not give any difficulty in comparing samples of the same solid with quite different specific surface areas or roughness factors, since we have no small pores.

2.5.3. Conclusion

The lowest surface areas which can be measured with the help of all these procedures, with a precision of about 10 per cent in comparing values for surfaces of the same nature, are of the order of some cm^2, chiefly by using xenon. Krypton is suitable to determine minimal areas of some tens of cm^2. For somewhat larger surface areas this kind of intercomparison can be more precise.

The accuracy of absolute measurements and of intercomparison between surfaces of different nature is dependent on σ, which cannot be accurately evaluated. In fact adsorption involves forces typical for each adsorbent–adsorbate system, and a fundamental question remains as to whether we can keep the model of a true surface at the areas occupied by molecules of an adsorbate in compact array at minimal and constant distance from the solid.

2.6. Miscellaneous

We report some methods which either do not seem to be of general application, or are developing now and perhaps may be of interest in the future, or are even subject to miscellaneous difficulties but have proved their ability to measure low surface areas.

2.6.1. Gas chemisorption

For the sake of specificity chemically interacting gases were used chiefly with metallic surfaces: hydrogen[91], carbon monoxide[92, 60], iodine[93], ^{14}C-formic acid[94]; the two latter provided the greatest sensitivity.

2.6.2. Negative adsorption[95]

After this method was shown to be a suitable means for measuring surface areas of about 1 m^2/g[96], it received a new theoretical and experimental development[97] and revealed its ability of going down to lower values. The limit depended on obtaining reasonable accuracy in estimating the relative concentration changes involved. These concentrations are low, and radiotracers can solve the problem.

2.6.3. Radioactive reagents

The areas of aluminium samples were assayed by reaction with a mixture of chromic acid and ^{32}P-phosphoric acid. The surface oxide layers were replaced by radioactive ones, and relative roughness factors could be obtained[98].

Radioactivated metals can conversely be extracted with long chain compounds adsorbed on them, and the transferred radioactivities give measurements of areas down to some cm^2 [99].

Heterogeneous non-isotopic ion exchange could be a more general method, but it has been little used (lead exchange with strontium[100] or barium[101] sulphate).

2.6.4. Emanation method

The emanating power of one solid particle is known to be proportional to its specific surface area, in the case of particles of dimensions larger than the recoil range of radon, i.e. for low specific surface areas[102]. In spite of the requirement of a special preparation of the solid, the method is of great interest because it provides a dynamical procedure for studying surface areas variations. Samples down to some tens of cm^2 were assayed previous to 1951[103]. In fact, the theory needs further development but some empirical work showed the validity of the proportionality law[104, 105], which is best known in the range of larger specific surface areas[106].

3. GENERAL DISCUSSION

For a complete review we must mention some methods together with the reasons why we do not intend to discuss them at any extent. Electrochemical methods are delicate[107] and generally electrochemists need to know surface areas of electrodes more accurately than they can measure them. Calorimetry misses sensitivity[3]. Sedimentation and turbidimetric seldom appear in the literature.

A new technique and method respectively, for which further developments are expected, are ellipsometry[108, 109] and Low Energy Electron Diffraction[110].

Our discussion will be made clear by making a quick comprehensive *intercomparison of the methods* described in Section 2. For this purpose we used the tables which are an appendix to reference 2, and the bibliography which we report in our present paper.

Optical and electron microscopy as a rule give areas which do not agree with other methods except in the case of solids with a roughness factor of unity, because it is difficult to take into account the particle irregularities. These methods are used to determine the geometric (apparent) area which is compared to the true one to calculate the roughness factor. Electron microscopy has great value in distinguishing primary solid particles from aggregates.

We do not know any comparison of *profilography* with other methods. Such work would be useful in a search for quite plane surfaces, chiefly by using electron microscopy of thin cross-sectional specimens and with the help of modern theories of surface state.

The *methods involving porosity* show rather good agreement with physical adsorption of gases, often better than 10 per cent, and it is not surprising since both are wholly 'dry' procedures. Unhappily there is no comparison with other methods, and in particular the question remains as to whether permeametry and BET measurements both agree with some 'wet' procedure.

As we pointed out at the end of Section 2.3, a similar situation exists with *heterogeneous isotopic exchange* chiefly from solutions, where the only available comparisons were made almost thirty years ago and showed an agreement within 20 per cent between this method and adsorption from solutions.

Dye adsorption could supply results agreeing within 10 per cent to those from microscopy, permeametry, and the BET method, in the range of some m^2/g. In a number of cases no agreement is apparent. With *fatty compounds* the situation is not very clear in that the observed discrepancies compared with permeametry and BET are either greater or smaller. The adsorption of stearic acid generally shows agreement to within a few per cent of the BET method; some measurements give lower values perhaps due to a roughness factor.

The values obtained from the *physical adsorption of gases* are often comparable to those from other methods, as has been mentioned above. So we think that in a number of cases the other methods fail in giving rather precise results, and we therefore propose the BET procedure as a standard (no clear conclusion seemed possible to us from the few available comparisons between BET and HJ or DKR treatments). The chief uncertainty that remains is on the elementary area, σ, of an adsorbed molecule. The use of different gases often results in measurements which agree within the reproducibility of the procedures, but it is not always clear whether they derive from absolute determinations of σ or from a calibration using the cross section for nitrogen.

Now we can try to develop *some conclusions as to the suitability of the methods.*

The miscellaneous methods referred to above are derived from different basic principles and can be useful within specific fields and conditions. On an atomic scale the different elementary interactions involved imply different concepts of the surface, from the consideration of either atomic sites, or electronic density, van der Waals radii and superficial bond energies. In this connection the nature of surface atoms and the eventual modifications induced by the procedure must be taken into account. For these reasons the agreement of two methods with each other within about 20 per cent can be regarded as good. Conversely, relative measurements on solids of the same nature by means of one method must show a precision of some per cent, except in the lower part of the range, where for a number of methods some error is encountered from the walls of the container.

The purpose of low surface area determinations is to obtain either the particle diameters of coarse powders or the roughness factors of massive solids; from these data a knowledge of the texture and the superficial properties of these substances follow. An idea therefore is to choose methods that involve the useful properties of the sample and which do not modify its surface. In fact the second requirement is seldom severe in the case of a coarse texture, in as far as it means the absence of narrow pores and of ageing processes (metallic thin films are an exception), and similarity of 'wet' and 'dry' procedures; as a rule the contact areas of particles cannot be large.

Of course the first question, when dealing with a typical solid, is to know whether it actually has a low surface area. Electron microscopy, low-angle x-ray scattering and the physical adsorption of gases are the available methods for a good answer. The first and second are necessary if a very narrow porosity is suspected. The third gives a rather precise value for any area in our range and seems to be the most suitable. It can also be proposed as a calibration method for some quicker or easier procedures (permeametry, adsorption from solutions, negative adsorption), as well as for further investigating of other methods.

For a good comparison of methods tests are needed with quite identical samples, a requirement which was not sufficiently obeyed up to now. An absolute calibration could be achieved if the roughness factor of some solid were known exactly, for instance, that of a perfectly plain metal surface obtained from very fine mechanical or electrolytical polishing or a heat polished glass. The examination of thin cross-sectional slides by electron microscopy could give a valuable information on the true surface state.

4. CONCLUSION

In briefly reviewing low surface area determination we have attempted to show the present state of the question and current trends in this field.

A number of methods, each with several variants, are available or will be available, in the near future, for measuring surface areas down to some square centimetres with a reproduibility within a few per cent. Studies of texture evolutions are therefore quite possible. Absolute values must be used cautiously for theoretical or experimental reasons, but the precision could be improved by means of suitable standard surfaces.

References

[1] J. H. de Boer, this Symposium.

[2] C. Orr, Jr. and J. M. Dallavalle. *Fine particle measurement*, The Macmillan Company, New York, 1959.

[3] S. J. Gregg and K. S. W. Sing. *Adsorption, surface area and porosity*, Academic Press, London, New York, 1967.

[4] T. Allen. *Particle size measurement*, Chapman and Hall Ltd., London, 1968.

[5] A. C. Wahl and N. A. Bonner. *Radioactivity applied to chemistry*, J. Wiley and Sons, New York, 1951.

[6] M. I. Barnett, this Volume, p. 369.

[7] A. I. Medalia, this Symposium.

[8] K. Bisa and E. Krücke. *Kolloid. Z.* **203**, 32 (1965).

[9] O. Erbacher. *Z. Phys. Chem.* **A163**, 215 et 231 (1933).

[10] I. L. Roikh, V. V. Ordynskaya and I. P. Bolotich. *Dokl. Akad. Nauk SSSR* **146**, 1316 (1962).

[11] R. M. Barrer, this Symposium.

[12] H. M. Rootare and C. F. Prenzlow. *J. Phys. Chem.* **71**, 2733 (1967).

[13] A. Renouprez, this Symposium.

[14] K. Klier and E. Kucera. *J. Phys. Chem. Solids* **27**, 1087 (1966).

[15] B. V. Enüstün and N. K. Tunali. *Intern. J. Appl. Rad. Isot.* **19**, 637 (1968).

[16] F. Paneth and W. Vorwerk. *Z. Phys. Chem.* **101**, 445 (1922).

[17] F. Paneth. *Radioelements as indicators*, McGraw-Hill Book Co, New York, 1928.

[18] J. H. Wang, in reference 5, p. 500.

[19] R. E. Fergusson and G. W. Leddicotte. *ORNL*-59-8-62 (1959).

[20] C. L. Nealy and G. R. Choppin. *J. Chem. Educ.* **41**, 597 (1964).

[21] G. C. Inks and R. B. Hahn. *Anal. Chem.* **39**, 625 (1967).

[22] J. D. Carruthers, J. Fenerty and K. S. W. Sing. 6th Symposium on the Reactivity of Solids, Schenectady 1968, publication number 2.4.1.

[23] J. C. Lagier and P. Bussière, to be published.

[24] E. R. S. Winter. *Adv. Catal.* **10**, 196 (1958).

[25] C. H. Giles, A. P. D'Silva and A. S. Trivedi, this Symposium.

[26] G. Schay, this Symposium.

[27] M. C. Kordecki and M. B. Gandy. *Intern. J. Appl. Rad. Isot.* **12**, 27 (1961).

[28] J. W. Shepard and J. P. Ryan. *J. Phys. Chem.* **63**, 1616 (1959).

[29] R. J. Adams, H. L. Weisbecker and W. J. McDonald. *J. Electrochem. Soc.* **111**, 774 (1964).

[30] C. O. Timmons, R. L. Patterson and L. B. Lockhart, Jr. *J. Coll. Interface Sci.* **26**, 120 (1968).

[31] O. Erbacher. *Z. Phys. Chem.* **A163**, 215, 231 (1933).

[32] H. P. Dibbs. *J. Appl. Chem.* **10**, 372 (1960).

[33] K. Schwabe. *Isotopentechnik* **1**, 175 (1961); *Electrochim. Acta* **6**, 223 (1962).

[34] L. Imre and J. Nagy. *Kolloid Z.* **183**, 134 (1962).

[35] J. Bénard. *Coloquio sobre Quimica Fisica de procesos en superficies solidas*, CSIC, Madrid 1965, p. 375.

[36] Fontana. *Mem. Mat. Fiz. Soc. Ital. Sci.* **1**, 679 (1777).

[37] Y. Lahrer. *J. Chim. Phys.* **62**, 604 (1965).

[38] S. Brunauer. *Pure Appl. Chem.* **10**, 293 (1965).

[39] S. Ross and J. P. Olivier. *On physical adsorption*, Interscience Publishers, New York, 1964.

[40] See reference 3.

[41] D. M. Young and A. D. Crowell. *Physical adsorption of gases*, Butterworths, London, 1962.

[42] S. Brunauer, P. H. Emmett and E. Teller. *J. Am. Chem. Soc.* **60**, 309 (1938).

[43] W. D. Harkins and G. Jura. *J. Chem. Phys.* **11**, 431 (1943).

[44] M. G. Kaganer. *Russ. J. Phys. Chem.* **33**, 352 (1959).

[45] A. L. McClellan and H. F. Harnsberger. *J. Coll. Interface Sci.* **23**, 577 (1967).

[46] See reference 2.

[47] N. Glossman and M. L. Corrin. *J. Coll. Interface Sci.* **23**, 237 (1967).

[48] G. A. Nicolaon and S. J. Teichner. *J. Chim. Phys.* **66**, 127 (1969).

[49] W. A. Cannon. *Nature* **197**, 1000 (1963).
[50] L. A. Wooten and C. Brown. *J. Am. Chem. Soc.* **65**, 113 (1943).
[51] X. Duval. *Ann. Chim.* **10**, 903 (1955).
[52] T. L. O'Connor and H. H. Uhlig. *J. Phys. Chem.* **61**, 402 (1957).
[53] D. M. Young and C. D. Anderson. *Can. J. Chem.* **43**, 309 (1965).
[54] D. P. Graham. *J. Phys. Chem.* **69**, 4387 (1965).
[55] T. J. Adams, J. N. Sherwood and F. L. Swinton. *J. Chem. Soc., Série A*, 1195 (1966).
[56] Y. Delaunois, A. Frennet and G. Lienard. *J. Chim. Phys.* **63**, 906 (1966).
[57] L. Lecrivain and R. Martin. *Bull. Soc. Fr. Céram.* No. 60, 55 (1963).
[58] J. Kremen, J. S. Lagarias and V. R. Deitz. *Rev. Sci. Instr.* **37**, 1265 (1966).
[59] N. E. Buyanova, G. B. Gudkova and A. P. Karnaukhov. *Kin. Kat.* **6**, 1085 (1965).
[60] T. Kabe, T. Mizuno and I. Yasumori. *Bull. Soc. Jap.* **40**, 2047 (1967).
[61] A. Schram. *Nuovo Cim., Suppl.* **5**, 291 (1967).
[62] J. Dollimore, G. R. Heal and D. McIlquam. *Chem. Ind.* No. 18, 742 (1963).
[63] A. J. Rosenberg. *J. Phys. Chem.* **62**, 112 (1958).
[64] J. L. Botts. TID-7015, Suppl. 5, 1105.1 (1963).
[65] V. Rudinger and A. Cassuto. *Le Vide* **123**, 240 (1966).
[66] D. W. Aylmore and W. B. Jepson. *J. Sci. Instr.* **38**, 156 (1961).
[67] G. Beurton, P. Bussière and B. Imelik. *Bull. Soc. Chim. Fr.* 1793 (1967).
[68] P. Chénebault and A. Schürenkämper. *J. Phys. Chem.* **69**, 2300 (1965).
[69] T. N. Rhodin, Jr. *J. Am. Chem. Soc.* **72**, 4343 (1950).
[70] F. M. Nelsen and F. T. Eggertsen. *Anal. Chem.* **30**, 1387 (1958).
[71] R. Stock. *Anal. Chem.* **33**, 966 (1961)
[72] A. Saint-Yrieix. *Bull. Soc. Chim. Fr.* 3407 (1965).
[73] K. V. Wise and E. H. Lee. *Anal. Chem.* **34**, 301 (1962).
[74] S. Thibault, J. Amouroux and S. Talbot. *Bull. Soc. Chim. Fr.* 1319 (1968).
[75] J. T. Clarke. *J. Phys. Chem.* **68**, 884 (1964).
[76] J. P. W. Houtman and J. Medema. *Ber. Bunsenges. Phys. Chem.* **70**, 489 (1966).
[77] J. Medema and J. P. W. Houtman. *Anal. Chem.* **41**, 209 (1969).
[78] G. A. Nicolaon and S. J. Teichner. *J. Chim. Phys.* **65**, 870 (1968).
[79] C. Moreau. *C.R. Acad. Sci.* **253**, 1044 (1961).
[80] G. Beurton and P. Bussière, to be published.
[81] G. L. Kington and J. M. Holmes. *Trans. Faraday Soc.* **49**, 417 (1953).
[82] R. A. W. Haul. *Angew. Chem.* **68**, 238 (1956).
[83] R. E. Ranc and S. J. Teichner. *J. Chim. Phys.* **64**, 401 (1967).
[84] J. M. Haynes. *J. Phys. Chem.* **66**, 182 (1962).
[85] P. J. Malden and J. D. F. Marsh. *J. Phys. Chem.* **63**, 1039 (1959).
[86] D. F. Klemperer and F. S. Stone. *Proc. Roy. Soc.* **243**, 1234 (1958).
[87] V. Ponec and Z. Knor. *Actes du 2ème Congrès International sur la Catalyse*, Technip, Paris, 1960, 195.
[88] L. Bonnetain and J. Cesmat. *Les solides finement divisés*, Direction de la Documentation Française, Paris, 1969, 165.
[89] Y. Lahrer and P. Maurice. *J. Chim. Phys.* **65**, 669 (1968).
[90] K. Kuchynka. *Coll. Czech. Chem. Comm.* **33**, 3049 (1960).
[91] J. R. Anderson and B. G. Baker. *J. Phys. Chem.* **66**, 482 (1962).
[92] C. S. Brooks and V. J. Kehrer, Jr. *Anal. Chem.* **41**, 103 (1969).
[93] M. K. Testerman and R. D. Hartman. *J. Appl. Physics* **34**, 1492 (1963).
[94] A. Lawson. *J. Catal.* **11**, 283 (1968).
[95] J. Lyklema, this Symposium.
[96] J. Belloni. *J. Chim. Phys.* **63**, 645 (1966).
[97] H. J. van den Hul and J. Lyklema. *J. Am. Chem. Soc.* **90**, 3010 (1968).
[98] R. C. Plumb and Lewis. *Nucleonics* **13**, No. 11, 22 (1955);
J. W. Swaine, Jr. and R. C. Plumb. *J. Appl. Phys.* **33**, 2378 (1962).
[99] F. P. Bowden and A. C. Moore. *Trans. Far. Soc.* **47**, 900 (1951).
[100] R. Singleton and J. Spinks. *Can. J. Res.* **27B**, 238 (1949).
[101] L. Imre. *Kolloid* Z. **106**, 39 (1944).
[102] S. Flügge and K. E. Zimens. *Z. Phys. Chem.* **B42**, 179 (1939).
[103] A. C. Wahl. in reference 5, 284.
[104] P. Harteck and H. Schmidt. *Z. Phys. Chem.* **B21**, 447 (1933).
[105] S. B. Skladzien. A.N.L.-6335 (1961).
[106] J. F. Gourdier, P. Bussiere and B. Imelik. *C.R. Acad. Sci.* **264**, 1625 (1967).
[107] H. A. Laitinen. *Anal. Chem.* **33**, 1458 (1961).
[108] W. T. Pimbley and H. R. Macqueen. *J. Phys. Chem.* **68**, 1101 (1964).
[109] G. A. Bootsma and F. Meyer. *Surf. Sci.* **13**, 110 (1969).
[110] J. J. Lander and J. Morrison. *Surf. Sci.* **6**, 1 (1967).

SURFACE ASPECTS OF FLOW IN MICROPOROUS MEMBRANES

R. M. Barrer

Physical Chemistry Laboratories, Chemistry Department, Imperial College, London, S.W.7., U.K.

In the transport of fluids through microporous membranes the quantities most readily measured are the steady-state flow and the sorption and desorption time-lags at the outgoing surfaces. These quantities can give much information about the nature of the membrane surface and pore structure. When the overall diffusion coefficients D are functions only of concentration, C, one may find the concentration dependence of D, concentration contours and local concentration gradients through the membrane. Steady state flows and concentration contours serve in their turn to evaluate sorption time-lags.

Expressions for time-lags and time-lag differences have been given which do not depend upon any assumed equation of flow and which, for diffusion flow, are valid when D is a function of C, distance x and time t singly or together. These lead in certain instances to very simple relationships. When D is a function only of C one such relation for simple boundary conditions allows the sorption isotherm and hence the monolayer equivalent surface area to be measured for membranes *in situ*, using only the steady state flow and the adsorption and desorption time-lags needed for their characterisation in other ways. Another absolute method of finding this area depends on measuring the breakthrough time for very rectangular isotherms. Blind pores can introduce a time-dependence into D and in absence of x-dependence of D combined time-lag and steady state flow measurements can give a porosity and surface area associated with blind pore character.

Flow measurements also serve to evaluate other properties of pores, through structure factors and through properties of surface flows. For example it is shown how surface diffusion coefficients are related to the reciprocal slopes of adsorption isotherms, and that broken surfaces generate less surface flow, area for area, than do smooth ones.

1. INTRODUCTION

The flow of sorbed or non-sorbed gases through microporous media is rapidly becoming a very important means of studying such media[1, 2] (pore geometry, blind-pore character, surface areas) and of investigating some equilibrium and non-equilibrium properties of the flowing species (for example, amounts sorbed, permeability and diffusion coefficients in the gas phase and on the adsorbing surfaces, concentration profiles across membranes, and separation factors for mixtures). In the present paper therefore an account will be given of some of the theoretical background of flow through membranes, together with examples of particular uses, actual or potential, which are of interest for surface chemistry.

2. THE MEMBRANE EXPERIMENT

For reasons given later in this communication the microporous membrane is best made by compaction of successive increments of high area powder, by appropriate hydraulic pressure in a steel tube. This method has been successful with such materials as alumina–silica cracking catalysts and carbons (Carbolac, Black Pearls, Graphon). In other cases the membranes may be obtained already in coherent form (porous ceramic, Vycor porous glass). Uncompacted membranes can be prepared by settling the powder in glass tubes (analcite spherulites, zeolite powders). In all systems the flow paths and pores have diameters or dimensions small compared with the macroscopic dimensions of the specimen. In this sense the porous membrane may be isotropic. Although ideally isotropic compacts may not be easy to make, the method of compacting in increments goes a long way towards this ideal.

The membrane is then made to separate a reservoir of fluid from a receiving volume. It is bounded by the planes $x = 0$ and $x = l$ and flow occurs in the direction of x increasing. The most general boundary conditions are

(i) $C = C_o$ at $x = 0$ for all t

(ii) $C = C_i(x)$ for $0 < x < l$ at $t = 0$

(iii) $C = C_l$ at $x = l$ for all t, with $C_l < C_o$

In most experiments (ii) and (iii) are respectively replaced by

(iv) $C = 0$ for $0 < x < l$ at $t = 0$

(v) $C \sim o$ at $x = l$ for all t.

Another significant alternative to (ii) is

(vi) $C = C_o$ for $0 < x < l$ at $t = 0$.

At $t = o$ the flow experiment is commenced. With boundary conditions (i), (iv) and (v) as an example the plot of pressure rise against time in the receiving volume approaches asymptotically to a straight line, as shown in *Figure 1*, curve 1. The intercept this asymptote makes on the axis of time is termed the adsorption time-lag at $x = l$, L_l^a, and the slope serves to calculate the steady state flux, J_∞. The experiment is so organised, for example by making the membranes of appropriately low permeability or by providing a large receiving volume at $x = l$, that the concentration in the receiving volume is always $\ll C_o$. The time-lag is called the adsorption time-lag because the microporous membrane fills its pores with gaseous and adsorbed molecules during the transient state. One may also in principle determine an adsorption time lag, L_o^a, at the ingoing surface, $x = 0$.

When the boundary conditions are (i), (v) and (vi) the membrane has initially an equilibrium loading, with $C = C_o$, of adsorbed and gaseous molecules, and the same steady state is now approached by desorption. The corresponding time lags at $x = l$ and $x = 0$ are L_l^d and L_o^d. L_l^d is indicated in *Figure 1*, curve 2. The significance of the membrane experiment then lies in the interpretation of the flux J_∞ and the time-lags, L, in terms of amounts sorbed, surface areas, surface and volume flows, diffusion coefficients and pore properties. Before considering some of these specific aspects,

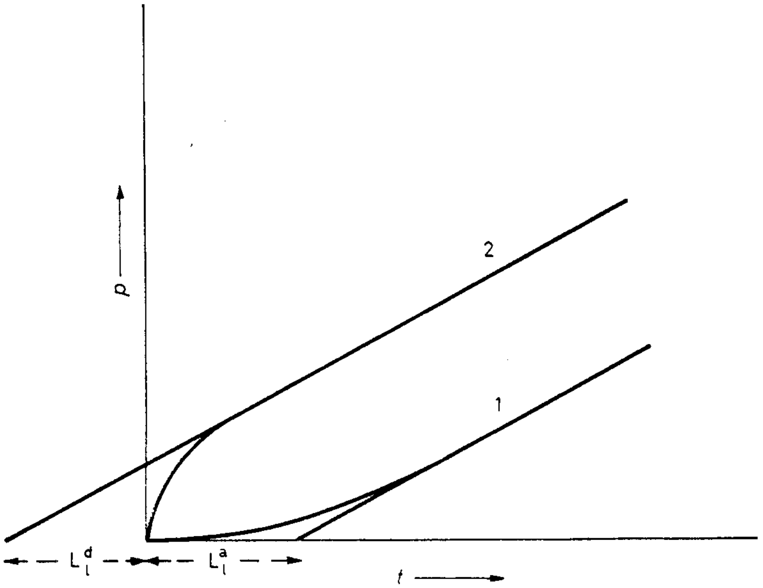

Figure 1. Pressure changes at the face $x = l$ as a function of t. Curve 1 indicates the adsorption time-lag and curve 2 the desorption time-lag.

however, basic aspects of the information given by the membrane experiment will be considered.

3. THE STEADY STATE FLUX

The steady state flux, J_∞, is often expressed, as appropriate, in terms of Fick's or Darcy's laws. In terms of the former, and considering steady state flow through unit-cross-section normal to x,

$$J_\infty = -D\,\mathrm{d}c/\mathrm{d}x \tag{1}$$

in an isothermal system. D may be constant, a function of x, a function of C, or a function of both x and C. In the transient state D may also be a function of t, but, by definition of the steady state, time dependence in this state will have disappeared from D in Eq. (1). We now consider the case where D is independent of x, but dependent upon C, since this is a very important practical case. If we integrate Eq. (1) from 0 to x and from 0 to l and express the two integrals as a ratio, we have, since J_∞ is independent of x (ref. 3)

$$\frac{x}{l} = \frac{\int_{C_x}^{C_0} D\mathrm{d}C}{\int_0^{C_0} D\mathrm{d}C} = \frac{\int_0^{C_0} D\mathrm{d}C - \int_0^{C_x} D\mathrm{d}C}{\int_0^{C_0} D\mathrm{d}C} = \frac{J(C_0) - J(C_x)}{J(C_0)} \tag{2}$$

A master graph is constructed by plotting $J(C_0)$ against C_0 (*Figure 2*). Here C_0^* is the concentration at $x = 0$ in a particular experiment. Then C_x will be the concentration at $x(0 < x < l)$; $J(C_0^*)$ and $J(C_x)$ are obtained, as shown, from *Figure 2* corresponding with C_0^* and C_x at $x = 0$, and hence their difference. The ratio x/l corresponding to C_x follows from Eq. (2). In

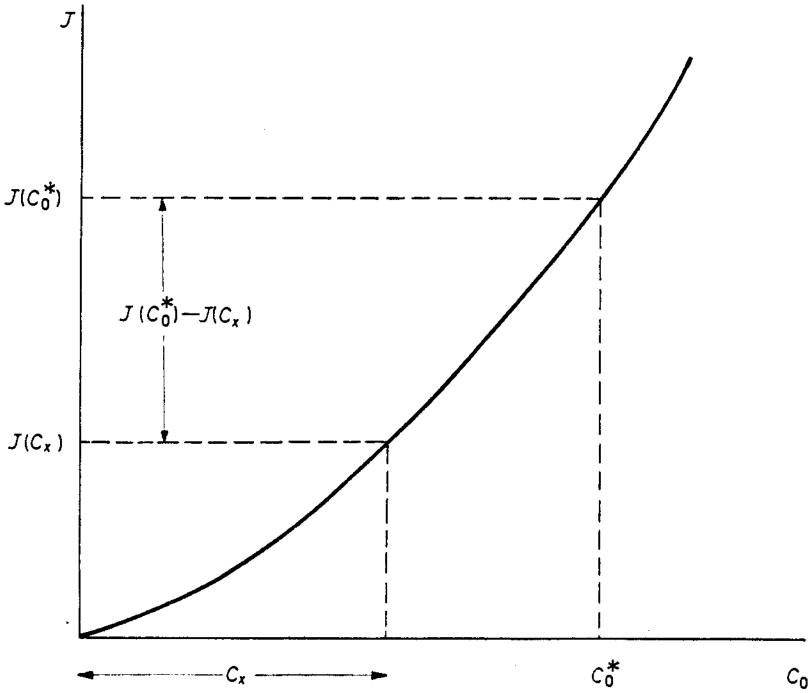

Figure 2. Master plot of J against C_o illustrating the method of obtaining concentration contours and gradients within the porous medium.

this way the whole concentration contour of C_x across the membrane can be found without knowing $D(C)$.

The flow experiments can equally well be used to find the concentration gradient at any point in the membrane without first finding the concentration contours across the membrane[3]. Thus in any particular experiment with $C_o = C_0^*$ the steady state relation is

$$J(C_0^*) = -D(C_x)\,(\mathrm{d}C/\mathrm{d}x)_x \tag{3}$$

where C_x is the concentration at x $(C_x < C_0^*)$. Integration of Eq. (3) from 0 to l and differentiation with respect to C_o gives for any C_o

$$D(C_o) = l(\mathrm{d}J/\mathrm{d}C_o) \tag{4}$$

which, for $C_o = C_x$ becomes

$$(\mathrm{d}C/\mathrm{d}x)_x = -\frac{J(C_0^*)}{l}\frac{\mathrm{d}C_x}{\mathrm{d}J_x} \tag{5}$$

The value of the differential on the right hand side of Eq. (5) then follows from the master plot of *Figure 2*.

Finally, from Eq. (4) and the master plot of *Figure 2* one may determine $D(C)$ for any value of $C = C_o$, since again $\mathrm{d}J/\mathrm{d}C_o$ is obtainable as the slope of J vs C_o in *Figure 2*. Thus the diffusion coefficient and its concentration dependence can be found. Since the concentration contour is also known, the variation of D with distance across the membrane is also available. All these very general aspects of the membrane experiment are valid as previously indicated, when D is a function only of concentration (or when D is a constant).

4. TIME-LAGS AND RELATED QUANTITIES

Frisch[4–6] some time ago was able to derive expressions for the time-lag, assuming Fick's law and when D was a function of C, without first requiring the explicit solution of the transient state equation of flow

$$\frac{\partial C}{\partial t} = \frac{\partial}{\partial x}\left(D(C)\frac{\partial C}{\partial x}\right) \tag{6}$$

Frisch's approach has subsequently been developed in various ways which have significance in the interpretation of membrane experiments[7–9]. Recently for example it has been shown[10] that one may obtain completely general expressions for the various time-lags and related quantities starting only from the conservation of matter condition

$$\frac{\partial C}{\partial t} = -\operatorname{div} J \tag{7}$$

so that there is no need to assume any formal flow equation. At any plane $x = X$ the adsorption time-lag is given for the boundary conditions (i), (iv) and (v) by

$$lJ_\infty L_x = \int_0^l xC(x)\mathrm{d}x - l\int_X^l C(x)\mathrm{d}x + \int_0^\infty\int_0^l (J_\infty - J(x,t))\mathrm{d}x\mathrm{d}t \tag{8}$$

In Eq. 8 $C(x)$ is the steady state concentration at x and $J(x,t)$ is the flux through this plane at time t. Similarly for $x = X$ and with the boundary conditions (i), (ii) and (v)

$$lJ_\infty L_X^d = \int_0^l x(C(x) - C_i(x))\mathrm{d}x - l\int_X^l (C(x) - C_i(x))\mathrm{d}x + \int_0^\infty\int_0^l (J_\infty - J(x,t))\mathrm{d}x\mathrm{d}t \tag{9}$$

From relation (8), by making $X = l$ and $X = 0$, respectively, one may find L_l^a, L_o^a and $(L_l^a - L_o^a) = \Delta L^a$. From relation (9) by making $X = l$ and $X = 0$ as before and setting $C_i(x) = C_o$ one may find L_l^d, L_o^d and $(L_l^d - L_o^d) = \Delta L^d$ Other quantities of interest are $(L_l^a - L_l^d) = \delta L$ and $(L_l^a - L_l^d) - (L_o^a - L_o^d) = \delta\Delta L$. All these quantities are summarised in *Table 1*. If for the last term in Eq. (7) and (8) the order of integration is changed one may write

$$\int_0^\infty\int_0^l (J_\infty - J(x,t))\mathrm{d}x\mathrm{d}t = \int_0^l (Q_\infty - Q(x))\mathrm{d}x \tag{10}$$

where

$$\int_0^\infty (J_\infty - J(x,t))\mathrm{d}t = Q_\infty - Q(x) \tag{11}$$

Thus $(Q_\infty - Q(x))$ is the difference between the steady state flow J_∞ and the flow $J(x,t)$ through the plane x, integrated between $t = 0$ and $t = \infty$.

Table 1. Time lags and related quantities

$$l\, J_\infty\, L_l^a = \int_0^l xC(x)\mathrm{d}x + \int_0^l (Q_\infty - Q^a(x))\mathrm{d}x \tag{12}$$

$$l\, J_\infty\, L_o^a = \int_0^l (x - l)C(x)\mathrm{d}x + \int_0^l (Q_\infty - Q^a(x))\mathrm{d}x \tag{13}$$

$$J_\infty\, (L_l^a - L_o^a) = J_\infty\, \Delta L^a = \int_0^l C(x)\mathrm{d}x = M_\infty \tag{14}$$

$$lJ_\infty\, L_l^d = \int_0^l xC(x)\mathrm{d}x - \frac{lM_o}{2} + \int_0^l (Q_\infty - Q^d(x))\mathrm{d}x \tag{15}$$

$$lJ_\infty\, L_o^d = \int_0^l (x - l)C(x)\mathrm{d}x + \frac{lM_o}{2} + \int_0^l (Q_\infty - Q^d(x))\mathrm{d}x \tag{16}$$

$$J_\infty\, (L_l^d - L_o^d) = J_\infty \Delta L^d = \int_0^l (C(x) - C_o)\mathrm{d}x = (M_\infty - M_o) \tag{17}$$

$$lJ_\infty\, (L_l^a - L_l^d) = lJ_\infty\, \delta L_l = \frac{lM_o}{2} + \int_0^l (Q^d(x) - Q^a(x))\mathrm{d}x \tag{18}$$

$$lJ_\infty\, (L_o^a - L_o^d) = lJ_\infty\, \delta L_o = -\frac{lM_o}{2} + \int_0^l (Q^d(x) - Q^a(x))\mathrm{d}x \tag{19}$$

$$J_\infty\, (\delta L_l - \delta L_o) = J_\infty\, \delta\Delta L = M_o \tag{20}$$

In *Table 1*, $M_\infty = \int_0^l C(x)\mathrm{d}x$ is the total amount of diffusant between $x = 0$ and $x = l$ per unit cross-section of the porous medium in the steady state, and $M_0 = C_0 l$ is this quantity at time $t = 0$. The relations (14), (17) and (20) are remarkably simple and in addition (17) and (20) hold not only when $C_i = C_0$ but in the general case $C_i = C_i(x)$. The time-lags and related quantities in *Table 1* have the following properties: (a) As already noted, they are valid for any equation of flow, since they are derived assuming only conservation of matter (Eq. 7). (b) They apply separately to every individual component in a mixture. The fluxes J are of course modified by the relevant cross-coefficients of the irreversible thermodynamic formulation and hence so are the L's, ΔL's or δL's. (c) If Fick's or other specific equations of flow are subsequently used to describe the flux, then the rate coefficient such as D may have separable or non-separable dependencies upon x, C or t.

5. *D* IS CONSTANT OR A FUNCTION OF *C*

When D is a constant or a function of C only, the relationships (8) and

(9) and many of those in *Table 1* become simpler. Thus, one may consider the term

$$\int_0^\infty \int_0^l (J_\infty - J(x,t))\mathrm{d}x\mathrm{d}t = I \tag{21}$$

which appears in Eqs. (8) and (9). Since

$$J(x,t) = -D(C)\,\mathrm{d}c/\mathrm{d}x$$

one may integrate with respect to x between o and l and obtain

$$\int_0 J(x,t)\mathrm{d}x = \int_0^{C_0} D(u)\mathrm{d}u = lJ_\infty \tag{22}$$

Accordingly I in Eq. (21) is zero and so $\int_0^l (Q_\infty - Q(x))\mathrm{d}x$ in *Table 1* is zero, when D is a function of C only, or is a constant[10]. It can also be seen that $\int_0^l (Q^d(x) - Q^a(x))\mathrm{d}x$ is zero for this case†, so that, for example, Eqs. (18) and (19) become respectively

$$J_\infty \delta L_l = C_0 l/2 = \tfrac{1}{2}M_o \tag{18a}$$

$$-J_\infty \delta L_o = C_0 l/2 = \tfrac{1}{2}M_o \tag{19a}$$

again two very simple results.

The adsorption time-lag, L_l^a, of *Figure 1* (curve 1) becomes for $D = D(C)$

$$lJ_\infty L_l^a = \int_0^l xC(x)\mathrm{d}x \tag{12a}$$

a relation first obtained by Frisch[4], and converted by him to

$$L_l^a = l^2 \int_0^{C_0} wD(w) \int_w^{C_0} D(u)\mathrm{d}u\,\mathrm{d}w \Bigg/ \left[\int_0^{C_0} D(u)\mathrm{d}u\right]^3 \tag{23}$$

in which form it has usually been employed. However Eq. (23) requires one to assume a functional form for $D(C)$, which is not very satisfactory, especially because $D(C)$ is a secondary quantity, obtained from the slope of plots of $J(C_0)$ vs. C_0 (Eq. 4). There are two ways of improving the procedure based on Eq. (23) for evaluating L_l^a from experimental measurements of steady state flows only[10].

Firstly, we have already seen above how $C(x)$ can be determined as a function of x. Accordingly $xC(x)$ can be found and plotted against x, so that $I = \int_0^l xC(x)\mathrm{d}x$ is found graphically. Then $L_l^a = I/lJ_\infty$. Secondly from Eq. (2) one finds

$$\mathrm{d}x = -\frac{l}{J(C_o^*)}\,\mathrm{d}J(Cx)$$

so that, substituting in Eq. (12a) for dx, and also for x from Eq. (2), we obtain

---

† $\int_0^l (Q^d(x) - Q^a(x))\,\mathrm{d}x$ can also be shown to be zero when D is a separable function of C and also of t[9]. Thus Eqs. (18a) and (19a) are independent of blind pore character (Section 6).

$$L_l^a = l \int_0^{J(C_o^*)} C_{J(Cx)} \{ J(C_o^*) - J(C_x) \} \, \mathrm{d}J(Cx)/(J(C_o^*))^3 \qquad (24)$$

The first term of the integral may be evaluated from the plot of C_o vs. $J(C_o)$ over the range $0 < C_o \leqslant C_0^*$ (*Figure 2*). This experimentally determined plot also provides the information needed to graph the product $C_{J(Cx)}$, $J(C_x)$ vs. $J(Cx)$ and so to obtain the second part of the integral.

From the experimental viewpoint the most easily determined quantities are the steady state flows, J_∞, and the time-lags L_l^a and L_l^d. From these three quantities and with no other measurements one may via Eq. (18a) find C_o or M_o, and hence the sorption isotherm by operating over a range of ingoing pressures and so of values of C_o. This isotherm is obtained with the membrane *in situ*. C_o is the total number of molecules per cm^3 of porous medium. Of these, $C_o'\varepsilon$ are in the gas phase, where C_o' is the number of molecules per cm^3 of gas phase at $x = 0$ which is known from the gas pressure at $x = 0$; and ε is the porosity in cm^3 per cm^3 which is also known from the density of the membrane material, its total mass and the volume into which it is compacted. Thus

$$C_o = C_o'\varepsilon + C_s \qquad (25)$$

where C_s is the Gibbs excess of sorbed molecules per unit volume of porous medium. The isotherm is conveniently presented as a plot of C_s against C_o' or p_0. From the isotherm the surface area of the porous medium can be found in the usual way by means for example of a BET plot.

Although this method of measuring surface areas follows from information which could rather easily be obtained in the course of normal membrane studies of J_∞ and of time-lags, it does not appear to have been used or even suggested previously.

6. TIME-DEPENDENCE OF *D*

Many porous media contain capillaries with some blind pore character. During the transient state of flow molecules penetrate and permeate all parts of the medium including the blind pores. In the steady state of flow on the other hand parts of the capillary system with blind-pore character are largely by-passed. Since the flow parameters in pores with blind pore character will not necessarily be the same as in channels without such character it was suggested[11] that diffusion coefficients determined in the transient state could differ from those in the steady state. If one considers separately the gas phase and surface transport within the porous medium four diffusion coefficients should be possible: D_g and D_{gs} which denote gas phase diffusion coefficients in transient and steady state respectively; and D_s and D_{ss} which are the corresponding quantities for surface transport. These diffusion coefficients were then related to ideal diffusion coefficients D^{cyl} in a long smooth cylindrical capillary having the same ratio ε/A as the actual porous medium, by means of the structure factors κ:

$$D_g = \kappa_g D_g^{cyl}; \; D_s = \kappa_s D_s^{cyl}$$

$$D_{gs} = \beta\kappa_{gs} D_g^{cyl}; \; D_{ss} = \beta\kappa_{ss} D_s^{cyl}$$

D_{gs} and D_{ss} involve the factor $\beta = (A/\epsilon)(\epsilon_s/A_s)$, ϵ_s and A_s being the porosity and surface area associated with the steady state flow only. κ_g and $\beta\kappa_{gs}$ in particular give useful information about pore character which will be referred to later (see Section 8).

A further inference of this argument is that D_g and D_s are distance- and time-averaged quantities across the membrane and over an interval at least equal to the time-lag; and that as flow in a membrane relaxes to its steady state the overall diffusion coefficient, D, for combined surface and gas phase flows must also be time dependent. This view can be usefully developed as follows[10]. Any local flow, j, may have a blind and a through pore component in the x-direction respectively denoted by j_B and j_T. If we sum these components per unit cross section of all local flows in the x-direction we obtain a total flow $J = J_B + J_T$ for which

$$\frac{\partial C}{\partial t} = -\frac{\partial}{\partial x}(J_B + J_T) \tag{27}$$

The total blind pore component, J_B, has the property of decaying to zero as the steady state is approached, while the total through pore component, J_T, becomes constant for $0 < x < l$. In terms of Fick's equation, if we define D_T and D_B by $J_T \equiv -D_T(\mathrm{d}C/\mathrm{d}x)$ and $J_B \equiv -D_B(\mathrm{d}C/\mathrm{d}x)$, Eq. (27) becomes

$$\frac{\partial C}{\partial t} = \frac{\partial}{\partial x}\left[D_T(1 + f(C,x,t))\frac{\partial C}{\partial x}\right] \tag{28}$$

where $D_B/D_T = f(C,x,t)$ and must, like J_B, approach zero as t increases. D_T, on the other hand, depends only on concentration and remains finite.

When the method of Frisch was applied to Eq. (27) to give the time-lag, L_l^a, this was found to be given by

$$lJ_\infty L_l^a = \int_0^l x\,C(x)\,\mathrm{d}x - \int_0^\infty\int_0^l J_B\,\mathrm{d}x\,\mathrm{d}t \tag{29}$$

The first term on the right hand side of Eq. (29) is the time-lag, L_l^a, for flow in a medium in which the steady state diffusion coefficient is a function of concentration only. The second term gives the correction $l.J_\infty.\Delta$ due to the time-dependent blind pore flow. That is, dropping the subscript 'l' from L_l^a,

$$L^a = L_1^a - \Delta \tag{30}$$

where

$$\Delta = \frac{\int_0^\infty\int_0^l J_B\,\mathrm{d}x\,\mathrm{d}t}{lJ_\infty} \tag{31}$$

If we assume that the order of integration in Eq. (31) may be changed, then $\int_0^\infty J_B\,\mathrm{d}t = Q_B(x)$ is the quantity of gas associated with J_B which has flowed through unit area of the yz plane at x by the time the steady state has been established. This is a finite quantity which for a given porous medium and flowing gas is a function only of x. Thus

$$\Delta = \frac{\int_0^l Q_B(x)\mathrm{d}x}{l J_\infty} \tag{32}$$

The x-dependence of $Q_B(x)$ should be related to that of $C(x)$. In the case of a non-sorbed gas, or when sorption obeys Henry's Law, one might expect for Knudsen flow that

$$Q_B(x) = Q_B(0)\ (1 - x/l) \tag{33}$$

so that from Eqs. (32) and (33)

$$2\Delta .\, l J_\infty = Q_B(0) \tag{34}$$

Accordingly time-lag and steady-state flow measurements with helium at a given pressure p_0 in each of a series of membranes of the same dimensions should allow comparison [through the $Q_B(0)$] of the blind pore character.

If the flowing gas is adsorbed according to Henry's law $Q_B(0)$ is given by

$$Q_B(0) = (\epsilon_b + A_b k_s)C_o' l \tag{35}$$

where ϵ_b and A_b are a blind pore porosity and area associated with $Q_B(0)$ and k_s is the Henry's law constant given by

$$k_s = C_s'/C_g' \tag{36}$$

C_g' is the number of molecules per unit volume of gas phase ($= C_o'$ at $x = 0$) and C_s is the number of adsorbed molecules per unit area of surface. If in addition the permeability coefficient K is related to the flux through unit cross section by

$$K = \frac{J_\infty l}{C_o} \tag{37}$$

(for $C_o' < C_l'$) then Eqs. (35) and (37) with Eq. (34) give

$$2K\Delta = l^2(\epsilon_b + A_b k_s) \tag{38}$$

while for a non-sorbed gas the term in k_s may be omitted. An estimate from the flow of helium through a Carbolac carbon membrane having $\epsilon = 0{\cdot}497$ cm^3 per cm^3 gave $\epsilon_b = 0{\cdot}026$ cm^3 per cm^3.[10]

This method of examining membranes for blind porosity is being studied further for various systems where Henry's law is obeyed. It is a procedure of considerable promise since the quantities ϵ_b and A_b have hitherto been important but inaccessible properties of porous media. However, ϵ_b and A_b are not necessarily total blind porosity and area.

7. *X*-DEPENDENCE OF *D*

It was earlier pointed out (see Section 4) that in the general time-lag equations (8) and (9) the term $\int_0^\infty \int_0^l (J_\infty - J(x,t))\mathrm{d}x\ \mathrm{d}t$ is zero for D a function of C. When D is a function of x or of t, or both, this term, is not necessarily zero. Correspondingly L^a will not equal L_1^a (Eq. 30) if D depends upon x. This can interfere with the Δ procedure for evaluating a blind pore porosity, ϵ_b, and surface area, A_b. It emphasises the importance of ensuring uniformity of porosity and pore size distribution throughout the membrane. Compaction of fine particles tends to compress the regions near $x = 0$ and $x = l$ more than the central region and so could result in smaller diffusion coefficients near $x = 0$ and $x = l$ than in the middle.

Such behaviour can be expressed conveniently by writing[10]

$$D = D_0/[1 - \alpha u(1 - u)] \tag{39}$$

where $u = x/l$ and α is a coefficient which for real and finite values of D lies in the range $0 \leqslant \alpha < 4$. With this model for the behaviour of D it was established that:

(a) Δ is negative for this x-dependence of D, whereas for the time-dependence due to blind pores Δ is positive.

(b) If a compacted membrane is made by compressing a succession of small increments of the powder [the procedure we have normally adopted (see Section 2)], then the periodic variation in D with x largely damps out this influence of x-dependence upon the time-lag, L^a, and hence upon Δ.

Experimentally it was observed, for various membranes each made by a number of compactions, that positive values of Δ were usual, so that the behaviour was dominated by time-dependence of D. However, for membranes made of one compaction both positive and negative values of Δ were found among different membranes.

8. THE STRUCTURE FACTORS, κ_g AND κ_{gs}

In Eq. (26) (Section 6) the ratios D_g/D_g^{cyl} or D_{gs}/D_g^{cyl} were used to define two structure factors κ_g or $\beta\kappa_{gs}$ for a porous medium of given ϵ/A. In the reference pore, a long straight cylindrical tube having ϵ/A equal to this ratio for the porous medium, D_g^{cyl} is given for Knudsen flow by

$$D_g{}^{cyl} = \frac{8}{3}\frac{\epsilon}{A}\sqrt{\left(\frac{2RT}{\pi M}\right)} \tag{40}$$

where M is the molecular weight of the flowing gas. Thus D_g^{cyl} can be found and κ_g or $\beta\kappa_{gs}$ evaluated. Some values are given in *Table 2*. As previously noted, $\beta = (A/\epsilon)(\epsilon_s/A_s)$ where ϵ_s and A_s are porosities and surface areas associated with the steady state of flow only. Therefore even if all other influences on κ_g and $\beta\kappa_{gs}$ are identical these two structure factors are not necessarily equal. ϵ_s and A_s are related to the porosities and areas evaluated by the Kozeny-Carman method[12], which is however too inaccurate for finding β.

If bottlenecks and tortuosity dominate κ_g then it will have values less than unity. On the other hand, if there are some through channels with considerably larger ϵ/A than the average, κ_g may become greater than unity. Examples of both situations are seen in *Table 2*. Flow in Vycor porous glass is evidently much affected by bottlenecks and tortuosity while in the catalyst plugs (5) and (8) some wider through channels are important. It is also possible for κ_g to approach unity so that all geometrical factors operating together give diffusion coefficients approaching those in cylindrical straight capillaries each with ϵ/A equal to that of the porous medium [e.g. Carbolac membrane (2)]. Nevertheless the actual channel system in the medium does not correspond physically with these reference cylindrical capillaries.

9. ADSORBED LAYERS

If the surface to volume ratio of the pores in a medium is not large surface flow is often not detectable by steady-state methods.

Table 2. Structure factors[11]

(a) Vycor porous glass; $\epsilon/A = 14{\cdot}4$Å

Gas	N_2	O_2	Ar	Kr	CH_4
T,°C	19	19	19	21	21
κ_g	0·17	0·17	0·17	0·17	0·17
$\beta\kappa_{gs}$	0·18	0·18	0·18	0·18	0·18

(b) Carbolac carbon membranes

(1) $\epsilon = 0{\cdot}37$ cm^3 per cm^3; $(\epsilon/A) = 3{\cdot}0$ Å (2) $\epsilon = 0{\cdot}64$; $(\epsilon/A) = 9{\cdot}3$ Å

Gas	N_2	N_2	Ar	Ar	Kr	N_2	N_2	Ar	Ar	Kr	Kr
T°C	0	25	0	25	25	0	25	0	25	0	25
κ_g	0·78	0·77	0·77	0·77	0·77	0·88	0·92	0·88	0·92	0·88	0·91
$\beta\kappa_g$	1·46	1·47	1·46	1·47	1·46	1·81	1·84	1·81	1·84	1·81	1·83

(c) Alumina-silica cracking catalyst membranes

(1) $(\epsilon/A) = 8{\cdot}4$ Å (4) $(\epsilon/A) = 8{\cdot}4$ Å (5) $(\epsilon/A) = 12{\cdot}3$ Å (8) $(\epsilon/A) = 12{\cdot}3$Å

Gas	N_2	N_2	N_2	Ar	N_2	N_2	N_2	N_2	N_2	N_2	N_2
T°C	0	30	50	30	0	30	50	0	30	50	30
κ_g	0·49	0·49	0·49	0·49	0·55	0·55	0·55	2·07	2·08	2·06	2·09
$\beta\kappa_g$	0·47	0·47	0·47	0·47	0·47	0·47	0·47	1·84	1·84	1·84	1·84

In the Knudsen flow range the permeability coefficients (defined as in Section 6) of helium, K_{He}, and of another gas are related at constant temperature by

$$K_{\mathrm{He}} \sqrt{(M_{\mathrm{He}})} = K \sqrt{(M)} \tag{41}$$

where the M's are molecular weights. Nevertheless adsorption, by delaying some of the flowing molecules, can still have marked effects upon the time-lags. Two limiting cases of adsorption are important: firstly when Henry's law is valid; and secondly when the isotherms are rectangular in shape.

The flow equation when Henry's law is valid is

$$\frac{\partial C_s}{\partial t} + \frac{\partial C_g}{\partial t} = D_s \frac{\partial^2 C_s}{\partial x^2} + D_g \frac{\partial^2 C_g}{\partial x^2} \tag{42}$$

The Henry's law relation gives $(C_s/C_g) = (AC'_s/\epsilon C'_g) = (Ak_s/\epsilon)$, so that Eq. (42) becomes

$$\left(1 + \frac{Ak_s}{\epsilon}\right)\frac{\partial C_g}{\partial t} = \left(D_g + \frac{D_s\,.\,Ak_s}{\epsilon}\right)\frac{\partial^2 C_g}{\partial x^2} \tag{43}$$

and the time-lag is accordingly

$$L_l^a = \frac{l^2(1 + Ak_s/\epsilon)}{6\,(D_g + D_s\,Ak_s/\epsilon)} \tag{44}$$

D_g can, like K, be determined from $D^{\mathrm{He}} = (l^2/6L_l^a)$ for helium ($D_g^{\mathrm{He}}\sqrt{M_{\mathrm{He}}} = D_g\sqrt{M}$). Eq. (44) then provides a relative method of determining the adsorption areas of membranes when $D_s\,Ak_s/\epsilon D_g \ll 1$. k_s is determined separately upon a sample of the parent material from which the compact has been made. On the assumption that k_s is the same in parent material and membrane, A for the membrane can be found. In media having larger values of A the quotient $D_s\,Ak_s/\epsilon D_g$ may no longer be small compared with unity. Then if A is determined for the membrane in a separate measurement of the sorption isotherm Eq. (44) serves to determine D_s. This has been the main use so far of Eq. (44).

In another time-lag procedure for a non-sorbed gas such as helium D_g in the time-lag expression is related to $D_g{}^{cyl}$ as given by Eq. 40, by means of the structure factor, κ_g, of *Table 2.* (i.e. $D_g = \kappa_g D_g{}^{cyl}$). If k_s in Eq. 44 is zero Eq. 44 then reduces to

$$L_l^a = \frac{l^2 A}{16\kappa_g\epsilon\sqrt{(2RT/\pi M)}}$$

from which A/κ_g follows. This method gives the area only if $\kappa_g \rightarrow 1$ (*Table 2*). However, it is an advance upon the Kozeny-Carman procedure[12] because in the transient state of flow (the time-lag period) all pores, including the blind pores, are involved.

The second limiting case arises when the isotherm is rectangular in shape so that the concentration contour of adsorbed molecules at all points reached by the gaseous molecules has the form of curve 1 of *Figure 3.* The gas phase concentration decreases from $x = 0$ to $x = \xi$, at which point $C_g \sim 0$. The front $x = \xi$ moves through the membrane, and the break-through time, t, at which $\xi = l$ is given by[13,14]

$$2\,J_\infty t_1 = lC_s = lAC_s' \tag{45}$$

This relation depends only on conservation of matter and is true for viscous flow, slip flow or molecular streaming of gas. Since C_s' is the number of molecules per unit area of surface its value is known from the co-area per molecule. Accordingly A, the monolayer equivalent surface area per cm^3 of porous medium, can be determined. This is an absolute procedure, but the rectangular isotherm is approached only in a limited number of sorbate-sorbent systems (e.g. for appropriate conditions in porous crystals of zeolites, or some microporous silica gels or carbons).

Where the adsorption follows other isotherm equations it is also possible, if there is no measurable surface flow or blockage of gas flow by the adsorbed

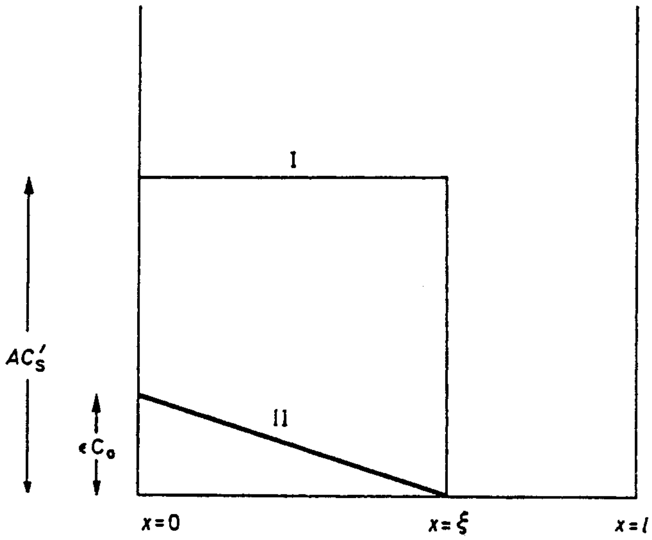

Figure 3. The distribution of adsorbed molecules (I) and of gaseous molecules (II) as functions of x in the limiting case of a rectangular sorption isotherm.

film, to calculate the time-lags. This has been done rigorously for long single capillaries[15] wherein the gas phase permeability obeys the slip flow equation (in which there is a viscous flow component). Time-lags were then obtained both in absence of adsorption and also when the isotherms associated with flow were those of Langmuir, BET, Huttig and Freundlich. The expressions are long and will not be discussed here, but that for Langmuir's isotherm in particular provides a further means of estimating surface areas.

10. SURFACE FLOWS

The reality of the extra flow associated with mobile films on high area microporous membranes can be demonstrated by plotting the quotient $K\sqrt{M}$ for constant temperature against any parameter which is related to the adsorbability of the medium (polarisability, α; energy of sorption, ΔE; Ak_s/ϵ; boiling or critical temperatures, T_B or T_C). If there is no viscous flow component in the gas phase, or surface flow, $K\sqrt{M}$ should be constant, and a straight line parallel to the abcissa would result. In the presence of surface flow the curve of $K\sqrt{M}$ rises above the limiting value for non-sorbed gases like helium. This behaviour is illustrated in *Figure 4*[16] for gas flows through a Carbolac carbon membrane showing no viscous flow component. The porosity was 0·498 cm^3 per cm^3 and the area 776 m^2 per cm^3. The correlations in *Figure 4* are very smooth, and the curves serve to evaluate surface permeability coefficients K_s, given by $K = \kappa_g + K_s$ where κ_g is obtained from the horizontal asymptote. For more strongly adsorbed gases the surface flow can easily outweigh that in the gas-phase, while for still more energetic sorption (e.g. SO_2) surface flow may exceed that in the gas phase by orders of magnitude[17].

This method of evaluating surface flow makes use of helium assumed to

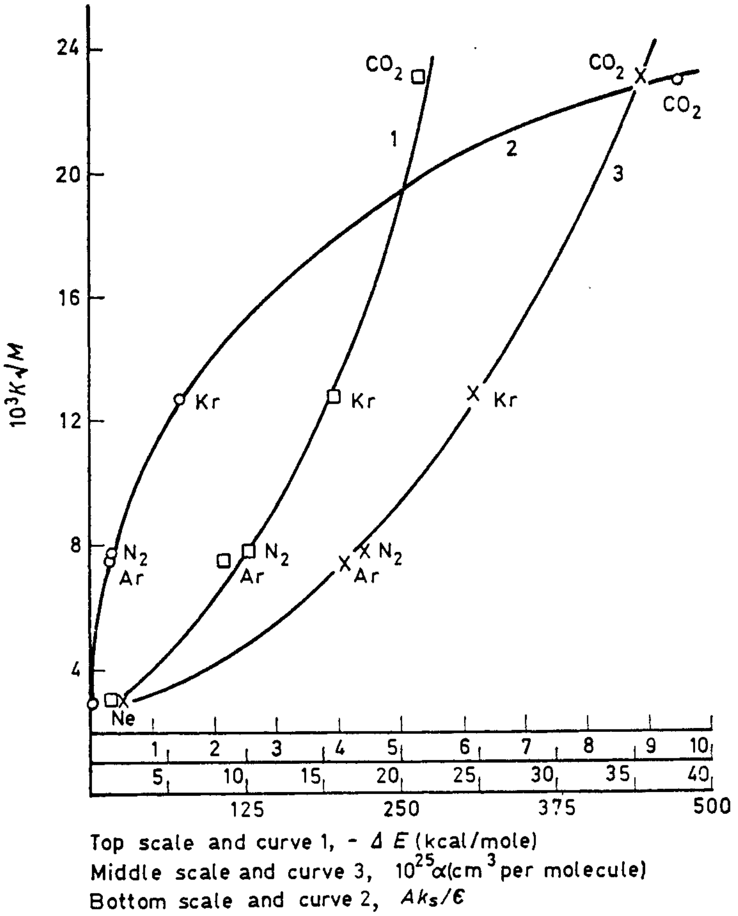

Figure 4. Correlations between $K\sqrt{M}$ at 0°C and quantities related to sorbability.

be a virtually non-sorbed calibrating gas. Per unit cross-section the relevant flows are

$$J_s = -D_{ss}\frac{dC_s}{dx}\;;\; J_g = -D_{gs}\frac{dC_g}{dx} \qquad (46)$$

The term 'surface flow' for J_s is in part a misnomer. J_s is the total flow called into play by the Gibbs surface excess present as a mobile sorbed film in a gradient of concentration. On broken surfaces such extra flows are partially in the gas phase and partially on the surface through any cross-section, since the flows have to pass from one exposed surface element to another, largely by evaporation through the gas phase[18].

The ratio J_s/J_g is then

$$J_s/J_g = \frac{D_{ss}}{D_{gs}}\frac{dC_s}{dC_g} = \frac{D_{ss}}{D_{gs}}\cdot\frac{A\sigma}{\epsilon} \qquad (47)$$

where $\sigma = \mathrm{d}C'_s/\mathrm{d}C'_g$ is the slope of the isotherm. When J_s and J_g are measured by the helium method one value of each is found for the membrane so that J_s/J_g is necessarily a constant and independent of x. At the outgoing face p is small and so is C_s. D_{ss} and D_{gs} tend to their constant limiting values, $D^0{}_{ss}$ and $D^0{}_{gs}$; while $\sigma \rightarrow k_s$, the Henry's law constant. Thus

$$\frac{J_s}{J_g} = \frac{D_{ss}A\sigma}{D_{gs}\epsilon} = \frac{D^0{}_{ss}}{D^0{}_{gs}}\frac{Ak_s}{\epsilon} = \text{constant} \tag{48}$$

so that finally

$$\frac{D_{ss}\sigma}{D_{gs}} = \frac{D^0{}_{ss}\,ks}{D^0{}_{gs}} = \text{constant} \tag{49}$$

In absence of a viscous flow component $D_{gs} = D^0_{gs}$ and so D_{ss} varies as $1/\sigma$. This interesting theorem has been examined and found to be correct for several experimental isotherms, as shown in *Figure 5*[3]. The SO_2 isotherm of *Figure 5a* is approximately of Freundlich type over the range for which D_{ss} and $1/\sigma$ are plotted. The argon isotherm of *Figure 5b* is of Type II in Brunauer's classification, and that of sulphur hexafluoride in *Figure 5c* is of Type V. Every isotherm type will show its own characteristic variation of D_{ss} (or D_{ss}/D_{gs}) with amount sorbed, predictable from Eq. (49).

The effectiveness of the surface in a microporous membrane in generating surface flow depends on the following factors[3]:

(a) The nature of the surface (roughness, continuity).
(b) Porosity (including blind pores).
(c) The nature of the gas.
(d) Temperature and pressure: and hence from (c) and (d)
(e) The extent of adsorption and the form of the isotherm.

Values of D_{ss} and of K_s/A are given in *Table 3* as alternative measures of the ability of surfaces to generate surface flows. The surfaces especially in the cracking catalyst but also to a degree in the Carbolac carbon membranes were of broken texture, and are seen from D_{ss} or K_s/A to be less efficient area for area in producing surface flow than are graphitised carbons such as Black Pearls and Graphon. These considerations are of much interest for membrane separations which depend upon surface flow. but will not be

Table 3. Values of D_{ss} and K_s/A for various surfaces[3]

Substance	A(m²/cm³) †	ε(cm³/cm³)	T(°K)	$10^5 D_{ss}$ (cm² sec⁻¹)	$10^{11} K_s/A$ (cm³ sec⁻¹)
Cracking catalyst	476	0·40	303	17	3·3
Carbolac carbon	1036	0·48	308	12·2	4·9
Carbolac carbon	776	0·50	273	10·9	9·9
Carbolac carbon	1233	0·37	298	16	9·3
Carbolac carbon	688	0·64	298	54	30
Carbolac carbon	392	0·50	273	132	54
Black Pearls	197	0·43	303	528	147
Graphon	90	0·42	303	990	344

†Values of A were measured by adsorption.

discussed further in this paper.

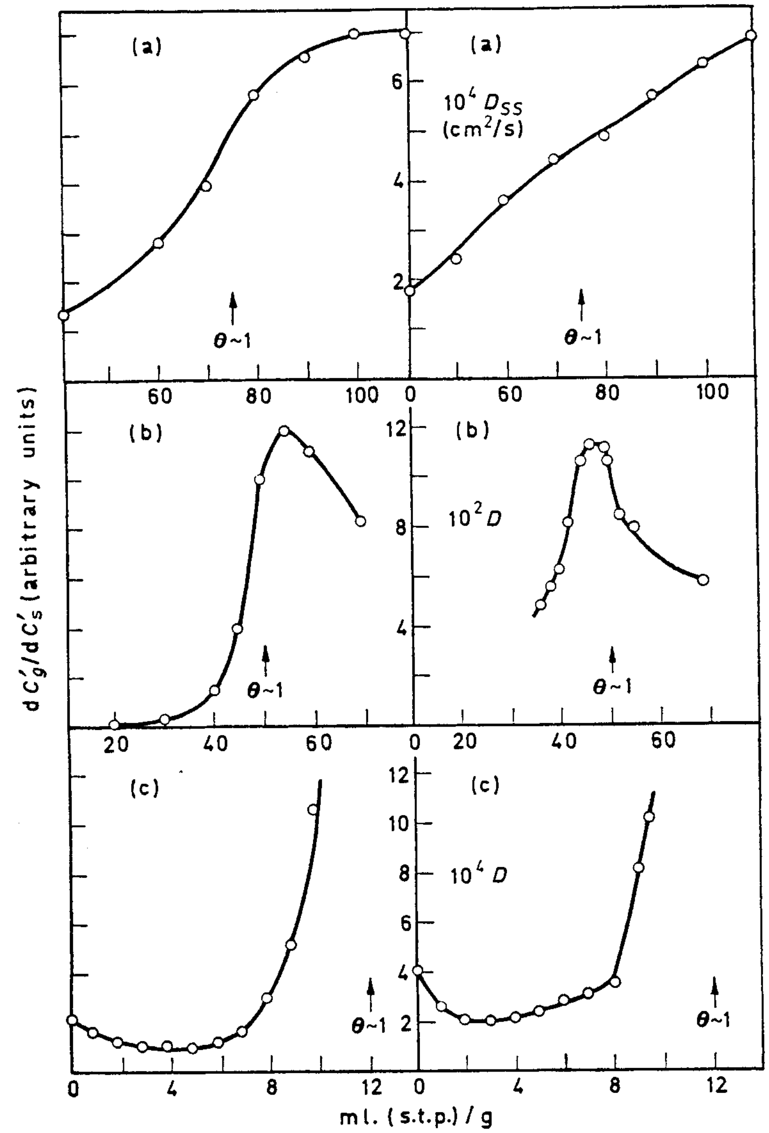

Figure 5. Comparison of the variation with coverage of $1/\sigma$ and either D_{ss} or overall diffusion coefficient D. (*a*) SO_2/Carbolac at −10·1°C. (*b*) Ar/Black Pearls at −183°C. (*c*) SF_6/Graphon at −50°C.

11. CONCLUSION

The aspects of flow in porous media which have been described tend, as shown in this paper, to be correlated, and may often be involved in evaluating the degree of approximation in flow methods of determining surface areas. An integrated treatment of the interpretation of the membrane experiment of Section 2 has therefore been presented, much of which may be relatively new and unfamiliar to those who have considered flow only in terms of the Kozeny-Carman procedure. Accordingly the several methods of using flow to evaluate surface areas are selected from the text for summarising mention:

1. The Kozeny-Carman steady state method. This does not take into account areas and porosities associated with cracks, crevices or blind pores. It has often been discussed before[12] and since it is not suitable for measuring total surface areas and porosities it has not been considered here.

2. Time-lag procedures. A time-lag procedure is described in Section 9, appropriate for immobile, dilute adsorbed films obeying Henry's law. This method is able to give the true adsorption area, but requires one to measure the Henry's law constant separately on a reference sample of the membrane forming particles. The result is also influenced to some extent by blind pore character. A second time-lag procedure for a non-sorbed gas is also referred to in Section 9. The required diffusion constant is related to the value for a single straight capillary times a structure factor. Although giving results nearer to the total area than the Kozeny-Carman procedure the structure factor may be greater or less than unity (*Table 2*) and introduces an uncertainty.

3. The breakthrough time method. This method can be used for gases and vapours which give very rectangular isotherms. It is an absolute method giving total areas and is independent of the presence of blind pores. Its basis is also described in Section 9.

4. Combined steady state flow and time-lag method. For a series of pressures of gas at the ingoing surface of the membrane one may measure the steady state flow and the adsorption and desorption time-lags at the outgoing surface (defined as in Section 4). From these measurements, needed to characterise the flow properties of the membrane, one may, without any additional information, obtain the complete adsorption isotherm for the membrane *in situ*, from which an adsorption area can be obtained using a BET plot. The basis of this method is developed in Section 5.

5. The Δ-method for a blind porosity and area. Time-lag theory for systems containing blind pores leads to a correction, Δ, to the time-lag, arising from blind pore character (Section 6). From this a blind pore volume and area may be derived, which however may not be the total volume and area of blind pores. Variations of porosity and surface area with distance through the membrane may arise from non-uniform compaction during preparation of the membrane. This can also influence the Δ correction (Section 7).

No prior use appears to have been made of methods (3) and (4) for measurements of surface area and very little use of methods (2). The study of blind porosity by method (5) is also very new.

Acknowledgement

I wish to thank Mr R. Ash of this Department for helpful comments.

References

[1] R. M. Barrer. In *The Gas Solid Interface*, Vol. 2 Chapter 19, p. 557 (Editor A. Flood) Dekker, New York, 1967.

[2] D. M. Grove. In *Porous Carbon Solids*, p. 155 (Editor R. L. Bond) Academic Press, New York, 1967.

[3] R. Ash, R. W. Baker and R. M. Barrer. *Proc. Roy. Soc.* **A**, **299**, 434 (1967).

[4] H. L. Frisch. *J. Phys. Chem.*, **61**, 93 (1957).

[5] H. L. Frisch. *J. Phys. Chem.*, **62**, 401 (1958).

[6] H. L. Frisch. *J. Phys. Chem.*, **63**, 1249 (1959).

[7] J. H. Petropoulos and P. P. Roussis. *J. Chem. Phys.*, **47**, 1491 and 1496 (1967).

[8] J. H. Petropoulos and P. P. Roussis. *J. Chem. Phys.*, **48**, 4619 (1968).

[9] R. Ash and R. M. Barrer, in preparation.

[10] R. Ash, R. W. Baker and R. M. Barrer. *Proc. Roy. Soc.* **A**, **304**, 407 (1968).

[11] R. M. Barrer and T. Gabor. *Proc. Roy. Soc.* A, **251**, 353 (1959).

[12] P. C. Carman. *The Flow of Gases through porous Media.*, Chapter IV, Butterworths, London, 1956.

[13] R. M. Barrer. *Brit. J. App. Phys., Suppl. No. 3*, 41 (1954).

[14] R. M. Barrer. *App. Mat. Res.* **2**, 129 (1963).

[15] R. Ash, R. M. Barrer and D. Nicholson. *Zeit. f. Phys. Chem.*, *Neue Folge*, **37**, 18 (1963).

[16] L. A. G. Aylmore and R. M. Barrer. *Proc. Roy. Soc.* **A**, **290**, 477 (1966).

[17] R. Ash, R. M. Barrer and C. G. Pope. *Proc. Roy. Soc.* **A**, **271**, 1 and 19 (1963).

[18] R. M. Barrer and T. Gabor. *Proc. Roy. Soc.* **A**, **256**, 267 (1960).

DISCUSSION

Dr J. H. Petropulos (*Democritos Nuclear Research Centre*, *Athens*) said: It is difficult to add something when Professor Barrer has finished dealing with a subject. Nevertheless, I would like to call attention to some additional results relevant to Sections 6 and 7 of his paper. There, attention is drawn to the possibility of obtaining a measure of the porosity and surface area pertaining to blind pores in a porous powder compact through the discrepancy (Δ in equation 30) between the time lag (L_l^a) calculated from equation (12a) and that actually observed. This discrepancy is considered to be the result of time dependence of the diffusion coefficient (D) due to the presence of blind pores. It is known that such discrepancies can also arise as a result of non-homogeneous packing of powder during compaction. During compression of the powder in a cylindrical mould fitted with two moveable plungers, higher compaction can be reasonably expected near the ends of the compact than in the middle. The diffusion coefficient will tend to increase in the same sense as the porosity, i.e., from the ends of the membrane to the mid-plane in a more or less symmetrical manner.

As Professor Barrer points out, in agreement with our own results (J. H. Petropoulos and P. P. Roussis, Internal Report CHEM 3/1, Democritos Nuclear Research Centre, Athens, Greece, June 1965), this variation of D with x yields a negative value of Δ. On the other hand, Professor Barrer's treatment of the effect of blind pores leads to $\Delta > 0$, the two effects being thus distinguishable.

Nevertheless, in a complete treatment of membrane heterogeneity, one should also take into account the x dependence of the solubility coefficient [J. H. Petropoulos and P. P. Roussis. *J. Chem. Phys.* **47**, 1496 (1967)] given by

$$S = \epsilon + Ak_s;$$

where, if we confine ourselves for convenience to the Henry law region of adsorption, k_s is simply the Henry law constant. In a membrane of the type discussed above, S for a reasonably strongly adsorbed gas should be higher near the ends of the compact than near the mid-plane [J. H. Petropoulos and P. P. Roussis. *J. Chem. Phys.* **48**, 4619 (1968)]. Then the effect of the x dependence of S on Δ counteracts that of D, the sign of Δ being, in fact, determined by the x dependence of the quantity S^2D. Hence, non-homogeneity in the x direction can give rise to $\Delta > 0$, in the case of a relatively strongly adsorbed gas. Pronounced departure from symmetry can have a similar effect irrespective of the adsorbability of the gas.

It has been shown [*J. Chem. Phys.* **47**, 1496 (1967)] that the effects of time dependence and x dependence of S and D on appropriate time-lag quantities can be distinguished, so that the presence of each of these types of 'non-Fickian anomaly' can be detected independently of the presence of the other. It, therefore, appears that time-lag analysis on these lines would be required, before application of Professor Barrer's treatment is attempted in practice.

Professor R. M. Barrer replied: Flow methods of studying pore systems, both for steady state and time lag measurements, are at their best when the compact is made by a number of successive additions and compressions of fine powder, as indicated in my paper. Under these circumstances any heterogeneity varies periodically through the medium and then the effect of x-dependence of D on Δ is almost damped out, as indicated in the paper. It would be expected also (although this has not yet been proved) that the influence on Δ of periodic x-dependence of $S = (\epsilon + Ak_s)$ would likewise be largely damped out. These are the circumstances under which, as made clear in the paper, the Δ-procedure may be helpful, not in membranes made by a single compaction such as that referred to by Dr Petropoulos.

Dr Ione (*Institute of Catalysis, Novosibirsk, U.S.S.R.*) said: We think that the technique of the time-lag method for diffusion coefficient determinations if applied to pressed porous membranes has some limitations. If such a membrane is obtained by pressing porous particles a non-uniform porous system is formed with a bidispersed porous structure; i.e. with micropores within the particles and macropores between the particles—their dimensions may differ by as much as two or three orders of magnitude.

Under the usual time-lag boundary conditions a pressure drop of gases along the plug exists which results in a viscous flow component. The latter is proportional to r^4_{macro} where r_{macro} is equal to the macropore radius. Hence in this case we are dealing with the process which is not purely diffusion controlled. Therefore application of a purely diffusion approach is not correct.

In the Institute of Catalysis of the U.S.S.R., C. A. Czachev and K. G. Ione have applied a method in which the time-lag values were found from the unsteady state part of the counter-diffusion technique. Under these conditions, the pressure drop along the plug and the viscous flow in the macropores were absent. Such a modified time-lag method permitted the more rigorous determination of diffusion coefficients and of surface area of catalysts in transient as well as under steady state conditions for bidispersed non-uniformed porous plugs from time-lag approaches.

Professor R. M. Barrer replied: The time-lag equations (see Section 3 and *Table 1* of my paper) are derivable on the basis only of the steady state flux and of conservation of matter (E. 7). It is not relevant in deriving them what is the mechanism of flow (turbulent, viscous, slip, Knudsen and surface flows and combinations of these are all possible). If an interpretation is attempted in terms of diffusional flow when diffusional flow is not occurring then naturally errors of interpretation will occur. Interpretation in terms of diffusional flow is given in the paper only under conditions where this is the mechanism. The proper use of the time-lag equations under any flow conditions is indicated in Sections 4 and 5.

Further, by definition the steady state is not achieved until every pore, blind or otherwise, has received its steady state quota of sorbed or gaseous molecules. Thus for a sorbable gas the time-lag is influenced by the entirety of pores and pore surfaces, whereas the steady state is not affected by blind pores. This makes the study of the time-lag particularly interesting.

Dr O. Kadlec (*Czechoslovak Academy of Sciences*) said: Our results of the study of the surface diffusion show a considerable difference in the values of the diffusion coefficients of benzene diffusion on a non-porous surface and on a surface of micropores of carbonaceous substances. The coefficients of surface diffusion of benzene on the surface of micropores of activated carbon and on carbonaceous molecular sieves are considerably lower than the coefficients of diffusion of benzene on the surface of non-porous black. According to our opinion, this difference in the diffusion coefficients is connected with the values of entropy of the adsorbed benzene on microporous and non-porous substances. As Professor Dubinin has shown, there is a considerable difference in the adsorption processes taking place on non-porous and microporous substances. This difference also shows in the different properties of the adsorbate in the course of adsorption on a flat surface and in micropores. The dependence of entropy of adsorbed benzene on the adsorbed volume and temperature, calculated from the measurements of adsorption equilibrium of benzene on activated carbons and graphitized carbon black, observed in the range from 20 to 350°C in our laboratory by Dr Zukal and shown in *Figure A*, indicates that the entropy of benzene in micropores of activated carbon is lower than the entropy of liquid benzene (standard state—liquid) over the whole adsorption range, in contrast to benzene adsorbed on the surface of graphitized carbon black, the entropy of which is higher than the entropy of the fluid. The increase in the entropy of benzene in the course of adsorption on graphitized carbon black in comparison to the liquid is among others the reason for the invalidity of the postulate of the potential theory of adsorption [B. F. Bering and V. V. Serpinskii. *Dokl. Akad. Nauk. SSSR* **148**, 1331 (1963)] for this system. The causes of this difference in entropies of the adsorbate are probably connected with the different mobility of the adsorbate on the surface, which in the case of micropores is hindered by their walls. The same effect also causes the said differences in diffusion coefficients on the surface of non-porous and microporous substances. The decrease in the values of the diffusion coefficient of benzene in the micropores which is connected with the considerable decrease of entropy in the course of adsorption on microporous activated carbons, can be the reason why the process of adsorption kinetics of ben-

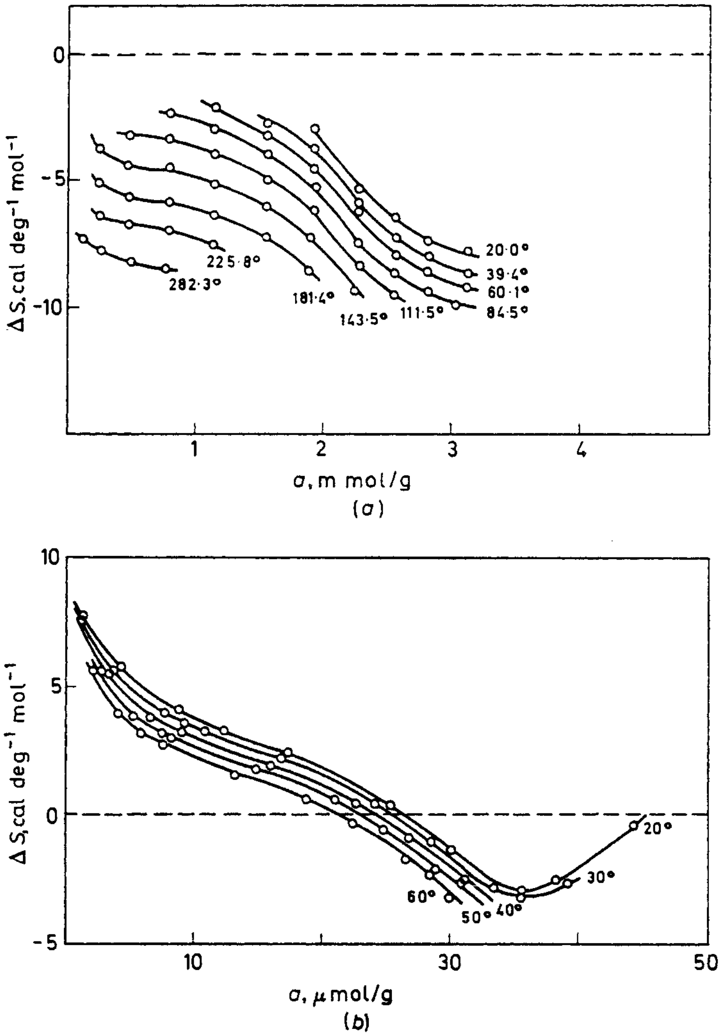

Figure A. Benzene adsorption entropy versus adsorbed volume [*a*, on microporous activated carbon at 20–282·3°C; *b*, on graphitized carbon black at 20–80°C].

zene (in vacuum) is controlled by diffusion through a system of micropores in case of activated carbon with a complicated structure of transitional and macropores.

EFFECTS OF ADSORPTION DYNAMICS ON SURFACE AREA DETERMINATION

Silviu Tilenschi

University of Bucharest, Bucharest, Rumania

In some earlier communications I have shown the striking difference which can sometimes be found between the desorption and the adsorption branches of vapours on porous adsorbents, in the domain of hysteresis, especially at lower pressures. In *Figure 1*, one can observe particularly the striking discontinuities of the desorption branch of an adsorption isotherm (N$_2$ on silica gel), over the range of 1 to 40 mm. We have therefore assumed that adsorption equilibrium cannot always be reached under the conditions ordinarily prevailing in adsorption measurements. It is well known incidentally that comparatively little work has been devoted to kinetic studies of adsorption.

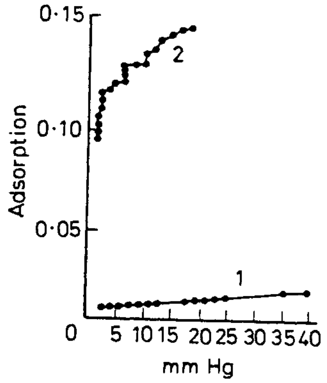

Figure 1. Adsorption of nitrogen on silica gel at 77°K (*1*, adsorption; *2*, desorption)

For the purpose of such a study we have constructed an adsorption beam microbalance using a gas flow meter and a photoelectric recorder as shown schematically in *Figure 2* (*a*, *b*).

In *Figure 3* (*a*, *b*, *c*, *d*) is shown the adsorption rise on N$_2$ admission at fairly constant flow rates, on four different adsorbents. Each adsorption time written on *Figure 3* relates to a given adsorption rate and pressure.

Figure 4 (*a*, *b*, *c*, *d*) shows the adsorption isotherm corresponding to the curves given in *Figure 3*, the relative pressures being recorded at the same time as the gas is admitted. From *Figure 4* it is clear that an adsorption isotherm must, according to its classical definition, be an assembly of equilibrium points reached after a given adsorption time; our curves in *Figure 4* were determined at different times.

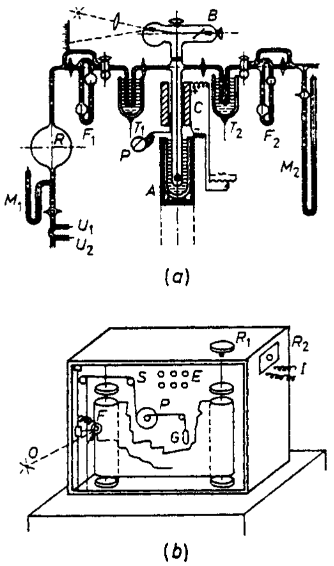

Figure 2. (*a*) The adsorption apparatus; (*b*) Recorder

However, it can be noted that: (i) most of the curves in *Figures 3* and *4* were obtained in periods of time longer than those normally used to determine an adsorption isotherm by static methods (from 6 to 24 hours), and (ii) in spite of the fact that the recorded isotherms differ, even in their BET-type, the final saturation values of adsorption (*Figure 3*) remain unchanged with time. We also find that the surface area determined by means of such curves is comparable, and sometimes even greater than that determined by the usual static methods.

Table 1. Effects of adsorption dynamics on the surface area determination

Adsorbent	*Surface area* (m^2/g)†	
	static	*dynamic*‡
Alumina (active)	500	525
Silica gel (E. Hickel)	500	700
Alumina-Silica gel	500	650
Zeolite-Ca A	—	—
Bentonite I	100	140
Bentonite II	100	140

† $a_{N_2} = 16{\cdot}2$ Å^2; $\theta = 0{\cdot}05$–$0{\cdot}3$
‡ or static by more points

Table 1 shows the agreement between the static (BET) method and our dynamic one. Most of the areas obtained by the latter method are larger. Such differences, between the areas of the same adsorbents determined by the same method, but by different authors are well known in the literature.

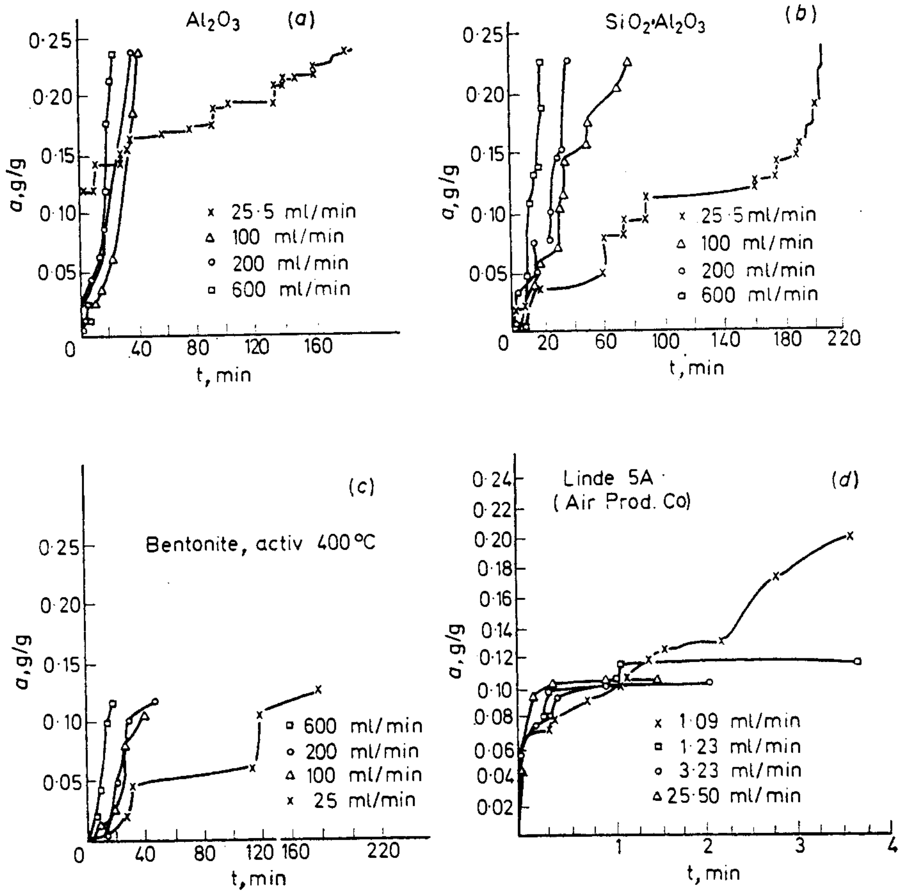

Figure 3. Variation of adsorption with time at different admission rates of nitrogen (77 °K). (*a*) alumina (*b*) alumina-silica (*c*) bentonite (*d*) molecular sieve linde 5A

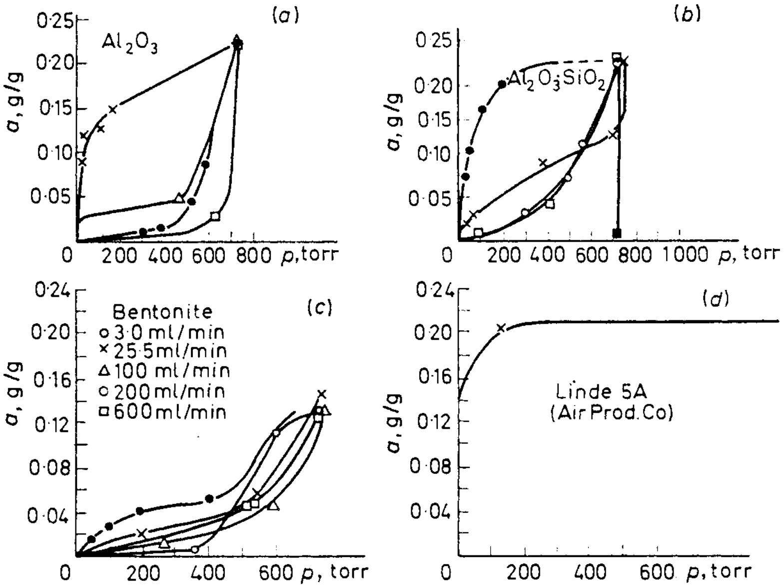

Figure 4. Adsorption isotherm dependence on the nitrogen admission rate. (*a*) alumina (*b*) alumina-silica (*c*) silica gel static (*d*) silica gel dynamic

Figure 5 gives curves of the surface areas of different silica gels, obtained at different pH-values between 2 and 12. The left-hand side of the curve, which begins with the unusual value for the silica gel of 850 m^2/g, agrees with a similar curve obtained by de Boer and Okkerse in 1960; the other side

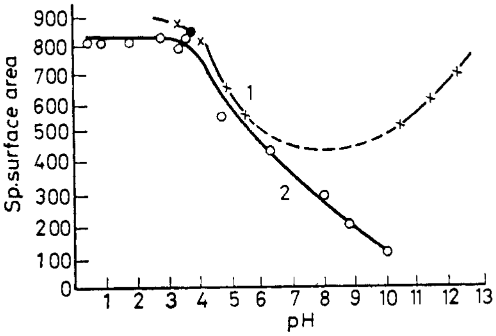

Figure 5. Variation of the specific surface area of silica gels as a function of pH

of the same curve was obtained by us, by preparing the respective alkaline-silica gels using a different procedure. A reason for the increased values of the surface area obtained by our method might be that shown in *Figure 6*—which shows several adsorption isotherms on the same adsorbent, but determined with a different point spacing. As shown in *Figure 6* the respective isotherms are as much different from one another as the curves of *Figure 4*.

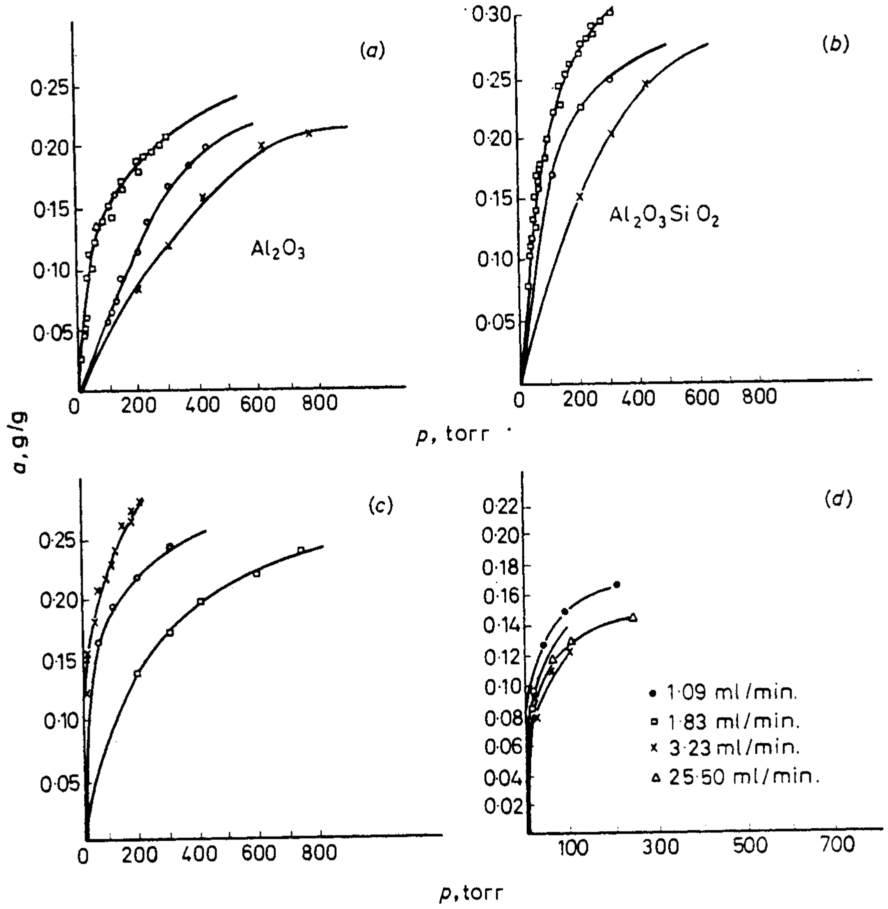

Figure 6. Adsorption isotherm dependence on point spacing as determined experimentally. *a*) alumina (*b*) alumina-silica (*c*) silica gel static (*d*) silica gel dynamic

Nevertheless the conditions for adsorption equilibrium had been carefully observed according to the classical definition. Cimino, Molinari and coworkers[3] showed previously the striking effects of gas admission at rising pressure. However, their experiments were on chemisorption on semiconductors, and carried out under different experimental conditions, *i.e.* at variable and uncontrolled flow rates and without automatic recording. Golay[3] also reported earlier that chromatographic adsorption on capillary columns, increased tenfold when compared to that on ordinary, large adsorbent columns.

It is possible to demonstrate on the basis of the general laws of adsorption equilibrium that adsorption at low admission rates increases as the adsorbent amounts put in contact with the adsorbate become smaller.

The quantitative effects on the adsorption equilibrium are rather plausible and necessary, the reasons for such effects undoubtedly being the dynamic factors of adsorption. Further developments of the method we have outlined, could show these reasons in greater detail.

References

[1] S. Tilenschi. 'Die Unstetigkeiten der Adsorptions isothermen von Gasen und Dampfen'. Private communication, University of Moscow, 1966 (Chairman Prof. A. V. Kiselev).

[2] A. Cimino, E. Molinari, C. Borgianni and E. Pepe. *J. Phys. Chem.* **67**, 2238 (1963).

[3] M. J. E. Golay. In *Gas Chromatography* (Eds: Coates, Noebelsa and Ferguson) p. 1, New York, 1958.

[4] C. Okkerse and J. H. de Boer. *J. chim. phys.* **57**, 534 (1960).

Note: If, instead of taking the whole quantity of the adsorbent and equilibrating this with a constant volume of a given adsorbate at a given initial pressure, one takes successively two separate fractions of it, the adsorption on the first fraction, expressed as a percentage, will be greater than that on the whole quantity. This occurs because with the smaller quantity of solid a smaller absolute amount of gas is adsorbed and a higher equilibrium pressure (p) is observed.

On addition of the second fraction of adsorbent, a further volume of gas will be adsorbed. If the gas adsorbed by the first fraction is not desorbed reversibly during this process, the total quantity of gas adsorbed will be greater than that adsorbed when the whole sample of solid is placed in contact with the gas at the same time.

DETERMINATION OF SURFACE AREAS OF CLAYS—EVALUATION OF METHODS

H. VAN OLPHEN

National Academy of Sciences, Washington D.C., U.S.A.

INTRODUCTION

The evaluation of the merits and limitations of methods for determining surface areas, sizes and shapes of particles in the colloidal size range requires the availability of reference colloidal materials of known surface area, surface composition, and particle size. For example, suspensions and powders of monodisperse spherical latex and silica particles have been used for this purpose. To extend the scope of reference systems, dispersions and powders of selected well-defined plate-like clay particles may well be considered. Their potential suitability as reference systems relates to the following unique features: (i) the particle surface is flat on an atomic scale, its area per unit weight is large, and the structure of the surface is known; surface areas can be derived from combined crystallographic and chemical data to serve as a reference for the evaluation of adsorption methods of surface area determination; (ii) the charge density of the particle surfaces can be determined and the ion species on the surface may be varied, hence, the effects of these variables on the results of area determination methods can be studied; (iii) usually, good electron micrographs can be obtained to serve as a reference for the evaluation of indirect methods for determining particle size and shape.

Only surface area determination methods will be discussed, although some occasional notes on particle size determination are included.

DETERMINATION OF SURFACE AREAS

Principles

Non-expanding clays. For non-expanding clays the particle area is the sum of the areas of the two exterior faces of the plates, and the edge area. Often, the edge surface area is small compared with the face area and may be neglected in the interpretation of the data. However, it is recommended that the fractional contribution to the total area by the edges be estimated from electron micrographs in each individual case.

For relatively thick kaolinite particles, the edge area estimated from indirectly determined axes ratios often amounts to as much as 20–35 per cent of the total area. However, Martin[28] pointed out that total surface area derived from particle geometry for a given carefully sized kaolinite appeared to be much less than that derived from adsorption methods, and he attributed this discrepancy to the existence of serrations at the particle edges as can be shown by electron micrographs. Due to this surface roughness of the edges the total face area is underestimated, and the fractional contribution of the edge area is overestimated.

The total area of a non-expanding clay may be determined by means of physical adsorption methods using either non-polar (e.g. nitrogen) or polar (e.g. water) compounds. It will be shown in the next section that considerable variations in the cross sectional areas for water molecules are derived using the nitrogen area of the clays as the reference area. Possible variations of the cross-sectional area for nitrogen molecules then are, of course, included in the derived water data.

Expanding clays. For expanding clays both the exterior and the interlayer areas must be considered. Since only polar molecules can penetrate between the unit layers, the exterior surface area can be determined separately by the adsorption of non-polar molecules. The total exterior and interlayer area combined is determined when using polar molecules as the adsorbate. Alternatively, however, this total area can also be computed from the unit cell dimensions and the unit cell weight. Hence, expanding clays offer the possibility of determining cross-sectional areas for water which are independent of adsorption methods with other molecules. Data for the cross-sectional area of water based on the crystallographic reference area again show considerable variation. The reasons for these variations will be discussed.

It may be noted that the average number of unit layers per particle, and hence the average thickness of the particles can be computed from the ratio of the nitrogen area and the water area, or preferably, from the ratio of nitrogen area and the total crystallographic area.

Area determination from vapour phase adsorption isotherms—Apparent molecular cross sectional areas for water

Most vapour phase adsorption isotherms for clays have a sigmoidal shape and may be classified as type II isotherms according to Brunauer's classification. In rare cases, Langmuir type isotherms are observed as will be discussed later. In the reviewed papers surface areas were routinely determined from BET plots applying the two-parameter BET equation.

Non-expanding clays: comparison of nitrogen and water areas—Keenan, Mooney, and Wood[23] determined nitrogen and water areas for a kaolinite, varying the species of exchange ion. The surface area per gram was varied by using both an ungraded sample ('N') and a small particle size fraction ('F') of the same mineral. The surface charge density of the F material was about 25 per cent lower than that of the N sample. The results are shown in *Table 1*.

The nitrogen areas within each series are nearly constant, although the authors claim that the slight increase in area with increasing ion size is outside the experimental error. The water areas, on the other hand vary considerably as shown by the computed apparent cross sectional areas for water based on the nitrogen areas as reference. In general, these areas increase with increasing ion size (with lithium ion taking an exceptional position) from 7·9 to 16·5 Å^2 for the N series, and from 10·2 to 16·5 Å^2 in the F series. For comparison we note that an area of 10·8 Å^2 frequently has been recommended for use in area calculations from water vapour isotherms. The number of cations per unit area also affects the results: the

Table 1. Nitrogen and water areas of a kaolinite in various ion forms†

Ion form	*Nitrogen* BET *area* (m^2/g‡)		*Water monolayer coverage* (mg/g)		*Apparent area per molecule water* (Å^2)	
	N	F	N	F	N	F
H	18·0	26·1	5·68	7·60	9·5	10·3
Li	18·0	26·3	3·27	4·77	16·5	16·5
Na	18·6	27·8	5·20	6·10	10·7	13·6
K	18·9	28·9	4·54	6·03	12·5	14·3
Rb	18·3	28·7	4·32	5·88	12·7	14·6
Cs	19·5	30·2	4·37	5·67	13·4	15·9
Ca	17·6	27·6	6·69	8·06	7·9	10·2
Sr	18·8	28·5	5·24	6·42	10·8	13·3
Ba	18·9	29·3	5·00	6·32	11·3	13·8

† Data from Keenan, Mooney, and Wood[23].
‡ Based on a nitrogen cross sectional area of 16·2 Å^2.
Note: Peerless No. 2 grade kaolin, Vanderbilt Co., mined near Bath, S.C., N: ungraded sample, F: fraction below 0·5 μ equivalent diameter. Exchange capacity N: 3·88 meq/100 g and F: 4·40 meq/100 g. Area occupied per monovalent ion for the N sample: 79 Å^2, and for the F fraction: 106 Å^2.

F fractions which have the lower charge density show consistently lower surface coverages (i.e. higher cross sectional areas for water) than the N samples. The area covered by a monovalent cation for the N and F samples are respectively 79 Å^2 and 106 Å^2. Hence, at monolayer coverage the data show that the number of water molecules per monovalent cation varies between about 5 and 10 for all samples, and per divalent cation between about 14 and 20. These figures are given for a rough orientation only, they may actually be somewhat smaller if the edge area were taken into account, since no exchange cations would be situated on the edge surfaces whereas nitrogen would cover the entire surface.

Expanding clays: comparison of nitrogen-, water-, and crystallographic areas—Mooney, Keenan, and Wood[30] prepared a number of ion forms of a Wyoming bentonite clay and measured both nitrogen and water adsorption isotherms. The results of this work are summarized in *Table 2*. In addition the Table includes total unit layer areas S calculated from

$$S = 2abN(1/w) \times 10^{-20}\ \mathrm{m^2/g}$$

in which a and b are the dimensions of the unit cell area in Å, w is the unit cell 'molecular' weight, and N is Avogadro's number.

From the ratio of nitrogen area and crystallographic area the average number of unit layers per particle is computed and listed in the table. These numbers vary between 6·3 and 18·6. These data apply to the dry clay powder. In suspension, the average degree of layer stacking in this clay is usually much smaller.

The apparent cross sectional areas for water listed in the table have been calculated using the crystallographic area as the reference area. Since the water molecules in the monolayer between the unit layers share opposite surfaces, the reference area is equal to half the crystallographic area. However, a small correction should be applied for external area which amounts to adding half the nitrogen area, therefore, the data still depend to a small extent on the nitrogen area data. Edge area certainly can be

Table 2. Nitrogen, water, and crystallographic areas of a bentonite in various ion forms†

Ion form	*Crystallographic area* (m²/g)	*Nitrogen* BET *area* (m²/g)	*Layers per particle*	H_2O *monolayer coverage* (mg/g)	*Apparent area* H_2O *molecule* (Å²)
H	767·2	44·7	17·2	100	12·2
Li	762·9	41·0	18·6	80	15·1
Na	751·8			§	
K	740·9	48·5	15·3	§	
Rb	711·3	64·2	11·1	57	20·3
Cs	675·7	108	6·3	62	16·3
Mg	759·2			120	10·0‡
Ca	753·5			120	10·0‡
Sr	737·8			90	13·0‡
Ba	721·7	42·4	17·0	90	12·7

† Data from Mooney, Keenan, and Wood[30].

‡ Estimated, assuming same nitrogen area as Ba-clay.

Note: Wyoming Bentonite: Volclay, SPV grade, 200 mesh, American Colloid Co. Exchange capacity 83 meq/100 g. Area occupied per monovalent ion: 160 Å² (or 80 Å² of cross sectional interlayer area).

§ No straight BET plot obtained.

neglected since the thickness of each unit layer (10 Å) is very small compared with the unit layer diameter.

Again, a considerable variation in cross-sectional area for water is observed with the variation of exchange ion species, ranging from about 10 to 20 Å². In the monolayer, the number of water molecules per ion varies from 4 to 6·5 for monovalent, and from 12 to 16 for divalent ions.

With regard to the determination of nitrogen areas of expanding clays, the effect of the presence of any residual water in the samples has been studied by Teichner[42], by Escard[10], and by Brooks[5]. In general the elimination of residual adsorbed water increases the accessibility of external surface areas for nitrogen, and a maximum is reached for the nitrogen area when the water is removed completely. Further dehydration, especially at elevated temperatures, causes removal of lattice hydroxyl water, and the consequent destruction of the lattice is accompanied by a decrease of the nitrogen area. This behaviour is observed for both illite and bentonite. For kaolinite, the nitrogen area appeared to be practically constant at water contents up to 8 per cent. Brooks observed that for calcium bentonite in a certain narrow range of water contents, the hydrated calcium ions keep the partially hydrated unit layers at such a distance that nitrogen molecules are able to penetrate into the interlayer space. Hence, in this range the nitrogen area shows a maximum.

In water vapour adsorption isotherms for expanding clays usually a significant amount of hysteresis between adsorption and desorption isotherms occurs. If the hysteresis loop does not close at monolayer coverage and below, different area values are derived from the adsorption and desorption isotherm. Since in general, the desorption isotherm more closely represents equilibrium, the calculation of areas from the desorption isotherms is preferred. The data in *Table 2* are actually obtained from the desorption branch.

During degassing of expanding clays prior to determining the water vapour adsorption isotherm, part of the unit layers may become unable to expand, they 'collapse'. This phenomenon is well known for potassium bentonites. Actually, determination of the water area can be used to monitor the degree of collapse as a function of degassing (or heating) history (H. van Olphen[46]).

Discussion of adsorption data for non-expanding and expanding clays—The results for the cross sectional area of water obtained for expanding clays using the crystallographic area as reference area confirm those for non-expanding clays using the nitrogen area as the reference area. The data show that 'BET areas' derived from water vapour sorption isotherms, applying the recommended cross-sectional area of 10·8 Å^2 for the water molecule in the monolayer may be off by as much as 50 to 100 per cent in extreme cases.

If surface charge density and ion species were indeed the variables determining the packing of the water molecules in the monolayer, one could in principle establish a set of cross-sectional areas as a function of these two variables. Unfortunately, no systematic data of sufficient reliability are available. The quoted data from one of the rare specimens of systematic work in this area do not yield consistent correlations between area and ion species for the two clays studied. This lack of consistency may well be due to the method of preparation of the different ion forms of the clays. Starting from the natural clay, first the hydrogen clay was prepared which was subsequently neutralized with a variety of metal hydroxides. At the time it was not known that in the hydrogen clay a substantial part of the exchange positions becomes occupied by Al ions, and these may not be completely replaced in the neutralization process. In later work by Orchiston[32] a direct exchange method was used to prepare monoionic clays from the natural clay, and the observed relations between ion species and molecular cross sectional area for water differ from those observed by Mooney, Keenan, and Wood. However, also a different source material was used.

The question should be raised whether the apparent spread in water monolayer packing on clay surfaces is real or merely an artifact resulting from inappropriate application of the BET theory. This question can be answered by studying interlayer adsorption of water in expanding clays since combined adsorption and x-ray observations afford an analysis of the packing geometry of the water molecules in the confinement of the interlayer space. A suitable system for such a study was observed by van Olphen[45], i.e. a high charge density vermiculite. This system is exceptional in that a monolayer and a two-layer hydrate are clearly separated in the adsorption process as shown by two-step isotherms and by the unit layer spacings measured during the adsorption process. The monolayer and two-layer coverages in this particular system can be derived from Langmuir plots, therefore, the applicability of BET plots is not involved in the analysis.

For the sodium form of the vermiculite it was found that the monolayer hydrate contains 1·6 sodium ions and 3·3 water molecules in planar arrangement between opposite unit cell surfaces with an area of 47·8 Å^2. The cross sectional area for the water molecules would thus be calculated to be 14·5 Å^2, although the actual value would be somewhat lower if allowance is made for the area occupied by the sodium ions.

In the two-layer hydrate the 1·6 sodium ions per unit cell are probably octahedrally coordinated with water, since according to x-ray analysis they are situated midway between the unit layers. There are 4·8 molecules of water per unit cell in each water layer, and thus their cross-sectional area under these conditions amounts to 10 Å^2.

For magnesium vermiculite the monolayer hydrate contains 2·78 water molecules and 0·8 Mg ion per unit cell from which a cross-sectional area for water of 17 Å^2 is calculated. In the two layer hydration stage, two different hydrates can be distinguished with respectively 10 and 11 molecules of water per Mg ion, and cross-sectional areas for water of 12 and 10·8 Å^2.

In the monolayer hydrates the water molecules are packed rather loosely, and they are probably clustered around the cations. Apparently, the formation of the two-layer hydrates involving the completion of the hydration shell around the ions takes preference over the completion of the monolayer. This would explain the occurrence of high cross-sectional areas for water on certain clays. The following observation on the magnesium vermiculite may also explain that sometimes rather low values (below 10 Å^2) are measured for water on clays: The monolayer hydrate of magnesium vermiculite is formed at very low relative pressures, i.e. below about 0·02, and beyond this pressure two-layer hydration takes place rapidly. Hence, in routine work the monolayer stage is easily missed, and the two-layer hydrate would be interpreted as the monolayer hydrate which would result in a calculated cross-sectional area of only 6 Å^2.

Obviously, since water adsorption on clays involves specific bonding forces, i.e. hydrogen bonding and ion hydration, surface coverage depends on surface structure, ion distribution, and ion species present. Hence, one cannot expect that a single value for the cross-sectional area of the water molecule at monolayer coverage will be applicable, neither for expanding nor for non-expanding clays.

It is also obvious from the above analysis that certain assumptions of the BET theory are not fulfilled in the clay–water vapour system. Due to the formation of a three-dimensional hydration shell around the cations the adsorption of the second layer will usually involve a finite amount of adsorption energy. Moreover, in expanding clays, adsorption of up to about four layers of water involves work of expansion of the lattice against unit layer attraction forces.

It must be concluded that the observed spread in apparent cross-sectional areas of water molecules at monolayer coverage on clay surfaces is partly real, and probably partly due to unjustified application of the two-parameter BET equation. (Since in expanding clays adsorption is limited to 2–4 layers the three-parameter BET equation should be applied, however, in view of the above basic considerations, such a refinement of the routine analysis does not seem warranted.) The same conclusions probably apply to the adsorption of water on other inorganic surfaces for which also wide variations of cross-sectional areas have been reported as shown by a survey of data from the literature by McClellan and Harnsberger[29]. An earlier review and critical discussion of literature data on vapour phase adsorption on clays and soils was presented by Quirk[37]. In addition to work mentioned above he reviews papers by Alexander and Haring[1], Makower, Shaw, and Alexander[27], Wadsworth[49], and Goates and Hatch[14]. Further work on area measurements on soils, clays and sediments has been published by Emmett, Brunauer, and Love[8], Purcell and Brooks[35], Johansen and Dunning[21], Okuda, Inoue, and Uei[31], Puri and Murari[36], and Farrar[11].

Surface areas derived from vapour phase adsorption of ammonia—Surface area derived from vapour phase adsorption isotherms of ammonia on clays, applying the BET analysis also vary considerably. Systematic work with Wyoming bentonite in the H, Na, and Ca form has been reported by Slabaugh and Siegel[41]. The homoionic clays were prepared by contacting the bentonite suspension with exchange resins in the respective ion forms. The results are shown in *Table 3*. Two series of experiments were run, one with oven-dried, and one with freeze-dried material. The average particle thickness derived from the ratio of nitrogen and crystallographic areas is smaller for the freeze-dried material. The cross-sectional areas for NH_3 vary from 14·3 to 16·3 Å^2 for the oven-dried, and from 12·7 to 16·4 Å for the freeze-dried material. Apparently oven-drying (at 105°C) causes a small degree of collapse, particularly in the calcium clay, according to these data. The cross-sectional areas were calculated from the observed monolayer coverage and the sum of half the crystallographic and half the nitrogen area, assuming monolayers of ammonia in the interlayer space.

Table 3. Nitrogen, ammonia, and crystallographic areas of a bentonite in various ion forms†

Ion form	*Crystallographic area* (m^2/g)	*Nitrogen* BET *area* (m^2/g)	*Layers per particle*	NH_3 *monolayer coverage* (mg/g)	*Apparent area* NH_3 *molecule* (Å^2)
H					
O.D.	767·2	40	19·2	92·3	16·3
F.D.		58	13·2	97·5	15·8
Na					
O.D.	751·8	33	22·8	90·7	16·2
F.D.		49	15·3	91·3	16·4
Ca					
O.D.	753·5	50	15·1	105	14·3
F.D.		70	10·7	121·3	12·7

† Data from Slabaugh and Siegel[41]

Note: Wyoming bentonite, O.D.: oven-dried at 105°C, F.D.: freeze-dried.

Surface area determination from heats of immersion of clays in water

The determination of surface area of clays and soils from data for the heats of immersion in water has been applied with some measure of success. For example, Puri and Murari[36] report obtaining reasonable values for soils using an average value of 186·8 erg/cm^2 for the heat of immersion. Okuda, Inoue, and Uei[31] applied the 'absolute' heat of immersion method of Harkins and Jura[19], and observed good agreement with the results from other methods.

Nevertheless, heats of immersion of clays are known to vary widely with charge density and ion species, as well as with variations in the conditions. Literature data are not numerous, and many are given for insufficiently characterized samples so that only estimates can be made in many cases of the effects of charge density and ion species. In *Table 4* reported data are summarized, and this list is fairly complete. For expanding clays, the crystallographic area may be used to estimate heats of immersion per unit area from the data reported per gram of clay. For the non-expanding clays

Table 4. Heats of immersion of clays in water in calories per gram clay (×4186 J/kg)

Serial No.	*Exchange ion species monoionic clays*								Nat.	CEC, meq p. 100 g	N_2 *area* m^2/g	*Notes*	*Lit. Ref.*
	Mg	Ca	H	Li	Na	K	Rb	Cs					
					BENTONITES—EXPANDING CLAYS								
1		22·1	20·1		12·1	9·1							38
2		22			16·1								9
3				18·2			9·0	10·0					26
4			26·5			10·7							22
5									11·8				34
6									11	80			33
									21	102			
									20	100			
									11	40		Beidellite	
7									13·3			Outgassed at 25°C	50
									22·0			Outgassed at 100°C	
8		21·28	21·02		14·29				12·88			Oven-dried at 105°C	39
					12·04				11·56			Freeze-dried	
9		13	16									Outgassed at 25°C	40
		25	21									Outgassed at 100°C	
10					17·11				24·19	112·7		Bent. Chmielnika	15
									24·88	112·7		(87%Ca, 12%Mg)	
									14·72	86·2		Bent. Machów	
									15·22	86·2		(66%Ca, 23·5%Mg,	
												10% Na)	
11	55·57				33·05					200		Llano Vermiculite	45
												Outgassed at 150°C	

Table 4 continued on p. 263

Table 4 (contd.)

									KAOLINITES—NONEXPANDING CLAYS				
12									1·24	9·85	48	Kaolinite Sedlec	15
									1·41	9·85	48	(87%Ca, 9% Mg)	
13		1·45	1·40		1·30	1·22							38
14									2·2				9
									1·9				34
16									1	9			33
17		0·99	1·05		0·89					1·65	11·6	0·4–0·8 μ	7
		0·89	0·92		0·81					1·15	8·5	0·8–1·6 μ	
18									0·95	2·40		10–20 μ	20
									0·99	2·60		0·5–10 μ	
									1·15	3·58		0·2–4 μ	
									1·38	3·76		0·1–0·5 μ	
									1·42	3·88		0·5–0·25 μ	
									1·87	5·43		0·25–0·1 μ	
19									1·61		13·3	Outgassed at 110°C	48
									1·68		13·3	150°C	
									1·82		13·3	210°C	
									2·03		13·3	250°C	
									2·12		13·3	360°C	

only in those cases where nitrogen or krypton areas are reported can the heats per unit area be calculated.

For the bentonites the heats of immersion are of the order of 10–25 cal/g, which amounts to roughly 55–140 ergs/cm^2 ($\times 10^{-3}$ J/m^2), and for the vermiculite the data correspond to 165 and 300 ergs/cm^2. For kaolinites for which nitrogen areas are reported the values correspond with 320–500 ergs/cm^2. Inspection of the values given for the cation exchange capacities reveal an increase in charge density from the bentonites to the vermiculites to the kaolinites, and the heats of immersion increase apparently with the charge density. In series of values for various monoionic forms of the samples, there is a clear trend of increase of heats of immersion with decreasing ion size. Orchiston[32] demonstrated a correlation between Brunauer's *c*-values for a series of homoionic bentonites and the hydration energy of the ions. Both observations suggest that the heat of immersion of clays is governed by the heat of ion hydration. Nevertheless, when the heats of hydration of the ions on the clay are estimated from the heat of immersion data, taking into account the electrical work of unit layer separation, these values are considerably lower than those for ions in solution. This could be shown from an analysis of the thermodynamic data which were determined in considerable detail for the sodium and magnesium vermiculites reported in *Table 4*, and discussed above (van Olphen[45]).

From the tremendous spread of the data (from 55 to 500 ergs/cm^2—though smaller within classes of clays) it must be concluded that the value of surface area determination of clays from heats of immersion would be very doubtful indeed.

Area determination methods based on adsorption from the liquid phase

Adsorption of polar molecules and of organic cations from the liquid phase may be considered as a basis for surface area determination of clays. Three different types of method may be distinguished: (i) adsorption of organic polar molecules by contacting the clay with the polar liquid; (ii) adsorption of polar molecules from a solution in a non-polar solvent; (iii) adsorption of organic cations from a solution in a polar solvent.

The first method, adsorption of polar molecules from the liquid phase, requires the establishment of conditions of monolayer coverage, and of cross-sectional areas of the adsorbate molecules. Reasonable methods have been developed for surface area determination of clays, particularly with glycerol as the adsorbate.

The second method, adsorption of polar compounds from solution, however, always involves simultaneous adsorption of the solvent molecules which takes place to an unknown extent, and no satisfactory method has been developed due to this unknown factor.

The third method, adsorption of organic cations from solution, does not pose serious problems of solvent adsorption since the organic cation adsorption is energetically so strongly preferred that any effects of solvent adsorption usually may be neglected. On the other hand, since the organic cation adsorption is dominated by exchange adsorption with the counter ions, the results are, in principle, more dependent on surface charge density than on surface area.

Surface area determination by adsorption of polar molecules from the liquid phase— Methods based on adsorption of polar molecules from the liquid phase require that the monolayer adsorption complex of the clay has a convenient stability range which is the same for all clays, allowing the desorption of polar molecules in excess of the monolayer by a standard evaporation procedure.

Dyal and Hendricks[6] were the first to introduce such a method using glycol as the adsorbed species. Excess glycol was desorbed by evacuation of the complex. They also devised a procedure to measure the external surface area of expanding clays separately, by measuring the glycol retention of a portion of the clay sample which had been heated at 600°C in order to 'collapse' the clay and thus make the interlayer area inaccessible to glycol.

Kinter and Diamond[24] introduced the use of glycerol as the adsorbed species. Due to its lower vapour pressure monolayer equilibrium conditions could be established more conveniently by heating of the adsorption complex at 110°C at normal pressures in the presence of glycerol vapour.

We will discuss the glycerol method in some detail. However, the main conclusions on its limitations will apply equally to the glycol method. For a more complete review of the adsorption of glycol and glycerol by clays and application to surface area determination, see Brindley[4].

In calculating the surface area from the glycerol retention at monolayer coverage, the authors assign a molecular cross sectional area of 26·9 Å^2 to the glycerol molecule. This is equivalent to an area of 17·65 m^2 of external or 35·3 m^2 of internal surface area for each 10 mg of glycerol adsorbed per gram of clay. The cross sectional area of the glycerol molecule was derived from the average thickness of the monolayer measured for a number of expanding clays, and assuming a normal liquid density for the monolayer of 1·26 g/cm^3. Of course, it is not certain whether normal density may be assigned to the adsorbed glycerol. Moreover, the liquid density at the measuring temperature (110°C) is 5 per cent less than the assumed value, which would increase the applicable cross sectional area by 5 per cent. The average thickness of the monomolecular layer is 4·5 Å, but it actually varies from about 4–5 Å depending on the clay. Hence, the cross-sectional area would vary ±10 per cent due to the variation in thickness. Taking the two effects into account, the cross-sectional area may vary from about 25·5 Å to 30·7 Å.

More recently, Hajek and Dixon[18] reported surface areas for expanding clays derived from glycerol vapour phase desorption isotherms. Linear Langmuir plots were obtained from which the following cross-sectional areas for glycerol at monolayer coverage were obtained: for Mg Wyoming bentonite 24·5 Å^2 (based on a monolayer coverage of 238 mg/g and a crystallographic area of 760 m^2/g), and for Mg Llano vermiculite 30·7 Å^2 (based on a monolayer coverage of 185 mg/g and a crystallographic area of 741 m^2/g). Taking external area into account, the value for the bentonite should be about 5 per cent higher, i.e. about 25·7 Å. For the Llano vermiculite the external area is negligible.

It is of interest to note that the packing of the glycerol molecules in the highly charged Mg Llano vermiculite apparently is relatively low at monolayer coverage, as is the case with the water molecules in the monolayer hydrate of this clay.

The cross-sectional areas derived from the vapour phase desorption isotherms are in agreement with the proposed value by Kinter and Diamond, allowing a 5–10 per cent spread. However, in a series of experiments on an impure bentonite converted to various homoionic forms a much larger spread in computed total area was observed, ranging from 374 m^2/g to 543 m^2/g for the sodium and magnesium forms respectively. For a number of non-expanding clays the authors obtained values for surface area which compared reasonably well with the results of other methods reported in the literature for similar clays, but no comparative data on identical samples were presented. Although the method may be reasonably accurate for certain practical applications, more comparative data will be needed to establish the limits of accuracy.

The method of determining external areas of expanding clays by measuring glycerol retention of the clay previously collapsed by heating at 600°C usually yields external areas for bentonites in the range of 5–10 per cent of the total area. However, some bentonites were found not to collapse completely by the heat treatment as was evident from x-ray analysis, and thus misleading high values for glycerol retention of the heated clays were obtained. No data have been reported on external areas measured by both glycerol retention and by nitrogen adsorption on identical samples.

Area determination by adsorption of cationic compounds from solution—As mentioned above, adsorption of cationic compounds will be dominated by exchange adsorption and would, therefore, be more dependent on surface charge density than surface area. This may be illustrated by the adsorption of pyridinium-type compounds. Using an excess of pyridinium chloride in aqueous solution, a Wyoming bentonite with a cation exchange capacity of 86 meq/100 g retains an equivalent amount of pyridinium ion after removal of the excess solution by washing with water. According to x-ray data, the pyridinium ions form a monolayer with the aromatic rings parallel to the unit layer surfaces. The projected cross sectional area of the cation in this position is about 40 $Å^2$. Since an area of about 70 $Å^2$ is available per exchange site, the molecules are loosely packed. The 3,4,6-trimethylpyridinium cation behaves in the same way, but its projected area is about 60 $Å^2$, hence, the organic cations are more densely packed (van Olphen[47]). Therefore, the monolayer coverage is dictated by the surface charge, rather than by the total available surface area. It was also found that for the highly charged Na Llano vermiculite (about 30 $Å^2$ per exchange site), exchange with the pyridinium ion was far from complete, amounting to a retention of pyridinium cations equivalent to about one fourth of the exchange capacity only.

Long chain quaternary bases have been suggested for surface area determination. These are often adsorbed in amounts of at least twice the exchange capacity. Adsorption of the first equivalent is due to exchange adsorption, and of the second equivalent to association of the hydrocarbon chains with the cationic group pointing away from the surface (Franzen[13]). The adsorption of the second equivalent then leads to reversal of charge of the surface.

A method for determining the cation exchange capacity of a clay has been based on this phenomenon (van Olphen[44]), using cetyltrimethylammonium bromide as the quaternary salt. Kivel, Albers, Olsen, and Johnson[25] studied adsorption of this compound as a means for determining surface area. Greenland and Quirk[16, 17] found that cetylpyridinium bromide (CPB) would be more suitable for this purpose since the packing of this molecule on clay surfaces appeared to be less variable. For non-expanding clays comparison with nitrogen areas led to an average cross-sectional area of CPB of 27 $Å^2$, which is half the projected area of the pyridinium compound, indicating that a bimolecular layer of CPB is adsorbed. However, the method is applicable only for surfaces in a limited range of charge densities. With expanding clays, bimolecular layers are adsorbed on external and monomolecular layers on internal surfaces, and an independent determination of external area is needed to interpret the adsorption data.

Because of the applicability of convenient colorimetric analytical techniques, adsorption of cationic dyes, particularly methylene blue, has been proposed for surface area determination. However, many complicating factors make the method unreliable. Dimerization occurs on the clay surface (Bergmann and O'Konski[2]), the projected cross-sectional area depends strongly on the orientation of the molecule on the surface, adsorption is dependent on electrolyte concentration (as shown for AgI by van den Hul[43]), and non-stoichiometric exchange has been observed (Bodenheimer and Heller[3]). Faruqi, Okuda, and Williamson[12] studied the adsorption of methylene blue by kaolinite as a function of charge density, and of pH. They also discuss previous literature in some detail, and reach the conclusion that methylene blue adsorption does not provide a reliable method for determination of either surface areas or the cation exchange capacity of clay minerals.

CONCLUSIONS

The packing density of polar molecules on clay surfaces in monolayer configuration varies widely for different clays with different charge densities, and different exchange cation species. Such variations are to be expected since specific forces dominate the adsorption, i.e. hydrogen bonding forces and charge-dipole interaction forces, rather than non-specific dispersion forces. Hence, the packing geometry will depend on the site distribution geometry.

Although for these reasons adsorption methods using polar molecules are inaccurate, such methods must be used if some particular application requires a knowledge of the total area of a clay sample which is accessible to polar molecules, in order to include the interlayer area of expanding clays which may be present in the sample. In such cases the possible spread in area data calculated from some average molecular cross-sectional area of the polar molecule should be considered in the interpretation of these data.

The sorption isotherms for polar molecules and expanding clays generally show considerable hysteresis. An important contribution to this phenomenon is the development of counteracting elastic stresses at the peripheries of the particles when polar molecules penetrate into the interlayer space during the adsorption process. Since such effects are less important during the desorption, the desorption data are preferred for the calculation of surface areas (van Olphen[45]). Due to this mechanism the BET plots show an upward bend at low pressures, and in extreme cases no linear section occurs in the BET plot in the customary pressure range (e.g. see note § in *Table 2*).

SUMMARY

Reviewed are principles and results of surface area determinations of expanding and nonexpanding clays by means of vapour phase and liquid phase adsorption isotherms using nitrogen, water, ammonia, glycol, glycerol, methylene blue, and quaternary bases. Also, heats of immersion of clays in water are evaluated from the point of view of area determination.

Surface areas of nonexpanding clays can be determined from vapour phase adsorption isotherms using either nonpolar (nitrogen, krypton) or polar molecules (water, etc.), applying BET theory. Considering the nitrogen area as a reliable reference area, molecular cross-sectional areas for polar molecules (e.g. water) are found to vary considerably with surface charge density and ion species of different clays.

External surface areas of expanding clays can be determined from nitrogen adsorption isotherms, whereas the combined internal and external surface areas can be determined from adsorption of polar molecules which are able to penetrate between the unit layers. This total area can be independently determined from crystallographic data and chemical analysis, and can be used as a reference area for the evaluation of the molecular cross sectional areas for polar molecules. Again, these cross-sectional areas vary considerably with surface charge density and ion species.

It is shown that the observed apparent variations in packing geometry of water molecules on clay surfaces at monolayer coverage are real. Specific adsorption forces (i.e. hydrogen bonding and charge-dipole forces) are involved in the adsorption of polar molecules, hence the packing geometry depends on the distribution geometry of the bonding sites. However, the variations may also be partly due to unwarranted application of the BET theory since assumptions underlying this theory are not fulfilled in the clay-surface/water system.

Also, because of the specificity of the adsorption processes involved, data on heats of immersion of clays in water, and data for the adsorption of ionogenic organic compounds, do not provide a highly accurate basis for surface area determination.

References

[1] L. T. Alexander and M. M. Haring. *J. Phys. Chem.* **40**, 195 (1936).
[2] K. Bergman and C. T. O'Konski. *J. Phys. Chem.* **67**, 2169 (1963).
[3] W. Bodenheimer and Lisa Heller. *Israel J. Chem.* **6**, 307 (1968).
[4] G. W. Brindley. *Clay Minerals* **6**, 237 (1966).
[5] C. S. Brooks *Soil Sci.* **79**, 331 (1955).
[6] R. S. Dyal and S. B. Hendricks. *Soil Sci.* **69**, 421 (1950).
[7] W. H. East. *J. Amer. Ceram. Soc.* **33**, 211 (1950).
[8] P. H. Emmett, S. Brunauer and K. S. Love. *Soil Sci.* **45**, 57 (1938).
[9] K. Endell, W. Loos, H. Meischeider and V. Berg. *Inst. Deut. Forsch. Bodenmechanik* **5**, (1938).

[10] J. Escard. *J. Chim. Phys.* **47**, 113 (1950).
Trans. Fourth Intl. Congress Soil Sci. **3**, 71 (1950).
[11] D. M. Farrar. *J. Soil Sci.* **14**, 360 (1963).
[12] F. A. Faruqi, S. Okuda and W. O. Williamson. *Clay Min.* **7**, 19 (1957).
[13] P. Franzen. *Clay Min. Bull.* **2**, 223 (1954).
[14] J. R. Goates and C. V. Hatch. *Soil Sci.* **75**, 275 (1953).
[15] B. Grabowska-Olszewska. *Biuletyn Geologiczny, University of Warsaw*, **10**, 5 (1968).
[16] D. J. Greenland and J. P. Quirk. *J. Phys. Chem.* **67**, 2886 (1963).
[17] D. J. Greenland and J. P. Quirk. *J. Soil Sci.* **15**, 178 (1964).
[18] B. F. Hajek and J. B. Dixon. *Soil Sci. Soc. Amer. Proc.* **30**, 30 (1966).
[19] W. D. Harkins and G. Jura. *J. Am. Chem. Soc.* **66**, 1362; 1366 (1944).
[20] C. G. Harmon and F. Fraulini. *J. Amer. Ceram. Soc.* **23**, 252 (1940).
[21] R. T. Johansen, and H. N. Dunning. *Clays and Clay Minerals*, Pergamon Press, **6**, 249 (1959).
[22] R. S. Johnson. Ph.D. Thesis, Stanford University (1954). [Diss. Abstracts, **57**, 2435 (1957)].
[23] A. G. Keenan, R. W. Mooney and L. A. Wood. *J. Phys. Coll. Chem.* **55**, 1462 (1951).
[24] E. B. Kinter and S. Diamond. *Clays and Clay Minerals*, Natl. Acad. Sci.—Natl. Res. Coun. Pub. 566 Washington D.C., 318, 334 (1958).
[25] J. Kivel, F. C. Albers, D. A. Olsen and R. E. Johnson. *J. Phys. Chem.* **67**, 1235 (1963).
[26] D. R. Longwell. Ph.D. Thesis, Stanford University (1963).
[27] B. Makower, T. M. Shaw and L. T. Alexander. *Soil Sci. Soc. Amer. Proc.* **2**, 101 (1938).
[28] R. T. Martin. *Clays and Clay Minerals*, Pergamon Press, **6**, 259 (1959).
[29] A. L. McClellan and H. F. Harnsberger. *J. Coll. Interface Sci.* **23**, 577 (1967).
[30] R. W. Mooney, A. G. Keenan and L. A. Wood. *J. Am. Chem. Soc.* **74**, 1367, 1371 (1952).
[31] S. Okuda, K. Inoue and I. Uei. Memoirs Faculty Industrial Arts, Kyoto Technical University, *Sci. and Technol.* **9**, 61 (1960).
[32] H. D. Orchiston. *Soil Sci.* **79**, 71 (1955).
[33] F. D. Ovcharenko and S. F. Bykov. *Kolloid Zhur.* **16**, 134 (1954).
[34] C. W. Parmelee and D. Frechette. *J. Amer. Ceram. Soc.* **25**, 108 (1942).
[35] W. R. Purcell and C. S. Brooks. *J. Petrol. Technol.* **195**, 289 (1952).
[36] B. R. Puri and K. Murari. *Soil Sci.* **96**, 331 (1963).
[37] J. P. Quirk. *Soil Sci.* **80**, 423 (1955).
[38] A. C. Siefert. Ph.D. Thesis, Pennsylvania State College (1942).
[39] W. H. Slabaugh. *J. Phys. Chem.* **59**, 1022 (1955).
[40] W. H. Slabaugh. *J. Phys. Chem.* **63**, 1333 (1959).
[41] W. H. Slabaugh and R. H. Siegel. *J. Phys. Chem.* **60**, 1105 (1956).
[42] S. Teichner. *J. Chim. Phys.* **47**, 118, 244 (1950);
C. R. Acad. Sci. Paris **231**, 1063 (1950).
[43] H. J. van den Hul. Ph.D. Thesis, Utrecht, The Netherlands. p. 45 (1966).
[44] H. van Olphen. *Clay Min. Bull.* **1**, 169 (1951).
[45] H. van Olphen. *J. Coll. Sci.* **20**, 822 (1965).
[46] H. van Olphen. *Clays and Clay Minerals*, Pergamon Press, **14**, 393 (1966).
[47] H. van Olphen. *J. Coll. Interface Sci.* **28**, 370 (1968).
[48] W. H. Wade and N. Hackerman. *J. Phys. Chem.* **63**, 1639 (1959).
[49] H. A. Wadsworth. *Soil Sci.* **58**, 225 (1944).
[50] A. C. Zettlemoyer, G. J. Young and J. J. Chessick. *J. Phys. Chem.* **59**, 962 (1955).

DISCUSSION

Dr R. Greene-Kelly (*Rothamsted Experimental Station*) said: Plate-like particles with large diameter-to-thickness ratios readily orient to form close-packed aggregates. This property may make it difficult to interpret surface area determinations in terms of particle size. Two examples are given below.

(a) A fractionated montmorillonite (sodium-saturated Wyoming-type), when prepared as an aerogel by the Kistler technique using ethanol and benzene, adsorbed nitrogen rapidly at -196°C; the isotherm was completely reversible and showed that the aerogel had a specific surface area of 54 m^2 g^{-1}. The same material compressed to form a plug (porosity 0·25) gave an isotherm with hysteresis (due to the formation of intermediate-sized pores) which indicated an apparent specific surface area of only 20 m^2 g^{-1}. Water-dried aggregates (porosity 0·15) adsorbed negligible amounts of nitrogen (specific surface area less than 1 $m^2 g^{-1}$) even if left for many hours and were evidently virtually impermeable to nitrogen. The powdered water-dried aggregates had variable specific surface areas and hysteresis in the isotherms indicated the presence of intermediate-sized pores. Obviously the BET surface areas of a Wyoming montmorillonite powder or plug are meaningless as a measure of particle size unless precautions are taken to limit aggregation. Not all montmorillonites show such marked changes in response to different methods of preparation although aggregation can result in the time required for equilibrium being several hours rather than minutes.

(b) A sodium-saturated Peerless Kaolinite consisting of well-defined hexagonal platelets was used to study the effect of pre-adsorbed water on both the heat of immersion in water (at 25°C) and the nitrogen adsorption (at −196°C) of the slowly cooled sample. In contrast to the results reported by Clint, Clunie, Goodman and Tate (p. 299) the heats of immersion were not independent of the amounts of pre-adsorbed vapour for θ (equal to volume adsorbed/volume required for monolayer coverage assuming a water molecule occupies 10×10^{-20} m^2, and the surface area is the BET surface area and a nitrogen molecule occupies 16×10^{-20} m^2) between 1 and 2; for $\theta = 2$ the apparent interfacial area was 20·5 $m^2 g^{-1}$ whereas the adsorption of nitrogen on the same sample corresponded to a specific surface area of 11 $m^2 g^{-1}$. The dried sample had a nitrogen specific surface area of 15 $m^2 g^{-1}$ and showed no intermediate-sized pore hysteresis. The isosteric heat of adsorption of water at $\theta = 2$ was therefore probably not yet equal to the heat of liquefaction; this is perhaps not unexpected with this system. The heat of immersion continues to decrease with further amounts of pre-adsorbed water reaching at a relative pressure (p/p_0) of 0·98 ($\theta = 12$) an apparent interfacial area of 8·6 $m^2 g^{-1}$. Other Kaolinites behaved similarly but samples of anatase and rutile gave interfacial areas in reasonable agreement with their nitrogen specific surface areas. The results suggest that reversible capillary condensation between the mutually-oriented platelets of Kaolinite started at relatively low p/p_0 (perhaps 0·6) so that when the isosteric heat approached the heat of liquefaction the interfacial area was already considerably less than the particle surface area (cf. anatase and rutile).

Dr H. van Olphen replied: I would like to thank Dr Greene-Kelly for his comments. I would also like to add the following reference to those cited in my paper: R. Greene-Kelly, *Clay Minerals Bulletin* **5**, November (1962).

Dr P. Connor (*Glaxo Ltd., Greenford*) communicated: I have recently made a study of the interaction of a series of long chain quaternary ammonium and pyridinium compounds (C_6–C_{16}) with well-characterized monodisperse polystyrene latices [P. Connor, Ph.D. Thesis, University of Bristol (1968); P. Connor, *Proc. 5th Congr. Surface Activity* (Barcelona 1968), in the press]. These latices were negatively charged owing to the presence of integrally bound carboxyl ions. The isotherms obtained had a two-stage nature and had an initial inflection where the amount adsorbed showed a precise one-to-one correspondence with the number of carboxyl groups present.

The packing density of the long chain ions at the first inflection was only one ion per *ca.* 1000–2500 Å^2 depending on the latex used. It was, however, independent of chain length. After this point the ions were adsorbed in the reverse orientation with the polar head groups pointing away from the latex surface. At surface saturation which occurred at the second inflection and around the critical micelle concentration the packing densities were very much higher and increased with chain length. For example, with the quaternary ammonium compounds, the areas per ion were 46·8, 56·3, 64·5 and 70·8 Å^2 for the C_{16}, C_{12}, C_{10} and C_8 compounds, respectively. Even the lowest of these figures is still higher than the 35 Å^2 calculated from a molecular model of the alkyl trimethylammonium ion.

These results indicate the complex nature of the adsorption process for long chain amphipathic compounds and suggest that considerable caution should be exercised if these compounds are used for surface area measurement. This is particularly true for adsorbents of low charge density where it is probable that the surface area will be considerably underestimated if this technique is employed.

ON THE USE OF ADSORPTION MEASUREMENTS FROM SOLUTIONS OF NON-ELECTROLYTES FOR SURFACE AREA DETERMINATION

G. Schay

Central Research Institute for Chemistry of the Hungarian Academy of Sciences, Budapest, Hungary

Adsorption methods for the determination of specific surface areas of solids are all based on the measurement of concentration changes caused by adsorption and an estimate of the monolayer capacity from these changes. The amounts of matter which seem to have disappeared from the bulk fluid by contact with the solid adsorbent are termed surface excesses. An adsorption isotherm is the functional relation between the surface excesses and the equilibrium concentrations in the bulk fluid phase at a given temperature. When the fluid is a one-component gas or vapour, concentration changes are equivalent to corresponding pressure changes. Liquids are, however, practically incompressible under ordinary conditions and, in consequence, thermal effects (heat of wetting, heat of immersion) can only be observed without concentration changes, when a pure liquid is brought into contact with an adsorbent. According to general convention, it is not usual to speak of adsorption in such cases, though it may be possible to define surface excesses by thermodynamic relations and to picture them as related to density changes caused by the adhesional forces acting in the interfacial layer. When liquids are concerned, adsorption as manifested by observable concentration changes can occur only with solutions or mixtures of at least two components. From the fact that in binary liquid solutions the concentrations of the two components are unambiguously interdependent, it follows that the same must be true for the surface excesses: positive surface excess of one of the components must be accompanied by a corresponding negative excess of the other, so that the adsorption process can be characterized by one single isotherm.

It may be noted incidentally that it would be false to connect concentration changes caused by adsorption with corresponding surface excesses without any restriction: this is permissible only if we can be confident that the surface of the solid is equally accessible to both of the solution components (if, e.g., water is removed from an organic liquid by a molecular sieve, this is more like an extraction process and thus a volume effect, though it can be described formally by an adsorption isotherm showing an apparent positive surface excess of water). All methods proposed for surface area determination (as different from determination of adsorption capacity!) by liquid adsorption are based tacitly or admittedly on the assumption of free accessibility.

Another point that must be stressed is the question of the limit of applicability of the surface area concept itself. We are faced with the same problem as in connection with vapour adsorption: if the adsorbent contains micropores with radii comparable with the diameters of the adsorbate molecules, then adsorption becomes a volume effect and computation of the specific surface area by the usual formalisms may result in more or less illusory values even if the micropores are equally accessible to the solution components.

The most usual experimental mode of determination of a single point of the pertinent adsorption isotherm of a binary solution is quite simple in principle: a known amount of initial solution (say n^0 moles or M^0 grams or V^0 cm^3) of known composition (mole fraction of component 1 x_1^0 etc.) is brought into contact with a weighed amount (m gram) of adsorbent in a vessel, at the required temperature (extremely careful thermostatting is mostly unnecessary, because liquid adsorption equilibrium is comparatively insensitive to temperature changes), and stirred for several hours. After equilibration, an aliquot part of the bulk liquid is separated and the concentration change, $\Delta x_1 = x_1^0 - x_1$, is determined by some suitable method (x_1 is the equilibrium mole fraction). The function

$$f(x_1) = n^0 \Delta x_1 / m, \tag{1}$$

called the specific adsorption proves to be really a function of x_1 only, independent of how the relative amounts n^0 and m have been chosen and of the initial concentration x_1^0, too, provided that the final equilibrium concentration x_1 remains the same. This independence is, in fact, the best check of reliability of any determination of liquid adsorption isotherms, a check not only of the required sensitivity of the chosen analytical method but also of the adsorbent being pure in the sense that it does not contain any contaminant soluble in the liquid which could falsify the analytical result. An often used method is the measurement of the refractive index and it is well known that this index is very sensitive to minimal amounts of water in organic solvents, so that any water contained in the adsorbent may become dangerous in connection with refractometric methods. Unfortunately, a lot of adsorption isotherms published in the literature have to be suspected of not having been determined with due circumspection.

It is easy to see that the adsorption, as defined in Eq. (1), is a surface excess, because $n^0 x_1^0$ is the total amount of component 1 present in the system, and $n^0 x_1$ the amount of it in the same number of solution moles of equilibrium composition. It has to be noted that it is not identical with the surface excess as defined by Gibbs in connection with his famous thermodynamical adsorption equation: the latter is $n^0 \Delta x_1 / (1 - x_1)$. It is well known that Gibbs introduced the notion of surface excess in order to be able to treat adsorption phenomena by exact thermodynamics without recurring to any detailed model of the interfacial layer, his treatment being equally compatible with monolayer as with multilayer adsorption. In view of this, we cannot expect to derive conclusive evidence as to the monolayer capacity (necessary for surface area determination) from any adsorption isotherm alone, without further information or assumptions.

In early times already (Williams, Wo. Ostwald, cf. Kipling[1]) attempts were made to interpret adsorption isotherms of solutions by some appropriate model. We have good reason to suppose that adsorption forces emanating from the solid surface do not reach far so that only a part of the solution in contact with it is under their influence (this is probably not true for quite narrow pores). If we denote the fraction of the total amount present (per gram adsorbent n^0 moles), supposed to be contained in the adsorption region, by n^s, and the respective amounts of the two components in it by n_1^s and n_2^s, and consider that in the 'free' liquid ($n^0 - n^s$ moles) the concentration is x_1, that of equilibrium, then we may write down the material balance for component 1:

$$n^0 x_1^0 = n_1^s + (n^0 - n^s)x_1,$$

$$\text{or} \quad n^0(x_1^0 - x_1) = n^0 \Delta x_1 = n_1^s - n^s x_1 (= n_1^s(1 - x_1) - n_2^s x_1). \tag{2}$$

It is remarkable that we get back in this way the same surface excess as by definition (1), but at the same time this may make us suspect that the separation of an adsorption layer is so far not more than a formal mental procedure. In fact, having once fixed some value of n^s provisionally, we may add mentally a further amount of equilibrium liquid to it, without upsetting the material balance expressed by Eq. (2), because any difference of two terms remains unaltered if we add and subtract an identical term.

There are cases, nevertheless, when the quantity n_1^s can be given an unequivocal meaning, provided that the surface excess of 1 is positive throughout so that it can be regarded upon as being the adsorbate. One important case is when the equilibrium concentration x_1 is negligibly small: evidently then the bulk liquid does not contain any appreciable amount of component 1, the whole of it is in the adsorbed state. On the other hand, because x_1 vanishes, the term $n^s x_1$ in Eq. (2) becomes negligible, so that in this way, too, we conclude $n^0 \Delta x_1 = n_1^s$. It has to be noted, however, that this is not really the expression of the adsorption isotherm, it can be valid only, in appropriate cases, for the very first part of an isotherm with a quite steep initial increase (strong adsorption of 1). The maximum value of n_1^s which complies with the foregoing equation (i.e. with the condition $x_1 \approx 0$) is what is called the adsorption capacity of the adsorbent in question, with respect to the species 1 in the given solvent. There is, however, no guarantee whatever that at this point the amount n_2^s has to be practically zero (which would mean that the amount n_1^s, equivalent with the adsorption capacity, should correspond to complete coverage of the adsorbent surface exclusively by component 1). In the case of the adsorption capacity being determined e.g. with dyestuff solutions, it is even quite probable that, at the decoloration limit, the adsorption layer contains more or less of the solvent, too, and this in different amounts depending on the nature of the solvent.

According to what has just been said, determination of the adsorption capacity cannot be identified with surface area determination, based on the assumption that this capacity should be equivalent with a complete monolayer of the sorbate molecules. The validity of such an assumption should be tested, for any kind of adsorbent in conjunction with a specified adsorptive in a given solvent, by some independent surface area determination. By such a test, an empirical surface occupancy of the adsorbate molecules may be computed, and such a value used for relative surface area determinations on different adsorbents of the same chemical nature. One has to bear in mind, however, that adsorption capacity can be best determined by sorptives having big molecules (physical adsorbability increases with molecular weight), and that for these the accessibility of the surface may be by far different for different adsorbent samples of 'identical' chemical character. On the other hand, the great practical value of such determinations of adsorption capacity should not be denied, by any means.

In the past, adsorption isotherms used to be studied mainly with dilute solutions only, and many formal similarities with vapour adsorption isotherms could be found (as e.g. validity of Traube's rule in connection with aliphatic homologous series, in their adsorption on charcoal). It was found that the empirical course of many adsorption isotherms can be fitted by an expression of the Freundlich or of the Langmuir type, and it was thought that the extrapolated asymptotic value of the latter may correspond to a definite surface coverage, supposedly to a complete monolayer of adsorbate molecules. It follows by definition, however, that when $n^0\Delta x_1$ is positive, it has to go through a maximum, if determined over a range of compositions wide enough. In case of completely miscible binary mixtures, it has to vanish at both ends of the composition range. Thus the eventuality that part of the ascending branch may be fitted by a Langmuir expression is not conclusive evidence for the existence of an asymptotic saturation value. From the interpretation of $n^0\Delta x_1$, as given by Eq. (2), one can see immediately the criterion for exclusive saturation coverage by component 1, from some value of x_1 onwards: if n_2^s is zero in this range, then constancy of n_1^s involves constancy of the expression $n^0\Delta x_1/(1 - x_1)$, containing measurable quantities only. This is not only a necessary but normally also a sufficient criterion: from the last form of Eq. (2), quoted in parentheses, it follows that $n^0\Delta x_1/(1 - x_1)$ cannot remain constant without n_2^s becoming zero (with exception of the case of equal molecular areas). This is then the other case, mentioned above, when n_1^s can be given an unequivocal meaning. Its interpretation as being equivalent with a complete monolayer should not be accepted, however, unconditionally.

Let us consider, in this context, first of all the case of an adsorptive, mostly a solid, of limited solubility in the given solvent, this being *par excellence* the case in which adsorption may be expected to be preferential to such a degree that the solvent should get displaced completely from the surface layer. Because of limited solubility, the adsorption isotherm cannot be followed up to $x_1 = 1$, and thus the above criterion has to be applied in the form that the plot of $n^0\Delta x_1/(1 - x_1)$ should reach a practically horizontal plateau before the solubility limit. If the specific surface area of the adsorbent is known from some other source (e.g. by the 'standard' BET method), then one may check whether the amount corresponding to the plateau is representative of a monolayer, based on some reliable estimate of the surface area occupied by a molecule of the sorbate.

In many instances, such checks give affirmative results. Thus, Kipling and Wright[2], on studying the adsorption of stearic acid on Graphon (a carbon black), have found the same asymptotic value when the solvent was cyclohexane, carbon tetrachloride, alcohol or benzene, and this common value fitted excellently with the picture of a saturated monolayer of dimeric acid molecules lying flat on the surface. It has to be stressed, however, that the procedure may be conclusive only when the limiting value in question can be reached effectively, but not if it is obtained by extrapolation. Thus the same authors studied the adsorption of stearic acid, dissolved in the same solvents as above, on another carbon black (Spheron 6), but in this case no plateau could be reached before the solubility limit. The accessible parts of the isotherms could be fitted, however, by Langmuir expressions, but the extrapolated asymptotic values showed a four-fold variation for the four different solvents, all of them being materially less than the calculated monolayer value. This is an indication that at the apparent limiting value, the presence of solvent molecules in the adsorbed layer cannot be generally excluded.

Even if an apparent limiting value of $n^0\Delta x_1/(1 - x_1)$ is reached before the saturation limit, this may not always be conclusive of this value corresponding to a pure monolayer: one has to think that sometimes, if the isotherm could be followed up to higher concentrations beyond the saturation limit, the limiting value would turn out to be really a maximum only. Adsorptions of butyl or amyl alcohol from aqueous solution on charcoal are examples of such behaviour, where Nagy and Schay[3] had to conclude that the apparent limiting value corresponds to a mixed layer containing water, too, besides alcohol. The findings of Kipling *et al.*[4] on the adsorption of malonic acid from aqueous solution on charcoal are instructive in this respect. There the solubility limit is considerably higher, and the above mentioned maximum could be actually observed. Beyond it, the function $n^0\Delta x_1$ falls off linearly, the extrapolated intersection of this straight portion with the base line does not lie far beyond the solubility limit of $x_1 = 0{\cdot}21$, indicative of a mixed adsorption layer (see Eqs. 10, 11). It may be mentioned that in cases of those kinds, a sharp rise of $n^0\Delta x_1$ can often be observed just before the solubility limit, apparently an indication of imminent phase separation. It may be pointed out that the second phase is then a mixed one, too (e.g. water in alcohol), so that a surface phase containing only one component in pure state would be most improbable, in fact.

As to the possibility of surface area or better of monolayer capacity determination, experiences with solutes of limited solubility may be summarized as follows. As explained, only a fairly long plateau of the function $n^0\Delta x_1/(1 - x_1)$ can be regarded as being conclusive, so that solutes with too low a solubility have to be excluded. It is advisable to plot also the function $n^0\Delta x_1$ and to see whether extrapolation of the linear part following the maximum gives the intersection with the base line at $x_1 = 1$, this corresponding to $n_2^s = 0$ at the limit. In order to ensure fulfilment of this latter condition, solvents have to be selected which are not supposed to produce strong solvation (mainly by hydrogen bonding, as in the cases mentioned above) of the adsorptive molecules. On the other hand, chemisorption (hydrogen bonding included) of the sorptive at the adsorbent surface may falsify the result, because the possibility of a physically adsorbed layer on top of the chemisorbed one may arise (see later). On the whole, the solute–solvent pair to be used has to be selected carefully, with regard not only at the chemical nature of the given adsorbent, but also at the accessibility of its surface by the sorptive, in case of a microporous material.

In view of the latter point, sorptives of relatively low molecular weight seem preferable, in which case, however, really strong preferential adsorption as compared with the solvent, can hardly be expected if chemisorption has to be excluded. We are thus led to the consideration of the adsorptive behaviour of pairs of completely miscible liquids comprising molecules of comparable sizes. A more intensive and systematic study of such systems is of recent date only. It has to be stated at once, that isotherms are met with in suitable cases, which exhibit a fairly long, practically straight portion on their ultimate course. Such a portion may be represented algebraically by an equation:

$$n^0 \Delta x_1 = a(1 - x_1), \tag{3}$$

a being a constant. Comparison with Eq. (2) and with what has been said in connection with limited solubility, prompts one to set[5]

$$n_1^s = a, n_2^s = 0 \tag{4}$$

along such a section. All of what has been said above in connection with limited solubility, applies here too. It has to be conceded, however, that on the whole, isotherms of this pure type are comparatively rare because preferential adsorption of one of the components is mostly not strong enough.

Much more frequent are isotherms whose final section is slightly curved, with the function $n^0 \Delta x_1/(1 - x_1)$ showing a slight linear increase to be described algebraically by:

$$n^0 \Delta x_1/(1 - x_1) = a(1 + cx_1), \tag{5}$$

c being another constant, with the restriction $c \ll a$. We have then, by the general relation (2):

$$n_1^s = n^0 \Delta x_1 + n^s x_1 = a + [n^s - a(1 - c)]\, x_1 - acx_1^2 = a + [n^s - a(1 + c)]x_1 \\ + acx_1(2 - x_1),\; n_2^s = - n^0 \Delta x_1 + n^s x_2 = [n^s - a(1 + c)]x_2 + acx_2^2. \tag{6}$$

Evidently, the amount of liquid represented by $n^s - a(1 + c)$ has the same composition as the equilibrium bulk liquid, and may thus be considered as not belonging really to the surface phase, if we are entitled to believe that the latter is representative of a monolayer (a mixed one, of course, in this case) having a composition different from that of the bulk phase. The amounts in the supposed surface phase proper will thus be:

$$n_1^s = a[1 + cx_1(2 - x_1)],\; n_2^s = acx_2^2, \\ n^s = a[1 + c(2x_1 + x_2^2 - x_1^2)] = a(1 + c) = \text{constant}. \tag{7}$$

The last result, involving a mixed monolayer of varying composition, but containing a constant total number of moles, may be realistic only when the surface occupancies of the two species constituting the mixture are materially equal. If this condition is observed, then the constants a and c are best determined by linear extrapolation according to Eq. (5), and the relevant value of n^s computed by Eq. (7). It has to be noted that, according to our experience, a final empirical course of the isotherm satisfying Eq. (5) may result also when the molecular sizes are substantially different, but no reliable monolayer value can be obtained by extrapolation of the function $n^0\Delta x_1/(1 - x_1)$, in this case.

At present, we are far from being able to predict whether with any liquid pair/adsorbent system, an isotherm will result which has the form required for the above analysis. But, if interested in surface area determination, we can say that, according to our experience, on oxidic or hydroxylic adsorbents such as silica or alumina gels, mixtures of benzene and n-hexane or n-heptane as well as mixtures of toluene and n-heptane proved to be satisfactory. The greater polarizability of the aromatic ring ensures sufficiently preferential adsorption, without any danger of chemisorption or of association akin to complex formation. The role of the last mentioned factors may be illustrated by the following observation[5]. Methanol in benzene yields on silica gel an isotherm the final part of which, from methanol mole fraction about 0·5 onwards, can excellently be represented according to Eq. (3), but $n_1^s = a$ corresponds practically to a double layer in this case, consisting probably of a physisorbed layer on top of a first chemisorbed one. This interpretation is corroborated by the further observation that the same mode of evaluation gives a good monolayer value when the gel has been pretreated with methanol (soaking followed by drying for two hours at 120°C), though the specific surface area is somewhat diminished by this pretreatment, as checked by adsorption measurements with mixtures of benzene and n-heptane, before and after pretreatment, respectively (see *Table 1*).

Table 1. Specific surface areas determined according to BET and graphical (G) methods

Adsorbent	s_{BET}† (m^2/g)	s_G (m^2/g)	*Mixture*	*Type of isotherm Eq. No.*
Silica gel	540	560	toluene + n-heptane	(3)–(5)
Silica gel	540	530	benzene + n-heptane	
Silica gel	210	202	benzene + n-heptane	
Alumina gel	240	236	benzene + n-heptane	
Alumina gel '240'			benzene + n-heptane	
(pretreated with methanol)	175	162	benzene + n-heptane	
Alumina gel	186	190	benzene + n-heptane	
Silica gel	450	460	benzene + n-heptane	
Silica gel '450' (pretreated with methanol)	320	340	benzene + n-heptane	
Charcoal	612	587	ethanol + benzene	(10)
Charcoal	840	870	ethanol + benzene	
Charcoal	1100	1200	ethanol + benzene	
Carbon black	68	72	ethanol + benzene	

† $a_{N_2} = 16{\cdot}2$ Å²

A different approach has been proposed by Everett[6], originally for so-called ideal adsorption only. A more general derivation is as follows. On the assumption again that n_1^s and n_2^s can be given a defined meaning, an enrichment factor α, characteristic of the surface layer, may be defined and expressed in terms of $n^0\Delta x_1$, making use of the general relation (2):

$$\alpha \equiv \frac{n_1^s x_2}{n_2^s x_1} = \left(\frac{n^0 \Delta x_1 + n^s x_1}{- n^0 \Delta x_1 + n^s x_2} \frac{x_2}{x_1} \right), \tag{8}$$

which gives, by suitable rearrangement, Everett's expression:

$$\frac{x_1 x_2}{n^0 \Delta x_1} = \frac{1}{n^s} \left(x_1 + \frac{1}{\alpha - 1} \right). \tag{9}$$

In case of the two components of the mixture having practically equal sizes so that n^s remains constant throughout the composition range, and when α happens to be more or less a constant independent of composition (according to the current thermodynamic theory of monolayer adsorption, approximate constancy of α may be brought about incidentally by favourable compensation effects even in the case of non-ideal behaviour), the plot of the left hand side of Eq. (9), containing directly measurable quantities only, will be a straight line from the slope of which n^s can be computed. Examples given by Everett[6] show that in favourable cases, good monolayer values may be obtained by this procedure.

The relation represented by Eq. (9) may be analysed, however, in a different manner, too. It has been stated above that isotherms with sufficiently strong preferential adsorption may be suitable for surface area determination. Strong preferential adsorption is equivalent, however, with α having a high value, and then the second term may become practically negligible besides the first one, at least towards the end of the composition range, on the right hand side of Eq. (9). As can be seen easily, Eq. (9) becomes then identical with Eq. (3), and it is thus not surprising that in cases of strong preferential adsorption of one of the components both methods yield fairly concordant values for n^s (in cases of practically exact validity of Eq. (3), there is complete equivalence), as has been shown recently, e.g. by Ramakrishna and Suri[7].

There is another type of isotherm to be encountered, too, which can be used for surface area determination, in suitable cases. These are isotherms in the course of which the maximum, occurring at some comparatively low mole fraction of one of the components, is followed sooner or later by an inflexion, so that either the end point is reached more or less asymptotically or $n^0 \Delta x_1$ changes its sign (occurrence of an adsorption azeotrope), to reach the end point, after a minimum, from the negative side. We shall discuss here only the latter type. Relying again on the thermodynamic theory of monolayer adsorption, such behaviour may be expected mainly with liquid pairs showing strong deviations from ideality (one of the decisive factors determining α is the ratio of the activity coefficients in the bulk liquid phase, and this ratio is strongly varying in the case of strong non-ideality, passing through the value 1, at some intermediate composition), a conclusion corroborated by experience. Strong deviations from ideality are connected, however, generally with considerable differences in polarity, and the most polar common liquids are hydroxylic compounds such as low molecular weight alcohols and weak organic acids (besides water, of course). Because of their tendency to hydrogen bonding, they may not be used, with the aim of surface area determination, on highly polar adsorbents of oxidic (or hydroxylic) character. They are, however, well suited in case of apolar or only slightly polar adsorbents, such as most carbonaceous adsorbents (charcoals and carbon blacks). As the other partner of the liquid mixture, benzene seems to be one of the best choices, because (i) deviations from ideality of such mixtures are quite strong and (ii) owing to its polarizability, the affinity of benzene for the adsorbents in question is mostly near to that of the other liquid component so that the ratio of activity coefficients may become the factor decisive for the course of the isotherm, as mentioned above. Further, being interested in monolayer values, a partner of benzene has to be selected the size of which is not too different, because the concept of a mixed monolayer (as will be seen presently, such a monolayer is involved in this case) loses its clear meaning in the case of molecular species of too widely different sizes. In view of all the points raised, mixtures of ethanol and benzene seem to be the most suitable choice.

Mixtures of ethanol and benzene give, on carbonaceous adsorbents, isotherms showing a fairly long practically linear section between their maximum and minimum (in case of more polar charcoals, the latter may become quite shallow or indistinct even, but this circumstance does not invalidate the following arguments). Such a section may be described algebraically by:

$$n^0 \Delta x_1 = a(1 - b x_1),\ b > 1,\ \text{constant.} \tag{10}$$

Comparison with Eq. (2) prompts the interpretation:

$$a = n_1^s,\ ab = n^s,\ a(b - 1) = n_2^s. \tag{11}$$

It can be shown[8] that this interpretation can be regarded as being correct, if we stipulate that n_1^s and n_2^s, respectively, should be characteristic of the minimum amount of liquid the composition of which differs from that of the equilibrium bulk liquid. Evidently, this amount has to be identified with the surface phase. The amounts n_1^s and n_2^s are given directly by the intercepts of the prolongations of the straight part of the isotherm with the ordinates at $x_1 = 0$ and $x_1 = 1$, respectively. It has been found[5] that with mixtures of ethanol and benzene on the said carbonaceous adsorbents, the amounts computed in this way correspond very satisfactorily to a mixed monolayer, so that this procedure is suitable for surface area determination. It has to be emphasized, however, that the occurrence of an isotherm of the above type is by no means a proof of monolayer adsorption in every case: here too, chemisorption and/or special association phenomena may result in double or even thicker layers on the one hand. On the other hand with microporous adsorbents the pore filling model may be more realistic (see the charcoal with specific 'surface area' of 1100 m^2/g in *Table 1*).

Though the above analysis works very well in practice, it has to be conceded that constancy of the composition of the surface layer over an extended range of compositions of the bulk liquid, as implied in the given analysis, has to be rejected on general thermodynamic grounds. This contradiction may be resolved by admitting that the linearity expressed by Eq. (10) exists only within the limits of experimental accuracy, but that in reality the section in question of the isotherm corresponds to a protracted inflexion. It can be shown then[8] that with this assumption, the right hand side of Eq. (10) is the analytical expression of the inflexion tangent, and thus the amounts indicated by Eq. (11) are strictly characteristic of the inflexion point of the isotherm only, without implying that they are really constant over a wider range.

Evidently, isotherms for systems which comprise an adsorption azeotrope cannot give a linear plot according to Everett's expression Eq. (9): at the azeotropic point, this plot must have a break with a jump from $+\infty$ to $-\infty$ (at the azeotropic point $n^0\Delta x_1 = \pm 0$, and $\alpha = 1$). Nevertheless, in cases when the maximum of $n^0\Delta x_1$ preceding the azeotrope is sharp enough, the initial section may be approximately linear if plotted according to Eq. (9), and values of n^s derived from the slope of this section are comparable with those resulting by Eq. (11), as has been shown by Ramakrishna and Suri[7].

When applying relations (4) or (11), respectively, to surface area determinations, suitable values of the surface occupancies of the molecular species involved have to be selected. The values recommended by Kipling[9] (which are near to those to be derived from liquid densities) seem to give most satisfactory results, as may be seen by *Table 1*, showing some comparisons of such surface area determinations with standard BET values. The molecular areas used for computation were: benzene: 180 m^2/mmole (30 Å^2); toluene: 204 m^2/mmole (34 Å^2); ethanol: 120 m^2/mmole (20 Å^2).

SUMMARY

Existing experiences on surface area determinations are discussed, using adsorption isotherms of solutions of non-electrolytes. Modes of evaluation are critically analyzed and most suitable kinds of solutions suggested.

References

[1] J. J. Kipling. *Adsorption from Solutions of Non-Electrolytes*, Academic Press, New York (1965)
[2] J. J. Kipling and E. H. M. Wright. *J. Chem. Soc.* 855 (1962).
[3] G. Schay, L. G. Nagy and T. Szekrényesy. *Periodica Polytechnica* **4**, 95 (1960).
[4] P. V. Cornford, J. J. Kipling and E. H. M. Wright. *Trans. Faraday Soc.* **58**, 74 (1962).
[5] L. G. Nagy and G. Schay. *M. Kém. F.* **66**, 31 (1960).
G. Schay and L. G. Nagy. *Acta Chim. Hung.* **50**, 207 (1966).
[6] D. H. Everett. *Trans. Faraday Soc.* **60**, 1803 (1964).
[7] V. Ramakrishna and S. K. Suri. *Acta Chimica Hung.*, in press.
[8] G. Schay. In *Surface and Colloid Science*, Vol. 2. (Ed. Matijević-Eirich, Wiley-Interscience, New York (1969).
[9] J. J. Kipling and D. B. Peakall. *J. Chem. Soc.* 4828, (1956); 4054, (1957).

DISCUSSION

Professor G. Schay (*Hungarian Academy of Sciences, Budapest*) said: In introducing my paper I wish only to illustrate the main points with some typical data. The quantity $n^s_{1,0}$, the amount of component 1 contained in the surface phase at the limit when component 2 is completely displaced from the surface layer, may be calculated from Eq. (2) as the limiting slope of $f(x_1)$ against x_1, or as the limiting value of $f(x_1)/(1 - x_1)$ as $x_1 \rightarrow 1$ and $n^s_{2,0} \rightarrow 0$. It must be stressed, however, that this quantity may correspond to more than a monolayer, especially when adsorption is not of the purely physical type, but chemisorption or strong association effects are involved.

For example, it has been found that mixtures of benzene or toluene with n-hexane or n-heptane when adsorbed on oxidic adsorbents such as silica gel, give isotherms from which monolayer values in good agreement with the BET values can be derived (*Figure A*). Mixtures of alcohol and benzene also give isotherms of this kind but the amount of alcohol, as computed from the final practically straight section of the isotherm, corresponds to more than a monolayer. This indicates a kind of chemisorption as is seen from the observation (see *Figure A*) that the surface area of silica gels, determined either by the conventional BET method or from adsorption of benzene + heptane, is diminished by pretreatment with alcohol.

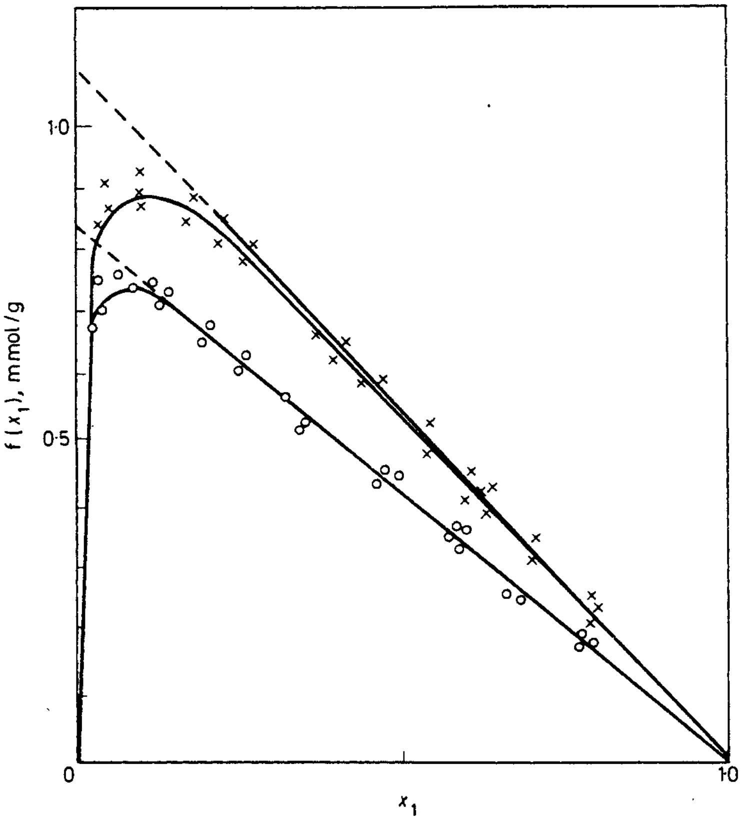

Figure A. Adsorption isotherms of benzene–heptane mixtures over silica gel at 20°C [× — × : not pretreated, $S_{BET} = 210\ m^2/g$, $S_G = 200\ m^2/g$. ○—○ : pretreated with ethanol, $S_{BET} = 160\ m^2/g$, $S_G = 152\ m^2/g$]

Alternatively, one may use Everett's equation (Eq. 9). The data of *Figure A* are shown plotted in this form in *Figure B*. The linearity is excellent and the monolayer capacity derived from the slope gives a surface area of 204 m^2/g.

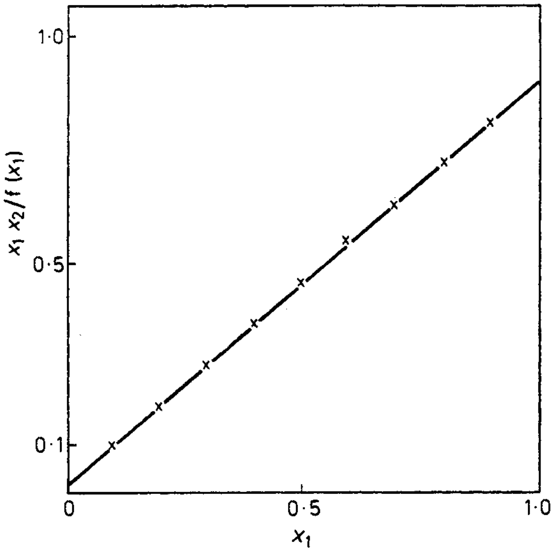

Figure B. Data of *Figure A* plotted according to Everett's equation, viz. Eq. (9). [benzene–n-heptane isotherms at 20° over silica gel] $S_{\mathrm{BET}} = 210\ \mathrm{m^2/g}$

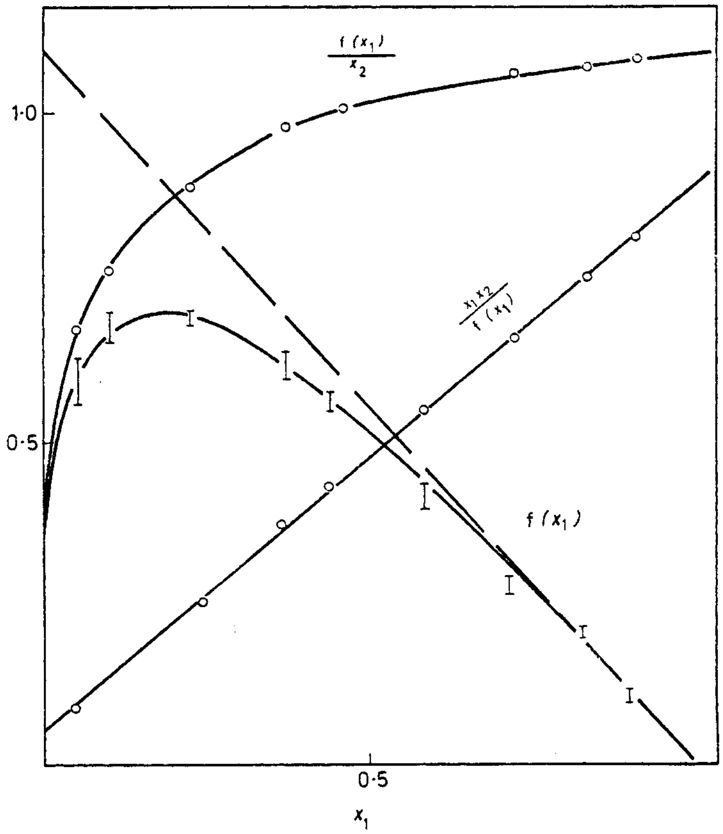

Figure C. Adsorption isotherms of benzene–cyclohexene mixtures over silica gel using the extrapolated value (as described in the text). $S_{\mathrm{BET}} = 210\ \mathrm{m^2/g}$

Equation (9) can be put in a form which allows for the different extents of surface occupied by the two components, namely,

$$\frac{x_1 x_2}{f(x_1)} = \frac{1}{n^s_{1,0}} \left[\frac{\beta}{\alpha - 1} + \frac{\alpha - \beta}{\alpha - 1} x_1 \right],$$

where $\beta = a_{m,2}/a_{m,1}$. Here $a_{m,1}$ and $a_{m,2}$ are the areas occupied respectively by components 1 and 2. The equation reduces to (9) when $\beta \approx 1$ and $\alpha \gg \beta$.

The use of the extrapolated value of $f(x_1)/(1 - x_1)$ to find $n_{1,0}^s$ is illustrated by *Figure C*. Both this method and the use of Eq. (9) lead to values of the surface area close to 210 m^2/g.

It has to be stressed that good linear plot of $x_1x_2/f(x_1)$ is not in itself a guarantee that the slope represents the monolayer capacity. For example, *Figure D* shows data for the adsorption of benzene + diethyl carbonate by charcoal. The apparent slope of the final tangent of $f(x_1)$ gives a value of 1·74 mmol/g for the monolayer capacity for benzene, while the slope of $x_1x_2/f(x_1)$ gives 2·24 mmol/g. The value should be 3·39. At the same time the separation factor, α, is small and decreases from 3·5 to 2·1, the variation being such that there results by an accidental compensation an empirically linear course of $x_1x_2/f(x_1)$.

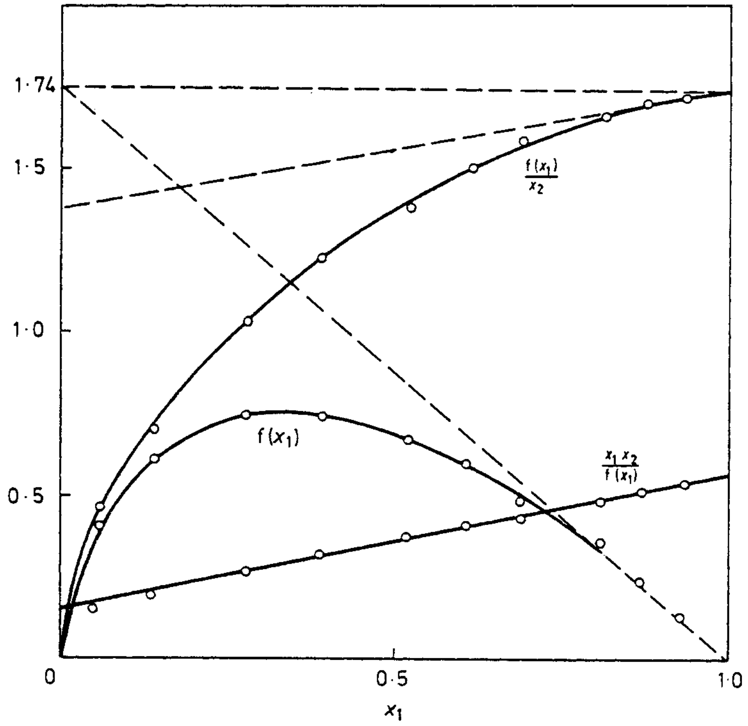

Figure D. Data for the adsorption of benzene + diethylcarbonate by charcoal. $S_{BET} = 620$ m^2/g

On the whole, we conclude that isotherms of the type under discussion can be applied to surface area determination only when preferential adsorption of one of the components is strong enough. A mechanical, uncritical use of apparently convenient isotherms for this purpose may lead to serious misinterpretations.

Finally, *Figure E* is an example of an isotherm with an adsorption azeotrope with a fairly long, practically straight section, from the slope and extrapolated intercepts of which a monolayer value of 570 m^2/g, can be derived† in very satisfactory agreement with the BET value of 590 m^2/g. As may be seen from the figure the experimental uncertainties are considerable enough to allow the apparently straight section to be really a protracted inflexion, as indicated in my paper. The pair ethanol + benzene prove to be a convenient mixture for the determination of the surface area of carbonaceous adsorbents.

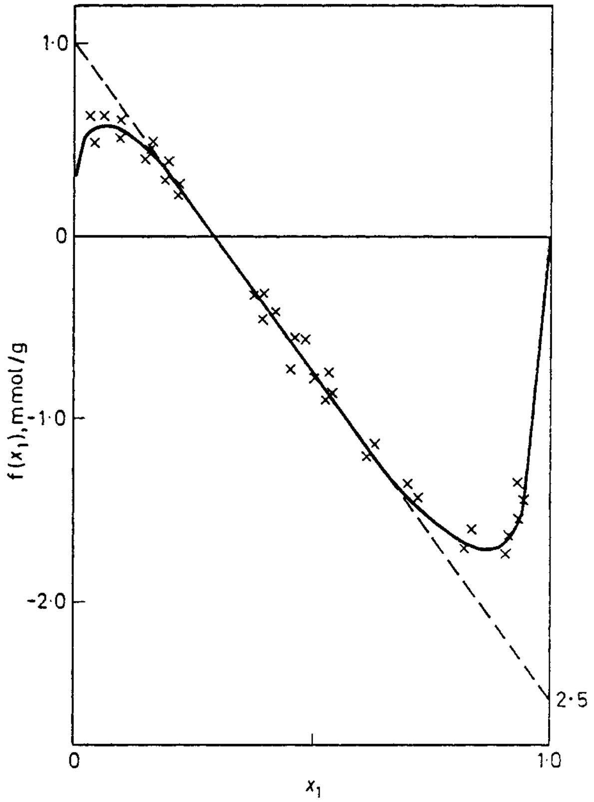

Figure E. Example of an isotherm with an adsorption azeotrope [ethanol–benzene mixture adsorption by charcoal at 20°C]. S_{BET} = 590 m^2/g; S_G = 570 m^2/g

Professor M. M. Dubinin (*Academy of Sciences, Moscow*) said: It is well known that in adsorption from solutions experimental isotherms of the surface excess of $\Gamma_2^{(N)}(N_2)$ or $\Gamma_2^{(V)}(C)$ often have a linear region‡. For such

---

† assuming 1 mmol of benzene covers 180m^2 and 1 mmol of ethanol 120m^2.

‡ N_2 denotes mole fraction and C concentration.

isotherms A. V. Kiselev and later G. Schay suggested a method for finding the limiting adsorption a_{m_2} (or specific surface area) by extrapolating the linear part of the isotherm to $C_2 = 0$ (Kiselev) or to $N_1 = 0$ and $N_2 = 0$ (Schay) as illustrated in *Figure F.* It is possible to show that both these methods are thermodynamically incorrect and cannot in the general case even be considered as approximate. From the accurate equation,

$$\Gamma_2^{(N)} = a_2 N_1 - a_1 N_2 \tag{A}$$

where a_1 and a_2 are the true amounts of the two components in the surface layer one can write for the linear region of the isotherm of $\Gamma_2^{(N)}(N_2)$

$$-\frac{d\Gamma_2^{(N)}}{dN_2} = K = a_1 + a_2 + N_2 \frac{da_1}{dN_2} - N_1 \frac{da_2}{dN_2} = a_1 + a_2 + \Delta \tag{B}$$

As can be seen from *Figure F*, the slope of K is numerically equal to $z = a_1 + a_2$. It is easy to show that Schay's supposition $z = a_1 + a_2$ can be fulfilled only on condition that,

$$\frac{da_2}{dN_2} = 0 \quad \text{and} \quad \frac{da_1}{dN_2} = 0 \tag{C}$$

This condition does not stem from the existence of the linear region in the isotherm of $\Gamma_2^{(N)}(N_2)$. It is an independent additional requirement, which is in contradiction with thermodynamics.

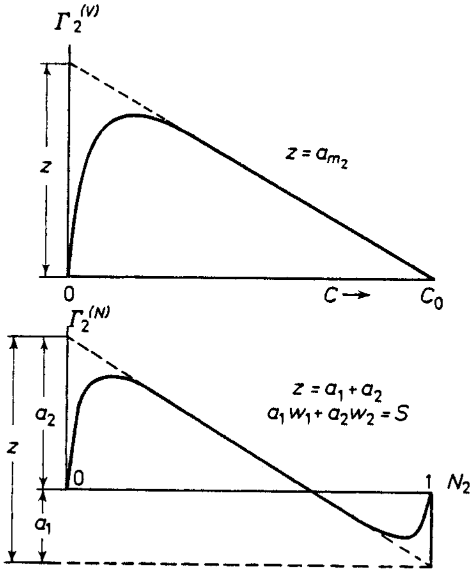

Figure F. Determination of limiting adsorption (G. Schay)

Indeed, from condition (Eq. C) it follows that $\mathrm{d}N_2^\sigma/\mathrm{d}N_2 = 0$, i.e. with a change in the composition of the bulk solution in the range corresponding to the linear region of the isotherm the composition of the surface solution should remain unchanged. This means that with a change in the chemical potential of a particular component in the bulk solution its chemical potential in the surface layer should remain constant, which is inconsistent with the condition of thermodynamic equilibrium. A rigorous proof of the impossibility of the equality $\mathrm{d}N_2^\sigma/\mathrm{d}N_2$ at far-from-critical temperatures has been given by Rusanov in his monograph *Thermodynamics of Surface Phenomena*. The value of the derivative $\mathrm{d}a_2/\mathrm{d}N_2$ cannot be determined from the curve of $\Gamma_2^{(N)}(N_2)$ alone, therefore Schay's or Kiselev's method cannot even be considered as approximate, since it is impossible to estimate the error in determining the specific surface area s or the adsorption volume W_0. We can only assert that the values of S or W_0 obtained by these methods will always be smaller than the true ones, because in Eq. (B) at $\mathrm{d}a_2/\mathrm{d}N_2 > 0$ $\Delta < 0$ in all cases [O. G. Larionov, L. G. Tonkonog and K. V. Chmutov. *Zh. fiz. Khimii* **39**, 2226 (1965)].

Professor G. Schay replied: Dubinin seems to have overlooked that, in order to eliminate any conflicts with thermodynamic requirements, we have dropped by now our previous assumption of the composition of the adsorbed layer remaining constant over an extended range of compositions of the equilibrium bulk liquid. In my present paper I state clearly that we think now that any observed linearity, mainly of isotherms having an infexion, is not rigorous but apparent only, existing only within the limits of experimental accuracy. The straight lines we draw through the scattered experimental points represent the asymptotic final tangent or the inflexion tangent of the isotherm, respectively, and thus the adsorption values derived from their slopes do not refer to extended regions but to single points of the respective isotherms only. It seems safe to assume that at these single points, the derivatives of the adsorbed amounts are, if not exactly zero, at least negligibly small.

Dubinin's theoretical arguments that our graphical procedure must give surface area values inferior to the true ones thus become pointless and his conclusions are refuted by experience, as may be seen from the data presented in *Table 1* of the paper which are but a small selection of a much greater number of similarly good results. So far our method, when handled with due circumspection, never failed to give results in very satisfactory agreement with conventional BET values calculated from nitrogen isotherms.

As far as we are aware, A. V. Kiselev's attempts to determine adsorption volumes have very little in common with our procedure, and we are of the opinion that any representation in terms of $\Gamma^{(V)}(C)$ can be adequate only in the case of practically ideal solutions, i.e. when the partial volumes of the mixture components are independent of composition.

Professor J. Th. G. Overbeek (*van't Hoff Laboratory, Utrecht, Netherlands*) said: At the end of the paper, areas per mole are mentioned for benzene, toluene and ethanol and it is added that they 'are near to those to be derived from liquid densities'. I do not consider it good practice to suggest that the molecules in the first adsorption layer are packed in the same way as in the liquid. For non-spherical molecules one has to expect a preferred orientation and an agreement between the area per molecule in the surface and the area calculated from the liquid density assuming that the molecules are spherical can at best be fortuitous. Incidentally the same remark applies to the nitrogen area (as derived from liquid-density) used in the BET method.

Professor G. Schay replied: Overbeek's remarks are certainly justified. We ourselves consider the quoted values as mainly empirically satisfactory and the remark in parentheses objected to by Overbeek was by no means meant to suggest that areas per molecule should be generally calculated from liquid densities. In fact, the value used for ethanol (20 Å^2 per molecule) is sensibly smaller and thus accounts for some orientation. In trying to explain the peculiar coincidence in other cases, one may perhaps bear in mind that in the case of liquid mixtures comprising not too big molecules of comparable sizes, any molecule at the surface is surrounded to more than half by other liquid molecules so that the orienting forces of the solid surface may be counteracted to a considerable extent by thermal motion in the liquid when chemisorption is excluded.

DETERMINATION OF THE SURFACE AREA OF SOLIDS FROM SOLUTION ADSORPTION

Yu. A. Eltekov

Institute of Physical Chemistry,
Academy of Sciences, Moscow, U.S.S.R.

The investigation of adsorption from binary liquid mixtures onto adsorbents of different chemical nature[1, 2] allows us to estimate the surface area of highly dispersed porous solids.

A number of cases of adsorption from solution which have been used for surface area determination have been discussed by Giles and Nakhwa[3] and Gregg and Sing[4]; both sets of authors discuss the possibilities and limitations of the method.

Analysis of the adsorption data obtained from solutions of two completely miscible liquids indicates that the Gibbs adsorption values $\Gamma^{(n)}$, as a rule, does not exceed the quantity a_{m_i}, the monolayer capacity. Therefore it is probable that the action of adsorption forces on the composition of the solution is limited mainly to the monolayer and that molecular reorientation in the adsorbed state does not take place in most cases.

The equation derived for monomolecular adsorption, in its simplest form, assumes ideal bulk and surface solutions, i.e. the solution component molecules are of the same chemical type and the molecular interaction forces are identical. This gives,

$$\Gamma_1{}^{(n)} = \frac{a_m K x_1 x_2}{1 + (K - 1)x_1} \tag{1}$$

where x_1 and x_2 are the mole fractions of components 1 and 2 in the bulk solution and K is an equilibrium adsorption constant. This equation has been derived by a number of different workers[1, 5].

Equation (1) can be written in the following linear form,

$$\frac{x_1 x_2}{\Gamma_1{}^{(n)}} = \frac{1}{a_m K} + \frac{K - 1}{a_m K} x_1 \tag{2}$$

For large K values a_m can be obtained from the slope and K from the intercept on the ordinate.

With the amounts adsorbed expressed as mol/g and solution conditions which are close to ideal we can find from equation (2) the monolayer capacity a_m in mol/g. Hence if ω_m is the area for one molecule of the adsorbed component the surface area of the adsorbent is given by,

$$S = a_m N_A \omega_m \tag{3}$$

With the introduction of γ_i and γ_i^s, activity coefficients of the components in the bulk and surface solutions respectively, equation (1) becomes,

$$\Gamma_1^{(n)} = \frac{a_m K\,(\gamma_1 x_1/\gamma_1^s)\cdot(\gamma_2 x_2/\gamma_2{}^s)}{1+(K-1)\gamma_1 x_1/\gamma_2^s} \tag{4}$$

However, the extra terms can be neglected in the case of large K values (high positive adsorption of component 1) and in the range of x_1 values at which γ_1/γ_2 and γ_1^s/γ_2^s are close to unity.

When equation (1) is applied to microporous adsorbents of active carbons and zeolites it gives not the monolayer capacity but the adsorption volume, i.e. essentially the microporous volume. Hence binary liquid mixtures, such as benzene–cyclohexane (or n-hexane) ($\omega_m \simeq 40$ Å^2) and dioxane–cyclohexane ($\omega_m \simeq 40$ Å^2), in which the molecules are of similar form and size

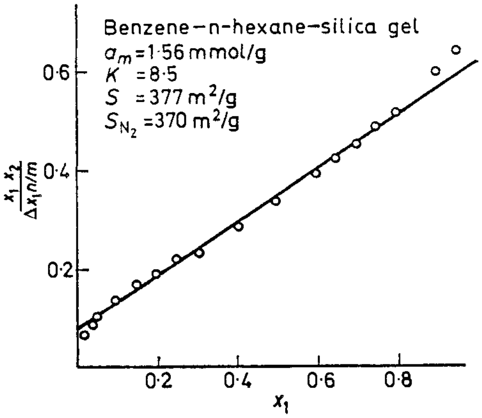

Figure 1. Isotherm of benzene adsorption from n-hexane solution on macroporous hydroxylated silica gel

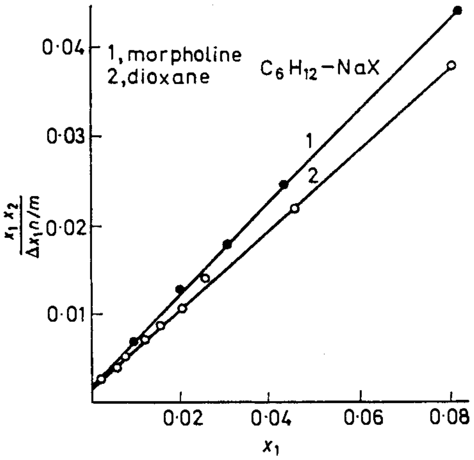

Figure 2. Morpholine and dioxane adsorption isotherms, from cyclohexane solution, by zeolite crystals NaX

are suitable for the surface area determination of macroporous and nonporous adsorbents.

An adsorption isotherm of benzene from n-hexane on a hydroxylated macroporous silica gel[5] (pore diameter d = 100 Å) is shown in *Figure 1.* The experimental points lie on a straight line over a wide range of equilibrium concentrations. A surface area of 376 m^2/g is obtained from an $a_m = 1{\cdot}56$ mmol/g. The surface area obtained is close to the value obtained by the adsorption of nitrogen at low temperatures using the BET method.

Adsorption isotherms of morpholine and dioxane from cyclohexane onto zeolite crystals are shown in *Figure 2.* The experimental points fit a straight line with $K = 980$ and $a_m = 1{\cdot}99$ mmol/g for morpholine and $K = 250$ and $a_m = 2{\cdot}2$ mmol/g for dioxane, as calculated from equation (2). A value of 480–500 m^2/g is obtained for the surface area of NaX from this value of a_m. The value of a_m should however be taken as the maximum micropore absorption capacity for the large crystal zeolite cavities of NaX and equation (4) should be used for this case and not equation (1).

References

[1] A. V. Kiselev. *Uspechi Chemii.* **25**, 705 (1955).
[2] J. J. Kipling· *Adsorption from Solution of Non-Electrolytes* Academic Press, London, New York, 1965.
[3] C. H. Giles and S. N. Nakhwa. *J. Appl. Chem.* **12**, 266 (1962).
[4] S. J. Gregg and K. S. W. Sing. *Adsorption, Surface Area and Porosity.* Academic Press, London, New York, 1967.
[5] Yu. A. Eltekov and A. V. Kiselev. *Molecular Sieves.* 1967, 267. Ed. Symes.
[6] A. V. Kiselev and L. F. Pavlova. *Neftechemie.* **2**, 861 (1962).
[7] D. A. Usmanova, Yu. A. Eltekov and E. A. Azipov. *Usbek. Zhurnal,* **1**, 31 (1969).

DETERMINATION OF THE ACCESSIBLE SURFACE AREA OF POROUS SILICAS BY THE ADSORPTION OF POLYSTYRENE

YU. A. ELTEKOV

Institute of Physical Chemistry,
Academy of Sciences, Moscow, U.S.S.R.

The maximum adsorption values of different vapours on active carbon and zeolites have shown that these amounts when expressed in ml of liquid adsorbed per g depend on the sizes and shapes of the adsorbate molecules rather than obeying the Gurvich Rule. This effect is caused by the ultraporous structure of the adsorbent or, the so-called, molecular-sieve effect[1–3].

The pore size distribution becomes more evident from a study of the interaction of large molecules and polymer macromolecules with porous silicas. It has also been shown that alumina and silica gels[4–6] with pore diameters less than 100 Å adsorb less polydimethyl siloxane and polystyrene than would be expected from the total surface area available[7–8].

At present many workers[9, 10] assume that the behaviour of linear polymer molecules can be described by a random coil. The mean square distance between the ends of the macromolecular chain in this coil is termed $\bar{r}^2$. In the general case for a macromolecule consisting of N links where the length and direction of each bond is described by the vector l then $\bar{r}^2$ is given by,

$$\bar{r}^2 = \sum_{i}^{N} \sum_{j}^{N} (l_i l_j) \qquad (1)$$

where the summations are taken over all pairs of links in the chain.

The particular solution of this equation under conditions of free rotation around the chain bonds for linear macromolecules leads to the expression[11],

$$\bar{r}^2 = Nl^2(1 - \cos\theta_1)(1 - \cos\theta_2)/(1 - \cos\theta_1 \cos\theta_2) \qquad (2)$$

where θ_1 and θ_2 are the bond angles in the chain. It is evident from equation (2) that $\bar{r}^2$ is directly proportional to the weight $M = M_z N$, where M_z is the mass of one element of the chain, and depends on the band angles in the chain. The ratio $\bar{r}^2/M = 49 \times 10^{-2}$ was obtained for polystyrene[12]. The values calculated for atactic polystyrene of different molecular weights are summarized in *Table 1* together with the values of the mean diameter of the polymer macromolecule. D was calculated from,

$$D = (M \,.\, [\eta]/\Phi)^{1/3} \qquad (3)$$

where $[\eta]$ = intrinsic viscosity and Φ is a parameter independent of the nature of the polymer and solvent which was put equal to $7{\cdot}8 \times 10^{23}$.

Table 1. The values $(\bar{r}^2)$ and D for polystyrene macromolecules of different molecular weights (M)

$M\,10^{-3}$	1	10	40	90	160	250	360	490	640	1000
$(\bar{r}^2)^{\frac{1}{2}}$	20	70	140	210	280	350	420	490	550	700
D	—	50	140	205	260	340	410	460	550	—

As can be seen from *Table 1* the diameters of polystyrene molecues having molecular weights in the range 10^3 to 10^6 lie in the region 20 to 100 Å. Many factors such as the nature of the solvent, temperature, concentration and field of force in the neighbourhood of the surface affect the macromolecule conformation and size. There is no doubt, however, that polymer fractions with narrow distributions of molecular weight are valuable materials for studying the accessible surface of different adsorbents and the transition into macroporous regions. The adsorption isotherms of macromolecules on nonporous adsorbents are usually characterized by a plateau on the isotherm and the maximum adsorption depends to some extent on the molecular weights within the limits of M from 10^4 to 10^6. Adsorption isotherms for materials within this range can be used for a comparison of the amounts adsorbed and for the estimation of accessible surface area.

We have investigated the adsorption of polystyrene (M_1 = 40 000 and M_2 = 300 000) from solution on to a nonporous silica with a surface area of 170 m^2/g and also on to silica gels with pores of different sizes (see *Figure 1*).

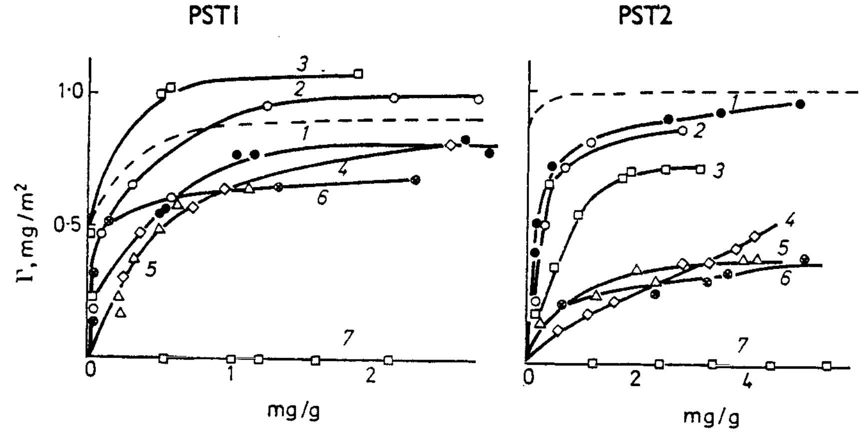

Figure 1. Adsorption isotherms of polystyrene on aerosil (broken line) and silica gels. Numbers on isotherms correspond to numbers on samples in *Table 2*

The surface areas of the silicas were determined by nitrogen adsorption using the BET method and taking 16·2 Å^2 for the area per nitrogen molecule. In the case of aerosil and macroporous silica gels with a pore size of 500–1000 Å, the adsorption isotherms, with adsorption expressed as mg/m^2, are almost coincident; the maximum adsorption of polystyrene for both fractions was approximately 0·9 mg/m^2. This coincidence probably indicates the complete and equal accessibility of nonporous and macroporous silica surfaces to the polystyrene molecule and to the nitrogen molecule. The values of the silica gel surface accessible to polystyrene molecules were calculated from the maximum values of polystyrene adsorption (*Table 2*).

Table 2 shows that the surface available to polymer molecules depends on molecular weight and silica gel pore size. The values for the surface area available to macromolecules are of great importance for highly dispersed porous solutes which are used as fillers in polymer compositions. For this case estimation of areas by nitrogen or vapour adsorption (e.g. benzene or butane) leads to high values.

It is to be noted that diffusion plays a significant role in the adsorption of macromolecules by porous solids. Molecules whose size is less than a silica gel pore diameter penetrate slowly into the silica gel pores and adsorption equilibrium is attained very slowly. In this case it is not relevant to speak about adsorption isotherms.

Table 2. The values of surface area of silica gels accessible for polystyrene macromolecule

Sample	*Pore diameter* *d* (Å)	S (m^2/g)			S_{PST1}/S_{BET}	S_{PST2}/S_{BET}
		BET	PST 1	PST 2		
Aerosil	—	170	170	170	1	1
Silica gel 1	800	24	23	23	0·95	0·95
2	550	50	50	45	1·0	0·9
3	410	95	95	70	1·0	0·7
4	280	120	100	60	0·8	0·5
5	220	130	85	45	0·65	0·35
6	140	340	220	120	0·65	0·35
7	110	300	5	3	0·02	~0·01

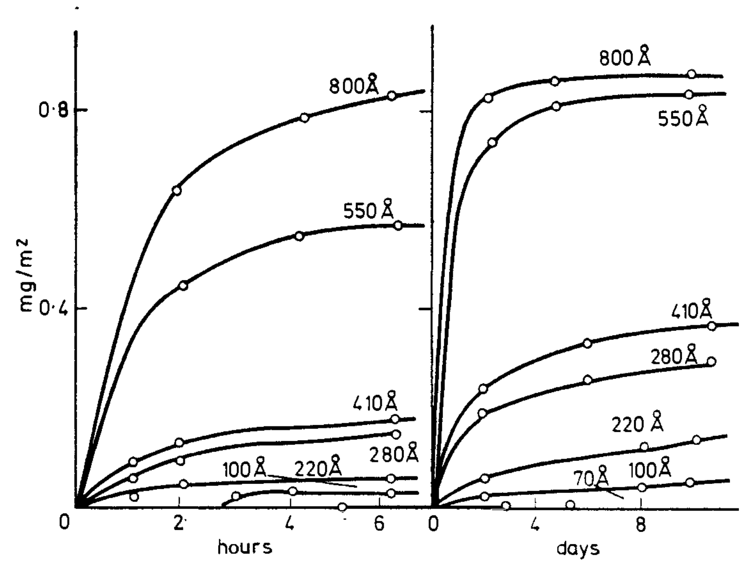

Figure 2. Kinetics of adsorption of polystyrene on silica gels at 20°C. Pore diameter is shown on isotherms

Kinetic polystyrene adsorption curves ($M = 300\,000$) on different silica gels are shown in *Figure 2*. The surface areas of the silicas were calculated by nitrogen adsorption using the BET method. Adsorption equilibrium on a silica gel specimen with a pore size of 220–410 Å is attained more slowly than with the other samples. This effect is shown more clearly when the time taken to reach half the equilibrium amount of adsorption is plotted against pore size (*Figure 3*). The extent of adsorption corresponding to an equilibrium situation was determined by stirring the silica gel suspension in a polystyrene solution for two weeks. The sharp maxima in the curves (*Figure 3*) indicate the hindrance of diffusion of macromolecules into pores of comparable size to the macromolecules. It should be noted that this curve allows an approximate estimate of the polymer molecule size, i.e. *ca.* 200 Å for the case shown. An increase in temperature affects the macromolecular penetration but does not significantly affect the amounts adsorbed at equilibrium.

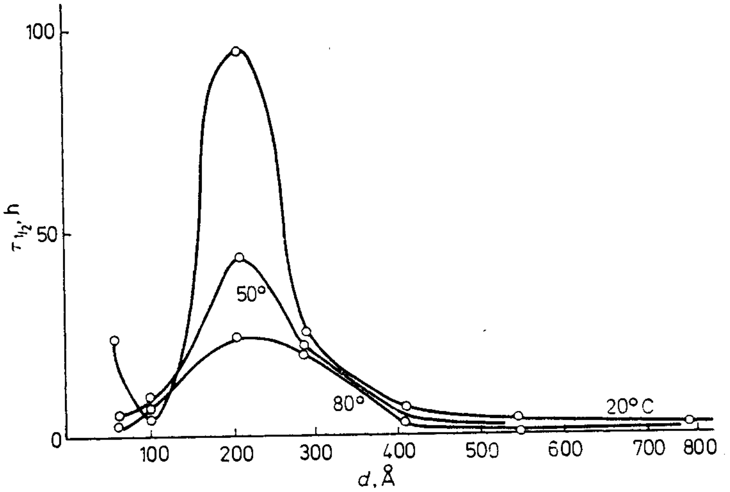

Figure 3. Amount adsorbed at half the time taken to achieve equilibrium adsorption plotted against the pore diameter of silica gels at 20, 50 and 80°C

Thus a set of polystyrene fractions, having a narrow range of molecular weights, allows a quantitative estimate of the accessible surface area to be made for molecules of different molecular weight. It also allows an estimate to be made of the inner and outer surface area of a solid.

References

[1] S. Brunauer. *The Adsorption of Gases and Vapours*, Oxford University Press, London, 1943.
[2] A. V. Kiselev, V. N. Semenova and Yu. A. Eltekov. *Kinetika i Katalis* **3**, 261 (1962).
[3] S. J. Gregg and K. S. W. Sing. *Adsorption, Surface Area and Porosity*, Academic Press, London and New York (1967).
[4] E. Jenkel and B. Rumbach. Z. *Elektrochem.* **55**, 612 (1951).
[5] W. Heller and W. Tanaka. *Phys. Rev.* **82**, 302 (1951).
[6] J. Koral, R. Ullman and F. R. Eirich. *J. Phys. Chem.* **62**, 541 (1958).
[7] A. V. Kiselev, V. N. Novikova and Yu. A. Eltekov. *Doklady Akad. Nauk* **149**, 131 (1963).
[8] E. K. Bogacheva, A. V. Kiselev, Yu. S. Nikitin and Yu. A. Eltekov. *Vysokomolek. soedineniya* **10A**, 574 (1968).
[9] P. J. Flory. *Principles of Polymer Chemistry*, Cornell University Press, Ithaca, 1953, p. 579.
[10] H. Morawetz. *Macromolecules in Solution*, Interscience Publishers, New York, 1965.
[11] H. Kuhn and W. Kuhn. *Helv. Chim. Acta* **28**, 1533 (1945).
[12] W. R. Krigbaum, D. K. Carpenter and S. Newmen. *J. Phys. Chem.* **62**, 1587 (1958).

SPECIFIC SURFACE AREAS OF GRAPHITIZED CARBON BLACKS FROM HEATS OF IMMERSION

J. H. CLINT, J. S. CLUNIE, J. F. GOODMAN and J. R. TATE

Procter & Gamble Newcastle Technical Centre, Basic Research Department, Newcastle upon Tyne, U.K.

The heats of immersion in liquid n-alkanes of two graphitized carbon blacks (Graphon, a high area solid, and Sterling MT, a low area solid) have been measured calorimetrically at 298°K. The heat of immersion data for the bare solids, and for the solids precoated with n-alkane from the vapour phase, have been used together with the measured enthalpies of the liquid n-alkane/air interface to calculate specific surface areas for the solids. The results obtained by this calorimetric method have been compared with specific surface areas obtained from nitrogen adsorption at 77°K and vapour phase adsorption of n-alkanes at 298°K.

For Graphon, there is good agreement between surface areas obtained by the calorimetric and gas adsorption methods, but, for Sterling MT, agreement is less satisfactory due to the low specific surface area involved.

INTRODUCTION

The most widely used method for determining the specific surface area of a solid is based on measurements of the physical adsorption of gases and analysis of the adsorption isotherms using the BET equation[1]. The method requires a knowledge of two quantities at monolayer coverage, namely the specific uptake, n_m^σ (in mol g^{-1}), and the area occupied per adsorbed molecule, a_l (in nm^2). Although the uptake, n^σ, can be accurately obtained by experiment, the exact point on the gas adsorption isotherm at which the monolayer is complete, i.e. n_m^σ, is less certain. The second parameter, a_l, can be estimated from the liquid density of the adsorbate, but the effective area per molecule, even for such a commonly used gas as nitrogen, is still in doubt. For example, estimates of a_l for nitrogen on graphitized carbon blacks range from 0·154 to 0·200 nm^2 (15·4 to 20·0Å^2)[2,3].

Alternatively, the surface area of a solid may be determined from heat of immersion studies. With the general availability of modern commercial calorimeters it has recently become much easier to measure heats of immersion and it seems appropriate to re-examine the calorimetric method for obtaining the specific surface area of a solid. The calorimetric method can be used in two ways: (i) immersion in pure liquid of the bare outgassed powdered solid[4], and (ii) immersion in pure liquid of the powdered solid precoated from the vapour phase with a duplex layer of the same liquid[5]. The first approach is open to several objections, in particular to the effects of surface heterogeneity and the limitation that the enthalpy of the solid/liquid interface, h_{SL}, must be known. These objections may be removed by precoating the surface with a layer of the liquid from the vapour phase.

The present investigation has been mainly confined to this second approach. Specific surface areas of a high and a low area graphitized carbon black, Graphon and Sterling MT respectively, have been determined from heats of immersion in liquid n-alkanes. The results have been compared with the specific surface areas obtained by gas adsorption methods.

EXPERIMENTAL

Materials

Graphon (Cabot Corporation) had a specific surface area of 92 m^2g^{-1} determined by a Cabot 'Adsorptograph' using nitrogen ($a_l = 0{\cdot}162$ nm^2, 16·2$Å^2$) at 77°K[6]. Examination in a Siemens Elmiskop 1 electron microscope showed that Graphon, even after ultrasonic dispersion, consisted of aggregates of roughly spherical primary particles with diameters in the range 25–35 nm (250–350Å). Selected area electron diffraction from areas 2 μm in diameter gave sharp ring patterns characteristic of aggregates of small crystallites. The patterns were indexed on the basis of reflections of the type (00.*l*) and (*hk*.0).

Sterling MT (Cabot Corporation) had a quoted specific surface area of 7–10 m^2g^{-1}. Examination in the electron microscope showed that the sample consisted mainly of individual polyhedral particles with diameters in the range 0·1 to 0·5 μm. Selected area electron diffraction gave sharp ring patterns from the smaller crystallites, as for Graphon, together with superimposed single crystal spot patterns from the larger crystallites.

n-Alkanes of even chain length from hexane to hexadecane (Fluka AG) were puriss grade ($\geqslant$99·9 per cent) for vapour adsorption studies and for precoating of adsorbents before immersion calorimetry, and purum grade ($\geqslant$99 per cent)for the immersion fluid in the calorimeter. Alkane purity was checked by gas–liquid chromatography using both polar (polyethylene glycol adipate) and non-polar (Apiezon L) columns.

Methods

(i) Surface tensions of the puriss grade n-alkanes were measured at four temperatures in the range 288 to 308°K by the pendant drop method[7]. Drops were suspended from a glass syringe in an enclosed optical cell, to provide a saturated atmosphere, and then photographed using parallel monochromatic light. The dimensions of the hanging drop profile were measured from the image on the photographic plate using a projectorscope (Precision Grinding Ltd.). With this technique, the surface tensions of the n-alkanes were measured to $\pm$ 0·05 mN m^{-1} (dyne/cm).

(ii) Adsorption isotherms for n-alkane vapours on the graphitized carbon blacks were determined at 298°K using a Cahn RG microbalance to measure the uptake of adsorbate and either a mercury manometer or a thermistor gauge to measure the equilibrium vapour pressure. The thermistor pressure gauge was calibrated against a low ratio McLeod gauge.

(iii) Heats of immersion were measured using an L.K.B. 8700 calorimeter system with recorder output. Precoated samples ($\sim$ 0·5 g) of the adsorbents were prepared in thin-walled glass bulbs attached to the manifold of a vacuum system containing a Cahn RG microbalance to monitor the amount of alkane adsorbed on a reference sample. The glass bulbs, containing adsorbent precoated with n-alkane to known coverages, were broken in liquid n-alkane, and the heat of immersion of the precoated material was measured. The heat evolved on breaking empty glass bulbs in each liquid n-alkane used was also determined and found to vary from 0·08 to 0·13 J (0·02–0·03 cal) with an uncertainty of 0·02 J (0·005 cal).

RESULTS

(i) The surface tensions, γ_{LV}, of the n-alkanes are recorded in *Table 1.* From the variation of γ_{LV} with temperature, the enthalpy, h_{LV}, of the liquid alkane/air interface at 298°K was calculated from the equation

$$h_{LV} = \gamma_{LV} - T\,(\partial \gamma_{LV}/\partial T)$$

and the values are listed in *Table 1.* Comparison of the present data with the literature[8] shows that the surface free energies (γ_{LV}) agree to ± 0·5 per cent and the surface enthalpies (h_{LV}) of the liquid n-alkane/air interface agree to ± 3 per cent.

Table 1. Thermodynamic quantities for the n-alkane/air interface

n-Alkane	*Surface free energy* (γ_{LV}) (mJ m^{-2}) (± 0·05)					*Surface entropy* ($-\partial\gamma_{LV}/\partial T$) (mJ m^{-2} K^{-1} (± 0·005)	*Surface enthalpy* (h_{LV}) (mJ m^{-2}) (± 1·5)
	288°K	293°K	298°K	303°K	308°K	298°K	298°K
n-Hexane	19·11	18·63	18·11	17·60		0·100	47·9
n-Octane		21·67	21·20	20·69	20·25	0·095	49·4
n-Decane		23·71	23·30	22·88	22·41	0·087	49·2
n-Dodecane		25·24	24·87	24·45	23·98	0·085	50·2
n-Tetradecane		26·33	25·89	25·51	25·01	0·087	51·8
n-Hexadecane		27·28	26·80	26·34	25·85	0·095	55·0

(ii) From vapour adsorption data at several temperatures, the isosteric heats of adsorption, q_{st}, for n-hexane and n-octane on Graphon, and for n-hexane on Sterling MT, were calculated using the Clausius-Clapeyron equation

$$\left(\frac{\partial \ln p}{\partial T}\right)_{n^\sigma} = \frac{q_{st}}{RT^2}$$

where n^σ is the measured uptake and p the equilibrium pressure. The variation of q_{st} with n^σ for n-hexane on Graphon is given in *Figure 1,* and the mean of several literature values for the heat of liquefaction, ΔH_L, of n-hexane at 298°K [31·2 ± 0·3 kJ mol^{-1} (7·45 ± 0·07 kcal mol^{-1})] is also shown.

(iii) Heats of immersion, ΔH_{imm}, for Graphon precoated with n-hexane into n-hexane are recorded graphically in *Figure 2* for the full coverage range. Results for other systems are listed in *Table 2.* The surface coverages are expressed as μmol g^{-1} and also in terms of θ, the number of BET monolayers, obtained from the adsorption isotherms. A finite limit to the precision of the measured heats of immersion is set by the small sample size (0·5 g) which, in turn, is determined by the size of bulb that can be accommodated in the L.K.B. calorimeter.

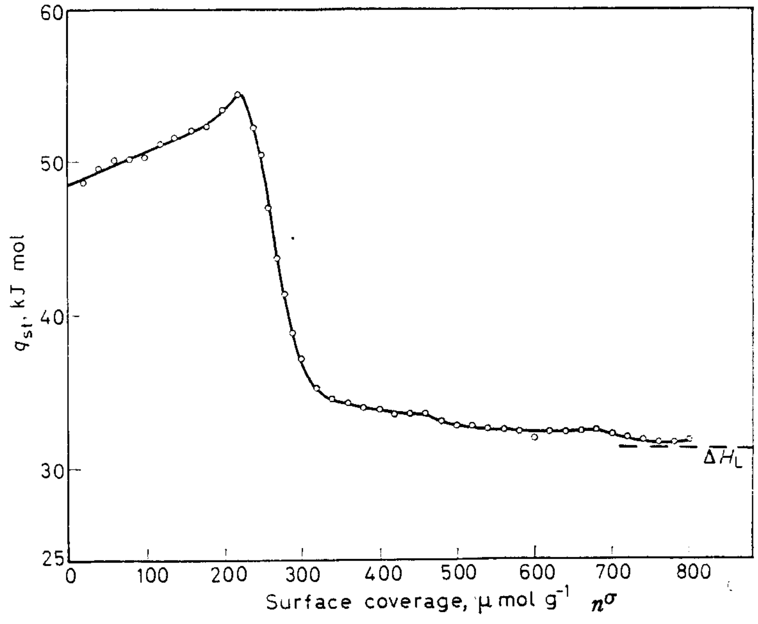

Figure 1. Mean isosteric heats of adsorption of n-hexane on Graphon in the temperature range 288–318°K (ΔH_L = heat of liquefaction at 298°K).

DISCUSSION

The Harkins and Jura calorimetric method[5] for the determination of surface areas was originally designed as a primary standard for other techniques. The method involves equilibration of the outgassed solid with saturated vapour ($p/p_0 = 1$) of the immersion fluid, followed by immersion of the equilibrated solid with its adsorbed layer in the pure liquid. It assumes that if the adsorbed layer is sufficiently thick its outer surface will have an enthalpy per unit area identical to that of the pure liquid surface. Under perfect wetting conditions, ($\cos\theta = 1$) the specific area of the outer surface of the adsorbed layer is given by

$$A' = \Delta H_{\mathrm{imm}}/h_{\mathrm{LV}}$$

where ΔH_{imm} is the measured heat of immersion (J g^{-1}) of the equilibrated solid and h_{LV} is the surface enthalpy (J m^{-2}) of the liquid/vapour interface. For small spherical particles, where the thickness of the adsorbed layer (t) is not negligible in comparison with the mean particle radius (r), A' will be larger than A, the specific surface area of the solid, and a correction must be applied:

$$A = \frac{A'r^2}{(r+t)^2}$$

Table 2. Heats of immersion versus coverage and derived specific surface areas

Solid	*Liquid*	*Coverage*		*Heat of immersion* ($\mathrm{J\,g^{-1}}$)	*Specific surface area*	
		μmol $\mathrm{g^{-1}}$	θ (BET monolayers)		*Measured* ($\mathrm{m^2g^{-1}}$)	*Corrected* ($\mathrm{m^2g^{-1}}$)
Graphon	n-Hexane	0	0	10·3	84 (122)†	
		518	2·0	4·72	98	86
		687	2·65	4·35	90	79
		1290	5·0	4·98	104	76
		2000	8·0	3·13	65	42
	n-Octane	0	0	11·6	91 (127)†	
		414	2·0	5·12	104	91
		460	2·3	5·1	103	90
		520	2·6	4·5	91	80
	n-Dodecane	0	0	13·3	85 (157)†	
		260	1·6	4·57	91	85
Sterling MT	n-Hexane	0	0	1·18	9·7 (122)†	Correction insignificant
		47·5	1·9	0·69	14·4	
		69·6	2·7	0·76	15·9	
		87·5	3·4	0·70	14·6	
	n-Octane	0	0	1·28	10·0 (127)†	Correction insignificant
		40·7	~2·0	0·57	11·5	

† Numbers in parentheses are enthalpies [mJ $\mathrm{m^{-2}}$ ($\mathrm{erg/cm^2}$)] of the corresponding Graphon/n-alkane interface obtained by Everett[10] and used to calculate the surface areas from heats of immersion of the bare solids.

For low area solids, this method has given reasonable agreement with areas obtained by other techniques, but, for high area solids, saturated vapour conditions can lead to condensation of liquid in the interstices between small particles, thus resulting in smaller surface areas than those obtained by gas adsorption methods. In the present study, the low surface area value for Graphon precoated with 8 monolayers of n-hexane (*Table 2*) constitutes direct confirmation of this viewpoint.

An added complication is the need to know the thicknesses of the adsorbed layers at $p/p_0 = 1$, and these Jura assumed[9] to be 2·5 nm (25Å) for water and 20 nm (200 Å) for n-heptane. Such thickness values correspond to more than eight and forty monolayers respectively. The present heat of immersion data for graphitized carbon blacks and n-alkanes indicate that such thick adsorbed layers are not necessary in order to obtain reasonable surface areas for homogeneous non-porous solids. This conclusion is directly confirmed by the results for the variation in isosteric heat of adsorption with surface coverage for n-hexane on Graphon (*Figure 1*). At coverages just above one BET monolayer, q_{st} is almost equal to the heat of liquefaction of the n-hexane, the residual difference ($<$ 10 per cent) having disappeared when the third adsorbed layer has been added at $p/p_0 = 0{\cdot}7$.

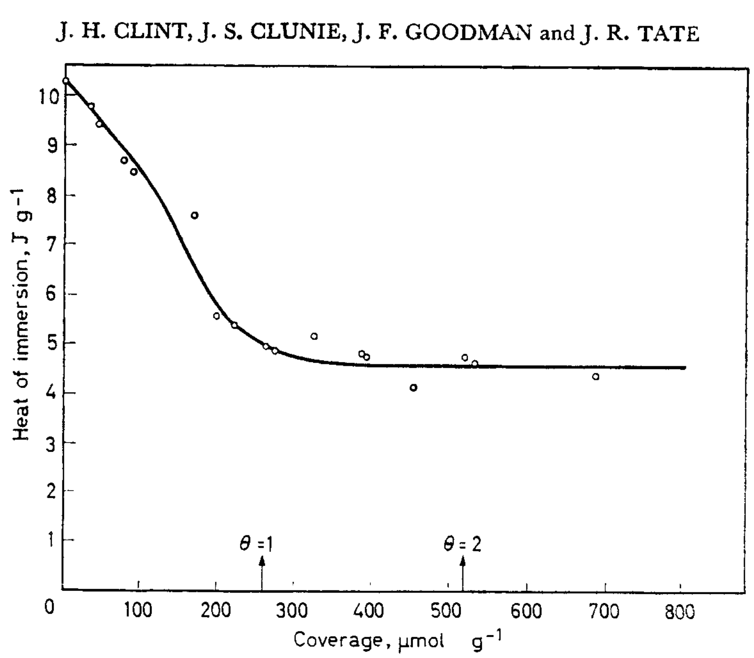

Figure 2. Heat of immersion of Graphon in n-hexane at 298°K.

Heats of immersion plotted against surface coverage (*Figure 2*) fall steeply over the first monolayer region and reach a limiting value above ~1·5 monolayer coverage. Taking the heat of immersion values above this coverage level and dividing by the surface enthalpy of the n-alkane/air interface (*Table 1*) gives the measured values for the specific surface areas shown in *Table 2*.

Surface areas obtained from heats of immersion of bare solid were calculated using values for the enthalpy per unit area of the Graphon/n-alkane interface (h_{SL}) obtained by Everett[10]. These values in mJ m^{-2} (erg/cm^2) are shown in parentheses in *Table 2*. This method is essentially comparative in nature since a value for the surface area of a reference sample is first required in order to determine h_{SL}.

Graphon

Since the average Graphon particle diameter is ~30 nm, it is necessary to correct the area calculated from heat of immersion data for precoated samples for the increase in area of each particle due to the presence of a layer of adsorbed liquid. At monolayer coverage the shorter chain length n-alkanes are lying flat on the surface[11], so that the adsorbed layer thickness is ~0·5 nm (5Å), giving a correction factor for an adsorbed layer *two* monolayers thick of ~6 per cent (*Table 2*).

Sterling MT

Although this graphitized carbon black has a more homogeneous surface than Graphon, the lower area tends to increase the experimental difficulties. This was particularly true with our calorimeter which was limited to 0·5 g samples. The combination of small sample size and low specific surface area probably accounts for the poor results obtained for Sterling MT when coated with n-alkane (*Table 2*).

Table 3. Comparison of specific surface areas from different methods

	Graphon Specific surface area (m^2 g^{-1})	*Sterling MT Specific surface area* (m^2 g^{-1})
CALORIMETRIC METHODS		
Mean results from all alkanes (*Table 2*)		
(i) Bare solid	86 ± 3	9·9 ± 0·2
(ii) Precoated solid	84 ± 5	14 ± 3
ADSORPTION METHODS		
(i) *Nitrogen*		
a_i = 0·162 nm^2 (16·2Å^2)		
(a) Volumetric apparatus (ref. 15) BET	83 ± 4	9·5 ± 0·7†
(b) Gravimetric apparatus		
Point B	84 ± 3	6·7 ± 0·5
BET	80 ± 2	7·5 ± 0·5
t-plot	81 ± 4	6·6 ± 0·4
(ii) *Alkanes*		
(a) n-Hexane		
a_i = 0·548 nm^2 (54·8Å^2)		
BET	85 ± 1	8·5 ± 0·2
(b) n-Octane		
a_i = 0·682 nm^2 (68·2Å^2)		
BET	86 ± 1	

† Krypton, a_i = 0·202 nm^2 (20·2Å^2).

Comparison of the results from calorimetric methods with those from other techniques

The specific surface areas obtained from a series of gas adsorption methods are shown in *Table 3*.† To derive the specific surface area from nitrogen adsorption at 77°K, three methods were used to obtain values for the monolayer capacity: (i) the 'Point B' method[12], (ii) the BET method[1], and (iii) the universal nitrogen isotherm (*t*-plot) method[13]. The molecular area, a_i, used was 0·162 nm^2 (16·2 Å^2). Specific surface area values were also obtained from n-alkane vapour adsorption at 298°K using values of a_i from Robert's equation[14] based on crystallographic data for solid n-alkanes and assuming that the adsorbate molecules are lying flat on the surface.

The comparison between the adsorption and calorimetric techniques is good for Graphon but poor for Sterling MT, probably because of the relatively low area. This emphasises the unsuitability of the immersion calorimetric method for solids with specific surface areas less than $\sim$20m^{2}g^{-1} unless large samples can be handled in the calorimeter.

---

† We are grateful to Mr. J. Dimery of the School of Chemistry, University of Bristol, for performing the volumetric adsorption measurements.

For Graphon the overall average surface area determined from the heats of immersion and alkane adsorption is 84 ± 5 m^2g^{-1}. From nitrogen isotherms the range of values of a_i required to give the same range for the specific surface area is 0·156 to 0·176 nm^2 (15·6–17·6 $Å^2$). Recent studies[3,16] have suggested that these values are too low for graphitized carbon blacks and that 0·20 nm^2 (20 $Å^2$) would be a better estimate. The general agreement obtained in the present work suggests, however, that 0·162 nm^2 (16·2 $Å^2$) is an appropriate value for the nitrogen molecular area and localised adsorption of the nitrogen molecules[3] need not be invoked.

CONCLUSIONS

(i) The calorimetric immersion method is not suitable for solids with surface areas less than ~20 m^2g^{-1}.

(ii) Precoverages greater than 2–3 monolayers are not necessary in the graphitized carbon black/n-alkane system and indeed equilibration at too high a value of p/p_0 can lead to low apparent areas.

(iii) Comparison of immersion calorimetry, n-alkane vapour adsorption and nitrogen adsorption indicates that 0·162 nm^2 (16·2 $Å^2$) is an appropriate value for the area occupied per nitrogen molecule on graphitized carbon blacks.

References

[1] S. Brunauer, P. H. Emmett, and E. Teller. *J. Amer. Chem. Soc.* **60**, 309 (1938).
[2] H. K. Livingston. *J. Colloid Sci.* **4**, 447 (1949).
[3] C. Pierce and B. Ewing. *J. Phys. Chem.* **68**, 2562 (1964).
[4] S. J. Gregg and K. S. W. Sing. *Adsorption, Surface Area and Porosity*, Academic Press, London, 1967.
[5] W. D. Harkins and G. Jura. *J. Amer. Chem. Soc.* **66**, 1362 (1944).
[6] P. G. Briggs, (Cabot Carbon Ltd.), Private communication.
[7] A. W. Adamson. *Physical Chemistry of Surfaces*, Interscience, New York, 2nd Edn., 1967.
[8] J. J. Jasper and E. V. Kring. *J. Phys. Chem.* **59**, 1019 (1955).
[9] G. Jura. In *Physical Methods of Chemical Analysis* (Ed. W. E. Berl), Academic Press, New York, 1951.
[10] D. H. Everett and G. H. Findenegg. *Nature, Lond.*, **223**, 52 (1969).
[11] A. V. Kiselev. *Proceedings 2nd International Congress on Surface Activity*, p. 168, Butterworths, London, 1957.
[12] D. M. Young and A. D. Crowell. *Physical Adsorption of Gases*. Butterworths, London, 1962.
[13] C. Pierce. *J. Phys. Chem.* **72**, 3673 (1968).
[14] L. Robert, C. Alexanian and J. Buzon. *Proc. 3rd World Petroleum Congress*, La Haye, 1951, p. 259.
[15] J. Dimery. (Bristol University). Private communication.
[16] A. C. Zettlemoyer. *J. Colloid and Interface Sci.* **28**, 343 (1968).

DISCUSSION

Dr F. A. P. Maggs (*C.D.E. Salisbury*) said: The differential heat of wetting data given in *Figure 2* of the paper can be used to provide measured values of the differential heat of adsorption (net) for comparison with the calculated isosteric differential heats (total) given in *Figure 1*. Cursory inspection suggests that a similar dependence on coverage will be obtained. Would the authors please make this comparison?

According to Harkins, the adfilm at saturation vapour pressure has liquid properties because it is a duplex film—but in earlier papers duplex films were defined as having liquid properties! Following Harkins, the present paper assumes a zero angle of contact between liquid and adfilm, a condition rarely encountered. The heat of wetting of unit area of a solid holding pre-adsorbed vapour is

$$\Delta h = \gamma_{\mathrm{LV}} \cos \theta - T\,\mathrm{d}(\gamma_{\mathrm{LV}} \cos \theta)/\mathrm{d}T$$

θ being the angle of contact with the adfilm. Clearly θ and its temperature dependence are all-important and should be known before the calculation of area can be made; the approach of heats of adsorption to heats of liquefaction is no criterion.

Dr J. H. Clint replied: (i) It is well known that the heat of immersion (ΔH_{imm}) of a solid with n^{σ} moles per gram pre-adsorbed is given by

$$\Delta H_{\mathrm{imm}} = \int_{n^{\sigma}}^{\infty} (q_{\mathrm{st}} - \Delta H_{\mathrm{L}})\,\mathrm{d}n^{\sigma} + Ah_{\mathrm{LV}}$$

Integration of the isosteric heat versus coverage plot (*Figure 1*) yields a heat of immersion curve almost identical to that shown in *Figure 2*.

(ii) Although, in principle, it is necessary to use the full equation involving the contact angle and its temperature dependence, in the system studied by us, and in many others [G. E. Boyd and H. K. Livingston. *J. Amer. Chem. Soc.* **64**, 2383 (1942)] the contact angle is zero. Furthermore, spreading coefficients in such systems are usually large and positive. For use in the immersional heat method of surface area determination for a given solid, one would obviously choose a liquid for which the contact angle on that solid is zero. Such systems are not unusual (cf. Boyd and Livingston, *loc. cit.*).

Dr J. F. Padday (*Kodak Limited*) said: It was indicated that when eight monolayers of adsorbate were present on the solid powder in equilibrium with the vapour at high relative pressure, a considerable reduction of area was found. Is there enough adsorbate present in eight monolayers to reduce the area by a half and, if so, will the adsorbate be uniformly distributed?

Secondly it appears from elementary geometry that a liquid bridge between two equal spheres does not result in any decrease in area of the magnitude indicated.

Dr J. H. Clint replied: Graphon consists of aggregates of polyhedral particles (roughly spherical) with diameters in the range 250–350 Å. If we consider a model system of close-packed spheres 300 Å in diameter, the centre of a 'tetrahedral' cavity will be 300 ($\sqrt{6}/4 - 1/2$) Å from the nearest solid surface, i.e. 34 Å. For a plane surface, 8 monolayers uniformly distributed with the n-alkane molecules lying parallel to the surface would have a thickness of approximately 40 Å. Hence, for a perfectly close-packed system of uniform spheres in the absence of swelling, the equivalent of 8 monolayers uniformly distributed would be more than adequate to fill all the interior space available, thus effectively reducing the measured surface area.

In reality the primary particles will be far from close-packed but it does seem reasonable to expect a reduction of the measured surface area by a factor of 0·5 with 8 monolayers adsorbed. It is unlikely that the adsorbate will be uniformly distributed. Preferential adsorption will take place at the points of contact of adjacent particles where interaction energies with the solid will be enhanced.

Dr J. C. Abram (*Tate and Lyle Limited*) said: We should like to support the findings of Clint *et al.* that the area occupied by the nitrogen molecule when adsorbed on graphitized carbon surfaces is 16·2 Å^2.

We have studied the adsorption from aqueous solution of tetrapentylammonium bromide (TPAB) on both non-graphitized and graphitized carbon surfaces. The idea behind the work was that this large symmetrical molecule would occupy equal areas/molecule on both types of carbon surface and thus enable us to determine the surface area of graphitized carbons, assuming a value of 16·2 Å^2 for nitrogen on the non-graphitized surfaces.

The surface areas and porosities of the non-graphitized carbon surfaces were determined using the Pierce V-n and the de Boer t-pbt methods. Combining these results with adsorption from solution data the areas found for TPAB were 143 Å^2 using the Pierce method and 106 Å^2 by the de Boer method.

Three graphitized carbon blacks were then investigated and their surface areas were determined by the BET method as well as by the de Boer and Pierce methods. We found good agreement between the areas calculated by the BET and de Boer methods to within 4 per cent, and again the Pierce treatment gave slightly higher values.

However, when a value of 16·2 Å^2 was used for nitrogen to calculate their surface areas, and thus the areas occupied by TPAB on these graphitized surfaces, we obtained values of 142 Å^2 for Pierce and 105 Å^2 for BET or de Boer. These values were in excellent agreement with the values obtained on the non-graphitized surfaces.

Thus if our initial contention is correct, that this symmetrical molecule will occupy the same areas on both types of surface, then one should use the same area/molecule for nitrogen on graphitized and non-graphitized surfaces, i.e. 16·2 Å^2.

Dr S. J. Gregg (*Brunel University*) said: This very interesting and comprehensive investigation was carried out on an adsorption system where the isotherm was of Type II. We have carried out a corresponding though less extensive study with a system showing a Type III isotherm, viz. TK800 (a non-porous silica of known surface area) in carbon tetrachloride. Since the isotherm is of Type III the heat of adsorption should be close to the latent heat of condensation, i.e. the net heat of adsorption should be close to zero. Thus even for pre-adsorption coverages of less than a monolayer the adsorbed film should act almost as a liquid; and the heat of immersion per unit area should therefore be close to the surface enthalpy of liquid carbon tetrachloride.

Mr Diano's results show that this expectation is fulfilled quite well. The plot of heat of immersion per unit area against the amount adsorbed is close to the surface enthalpy of carbon tetrachloride, except at very low coverages where it is significantly higher; this region of higher values corresponds to the very small 'knee' on the isotherm (which is therefore not quite pure Type III) and this is probably to be attributed to the presence of a very small proportion of active sites.

It could well be that systems showing Type III isotherms are particularly suitable for the application of the Harkins–Jura absolute method.

Dr J. Rouquerol (*Centre de Microcalorimetrie, France*) said: I would like to give some results obtained on the same Sterling MT carbon black as used by Dr Clint. But, instead of studying it by *immersion* calorimetry, we have used *adsorption* calorimetry *at liquid nitrogen temperature*. And I would like to give some optimism to Dr Clint, because I feel that the calorimetric method is suitable even for solids having a specific surface area as low as 7·5 m^2 g^{-1}, like this Sterling black.

We have performed adsorption calorimetry of argon on this sample, at liquid nitrogen temperature. Here we must remember that R. A. Beebe, who has been working on low temperature adsorption calorimetry for a long time has published several curves giving the differential heats of adsorption of argon on carbon black. *Figure A* shows typical ones [R. A. Beebe and D. M. Young, *J. Phys. Chem.* 93–96 (1954)]. The last curve shows a first maximum, attributed to lateral interaction between adsorbed molecules near the completion of the monolayer, and a second maximum, attributed to a change in the physical state of the adsorbed phase, when arriving

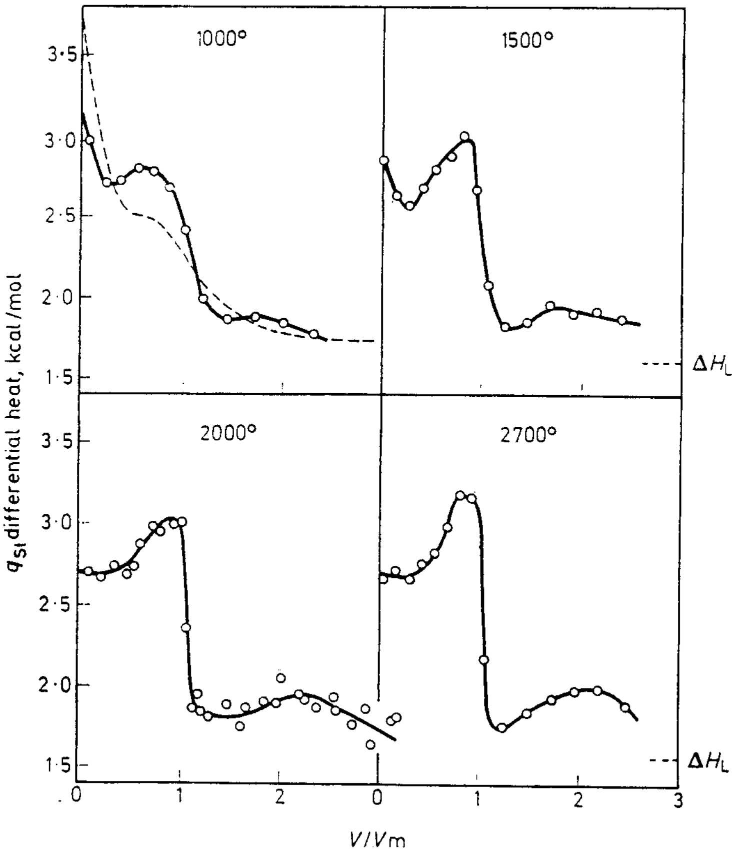

Figure A. Differential heat of adsorption curves of argon on carbon black [R. M. Beebe and D. M. Young] at the completion of the second layer. In another paper [R. A. Beebe, B. Millard and J. Cynarski, *J. Am. Chem. Soc.* 839–45 (1953)] we can read: '. . . there is even some indication of a third maximum in the argon-Graphon heat curve. We feel that the evidence for this third maximum is not very convincing, since it depends on only two experimental points. However, the possibility of a third maximum is at least suggested and perhaps should be investigated by a method capable of giving finer detail than that attainable with our present instrument'.

Figure B shows our recorded curve. One can distinguish a second, a third and may be a fourth maximum, corresponding to the second, the third, and may be the fourth layer. Each maximum is possibly due to the same lateral interaction forces which, in the case of a very uniform surface, act all together just before the completion of each layer. I shall ask you to ignore the first rising part of the recorded curve, which is due to the response time of the whole apparatus, but I would like to point out that, with the technique we are using now, the recorded curve gives us differential heats of adsorption versus coverage; besides, we have made here a continuous and slow introduction of gas into the sample. The measurement itself is all performed within half a day. The continuous recording avoids any error in the drawing of the curve and avoids one to wonder whether the number of experimental points is sufficient to prove the existence of any irregularity. The qualitative interpretation of the recorded curve can therefore be made faithfully; nevertheless, we have to remember that before using this curve for computations one has to make the corrections due to the response time of the apparatus (they are not shown here).

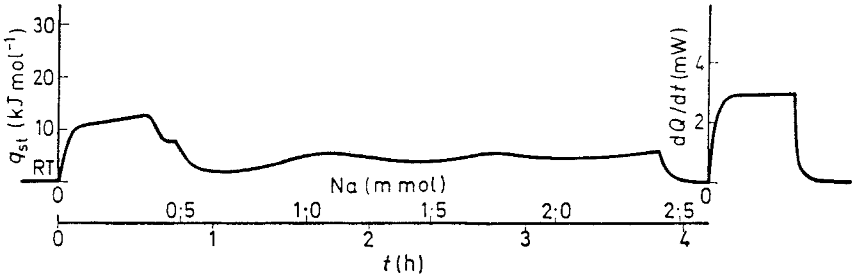

Figure B. Argon–Graphon heat curve showing a second, a third and possibly a fourth maximum, corresponding to the second, the third and possibly a fourth layer

If we now come back to Dr Clint's *Figure 1*, which gives isosteric heats *versus* coverage for a Graphon black, we can see two little waves which correspond more or less, I think, to the end of coverage of the second and third layer.

To conclude, I would like to point out the help which can be brought by adsorption calorimetry to the measurement of specific surface areas. I think this help can be at least threefold. First, in the case of a very homogeneous surface, it seems that the sharp drop in the differential heats of adsorption at the end of the coverage of the monolayer could be used to determine the

V_M. Secondly, only one glance at the differential heat curve allows one to know whether the hypothesis of constant energy of adsorption, on the monolayer on one hand, and on the following layers on the other hand, is valid, and therefore, to have an idea of the care necessary in applying the BET method for the studied system. Thirdly, in the very frequent case when there is no clear experimental calorimetric distinction between the first and the second layer, would it not be significant, I ask the question, to figure out thoroughly, not the V_M, but instead of it, the number of moles for which the differential heat of adsorption exceeds the liquefaction energy, that is to say the number of moles which are in interaction with the surface. It is likely that this number will usually be higher than V_M but would nevertheless be representative of the action of the surface.

Dr R. B. Gammage (*Oak Ridge National Laboratory, U.S.A.*) said: The surface of a low-area (2·96 m^2/g), non-porous thorium oxide is another example where the heat of immersion reaches the limiting value of h_L, the surface enthalpy, after only a few layers of immersing fluid are preadsorbed; surprisingly the adsorbate is water. The heat of immersion plotted against preadsorbed water (*Figure C*) shows three linear sections before

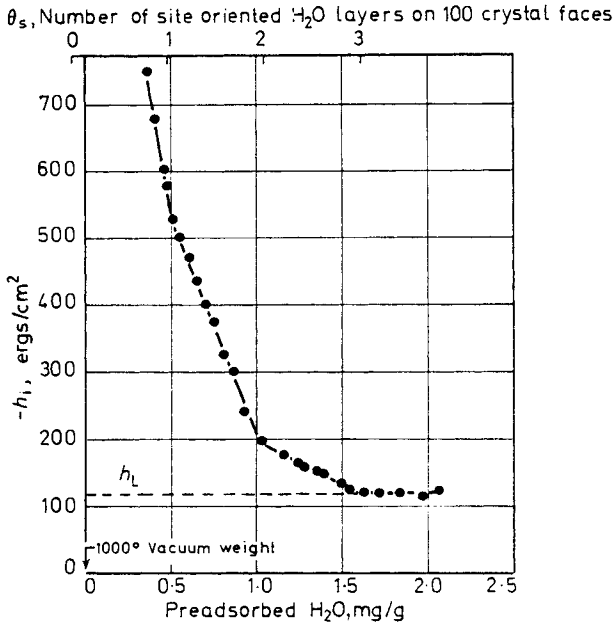

Figure C. Heat of immersion of non-porous thorium oxide in water at 25°C

reaching h_L. The chemisorptive capacity (θ_s) of an ideal 100 crystal face is 0·192 mg/m^2 or 12·7 hydroxyls/100 Å^2. If the preadsorbed water is expressed in terms of θ_s, then working backwards from $3\theta_s$ at h_L, the other breaks occur quite close to $2\theta_s$ and θ_s. The most probable explanation is for a site oriented, layer buildup of water on a surface having considerable uniformity. The initial interaction of water with the oxide surface is very strong but by the third layer, shielding of the oxide surface seems to be complete.

Although the abscissa is based on the 1000C° vacuum weight, all the heat of immersion measurements were actually made on surface outgassed at 500°C prior to preadsorbing water. From the weight *in vacuo* at 1000°C it can be seen that the surface was able to retain the best part of a chemisorbed layer of water at 500°C.

DETERMINATION OF BASAL PLANE AND POLAR SITE AREAS IN GRAPHITES AND GRAPHITIZED CARBONS

A. J. Groszek

British Petroleum Company Ltd., Sunbury on Thames, U.K.

Much of the discussion at this meeting has been concerned with measurement of total surface areas. In practice, discrimination between different kinds of surface is important and this is particularly true for a proper understanding of the lubricating and adsorptive behaviour of graphite.

Graphite consists of particles having two different kinds of site, those on the basal planes and polar sites at the edges of crystallites. It has been known since Breshchenko's work in 1957[1] that the basal planes adsorb long-chain n-paraffins and we have found that they do so in preference to polar compounds such as alcohols. The polar sites exhibit the opposite behaviour and will preferentially adsorb polar solutes from non-polar liquids.

The integral heat of adsorption of n-dotriacontane ($C_{32}H_{66}$) onto various graphites and graphitized carbons from solution in n-heptane is proportional to the amount adsorbed[2], in fact 55 kJ/mol. Furthermore, the same heat effect is obtained if the n-C_{32} is adsorbed from solution in heptane containing 2 g/l n-butanol, if the absorbent has previously been saturated with the mixed solvent.

Figure 1 shows the heat evolution accompanying adsorption of n-C_{32} on to

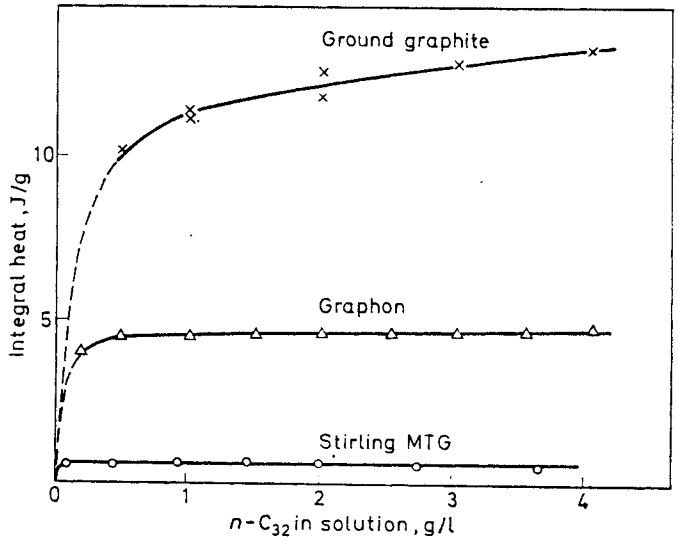

Figure 1. Variation of integral heat of adsorption of n-C_{32} from n-heptane with solute concentration

different graphitized carbon blacks and graphite from solutions in n-heptane. The curves correspond to adsorption isotherms and the adsorption reaches near saturation at a solution concentration of 2 g/l. Assuming that, at saturation, there is monolayer coverage of molecules lying flat (178 $Å^2$ per molecule), one obtains surface areas from the heat evolution at saturation, using a conversion factor of 19·3 m^2/J (ref. 2).

Similarly by measuring the heat evolution on saturating the graphite with dilute solutions of n-butanol in n-heptane and using a conversion factor of 6·7 m^2/J, obtained from measurements on various samples of graphite, one obtains the polar site area[2].

The heat effects are conveniently and rapidly measured in a flow microcalorimeter by successive percolation of 2 g/l solutions of n-butanol and n-dotriacontane in n-heptane through the same sample of powder, the n-butanol being desorbed with pure solvent before starting percolation with the long-chain paraffin. The sensitivity of the calorimeter, 2×10^{-5} J, is such that specific surface areas ranging from 0·05 to 100 m^2/g can be measured on 100 mg samples[3].

Table 1 gives data obtained in this way for graphitic materials of varied type and BET areas for comparison. Reproducibility tests on seven replicates of the synthetic graphite showed standard deviations of 0·38 on 5·2 m^2/g and 0·28 on 2·6 m^2/g.

Table 1. Surface area determinations for graphites

Type of graphite	*Integral heat of adsorption from* n-*heptane* (J/g)		*Calorimetric surface area* (m^2/g)		*BET surface area* (m^2/g)	
	n-Dotri-acontane	n-Butanol	Basal plane	Polar	N_2 = 16·2 $Å^2$	N_2 = 20·2 $Å^2$
Graphon	4·18	0·209	81	1·4	81	101
Sterling MTG	0·485	0·293	9·4	2·0	7·7	9·6
Synthetic graphite	0·268	0·377	5·2	2·6	5·0	6·2
Ground graphite	12·55	11·30	243	76	436	—

It is interesting that the area derived from heat of adsorption for the Sterling MTG agrees better with the N_2 adsorption using 20·2 $Å^2$ for the N_2 area, whereas the Graphon figure of 81 m^2/g agrees with the BET surface area based on 16·2 $Å^2$. This is probably a reflection of the significant structural differences between these materials. Also, it is evident that the surface measured by N_2 adsorption in the ground graphite is not all accessible to the larger molecules.

May I add a comment relevant to Dr Gammage's and Professor de Boer's contributions (described elsewhere in this publication) about the effects of water? In many practical situations, it is more useful to measure the surface areas under moist conditions than in the dehydrated state. In these cases it is perhaps fortunate that reproducible surfaces having water hydrogen-bonded to oxide or hydroxyl groups give good agreement with BET measurements. *Table 2* shows surface areas of a variety of oxides derived from flow

Table 2. Surface area determinations for iron and iron oxides

Adsorbent	*Integral heat of adsorption of* n-butanol (J/g)	*Calorimetric surface area* (m^2/g)	BET, N_2 (m^2/g)
Iron	0·0092	0·1	0·1†
α-Fe_2O_3	0·031	3·7	3 ± 1
γ-Fe_2O_3	1·03	11·5	12 ± 2
Fe_3O_4	1·17	13·4	9 ± 2
γ-Fe_2O_3/Fe_3O_4	0·755	8·6	6 ± 2
TiO_2 (rutile)	1·58	18·2	22·6†

† Values supplied to the author from external sources, precision unknown.

calorimeter data of the adsorption of n-butanol from 2 g/l solution in n-heptane by the method described for graphite. The conversion factor, 11·5 m^2/J was obtained from calibration runs on a non-porous alumina[3]. The standard deviation in eight replicates of the α-Fe_2O_3 was 0·13 m^2/g on the mean 3·7 m^2/g and the agreement with BET areas is good.

References

[1] E. M. Breshchenko. *Khim Tekh Topliv i Masel* **9**, 32 (1957).
[2] A. J. Groszek. *Proc Roy Soc.*, **A314**, 473 (1970).
[3] A. J. Groszek. *Chem. & Ind.* 1754 (1966).

USE OF DYES FOR SPECIFIC SURFACE MEASUREMENT

C. H. GILES, A. P. D'SILVA and A. S. TRIVEDI

T. Graham Young Laboratory, University of Strathclyde, Glasgow C. 1, *U.K.*

INTRODUCTION

The following classes of solutes have been used for measuring specific surface by adsorption: aliphatic substances, mainly long-chain surface-active compounds, phenols, and dyes. In this laboratory after a large number of trials with a variety of solutes and adsorbents, we have chosen *p*-nitrophenol and a few selected dyes as being the most suitable for general use. They offer a remarkably simple, rapid and versatile method which can be used for the measurement of (i) external specific surface of non-porous solids, over a wide range of values from *ca.* 0·01 m^2/g; (ii) internal specific surface of porous solids accessible to solute molecules of a range of sizes respectively; (iii) external specific surface of porous powders and fibres; and (iv) specific surface of solids, e.g., dyes, adsorbed in cellulose fibres.

DYES: CAUSES OF INCONSISTENT RESULTS

Dyes have been used by many investigators for measuring the specific surface of powders. The method has not been widely accepted apparently because of the inconsistency of the results reported, both between different dyes, and in comparison with other methods, especially the nitrogen adsorption procedure. We have identified a number of causes of such inconsistencies, and their identification enables more reliable results to be obtained. These causes include: (a) Effects of specific dye-substrate bonding; (b) Association of dyes adsorbed by non-specific bonding; (c) Interference by chemical reaction between the dye, and either the solid, or adventitious ions introduced into solution from the solid; (d) Molecular sieve action of porosity in solids; and (e) Ageing effects on the solid surface.

The details of these causes are as follows.

(a) Some dyes form specific bonds with groups in the substrate, usually hydrogen bonds or covalent bonds, which clearly will determine their orientation, but they may form both specific and non-specific bonds. Thus sulphonated dyes can be adsorbed on anodic alumina films both by covalent bonds between the sulphonate groups and aluminium atoms and also by electrostatic attraction of anionic dye micelles by the positively charged surface.

It is advisable generally to avoid the use, for specific surface determination, of dyes which may be adsorbed in this dual manner and indeed any dyes which may form covalent bonds with the surface, since they may be liable to selective adsorption on particular sites.

(b) A plot of number of moles of mono-ionic dyes adsorbed by non-specific bonding, on a given area of a non-porous solid, against weight of the coloured ion for a series of such dyes gives the type of result shown in *Figure 1.* The number of moles adsorbed *rises* markedly with ionic weight, and thus with the size of ion. If the dyes were all adsorbed in a condensed monolayer of monodisperse dye colour ions or molecules the number of moles adsorbed would clearly tend to *fall* with molecular weight. This apparent anomaly has been shown to be due to adsorption of the dyes as ionic micelles, with an average aggregation number which rises with the cube of the ionic weight of the dye and is apparently independent of the nature of the surface over a wide range of solids, and of the charge on the dye ion; provided as stated, each molecule carries only one ionic group and no *specific* bonds are formed between dye and surface (*Figure 2*). Thus each such dye can be alloted an aggregation number N or *coverage factor*, for use in calculations of specific surface, as described below (cf. *Table 1*). Statistical tests suggest that the dye micelles are composed of dye ions packed face-to-face and adsorbed flatwise on the surface[3].

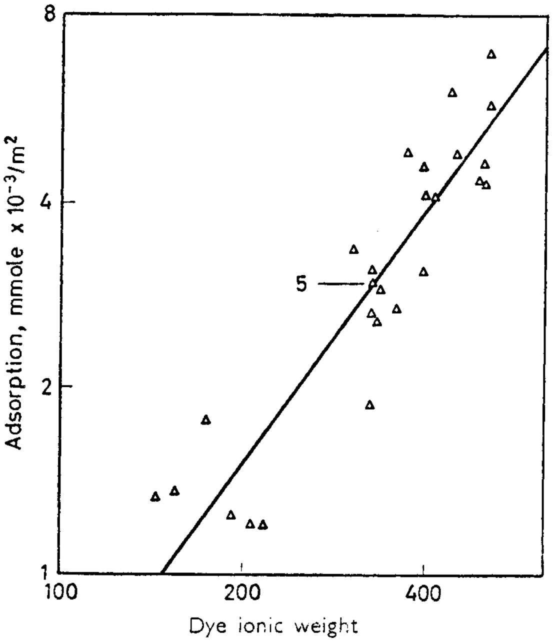

Figure 1. Relation between adsorption of dyes by unit area of various non-porous solids, and the weight of the colour ion[3]. (Five results are shown as one point, as indicated)

(c) Some anionic dyes tend to be precipitated by cations, e.g. Fe^{3+} or Ca^{2+} in the solid and should not be used, e.g., with Fe_3O_4 or $CaCO_3$ powders; and some cationic dyes, e.g., Crystal Violet, are particularly sensitive to alkali and thus give unreliable results with certain technical aluminas with alkaline reaction.

(d) Many porous solids, e.g., charcoals and silicas, act as molecular sieves towards the dye micelles mentioned above. This is an advantage in making estimates of porosity[4] (*Figures 3* and *4*).

(e) Some silica and titania powders have been found to lose specific surface by ageing on prolonged storage at room temperature[5].

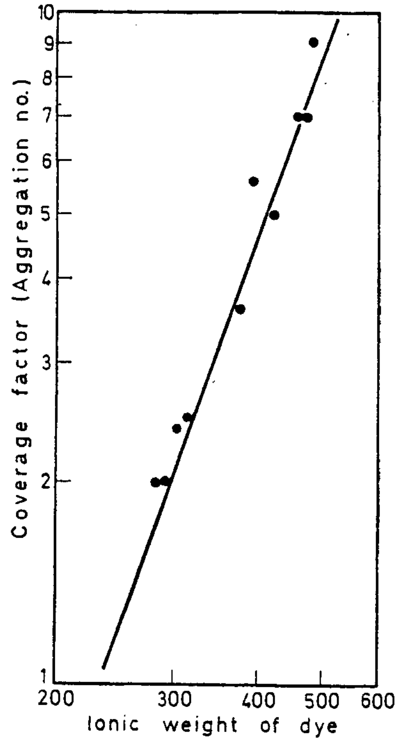

Figure 2. Relation between aggregation number of adsorbed dyes on various non-porous solids, and their colour ionic weights. Flatwise adsorption assumed. Other data are given elsewhere[3].

As a result of the above observations, we have made efforts to select, from the very large number available, a limited number of mono-ionic dyes which can be recommended for general use. Criteria of selection were that the dyes can readily be obtained pure, are adsorbed by most surfaces in the form of ionic micelles of known aggregation number, are not affected chemically by most solids likely to be tested, and cover a range of micellar sizes so that porosity measurements can be made if desired.

From a large number of dyes tested, we at present recommend those in *Table 2*, which includes other necessary data.

The two BP quality dyes are sufficiently pure for use without further treatment; the two anionic dyes can readily be purified by recrystallization two or three times from an approx. 50:50 ethanol–water mixture, and Victoria Pure Lake Blue BO from dry acetone.

Table 1. Dye aggregation numbers, determined by various methods

Dye	*In aqueous solution, by*		*Aggregation No. N Adsorbed on solid*					*In monolayer on water*†
	Diffusion[1]	*Polarography*[2]	*By comparison with N_2 area, on*[3]			*By streaming potential, on*[1]		
			C	SiO_2	Al_2O_3	SiO_2	C*	
Cationic								
Methylene Blue BP	1·6–1·7	1·6–2·0	2·0	2·0	2·0	2·4		1·9
Brilliant Basic Red B (C.I. 50250)			3·5		3·9	3·5	3·5	
Crystal Violet BP		1·5–5·0	3·3	3·8		2·6		
Victoria Pure Lake Blue BO	8·9–9·9		9·0	9·0		8·9		8·0
Anionic								
Orange II	1·2–2·6		2·6		3·0			
Solway Ultra Blue B (C.I. 62055)	2·2–2·5	*ca.* 1–5	5·6					

* Anthracite powder.
† V. G. Agnihotri, unpublished results by new method.

The molecular areas have been measured from Catalin models and are for the *smallest enclosing rectangle*. We find it advisable to use this standard method of measurement, which proves to give consistent results, rather than to attempt to estimate the (uncertain) areas which might be covered if some interlocking of micelles were to occur. It seems probable anyway that since the adsorption state is one of dynamic equilibrium, with dye micelles constantly striking and rebounding from the solid surface, interlocking is very unlikely to occur.* Similarly the aggregation number N or coverage factor is an average based on results for different solids, though there is in fact little variation in its value between one solid and another, provided the chemical factors already mentioned do not interfere[1, 3].

The value of N for each dye was initially found from tests on a few non-porous solids for which a nitrogen area was known. Once established it was used in future tests without reference to nitrogen areas. Recent work here, however, has shown promise of determining N values absolutely by the Langmuir film balance (*Table 1*).

---

* It may be mentioned that the degree of uncertainty in estimating dye molecular areas is probably less than that for nitrogen, for which values ranging from 13 to 20 Å^2 have been quoted[6], though 16·2 Å^2 is that usually adopted[7].

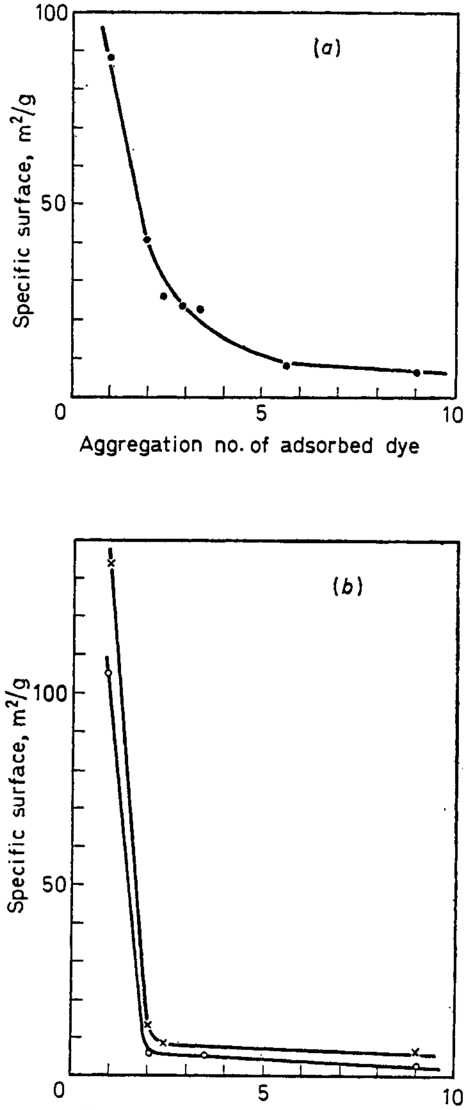

Figure 3. Relation between aggregation number of various dyes (and PNP) and accessible specific surface of porous solids. (a) bone char; (b) two varieties of micro-porous silica.

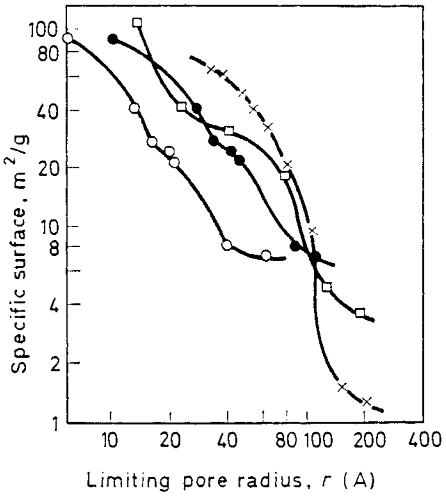

Figure 4. Pore surface distribution data for bone char by various methods[4]. ×, Mercury porosimetry; □ benzene desorption; ●,○ PNP and dye adsorption; ●, assuming $r = 3l$ (r = pore radius, l = dye micelle thickness); ○, assuming $r = 1{\cdot}5l$.

Table 2. Details of recommended dyes

Name	*C.I. No.*	*Ionic Weight*	*Mol. area flat* (Å²)	*Aggn. No. N*	*Molar extincn. coeff.* (× 10⁻⁴)	λ_{max} (nm)
		ANOINIC DYES				
Orange II	15510	327	120	3·0	2·4	480
Naphthalene Red J.	15620	400	150	3·6	2·1	500
		CATIONIC DYES				
Methylene Blue BP	52015	302	120	2·0	4·0	610
Crystal Violet BP	42558	372	225	3·6	3·6	590
Victoria Pure Lake Blue BO	42598	478	270	9·0	6·8	620

We also recommend *p*-nitrophenol (PNP) as a very useful supplementary solute. It is stable, readily purified (from water), soluble both in water and several organic solvents, easily analysed by a spectrophotometer, and its molecular size is easily measured[8].

External surface of porous solids

This is determined (e.g., for fibres[9]) by making a series of adsorption tests for short periods of time, say 2,5, and 10 min and plotting an isotherm for each. These are not equilibrium isotherms and the measured area increases with time, because of slow-penetration into the pores, but by plotting area against time and extrapolating back to zero time, an estimate of the external area can be made (*Figure 5*).

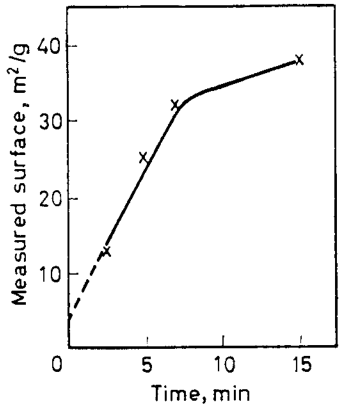

Figure 5. Surface of a bone char measured after various periods of time by PNP in aqueous solution. Back extrapolation to zero time, as shown, gives an indication of external surface.

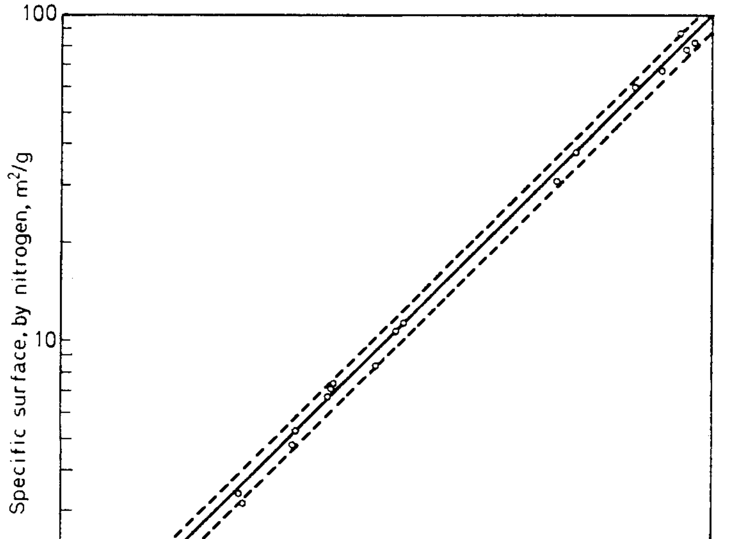

Figure 6. Comparison of specific surface of non-porous powders measured by dyes and nitrogen. The points refer to tests on varieties of the following: alumina, calcium carbonate, ferric oxide, graphite, manganese dioxide, silica, silver halides, titania (anatase and rutile). The broken lines are the ± 10% limits.

Specific surface of adsorbed dyes and pigments in fibres

Recent work here shows that the surface of particles or aggregates of dyes or pigments in cellulose fibres can be determined by adsorption of PNP from water. PNP is adsorbed by the colouring matters but not by cellulose. The method might be useful for other types of solid in or on cellulose fibres.

Comparison with results by other methods

Some comparisons are given in *Figure 6* and *Table 3*. The latter includes some data on the external surfaces of fibres and on certain powders which give lower values with nitrogen than with PNP*; other comparisons of the latter types are given in ref. 8; additional comparisons (PNP as solute) are given in the same publication; for oxides (PNP and dyes) see ref. 5; and for porosity measurement, ref. 4.

Table 3. External specific surface (m²/g) of solids, by various methods

Solid	*Method*						
	Adsorption				*Air perm.*	*Opt. micr.*	*Elect micr.*
	PNP	*Dyes*	*N_2*	*Kr*			
Alumina[8]	5·0				0·04	1·5	
Cement[8]	50·0				0·27	0·35	
	1·2		< 1·0		0·22		
Fibres[9]: nylon	0·46				0·15	0·16	
rayon	0·84				0·28	0·24	
Terylene	0·44				0·18	0·14	
wool	0·61				0·16	0·13	
Graphite	2·9						2·4
Iron Powder	4·6		1·6				
Organic (azo)	24·4		11·6				
pigments[8]	31·8		33·4				
Silica[5]		3·6	4·2	3·9			
Silver bromide		0·17	0·11				
Silver iodide		0·36	0·36				
Silver iodide[10]		0·48[11]	0·45			0·25	
Silver iodide[10]		0·34[11]	0·38		0·35† (0·27)	0·18	
Silver iodide[10]		0·54[11]	0·52		0·51† (0·34)	0·32	
Silver iodide[10]		0·36[11]	0·30		0·26† (0·19)	0·22	
Silver iodide[10]		1·21[11]	0·97		0·88† (0·48)	0·45	
Silver iodide[10]		1·19[11]	1·99				
Sugar[8]	0·018				0·008		

† "Internal areas," "external areas" in parentheses

METHOD

0·05–0·50 g samples of powder, depending on the specific surface, are tumbled gently with 10 ml aliquots of aqueous solutions of dye or PNP at room temperature; though for materials which are swollen, dissolved, or

---

* This fact was attributed to the high specific gravities of the powders concerned, which may cause them to adhere under the outgassing conditions. Other cases are known where nitrogen gives lower values than a solute adsorption method (A. J. Groszek, private communication).

otherwise chemically affected by water, PNP in xylene or *n*-hexane may be used[8, 9]. 10–30 min is a sufficient time for equilibration with non-porous powders, but 12–48 h or even longer may be required for porous powders. (Initially a rate curve should be obtained.) The tubes are then centrifuged and the solutions analysed spectrophotometrically.

A semi-micro method has been developed[12], requiring 5–200 mg powder and 2 ml solution per tube; dilution of solutions for analysis may be avoided by use of a very thin cuvette in the spectrophotometer, e.g. a 1 mm cell with a glass plate spacer 0·9 mm thick inserted (variable path-length cells are not well suited to use on this scale). Staining of tubes and cells by cationic dyes can be minimised by treatment with a chloroform solution of dimethyldichlorosilane (Hopkin and Williams Ltd.) followed by rinsing with acetone and drying, which confers water-repellency. If required, the coating is removable by hot alkaline solutions.

The isotherms (cf. *Figures 7–9*) with dyes usually have a long plateau, enabling a good estimate of the monolayer capacity to be made; this is assumed to be a condensed monolayer of ionic micelles of dye. The long plateau enables a 'one-point' method to be used readily.

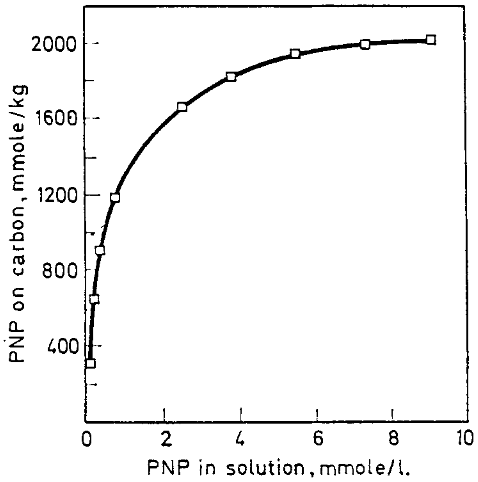

Figure 7. Typical isotherm for PNP adsorption from water (18°C). Substrate: a high surface carbon (Actibon C).

The time for a complete test is *ca.* 60–90 min, excluding time of tumbling. For a 'one-point' test this can be cut to *ca.* 25 min.

The specific surface, $S = Y_m N a/n$, where Y_m is the amount of dye adsorbed (mmol/g) at the plateau, N the Avogadro number, a the (flat) molecular area of the dye (smallest enclosing rectangle) and n is the aggregation number or *coverage factor* of the adsorbed dye (*Table 1*), representing the average number of dye colour ions in the adsorbed micelle.

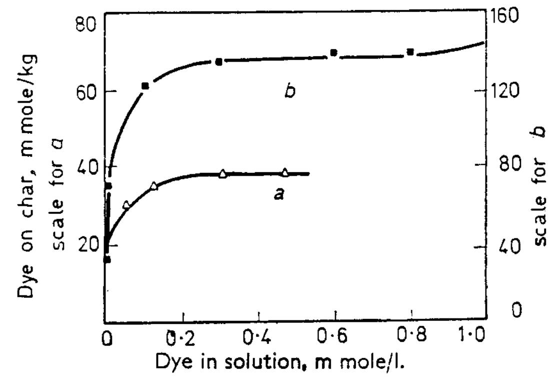

Figure 8. Typical isotherms for cationic dye adsorptions (18°C). Substrate: bone char. Dyes: *a*, Victoria Pure Lake Blue BO; *b*, Methylene Blue BP.

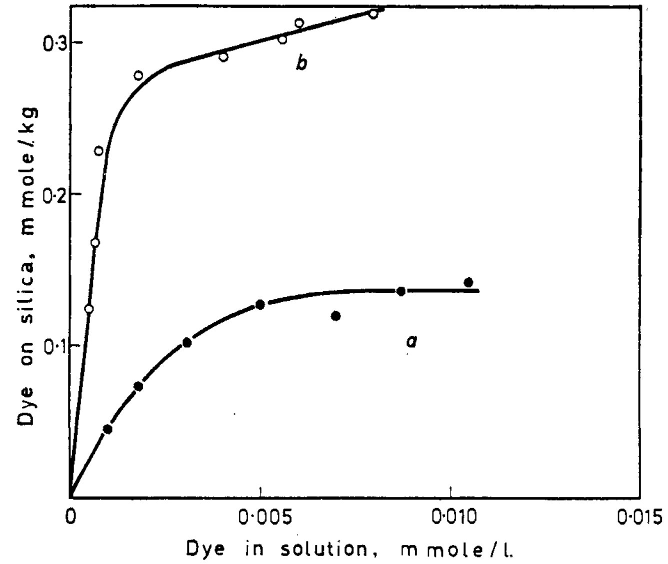

Figure 9. Isotherms for Methylene Blue BP adsorption on low surface area silica. *a*, initial condition, specific surface, 0·05m^2/g; *b*, ground 2 min, specific surface, 0·12 m^2/g.

SUMMARY

Results are given of specific surface (SS) measurements on a variety of finely divided solids, using *p*-nitrophenol (PNP) and dyes. Cationic dyes, especially Methylene Blue, Crystal Violet, and Victoria Pure Lake Blue BO, are recommended for use, in water, to measure SS on both non-porous and porous solids. PNP can also be used either in water, or where water would affect undesirably the solid being measured, in a non-aqueous solvent, e.g., n-hexane or xylene. With a number of nonporous solids results are in good agreement with nitrogen areas. Micro-porous solids act as molecular sieves

towards the above-mentioned solutes, which can thus be used for determining surface accessible to different sizes of solute molecule. A method is described for measuring only external surface of porous solids.

The recommended methods are simple and rapid. Reasons for previous inconsistencies in results from measurements with dyes are explained.

References

[1] C. H. Giles and A. P. D'Silva. *Trans. Faraday Soc.* **65**, 2516 (1969).
[2] P. J. Hillson and R. B. McKay. *Trans. Faraday Soc.* **61**, 374 (1965).
[3] C. H. Giles, I. A. Easton, R. B. McKay, C. C. Patel, N. B. Shah, and D. Smith. *Trans. Faraday Soc.* **62**, 1963 (1966);
I. A. Easton, C. H. Giles, and R. B. McKay. *Chem. and Ind.* 1863 (1964).
[4] C. H. Giles, A. P. D'Silva, and A. Cameron. *Chem. and Ind.* 239 (1969); *Trans. Faraday Soc.* **65**, 1943 (1969).
[5] C. H. Giles, I. A. Easton, and A. S. Trivedi. *J. Appl. Chem.* **19**, 18 (1969).
[6] S. J. Gregg and K. S. W. Sing. *Adsorption, Surface Area and Porosity*, p. 116 (Academic Press, London), 1967.
[7] B.S.I. *Methods for the Determination of Specific Surface of Powders. Nitrogen adsorption* (*B.E.T. Method*). B.S. 4359: Part 1: 1969.
[8] C. H. Giles and S. N. Nakhwa. *J. Appl. Chem.* **12**, 266 (1962).
[9] C. H. Giles and A. H. Tolia. *J. Appl. Chem.*, **14**, 186 (1964).
[10] H. J. van den Hul and J. Lyklema. *J. Amer. Chem. Soc.* **90**, 3010 (1968).
[11] C. H. Giles. *J. Amer. Chem. Soc.* **91**, 759 (1969).
[12] C. H. Giles and A. S. Trivedi. *Chem. and Ind.* 1426 (1969).

DISCUSSION

Professor J. Lyklema (*Agricultural University, Wageningen, The Netherlands*) said: The dye adsorption areas on silver iodide quoted in *Table 3* are (except for the first one) apparently taken from our results (reference 10), with the only difference that you took a molecular cross section that yielded a 1:1 correspondence with the BET area obtained after drying. Does this imply that you use in fact the BET area for calibration, or do you consider your dye adsorption areas still absolute?

Dr C. H. Giles replied: Yes, we used the BET area for calibration.

N. K. Sandle (*Imperial College, London*) said: When we consider the adsorption from binary solutions by solid adsorbents, it is very well known that both the components of the solution compete for selective adsorption. In the case of adsorption of PNP from aqueous solutions onto porous adsorbents such as silica gel or carbons, the competitions of water molecules for the surface will be quite significant and is difficult to ignore. Consequently the results of surface area obtained by considering only the PNP adsorbed may be misleading.

In the case of adsorption at the solid–liquid interface interaction in the liquid phase between solute and solvent plays a significant role in the orientation of the adsorbed molecules at the solid–liquid surface, and the total amount of the adsorbed species which may sometimes exceed a monolayer. The results of surface areas measured by ignoring the solute–solvent interaction may be erroneous.

Dr C. H. Giles replied: With non-porous silica and graphite, PNP adsorbed from *appropriate solvents* gives results comparable to those obtained by the standard nitrogen adsorption method. It is therefore reasonable to use it for porous samples of these materials.

If *water* is used as solvent, complete coverage is not obtained with certain acidic solids, e.g. silica, and we do not therefore recommend the use of PNP in these cases.

Dr J. F. Padday (*Kodak Ltd., Harrow, U.K.*) said: The data of *Figure 6* and of *Table 3* suggest that the site area of a single adsorbed dye ion or molecule possesses some constant value for many different types of solid surfaces. However, it appears that the coverage factor, which is equivalent to the site areas, are themselves derived from the nitrogen area; hence the data do not appear to represent an independent confirmation of the dye method for measuring the surface area of a solid.

Dr C. H. Giles replied: This is correct, but cross-checking of the aggregation number between different methods appears to confirm the results (e.g. *Table 1*).

Dr J. C. Abram (*Tate and Lyle Limited, U.K.*) said: Dr Giles mentioned in his paper some of the causes of inconsistent results when adsorption from solution techniques are used to measure specific surface areas. I should like to draw your attention to two more.

The first concerns the interaction between the solid and the solute, and more specifically between bone char, one of the materials studied by Dr Giles, and cationic solute molecules. Bone char is a mixed adsorbent containing both calcium phosphate and carbon surfaces. We have studied the adsorption of both anionic and cationic molecules on this surface and found that whereas anionic molecules such as sodium di-2-ethylhexyl-sulphosuccinate are adsorbed from aqueous solution over the whole of the bone char surface, cationic molecules such as methylene blue (MB) and cetyltrimethylammonium bromide are adsorbed only on the carbon surface. This is illustrated in *Figure A* where the amount of methylene blue adsorbed on the bone char is plotted as a function of the carbon content of bone char. Thus the use of cationic dyes to measure the pore size distribution of this material will yield incorrect results as they are only adsorbed on part of the surface.

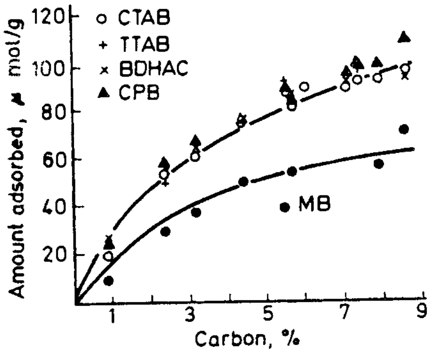

Figure A. Methylene blue adsorbed *vs.* carbon content in the case of bone char

The second concerns the possible effect of pH on the adsorption of dyes from solution. Methylene blue has been used frequently to measure the surface areas of powders and, in particular, carbons. The pH of the aqueous extract from carbons can vary between 3 and 11. We have measured the adsorption of methylene blue on two very different carbon surfaces, Spheron 6 and Graphon from buffered solutions.

Table A. Adsorption of methylene blue on Spheron 6 and Graphon from buffered solutions

pH	*Buffer*	*Amount methylene blue adsorbed* (μmoles/g)	
		Spheron 6	Graphon
5·3	Water	74	103
6·3	KH_2PO_4/NaOH	125	145
7·2	KH_2PO_4/NaOH	143	155
7·9	KH_2PO_4/NaOH	—	143
8·0	Na_3BO_4/HCl	149	—
8·2	KH_2PO_4/NaOH	149	148
9·0	Na_3BO_4/HCl	149	—
9·0	KH_2PO_4/NaOH	—	147
9·2	Na_3BO_4/HCl	148	146
9·2	KH_2PO_4/NaOH	—	146
10·0	Na_3BO_4/NaOH	159	—
10·0	$NaHCO_3$/NaOH	161	170
11·0	$NaHCO_3$/NaOH	203	220

The results are shown in *Table A*. It can be seen that the adsorption is dependent on the pH of the system, but the buffer is not affecting the adsorption. The adsorption reaches a plateau between pH 7–9 and consequently the adsorption of methylene blue should be measured at pH 8 if consistent results are to be obtained.

Dr C. H. Giles replied: Bone-char was first treated with 2N HCl at 40°C and later washed with distilled water, until all trace of acidity disappeared; measurements of porosity were then made. We agree that pH of the test solutions is important, and advise against tests being made from solutions which are outside the range of pH *ca.* 5–8.

MEASUREMENT OF SURFACE AREA BY THE ADSORPTION OF DYES FROM SOLUTION

J. F. PADDAY

Research Laboratories,
Kodak Limited, Wealdstone, Middlesex, U.K.

INTRODUCTION

Recent reviews[1] show that in order to measure the surface area of a solid powder by the adsorption of dye (or other large molecule) from solution it is necessary to ensure that thermodynamic equilibrium is reached between dye adsorbed and dye in solution, that all the surface of the powder is accessible to the dye, that the dye is present preferably in one form only and not in several aggregation states, that the adsorbed dye forms a physically adsorbed monolayer and not multilayers, and that the site area of a single dye ion or molecule, at saturation adsorption, is clearly and unambiguously known. It will be assumed that published literature reviewed here meets some of these general requirements. The purpose then is to show whether or not the site area of the adsorbed dye changes when the parameters of the system are changed.

SPECIFIC AREA OF THE SOLID SURFACE

The site area of the adsorbed dye is given by the amount of dye adsorbed at the plateau of the isotherm per unit weight of substrate, divided by the specific area of the substrate. The specific area in many earlier studies involving silver-halide surfaces was obtained from particle size analyses of heterodisperse systems[2-4], from the adsorption of nitrogen, argon or krypton at low temperatures[5-10], and from the projected area of monodisperse silver-halide particles of very regular shape[11, 12]. Herz and Helling[12] used three different methods other than dye adsorption and obtained very good agreement for the specific surface area of the solid. The use of *p*-nitrophenol[13] as an intermediate adsorbate appears to have little absolute accuracy for surface area measurement, mainly because many isotherms show no clearly defined plateaux. Of the studies listed references 5–12 are probably the most precise.

AGGREGATION OF THE DYE IN SOLUTION

Recent reviews[14-16] indicate that many of the dyes used for adsorption studies aggregate in aqueous solution to form dimers and higher aggregates in the concentration range covered by the adsorption isotherm. *Figure 1* shows that a thiacarbocyanine dye may have half its concentration in solution at equilibrium with saturation adsorption, present as dimers. The reduction in the concentration of the monomer due to aggregation has the effect of contracting the plateau of the isotherm as shown in *Figure 2.*

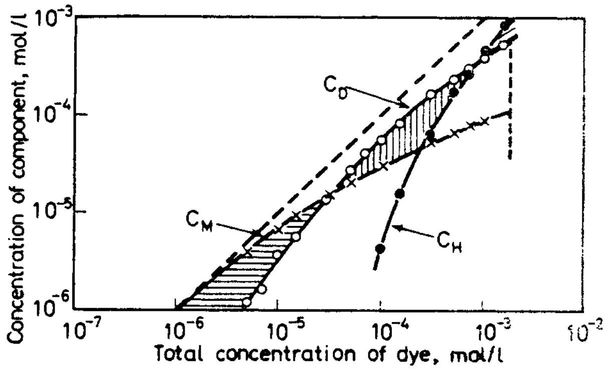

Figure 1. Logarithm of concentrations of monomer (C_M), dimer (C_D) and trimer (C_H) of a thiacarbocyanine dye in water a~ a function of the logarithm of the total dye concentration.

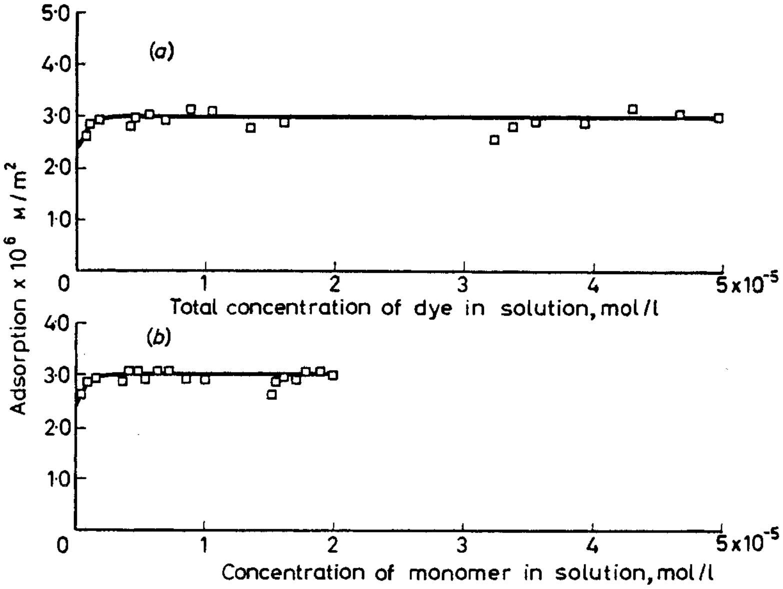

Figure 2. Adsorption isotherm of a thiacarbocyanine dye adsorbed onto silver bromide from water; *a* as a function of total dye concentration; *b* as a function of the concentration of monomer.

However such a contraction can be applied when it is certain that only the monomer is adsorbed as then the conditions of reversible adsorption of a single species are met. For other systems adsorption should be regarded as complex and unlikely to follow Langmuir's conditions for adsorption.

AGGREGATION OF DYES ADSORBED AT THE SURFACE

It is well known that many cyanine and other dyes adsorb on the solid in the aggregated form. Although many dyes aggregate in solution, the data referring to cyanine dyes indicates that the aggregation giving rise to metachromasy in solution produces similar metachromatic changes with the dye in the adsorbed state. For this reason adsorption isotherms of some cyanine dyes have been accompanied by spectral reflectance measurements as an additional probe for the surface state of the dye. Examination of published spectra[2, 6–9, 17–19] indicates that some dyes are present in at least two forms. However, Herz *et al.*[20, 21] consider that only one species is adsorbed at the saturation plateau of 1,1′-diethyl-2,2′-cyanine and that all the dye is in the aggregated form.

The wavelength of the band due to monomer (M-band) is shifted towards the red region when the dye is adsorbed onto a silver halide as monomer[22]. This shift is due to the change in refractive index of the environment of the dye. Apart from this the spectrum of a dye in its adsorbed state shows metachromatic changes very similar to those that occur in solution and are attributed to aggregation. Herz and Helling[20, 21] have analysed reflectance spectra of dyes in the adsorbed state in terms of Kubelka and Munk's equation. This method takes account of the non-linearity of absorbance, as measured by the reflectance method, when the surface concentration of dye is increased. Herz and Helling have further shown that adsorption isotherms may be obtained, without separating the liquid and solid phases, by using this method of spectral analysis[20]. However the method works best when the dye is adsorbed in a single state. Comparison of the spectra of the dye 1,1′-diethyl-2,2′-cyanine in the adsorbed state[7, 8, 20, 21] indicates that reflectance spectra agree in general features but not in detail. For instance, there is no clear agreement as to how much dye, if any, is present in the monomer form when the surface concentration is at its maximum value. The reason for this difficulty is that the adsorption spectrum of the dye in the aggregated state has an absorption shoulder that lies near the main peak of the dye in its monomer state, and discriminating between them is complex. Resolution of M and D states (the D state being the first aggregation state composed of dimers) is somewhat easier but is still complex, as a similar overlap may exist. However, 1,1′-diethyl-2,2′-cyanine appears to adsorb onto silver bromide in predominantly one state, whilst other dyes appear to show adsorption in two or more states at saturation coverage.

EFFECT OF SOLVENT

It is well known that aggregation of many of these dyes is greatly inhibited by dissolving the dye in alcoholic solution[15, 16]. Silver bromide adsorbs less dye from alcoholic solution than from aqueous solution, and the dye adsorbed is in its monomeric state.[7, 19, 23] However, although in some instances dyeing from alcoholic solution appears to produce a uniform flat-oriented monolayer of adsorbed dye, this cannot be relied upon, and the site area appears to vary with electrolyte concentration and the counterion of the dye. Also the same dye is found to aggregate when adsorbed onto a silver-iodide surface from alcoholic solution[6]. Site areas obtained by adsorption from an alcohol–water mixture[12, 30] were found not to vary, adsorption being very much akin to that from pure water. It thus seems that the site area of a dye can depend critically on the solvent.

EFFECT OF SUBSTRATE

As already noted the adsorption of a cyanine dye from alcohol or from water onto a silver halide surface leads to different coverages according to whether the surface is formed of AgCl, AgBr or AgI[6, 7, 8, 23]. A comparison of the surface spectra of a cyanine dye on AgBr, TlCl and Al_2O_3 shows that the dye is adsorbed in very different ways on each of the surfaces[18, 21] and that on AgBr and TlCl the dye appears to be present in two or more states. Although it is claimed that the site area of the adsorbed dye aggregate is constant for many surfaces[24], (i.e. coverage factor is constant) this is at variance with the work from other laboratories as reported here (see for instance *Table 1* where the site area of a dye on AgBr is larger than on AgI).

Table 1. Site area of 1,1′-diethyl-2,2′-cyanine

Worker	*Substrate*	*Surface area*	*Site area* (Å^2)
Sheppard *et al.* (1938)[2a]	AgBr/AgI	Particle size	80
Skerlak (1941)[27]	Mica		52–76
Hoppe (1944)[28]	Glass	X-ray	80
West *et al.* (1952)[2b]	AgBr	Particle size	79
Klein and Moll (1959)[3]	AgBr	Particle size	75
Pradvik and Mirnik (1960)[4]	AgBr	Particle size	63
Stanienda (1962)[31]	Hg	Polarography	54
Boyer and Cappelaere (1963)[18]	AgBr	Particle size	(70)
Jaycock (1963)[5]	AgBr	Gas adsorption	55
Curme and Natale (1964)[29]	AgBr	Projected area	63
Gunther and Moisar (1965)[26]	AgBr	Projected area	64
Padday and Wickham (1966)[7]	AgBr	Gas adsorption	58
	AgI	Gas adsorption	15
Herz and Helling (1966)[12]	AgBr	Projected area and other methods	54±4
Boyer and Preteseille (1966)[32]	AgBr	Projected area	52–55
Lyjklema and van den Hul (1968)[9]	AgI (alcohol)	Gas adsorption	70–80
Kragh *et al.* (1966)[8]	AgBr	Projected area	82
Peacock and Kragh (1968)[30]	AgBr	Gas adsorption	54
Peacock and Kragh (1968)[30]	AgI	Gas adsorption	43
Herz *et al.* (1966)[21]	AgBr	Projected area	57
Tani and Kikucki (1969)[10]	AgBr	Gas adsorption	60
Tani and Kikucki (1969)[10]	AgI	Gas adsorption	40

If a silver-halide surface is dyed to saturation with a cyanine dye from aqueous solution, it is found in some instances that all the aggregated dye may be removed by washing with alcohol. This process leaves behind an adsorbed layer of monomeric dye which itself can be removed by treating the powder with silver nitrate. Thus it seems that only a proportion of the dye is adsorbed reversibly.

It is well known that the amount of a charged dye adsorbed to a solid depends on the initial surface charge[18]. Thus the site area of 1,1′-diethyl-2,2′-cyanine on silver bromide successively increased (i.e. surface concentration decreased) as the pAg of the solution from which adsorption took place was lowered[26]. Similarly the negatively charged dye erythrosin showed corresponding inability to adsorb on to a negatively charged silver-halide surface at high pAg. Most adsorption data refer to silver halides, the surface of which are saturated with an excess of negative halide ions[25] and under these conditions reproducible site areas of many cationic dyes were obtained.

The adsorption of dyes onto surfaces of different crystallographic index[8, 21, 26] (100 and 111 planes of AgBr) appears to be complex, in that the reflectance spectra at the same surface concentration are different for the two planes. Although constant site area of the adsorbed dye is obtained on each crystal plane with some dyes, the variation in the heat of adsorption with coverage and with the pAg of the dyeing solution[26] suggests that the adsorption process is complex and involves two types of adsorption bonds.

COMPARISON OF RESULTS WITH 1,1′-DIETHYL-2,2′-CYANINE

Many adsorption isotherms of the dye 1,1′-diethyl-2,2′-cyanine have been published and the results of these are given in *Table 1*. These investigations have measured the specific surface area of the substrate by some independent means which was then used to calculate the site area from the adsorption plateau. The determination of specific area prior to Jaycock's work[5] in 1963 was subject to considerable error because the particles forming the powder were distributed over a wide range of size and shape. Following this the more accurate studies with better characterized surfaces showed a remarkably good agreement for the site area of this dye on a silver-bromide surface. This site area is considerably smaller than the 'flat area' of a single dye ion. The site area of this dye on a silver iodide surface, measured by similar methods, was very much smaller than that of the dye on silver bromide and showed greater variation.

The dye 1,1′-diethyl-2,2′-cyanine has certain properties that favour its use for surface area measurement. It is more stable chemically than many other dyes, has relatively high solubility and has good light absorption characteristics. When adsorbed from water its site area appears to be independant of the crystal face onto which adsorption takes place[21], of the temperature, of salts, of hydrogen ion concentration in the region pH 5–10, and of the presence of gelatin. The main disadvantage of this particular dye is that, like other dyes the site area does not appear to be independent of the composition of the substrate.

Methylene blue has been employed extensively for attempts at surface area measurement but is known to give variable extinction coefficients due to demethylation[33], as well as showing the disadvantages of the cyanine dyes.

SITE AREA OF THE ADSORBED DYE

Molecular models indicate that the single dye ions of many of the dyes used for surface-area measurement are not regular in shape. Many of the cyanine dyes have the proportions of a rectangular block. It is to be expected that a single dye ion would rest on the surface in the flat-on orientation, as this should be of lowest energy. As the site area of the dye 1,1′-diethyl-2,2′-cyanine at saturation, particularly when the dye is adsorbed from aqueous solution, is smaller than the flat-on area, alternative methods of accommodating the dye on the surface are needed in explanation. Three alternatives are suggested.

The oldest is simply that the dye ions first adsorb flat-on and then, at higher surface concentrations, tip up into a side-on orientation, while at saturation all the dye is oriented side-on. Such an explanation suggests that the first amounts of dye adsorbed are easily removed to their new position, but experimentally it is found that the dye adsorbed in the lower part of the isotherm is very difficult to move[18]. West[1b] attributes the high initial energies of adsorption as being due to active sites but considers that even at these sites reorientation from flat to side-on arrangement can take place. In addition the site area of 58 Å^2 for 1,1′-diethyl-2,2′-cyanine is very small and involves an edge-on orientation with some interlocking or close packing[21] and no free space. Such an array would, in my opinion, come to equilibrium very much more slowly than is found experimentally.

A second explanation is that the dye first goes on as flat-on dye ion irreversibly adsorbed at low surface coverage, and then a second monolayer of aggregated dye adsorbs on top of the first layer at higher coverages[7]. Such an explanation allows for two species of dye coexisting at the same time on the surface of the solid and at the same time takes account of the partial reversibility of the adsorption process. Some doubt[21] has been cast on the spectral evidence for two species coexisting on the surface in the adsorbed state. However, such doubt rests on the extinction coefficient of the J state at the wavelength of the M band being equal to that of the M state (*i.e.* an isosbestic region) and this has not been decided experimentally. The explanation does not account for the site area of the dye 1,1′-diethyl-2,2′-cyanine adsorbed on silver bromide being very much larger than that on silver iodide.

A third explanation[11] supposes that the dye adsorption process is heterogeneous and that the site area is variable from one part of the surface to another. Such an explanation allows for monomer, dimer and multimer to adsorb first independently on different parts of the surface. As the amount of adsorbed dye increases, so the remaining free area is filled with dye monomer and aggregates depending both on steric effects and on cooperative effects. Thus near saturation coverage some parts of the surface are covered with monomer, but a much larger part is covered with aggregated dye which must be piled above the surface. This explanation takes account of the varying heat of adsorption that is found experimentally and the near certainty that the solid surface has many defects in the surface which may well act as active centres for adsorption at very low concentrations. The explanation is somewhat at variance with the surface spectra data of Herz and Helling[21] but could possibly be compatible with other spectral data[7, 19].

CONCLUSIONS

The information obtained from the adsorption of cyanine and a few other dyes suggests that (i) The surface area of silver bromide, but not of silver iodide, may be measured with the dye 1,1′-diethyl-2,2′-cyanine providing a number of conditions are defined (i.e. pAg and solvent in water). The site area of this dye on AgBr is 58 Å^2 under these conditions. (ii) Generally the site area of a cyanine dye adsorbed from water is too small to accommodate the dye in a simple flat-on orientation. (iii) Spectra of the dye in the adsorbed state indicate clearly that in many systems some of the dye, and in some instances all the dye, is adsorbed in the aggregated state. (iv) As the degree of aggregation of a dye at a solid surface and consequently its site area, cannot be forecast with any certainty, *measuring surface area by the adsorption of dye from solution invariably involves a precalibration of the method against some more reliable method* such as gas adsorption at low temperatures or the geometry of regular monodisperse crystals.

Acknowledgement

I would like to express my warmest appreciation for the advice and help I have received from Dr. A. H. Herz of the Kodak Rochester Laboratories in Rochester.

References

[1a] J. J. Kipling. *Adsorption from solution of non–electrolytes*, Academic Press, London (1966), p. 288.
[1b] A. W. Adamson. *Physical chemistry of surfaces*, 2nd Edn., John Wiley, New York (1967), p. 412.
[2a] S. E. Sheppard, R. H. Lambert and R. D. Walker. *J. Chem. Phys.* **7**, 265 (1938).
[2b] W. West, B. H. Carroll and Whitcomb. *J. Phys. Chem.* **56**, 1054 (1952).
[2c] C. E. K. Mees. *The Theory of Photographic Process*, 3rd Edn., Macmillan, New York.
[3] E. Klein and F. Moll. *J. Phot. Sci. and Eng.* **3**, 232 (1959).
[4] V. Pravdic and M. Mirnik. *Croat. Chem. Acta*, **32**, 1 (1960).
[5] M. J. Jaycock. Thesis, Cambridge (1963).
[6] J. F. Padday. *Trans. Farad. Soc.* **60**, 1325 (1964).
[7] J. F. Padday and R. S. Wickham. *Trans. Farad. Soc.* **62**, 1283 (1966).
[8] A. M. Kragh, R. Peacock and G. S. Reddy. *J. Phot. Sci.* **14**, 185 (1966).
[9] J. Lyklema and H. J. van den Hul. *J. Amer. Chem. Soc.* **90**, 301 (1968).
[10] T. Tani and S. Kikuchi. *J. Phot. Sci.* **17**, 33 (1969).
[11] E. Gunther and E. Moisar. *J. Phot. Sci.* **13**, 280 (1965).
[12] A. H. Herz and J. O. Helling. *J. Coll. Sci.* **22**, 291 (1966).
[13] C. H. Giles and S. N. Nakau. *J. Appl. Chem.* **12**, 166 (1962).
[14] J. A. Bergeron and M. Singer. *J. Biophys. Biochem. Soc.* **4**, 433 (1958).
[15a] J. Nys. *Symposium on special sensitization*, Bressanone Aug. 1967 (preprints).
[15b] J. F. Padday. *Proc. N.A.T.O. Advanced Study Institute on Connective Tissue Research*, Santa Mergherita, Italy, Academic Press, London (1969) (in press).
[16] J. F. Padday. *J. Phys. Chem.* **72**, 1259 (1968).
[17] W. West and B. H. Carroll. *The Theory of the Photographic Processes* 3rd Edition. Ed. C. E. K. Mees and T. H. James. Macmillan, New York (1966), p. 233.
[18] S. Boyer and J. Cappelaere. *J. Chim. Phys.* **63**, 1123 (1963).
[19] S. V. Natanson and N. I. Sennikova. *Trudy Vsesoyuz Nauch-Issledovatel. Kinefotoinst.* No. 40, 34 (1960).
[20] A. N. Herz and J. O. Helling. *Kolloid Z.* **218**, 157 (1967).
[21] A. H. Herz, R. B. Danner and G. Janusonis. *Advances in Chemistry Series* "*Adsorption from Solution.*" No. 78. American Chemical Society (1967).
[22] W. West and S. Pearce. *J. Phys. Chem.* **69**, 1894 (1965).
[23] H. J. van den Hul. Thesis Utrecht 1966.
[24] C. H. Giles, A. P. D'Silva and A. S. Trivedi. This symposium, p. 317.
[25] A. H. Herz and J. O. Helling. *J. Colloid Sci.* **17**, 293 (1962).
[26] E. Gunther and E. Moisar. *J. Phot. Sci.* **13**, 280 (1965).
[27] T. Skerlak. *Kolloid Z.* **95**, 265 (1941).
[28] W. Hoppe. *Kolloid Z.* **109**, 21 (1944).
[29] H. C. Curme and C. C. Natale. *J. Phys. Chem.* **68**, 2009 (1964).
[30] R. Peacock and A. M. Kragh. *J. Phot. Sci.* **16**, 229 (1968).
[31] A. Stanienda. *Z. Physik. Chem.* (Frankfurt), **32**, 238 (1962).
[32] S. Boyer and M. Preteseille. *Sci. Ind. Phot.* **37**, 129 (1966).
[33] K. Bergmann and C. O'Konski. *J. Phys. Chem.* **67**, 2169 (1963).

DISCUSSION

Dr. W. Carr (*Geigy* (*U.K.*) *Ltd.*) said: Surface area measurement by adsorption of dyes from solution is a technique that is simple, rapid and versatile. There is however, to my mind, one question mark which hangs over the whole technique and which casts doubt on its validity. This question is whether the amount of dyestuff adsorbed by a powdered substrate is dependent on the degree of dispersion of the solid. The normal experimental technique used in adsorption experiments comprises simple mechanical stirring or end over end tumbling of the powdered solid in the dyestuff solution. It is known that under these conditions, the degree of dispersion of the solid, especially with hydrophobic materials such as carbon blacks and organic pigments, is poor and that the solid is present in the suspension in the form of dense aggregates and not as individual particles. Do these aggregates have the same adsorption capacity as the individual basic particles? An idea of the tremendous degree of aggregation can be obtained from electron micrographs of a yellow organic pigment (C.I. Pigment Yellow) and a carbon black taken under conditions of light and heavy dispersion.

Whether the aggregates have or have not a reduced capacity for adsorption from solution compared with the unaggregated particles has not been rigorously established but the weight of indirect evidence is heavily on the side of reduced adsorption.

Dr. J. F. Padday replied: Most of the dyes used for surface area measurement do not lower the surface tension of water and do not help the water to wet a low energy surface. Thus when measuring the adsorption of a dye from aqueous solution onto finely divided carbon black it is well known that errors arise due to poor wetting of clusters or aggregates of the solid powder. Tumbling or shaking is often insufficient to ensure good wetting but in my own experience two minutes' exposure to ultrasonic vibration is usually sufficient to break up these clusters. When this is done the powder is then allowed to come to equilibrium with the solution in the usual way.

Dr. A. J. Groszek (*BP Laboratories, Sunbury*) said: Referring to different ways in which certain dye molecules are orientated at the interface between silver halides and water, I would like to report similar phenomena occurring in for n-octadecanol adsorbed at iron oxide/n-heptane interfaces. This long-chain alcohol is adsorbed strongly by α-Fe_2O_3 and Fe_3O_4 from dilute solutions in n-heptane and it was thought therefore that the adsorption could be used for the estimation of specific surface areas of polar solids, such as the iron oxides. An indication was obtained, however, from the heat of adsorption measurements in the flow microcalorimeter, that n-octadecanol is adsorbed on the iron oxides in two positions occupying different areas on the surface. An example of this effect is shown in *Figure A* for Fe_3O_4. As can be seen the heat of preferential adsorption increases with solute concentration in two steps, a steep increase in the heat occurring with the concentration of n-octadecanol is about 1·5 g/l. The adsorption isotherm for this system at 21°C also shows two distinct steps. The amount of adsorption at the lower step corresponds approximately to the areas occupied by horizontally oriented molecules (area per molecule 90 Å^2) whilst at the higher step the

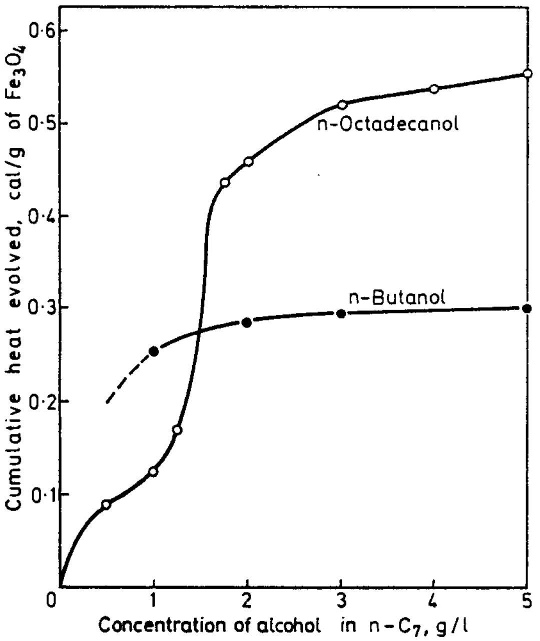

Figure A. Effect of concentration on heat of adsorption of n-alcohols at Fe_3O_4/n-heptane interface.

area is 20 Å^2, i.e. is more in line with the close-packed vertically oriented molecules.

The change in the orientation of the adsorbate makes it difficult to use n-octadecanol and other similar long-chain compounds for the estimation of surface areas, as the transition from the 'horizontal' to 'vertical' orientations the solid/liquid interface for such compounds may occur at varying solute concentrations for different metal oxides. In contrast, the adsorption of a short-chain alcohol, such as n-butyl alcohol, occurs in most cases with the formation of a single distinct plateau, as shown for Fe_3O_4 in the figure. The amount of adsorption and the integral heat of preferential adsorption corresponding to the plateau can be used therefore for the estimation of specific surface areas with more confidence than the estimation made on the basis of adsorption of the long-chain polar compounds.

It has been shown in fact, that the integral heats of preferential adsorption of n-butanol from n-heptane determined in the flow microcalorimeter correlate well with the specific surface areas of several non-porous metals and metal oxides measured by the BET method [A. J. Groszek. *Chem. & Ind.* 1754 (1966)], demonstrating the suitability of the preferential adsorption of n-butanol from n-heptane for the estimation of specific surface areas of polar solids.

Dr. J. F. Padday replied: I think it could be stretching assumptions too far to estimate any sort of orientation from the shoulder of the n-octadecanol curves of Fig. *A* as suggested in the comments. At the concentration corresponding to the inflexion point one would expect a statistical distribution of heptane in its several orientations and n-octadecanol in its several orientations. A more informative plot would be the integral heat per mole adsorbed plotted as a function of concentration as then one would detect the difference between adsorption energy at the initial stages and that at saturation of the isotherm.

SPECIFIC SURFACE AREAS BY NEGATIVE ADSORPTION

J. LYKLEMA and H. J. VAN DEN HUL†

Laboratory for Physical and Colloid Chemistry,
Agricultural University, Wageningen,
Netherlands

INTRODUCTION

When a solid is suspended or colloidally dispersed in an electrolyte solution, an electrical double layer will develop around the particles, provided that they are charged. If for example the particle charge is negative, a positive countercharge of equal magnitude arises on the solution side of the double layer. This positive charge is made up of the following three contributions (henceforth called the ionic components of charge): (i) an excess of cations (counterions) in the Stern layer; (ii) an excess of cations in the Gouy layer; (iii) a deficit of anions (co-ions) in the Gouy and the Stern layer, the latter of which is negligible.

The accumulation of counterions according to (i) and (ii) is an example of 'positive adsorption', or simply 'adsorption'. It is characterized by a positive surface excess. The deficit of co-ions according to (iii) is an example of 'negative adsorption', characterized by a negative surface excess.

A number of methods for the determination of specific surface areas are based on various forms of positive adsorption, e.g. gas adsorption, such as the BET-method, and adsorption from solution of solutes such as dyes, surfactants, and fatty acids. These methods involve essentially three steps: (i) The experimental determination of the amount adsorbed as a function of gas pressure or solute concentration at constant temperature, the so-called adsorption isotherm; (ii) The derivation of the amount adsorbed in a monolayer, v_m, from the shape of the isotherm and/or theoretical considerations; (iii) Calculation of the surface area of the adsorbent from v_m, after assignment of an effective cross-sectional area a_0 to the adsorbate molecule. This is often a vexed problem, as a_0 depends on a number of factors, such as the nature of the adsorbent, its surface charge, and—in the case of adsorption from solution—on the nature of the solvent. Thus, we cannot generally assign a universal value to a_0.

The negative adsorption (NA) method for the determination of specific surface areas is based on the expulsion of co-ions. It has the following advantages and limitations.

(i) The NA is measured as an, usually small, increase in concentration (Δc), requiring accurate analytical techniques and setting a lower size limit

---

† The Plastics Laboratory, The Dow Chemical Co., Midland, Michigan, U.S.A.

to the specific area that can be measured. (ii) The surface area is directly proportional to Δc; the proportionality constant does not contain a cross-sectional area. This is an important advantage over the positive adsorption methods. (iii) Instead of a_0, the potential or charge of the diffuse part of the double layer is a parameter in the equations. However, in the limiting case where the potential or the charge is sufficiently high, the NA is independent of it, and is thus insensitive to the electrical properties of the expelling surfaces. (iv) As the method is applied in solution, drying artefacts are excluded. This is an advantage in the case of colloidal or suspended systems, where the measurements can be carried out *in situ*.

The advantages outlined under (ii), (iii), and (iv) make the NA method principally attractive in those cases in which it is applicable. On the other hand, the inherent limitations will prevent the method from becoming a routine tool.

Below we shall briefly discuss the theoretical outlines, survey the present status, and present a comparative study of areas, determined by NA and by other methods.

NEGATIVE ADSORPTION IN THE ELECTRICAL DOUBLE LAYER

Although the NA of co-ions has been treated in a number of papers, in very few cases was the proportionality between the surface deficit and the expelling area explored to estimate the latter. Historically, the contribution of the NA is an integral part of the Gouy–Chapman theory[1, 2]. The expulsion of salt from a colloidal dispersion in a Donnan membrane equilibrium[3–5] is also well known.

Grahame *et al.*[6, 7] determined the ionic components of charge on mercury, except for a constant, from the concentration dependence of the surface charge σ_0. The constant was evaluated by comparison of the thus obtained NA with the NA calculated from the Gouy theory, and agreed with the constant derived from the shift in the electrocapillary maximum. As the Gouy calculation involves the area of the mercury electrode, Grahame's results implicitly amount to a corroboration of the relation between NA and surface area in the Gouy theory. After modification, his procedure can also be applied to reversible systems, such as AgI[8] and SiO_2.[9]

In a number of practical cases, NA is also important. The ion exclusion from ion-exchange membranes or resins is used both in industry and in the laboratory for the separation of electrolytes and non-electrolytes[10] and desalting by electrodialysis[11]. Another example is salt sieving by clays and sands in agriculture[12]. Groenevelt and Bolt[13], for example, calculated the coefficients in the phenomenological equations of irreversible thermodynamics describing this process. These coefficients depend on the extent of the co-ion expulsion. The ion exclusion found by Horne *et al.*[14] when electrolyte solutions were filtered over columns containing silica or alumina, may thus also be partly due to expulsion of ions in the electrical double layer and is not necessarily evidence for the existence of structured water layers at the surface.

Vrij and Overbeek[15] accounted for the contribution of the NA of co-ions from charged colloidal particles in the fluctuation theory of light scattering. Stigter and Huisman[16] considered the NA around micelles.

A number of authors have derived relations between the NA and various double layer parameters, including in some cases the specific surface area. Especially relevant to our subject are the calculations of Loeb *et al.*[17], who treat the NA as a function of surface potential and curvature, and those of de Haan and Bolt[18, 19] who take into account double layer overlap and exclusion in mixed electrolytes. Other references will be mentioned below.

SURFACE AREAS FROM NEGATIVE ADSORPTION

Surface areas can be calculated from the experimental NA by either of two methods. Both are based on the Gouy theory of the diffuse part of the double layer and disregard double layer overlap; however, their elaboration is quite different. In the first method, advanced by Schofield *et al.*[20], the surface charge is taken as the primary variable, in the second method, used by van den Hul and Lyklema[21], the surface potential.

In the latter approach the NA, Γ_i of a given co-ion *i* is derived from the ion distribution in the double layer, which is shown schematically in *Figure 1*†.

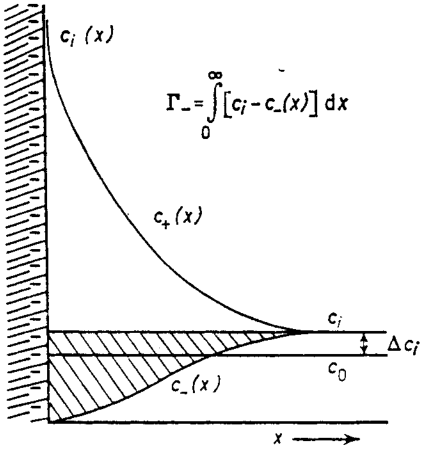

Figure 1. Equilibrium distribution of ions at an uncharged surface (c_0) and a negatively charged surface (c_i) assuming $\psi_0 = -\infty$

The surface deficit Γ_i is indicated by the shaded area and is given by

$$\Gamma_i = \int_0^\infty [c_i - c_i(x)]\,dx \qquad (1)$$

where c_i is the equilibrium concentration in moles/cm^3; Γ_i has the dimension of moles/cm^2. The total ion exclusion from a surface of S cm^2 of expelling surface area is $S\Gamma_i$ moles. On the other hand we can derive from a material balance that

$$S\Gamma_i = V_t\Delta c_i \qquad (2)$$

---

† Figures 1–4 in this communication are reproduced from *J. Colloid Interface Sci.* by the courtesy of Academic Press.

in which V_t is the total liquid volume in which the dispersion with area S cm^2 is suspended. S can be calculated after combination of Eqs. (1) and (2) if the integration can be carried out. This is done as follows. The distribution $c_i\ (x)$ is given by the Boltzmann equation,

$$c_i(x) = c_i \exp(-z_i e\psi(x)/kT) \tag{3}$$

where $\psi(x)$ is the potential in the double layer at a distance x from the surface and z_i is the valency of the ion i, sign included. Now, x is replaced as a variable by ψ, making use of the following equation of the diffuse double layer theory[22] holding for flat double layers:

$$\left(\frac{\mathrm{d}\psi(x)}{\mathrm{d}x}\right)^2 = \frac{8\pi NkT}{\epsilon}\sum_j c_j\{\exp(-z_j e\psi(x)/kT) - 1\} \tag{4}$$

where the summation is extended over all ionic species present. Combination of Eqs. (1) through (4) results in a general relation between S and Δc, containing the integration over the co-ion distribution between the limits[21] $\psi(x = 0)$ and $\psi(x = \infty)$. This integration easily leads to a simple solution if two assumptions are made: (i) only one electrolyte is present; (ii) the surface potential is infinitely high, which is equivalent to setting the concentration of expelled co-ions at the surface to zero (see *Figure 1*). Then:

$$S = V_t(\Delta c_1/c_1).(\varkappa/A)\ \mathrm{cm}^2 \tag{5}$$

where $1/A$ is the solution of the integral, and $\varkappa$ is the so-called reciprocal double layer thickness, defined in the usual way.

For aqueous solutions at 20°C we calculate:

$$S = B\mathrm{x}10^7 V_t(\Delta c_1/c_1)\ \sqrt{c_1}\ \mathrm{cm}^2 \tag{6}$$

with c_1 now in moles/l. Values for the constants A and B are given in *Table 1* for various electrolyte types at a negatively charged surface.

The approach taken by Schofield does not differ principally from the one outlined above, but aims at systems of known charge density (such as clays). For mathematical convenience, Schofield extended the concentration-distance curves beyond the surface over a distance δ to the point where $c_1(x) = 0$ as shown in *Figure 2*. For δ he derived the approximation $\delta \approx 4\beta\Gamma_0$, in which Γ_0 is the surface charge density in g.ions/cm^2 and $\beta = 8\pi \mathrm{Ne}^2/\epsilon kT$. The relative NA is then given by

$$\frac{\Gamma_1}{c_1} = \frac{q}{(\beta c_1)^{\frac{1}{2}}} - \frac{4}{\beta\Gamma_0} \tag{7}$$

with c_1 again in moles/l and q a constant given in *Table 1*.

In the limiting case of infinitely high Γ_0

$$\frac{\Gamma_1}{c_1} = \frac{q}{(\beta c_1)^{\frac{1}{2}}} - \frac{q\lambda}{\varkappa} \tag{8}$$

with λ defined by $\lambda^2 = (z_+ + z_-)/2z_+$. This case is equivalent to our solution for high surface potential. Combination of Eqs. (2) and (8) leads to Eq. (5) with $A = q\lambda$ (see *Table 1*). Thus we conclude that in the limiting case of high charge and high potential both theories are identical. In case these conditions are not fulfilled (see below) it is a question of convenience rather than principle whether the surface charge or the surface potential is chosen as the primary variable.

Table 1. Constants A and B of Eqs. (5) and (6) for various electrolytes and values of q and λ of Eq. (8), at a negative surface†

z_+	z_-	A	B	λ	q
z	z	2	1·64z	1	2
2	1	1·268	4·48	0·866	1·464
3	1	0·943	8·51	0·816	1·16
1	2	3	1·89	1·225	2·46
1	3	3·743	2·14	1·414	2·65

†For positive surfaces, z_+ and z_- have to be interchanged.

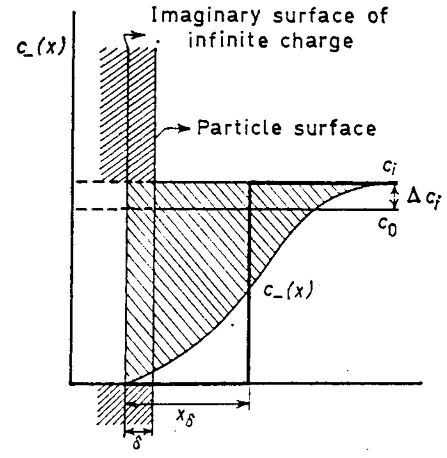

Figure 2. Equilibrium distribution of co-ions at a negatively charged surface of low surface charge density

EXPERIMENTAL DETERMINATION OF NEGATIVE ADSORPTION

Generally, two experimental methods can be distinguished. In the first, a known quantity of solid is dispersed in an electrolyte solution, equilibrated, and a clear supernatant obtained by sedimentation of the solid by gravity[20, 21] or by centrifugation[23]. The equilibrium concentration of co-ions is determined analytically in the supernatant, and if desired in the sediment. The NA is then calculated from the increase in co-ion concentration in the bulk liquid due to introduction of the solid.

The following example may illustrate this. A wet paste, containing about 5 g AgI, is weighed into a 100-ml wide-mouthed bottle. A calculated amount of KI solution was added to provide the necessary surface potential. Then, 10 ml of a 10^{-4} N K_2SO_4 solution was added. The suspension was stirred for 1 h, allowed to settle for two days, the supernatant pipetted off and analyzed.

In cases where the dispersed particles do not settle by gravity, they can be centrifuged off, although one should be aware of the centrifugation potential thus generated; this tends to compensate the NA. This effect is most pronounced in solutions of low x at high centrifugal velocity[12]. Also, if the sediment is too tightly packed, double layer overlap will result in a decrease in NA. In those cases an alternative method can be used based on a membrane equilibrium[18, 24]. A dispersion is measured into a cellulose dialysis bag and the bag immersed in the electrolyte solution (or vice versa), and the system equilibrated. Then, the co-ion concentration on both sides of the membrane is determined.

FACTORS AFFECTING THE NEGATIVE ADSORPTION

Concentration of co-ions

According to Eq. (6), S can be calculated from one NA measurement at one concentration. However, in order to check the validity of this equation, measurements have to be performed at several concentrations. One could then plot $10^7\ V_tB\Delta c_1/c_1$ against $c_1^{-\frac{1}{2}}$, which should yield a straight line through the origin with slope S. A more elegant way is obtained, if the smooth $c_-(x)$ curve in *Figure 1* is replaced by a step function (*Figure 2*) in which $c_-(x)$ is zero over a distance X_δ, the distance of exclusion, then jumps to the bulk value c_1. In that picture, a volume $\Delta V = SX_\delta$ can be considered void of co-ions. As analytically this volume of exclusion $\Delta V = V_t\Delta c_1/c_1$, Eq. (5) can be written as $\Delta V = SA/\varkappa$ and a plot of ΔV versus $A/\varkappa$ $(=X_\delta)$ should again be linear with slope S. In *Figure 3* an illustration of such a plot is given for the NA of HPO_4^{2-} and SO_4^{2-} ions from negative AgI[21c].

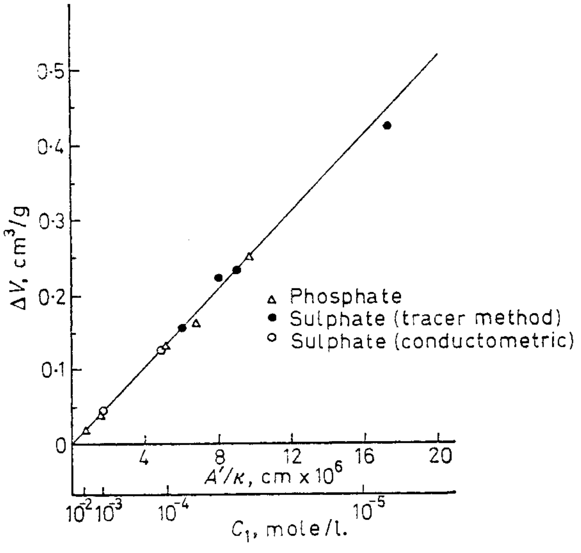

Figure 3. Concentration dependence of the negative adsorption on AgI. S(NA) = 2·6 m²/g

Presence of other ions

If another electrolyte, e.g. a potential determining one is present in a concentration of the order of c_1 or larger, the equations are more elaborate. For negative particles, $\sqrt{c_1}$ can simply be replaced by $\sqrt{(c_1 \pm c_2)}$ for both (1:1) and (2:1) electrolytes, if c_2 is the concentration of the second electrolyte. A solution for (1:2) electrolytes has been given by van den Hul and Lyklema[21a, b]. A more complete set of results for various mixed electrolytes, calculated by using Schofield's approach, has been published by de Haan and Bolt[18, 19].

Double layer overlap

The NA, measured from closely-packed sediments or very concentrated suspensions, will be lower than the theoretical one because of double layer overlap. Quantitative examples are given in the literature[18, 25, 26]. The most extensive treatment of the effect of double layer overlap has been given by de Haan[18]. From his paper it can be derived that the NA is depressed by less than 5 per cent, if the interparticle distance is $>8/\varkappa$.

Curvature

Both approaches discussed earlier are based on the theory for isolated flat double layers. In real suspensions, however, the particles are often more nearly spherical. Stigter[16] and Loeb *et al.*[17] have given calculations of the NA from spherical particles of known radius a.

For the calculation of an unknown radius or surface area from the experimental NA, van den Hul and Lyklema[21] derived the following equation—valid if either z_+ or $z_- = 1$:

$$S = 1{\cdot}638 \times 10^7 \sqrt{z_-} V_t(\Delta c_1/c_1) \sqrt{c_1}(1/I_-) \text{ cm}^2 \tag{9}$$

with z_- = the valency of the co-ion and I_- = a parameter tabulated by Loeb *et al.* as a function of the potential and of the 'reduced radius' $q_2 = \varkappa a/\lambda$. Thus, the unknown parameter a is required in its own calculation and Eq. (9) cannot be used directly, except by a successive approximation method. However, in the case of homodisperse systems, $S = 3/\rho a$, in which ρ is the solid density. If this is substituted in Eq. (9), then, after rearrangement and introduction of numerical constants:

$$V_t(\Delta c_1/c_1)\ \rho = \Delta V\rho = 6I_- z_+/q_0 \tag{10}$$

One can now construct theoretical plots, for each potential, of $\Delta V\rho$ versus z_+/q_0, by calculating the right-hand-side of Eq. (10) for various combinations of particle size and concentration. To calculate a or S from experiment we express the data as $\Delta V\rho$, determine the corresponding z_+/q_0 value from the plot and calculate a from q_0. This value of a may be called the 'negative adsorption average radius' a_{NA}. For non-uniform size distributions, the average calculated by this method is generally close to the volume/surface average a_{VS}. Model calculations[27] show a_{NA} to be within a few per cent of a_{VS} for many bimodal, normal, and log normal distributions. Only if the relative number of small particles is large, or the distribution very wide, will a_{NA} shift to lower values and approach the number average.

For other shapes (spheroids, rods), the effect of curvature will be overestimated by the use of Eq. (10) and the calculated areas will be too low.

Surface roughness

NA areas are measured with $1/\varkappa$ as a yardstick. Hence, irregularities, pores, etc. $< 1/\varkappa$ are not seen. Moreover, in pores of radii $< 4/\varkappa$ double layer overlap decreases the NA even more. Thus, the method applies to smooth, non-porous surfaces only. On the other hand, it is possible to assess the extent of porosity by comparing the (smoothed) NA area with the internal (e.g. gas adsorption) area[9].

Potential or charge

As was mentioned above, the concentration of co-ions at the surface is only zero for infinitely high potential or charge. However, in real systems these parameters have a finite value. Moreover, it should be realized that NA occurs in the diffuse part of the double layer. The determinative parameters are the potential of the outer Helmholtz plane ψ_δ or the diffuse double layer charge $\sigma_d = F\Gamma_d$. This means that a high surface charge in itself is not sufficient argument for the applicability of the NA method, because ψ_δ may be low due to extensive counterion adsorption in the Stern layer. Conversely, the opposite situation is imaginable: an uncharged surface (e.g. carbon black) with a high Stern charge (e.g. due to the adsorption of anionic surfactants) may lead to a high ψ_δ.

The problem of how to deal with a low ψ_δ or Γ_d has been considered both by Schofield and by van den Hul and Lyklema. As mentioned above, Schofield tried to solve this problem by defining a hypothetical plane of infinite charge at a distance δ from the surface (actually the outer Helmholtz plane) for which he derived $\delta \approx 4/\beta\Gamma_0$, which is the second term in the Schofield equation (Eq. 7). Thus, S can be calculated if Γ_0 is known, or can be obtained from a plot of ΔV versus $q/(\beta c_1)^{\frac{1}{2}}$. As one can see by substituting Γ_1 from Eq. (2) into Eq. (7), this plot should be linear with slope S and intercept $4S/\beta\Gamma_0$. It must be realized, that Eq. (7) is only valid when the first term on the right is at least 5 times the second[20a, 28], which requires for example a charge of $\gtrsim 3 \mu C/cm^2$ for $c_1 = 10^{-2}$M.

Hunter and Alexander[29] have derived an equation for the charge dependence at very low surface charge or potential (<25 mV).

In our approach, the introduction of a non-infinite ψ_δ is introduced in a straightforward manner because the integration in Eq. (1) is now carried out with $\psi(x = 0) = \psi_\delta$ as the upper limit, instead of $\psi(x = 0) = \infty$. The result for a (1:1) electrolyte and flat plates reads for example

$$S = 1{\cdot}64 \times 10^7 \, V_t(\Delta c_1/c_1)\sqrt{c_1}[1 - \exp(e\psi_\delta/2kT)]^{-1} \qquad (11)$$

This equation is equivalent to Eq. (6), except for the term between brackets. It is obvious, that on increasing negative ψ_δ, the exponential will decrease, and the term between brackets will approach unity. Thus, at high potential the NA becomes potential independent. E.g. for $\psi_\delta = -50$ mV this term is 0·566, for -100 mV 0·865, for -150 mV 0·952 and for -250 mV 0·994.

For spherical particles, the potential dependence can be accounted for by choosing the value of I_- in Eqs. (9) or (10) from the tables of Loeb *et al.* at the proper value of the potential. The effect of potential is relatively more pronounced at low $\varkappa a$, e.g. the NA at $\varkappa a = 1$ is decreased by a factor 0·495, 0·733, 0·885 and 0·990 at potentials of −50, −100, −150 and −250 mV respectively. The effect of potential is somewhat smaller for bi- and trivalent ions.

The above relation has been checked successfully for the silver iodide system. In this case, $\psi_\delta = \mathrm{f}(\psi_0)$ can be evaluated from the adsorption isotherms of the potential determining ions[8, 30], assuming absence of specific adsorption, which is an acceptable approximation in the low salt concentrations considered. The result in *Figure 3* shows that the NA is independent of the surface potential for ψ_0 more negative than −200 mV in the case of SO_4^{2-}, and −250 mV in the case of HPO_4^{2-} ions. At lower potentials specific adsorption in the Stern layer reduces the NA, so that close to the point of zero charge even positive adsorption of these ions occurs.

For materials, where the $\psi_\delta = \mathrm{f}(\psi_0)$ relation is not available, measurements at two or three potentials may be necessary. For example, recent measurements by Breeuwsma[31] show that the NA of several cations from positively charged haematite (α-Fe_2O_3) was independent of pH (i.e. independent of ψ_0) over several pH units, suggesting that the maximum level is reached.

Another possibility to assess ψ_δ is identification with the zeta potential, assuming $\zeta = \psi_\delta$ which is probably a reasonable approximation at low ionic strength. At high potential deviations may be expected with $\zeta < \psi_\delta$, but there the effect of the potential on the NA will be less. An attempt to relate ζ to the NA has been made by Saleeb and Kitchener[26].

It would be worthwhile to study systematically the NA as a function of the zeta potential for several systems.

COMPARISON OF SURFACE AREAS

In comparing NA-areas with areas determined by another method, it should be kept in mind that agreement may be expected only when the premises underlying both methods are satisfied. A comparison might still be useful, even when all conditions are not met, because interesting information regarding the surface properties of the system can be derived from it. For example, comparison of the smoothed NA-area with a BET- or t-plot area on a porous system can yield useful information on the surface porosity. In addition, comparison between the 'wet' NA-area and the 'dry' BET-area could reveal drying artefacts. However, systematic comparative studies are scarce. The systems studied most extensively are clays and AgI. Part of this work has already been reviewed[21b, 25].

Clays

Clays derive their charge from isomorphic substitution and from dissociation of surface groups (silanols and others). The surface charge, as calculated from the exchange capacity is quite high and the particles are platelets. Hence, if complications such as adsorption at positively charged edges or incomplete swelling are absent, this is an ideal system to apply the NA-method.

Schofield[19a, b] first tested his equation using data of Mattson[32] for the NA of Cl^-, NO_3^-, SO_4^{2-}, and $Fe(CN)_6^{4-}$ ions from Na- bentonites. He found a NA-area of 482 m^2/g as compared to 700–800 m^2/g from x-ray determination of the basal spacings. Schofield suggested that incomplete dispersion was responsible for the discrepancy. In a subsequent paper, Schofield and Samson [19c] gave NA-areas for three kaolinites under conditions of complete swelling, 8, 9, and 18 m^2/g respectively. These results compare very well with the BET (N_2)-areas: 6, 10 and 16 m^2/g. In one other kaolinite sample the NA-area of 25 m^2/g fell below the BET-area of 39 m^2/g, which could be ascribed to contamination of the sample by iron oxide, which is positively charged under the experimental conditions and hence tends to adsorb anions positively.

As Schofield pointed out, the positive adsorption at the positively charged edges should be eliminated or accounted for in order to arrive at reliable NA values. Bolt and Warkentin[24] 'blocked' these positive edges by specific adsorption of poly-metaphosphate or low molecular weight polyacrylic acid and arrived at the very reasonable value of 700 m^2/g for Na-montmorillonite. Untreated clays gave lower areas, as was confirmed by Edwards and Quirk[33]. However, these authors attributed the low observed NA not to positive adsorption at the edges, but to double layer overlap. In the case of Ca-montmorillonite, Bolt and Warkentin found a slightly greater discrepancy with the crystallographic area than with the sodium clay, whereas Edwards and Quirk (on untreated samples) found an area as low as 85 m^2/g. In relation to this, the strong chemisorption of Ca^{2+} onto surface silanol groups should be mentioned, as this tends to lower ψ_δ (or Γ_d) and hence the NA[34]. The measurements have been extended by de Haan and Bolt[19] to systems with Cl^-, SO_4^{2-}, as well as mixtures of these ions. Again satisfactory agreement with the crystallographic area was achieved under conditions where the NA-method would be expected to apply.

Some unexpected results have recently been obtained by Edwards *et al.*[35] on homo-ionic Fithian illites, non-expandable clays saturated with various mono- and bivalent cations. The BET-area was 110 m^2/g, but the NA-areas (slope of the linear ΔV versus $q/(\beta c_1)^{\frac{1}{2}}$ plots) ranged from 0 m^2/g for Cs^+ and most of the bivalent ions, to 80 m^2/g for the Li-clay. Double layer overlap, or a low charge density due to ion association were excluded as possible explanations. A discreteness of charge effect is suggested instead. The model the authors give for the ion specificity is not very convincing, therefore their results remain largely unexplained.

Bower and Goertzen[36] measured the NA of chloride ion from twelve Ca-saturated soils and plotted the results against the total surface area as determined by the glycol retention method (see below). The reciprocal slope of the so obtained linear plot, is the average NA per unit area, and is 0·306 μeq./cm^2. With Eq. (6) we calculate for this case a theoretical NA of 0·315 μeq./cm^2. Thus, the agreement between the average glycol retention and NA-areas is very good. The glycol retention method[37], in which the surface area is found from the amount of glycol retained in the suspension, has the same drawbacks as other adsorption methods, such as the uncertainty of the effective cross-section a_0 of the adsorbed glycol molecule and its dependence on the nature of the solid and the surface charge.

Later, de Haan[38] found NA-areas (after treatments with Na_3PO_4) 2–7 times lower than glycol retention areas on twelve Dutch soils and one pure illite fraction. The surface charge density calculated with the NA-area was the most realistic. The discrepancy correlated more or less with the per cent organic matter in the soil. In view of the above and some results obtained with a soil from which the organic matter had been removed, de Haan suggests that the glycol retention areas are too high.

Summarizing, in a number of cases where comparison between NA-areas and areas determined otherwise (x-ray, BET, glycol retention) is possible, excellent agreement is obtained, showing that these methods are mutually consistent. However, in some cases notable discrepancies were observed, indicating that one of the methods did not apply. Further systematic studies on well-defined systems would be welcome.

Silver iodide

Silver iodide derives its charge from adsorption of Ag^+ or I^- ions. Surface charge and surface potential depend on pI and can be determined except for a constant[30].

An extensive comparative study has been published by van den Hul and Lyklema[21b, 25]. Some results are given in *Table 2*, from which the following is deduced.

Table 2. Comparison of surface areas (m^2/g) as determined by various methods

AgI *Sample*	S_{cap}†	S_{NA}	S_{BET}	S_{MB}‡	S_{DEC}§
A2	1·35	1·3	0·38	0·61	0·65
B2	1·5	1·6	0·52	0·98	1·00
B3	0·85	0·9	0·30	0·65	—
C1	3·5	3·3	0·97	2·18	1·92

† Capacitance method;
‡ Methylene blue, $a_0 = 108$ Å^2;
§ 1,1′-Diethyl-2, 2′-cyanine bromide $a_0 = 138$ Å^2

Agreement between the NA and capacitance area is excellent, however both are on the average 3·3 times higher than the BET-areas. A detailed discussion in the original references shows that both areas are correct, but do apply to different states of the precipitates, i.e. the BET-area is the 'dry area', whereas the electrochemical area is the 'wet area'. Some of the arguments are summarized below.

The BET-areas were in one case (AgI B_2) determined in four different laboratories, using five different adsorbates (N_2, Ar, Kr, C_6H_6, and CCl_4), with a standard deviation of the average of less than 9 per cent. Moreover, different drying and outgassing conditions had no significant effect. Also, the results of the air permeability measurements (not shown), confirmed the BET-areas.

The dye adsorption areas were calculated from the isotherm plateaus of methylene blue (MB) adsorbed from H_2O and 1,1′-diethyl-2,2′-cyanine bromide (DEC) adsorbed from alcohol on neutral AgI, using the theoretical cross-section for a flat adsorbed dye molecule. This is rather arbitrary, as the adsorption depends on surface charge, nature of the solvent and of indifferent electrolyte, and on the dye counterion. The reported surface areas are therefore ambiguous. It is interesting to note, that when DEC bromide is adsorbed from aqueous solution, a much higher adsorption occurs, from which areas of the order of the NA-area are estimated—(the isotherm plateau could not be reached because of the low dye solubility). This is in general accord with the careful work of Herz *et al.*[37], who found agreement between geometrical and dye adsorption areas of crystallographically defined AgBr crystals, if the proper counterion was chosen and the cyanine dyes were dissolved in methanol–water mixtures to enhance their solubility.

The results of Herz *et al.* have been confirmed recently by Peacock and Kragh[38] for the adsorption of cyanine dye from aqueous solutions containing both gelatine and potassium halide (10^{-3}M), onto AgBr or AgI suspensions. The procedures of Herz *et al.* and Peacock *et al.* have not been tried on the samples mentioned in *Table 2.*

The NA-areas were calculated with Eq. (6). The concentration dependence predicted by this equation, as well as the potential dependence, have been verified experimentally (*Figures 3* and *4*). One should keep in mind that all corrections discussed in the preceding section, except for curvature, would lead to still higher NA-areas. It is obvious that the curvature correction is negligible for fairly regular, hexagonal crystals of 0·5–2μ.

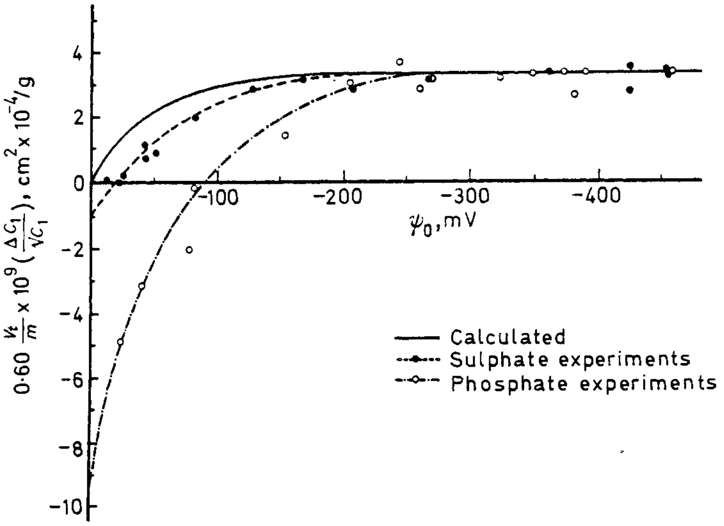

Figure 4. Comparison of theoretical and experimental values of the negative adsorption at different surface potentials on AgI. $S(\text{NA}) = 3{\cdot}3\ \text{m}^2/\text{g}$

The capacitance area is calculated by comparing the experimental double layer capacitance in 10^{-3}M KNO_3 at the point of zero charge (p.z.c.), with the theoretical capacitance per unit area, 5·3 ± 0·5 μF/cm². This value is derived from the Gouy-Stern theory using Lyklema's results for the Stern capacity[30]. The experimental value is derived from the potentiometrically determined surface charge as a function of surface potential. This method is independent of the NA-method, e.g. it is applied at the p.z.c. and is based on the positive adsorption of potential determining ions, whereas the NA of indifferent anions is measured at high potential.

The above mentioned capacitance was recently confirmed by direct measurement by Engel[41], using an a.c.-bridge technique. At the lowest possible concentration, 0·003 M KNO_3, he measured 10 $\mu F/cm^2$ at the p.z.c., which reduces to 5·8 $\mu F/cm^2$ at 10^{-3} M. At higher concentrations and with other electrolytes, his capacities also agree generally with those of Lyklema[30], if these are based on the NA or capacitance area. Engel states explicitly that in all cases in which aqueous AgI suspensions are studied, the NA-area should be preferred over the BET-area.

It must be concluded, that the discrepancy between the 'wet' and the 'dry' area is due to a loss in surface area during drying. This was recently substantiated by electron reflectance photography†. The photographs showed extensive stacking of the AgI particles, whereas the specific surface area assessed from the size of the individual particles was close to the NA-area.

We have shown[25] that a number of results involving adsorption on AgI could be interpreted more elegantly if they were based on the NA-area, rather than on the BET-area.

Other systems

A very typical example concerns a porous sample of precipitated silica[9, 25]. A t-plot following de Boer *et al.*[42] for the N_2 adsorption on this sample, revealed an initial area of 56·5 m^2/g, the filling of micropores at relative pressures $x < 0{\cdot}3$, and a non-porous outer area of 40 m^2/g at high x, agreeing reasonably well with the NA-area of 34·5 m^2/g. This example illustrates how comparison between NA and other areas can be helpful in the characterization of surface features.

A few other studies can be mentioned. Parks and de Bruyn[43] report a capacitance area for haematite of about 60 m^2/g, while the NA-and BET-area where both lower by a factor of 5. Evaluation of these results is impossible, as no experimental details are given. The capacitance area is most likely to be too high because of surface porosity[44].

Saleeb and Kitchener[26] measured the NA of chloride ions from graphon, charged by adsorption of an anionic, sulphonate-type surfactant. The results were much lower than the NA calculated after identification of ψ_δ and ζ on the basis of the BET-area with the aid of the Loeb *et al.* tables, as shown in *Table 3*. However, as the suspensions were centrifuged, the discrepancy may be due to double layer overlap in the sediment. If the results in 10^{-3}N may be used to calculate the average interparticle distance in the sediment from de Haan's[18] figure 3, and it is assumed that this distance is not changed in 10^{-2}N NaCl, then the calculated NA in 10^{-2}N, corrected for double layer overlap, agrees very well with the experimental value (see *Table 3*).

Finally, Belloni and Pavlov[45] measured the adsorption of various radioactive ions on metal oxides, NA occurred in a number of cases, such as Cs^+, Pm^{3+}, and Sm^{3+} from HgO and ThO_2, Cs^+ from ZrO_2 and Ag_2O,

---

†Courtesy of Dr K. E. Lewis of the Unilever Research Laboratory, Port Sunlight, U.K.

and SO_4^{2-} from WO_3 and GeO_2. Although measurements under better defined conditions (e.g. pH) are required to evaluate specific surface areas in these cases, their work demonstrates that the NA method may be applicable here.

Table 3. Negative adsorption from graphon; data of Saleeb and Kitchener[26]

	ζ (mV)	Γ_- exp.	Γ_- calc.	Γ_- overlap
10^{-2} N NaCl	61	1·7	6·0	3·6
	73	4·1	6·6	4·0
	74	4·3	6·7	4·0
	75	4·2	6·8	4·1
10^{-3} N NaCl	60	0·6	3·1†	—
	75	0·8	3·7†	—

† The erroneously high values calculated by the authors have been corrected.

SUGGESTIONS FOR FURTHER RESEARCH

Further research on NA can be fruitful for the surface area method as well as for double layer electrochemistry in general. The method can probably be expanded to a number of oxides and other, poorly soluble inorganic solids, and to dispersed solids with a high coverage of an ionic surfactant. It may be especially helpful in those cases where the identity of the 'wet' and 'dry' areas has not yet been established.

In view of the fact that colloidal stability, electrokinetics, as well as NA depend on ψ_δ, simultaneous measurements of these properties as a function of surface potential or surface charge would be useful. Well-characterized uniform latexes[46] can be especially useful for such studies.

SUMMARY

The negative adsorption method for the determination of surface areas, based on the exclusion of co-ions from the electrical double layer around a charged particle, is an attractive method for the measurement of surface areas of dispersions of solids in a liquid. As compared to many other surface area methods, it has the principal advantage that absolute areas are obtained, as the size of the co-ion does not enter into the calculations. However, as the negative adsorption is usually small, and the measurements rather tedious, it is not a routine method.

The principal conditions are: (i) rather smooth, non-porous particles; (ii) a Stern potential >150 mV, or at least fairly accurately known; (iii) specific areas of 1 m^2/g or more; (iv) an interparticle distance of $>8/\varkappa$. If these conditions are met, surface areas can be determined with an accuracy of 10 per cent or better.

In the paper, NA-areas are compared with a number of areas obtained by other methods. In several cases excellent agreement is found, indicating the correctness of either method. However, in some instances definite discrepancies were observed, indicating special conditions with respect to the state of aggregation or surface porosity, limiting the applicability of one of the methods.

References

[1] G. Gouy. *J. Phys.* **9** (4), 457 (1910); *Ann. Phys.* **7** (9), 129 (1917).

[2] D. L. Chapman. *Phil. Mag.* **25** (6), 475 (1913).

[3] F. G. Donnan and A. B. Harris. *J. Chem. Soc.* **99**, 1554 (1911);
F. G. Donnan. *Z. Elecktrochem.* **17**, 572 (1911); *Chem. Revs.* **1**, 73 (1924).

[4] F. W. Klaarenbeek. Thesis, State University, Utrecht, 1946.

[5] J. Th. G. Overbeek. *Progr. Biophys. Biophys. Chem.* **6**, 57 (1956).

[6] D. C. Grahame. *Chem. Revs.* **41**, 441 (1947).

[7] D. C. Grahame and B. A. Soderberg. *J. Chem. Phys.* **22**, 449 (1954).

[8] J. Lyklema. *Trans. Faraday Soc.* **59**, 418 (1963); *Discuss. Faraday Soc.* **42**, 81 (1966).

[9] Th. F. Tadros and J. Lyklema. *J. Electroanal. Chem. Interfacial Electrochem.* **17**, 267 (1968).

[10] W. C. Bauman, U.S. Patent 2 684 331 (1954); W. C. Bauman, R. M. Wheaton, and D. W. Simpson, in *Ion Exchange Technology*, F. C. Nachod and J. Schubert, Eds., Academic Press Inc., New York, N.Y., 1956, Ch. 7.

[11] U. Merten. *Desalination by Reverse Osmosis*, M.I.T.-Press, Cambridge, Mass., 1966, p. 30–35.

[12] G. H. Bolt. *Kolloid-Z.* **175**, 33, 144 (1961).

[13] P. H. Groenevelt and G. H. Bolt. *J. Hydrology* **4**, 345 (1968).

[14] R. A. Horne, A. F. Day, R. P. Young, and N. T. Yu. *Electrochim. Acta* **13**, 397 (1968).

[15] A. Vrij and J. Th. G. Overbeek. *J. Colloid Sci.* **17**, 570 (1962).

[16] D. Stigter. *Rec. Trav. Chim. Pays-Bas* **73**, 593 (1954);
H. F. Huisman. *Proc. Koninkl. Ned. Akad. Wetenschap.* **B67**, 407 (1964).

[17] A. L. Loeb, P. H. Wiersema, and J. Th. G. Overbeek. *The Electrical Double Layer around a Spherical Colloid Particle*, M.I.T.-Press, Cambridge, Mass., 1960.

[18] F. A. M. de Haan. *J. Phys. Chem.* **68**, 2970 (1964); Thesis, Agricultural University, Wageningen, 1965.

[19] F. A. M. de Haan and G. H. Bolt. *Soil Sci. Soc. Amer. Proc.* **27**, 636 (1963).

[20] (a) R. K. Schofield. *Nature* **160**, 408 (1947); (b) R. K. Schofield and O. Talibuddin. *Discuss. Faraday Soc.* **3**, 51 (1948); (c) R. K. Schofield and H. R. Samson. *Discuss. Faraday Soc.* **18**, 135 (1954).

[21] (a) J. Lijklema. Thesis, State University, Utrecht, 1956; (b) H. J. van den Hul. Thesis, State University, Utrecht, 1966; (c) H. J. van den Hul and J. Lyklema. *J. Colloid Interface Sci.* **23**, 500 (1967); (d) *Ibid.*, Proc. IVth Int. Congress on Surf. Active Substances, Gordon and Breach Pub., New York, London, 1967, Volume II, p. 141.

[22] J. Th. G. Overbeek, in *Colloid Science*, H. R. Kruyt, Ed., Elsevier, Amsterdam, 1952, Volume I.

[23] J. P. Quirk. *Nature* **188**, 253 (1960).

[24] G. H. Bolt and J. P. Warkentin. *Trans. Int. Soil Sci. Congr.*, VIth Congress, Paris, **B33**, 1956; *Kolloid-Z.* **156**, 41 (1958).

[25] H. J. van den Hul and J. Lyklema. *J. Amer. Chem. Soc.* **90**, 3010 (1968).

[26] F. Z. Saleeb and J. A. Kitchener. *Proc. IVth Int. Congress on Surf. Active Substances*, Gordon and Breach Pub., New York, London, Volume II, 1967, p. 129.

[27] H. J. van den Hul, unpublished calculations.

[28] M. G. T. Shone. *Trans. Faraday Soc.* **58**, 805 (1962).

[29] R. J. Hunter and A. E. Alexander. *J. Colloid Sci.* **18**, 843 (1963).

[30] J. Lijklema. *Kolloid-Z.* **175**, 129 (1961); J. Lyklema and J. Th. G. Overbeek. *J. Colloid Sci.* **16**, 595 (1961).

[31] A. Breeuwsma, unpublished results, 1968.

[32] S. Mattson. *Soil Sci.* **23**, 179 (1929).

[33] D. G. Edwards and J. P. Quirk. *J. Colloid Sci.* **17**, 872 (1962).

[34] Th. F. Tadros and J. Lyklema. *J. Electroanal. Chem. Interfacial Electrochem.*, **22**, 1 (1969).

[35] D. G. Edwards, A. M. Posner, and J. P. Quirk. *Nature, Lond.* **206**, 168 (1965); *Trans. Faraday Soc.* **61**, 2808, 2816, 2820 (1965).

[36] C. A. Bower and J. O. Goertzen. *Soil Sci. Soc. Amer. Proc.* **19**, 147 (1955).

[37] R. S. Dyal and S. B. Hendricks. *Soil Sci.* **69**, 421 (1950);
C. A. Bower and J. O. Goertzen. *Soil Sci.* **87**, 289 (1959).

[38] F. A. M. de Haan. *Soil Sci.* **99**, 379 (1965).

[39] R. Peacock and A. M. Kragh. *J. Photogr. Sci.* **16**, 229 (1968).

[40] A. H. Herz and J. O. Helling. *J. Colloid Interface Sci.* **22**, 391 (1966); *Kolloid-Z.Z. Polymere* **218**, 157 (1967).

[41] D. J. C. Engel. Thesis, State University, Utrecht, 1968.

[42] J. H. de Boer, B. C. Lippens, B. G. Linsen, J. C. P. Broekhoff, A. van den Heuvel, and Th. J. Osinga. *J. Colloid Interface Sci.* **21**, 405 (1966).

[43] G. A. Parks and P. L. de Bruyn. *J. Phys. Chem.* **66**, 967 (1962).
[44] J. Lyklema. *J. Electroanal. Chem. Interfacial Electrochem.* **18**, 341 (1968).
[45] J. Belloni and D. Pavlov. *J. Chim. Phys.* **62**, 458 (1965);
J. Belloni. *J. Chim. Phys.* **63**, 645 (1966).
[46] H. J. van den Hul and J. W. Vanderhoff. *J. Colloid Interface Sci.* **28**, 336 (1968).

DISCUSSION

Mr. A. M. Kragh (*Ilford Ltd.*) said: With silver halides, very good agreement has been obtained between the surface area determined from electronmicrographs, from turbidity measurements in solution, and from gas adsorption measurements. The adsorption of 1,1′-diethyl-2,2′-cyanine chloride (DEC) from water has been used as a standard for comparison.

The results of dye adsorption are required since the surface areas cannot be measured accurately by all methods on the same suspensions. Silver bromide can be produced in the presence of gelatin in very well defined monosized cubic crystals whose surface area can be determined accurately by electronmicrographs or by turbidity in solution. From these areas a molecular area of DEC adsorbed from water of about 58 Å^2 has been obtained. The surface area of these suspensions cannot be measured by gas adsorption because of the presence of gelatin, but with suspensions prepared from aggregated silver bromide powder, whose area has been measured by gas adsorption, the same molecular area for the dye is obtained. The very good agreement obtained by different workers is shown in *Table A*.

Table A. Molecular Area of DEC adsorbed on AgBr (in Å^2)

Suspension	*Method of surface area measurement*	*Authors*	*Molecular area*
Monosized cubes in gelatin	Electronmicrography	Herz & Helling[a, b]	58
	Turbidity	Gunter & Moisar[c]	56–64
Less well defined crystals	Electronmicrography	Herz & Helling[b]	50–58
	Electronmicrography	Peacock & Kragh[d]	52
Sols	Electronmicrography	Curme & Natale[e]	63
Aggregated sols	Gas adsorption	Padday & Wickham[f]	58
	Gas adsorption	Peacock & Kragh[d]	64
	Gas adsorption	Tani *et al.*[g]	60

[a] A. H. Herz and J. O. Helling. *J. Coll. Sci.* **22**, 291 (1966).
[b] A. H. Herz. Private communication.
[c] E. Gunther and E. Moisar. *J. Phot. Sci.* **13**, 280 (1965).
[d] R. Peacock and A. M. Kragh. *J. Phot. Sci.* **16**, 229 (1968).
[e] H. C. Curme and C. C. Natale. *J. Phys. Chem.* **68**, 3009 (1964).
[f] J. F. Padday and R. S. Wickham. *Trans. Faraday Soc.* **62**, 1283 (1966).
[g] T. Tani and S. Kikuchi. *J. Phot. Sci.* **17**, 33 (1069).

It is clear from these results that for silver bromide there is no possibility of a discrepancy of three times between the gas-adsorption and geometric surface areas as was obtained by Lyklema and van den Hul for silver iodide. (It has been clearly established that the maximum adsorption of DEC is not affected by gelatin.)

Far fewer results are available for silver iodide but they suggest the same conclusion and they would not in fact be expected to differ markedly from those for silver bromide.

Table B. Molecular area of DEC adsorbed on AgI (in Å^2)

From gas adsorption	*Molecular area*	*From electronmicrography*	*Molecular area*
Aggregated sols		Well defined crystals in gelatin	
Peacock & Kragh[d]	43	Peacock & Kragh[d]	39
Tani *et al.*[g]	42		

[d, g] For details of these references *See* Table A.

It can be seen from *Table B* that the molecular area of DEC is rather less on silver iodide than on silver bromide, but it still agrees well with the one result reported based on electronmicrographs. Well defined and near monosized crystals were used and Peacock & Kragh gave an estimated error of 20 per cent for the size determination. It may be thought that a 50 per cent error was possible but a 300 per cent error seems inconceivable.

It seems difficult to escape the conclusion that the negative adsorption method of surface area measurement gives values which are about 3 times too high on silver iodide.

Professor J. Lyklema replied: Although I can accept the experiments underlying Kragh's interpretation, I do not agree with his conclusion that the NA-area on AgI is 3 times too high.

The experiments, quoted by Kragh say that in a number of well-defined systems, the dye adsorption area is *proportional* to the BET-area, which in turn is equal to the electronmicrographic area. More than this cannot be concluded, but if one accepts 58 Å^2 (on AgBr) or 40 Å^2 (on AgI) as the cross-sectional area of the adsorbed DEC molecule as the adaptable parameter, the dye adsorption of course becomes *equal* to the other ones.

In the experiments with suspended AgI samples quoted in the paper no such adaptable parameter is available in the NA-method. The NA-method is internally consistent and the NA-area agrees with the capacitance area (both directly and indirectly measured) with electron reflectance photography and the results based on the NA-area are in good agreement with electrochemical work on other systems, like mercury. The BET area agrees with none of these, although it agrees with the air permeability area and can be made to agree with the dye adsorption area if we are willing to assume some specific value for the dye cross-sectional area. We attributed the observed discrepancy tentatively to reversible stacking of the AgI particles upon drying.

By consequence, the problem is not failure of NA but aggregation of our AgI-particles. This type of aggregation does apparently not occur in the AgBr-samples mentioned by Kragh. It would be worthwhile to make these samples in large amounts (in absence of gelatine) so that NA measurements could be performed on them. Doubtless, the NA-area would then agree with the electron micrographic one.

Dr. A. W. Flegmann (*University of Cambridge*) said: In his paper Professor Lyklema has quoted some interesting results published recently by D. G. Edwards, A. M. Posner and J. P. Quirk [*Trans. Faraday Soc.* **61**, 2808 (1965)] who have measured the specific surface areas of Fithian illites saturated with various monovalent and divalent cations by negative adsorption of co-ions and by low temperature nitrogen adsorption respectively. Application of BET theory to the nitrogen adsorption by monovalent cation saturated illites gave a surface area of 110 ± 7 m^2/g. By contrast, the area derived from the negative adsorption measurements obtained by applying Schofield's equation varied from 80 m^2/g for Li-illite to 0 m^2/g for Cs-illite. This is a discrepancy of first order magnitude and I share Professor Lyklema's view that it is as yet largely unexplained.

Without assuming differences in particle aggregation which have been ruled out by D. G. Edwards *et al.* an explanation of their results might be as follows.

It appears that, in this instance, our uncertainty with regard to the charge density of the Gouy layer is greater than that concerning the electrochemical surface area. Let it therefore be assumed that the latter parameter is known (= 110 m^2/g, the BET area) and that it is the former which needs calculating. Since it is by no means certain that the charge density of, or the potential drop across the Gouy layer will turn out to be as large as is required by the Schofield equation, it is better to start off with the unapproximated expression given by J. Th. G. Overbeek [*Progr. Biophys.* **6**, 58 (1956)]:

$$\frac{n_-}{n_\infty} = \left(\frac{\epsilon kT}{2\pi e^2 n_\infty}\right)^{\frac{1}{2}} \left[1 - \exp\left(-\frac{e\psi_\delta}{2kT}\right)\right] \text{cm}$$

Here n_- is the number of counterions repelled per unit area, n_∞ is the number of counterions per unit volume in the bulk solution, ψ_δ is the electrical potential drop across the Gouy layer, and the other symbols have their usual significance. If the equation is to be used for the evaluation of ψ_δ, the electrochemical surface area must be known from independent measurements. Introducing the identities

$$\left(\frac{\epsilon kT}{2\pi e^2}\right)^{\frac{1}{2}} \equiv K \qquad \text{and} \qquad \frac{e\psi_\delta}{kT} \equiv z,$$

the equation can be rewritten:

$$\frac{n_-}{K} = \left[1 - \exp\left(-\frac{z}{2}\right)\right] n_\infty^{\frac{1}{2}}$$

ψ_δ can then be evaluated for each cation from the slopes of the curves of n_-/K against $n_\infty{}^{1/2}$. These curves need be straight lines only if, in the experimental range, ψ_δ is independent of the electrolyte concentration.

When the results were replotted in this way they turned out to be straight lines. The resulting values of ψ_δ were sufficiently low to account for the discrepancy between the BET and the negative adsorption surface areas. Experiments are now in progress for measuring the electrokinetic potentials directly for comparison with the ψ_δ values calculated from negative adsorption results.

I would be grateful for Professor Lyklema's comments on this tentative explanation.

Professor J. Lyklema replied: The quoted results by Edwards *et al.* constitute one of the few cases in which no satisfactory explanation is available for the observed discrepancy between BET and NA area. In view of the linearity of the expelled volume vs. $2\,n_{-}K^{-1}$ plots the most logical interpretation would be that the surface area decreases due to platelet aggregation. Dr. Flegman suggests an alternative explanation which in fact boils down to stating that ψ_{δ} is low due to extensive counterion adsorption in the Stern layer.

It should at the very outset be noted that under the experimental conditions (surface charge of the order of 27 μC cm^{-2} and electrolyte concentration between 0·003 and 0·5 N) the double layer is indeed almost entirely non-diffuse. However, good NA measurements have been done with other highly-charged clays, also at relatively high salt content, implying that it is possible that sufficient charge remains in the diffuse part of the double layer to warrant the applicability of the Schofield equation (8) or our equations (5) and (6). In order to make the argument quantitative the counterion adsorption in the Stern layer and/or the electrokinetic potential (assuming $\psi_{\delta} \sim \zeta$) should be known. In the Cs^{+} case this should amount to 27 μC cm^{-2} of Cs^{+} adsorption on the illite platelets, which is a very high but not impossible value (H. van Olphen and G. H. Bolt, private communications). At any rate, electrokinetic measurements would be useful, notably streaming potential measurements in conjunction with permeability studies which would reveal extensive aggregation.

There is one objection to be made in this respect Dr. Flegmann states that plots of (in his notation) n_{-}/K against $n^{1/2}{}_{\infty}$ are straight lines, implying constancy of ψ_{δ} with salt concentration. This is improbable. With increasing electrolyte content, the Stern charge should go up and ψ_{δ} should decrease because the surface charge remains unaltered. Perhaps this point is not extremely critical because the experiments are not entirely satisfactory. For example, in the original data by Edwards *et al.* in some instances *positive* adsorption of Cs^{+} has been observed, indicating experimental artefacts.

Dr. P. Connor (*Glaxo Ltd.*, *Greenford*) communicated: Recently I have made some measurements on the negative adsorption of iodide ions from negatively charged polystyrene latices. These latices were highly monodisperse and non-porous as shown by the good agreement between gas adsorption and electron microscopy surface areas. The adsorption measurements were carried out at 20°C using dialysis membranes and an interferometer to analyse the solutions.

Initially, results were calculated using Eq. (6) as given by Lyklema and van den Hul and in every case the surface areas calculated from negative adsorption were about half the areas derived from the BET method. However, I have recently recalculated the surface areas using Eq. (11) given by Lyklema and van den Hul for flat plate systems and obtained surface area values which were only about ten per cent lower than the BET figures.

The results are obviously explained by the low ψ_{δ} of the polystyrene latices, which never exceeded about $-$ 50 mV, and their low surface charge density ($<$ 1·0 μC/cm^{2}). Considering that an equation for flat plates has been used instead of an equation for spheres, the agreement can be considered as very good.

Dr. L. Barclay (*BP Laboratories, Penarth*) communicated: Polymer latices provide a system having particles of well-defined shape which afford an ideal adsorbent for surface area studies. A comparison of surface areas determined on a non-porous polystyrene latex has recently been carried out [L. M. Barclay, M.Sc. thesis, Bristol (1966)]. The latex used in this work gave a geometrical surface area, based on electron microscopy, of 27 m^2/g from a 2000 particle count. *Table C* summarises the results from nitrogen and krypton adsorption at liquid nitrogen temperature using the BET method.

Table C. Nitrogen and krypton adsorption at liquid nitrogen temperature

Adsorbate	*p_0 value used* (mm Hg)	*Adsorbate molecular area A_0* (Å^2)	*BET surface area* (m^2/g)
Nitrogen	760	16·2$^{(c)}$	35·6 ± 0·3
		15·4$^{(d)}$	33·9 ± 0·3
Krypton	1·83^{a}	19·5	24·8 ± 0·5
	2·63^{b}	19·5	27·6 ± 0·5

[a] p_0 value of solid krypton determined in the adsorption vessel at liquid nitrogen temperature

[b] Quoted value for the vapour pressure of liquid krypton at −195·5°C (R. A. Beebe, J. B. Beckwith and J. M. Honig. *J. Amer. Chem. Soc.* **67**, 1554 (1965)

[c] P. H. Emmett and S. Brunauer. *J. Amer. Chem. Soc.* **59**, 1553 (1937).

[d] H. K. Livingston. *J. Coll. Sci.* **4**, 447 (1949).

Adsorption of 1,1′-diethyl-2,2′-cyanine chloride from aqueous solution at 25°C gave a Langmuir-type isotherm. This gave a specific surface area of 19·2 m^2/g for the latex, assuming the flat oriented dye molecule occupied an area of 138 Å^2 [W. West, B. H. Caroll and D. H. Whitcomb. *J. Phys. Chem.* **56**, 1054 (1952)].

Preliminary work [L. M. Barclay and R. H. Ottewill, to be published] on the negative adsorption of chloride on these negatively charged latex particles indicates a specific surface area of 50 m^2/g, using the approximate expression for a flat plate system as given by H. J. van den Hul and J. Lyklema [*J. Coll. Sci.* **23**, 500 (1967); *J. Amer. Chem. Soc.* **90**, 3010 (1968)].

The nitrogen molecular area of 16·2 Å^2 was originally proposed by P. H. Emmett and S. Brunauer [*J. Amer. Chem. Soc.* **59**, 1553 (1937)] and is considered almost as a universal value. However, since the nitrogen molecule is diatomic, there may be justification in proposing that the adsorbed nitrogen molecule, and hence its area, may be subject to orientation determined by the nature of the adsorbent surface. The 'universal' nitrogen molecular area has in the past appeared to give good correlation with other surface area methods using 'universal carbons'. It would therefore be of great interest if nitrogen adsorption work was carried out on a series of geometrically well-defined adsorbents such as latices of different polymers and drawn fibres. In a review by A. L. McClellan and H. F. Harnsberger [*J. Coll. Sci.* **23**, 577 (1967)] on cross-sectional areas of adsorbed molecules, a wide range of molecular areas is apparent for individual adsorbates. On this basis, it is of interest to quote the calculated nitrogen molecular area from this work (L. M. Barclay, *loc. cit.*) as 12·3 Å^2, assuming the latex geometrical area by electron microscopy as absolute.

SMALL ANGLE SCATTERING OF X-RAYS

A. RENOUPREZ

Institut de Recherches sur la Catalyse,
Villeurbanne, France

Our object has been to show how finely divided or porous solids can be characterized by means of small angle x-ray scattering. The practical way to obtain the specific surface and the pore or particle size, distribution curves, is given; results are compared with information obtained by other physical methods.

SPECIFIC SURFACE DETERMINATION

The first step is to obtain the complete scattered intensity curve, $I(\theta)$, from 0 up to the angle at which the intensity is two or three times the background.

When the specific area is low ($10\ \mathrm{m}^2\ \mathrm{g}^{-1}$) it is unnecessary to go farther than $2\theta = 2°$ (CuKα). On the contrary with dense samples and high values of the surface area, one must go up to 2θ values of 6 or even 8 degrees.

Then one can calculate the specific area by the Porod method[1-3] for large values of the scattering angle, the product Is^3 (with a rectangular x-ray beam) remains constant over a reasonable range and the expression for the surface area S in $\mathrm{m}^2\ \mathrm{g}^{-1}$ is:

$$S = \frac{16\pi^2 \cdot 10^4}{m \nu a_T \mu^2} \cdot \lim.\ Is^3,$$

where

I = scattered intensity;

$s = \frac{2\theta}{\lambda}$; θ is the scattering angle in radians; λ is the wavelength in Å;

m is the sample weight in g;

$\nu = 0{\cdot}00716\ \lambda^2$;

a_T is the total energy of the transmitted beam; and

μ is the density of the material in $\mathrm{g\ cm}^{-3}$.

Practically, one must check that the curve of the product Is^3 versus s^3 is a straight line: in some cases it has a positive slope caused by the background; then the correct value of the Is^3 limit is given by the intercept on the Is^3 axis.

The value of a_T is calculated either by manual planimetry of the transmitted beam or by computer integration of the step-by-step recorded curve.

Remarks—The measured value of S includes pores, both open and closed, from about 2 Å to 500 Å diameter; of course it includes too, the external surface of particles of a similar size. For compounds of low density, it is necessary to desorb the water contained in the sample.

Comparison with the BET measurements[4–6]

This method is suitable for the measurement of both low and high specific surface areas.

Low specific surfaces—We have measured the surface area of a silicon carbide sample with a particle diameter of 12–30 μ. The x-ray value of the surface area is 0·35 $m^2 g^{-1}$, the BET value, 0·34 $m^2 g^{-1}$. In fact this is an exceptional case; effectively, the Porod law is followed between 1 and $1{\cdot}8 \times 10^{-3}$ $Å^{-1}$ and if the direct beam is not well collimated the parasitic scattering is as important as the scattered one; then the lowest measurable value is about 1 $m^2 g^{-1}$.

High specific surfaces—In the range of high specific surfaces, it is easy to investigate low density samples with surface areas of several hundred $m^2 g^{-1}$ and the agreement with the BET values is generally good. For example, for a silica–alumina sample the calculated values were 701 and 715 $m^2 g^{-1}$ for the BET and x-ray measurements respectively. However, if the density of the material is high some difficulties occur in measuring specific surfaces in the range of two or three hundred $m^2 g^{-1}$. In this case, the Porod law is not followed at angles lower than six or seven degrees and by then the measured intensity falls down to five to ten impulses per second; under these conditions the precision of the measured surface area depends on the statistical counting error.

The x-ray method does not depend on the same hypotheses as the BET method, and in some cases, the results obtained by the two methods are very different. For example, two samples of petroleum coke used as oxidation catalysts were studied by both methods. Before use the BET and x-ray values were 0·9 and 15 $m^2 g^{-1}$; after use 0·8 and 40 $m^2 g^{-1}$. This shows that in both catalysts there are closed pores and that an important volume of closed pores is produced during the reaction.

In some cases, however, the values obtained by the x-ray method are lower than those obtained using the BET procedure; at present no satisfactory explanation has been found for the discrepancy. It is possible that boiling nitrogen could modify the texture of the sample.

PORE OR PARTICLE SIZE DISTRIBUTION CURVES

By virtue of the Babinet theorem, x-rays do not distinguish between holes and particles; so the curves must be compared in most cases with those calculated from gas adsorption measurements using the Barrett, Joyner and Halenda (BJH) method[10] to know whether peaks are caused by particles or pores.

Two methods have been developed recently to compute these distribution curves[8–10].

A knowledge of the Patterson function of the sample is required, namely,

$$P(r) = -(1/\pi)\int_0^\infty [q(\sqrt{\{r^2+z^2\}})/\sqrt{\{r^2+z^2\}}]\mathrm{d}z,$$

where $q(t)$ is the cosine Fourier transform of the scattered intensity.

From $P(r)$ three distribution functions are computed:

$f_N(D)$ the numerical distribution function of particle diameter,
$f_s(D)$ the surface distribution function,
$f_v(D)$ the volume distribution function.

That means, in the second case, for example, $f_s(D)\,\mathrm{d}D$ is the surface area of particles whose diameters are in the range D to $D + \mathrm{d}D$.

$$f_N(D) = -\frac{1}{D^2P''(0)}\,[P''(D) - DP'''(D)]$$

$$f_s(D) = -[P''(D) - DP'''(D)]/2P'(0)$$

$$f_v(D) = [DP''(D) - D^2P'''(D)]/3P(0)$$

This method was tried successfully. However, as it requires complex mathematical treatment, we prefer, when the sample is thin, the second method which does not require numerical differentiation. The expression for $f_s(D)$ is

$$f_s(D) = \tfrac{1}{2}[\int_0^{s\,\max} G(s)\mathcal{J}_0''(2\pi sr)\,\mathrm{d}s - 2\pi r\int_0^{s\,\max} s\,.\,G(s)\mathcal{J}_0'''(2\pi rs)\,\mathrm{d}s]$$

where $G(s) = A(B - Is^3)$, $\mathcal{J}_0(2\pi rs)$ a Bessel function, and B is the limit of Is^3 for comparatively high angles.

These calculations have of course to be carried out on a computer.

Experimental equipment[11]

The knowledge of the complete scattered intensity curve requires the use of a special low angle goniometer. For this purpose, we have built a special apparatus whose main characteristics are (i) high accuracy of the step-by-step movement (step of one second of arc is necessary); (ii) high definition of the counter slit; (iii) monochromatization of the radiation ($K\alpha_1$); and (iv) a collimating system with tantalum edged slits.

However, photographic measurements can be used if only the specific surface is needed.

Experimental results. Comparison with other methods

We have chosen two characteristic examples. The first sample is a collection of spherical particles of colloidal gold prepared by reduction of gold chloride with sodium citrate. Electron micrographs showed spherical particles whose diameters ranged between 150 and 300 Å.

As is shown in *Figure 1* the x-ray intensity curve decreases rapidly at $1{\cdot}5 \times 10^{-2}$ Å^{-1} (2θ 1° 20′); the Porod law is followed from $2{\cdot}5 \times 10^{-3}$ Å^{-1}. In this region, the product Is^3 is constant (*Figure 2*). The distribution curves $F_s(D)$ and $F_v(D)$ show a maximum at 240 Å (*Figure 3*).

The second example consists of two Ketjen samples (silica–alumina, 13 per cent Al_2O_3) from which Al_2O_3 was extracted.

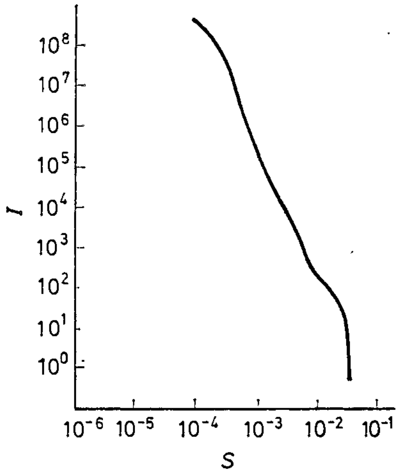

Figure 1. Gold sample: scattered intensity I, versus s, logarithmic scale

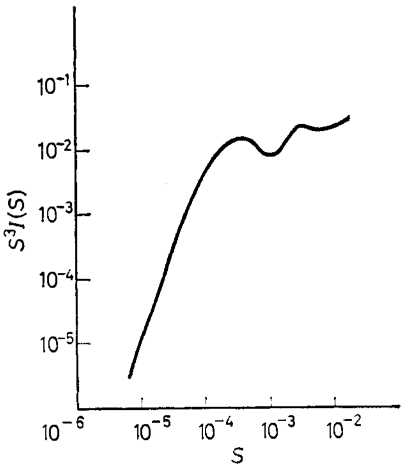

Figure 2. Gold sample: Is^3 versus s, logarithmic scale

In the first sample, in which 0·6 per cent Al_2O_3 was left, the x-ray surface is 900 m^2 g^{-1} and the BET, 774 m^2 g^{-1}. This difference is easy to explain if we consider the F_v curves and BJH pore distribution (*Figure 4*).

The F_v curve shows two peaks at 12 and 28 Å; while on the BJH curve there is only one maximum at 37 Å.

For the second sample in which only 0·3 per cent of Al_2O_3 was left (*Figure 5*) the values of the specific area were 701 and 715 m^2 g^{-1} and there

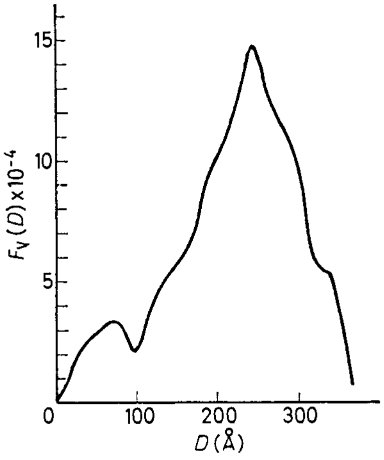

Figure 3. Gold sample: particle diameter distribution

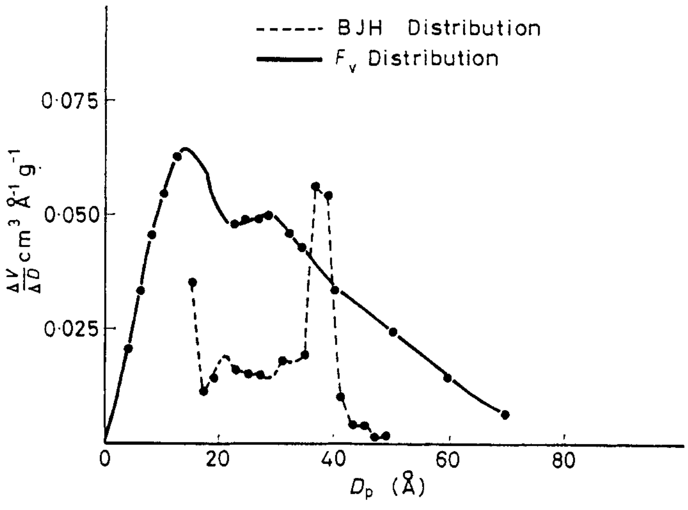

Figure 4. Silica–alumina: 0·6 per cent alumina, pore size distribution

is only one maximum on the F_v curve for a diameter of 23 Å; on the BJH curve, the peak has an abcissa of 40 Å.

In conclusion it is obvious that small angle scattering of x-rays is a powerful method especially if results can be compared with information afforded by other techniques.

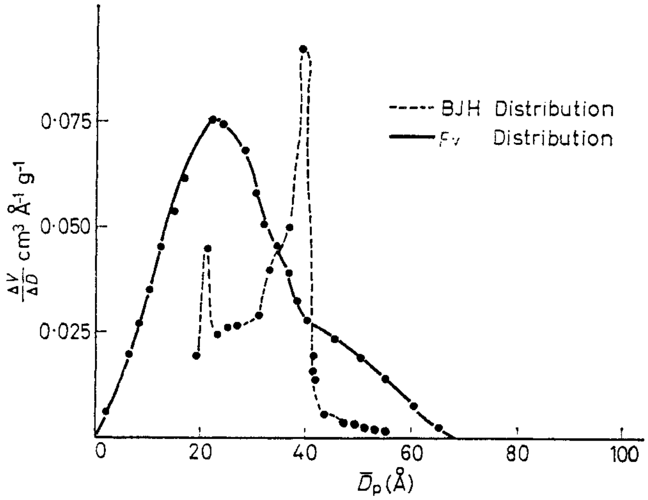

Figure 5. Silica–alumina: 0·26 per cent alumina, pore size distribution

References

[1] G. Porod. *Kolloid Zeitschrift.* **124**, No. 2, 84 (1951).
[2] J. L. Soule. *J. Phys. Rad.* **18**, 90 (1957).
[3] D. Weigel, A. Renouprez, and B. Imelik. *J. Chim. Phys.* **62**, 125 (1965).
[4] A. Renouprez, G. Dalmai, D. Weigel, and B. Imelik. *J. Chim. Phys.* **64**, No. 6, 934 (1967).
[5] R. Baro and V. Luzzati. *Acta Cryst.* **12**, No. 2, 144 (1959).
[6] C. Alexanian, J. L. Soule, and J. Durif. *J. Phys. Rad.* **20**, No. 12, suppl. 139 A (1959).
[7] H. Brusset, J. R. Donati, and B. Pascal. *C.R. Acad. Sci.* **264**, No. 2, 175 (1967).
[8] J. R. Donati, B. Pascal, and A. Renouprez. *Bull. Soc. Fr. Minéral. Cristallogr.* 1967, XC 452.
[9] A. Renouprez and B. Imelik. *C.R. Acad. Sci.* **268**, 69, série B (1969).
[10] E. P. Barrett, L. G. Joyner, and B. P. Halenda. *J. Amer. Chem. Soc.* **73**, 373 (1951).
[11] A. Renouprez, H. Bottazzi, D. Weigel, and B. Imelik. *J. Chim. Phys.* **62**, 131 (1965).

DISCUSSION

Dr P. Connor (*Glaxo Ltd., Greenford*) communicated: Some years ago, a method was developed for the measurement of particle size based upon the backscattering of β-particles [P. Connor, W. H. Hardwick and B. J. Laundy. *J. Appl. Chem.* **2**, 525 (1959); P. Connor and W. H. Hardwick. *Industrial Chemist*, **36**, 427 (1960)]. In this method the β-particles from a sealed ^{90}Sr–^{90}Y source are backscattered from a solid particulate deposit which has sedimented in either gas or liquid media under well-controlled conditions.

The efficiency of the scattering process is dependent on the energy of the β-particles and the mean atomic number of the scattering materials.

The effective atomic number, *Z*, for backscattering from compounds is defined as

$$\frac{n(\text{Ab}\ Zb) + m(\text{Ac}\ Zc)}{\text{molecular weight of } \text{B}_n\ \text{C}_n}$$

where Ab and Ac are the atomic weights of B and C for the compound $\text{B}_n\ \text{C}_n$.

Using a two-layer technique and by applying Stokes' law it is possible to obtain the particle size distribution. With recent electronic improvements [W. H. Hardwick and B. J. Laundy. Society for Analytical Chemistry. Particle Size Analysis Conference, Loughborough (1966)] the apparatus may be used to measure the particle size of very low atomic number materials such as beryllium and carbon. If centrifugal sedimentation is used, then particles as small as $0 \cdot 1\ \mu$ may be measured.

OPTICAL MICROSCOPY FOR PARTICLE SIZE ANALYSIS

MICHAEL I. BARNETT

Welsh School of Pharmacy, University of Wales Institute of Science and Technology, Cathays Park, Cardiff, U.K.

Microscopy is the most direct method for determining the size and shape of particles, and the size distribution of particles in a system. The majority of techniques employed are relatively simple but suffer from the disadvantages of being slow to perform, with resulting tedium to the observer and a consequent loss in precision of measurement. Microscopy is the only method of size analysis in which individual particles are measured, and in order to obtain an accurate assessment of a distribution a great number of particles have to be measured. The practical lower limit of measurement by microscope methods is between 0·8 μ and 1 μ using a good optical system, flat field objectives and a monochromatic light source. The lower limit of resolution is theoretically related to the wavelength of light and the numerical aperture of the objective and is usually quoted at 0·2 μ for white light and an oil immersion objective[1]. The detecting power of the microscope is far below this level, Loveland[2] quotes 0·005 μ, and is dependent upon illumination intensity and refractive index differences. The normal microscope image is two-dimensional and as size is essentially a three-dimensional quantity, conversion of microscope linear data into weight, volume or surface area data may often be misleading. The microscope remains, however, a useful tool for analysis[3] both singularly and in conjunction with other techniques, where the degree of dispersion of particles requires assessment and where shape factors need to be calculated.

SAMPLING METHODS AND SLIDE PREPARATION

The preparation of a slide containing a representative sample from a bulk powder or from a concentrated suspension of particles, is one of the greatest problems involved in particle size determination by optical techniques. Errors in sampling affect the accuracy of any method of particle size determination, and a statistical treatment of the errors involved in sampling procedures has been carried out by Herdan[4].

The original batch of material should be thoroughly mixed and then subdivided to produce a sample of between 1·0 g and 5·0 g. The gross sample may be subdivided by halving, coning and quartering or by the use of mechanical subdividers as described in the British Standard B.S. 3406 pt. 15, or by any other method that gives accurate and representative samples, some of which have been described by Allen[6]. The small sample obtained must be further subdivided prior to dispersion on a slide. The powder may be dispersed in a small quantity of fluid, in which it is insoluble, and a small drop of the suspension placed on a slide[7]. A dispersing agent may be required to prevent flocculation or aggregation of the particles[8]. Alternative procedures for dispersion are described in the British Standard on optical microscopy[9] for size analysis. Green[10] and Dunn[11] have described standard procedures for slide preparation and Harwood[12] has suggested special methods for powders which are difficult to disperse. Fairs[13] and Orr and Dallavalle[14] have described techniques for making permanent slides, whilst Rosinski *et al.*[15] have investigated several techniques to find the most reproducible ones.

DIAMETERS AND GRATICULES

An irregularly shaped particle has no unique dimension and consequently before a microscope analysis is attempted, the particular statistical diameter being measured, must be defined in an unambiguous manner. A statistical diameter is the mean of a large number of measurements on a particle population, all the measurements being taken in a fixed arbitrary direction[16], Martin's diameter[17], the mean length of a line which approximately bisects the particle profile, and Feret diameter[18], the mean distance between two parallel tangents on opposite sides of the outline of the particle, are such statistical diameters. The inter-relationship of these diameters have been discussed by Heywood[19] and by Herdan[20]. These diameters may be determined by simple linear eyepiece graticules previously calibrated against standard stage micrometers; or by the use of an optical eyepiece micrometer having a movable cross-hair and a calibrated micrometer drum.

Projected-area diameter is the diameter of a circle equal in area to the profile of the particle when viewed normally to a plane surface, on which it is at rest in a stable position. The globe and circle graticule first described by Patterson and Cawood[21], is used to estimate projected area diameter. This type of graticule was further developed by Fairs[22,23] who introduced a $2^{\frac{1}{2}}$ progression of reference circles, and later was accepted as the British Standard graticule. May[24] introduced a graticule with a grid containing a series of parallel lines whose distances from a centre zero line increase in $2^{\frac{1}{2}}$ progression, in addition to having a $2^{\frac{1}{2}}$ progression of circle diameters. He improved this graticule[25] to accommodate wider size ranges of particles and to minimize difficulties arising from line thickness. A graticule designed to facilitate rapid calculation of statistical parameters from experimental results was recently described by Guraswamy[26].

The use of eyepiece graticules often gives rise to errors in the assessment of the size of irregular particles; untrained observers particularly, having a tendency to oversize the particle profile. Heywood[27] has described the application of a particle profile test card for assessing bias and for training observers in the estimation of equivalent circles. A test strip suitably reduced in size, has been used by Watson and Mulford[28] to assess the accuracy of sizing of irregular particles by a microscope method. Hamilton *et al.*[29] have discussed the limitations of existing eyepiece graticules for use in routine particle counting, and have compared the consistency and accuracy obtained with globe and circle graticules and a parallel line graticule. The bias in particle size analyses by counting methods has been investigated[30] and simple corrections proposed for obtaining unbiased estimates of particle size distribution based on number, area and volume.

DOUBLE IMAGE MICROSCOPY

The measurement of particles by double-image microscopy requires the use of a beam-splitting device between the objective and eyepiece, so that two identical images are formed in the field of view. The device is fitted with a means of shearing the images apart, and with a scale to indicate the amount of shear. Two methods have been used to produce these images; a mechanical–optical method described by Dyson[31,32] and an electrical–optical method described by Timbrell[33,34].

Dyson's method of image splitting is achieved by using two prism blocks, rotated by means of a micrometer screw drive about a vertical axis, the shear obtained being directly proportional to the micrometer reading. An alternative mechanical–optical method has been described by Barer[35]. The electrical–optical method employs an electromagnetic vibrator inserted between the objective and the eyepiece of the microscope. A small mirror inclined at 45° to the vertical reflects a light-beam from the objective to the eyepiece. The back of the mirror is mounted on the diaphragm of a loudspeaker type transducer and can be vibrated by energising the loudspeaker with an alternating current of 50 c/s. The amplitude of the vibration is controlled by the strength of the current. The source of illumination is arranged to flash when the mirror is at the extremities of its vibration, resulting in two beams being formed fifty times a second, and due to persistence of vision the observer sees two stationary images of each object in the field of view. The separation or amount of shearing of the images is proportional to the energising current and an ammeter can be graduated to show directly, the double-image diameter of the particle in microns. The images follow collinear tracks and a perfect zero shear setting is obtained when the vibrator is switched off. This is in contrast to the mechanical–optical method where Powell and Erington[36] found some deviation in the zero readings. The electrical–optical method has facilities for placing particles in relatively narrow size ranges in preference to making precise measurements on each particle. This procedure has been described elsewhere[37]. Barnett and Timbrell[38] claim extremely high reproducibility for this method down to 2·0 μ, and low inter-observer and intra-observer errors. The apparatus can be made semi-automatic by the addition of data processing equipment to the basic unit.

AUTOMATIC COUNTING AND SIZING

Size analysis by optical microscope techniques is tedious and time consuming and in an attempt to overcome these factors and the subjectiveness of the available methods, a number of automatic and semi-automatic sizing and counting devices have been developed. The principle of many of these instruments, is to record the change in the intensity of a light beam as it traverses a microscope field in which the particles to be measured, have been dispersed. The instruments can be generally classified as "spot-scanners", or "slit-scanners" depending upon the nature of the light beam.

The spot-scan methods are based on the flying-spot microscope described by Roberts and Young[39], where an intense light spot moving on a cathode-ray tube is directed on to a particle distribution through a conventional microscope. Interruption of the light beam by a particle activates a photocell and the particle is recorded. Developments of this technique have been described by Dell[40] and by Taylor[41]. The Mullard particle size analyser utilises a flying-spot to scan a 35 mm film record of the particles. This technique extends the range of the instrument to electron photomicrographs of submicron particles. A critical assessment of this instrument has been made by Collins[42] who investigated operator error and intrinsic instrument errors.

A theoretical treatment of slit-scanning has been given by Hawksley[43] who demonstrated the relationship between the number and size distribution of particles dispersed in the field, and the number of particles interrupted by a scanning slit passed across the field. In this method, an image of the slide is projected on to a slit through a microscope. The slide is scanned mechanically and signals are produced and recorded as the images pass over the slit. A number of different slit-scanners have been described in a review by Connor[44]. It must be realised that the limitations of these automatic instruments, are essentially the same as those of the optical microscope, with the added difficulty of poor signal to noise ratios giving inadequate resolution at the lower end of the scale.

Endter and Gebaur[45] constructed a semi-automatic instrument for measuring particle size from photomicrographs. In this method an illuminated iris diaphragm is imaged by a lens on to the plane of a Plexiglass plate, where, by adjustment of the diaphragm, the area of a spot of light can be matched with the area of a particle on the photograph. The sizes of the particles are recorded on a forty-eight channel register. The method is subject to errors produced by photographing particles and measuring their images from prints, but it does minimize operator fatigue. Chatfield[46] describes a similar instrument but employs projection of 35 mm negative photographs and light spots for area comparison that are in a $2^{\frac{1}{2}}$ progression of size, rather than infinitely variable as in the previous method.

The Metals Research image-analysing computer is the most recent of the automatic techniques. A microscope fitted with a beam splitting prism projects an image into a binocular eyepiece for direct viewing and simultaneously into a television camera, the output of which is displayed on a monitor. The camera output is also fed to a detector which responds to changes in output voltage as a scanning spot in the camera tube passes over particles in the field. The detected signal passes to a computer unit which can be set to measure total projected area, particle number, length or size distribution. An appraisal and full description of the instrument has been given by Fisher[47] who also indicates its use in the estimation of the specific surface area of powder samples.

SPECIFIC SURFACE AREA FROM NUMBER DISTRIBUTION

When the size distribution has been determined microscopically in terms of the projected diameter d_a, the total surface area of the particles is given by[48]:

$$\text{Surface} = \pi \Sigma d_{a_i}{}^2 n_i;$$

and their volume by

$$\text{Volume} = \frac{\pi}{6} d_{a_i}^3 n_i$$

Assuming the particles are non-porous and spherical, the ratio of surface to volume gives the specific surface S_V

$$S_V = \frac{6\Sigma d_{a_i}^2 n_i}{\Sigma d_{a_i}^3 n_i}$$

For irregular particles, surface projected area and volume projected area shape factors are included in the expression. So that

$$S_V = \frac{\alpha_s \, \Sigma d_{a_i}^2 n_i}{\alpha_V \, \Sigma d_{a_i}^3 n_i}$$

where α_s and α_V are the shape factors. These factors have been described by Heywood[49] who also presented tables for use in estimating them from microscopic measurements.

References

[1] H. Heywood. *J. Pharm. Pharmac.* **15**, 56T (1963).
[2] R. P. Loveland. *Symposium on Particle Size Measurement.* Special Technical Publication No. 234, p. 57, A.S.T.M. Philadelphia Pa. (1958).
B. Scarlett. *Chem. and Process. Eng.* **46**, 197 (1965).
[4] G. Herdan. *Small Particle Statistics*, p. 42, Butterworths, London (1960).
[5] B.S. 3406 Part 1. *Subdivision of gross sample.* British Standards Institution (1963).
[6] T. Allen. *Particle Size Measurement.* Chapman and Hall, London (1968).
[7] M. I. Barnett. M. Pharm. Thesis. University of Wales (1962).
[8] M. J. Groves. *Lab. Pract.* **14**, 1282 (1965).
[9] B.S. 3406 Part 4. *Optical Microscope Method.* British Standards Institution (1963).
[10] M. Green. *J. Franklin Inst.* **192**, 657 (1921).
[11] E. J. Dunn. *Ind. Eng. Chem. Anal. Ed.* No. 2, 59 (1930).
[12] M. G. Harwood. *Brit. J. Appl. Phys. Suppl.* **3**, S. 193 (1954).
[13] G. L. Fairs. *Chem. and Ind.* **62**, 374 (1943).
[14] C. Orr and J. M. Dallavalle. *Fine Particle Measurement.* Macmillan, New York (1959).
[15] J. Rosinski, H. E. Glaess and C. R. McCully. *Anal. Chem.* **28**, 486 (1956).
[16] H. Heywood. *Bull. Instn. Min. Met.* No. 477 (1946).
[17] G. Martin, C. E. Blythe and H. Tongue. *Trans. Br. Ceram. Soc.* **23**, 61 (1923–24).
[18] L. R. Feret. Assoc. Int. pour l'essai des Mat. 2, group D, Zurich (1931).
[19] H. Heywood. *Trans. Inst. Min. and Met.* **55**, 391 (1946).
[20] G. Herdan. *Small Particle Statistics*, p. 140, Butterworths, London (1960).
[21] H. S. Patterson and W. Cawood. *Trans. Faraday Soc.* **32**, 1084 (1936).
[22] G. L. Fairs. *Chem. and Ind.* **62**, 374 (1943).
[23] G. L. Fairs. *J. Roy. Micro. Soc.* **71**, 209 (1951).
[24] K. R. May. *J. Sci. Instrum.* **22**, 187 (1945).
[25] K. R. May. *J. Sci. Instr.* **42**, 500 (1965).
[26] S. Guruswamy. *Proc. Particle Size Analysis Conference*, Loughborough, p. 29 (1966), Society for Analytical Chemistry, London (1967).
[27] H. Heywood. *Bull. Inst. Min. Met.* Nos. 477, 478 (1946).
[28] H. H. Watson and D. L. Mulford. *Brit. J. Appl. Phys. Suppl.* **3**, S 105 (1954).
[29] R. J. Hamilton, J. F. Holdsworth and W. H. Walton. *Brit. J. Appl. Phys. Suppl.* **3**, S 101, (1954).
[30] J. E. Gwyn, E. J. Crosby and W. R. Marshall, Jr. *Ind. Eng. Chem. Fund.* **4**, 204 (1965).
[31] J. Dyson. *Nature, Lond.* **184**, 1561 (1959).
[32] J. Dyson. *J. Opt. Soc. Amer.* **50**. 754 (1960).
[33] V. Timbrell. *Nature, Lond.* **170**, 318 (1952).
[34] V. Timbrell. *Lab. Pract.* **8**. 33 (1959).
[35] R. Barer. *Nature, Lond.* **188**, 398 (1960).
[36] E. O. Powell and F. D. Errington. *J. Roy. Micr. Soc.* **82**, 39 (1963).

[37] M. I. Barnett. *Annals N.Y. Acad. Sci.* in Press.
[38] M. I. Barnett and V. Timbrell. *Pharm. J.* **189**, 379 (1962).
[39] F. Roberts and J. Z. Young. *Nature, Lond.* **167**, 231 (1951).
[40] H. A. Dell. *Brit. J. Appl. Phys. Suppl.* **3**, S 156 (1954).
[41] W. K. Taylor. *Brit. J. Appl. Phys. Supp.* **3**, S 173 (1954).
[42] G. F. Collins. *Proc. Particle Size Analysis Conference*, Loughborough, p. 65 (1966), Society for Analytical Chemistry, London (1967).
[43] P. G. W. Hawksley. *Brit. J. Appl. Phys. Suppl.* **3**, S. 125 (1954).
[44] P. Connor. *Ind. Chemist* **39**, 74 (1963).
[45] F. Endter and H. Gebauer. *Optik*, **13**, 87 (1956).
[46] E. J. Chatfield. *J. Sci. Instrum.* **44**, 615 (1967).
[47] C. Fisher. *Proc. Particle Size Analysis Conference*, Loughborough, p. 77 (1966), Society for Analytical Chemistry, London (1967).
[48] G. Herdan. *Small Particle Statistics*, p. 192, Butterworths, London (1960).
[49] H. Heywood. *Symposium on Particle Size Analysis, Inst. Chem. Eng. Suppl.* **25**, 14 (1947).

CALCULATION OF THE SPECIFIC SURFACE OF A POWDER

H. Heywood

Loughborough University of Technology, Loughborough, Leics., U.K.

INTRODUCTION

Different methods of assessing surface area may give vastly different numerical values according to the procedure adopted. The calculated specific surface is assumed to be that of a smooth, impermeable skin of negligible thickness which contacts the external surface of the particle. Whilst such a skin can follow the major irregularities in shape of the particle, it cannot follow the micro-roughness of the surface and would seal off any internal porosity. Hence the numerical value of the calculated specific surface for a given powder will be somewhat less than that determined by the permeability method and may be very much less than that determined by gas adsorption.

The specific surface area of a powder can be calculated from the particle size distribution derived from the sizing analysis, but difficulties arise due to the uncertainty of the analysis, especially of the content of relatively fine particles whose influence predominates in the result and to variations in particle shape. There are, however, circumstances in which calculation is the only possible manner by which specific surface may be assessed, such as when only a minute sample is available on a microscope slide. A similar situation occurs at the coarse end of the scale of particle size, when the particles are too large for the application of direct methods of surface determination.

The procedure for calculation is therefore of importance in the study of particle characterization and the British Standards Institution has prepared a draft standard thereon which will shortly be ready for publication. The sub-committee involved forms part of the main committee CHE/50 whose terms of reference are the sampling and determination of particle size. The purpose of this paper is to summarise the main contents of the proposed B.S. specification and also to describe additional methods of calculation, which although not included in the specification for reasons explained later, may be applicable in certain circumstances.

The basis of the procedure for calculating specific surface is shown below: The specific surface on a volume basis for a single particle

$$= \frac{\text{smoothed external surface area of particle}}{\text{volume of particle}}$$

$$= \frac{\text{surface shape coefficient} \times (\text{characteristic dimension})^2}{\text{volume shape coefficient} \times (\text{characteristic dimension})^3} \qquad (1)$$

and for a system consisting of various sizes of particles

$$= \frac{\text{combined shape coefficient}}{\text{(mean characteristic dimension representing the properties surface and volume)}} \qquad (2)$$

Specific surface on a weight basis is obtained by dividing by the particle density.

In principle the procedure is simple, the problems are concerned with defining adequately the characteristic dimension of an irregularly shaped particle, the numerical definitions of particle shape and the derivation of the appropriate mean size for a system of particles. The succeeding sections of the paper consider each of these in turn.

DEFINITION OF PARTICLE SIZE

The size of an irregularly shaped particle may be expressed in terms of the diameter of a circle or of a sphere which is equivalent to the particle in some stated property[1]. Such equivalents are: (i) The circle having the same projected area as the profile of the particle; symbol d_a. (ii) The sphere having the same volume as the particle; symbol d_v. (iii) The sphere having the same surface as the particle; symbol d_s. (iv) The sphere having the same terminal velocity of fall in a fluid as the particle: symbol d_{st} if the conditions of motion fulfill those of Stokes' Law.

The equivalent diameter d_a is measured by means of the microscope; it is a two-dimensional mean approximating to the average of the length and breadth of the particle and ignoring the thickness. The other equivalents are three dimensional; the diameter d_v can be calculated if the particle is large enough for the volume to be measured directly, but this cannot be done for small particles except by means of the Coulter Counter. There is no simple method of measuring directly the envelope surface of individual particles unless these exceed a size of say 1 inch. The Stokes' diameter d_{st} is measured when a sizing analysis is performed by one of the sedimentation techniques.

All these equivalent diameters differ numerically except for spherical particles and the divergence may be considerable for non-equiaxial particles such as flakes and needles. The selection of one of the above equivalent diameters as the characteristic dimension of the particle as in equation (1) is therefore the first factor to be taken into account for the calculation of specific surface.

DEFINITION OF PARTICLE SHAPE

Equation (1) shows that the volume and surface of a particle are functions of the diameter raised to an appropriate power, and since these properties are fixed for a given particle the numerical values of the shape coefficients must be linked with the characteristic dimension chosen to represent the particle.

If the volume coefficient is denoted by α_v and the surface coefficient by α_s then an additional subscript which is the same as that used to define particle size must be added to these symbols. Thus $a_{v,a}$ denotes the volume coefficient calculated from the projected area measurement of the particle.

Consequently:

$$\text{Volume of particle} = a_{v,a}d_a^3 = a_{v,v}d_v^3 = a_{v,s}d_s^3 = a_{v,st}d_{st}^3 \qquad (3)$$

$$\text{and surface of particle} = a_{s,a}d_a^2 = a_{s,v}d_v^2 = a_{s,s}d_s^2 = a_{s,st}d_{st}^2 \qquad (4)$$

Note that $a_{v,v} = \pi/6$ and $a_{s,s} = \pi$, the respective values for a sphere.

Equation (2) shows that the ratio of these two coefficients is ultimately used for the calculation of specific surface, hence:

$a_{sv,x} = \dfrac{a_{s,x}}{a_{v,x}}$ x being replaced by the appropriate subscript according to the procedure used for size definition.

The shape coefficients and the method of measurement of particle size are related according to equations (3) and (4); hence conversion of shape coefficients from one system of measurement to another may be made by expressions such as those shown below, the equivalent Stokes' and projected area diameter being used as an example.

$$a_{v,st}/a_{v,a} = (d_a/d_{st})^3;\; a_{s,st}/a_{s,a} = (d_a/d_{st})^2 \qquad (5)$$

and $a_{sv,st}/a_{sv,a} = d_{st}/d_a$ for the combined coefficient (6)

Table 1 gives statistical values for the equivalent diameter ratios, as affected by the volume coefficient $a_{v,a}$; values of $a_{v,a}$, $a_{s,a}$ and $a_{sv,a}$ for various types of material are given in *Table 2*.

Table 1. Equivalent diameters in terms of projected area diameter d_a for angular particles

	Volume coefficient $a_{v,a}$			
	0·1	0·2	0·3	0·4
A†$/d_a$	0·60	0·70	0·81	0·91
d_v/d_a	0·57	0·72	0·83	0·91
d_s/d_a	0·77	0·87	0·99	1·05
d_{st}/d_a	0·50	0·63	0·75	0·85

† A = equivalent sieve aperture

Table 2. Average values of shape coefficients for different types of powder[2]

Type of powder	$a_{v,a}$	$a_{s,a}$	$a_{sv,a}$
Spherical particles	0·524	3·14	6·0
Rounded particles; water worn sands, fused flue dust, atomised metals	0·32–0·41	2·7–3·4	8·5
Angular particles of pulverised minerals: coal, limestone, silica	0·18–0·28	2·3–3·2	13–11
Flaky particles: plumbago, talc, gypsum	0·08–0·16	1·8–2·8	22–17
Very thin flakes: mica, graphite, aluminium	0·01–0·03	1·6–1·7	160–50

Finally, because of the difficulty of determining experimentally the numerical value of α_s for fine particles, a statistical relationship between $\alpha_{v,a}$ and $\alpha_{s,a}$ was obtained by measurements on stones of various shapes sized 1 to 2 inches[3]. Since this relationship is purely geometrical and independent of particle size, the results are applicable to the smallest particles, provided that the geometrical form can be estimated by observation.

$$\alpha_{s,a} = 1{\cdot}57 + C\,(\alpha_{v,a})^{4/3}\,\frac{(n+1)}{n^{\frac{1}{3}}} \tag{7}$$

where n is the elongation of the particle, equal to the ratio length/breadth, and C is a parameter depending on the geometrical form of the particle as set out below

Angular, tetrahedral	$C = 3{\cdot}3$
Angular, prismoidal	$C = 3{\cdot}0$
Sub-angular	$C = 2{\cdot}6$
Rounded	$C = 2{\cdot}1$

The theoretical approach described above was first proposed by the author[4] in a paper published in 1933. It has been extended and amplified during the intervening period and, with modifications suggested by other members of the sub-committee, has been included in the proposed B.S. on specific surface calculation. Numerical values obtained from various sources for these materials will be included in the specification.

THE MEAN SIZE OF A PARTICULATE SYSTEM

The determination of this factor is the major problem in the calculation of specific surface, and the first approach is to consider the relationship between the various size-dependent properties of a particulate system.

A particulate system may be characterized by the size dependent properties of total number, length, surface area and volume, or weight if the density of the material is uniform. All particles are assumed to have the same shape, not necessarily spherical and as the method of size assessment is not involved, particle size is denoted by the symbol x. Hence, if there are $\mathrm{d}N$ particles in a group with narrow size limits which may be represented by a single size x, then the above size-dependent properties may be expressed in terms of x raised to the power r and multiplied by $\mathrm{d}N$, as shown in *Table 3*.

Table 3. Size dependent properties of a particulate system

r	*Property within group*	*Total of property in system*
0	Number $= x^0\mathrm{d}N$	$\Sigma x^0\mathrm{d}N = N$
1	Length $= x^1\mathrm{d}N$	$\Sigma x^1\mathrm{d}N = L$
2	Surface $= x^2\mathrm{d}N$	$\Sigma x^2\mathrm{d}N = S$
3	Volume $= x^3\mathrm{d}N$	$\Sigma x^3\mathrm{d}N = V$

If the mathematical law relating the size and relative frequency of any of the above properties were known, then the transformation from one property to another could be performed by integration. As no law for size distribution yet devised is completely satisfactory, the transformation must be accomplished by dividing the complete size range of the powder into a number of groups as described above and assuming as a first approximation that the mean size for each group is x_{am}, the arithmetic mean of the limiting sizes.

The size distribution on a number basis used throughout this paper as an example for the calculation of specific surface is given in *Table 4*. Although the groups are finite in size range, it is convenient to use the calculus notation and represent the relative frequency for each group by the expression dN/dx at size x_{am}.

Table 4. Frequency distribution of particles by number

Size range dx	0–1	1–2	2–3	3–4	4–6	6–8	8–10	10–12	12–16	16–20
Number of particles in group dN	310	175	108	74	100	64	44	31	36	10
Relative frequency dN/dx	310	175	108	74	50	32	22	15·5	9	2·5
Mean size for group x_{am}	0·5	1·5	2·5	3·5	5·0	7·0	9·0	11·0	14·0	18·0

The above figures for relative frequency have been plotted against the arithmetic mean size x_{am} for each group in *Figure 1*. The stepped form is inevitable as a first stage since no information is available on the frequency variation within the groups, but a more probable frequency distribution would be obtained by constructing a frequency polygon through the steps. The number of particles in each group is represented by the area of the appropriate block, and the total number in the sample by the complete area enclosed.

The transformation from a number frequency curve to curves representing properties corresponding to higher orders of x, as set out in *Table 3*, is

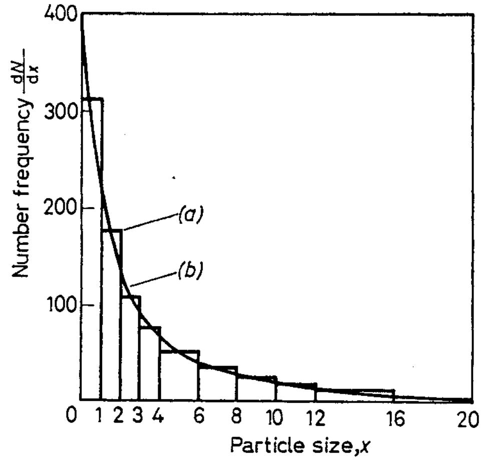

Figure 1. Frequency distribution by number [(*a*), stepped diagram; (*b*) frequency polygon]

performed by calculating the first, second and third moments of the number frequency curve about the $x = 0$ axis and thus determining the frequency curves for the properties length, surface and volume respectively. The mean diameter of a system of particles is obtained by dividing the moment of a specific frequency curve by the area enclosed; this process can be expressed in symbols as:

Area enclosed by frequency curve $= \Sigma x^r \mathrm{d}N$

First moment of the area $= \Sigma x^{r+1}\,\mathrm{d}N =$ area of the $(r + 1)$ frequency curve.

Therefore, mean of the r frequency curve $= \Sigma x^{r+1}\,\mathrm{d}N/\Sigma x^r \mathrm{d}N = x_{r,r+1}$ (8)

This system of nomenclature is summarised in *Table 5*. The properties surface and volume are relative, and to make them absolute must be multiplied by the surface and volume coefficients respectively; but since these factors are assumed constant for all particles in a given sample, they need not be introduced until the end of the calculation.

Table 5. Derivation of mean diameters of a particulate system

Nomenclature and properties concerned	*Expression for means*	*Symbols*
Number length mean diameter	$\Sigma x\,\mathrm{d}N/\Sigma \mathrm{d}N$	x_{nl}
Length surface mean diameter	$\Sigma x^2\mathrm{d}N/\Sigma x\mathrm{d}N$	x_{ls}
Surface volume mean diameter	$\Sigma x^3\mathrm{d}N/\Sigma x^2\mathrm{d}N = \Sigma \mathrm{d}V/(\Sigma \mathrm{d}V/x)$	x_{sv}
Volume moment mean diameter	$\Sigma x^4\mathrm{d}N/\Sigma x^3\mathrm{d}N = \Sigma x\mathrm{d}V/\Sigma \mathrm{d}V$	x_{vm}
Weight moment mean diameter	or $\Sigma x\mathrm{d}W/\Sigma \mathrm{d}W$	x_{wm}

PROCEDURES FOR CALCULATING x_{sv} FROM A NUMBER-SIZE DISTRIBUTION

It is assumed in the proposed B.S. specification that the effective mean diameter of the group is equal to the arithmetic mean of the limiting diameters of the group, namely x_{am}. It is known that this assumption introduces an error, but for two reasons that are explained later, this error is generally small compared with the probable error of the sizing analysis and the simple procedure of using a constant multiplier of x_{am} for each group was adopted in the B.S. specification. The procedure, which it is not necessary to set out in detail in this paper, is to construct a table with the column headings x_{am}, $\mathrm{d}N$, $x_{am}{}^2\mathrm{d}N$ and $x_{am}{}^3\mathrm{d}N$ in which the values for each group are inserted and the total for the last two columns is obtained. The mean diameter of the system that relates the properties of surface and volume, x_{sv}, is then equal to $\Sigma x^3\mathrm{d}N/\Sigma x^2\mathrm{d}N$ and is the diameter corresponding to the centroid of the area enclosed by the surface frequency curve.

A more precise method of calculation is based on the following theory. As has been explained above, if the area of a frequency curve of the order x^r is multiplied by the mean value of x which passes through the centroid of the area, then the area representing the property having the order x^{r+1} is obtained, since this process corresponds to taking moments. The first error of the simple procedure arises from the fact that if a group of particles between the size limits x_1 and x_2 is considered and the value of dN/dx over this range is constant so that $(dN/dx)_1 = (dN/dx)_2$ then the next higher order property will be calculated correctly as $x_{am} \,.\, dN$ since in this case the centroid size is identical with the arithmetic mean of limiting sizes, but for the next stage of transformation, however, $x dN/dx$ will not be constant and $(x dN/dx)_2$ will be greater than $(x dN/dx)_1$ since x_2 is greater than x_1. Therefore the centroid size which is the multiplying factor for the second transformation will be greater than x_{am}, and this disparity will increase with each transformation, thus leading to a greater relative surface and volume than would be calculated by means of the simple procedure. The change in shape of such a section of a frequency curve is shown by the upper series of diagrams in *Figure 2*.

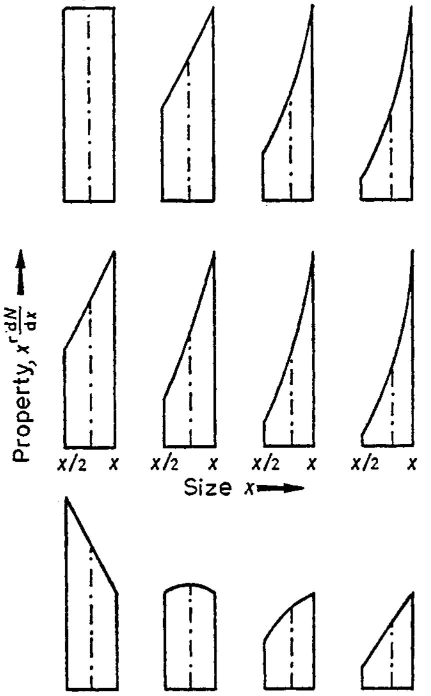

Figure 2. Change in shape of a section of a frequency curve as the property number is transformed to other size-dependent properties. Chain-dotted lines pass through centroid of area.

The second error is due to the fact that dN/dx between x_1 and x_2 is not generally constant but that $(dN/dx)_2$ differs from $(dN/dx)_1$. If the former is greater than the latter as in the middle series of diagrams in *Figure 2* then the effect described above will be intensified, since the centroid size is always greater than the arithmetic mean size. If the converse is the case, as in the lower series of *Figure 2* then for the first transformation the centroid size will be less than x_{am}, for the second transformation will become approximately equal to x_{am} and eventually becomes greater than x_{am}. Thus the error in the simple calculation is variable, depending upon the shape of the basic frequency curve, and for an initial frequency curve of approximately Gaussian distribution there would be virtually no error.

An equation providing a general solution to this problem has been developed and the theory is explained in Appendix 1. The assumption is made that in a section of the area below a frequency curve that is bounded by two size limits x_1 and x_2, the portion of the frequency curve between the two limits may be regarded as a straight line, of either positive or negative slope. The equation obtained is somewhat formidable, and it will be appreciated why the simple method of calculation was chosen for the B.S. specification. Nevertheless, there may be special circumstances where the simple theory is inadequate and in any case it was necessary to justify the simple theory by comparison with a more rigorous treatment before the former could be accepted for normal use. There is, however, another aspect to be considered; the B.S. specification is concerned solely with the calculation of specific surface and the reason why the error in the proposed method is so small is that whilst there may be considerable error in the calculated magnitudes of both the relative volume and surface, the ratio of these two quantities is much less affected. If, however, the intention is to calculate the volume or weight distribution from a number count, then the error by the simple method may exceed 10 per cent at the extreme ends of the size range, though the average error over the whole range will be considerably less.

A comparison of the two forms of calculation is given in *Table 6*, using the data quoted in *Table 4*.

Table 6.

	Simple method	*General equation*	*Error of simple method* (%)
Number of particles ΣdN	952	952	—
Relative surface = $\Sigma x^2 dN$	25 307	24 670	+ 2·58
Relative volume = $\Sigma x^3 dN$	270 390	259 540	+ 4·18
Surface volume diameter, x_{sv}	10·68	10·52	+ 1·56

The error of the specific surface calculation is very much less than the probable error between sizing analyses, even if these were determined by the same procedure[5].

CALCULATION OF THE SPECIFIC SURFACE FROM A WEIGHT-SIZE DISTRIBUTION

The procedures described above for transforming frequency curves in ascending powers of x may be used for transforming in descending powers of x, but there are significant differences. In this case the elements or groups of the basic frequency curve, i.e. the curve derived from measurements, are divided by the effective mean size of the group. The principle now is that the group property must be divided by the centroid size of the group property with one lower power of x than the basic property. This involves no problem by the simple method where the effective size is taken as x_{am}

throughout the transformations, but if a rigorous solution is required then the general equation must be used. Another problem is that when dividing successively by small values of effective size, any error in the sizing analysis or in the numerical value of the dividing factor will result in gross errors in the final answer. In fact, if the volume frequency curve of $x^3\mathrm{d}N/\mathrm{d}x$ against x is not zero at $x = 0$, then the calculated surface area will be infinite, and this raises the problem as to the selection of a mean effective size for the 0 to x_1 group when this is expressed in a block form. The B.S. specification recommends in such circumstances the use of a dividing factor of one quarter of the upper size limit of the finest fraction as a dividing factor, instead of one half, but this is arbitrary and can only be approximate. In order to avoid this situation occurring, the sizing analysis by weight should be continued to a particle size that is smaller than that of the modal frequency of the weight distribution curve.

Figure 3 shows the volume-size frequency curve calculated from the data in *Table 4* by means of the general equation. The groups are both shown as a stepped diagram and as a frequency polygon, also as a correct curve where this differs appreciably from the frequency polygon.

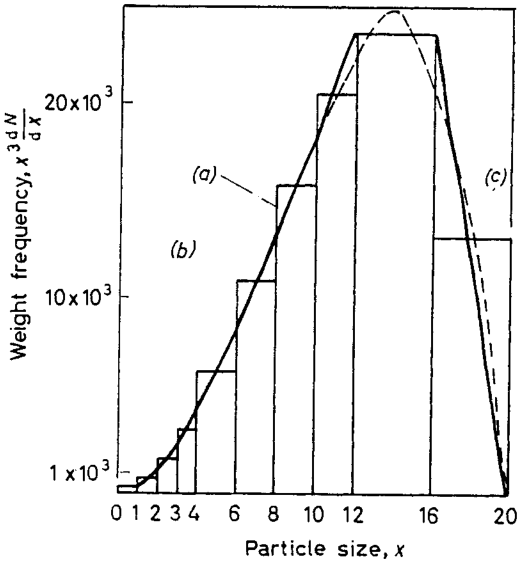

Figure 3. Frequency distribution by volume or weight [(*a*), stepped diagram; (*b*) frequency polygon; (*c*) frequency curve].

The relative surface has been calculated from the data in *Figure 2* by the simple method of using x_{am} as a dividing factor for each group and also by the general equation, and the results are given below.

	Simple method	*General equation*
Relative volume, $\Sigma x^3\mathrm{d}N$	259 540	259 540
Relative surface, $\Sigma x^2\mathrm{d}N$	24 624	24 640
Surface volume diameter, x_{sv}	10·54	10·53

The difference between the two methods is negligible, due to the fact that the basic frequency curve has an approximately Gaussian distribution, though there would be considerable greater error with a distribution that was markedly skewed.

ALTERNATIVE METHODS OF CALCULATING SPECIFIC SURFACE

If a volume-size frequency curve such as *Figure 3* is re-plotted to a base of log x, either as a stepped diagram or as a polygon, then the area enclosed represents the relative surface of the particles. This follows from the fact that $d(\ln x)/dx$ equals $1/x$, hence the property of the original curve is reduced by one order of x. The relative surface of a group is obtained by multiplying the height of the step by $2{\cdot}303 \log (x_2/x_1)$, and adding the products to obtain the total surface. For the step covering the range 0 to x_1 the theoretical area is infinity, so that an arbitrary lower limiting size must be assumed, say $0{\cdot}1\ x_1$. Calculation by this method gave x_{sv} equal to 10·46, the slight difference from the other calculations being due to the assumption of a stepped shape diagram.

The size analysis of a powdered material is conveniently expressed by a graph relating the cumulative weight percentage residue or the undersize against particle size. Preference is now given to the use of undersize curves and this is the integral curve of the weight frequency distribution as shown in *Figure 3* and used in the calculations described earlier in the paper. Such curves are normally plotted to a base of log particle size. The percentage weight undersize may be plotted to some functional scale, such as log. probability or the Rosin-Rammler scale (see Appendix 2) in an attempt to transform the graph from a curve to a straight-line relationship. In fact, however, a straight-line relationship is only obtained over a limited portion of the size range, so that a summation procedure is still necessary for transformation from one property to another.

In the discussion on the paper by the author already referred to[4], a description was given of a graphical method by which the specific surface of a powder could be determined directly from a cumulative plot on the Rosin–Rammler scales. This has since been modified so that the calculation can be computerized, though this is not essential, and the surface-volume mean diameter, x_{sv}, may be determined directly from the undersize curve. A description of the procedure as applied to the Rosin–Rammler scales is given in Appendix 2, and the value of x_{sv} for the example of size distribution used throughout this paper came to 10·35, compared with 10·5 by use of the general equation.

DENSITY OF THE PARTICLES

The appropriate density to be used in the conversion of specific surface from a volume to a weight basis is defined in B.S. 2955 as the effective particle density, viz., the mass of a particle divided by the volume of the particle including open and closed pores.

SUMMARY OF METHOD OF CALCULATION

Two examples will be considered; the first assumes that a number-size count of the particles has been made to obtain the data given in *Table 4*.

The appropriate surface volume mean diameter of the particles is calculated, either by the simple proposed B.S. method or by the general equation if warranted; let this be x_{sv} in μm. Since the measurements have been made by microscope the appropriate shape coefficient is $a_{sv,a}$, which may have been determined by measurement or an assumed value abstracted from *Table 2*.

$$\text{Hence specific surface on a volume basis, } S_v = a_{sv,a} \cdot \frac{1}{d_{a,sv}}\text{, m}^2/\text{cm}^3 \qquad (9)$$

and if the effective density of the particles is ρ_e g/cm^3, then

$$S_w = S_v/\rho_e\text{, m}^2/\text{g}$$

The second example assumes that a weight-size distribution has been obtained by a sedimentation analysis procedure. The first step is to calculate the value of x_{sv} and since particle size has been deduced from Stokes' law, this becomes $d_{st,\,sv}$ in μm.

S_v now equals $a_{sv,\,st} \cdot \frac{1}{d_{st,\,sv}}$, m^2/cm^3, but as values of $a_{sv,\,st}$ are not tabulated the following conversion is made:

$$a_{sv,\,st} = a_{sv,\,a} \cdot \frac{d_{st,\,sv}}{d_{a,\,sv}} = 0{\cdot}63\, a_{sv,\,a} \text{ (from } \textit{Table 1} \text{ if } a_{v,\,a} = 0{\cdot}2\text{).}$$

$$\text{Therefore: } S_v = a_{sv,a} \frac{0{\cdot}63}{d_{st,\,sv}}\text{, m}^2/\text{cm}^3 \qquad (10)$$

When the specific surface has been measured by a direct method, such as permeability or adsorption, an equivalent mean particle diameter is often calculated in order to give a physical interpretation of the particle size. Spherical particles are assumed, for which $a_{sv} = 6$, and the mean diameter cannot be other than a surface volume mean. The following system of notation might be used to define this procedure:—

$d_{per.}$ or $d_{ads.}$ in μm $= 6/(S_v$ by permeability or adsorption in m^2/cm^3) (11)

CONCLUSIONS

The author hopes that this paper has not given the impression that calculation of the specific surface of a powder is necessarily a complicated procedure. The accuracy of the calculation is limited by that of the sizing analysis, but since the error of the simple method in the proposed British Standard is generally less than the probable error in sizing, the use of a more rigorous mathematical treatment is not normally justified. Nevertheless, the more rigorous method had to be investigated, both to justify the general use of the simple method and to enable transformations from one size-dependent property to another to be performed with a higher degree of accuracy when this is required.

APPENDIX 1

Derivation of a general equation for transformations from one property to another.

Consider a portion of the basic frequency curve which represents a group of particles limited by two diameters x_1 and x_2 as shown in *Figure 4*. The basic frequency curve is that to which the size analysis measurements apply, whether this be number, weight or any other property. The assumption is made that the portion of the frequency curve between the size limits is a straight line, which may have a positive slope, as shown, a negative slope or zero slope.

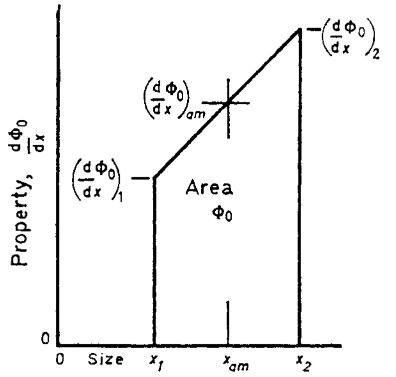

Figure 4. Section of frequency curve representing the property Φ_0

The procedure is to denote the basic property by Φ_0, this being the area of the portion of the basic frequency curve between the limits x_1 and x_2, including the case where $x_1 = 0$. Ascending properties in increasing order of r are obtained by calculating the first, second and third moments respectively of the basic property. Descending properties are calculated by negative or inverse moments of the basic property in decreasing order of r. Thus the properties Φ_1 to Φ_4 or the properties Φ_{-1} to Φ_{-4} may be calculated in terms of the property Φ_0.

The rth moment of Φ_0 may thus be calculated to obtain the general equation, from which the equations for specific values of r are obtained. The complete value for the property Φ_r is obtained by summation of the individual values of Φ_r for the size-limited groups into which the frequency curve has been divided. The procedure for deriving the general equation for Φ_r is shown below.

$$p = \left(\frac{d\Phi_0}{dx_1}\right)_1 \bigg/ \left(\frac{d\Phi_0}{dx_2}\right)_2 \text{, can vary from 0 to infinity}$$

$$q = (x_1/x_2)\text{, can vary from 0 to 1.}$$

$$\frac{d\Phi_0}{dx_{am}} = \left\{\left(\frac{d\Phi_0}{dx}\right)_1 + \left(\frac{d\Phi_0}{dx}\right)_2\right\}\bigg/2;$$

$$\left(\frac{d\Phi_0}{dx}\right)_2 - \left(\frac{d\Phi_0}{dx}\right)_1 = 2\left(\frac{d\Phi_0}{dx}\right)_{am}\frac{(1-p)}{(1+p)} \qquad (1)$$

$$x_{am} = (x_1 + x_2)/2; \quad x_2 - x_1 = 2x_{am}\frac{(1-q)}{(1+q)} \qquad (2)$$

The magnitude of the property represented by the index r is equal to the rth moment of the property Φ_0 and is obtained by integration.

$$\text{Since } \frac{d\Phi_0}{dx} = \left(\frac{d\Phi_0}{dx}\right)_1 + \frac{(x - x_1)}{(x_2 - x_1)}\left\{\left(\frac{d\Phi_0}{dx}\right)_2 - \left(\frac{d\Phi_0}{dx}\right)_1\right\}$$

$$\Phi_r = \int_{x_1}^{x_2} x^r \frac{d\Phi_0}{dx}\, dx$$

$$= \left(\frac{d\Phi_0}{dx}\right)_1 \int_{x_1}^{x_2} x^r\, dx + \left\{\left(\frac{d\Phi_0}{dx}\right)_2 - \left(\frac{d\Phi_0}{dx}\right)_1\right\}$$

$$\left[\frac{1}{(x_2 - x_1)} \int_{x_1}^{x_2} x^{r+1}\, dx - \frac{x_1}{(x_2 - x_1)} \int_{x_1}^{x_2} x^r\, dx\right]$$

Substituting for $(x_2 - x_1)$ and for $(d\Phi_0/dx)_2 - (d\Phi_0/dx)_1$ from equations (1) and (2)

$$\Phi_r = \frac{2^{r+2}}{(r+1)\,(r+2)} \left(\frac{d\Phi_0}{dx}\right)_{am} {}^{r+1}_{am} \frac{(1 - q^{r+1})}{(1 + q)^{r+1}} \left[\quad\right] \tag{3}$$

$$\left[\quad\right] = \left[\frac{p(r+2)}{(1+p)} + \frac{(1-p)}{(1+p)\,(1-q)} \left\{\frac{(r+1)\,(1-q^{r+2})}{(1-q^{r+1})} - (r+2)q\right\}\right]$$

applicable for r having any positive or negative integer value except -1 and -2. Alternatively

$$\left[\quad\right] = \left[\frac{p(r+2)}{(1+p)} + \frac{(1-p)}{(1+p)} \left\{\frac{(r+1) + rq + (r-1)\,q^2 \ldots . q^r}{(1 + q + q^2 \ldots q^r)}\right\}\right] \tag{4}$$

applicable for r zero or any positive integer value.

When r is equal to -1 or -2 integrations involve $\ln(1/q)$ and the general equation cannot be used.

The equations for specific values of r are given below:

$$\Phi_{-2} = \left(\frac{d\Phi_0}{dx}\right)_{am} \frac{1}{x_{am}} \left[\frac{(p-q)}{(1+p)} \frac{(1+q)}{q} + \frac{(1-p)}{(1+p)} \frac{(1+q)}{(1-q)} \ln \frac{1}{r}\right]$$

$$\Phi_{-1} = 2\left(\frac{d\Phi_0}{dx}\right)_{am} \left[\frac{(1-p)}{(1+p)} + \frac{(p-q)}{(1+p)\,(1-q)} \ln \frac{1}{r}\right]$$

$$\Phi_0 = 2\left(\frac{d\Phi_0}{dx}\right)_{am} x_{am} \frac{(1-q)}{(1+q)} [1]$$

$$\Phi_1 = \frac{4}{3}\left(\frac{d\Phi_0}{dx}\right)_{am} x_{am}^2 \frac{(1-q^2)}{(1+q)^2} \left[\frac{3p}{(1+p)} + \frac{(1-p)}{(1+p)} \frac{(2+q)}{(1+q)}\right]$$

$$\varPhi_2 = \frac{4}{3}\left(\frac{\mathrm{d}\varPhi_0}{\mathrm{d}x}\right)_{am} x_{am}^{3}\frac{(1-q^3)}{(1+q)^3}\left[\frac{4p}{(1+p)} + \frac{(1-p)}{(1+p)}\,\frac{(3+2q+q^2)}{(1+q+q^2)}\right]$$

$$\varPhi_3 = \frac{8}{5}\left(\frac{\mathrm{d}\varPhi_0}{\mathrm{d}x}\right)_{am} x_{am}^{4}\frac{(1-q^4)}{(1+q)^4}$$

$$\left[\frac{5p}{(1+p)} + \frac{(1-p)}{(1+p)}\,\frac{(4+3q+2q^2+q^3)}{(1+q+q^2+q^3)}\right]$$

The equations for $\varPhi_1$ to $\varPhi_3$ are considerably simplified if p is equal to 1, as in a stepped frequency diagram, for all the terms in square brackets are then reduced to $(r+2)/2$. This special case was investigated by Morgan[6], but in certain circumstances the assumption that $p = 1$ may result in over-correction of the calculations.

The statistics of small particles and the use of probability functions have been discussed fully in a book by Herdan[7], and methods of calculation based on probability functions have been developed by Wise[8] and by Kottler[9].

APPENDIX 2

Derivation of specific surface from the cumulative undersize curves.

This procedure makes use of a graph of percentage by weight undersize plotted according to a functional scale derived from the Rosin–Rammler law, against log of particle size. The law[10] is expressed as

$$\frac{100}{R} = \exp\,(bx^n)$$

where R is the cumulative residue per cent by weight, n and b are constants. This may be reduced to the form

$$\log\log\frac{100}{100-U} = n\log x + \log b,$$

where U is the cumulative undersize per cent by weight. The data derived from *Figure 3* are plotted in this manner in *Figure 5*.

The object is to construct a curve which encloses an area proportional to the surface of the particles and which converges to the axis as x tends to 0. The theoretical basis of the procedure is described in detail on p. 456 of reference 4. The essential features are that at any size x the surface of the particles is proportional to $1/x$ but that as the area representing surface is to be plotted in arithmetical scales then the value of $1/x$ must be multiplied by the ratio of the functional scale to the arithmetical scale appropriate to the value of corresponding to x. This latter ratio is termed the scale ratio Ω, and is calculated as follows:

Let y = the length from $U = 0{\cdot}1$ to $U = 99{\cdot}9$ on both the log log scale and the arithmetic scale of plotting. Then the mean scale ratio over this length y is:

$$\frac{99.9 - 0.1}{\log\log\dfrac{100}{100-99{\cdot}9} - \log\log\dfrac{100}{100-0{\cdot}1}}$$

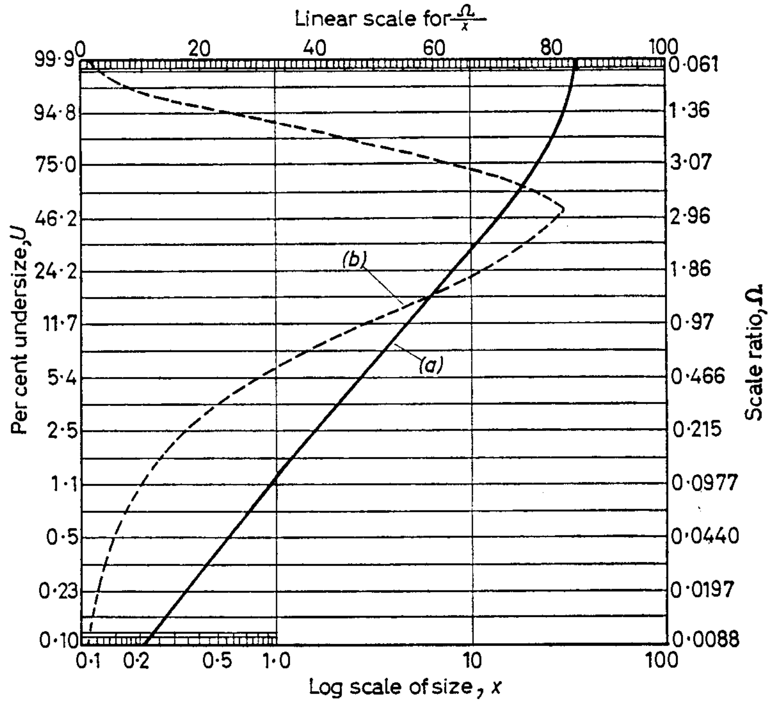

Figure 5. Construction of surface area diagram from per cent undersize weight curve to scale log log $\{100/(100-U)\}$ [(*a*) undersize curve, log x base; (*b*) surface area diagram, linear scale of Ω/x]

$$= \frac{99{\cdot}8}{0{\cdot}4771-(-3{\cdot}3620)} = \frac{99{\cdot}8}{3{\cdot}8391}$$

The log log scale is variable however, and at any given value of U is equal to

$$\frac{\mathrm{d}U}{\mathrm{d}y} = \frac{\mathrm{d}U}{\mathrm{d}\log\log\{100/(100-U)\}}$$

$$= 2{\cdot}303^2\,(100-U)\log\frac{100}{100-U}$$

Therefore the scale ratio $\Omega = 2{\cdot}303^2\,(100-U)\log\frac{100}{100-U}\bigg/\frac{99{\cdot}8}{3{\cdot}8391}$

$$= 0{\cdot}204\,(100-U)\log\frac{100}{100-U}$$

The functional scale of U in *Figure 5* has been divided equally into 22 sections and against alternate dividing lines the undersize percentage and corresponding scale ratio have been marked. The procedure is to read x from the curve at each dividing line, convert to $1/x$ and multiply by the scale ratio. In symbols:

$$dS = \frac{1}{x} . \Omega . dW.$$

The mean value of $1/x$ is obtained by dividing the sum of the individual values obtained from the above equation by 23, and using this in the specific surface equation as described in the paper.

SUMMARY

The calculated specific surface of a particle is that of a smooth impermeable skin of negligible thickness which contacts the external surface. The specific surface of a powder is calculated from the size distribution of the constituent particles and allowance can be made for the effect of particle shape.

The problems are to define the characteristic dimension of an irregularly shaped particle, the various shape factors and the appropriate mean size for a system of particles. Each of these problems is discussed fully.

The British Standards Institution intends to publish a standard describing a simple method for performing these calculations, and this procedure is summarized in the paper. A more exact procedure has been devised by the author to show that certain approximations that are made in the B.S.I. method do not introduce any significant error in the calculated specific surface, whilst they reduce greatly the possibility of arithmetical mistakes and the time required for the calculation.

References

[1] H. Heywood. *J. Pharm. and Pharmac. Supplement* **15**, 56T (1963).
[2] Institute of Chemical Engineers. *Report on storage and recovery and particulate solids* (1966).
[3] H. Heywood. *J. Imper. Coll. Chem. Eng. Soc.* **8**, 25 (1954).
[4] H. Heywood. *Proc. Inst. Mech. Engrs.* **125**, 383 (1933).
[5] B.S. 3406 Part 2, Appendix B (1963).
[6] V. T. Morgan. *Powder Metall.* No. 10, 237 (1962).
[7] G. Herdan. *Small Particle Statistics.* Butterworths, London (1960).
[8] M. E. Wise. *Philips Res. Reports* **9**, 231 (1954).
[9] F. Kottler. *J. Franklin Inst.* **251**, 499, 617 (1951).
[10] P. Rosin and E. Rammler. *J. Inst. Fuel* **7**, 29 (1933).

WORK OF THE BRITISH STANDARDS INSTITUTION COMMITTEE ON SURFACE AREA DETERMINATION

A. S. Joy

Warren Spring Laboratory, Stevenage, Herts, U.K.

It is well known that any two operators working in isolation, using apparatus constructed to their own design, different methods of preparing the samples or specimen, and their personally preferred operational techniques, frequently have a negligible chance of getting the same result. In research work the chance is greatly improved owing partly to a greater awareness by the worker of the hazards and possible sources of error, partly to a careful briefing in the literature and partly to exchange of information with groups working on the same problem. Manipulative skill may nevertheless vary widely, and one is constantly reminded of the remark of Professor Partington that "He would accept a result by T. W. Richards in preference to one obtained by a young post-graduate student operating the controls of an instrument, the working of which he only barely understood". Nevertheless, surprisingly good agreement is often obtained under such circumstances, although, that scepticism exists is evidenced by the frequency with which manipulative details are queried in the discussions following the presentation of scientific papers.

In industrial laboratories, concerned with production control, the quality of raw materials and products, pressures are great, circumstances are different and consequences may be extremely serious. A disagreement which resulted in nothing more than friendly argument between research workers could in industry quite easily lead to legal action or loss of production costing many thousands of pounds. Professional consultants may act as referees to offer an 'umpire' analysis, but even when this is done, the method used by the referees must be acceptable to both parties and known to give reproducible results. The actual result must also be accepted to be a 'true' result within permissible limits of error. It is not always a simple matter to decide what constitutes the 'true' result. If an absolute value is required and an acknowledged 'absolute' method is known, then the referee method should give a result very close to that given by the absolute method, preferably without the use of correlation or weighting factors.

In the absence of an absolute method, or, as very frequently occurs, an absolute value is not required, then the worth of the 'referee' method tends to be adjudged on subjective grounds. These may vary in subjectivity, from a semi-quantitative argument that it gives a result which is a mean of the results obtained by other methods, to an entirely qualitative argument that the result accords with expectations and experience. A value based on experience is not to be disregarded, especially if it relates to technical or industrial usage. Such usage can, and frequently does, influence the choice of method. This is particularly important when a number of methods are available for the determination of a property which by absolute scientific standards ought to have a unique value. The absolute value may have little or no relation to the industrial process or usage. A simple example is the use of a powder as an adsorbent for oils. The total specific surface as determined, for instance, by the adsorption of small gas molecules can be totally unrelated to the technical efficiency of the powder, if an appreciable fraction of the area is contributed by pores which are too small to permit the entry of large oil molecules.

If a particular 'referee' method is required to meet the needs of a particular industry of a particular material, then it is appropriate and not too difficult to select a method which directly satisfies the particular industrial needs. It is much more difficult to propose 'referee' methods which are not for any one definite industry or material. Nevertheless, there are several reasons for the production of standard methods of this kind. The progress of technology and the large number of new materials and processes which appear at an ever-increasing rate make it impossible to produce particular standards fast enough to meet all possible demands, even if this were desirable. Where applicable, a standard method specification forms a basis for a mutually agreed 'referee' method, and eventually can be incorporated in whole, in part, or merely by reference, in a Standard for a specific material. General method specifications are comparatively rare; the majority of B.S. specifications specify weights, dimensions and technically significant properties of manufactured goods. Many of these specifications do include methods for testing the articles and for determining the values of the significant properties. A very large number of Standards, particularly those which deal with materials, are mainly concerned with specifying properties and methods for the determination of these properties.

It is of historical interest that the first specification (B.S.1: 1898) Rolled Steel Joists, was the direct result of a meeting of Civil Engineers and Ironmasters in an attempt to rationalise production. This lead was taken up very quickly by the cement industry with the publication in 1904 of B.S.12—Portland Cement. This Standard is of particular interest because it was the first Standard—by amendment in 1947—to incorporate a test method for the determination of specific surface. The specification underwent revisions but it is still an essential, basic, description of an apparatus and operating procedure for quality control in the cement industry—and in other industries.

B.S.12 specifies the constant-flow Lea and Nurse air-permeability apparatus; a later specification (B.S.3892: 1965—Pulverized Fuel Ash for use in Concrete) described the constant volume method due to Rigden as an alternative to the Lea and Nurse method. The dimensions and method of filling the permeability cell are rigorously specified and no choice is allowed in this respect. Thus, prior to 1965 there was only one specified method for specific surface determination available to cover the whole of the industrial needs. In 1952 a Technical Committee (CHE/80) was set up to examine the whole question of Test Methods for Powder Properties. It was decided that the methods described in the then current Standards for the Determination of Particle Size of Powders and for the Determination of Specific Surface of Powders were inadequate to cope with industrial needs. Particle size determination was considered to be the more urgent problem and a Sub-Committee (CHE50/1 with Dr Heywood as Chairman) was established in 1952. The B.S.3406 series of Standards was published in 1963 as a result of the work of this Sub-Committee.

In 1964 a referendum was put to the CHE/50 Committee for a decision to proceed with the production of general Standards on Methods for the Determination of Specific Surfaces of Powders. It was envisaged that the Standards would follow the pattern of the B.S.3406 series. Initially, a small Panel was appointed to ascertain whether there was a real industrial need for such Standards and if the need were confirmed, to list possible methods and to contact the relevant U.K. experts. The industrial response was encouraging and the first meeting of the new Sub-Committee CHE50/5 took place in September 1964.

The list of possible methods presented to the Committee at that time was:—

I. Volumetric Gas or Vapour Adsorption
  (a) Nitrogen adsorption (BET method)
  (b) Krypton (or other inert gas) adsorption
  (c) Vapour (benzene, cyclohexane, etc.) adsorption[1]
  (d) 'Single-point' adsorption methods
  (e) Haynes air adsorption method[2]
  (f) Flow or 'chromatographic' methods[3]

II. Gravimetric Gas or Vapour Adsorption
III. Gas or Liquid Flow Constant
  (a) Constant flow rate methods
  (b) Constant volume flow-time methods
  (c) Transient gas-flow methods[4]

IV. Adsorption of Liquids or from the Liquid Phase
  (a) Dye-stuff adsorption[5]
  (b) Glycerol or ethylene glycol adsorption
  (c) Negative adsorption[6]
  (d) Double layer capacity[7]

V. Thermal Effects
  (a) Direct heat of wetting
  (b) Flow calorimetry

VI. Dimensional Effects
  (a) Photo-sedimentation
  (b) Electron and optical microscopy
  (c) Calculation from size distribution and shape factors

The primary industrial demand[8] was clearly for Standards based on gas adsorption and air permeability methods. The choice was complicated by the availability of a variety of commercial instruments although in principle there is no objection to the selection of a commercial instrument for inclusion in a Standard. A large number of Standards in various fields rely upon commercial apparatus. The Roller and the Bostock machines were described in the B.S.3406 series and B.S.3181: 1959 (Determination of Cotton Fibre Fineness by the Airflow Method) is entirely based on the Porton, Shirley WIRA and Micronair constant flow air-permeability machines. A commercial instrument should be chosen only if it is readily available, has sufficient constancy of operation, is not likely to be superseded by a new, or modified, version in a reasonable space of time, and can cope with all of the materials and range of values which the Standard is expected to cover. Very often the sequence of events is reversed and the publication of a Standard is followed by the production of an apparatus by an equipment manufacturer.

Greater freedom in the choice of methods and equipment for standardization is possible if the Standard is not necessarily expected to be suitable for daily routine use, but to define procedures for referee purposes. Even then, the choice is restricted by considerations of sophistication and expense.

Finally, the methods selected must be accepted by industry; the results should have some understandable significance and relevance to industrial usage. For these reasons negative adsorption and double layer capacity were rejected at the first meeting of CHE50/5.

A standard heat-of-wetting apparatus is perfectly feasible and a few industries—notably the cement industry—do use an internally standardised method; the results are accepted to be only partially related to specific surface and are more commonly taken as a measure of reactivity. The flow-calorimeter is a refinement which should have a wider applicability and commercial versions—such as the Microscal—are available. However, a major obstacle to its adoption as a Standard is that, so far, the acceptance level is very low. It was for this reason, also, that the benzene and cyclohexane vapour adsorption and the transient gas-flow methods were rejected, even though suitable apparatus and procedures have been described in the literature[1, 4].

Glycerol or glycol adsorption is quite commonly used for bentonite, clay and soil characterization, but, although it can give results[8] in surprisingly good agreement with the BET method, quantitative interpretation is frequently difficult. The technique is ideally suited for a specific Standard for a particular material.

Of the remaining methods, conventional nitrogen adsorption and constant flow and constant volume air-permeability were obvious choices for the first Standards. Of the large number of adsorption systems described in the literature, that proposed by Dr V. Crowl was agreed to be taken as the basis of a Standard. It had the merits of simplicity combined with adequate accuracy and versatility. Consequently a small Panel was elected and given the task of preparing draft Standards for consideration. A similar Panel, chaired by Mr Grant of the E.R.D.E., Waltham Abbey, started work at the same time on a Standard intended to cover the Lea and Nurse, the Rigden and the Blaine air permeability methods.

At that time it was thought best not to include commercially available equipment in the main text of the Standards, but to refer to them in Appendices.

It was found particularly difficult to decide whether to accept or reject the Haynes' air adsorption apparatus, the continuous flow or chromatographic methods, and dye-stuff adsorption methods. The Haynes' method has the merit of outstanding simplicity and speed of operation without being limited to a single-point determination. It is definitely a secondary Standard in that it needs to be calibrated by reference to a more fundamental method. This does not exclude it provided that a calibration factor can be applied which is constant for a given material over the expected range of usage. In this respect it appeared to be comparable to commercial apparatus such as the Strohlein Area-meter and the Aminco Sorbet.

Flow-methods have been gaining in popularity and numerous improvements and modifications have been made to the original Innes[9] method. The Atlas Betograph is one such modern variant. More recently attention has been diverted to the application of the techniques of gas chromatography[10–12]. The equipment is relatively simple, rapid, sensitive, and avoids the complications of high-vacuum technology which so often render the conventional methods unsuitable for small industrial laboratories. Commercial apparatus—the Engelhard Isorpta and the Perkin-Elmer Sorptometer—are available and most manufacturers of gas chromatographic equipment now provide accessories for surface area determination.

Dye-stuff adsorption is the oldest method and recent work by Giles[13] and others has shown that consistent results can be obtained.

In an attempt to establish a basis for selection a sample exchange and test scheme was set up. Samples provided by the Sub-Committee members were sent to their own and to other laboratories. It had been anticipated that the number of laboratories possessing any one particular type of apparatus would be roughly in proportion to the popularity of that apparatus. Unfortunately, the bias was such that by the time the first draft Standards were ready it had not been possible to get a statistically significant number of results relating to the less conventional methods. Surprisingly this was also found to be the case for all but a few of the commercial versions of conventional apparatus. Consequently, the original plan was abandoned. Commercial equipment—with the exception of the very popular Fisher Sub-sieve Sizer—has been omitted from the current series of Standards and only those methods dealt with by the existing Panels have been standardized.

The intention is to re-convene CHE50/5 as soon as evidence is obtained that there is a real need to produce Standards relating to the other methods listed.

In addition to the two Panels working on B.S. equipment specifications, a third Panel, led by Mr Morgan of British Coal Utilization Research Association was asked to tackle the extremely difficult task of preparing a document recommending procedures for the Calculation of Specific Surface from Particle Size Distributions. The Sub-Committee considered this to be the only practical way to standardize the wide variety of possible methods based on direct and indirect determination of particle dimensions. Thus, this might be termed an indirect Standard in that its purpose is to ensure the existence of a common basis for specific surface estimation from other data. It would be presumptuous to assert that the recommendations, formulae and conversion factors to be given in the Standard are necessarily more correct than those to be found in the numerous literature publications.

What is important is that any two laboratories can ensure by referring to the Standard and agreeing to use the same appropriate factors that any difference in their results is at least not due to the methods of calculation.

One Standard—Part I Nitrogen adsorption (BET) method has been issued as B.S. 4359 Part I, 1969. The papers on Permeability Methods and on Calculation of the Specific Surface of a Powder from the Particle Size Distribution are in the proof stage and will be published as B.S.4359 Part II and Part III.

A further extension of the sample testwork in relation to the reproducibility and repeatability of the air-permeation methods has been carried out by the members of the Permeability Methods Panel. The results of this work, and of the main sample exchange test scheme, will be published elsewhere as separate papers.

References

[1] J. F. Padday (Kodak Ltd., Harrow), Private communication.
[2] J. M. Haynes. *Clay Minerals Bull.* **4**, 1 (1959).
[3] A. J. Haley. *J. appl. Chem.* **13**, 392 (1963).
[4] T. Allen, N. G. Stanley-Wood and T. S. Krishnamoorthy. *Particle Size Analysis*, Society for Analytical Chemistry, London, 1966, p. 297.
[5] C. H. Giles and A. H. Tole. *J. appl. Chem.* **14**, 186 (1964).
[6] R. K. Schofield and O. Talibudeen. *Disc. Farad. Soc.* No. 3 (1948) p. 51.
[7] E. L. Mackor. *Rec. trav. Chim.* **70**, 763 (1951).
[8] A. N. Puri and K. Murari. *Soil Sci.* **96**, 331 (1963).
[9] W. B. Innes. *Analyt. Chem.* **23**, 759 (1951).
[10] F. M. Nelson and F. T. Eggerton. *Analyt. Chem.* **30**, 1387 (1958).
[11] R. Stock. *Analyt. Chem.* **33**, 966 (1961).
[12] P. J. Kipling, P. G. Jeffrey and C. A. Savage. *Research & Development*, Feb. 1965, p. 18.
[13] C. H. Giles & S. Nakhwa. *J. appl. Chem.* **12**, 266 (1962).

DISCUSSION

Dr E. Roben (*Battelle-Institute e.V., Frankfurt/Main, Germany*) *said:* I would like to remark that the German Standards Institution, the Deutscher Normenausschuss (DNA), Fachnormenausschuss: Siebböden und Korngrösse, Arbeitsausschuss: Oberfläche experimentell has work in progress on standard methods for BET surface determination.

THE DETERMINATION OF SURFACE AREAS ON TITANIUM DIOXIDE PIGMENTS

D. URWIN

British Titan Products Company Limited, Billingham, U.K.

There are now a large number of commercial instruments designed to measure the BET surface area. Some of these instruments provide data from which a full adsorption/desorption isotherm can be calculated, others actually print out a value for the surface area.

Two instruments are used in the laboratories of British Titan Products Co. Ltd., to help define the surface of TiO_2 pigments. These are (i) a very simple apparatus, the Strohlein AREA-meter, used for the determination of surface areas by a single point method; and (ii) a more sophisticated instrument, the Carlo Erba Sorptomatic, which provides data from which a complete adsorption/desorption isotherm can be calculated.

The Area-meter is very simple and does not require vacuum techniques. The instrument is flushed with N_2 at atmospheric pressure. Two matched sample tubes are attached to the arms of a manometer. On immersion of the tubes, in liquid N_2, a differential pressure is set up due to adsorption of N_2 on the sample. The pressure difference, which is proportional to the surface area, is measured on the manometer.

Before the area can be measured the sample must first be treated so that a clean surface is presented. This pretreatment is carried out on a separate rig and entails flushing the samples, at elevated temperatures, with N_2. The conditions necessary to give a clean surface, free from adsorbed vapours, must be determined experimentally. *Figure 1* shows the results. It is clear that a temperature in the range 150–200°C for a time exceeding 6 hours gives the optimum figure for the surface area. *Figure 2* shows that at temperatures above 250°C collapse occurs with a consequent decrease in surface area.

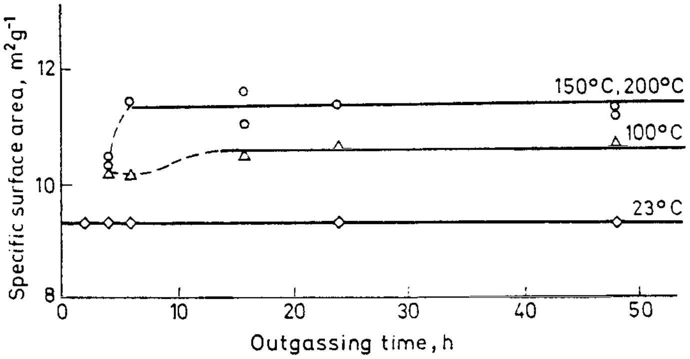

Figure 1. Changes in the surface area of a titanium dioxide sample with outgassing conditions

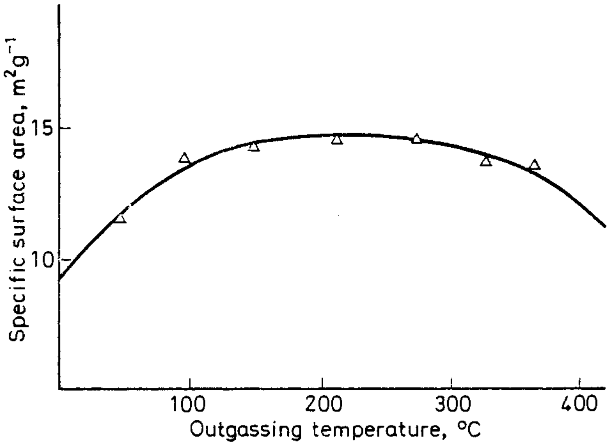

Figure 2. Variation in surface area of a titanium dioxide sample with temperature after outgassing for 16 h at $< 10^{-5}$ torr.

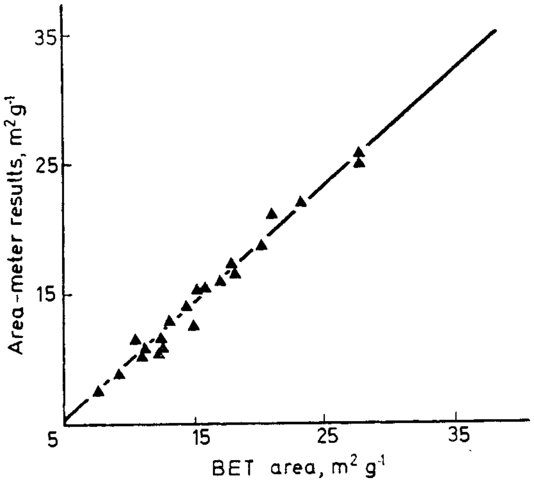

Figure 3. Comparison of the areas obtained for various titanium dioxide samples using the Area-meter and the BET method.

It is evident from these graphs that there is a considerable variation in surface area obtained under different conditions and it cannot be emphasised too strongly that the correct outgassing conditions must be determined experimentally for each type of material being examined.

Using these optimum outgassing conditions it was possible to proceed and to evaluate Area-meter results using, as a standard, results from the high vacuum apparatus. *Figure 3* shows the results for 50 samples. The difference between BET and Area-meter results, in the range 5–30 m^2 g^{-1}, is constant, the Area-meter yielding figures 10 per cent lower than the corresponding BET result. This is to be expected as a consequence of the single point determination. Using this single point technique it is possible to determine the surface areas of up to 16 samples each day.

The Carlo Erba Sorptomatic instrument automatically injects fixed amounts of N_2 into the sample bulb and determines the equilibrium pressure after each injection. Both adsorption and desorption isotherms can be determined after a little calculation. From this data the pore size distribution can be determined by whichever method is most suitable. Results can be obtained quickly. For a low surface area material a full adsorption/desorption isotherm can be obtained in about 10 hours. This is much quicker than using conventional high vacuum techniques. *Figure 4* compares results from the Carlo Erba Sorptomatic, the Micromeretics 2100, a BTP high vacuum volumetric apparatus and gravimetric data. The very good agreement indicates that the Sorptomatic can be used to obtain adsorption/desorption isotherms with a very considerable saving in both time and labour.

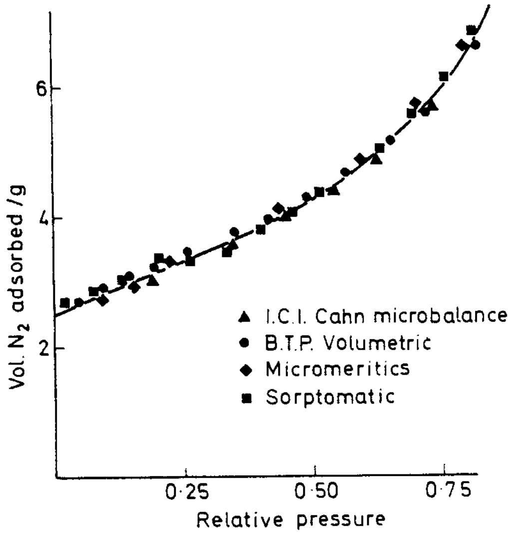

Figure 4. Nitrogen adsorption isotherms obtained on a rutile sample of surface area 13 m^2/g using various methods

A COMPARISON OF THE SURFACE AREA OF A STANDARD SAMPLE OF SILVER IODIDE AS MEASURED BY DIFFERENT METHODS IN DIFFERENT LABORATORIES

J. F. Padday

Kodak Limited, Harrow, Middlesex, U.K.

The surface area of a standard sample of silver iodide has been measured by a number of gas adsorption methods and by some solution adsorption methods in different laboratories. The results have been collected and tabulated for the purposes of comparison.

The comparison showed that surface area as measured by vapour adsorption and the BET equation gave good reproducibility but that adsorption from solution methods gave values greater than those obtained by the BET method.

PREPARATION OF THE SILVER IODIDE SAMPLE

Five litres of 1 M silver nitrate were added slowly to a little over 5 l of 1 M potassium iodide contained in a large clean vessel and stirred vigorously. The mixture was maintained at about 30°C and the pAg was not allowed to drop below 13·5 units as measured from the e.m.f. of a silver/silver iodide electrode backed with a saturated calomel electrode and porous pin salt bridge.

The preparation was carried out in a darkroom fitted with safelights to cut out blue and u.v. light (Wratten OB safelight) and the water used for the preparation and subsequent washing was distilled and checked for surface active impurities by surface tension measurement.

The slurry of silver iodide in potassium nitrate solution was heated to a temperature between 60–80°C with gentle stirring for two periods of eight hours each on successive days. Previous experience had shown that this treatment was about four times as long as needed for the surface growth to reach a stable state.

The mixture was then flocculated by reducing the pAg to a value of about 8·5 and decanted slowly. The precipitate was then washed with about 5 litres of distilled water, decanted and further washed by repeated water addition and decantation about 50 times until the specific resistance of the wash water became greater than 4×10^5 ohms/cm^3. The slurry was now centrifuged, washed with two successive volumes of 500 ml of ethanol and dried in a vacuum oven at 105°C for a few hours. The dried silver iodide was then gently crumbled and passed through a stainless steel mesh (approximately X30). The whole batch was coned and quartered according to standard procedures and samples were placed in clean dark-glass bottles for dispatch to other laboratories.

PRETREATMENT PRIOR TO MEASUREMENT

Silver iodide is only slightly sensitive to light, but prolonged exposure to both light and vacuum has the effect of reducing the surface to silver and iodine vapour. The suggested pretreatment was 2 hours evacuation at 105°C in the absence of u.v. and blue light.

METHODS OF MEASUREMENT

The method of measuring surface area by low-temperature adsorption of nitrogen or inert gases varies from laboratory to laboratory. A general guide to such methods is given in British Standard 4359 Part I: 1969. As certain parameters are important for the purposes of calculating the surface area by the BET method these details are listed below for each laboratory taking part in the exercise together with the name of the worker and the location of his laboratory. They were:

Dr. M. Jaycock, Loughborough University

Sample degassed at 100°C. Nitrogen adsorption at $-77{\cdot}5$°K in the range p/p_0 0·05 to 0·30. The specific area of a nitrogen molecule was taken as 16·2Å^2.

Mr. A. S. Joy, Warren Spring Laboratory

Nitrogen adsorption at liquid nitrogen temperatures in a continuous flow apparatus[1]. Range of p/p_0 0·01–0·3 the value of p_0 was 835 mm and the specific area of a nitrogen molecule was taken as 15·8Å^2.

The late Dr. J. J. Kipling, Hull University

Krypton adsorption at liquid nitrogen temperatures. Details of the measurements were not stated but they are believed to follow very closely those of Professor Sing of Brunel University. Dr. Kipling gave two results the second (lower value) of which he suspected as being too low.

Professor J. Lyklema and Dr. H. J. van den Hul, Wageningen University, Netherlands

1. Adsorption of cetylpyridinium bromide in aqueous solution assuming a site area of 54Å^2 per adsorbed cetylpyridinium ion.
2. Adsorption of methylene blue in aqueous solution assuming a site area of 61·6Å^2 per adsorbed ion.
3. Negative adsorption of $^{35}SO_4^{2-}$ ion.
4. Differential capacity.

Dr. A. P. Prosser and Dr. Eadington, Imperial College of Science, London

Krypton adsorption at liquid nitrogen temperatures over the partial pressure range p/p_0 0·01 to 0·5. p_0 of krypton was 2·905 mm Hg and the specific area of a krypton atom was taken as 18·5Å^2. Weight of silver iodide was in the range 0·5g to 2·5g.

Professor K. S. W. Sing, Brunel University

Krypton adsorption at 77°K. An extrapolated value of p_0 was used which was about 2·5 mm Hg. The specific area of krypton was taken as 19·5Å^2 per atom.

SURFACE AREA MEASUREMENTS OF SILVER IODIDE

The results of surface area measurement of silver iodide obtained by the various investigators are given in *Table 1*.

Table 1. Results of surface area measurement of silver iodide

Name		*Method*		*Result*
Jaycock		Nitrogen BET		0·52(5) m^2/g
Joy		Nitrogen continuous flow		0·60
Kipling		Krypton BET		0·59 (0·23) See text
Lyklema		Cetylpyridium ion		0·92
		Methylene blue		1·03
		Negative adsorption $^{35}SO_4^{2-}$		1·34
	After ageing sample	Methylene blue		0·71
		Negative adsorption $^{35}SO_4^{2-}$		1·07
		Differential capacity		2·96
Prosser		Krypton BET		0·60
		Krypton BET		0·57
		Krypton BET		0·56
		Krypton BET		0·57
	Sample aged	Krypton BET		0·50
Sing		Krypton BET		0·9
		All values	*BET only*	*Wet methods only*
Mean surface area		0·85 m^2/g	0·60 m^2/g	1·34 m^2/g
Standard deviation		0·62(4) m^2/g	0·12 m^2/g	0·82 m^2/g

CONCLUSIONS

1. Except for the suspect result from Dr. Kipling's laboratory which he was anxious to repeat the BET results show a degree of reproducibility of about ± 20%.
2. The original instructions indicated erroneously that pretreatment should take place at 150°C (instead of 105°C) with evacuation. This error may have caused the high results obtained in Professor Lyklema's laboratory.
3. The adsorption isotherms of cyanine and other dyes carried out at Harrow did not possess clear plateaux. Complex adsorption, which was found with silver iodide, could account for the high values obtained by Professor Lyklema.
4. The large standard deviation of results by the wet methods is strongly affected by the high single value obtained by differential capacity measurements. If this one value is omitted then the standard deviation is reduced to 0·6.
5. Some ageing effects are suggested but these cannot explain the difference between wet methods and BET methods.

Reference

[1] P. J. Kipling, P. G. Jeffrey and C. A. Savage. *Research and Development in Industry*, Feb./March 1965, pp. 18—22.

AUTHOR INDEX

Original contributions in bold type
Discussion contributions in roman